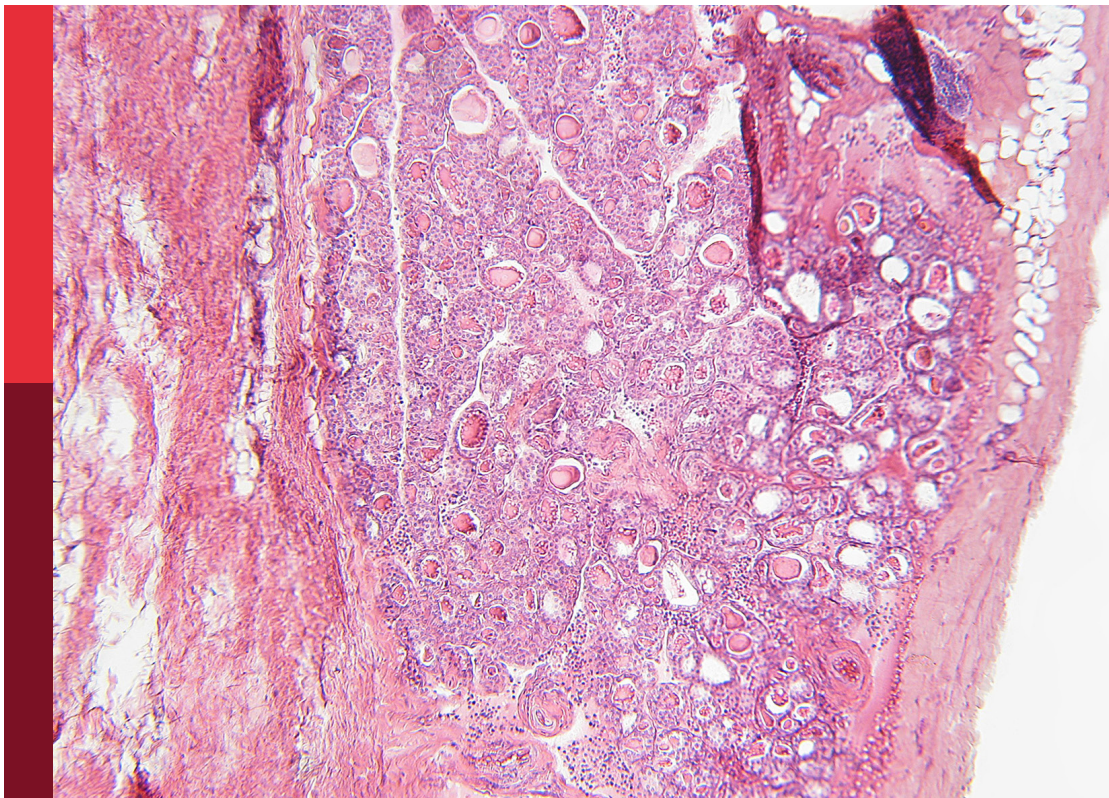
frontiers | Research Topics

Maternal-fetal interface: New insight in placenta research

Edited by
Cilia Abad, Mariana Farina, Alicia E. Damiano and Reinaldo Marín

Published in
Frontiers in Endocrinology



FRONTIERS EBOOK COPYRIGHT STATEMENT

The copyright in the text of individual articles in this ebook is the property of their respective authors or their respective institutions or funders. The copyright in graphics and images within each article may be subject to copyright of other parties. In both cases this is subject to a license granted to Frontiers.

The compilation of articles constituting this ebook is the property of Frontiers.

Each article within this ebook, and the ebook itself, are published under the most recent version of the Creative Commons CC-BY licence. The version current at the date of publication of this ebook is CC-BY 4.0. If the CC-BY licence is updated, the licence granted by Frontiers is automatically updated to the new version.

When exercising any right under the CC-BY licence, Frontiers must be attributed as the original publisher of the article or ebook, as applicable.

Authors have the responsibility of ensuring that any graphics or other materials which are the property of others may be included in the CC-BY licence, but this should be checked before relying on the CC-BY licence to reproduce those materials. Any copyright notices relating to those materials must be complied with.

Copyright and source acknowledgement notices may not be removed and must be displayed in any copy, derivative work or partial copy which includes the elements in question.

All copyright, and all rights therein, are protected by national and international copyright laws. The above represents a summary only. For further information please read Frontiers' Conditions for Website Use and Copyright Statement, and the applicable CC-BY licence.

ISSN 1664-8714
ISBN 978-2-8325-4106-7
DOI 10.3389/978-2-8325-4106-7

About Frontiers

Frontiers is more than just an open access publisher of scholarly articles: it is a pioneering approach to the world of academia, radically improving the way scholarly research is managed. The grand vision of Frontiers is a world where all people have an equal opportunity to seek, share and generate knowledge. Frontiers provides immediate and permanent online open access to all its publications, but this alone is not enough to realize our grand goals.

Frontiers journal series

The Frontiers journal series is a multi-tier and interdisciplinary set of open-access, online journals, promising a paradigm shift from the current review, selection and dissemination processes in academic publishing. All Frontiers journals are driven by researchers for researchers; therefore, they constitute a service to the scholarly community. At the same time, the *Frontiers journal series* operates on a revolutionary invention, the tiered publishing system, initially addressing specific communities of scholars, and gradually climbing up to broader public understanding, thus serving the interests of the lay society, too.

Dedication to quality

Each Frontiers article is a landmark of the highest quality, thanks to genuinely collaborative interactions between authors and review editors, who include some of the world's best academicians. Research must be certified by peers before entering a stream of knowledge that may eventually reach the public - and shape society; therefore, Frontiers only applies the most rigorous and unbiased reviews. Frontiers revolutionizes research publishing by freely delivering the most outstanding research, evaluated with no bias from both the academic and social point of view. By applying the most advanced information technologies, Frontiers is catapulting scholarly publishing into a new generation.

What are Frontiers Research Topics?

Frontiers Research Topics are very popular trademarks of the *Frontiers journals series*: they are collections of at least ten articles, all centered on a particular subject. With their unique mix of varied contributions from Original Research to Review Articles, Frontiers Research Topics unify the most influential researchers, the latest key findings and historical advances in a hot research area.

Find out more on how to host your own Frontiers Research Topic or contribute to one as an author by contacting the Frontiers editorial office: frontiersin.org/about/contact

Maternal-fetal interface: New insight in placenta research

Topic editors

Cilia Abad — Charles University, Czechia

Mariana Farina — CONICET Centro de Estudios Farmacológicos y Botánicos (CEFYBO), Argentina

Alicia E. Damiano — University of Buenos Aires, Argentina

Reinaldo Marín — Instituto Venezolano de Investigaciones Científicas (IVIC), Venezuela

Citation

Abad, C., Farina, M., Damiano, A. E., Marín, R., eds. (2023). *Maternal-fetal interface: New insight in placenta research*. Lausanne: Frontiers Media SA. doi: 10.3389/978-2-8325-4106-7

Table of contents

05 Editorial: Maternal-fetal interface: new insight in placenta research
Cilia Abad, Mariana Farina, Alicia E. Damiano and Reinaldo Marín

08 Vitamin D Supplementation Improves Mitochondrial Function and Reduces Inflammation in Placentae of Obese Women
Elysse A. Phillips, Nora Hendricks, Matthew Bucher and Alina Maloyan

20 Detection of Shiga Toxin-Producing *Escherichia coli* (STEC) in the Endocervix of Asymptomatic Pregnant Women. Can STEC Be a Risk Factor for Adverse Pregnancy Outcomes?
María Luján Scalise, Nicolás Garimano, Marcelo Sanz, Nora Lia Padola, Patricia Leonino, Adriana Pereyra, Roberto Casale, María Marta Amaral, Flavia Sacerdoti and Cristina Ibarra

29 Chronic histiocytic intervillositis (CHI): current treatments and perinatal outcomes, a systematic review and a meta-analysis
Laurel Moar, Chloe Simela, Surabhi Nanda, Andreas Marnerides, Mudher Al-Adnani, Catherine Nelson-Piercy, Kypros H. Nicolaides and Panicos Shangaris

46 Kisspeptin treatment improves fetal-placental development and blocks placental oxidative damage caused by maternal hypothyroidism in an experimental rat model
Bianca Reis Santos, Jeane Martinha dos Anjos Cordeiro, Luciano Cardoso Santos, Erikles Macedo Barbosa, Letícia Dias Mendonça, Emilly Oliveira Santos, Isabella Oliveira de Macedo, Mário Sergio Lima de Lavor, Raphael Escorsim Szawka, Rogeria Serakides and Juneo Freitas Silva

64 Identification of unusual oxysterols biosynthesised in human pregnancy by charge-tagging and liquid chromatography - mass spectrometry
Alison L. Dickson, Eylan Yutuc, Catherine A. Thornton, Yuqin Wang and William J. Griffiths

83 Protein *O*-GlcNAcylation as a nutrient sensor signaling placental dysfunction in hypertensive pregnancy
Rinaldo Rodrigues dos Passos Junior, Raiany Alves de Freitas, Vanessa Dela Justina, Sebastián San Martín, Victor Vitorino Lima and Fernanda Regina Giachini

95 Serotonin system in the human placenta – the knowns and unknowns
Maja Perić, Ivona Bečeheli, Lipa Čičin-Šain, Gernot Desoye and Jasminka Štefulj

114 Cell-type specific distribution and activation of type I IFN pathway molecules at the placental maternal-fetal interface in response to COVID-19 infection
Yuping Wang, Yang Gu, David F. Lewis, Xin Gu, Karisa Brown, Courtney Lachute, Miriam Hankins, Rona S. Scott, Caitlin Busada, Danielle B. Cooper, Charles E. McCathran and Perry Barrilleaux

127 Regulators involved in trophoblast syncytialization in the placenta of intrauterine growth restriction
Hanjing Zhou, Chenqiong Zhao, Peixin Wang, Weijie Yang, Haiyan Zhu and Songying Zhang

143 Inhibition of diacylglycerol lipase β modulates lipid and endocannabinoid levels in the *ex vivo* human placenta
Natascha Berger, Tom van der Wel, Birgit Hirschmugl, Thomas Baernthaler, Juergen Gindlhuber, Nermeen Fawzy, Thomas Eichmann, Ruth Birner-Gruenberger, Robert Zimmermann, Mario van der Stelt and Christian Wadsack

155 Cellular mechanisms linking to outdoor and indoor air pollution damage during pregnancy
Delia I. Chiarello, Javier Ustáriz, Reinaldo Marín, Ivo Carrasco-Wong, Marcelo Farías, Ady Giordano, Felipe S. Gallardo, Sebastián E. Illanes and Jaime Gutiérrez

170 Identification of altered miRNAs and their targets in placenta accreta
José M. Murrieta-Coxca, Emanuel Barth, Paulina Fuentes-Zacarias, Ruby N. Gutiérrez-Samudio, Tanja Groten, Alexandra Gellhaus, Angela Köninger, Manja Marz, Udo R. Markert and Diana M. Morales-Prieto

185 Endometrial stromal cell miR-19b-3p release is reduced during decidualization implying a role in decidual-trophoblast cross-talk
Ellen Menkhorst, Teresa So, Kate Rainczuk, Siena Barton, Wei Zhou, Tracey Edgell and Evdokia Dimitriadis

194 Expression of placental glycans and its role in regulating peripheral blood NK cells during preeclampsia: a perspective
Julio C. Bueno-Sánchez, Alejandra M. Gómez-Gutiérrez, Juan G. Maldonado-Estrada and Juan C. Quintana-Castillo

211 Machine learning applied in maternal and fetal health: a narrative review focused on pregnancy diseases and complications
Daniela Mennickent, Andrés Rodríguez, Ma. Cecilia Opazo, Claudia A. Riedel, Erica Castro, Alma Eriz-Salinas, Javiera Appel-Rubio, Claudio Aguayo, Alicia E. Damiano, Enrique Guzmán-Gutiérrez and Juan Araya

233 Expression of nutrient transporters in placentas affected by gestational diabetes: role of leptin
Pilar Guadix, Isabel Corrales, Teresa Vilariño-García, Carmen Rodríguez-Chacón, Flora Sánchez-Jiménez, Carlos Jiménez-Cortegana, José L. Dueñas, Víctor Sánchez-Margalet and Antonio Pérez-Pérez

249 Ferroptosis and its potential role in gestational diabetes mellitus: updated evidence from pathogenesis to therapy
Yan Zhao, Qianqian Gao, Baoxuan Li, Yang Wang and Yue Wang

frontiers | Frontiers in Endocrinology

TYPE Editorial
PUBLISHED 28 November 2023
DOI 10.3389/fendo.2023.1325568

Check for updates

OPEN ACCESS

EDITED BY
Wei Ge,
University of Macau, China

REVIEWED BY
Chun Peng,
York University, Canada

*CORRESPONDENCE
Cilia Abad
clabad@gmail.com
Mariana Farina
marifarina@yahoo.com
Alicia E. Damiano
aedamiano@gmail.com
Reinaldo Marín
reinaldomarin@gmail.com

RECEIVED 21 October 2023
ACCEPTED 21 November 2023
PUBLISHED 28 November 2023

CITATION
Abad C, Farina M, Damiano AE and Marín R (2023) Editorial: Maternal-fetal interface: new insight in placenta research. *Front. Endocrinol.* 14:1325568. doi: 10.3389/fendo.2023.1325568

COPYRIGHT
© 2023 Abad, Farina, Damiano and Marín. This is an open-access article distributed under the terms of the Creative Commons Attribution License (CC BY). The use, distribution or reproduction in other forums is permitted, provided the original author(s) and the copyright owner(s) are credited and that the original publication in this journal is cited, in accordance with accepted academic practice. No use, distribution or reproduction is permitted which does not comply with these terms.

Editorial: Maternal-fetal interface: new insight in placenta research

Cilia Abad[1]*, Mariana Farina[2]*, Alicia E. Damiano[3,4]* and Reinaldo Marín[5]*

[1]Department of Pharmacology and Toxicology, Faculty of Pharmacy in Hradec Kralove, Charles University, Hradec Králové, Czechia, [2]Faculty of Medicine, Center of Pharmacological and Botanical Studies (CEFYBO-CONICET), University of Buenos Aires, Buenos Aires, Argentina, [3]Department of Biological Science, Faculty of Pharmacy and Biochemistry, University of Buenos Aires, Buenos Aires, Argentina, [4]Institute of Physiology and Biophysics Bernardo Houssay 018(IFIBIO Houssay), CONICET, University of Buenos Aires, Buenos Aires, Argentina, [5]Center for Biophysics and Biochemistry (CBB), Venezuelan Institute for Scientific Research (IVIC), Caracas, Venezuela

KEYWORDS

pregnancy, placenta, maternal-fetal health, maternal-fetal interface, placental pathology

Editorial on the Research Topic
Maternal-fetal interface: new insight in placenta research

Pregnancy, a complex and multifaceted biological process, often goes underappreciated despite involving intricate mechanisms to ensure the well-being of both the mother and the fetus. The placenta, often regarded as the bridge between mother and baby, plays a central role in this process. Recent studies have shed light on the importance of placental health, revealing potential therapeutic targets (1).

The objective of the Research Topic "*Maternal-Fetal Interface: New Insights in Placenta Research*" was to bring together original research articles and reviews that highlight recent advances in understanding the functions of the placenta and its impact on the health of both the mother and her future child. This Research Topic includes a diverse range of studies, encompassing ten original articles, six reviews, and one systematic review.

One significant concern is obesity, affecting approximately 30% of expectant mothers in the US (2). Its adverse effects on pregnancy, including issues like mitochondrial dysfunction and placental inflammation, may be linked to reduced Vitamin D levels. Encouragingly, Vitamin D supplementation emerges as a potential remedy, offering a relatively straightforward solution to a complex problem.

Furthermore, maternal hypothyroidism is associated with fetal growth, placental dysfunction, and reduced kisspeptin/Kiss1R at the maternal-fetal interface (3, 4). In this regard, daily treatment with kisspeptin improves fetal development and placental

morphology in an experimental model of hypothyroid rats, blocking placental oxidative damage, and increasing the expression of growth factors and antioxidant enzymes in the placenta.

Chronic histiocytic intervillositis (CHI) is a rare placental lesion associated with recurrent pregnancy issues (5). A systematic review and meta-analysis aimed to understand the perinatal consequences of CHI pregnancies and the potential benefits of treatment. While various drugs show potential, more research is needed to validate their safety, efficacy, and optimal dosage.

Shiga toxin-producing *Escherichia coli* (STEC) in the endocervix of asymptomatic pregnant women could have a potential role in adverse pregnancy outcomes (6). Bacterial findings reveal that a significant percentage of asymptomatic pregnant women with STEC in their endocervical samples. These findings suggest that STEC may be present in the lower female reproductive tract during pregnancy, raising new questions about its potential impact on pregnancy complications.

The impact of COVID-19 on pregnant women has been a cause for concern (7, 8). Findings suggest that certain molecules are upregulated in placentas exposed to COVID-19, indicating a potential innate defense mechanism of the placenta against the SARS-CoV-2 virus.

Advanced techniques have allowed for the study of microRNAs (miRNAs) in placenta accreta, revealing altered expressions and potential regulatory networks (9). Similarly, research into the serotonin system in the human placenta has illuminated its potential pathways and alterations, which could have consequences for the fetus.

Oxysterols, small molecules with a potentially monumental role in maternal-fetal health, hypertension during pregnancy, and the placental serotonin system are other areas being thoroughly investigated (10). The research aims to detect oxysterols and their subsequent metabolites in the placenta, umbilical cord blood plasma, maternal plasma, and amniotic fluid. This study contributes to a deeper understanding of the role of these molecules at the maternal-fetal interface.

Placental dysfunction can lead to gestational hypertension (11). In fact, it is well established that defective placental development/function is the root cause of early-onset preeclampsia and fetal growth restriction (12). Protein modifications (O-GlcNAcylation) are linked to hypertension, but their impact on placental function remains unclear (13). Female Wistar and spontaneously hypertensive rats (SHR) were studied during pregnancy, revealing that SHR had higher blood pressure, smaller fetuses, and reduced placental efficiency. Morphological changes in the placenta were observed, with lower O-GlcNAc protein expression and enzyme levels in hypertensive rats. This suggests that insufficient placental O-GlcNAcylation impairs fetal growth by disrupting placental function.

Environmental factors, especially air pollution, have been shown to pose risks to pregnancy, emphasizing the need for global efforts to improve air quality (14).

The pattern of glycan expression at the maternal-fetal interface could have a crucial role in driving the physiological alterations during pregnancy (15). Glycans' role emerges as a key player in understanding disorders like preeclampsia. On the other hand, lipids and fatty acids are essential elements in the metabolic processes within the human placenta, actively participating in fetal development (16). Dysregulated lipid metabolism and abnormal functioning of lipases in the placenta have been associated with various pregnancy-related complications, including conditions like preeclampsia and preterm birth. In this regard, the significance of diacylglycerol lipase β (DAGLβ) highlights the importance of intracellular lipases in lipid network regulation, with potential implications for placental function in normal and compromised pregnancies.

Addressing complications like fetal intrauterine growth restriction (IUGR), which results from impaired trophoblast syncytialization, requires a deeper understanding of the involved regulators (17). Machine learning is innovatively employed to identify patterns and predict perinatal disorders, marking a new era in maternal and fetal healthcare.

The successful implantation of a blastocyst in a healthy pregnancy relies on the decidualization of uterine endometrial stromal fibroblast cells (hESF) (18). MicroRNAs (miRs) play a critical role in cellular function and can influence recipient cells. Investigating how decidualization affects miR release by hESF, with a focus on miR-19b-3p linked to recurrent pregnancy loss, reveals that *in vitro* decidualization reduces the release of several miRs. Notably, miR-19b-3p is elevated in the endometrium of patients with a history of early pregnancy loss. Functionally, miR-19b-3p overexpression impedes trophoblast cell proliferation and increases HOXA9 expression, suggesting that miR release by decidualized hESF may regulate other cell types in the decidua, emphasizing the importance of proper miR release for healthy implantation and placental development.

Nutrient transport, especially in conditions like gestational diabetes mellitus (GDM), plays a crucial role (19). Leptin's role in modulating this transport, particularly in GDM, emerges as a critical research avenue.

Traditional Chinese medicine (TCM) offers potential solutions for complications like GDM (20). The discovery of the significance of ferroptosis in GDM pathogenesis and the potential therapeutic properties of *Coptis chinensis* underscore the harmonious integration of traditional knowledge and modern science.

In conclusion, placental health is a diverse and intricate field. Advances in research, a deeper understanding of molecular mechanisms, and innovative solutions are converging to shape a brighter future for maternal and fetal health. Interdisciplinary collaboration and a commitment to scientific excellence hold the promise of better interventions and therapies. We aspire to a future where every pregnancy is celebrated with the expectation of a healthy and thriving outcome, free from complications and disease.

This journey of discovery and understanding opens the door to innovations that can transform maternal-fetal health, offering hope and happiness for all mothers and unborn children. It is a future that honors the miracle of life in all its wondrous and complex forms, where each step brings us closer to realizing a vision of a brighter and healthier future for all.

Author contributions

CA: Writing – original draft, Writing – review & editing. MF: Writing – original draft, Writing – review & editing. AD: Writing – original draft, Writing – review & editing. RM: Writing – original draft, Writing – review & editing.

Conflict of interest

The authors declare that the research was conducted in the absence of any commercial or financial relationships that could be construed as a potential conflict of interest.

Publisher's note

All claims expressed in this article are solely those of the authors and do not necessarily represent those of their affiliated organizations, or those of the publisher, the editors and the reviewers. Any product that may be evaluated in this article, or claim that may be made by its manufacturer, is not guaranteed or endorsed by the publisher.

References

1. Cindrova-Davies T, Sferruzzi-Perri AN. Human placental development and function. *Semin Cell Dev Biol* (2022) 131:66–77. doi: 10.1016/j.semcdb.2022.03.039

2. Catalano PM, Shankar K. Obesity and pregnancy: mechanisms of short term and long term adverse consequences for mother and child. *Bmj* (2017) 356:j1. doi: 10.1136/bmj.j1

3. Krassas GE, Poppe K, Glinoer D. Thyroid function and human reproductive health. *Endocr Rev* (2010) 31:702–55. doi: 10.1210/er.2009-0041

4. Santos BR, Dos Anjos Cordeiro JM, Santos LC, De Oliveira LS, Mendonça LD, Santos EO, et al. Maternal hypothyroidism reduces the expression of the kisspeptin/Kiss1r system in the maternal-fetal interface of rats. *Reprod Biol* (2022) 22:100615. doi: 10.1016/j.repbio.2022.100615

5. Goldstein JA, Gallagher K, Beck C, Kumar R, Gernand AD. Maternal-fetal inflammation in the placenta and the developmental origins of health and disease. *Front Immunol* (2020) 11:531543. doi: 10.3389/fimmu.2020.531543

6. Sacerdoti F, Scalise ML, Burdet J, Amaral MM, Franchi AM, Ibarra C. Shiga toxin-producing escherichia coli infections during pregnancy. *Microorganisms* (2018) 6:111. doi: 10.3390/microorganisms6040111

7. Ayala-Ramírez P, González M, Escudero C, Quintero-Arciniegas L, Giachini FR, Alves De Freitas R, et al. Severe acute respiratory syndrome coronavirus 2 infection in pregnancy. A non-systematic review of clinical presentation, potential effects of physiological adaptations in pregnancy, and placental vascular alterations. *Front Physiol* (2022) 13:785274. doi: 10.3389/fphys.2022.785274

8. Marín R, Pujol FH, Rojas D, Sobrevia L. SARS- CoV-2 infection and oxidative stress in early-onset preeclampsia. *Biochim Biophys Acta Mol Basis Dis* (2022) 1868:166321. doi: 10.1016/j.bbadis.2021.166321

9. Long Y, Chen Y, Fu XQ, Yang F, Chen ZW, Mo GL, et al. Research on the expression of MRNA-518b in the pathogenesis of placenta accreta. *Eur Rev Med Pharmacol Sci* (2019) 23:23–8. doi: 10.26355/eurrev_201901_16743

10. Chatuphonprasert W, Jarukamjorn K, Ellinger I. Physiology and pathophysiology of steroid biosynthesis, transport and metabolism in the human placenta. *Front Pharmacol* (2018) 9:1027. doi: 10.3389/fphar.2018.01027

11. Qu H, Khalil RA. Vascular mechanisms and molecular targets in hypertensive pregnancy and preeclampsia. *Am J Physiol Heart Circ Physiol* (2020) 319:H661–h681. doi: 10.1152/ajpheart.00202.2020

12. Marín R, Chiarello DI, Abad C, Rojas D, Toledo F, Sobrevia L. Oxidative stress and mitochondrial dysfunction in early-onset and late-onset preeclampsia. *Biochim Biophys Acta Mol Basis Dis* (2020) 1866:165961. doi: 10.1016/j.bbadis.2020.165961

13. Ning J, Yang H. O-glcNAcylation in hyperglycemic pregnancies: impact on placental function. *Front Endocrinol (Lausanne)* (2021) 12:659733. doi: 10.3389/fendo.2021.659733

14. Saenen ND, Martens DS, Neven KY, Alfano R, Bové H, Janssen BG, et al. Air pollution-induced placental alterations: an interplay of oxidative stress, epigenetics, and the aging phenotype? *Clin Epigenet* (2019) 11:124. doi: 10.1186/s13148-019-0688-z

15. Rahnemaei FA, Fashami MA, Abdi F, Abbasi M. Factors effective in the prevention of Preeclampsia:A systematic review. *Taiwan J Obstet Gynecol* (2020) 59:173–82. doi: 10.1016/j.tjog.2020.01.002

16. Delhaes F, Giza SA, Koreman T, Eastabrook G, Mckenzie CA, Bedell S, et al. Altered maternal and placental lipid metabolism and fetal fat development in obesity: Current knowledge and advances in non-invasive assessment. *Placenta* (2018) 69:118–24. doi: 10.1016/j.placenta.2018.05.011

17. Colson A, Depoix CL, Baldin P, Hubinont C, Sonveaux P, Debiève F. Hypoxia-inducible factor 2 alpha impairs human cytotrophoblast syncytialization: New insights into placental dysfunction and fetal growth restriction. *FASEB J* (2020) 34:15222–35. doi: 10.1096/fj.202001681R

18. Gellersen B, Brosens JJ. Cyclic decidualization of the human endometrium in reproductive health and failure. *Endocr Rev* (2014) 35:851–905. doi: 10.1210/er.2014-1045

19. Pérez-Pérez A, Vilariño-García T, Guadix P, Dueñas JL, Sánchez-Margalet V. Leptin and nutrition in gestational diabetes. *Nutrients* (2020) 12:1970. doi: 10.3390/nu12071970

20. Xu YXZ, Xi S, Qian X. Evaluating traditional chinese medicine and herbal products for the treatment of gestational diabetes mellitus. *J Diabetes Res* (2019) 2019:9182595. doi: 10.1155/2019/9182595

frontiers | Frontiers in Endocrinology

ORIGINAL RESEARCH
published: 31 May 2022
doi: 10.3389/fendo.2022.893848

Vitamin D Supplementation Improves Mitochondrial Function and Reduces Inflammation in Placentae of Obese Women

Elysse A. Phillips[1†], *Nora Hendricks*[1†], *Matthew Bucher*[2] *and Alina Maloyan*[1*]

[1] Knight Cardiovascular Institute, Oregon Health & Science University, Portland, OR, United States, [2] Department of OB/GYN, Oregon Health and Science University, Portland, OR, United States

OPEN ACCESS

Edited by:
Reinaldo Marín,
Instituto Venezolano de Investigaciones Científicas (IVIC), Venezuela

Reviewed by:
Madan Madhav Godbole,
Sanjay Gandhi Post Graduate Institute of Medical Sciences (SGPGI), India
Luis Sobrevia,
Pontificia Universidad Católica de Chile, Chile

***Correspondence:**
Alina Maloyan
maloyan@ohsu.edu

[†]These authors have contributed equally to this work

Specialty section:
This article was submitted to Developmental Endocrinology, a section of the journal Frontiers in Endocrinology

Received: 10 March 2022
Accepted: 25 April 2022
Published: 31 May 2022

Citation:
Phillips EA, Hendricks N, Bucher M and Maloyan A (2022) Vitamin D Supplementation Improves Mitochondrial Function and Reduces Inflammation in Placentae of Obese Women. Front. Endocrinol. 13:893848. doi: 10.3389/fendo.2022.893848

Background: About 30% of women entering pregnancy in the US are obese. We have previously reported mitochondrial dysregulation and increased inflammation in the placentae of obese women. Vitamin D (VitD) is a major player in calcium uptake and was shown to modulate mitochondrial respiration and the immune/inflammation system. Studies show decreased VitD levels in obese individuals; however, the effect of maternal obesity on VitD metabolism and its association with placental function remains understudied.

Methods: Maternal and cord blood plasma and placental samples were collected upon C-section from normal-weight (NW, body mass index [BMI]<25) and obese (OB, BMI>30) women with uncomplicated pregnancies at term. We measured 25(OH)D_3 (calcidiol) levels in maternal and cord blood plasma using ELISA. We assessed the expression of CYP27B1, an activator of calcidiol, and Vitamin D receptor (VDR) in placentae from NW and OB, and women with gestational diabetes and preeclampsia. In addition, we examined the effects of VitD supplementation on mitochondrial function and inflammation in trophoblasts from NW and OB, using the Seahorse Bioanalyzer and Western blot, respectively.

Results: Vitamin D levels in blood from OB but not NW women and in cord blood from babies born to NW and OB women showed a significant inverse correlation with maternal pre-pregnancy BMI (r=-0.50, p<0.1 and r=-0.55, p=0.004 respectively). Cord plasma VitD levels showed a positive correlation with placental efficiency, i.e., the ratio between fetal and placental weight, as well as with maternal blood VitD levels (r=0.69 and 0.83 respectively, p<0.00). While we found no changes in CYP27B1 in OB vs. NW women, VDR expression were decreased by 50% (p<0.03) independent of fetal sex. No changes in VDR expression relative to BMI-matched controls were observed in the placentae of women with gestational diabetes or preeclampsia. Cytotrophoblasts isolated from placentae of OB women showed a dose-dependent increase in VDR expression after 24-hour treatment with calcitriol (10 nM and 100 nM), an active form of VitD. Trophoblasts

isolated from OB women and treated with calcitriol improved mitochondrial respiration ($p<0.05$). We also found a two-fold increase in expression of the NLRP3 inflammasome and the pro-inflammatory cytokine IL-18 in trophoblasts isolated from placentae of OB women ($p<0.05$), with IL-18 expression being reversed by calcitriol treatment (100 nM).

Conclusions: We show that VitD deficiency is at least partially responsible for mitochondrial dysfunction and increased inflammation in the placentae of obese women. Vitamin D supplementation could be beneficial in improving placental dysfunction seen in obese women.

Keywords: maternal obesity, Vitamin D, cord blood, maternal blood, placenta, mitochondrial function, placental inflammation

INTRODUCTION

Epidemiological studies have shown that obese individuals have lower levels of circulating Vitamin D (VitD) compared with normal-weight people (1), though the mechanism for this has not yet been extensively studied. Vitamin D is a lipid-soluble vitamin that performs many important functions in the human body, including aiding in calcium absorption (2), exerting antimicrobial properties (3), and helping to reduce inflammation (4). Once VitD is obtained, either through sunlight or the diet, it enters the bloodstream, where it is transported to the liver for hydroxylation to its inactive form, calcidiol [$25(OH)D_3$], and subsequently to the kidney for its final hydroxylation by cytochrome P450 family 27 subfamily B member 1 (CYP27B1) to the active form, calcitriol [$1a,25(OH)_2D_3$] (5). During pregnancy, VitD plays important roles in supporting calcium absorption and the healthy growth of bones in the developing fetus; it also aids immune system function (6).

In the United States, it is estimated that over one-third of the adult population is obese, defined as having a body mass index (BMI) greater than 30 (7). More than 65% of women entering pregnancy in the US are either overweight or obese. Pregnancies in obese mothers generate an adverse intrauterine environment *via* both their inflammatory milieu (8) and metabolic and endocrine derangements (9). Obesity impacts the outcome of the pregnancy *per se*, and is associated with hypertensive disorders, gestational diabetes, preeclampsia, and thromboembolic events (10). It also affects the fetus and newborn, causing congenital malformations, large- and small-for-gestational-age infants, and stillbirth. Importantly, maternal obesity leads to cardiovascular dysregulations (11–13) and to obesity and metabolic diseases in offspring (10). In addition, data also show that maternal obesity results in metabolic inflammation in the mother and programs inflammation in the offspring (14).

The placenta is now recognized as a critical regulator of fetal growth and development and as the transducer for communication of maternal and uterine environments to the fetus, whether normal or adverse (15). Thus, despite its short lifespan, the placenta plays a crucial role in offspring health. Several groups including our own have shown that maternal obesity compromises placental function, even in pregnancies having apparently "normal" outcomes (10, 16–18). In particular, maternal obesity has been reported to dysregulate placental metabolism, leading to abnormal mitochondrial respiration and excessive production of reactive oxygen species (16), accumulation of inflammation (19), dysregulated autophagy (17), and changes in miRNA expression (20) and epigenetic modifications (21).

At the molecular level, placentae from obese women were demonstrated to have increased expression of the nucleotide-binding oligomerization domain, leucine-rich repeat-, and pyrin domain-containing 3 (NLRP3) inflammasome, a key mediator of sterile inflammation (22). Inflammasomes are multiprotein complexes, assembly of which is triggered by both microbial and endogenous danger signals and results in activation and cleavage of caspase-1. When activated, caspase-1 cleaves gasdermin D (23) to generate an N-terminal cleavage product that triggers inflammatory cell death (pyroptosis) and the release of pro-inflammatory cytokines interleukin-1β (IL-1β) and IL-18 (24). Excessive activation of the NLRP3 inflammasome has been shown to lead to diabetes, atherosclerosis, and obesity-induced insulin resistance (25). Vitamin D has been found to inhibit the NLRP3 inflammasome either by direct binding between NLRP3 and the Vitamin D receptor (VDR) (26) or *via* VDR signaling-mediated inhibition of cytokine secretion (27). However, the specific role of VitD in maternal obesity-mediated placental inflammation remains understudied.

The aim of this study was to determine whether obesity in pregnancy affects circulating Vitamin D levels. Using maternal and umbilical cord blood collected from normal-weight and obese women at term, we found maternal BMI-dependent changes in the levels of VitD and its receptor. We also assessed the role of VitD supplementation in addressing the placental mitochondrial dysfunction and increased placental inflammation seen in the setting of maternal obesity.

MATERIALS AND METHODS

Ethics Statement

The studies involving human participants were reviewed and approved by the Institutional Review Board of Oregon Health & Science University. Maternal blood, cord blood, and placental tissue were collected from labor and delivery units with informed consent from the patients.

Collection and Processing of Placental Tissue

Placentae were collected at term, immediately after elective C-section (gestational weeks 39-40) with no labor. C-sections deliveries prior to labor were chosen because uterine contractions during labor have been shown to be associated with activation of oxidative stress and pro-inflammatory signaling, with increased accumulation of COX-2, TNFα, and IL-1β as well as stabilization of HIF-1α in placental tissue (28). In addition, the duration of labor increases the severity of the impact, which is to be expected. This study was supported by report from Lager et al. (29). These findings indicate that in many respects a vaginally delivered placenta does not accurately reflect the organ's normal *in vivo* state and caution against the use of such placentae for biochemical and molecular studies. Placental tissues for this study were collected from subjects who: 1) Had a singleton pregnancy; 2) Delivered by C-section; 3) Had either normal or high pre-pregnancy body mass index (BMI), respectively grouped as normal-weight (NW; BMI=18.5-24.9) or obese (OB; BMI=30-45); 4) Had either uncomplicated pregnancy or developed gestational diabetes A2GDM controlled by insulin; and 5) Were either normotensive or developed severe preeclampsia defined as presence of hypertension (systolic blood pressure >160 mmHg and/or diastolic blood pressure >110 mmHg on two occasions 2 - 240 hours apart) and proteinuria (≥2 protein on dipstick) occurring after 20 weeks of gestation in a previously normotensive woman. Exclusion criteria included multifetal gestation; pre-gestational chronic inflammatory diseases (asthma, type 2 diabetes, rheumatoid arthritis, Crohn's disease, etc); use of tobacco or illicit drugs, or both; and recent bariatric surgery. The placentae were randomly sampled as described previously (30). Placental efficiency was calculated as the ratio between birth weight and placental weight.

Plasma Collection

Maternal blood was collected from fasting patients before C-section. Cord blood was collected and placed in EDTA-containing collection tubes. Plasma was immediately separated from whole blood by centrifugation at 2000 g for 10 min at 4°C, then flash-frozen in liquid nitrogen and stored at -80°C for further analyses.

Materials

ELISA kits to detect circulating 25(OH) Vitamin D (calcidiol) were purchased from Abcam (Cambridge, MA). Antibodies against Vitamin D receptor (VDR) and against mouse and rabbit IgG were purchased from Cell Signaling Technology (Danvers, MA), and the antibody against cytochrome P450, family 27, subfamily B, polypeptide 1 (CYP27B1) was purchased from ThermoFisher (Waltham, MA). Anti-NLRP3 was purchased from Novus Biologicals (Centennial, CO), and antibodies against gasdermin D and anti-IL-18 were purchased from Biolegend (San Diego, CA). Antibodies against caspase-1 that recognized both total and cleaved forms were purchased from Cell Signaling, and the antibody against endogenous control β-actin (ACTB) was purchased from Sigma-Aldrich St. Louis, MO). Pierce™ BCA Protein Assay Kits were also purchased from ThermoFisher. For cell culture experiments, calcitriol was purchased from Cayman Chemical Company (Ann Arbor, Michigan). Mitochondrial inhibitors oligomycin, FCCP, antimycin A, and rotenone were purchased from Sigma.

Maternal Serum and Cord Blood Vitamin D Content

Circulating levels of 25(OH) Vitamin D were measured using an enzyme-linked immunosorbent assay (ELISA) according to manufacturer instructions.

Tissue Processing and Sampling

Villous tissue was dissected from placentae and flash-frozen in liquid nitrogen for protein expression measurements. Cytotrophoblasts (CTBs) were isolated by enzymatic digestion followed by density gradient purification as we previously described (30). CTBs were plated in Iscove's Modified Dulbecco's Medium (ThermoFisher Scientific, catalog # 12440), containing 25 mM D-glucose (dextrose), and supplemented with 10% FBS and penicillin/streptomycin. Cells were allowed to fuse and form a multinucleated syncytium for 72 hours before measurements were taken.

Protein Isolation

Proteins were isolated from flash-frozen villous tissue or from cytotrophoblasts that were cultured for 72 hours. Samples were lysed using ice-cold radioimmunoprecipitation assay (RIPA) buffer with freshly-added protease and phosphatase inhibitors. The resulting mixture was transferred to a 1.5 ml tube and centrifuged at 1000 x *g* for 10 minutes at 4°C to remove cellular debris. The supernatant was transferred to a fresh tube and protein concentration was quantified using a Pierce Bicinchoninic Acid (BCA) Protein Assay Kit.

Western Blotting

About 25 μg of protein was separated on a 4-20% SDS-PAGE gel, then transferred to a polyvinylidene difluoride (PVDF) membrane and blocked for one hour in 5% (w/v) milk in TBS solution with 0.1% Tween 20. Membranes were subsequently incubated with primary antibodies, then washed, blocked in 1% milk, and probed with secondary antibodies conjugated to HRP. Western blot membranes were visualized using the G: Box from Syngene (Frederick, MD) and analyzed using Genetools software (Syngene). All samples were normalized to β-actin (ACTB).

Cell Culture Experiments

Cytotrophoblasts (CTB) were isolated from term placentae collected at C-section. At 24 hours after plating, the CTBs were treated with two concentrations (10 nM and 100 nM) of the active form of Vitamin D (calcitriol) for 24 hours. CTBs were then cultured another 24 hours for a total of 72 hours, after which the cells were harvested for protein detection by Western blot. Mitochondrial respiration in isolated trophoblasts was assessed using a Seahorse Bioscience XFe96 analyzer (Agilent, USA).

Mitochondrial Respiration Assay

Twenty-four hours before mitochondrial respiration was measured, a sensor cartridge was calibrated using Seahorse Calibrant Solution (Agilent, CA) and placed in a non-CO_2 incubator overnight. One hour before the assay, complete Iscove's Modified Dulbecco's Medium (IMDM) media was exchanged for Seahorse base media supplemented with 25 mM glucose, 4 mM glutamine, and 1 mM pyruvate (same as culture media). Cells were then placed in a non-CO_2 incubator for one hour and were allowed to equilibrate before the oxygen consumption rate (OCR) was measured using a Seahorse XFe96 Analyzer. Basal respiration was calculated from four baseline OCR readings. ATP-coupled respiration, maximum respiration, spare capacity, proton leak, and non-mitochondrial respiration was calculated from OCR readings following the injection of oligomycin (1 μM), FCCP (1 μM), and a mixture of rotenone (3 μM) and antimycin A (1.5 μM) as we described previously (16). The effect of Vitamin D treatment was calculated by taking the ratios of parameters in treated and untreated cells. All assays were normalized to total DNA content per well using the Quant-iT Picogreen dsDNA assay kit.

Statistical Analysis

The Shapiro–Wilk test was used to test for normal distribution in all data sets. For normally distributed data, significant differences between groups were tested as an interaction between fetal gender (M, F) and pregnancy complications such as maternal obesity with a two-way ANOVA followed by Student's *t*-test. For non-parametric data, the Kruskal–Wallis test was applied for the same factors (fetal sex and maternal adiposity), followed by the Mann–Whitney U *post hoc* test. Data from males and females were pooled when no fetal sex-dependent differences were observed. *P*-values < 0.1 are reported as statistically significant.

RESULTS

Clinical Characteristics of Study Participants

Table 1 shows the clinical characteristics of the patients participating in this study. By experimental design, maternal BMI was significantly different between the groups. The gestational weight gain in OB mothers with female fetuses was significantly smaller than that in NW mothers ($p<0.05$). No significant differences in maternal age, gestational age, birth weight, or placental weight were detected between the groups.

Effect of Maternal BMI on Fetal and Maternal Circulating Vitamin D

Inactive Vitamin D (VitD) is synthesized primarily in human skin and converted to its active form of 1α,25-dihydroxyvitamin D_3, or calcitriol, in the kidney, placenta, and other target organs by 25-hydroxyvitamin D-1 alpha hydroxylase (CYP27B1) (31) (**Figure 1A**). The actions of calcitriol are mediated by the Vitamin D receptor (VDR), a ligand-dependent nuclear receptor. As circulating levels of VitD are reported to be decreased in obese individuals (32), we hypothesized that Vitamin D status could also be affected by maternal obesity. In the group of normal-weight (NW) women, we observed no correlation between maternal plasma VitD levels and maternal BMI (**Figure 1B**). However, an inverse correlation between maternal circulating VitD and maternal BMI was present in OB women (r=-0.5, $p<0.1$), independent of fetal sex (**Figure 1C**). In addition, male and female cord blood levels of VitD inversely correlated with maternal BMI (r=-0.47, $p<0.001$), but showed positive correlation with maternal plasma VitD (r=0.83, $p<0.000$; **Figures 1E, F**). We also observed a significant correlation between cord blood levels of VitD and placental efficiency, calculated as the ratio of fetal and placental weights (r=0.69, $p<0.0001$, **Figure 1G**). No relationship, however, was observed between maternal blood VitD concentrations and placental efficiency ($p=0.35$, **Figure 1D**).

Placental Expression of CYP27B1 Is Not Affected by Maternal Obesity

CYP27B1 is the sole Vitamin D 1α-hydroxylase responsible for the last activation step to produce the fully-active VitD hormone calcitriol (31). Since VitD levels were decreased in maternal and cord blood of obese women, we wanted to understand if the placenta plays a role in this process. We began by measuring protein levels of CYP27B1 in placentae from NW and OB women. As shown in **Supplemental Figures 1A, B**, we observed no differences in CYP27B1 expression between the groups. However, within the OB group, levels of CYP27B1 were significantly lower in placentae of female offspring vs. males. Since the placenta is composed of multiple cell types, we next measured expression of CYP27B1 in primary trophoblasts isolated from NW and OB women. We found no statistically significant differences between groups or between sexes (**Supplemental Figures 1C, D**).

Vitamin D Receptor Protein Expression Is Decreased in Placentae From Obese Women

The genomic functions of VitD are mediated through its binding to the Vitamin D receptor (VDR) in target tissues (33). It has been estimated that binding of calcitriol to VDR regulates the expression of about 2000 genes involved in numerous intracellular functions (34). We next hypothesized that the reduced circulating VitD in OB women is a result of decreased VDR expression in the placenta. Western blot analysis of placental tissue from NW and OB women showed a significant 50% reduction in VDR expression in OB vs. NW women, whether having male ($p<0.001$) or female ($p<0.1$) fetuses (**Figures 2A, C**).

Vitamin D deficiency in pregnant women is associated with increased risk for pregnancy complications (35) such as gestational diabetes mellitus (GDM) (36) and preeclampsia (37). We next examined VDR expression in placentae from pregnancies complicated by gestational diabetes regulated by insulin (A2GDM) and preeclampsia (PE). To rule out an effect of maternal adiposity, control samples were matched by maternal BMI. Clinical characteristics of the A2GDM and PE groups and corresponding controls are presented in **Supplemental Tables 1 and 2 (S1 and S2)**. The A2GDM women were slightly older compared to the control group, whether with male or female

TABLE 1 | Clinical characteristics of study patients.

Clinical Characteristics	NW		OB	
	Females n = 26	Males n = 29	Females n = 25	Males n = 28
Pre-pregnancy BMI (kg/m^2)	22.77 (18.3-24.9)	22.43 (19.2-24.7)	**36.49*** (30.03-43.8)	**35.78*** (29.0-45.5)
Maternal Age (years)	31.60 (24-41)	32.70 (23-46)	31.32 (22-43)	30.40 (20-41)
Gestational age (weeks)	39.32 (39.0-39.7)	39.23 (39.0-39.6)	39.305 (39.0-39.8)	39.24 (39.0-40.0)
Fetal Birth Weight (g)	3477 (2370-4975)	3448 (2845-3941)	3346 (2865-3980)	3392 (2220-4305)
Placenta Weight (g)	581.94 (457.4-758.6)	512.39 (273.6-649.9)	530.53 (389-719.7)	549.13 (349-762.6)
Maternal Weight Gain (kg)	16.65 (6.1-30.7)	13.02 (-3.2-20.4)	**11.25*** (0.7-45.4)	10.23 (-5.5-20.9)

*Maternal and cord plasma samples were collected from male and female offspring of normal-weight (NW) and obese mothers (OB). BMI, body mass index. Data are presented as median (range). *, p<0.05 OB vs. NW group with same fetal sex.*
The bold values are statistically significant.

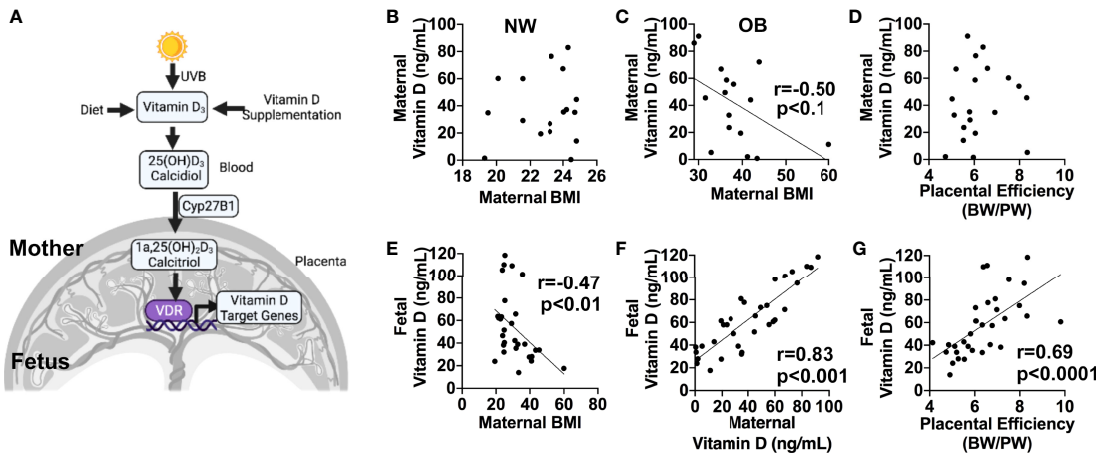


FIGURE 1 | **(A)** Simplified diagram showing pathways for Vitamin D synthesis, bioactivation, and function. Created in Biorender.com. **(B–G)**, 1α,25-dihydroxyvitamin D_3 (calcidiol) levels in maternal and cord blood plasma from normal-weight (NW) and obese (OB) women, measured by ELISA. **(B–D)**, Correlations between maternal blood plasma Vitamin D concentration and maternal pre-pregnancy BMI in normal-weight **(B)** and obese **(C)** women, and placental efficiency calculated as the ratio between birth weight (BW) and placental weight (PW) **(D)**. **(E–G)**, Correlations between cord blood plasma vitamin D levels and maternal pre-pregnancy BMI **(E)**, maternal plasma Vitamin D **(F)**, and placental efficiency **(G)**. Sample sizes are given in **Table 1**.

fetuses (p<0.01, **Supplemental Table S1**). Since the C-sections in pregnancies complicated by preeclampsia were performed prior to term, there were significant differences in gestational age and fetal birth weight in the PE group relative to normotensive controls (**Supplemental Table S2**). Nonetheless, when stratified by maternal pre-pregnancy BMI, no statistically significant differences in VDR expression were seen in placentae from women with A2GDM or PE vs. corresponding control groups (**Figures 2B, D–F**).

Treatment With Vitamin D Increases VDR levels in Primary Trophoblast Cells

Given ongoing debate concerning the efficacy of VitD supplementation and the proper dosage for optimal health during pregnancy (38), we conducted *in vitro* studies to determine the effect of VitD supplementation on placental function. We treated cytotrophoblasts (CTBs) with calcitriol, an active form of VitD, in concentrations previously reported to be effective in cell culture studies using various types of cells, including trophoblasts (39–41). Measuring VDR expression in calcitriol-treated trophoblasts revealed a dose-dependent increase over the 24 hours following treatment, independent of fetal sex and maternal adiposity (**Figure 3**).

Vitamin D Improves Mitochondrial Respiration in Primary Trophoblasts

It has been previously reported that VitD supplementation of deficient individuals improves mitochondrial function (42). Reports from our group indicate mitochondrial dysfunction to occur in trophoblasts isolated from the placentae of obese women

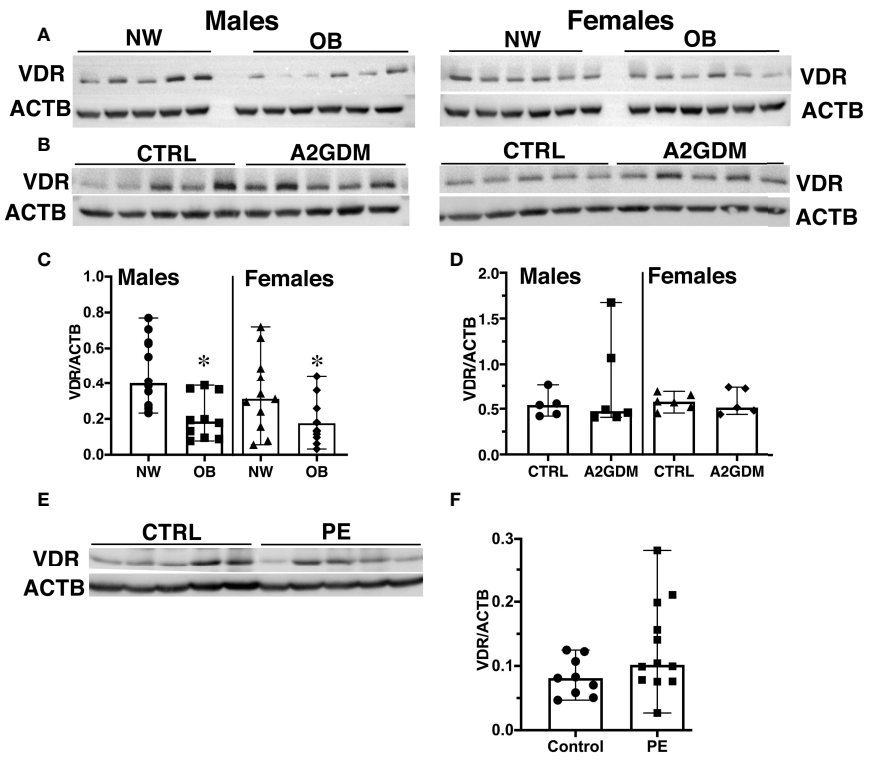


FIGURE 2 | Effect of maternal obesity, gestational diabetes, and preeclampsia on placental expression of Vitamin D receptor (VDR). **(A, C),** Representative images **(A)** and quantification **(C)** by Western blot of VDR in placentae from normal-weight and obese women with male and female fetuses. **(B, D)**, Representative images **(B)** and quantification **(D)** by Western blot of VDR in placentae from pregnancies complicated by gestational diabetes regulated by insulin (A2GDM). **(E, F)**, Representative images **(E)** and quantification **(F)** by Western blot of VDR in placentae from pregnancies complicated by preeclampsia (PE). Control samples for A2GDM and PE were matched by BMI. Data were normalized to β-actin; values are mean ± SEM.*, $p<0.05$. Sample sizes are given in **Table 1** and **Supplemental Tables 1, 2**.

(16). We therefore next aimed to determine whether VitD supplementation would be sufficient to improve mitochondrial respiration in primary trophoblasts isolated from NW and OB women. To this end, trophoblasts were either left untreated or treated with 10 or 100 nM of calcitriol. Oxygen consumption rates were measured using a Seahorse XF Analyzer (**Figure 4**). No changes associated with calcitriol treatment were observed in trophoblasts isolated from placentae of NW women. However, treated trophoblasts from OB women showed significant improvements in spare capacity (**Figure 4F**) and proton leak (**Figure 4G**), independent of fetal sex.

Vitamin D Reduces Expression of the NLRP3 Inflammasome in CTBs From Obese Women

Vitamin D has been shown to inhibit the NLRP3 inflammasome either by direct binding between NLRP3 and VDR (26) or *via* VDR signaling-mediated inhibition of cytokine secretion (27). We measured the protein expression of NLRP3 and its downstream factors such as gasdermin D, caspase-1, and IL-18 in primary trophoblasts isolated from male and female placentae from normal-weight and obese women, and further assessed the effect of calcitriol in that context. Protein levels of NLRP3 and IL-18 were significantly increased in trophoblasts from OB women vs. NW women (**Figures 5A–C**), whether with male or female fetuses. Calcitriol treatment reduced expression of IL-18 but not NLRP3 ($p<0.05$) in trophoblasts of OB women, independent of fetal sex. No change in IL-18 or NLRP3 expression was detected in trophoblasts from NW women. Likewise, levels of gasdermin D and total and cleaved (p20) caspase-1 remained unchanged across the groups (**Figures 5D–F**).

We also measured expression of NLRP3 and IL-18 in whole placentae collected from NW and OB women, but found no changes associated with maternal adiposity, suggesting that the increases in these proteins were trophoblast-specific (**Supplemental Figure 2**). Importantly, we found that expression of NLRP3 was two-fold higher in female NW placentae and that of IL-18 was two-fold higher in female OB placentae when compared with males within the same maternal BMI group ($p<0.05$).

DISCUSSION

In this study, we investigated the effect of maternal obesity on maternal and fetal circulating Vitamin D levels, along with the effect of VitD supplementation on VDR expression and on mitochondrial respiration and inflammation in human

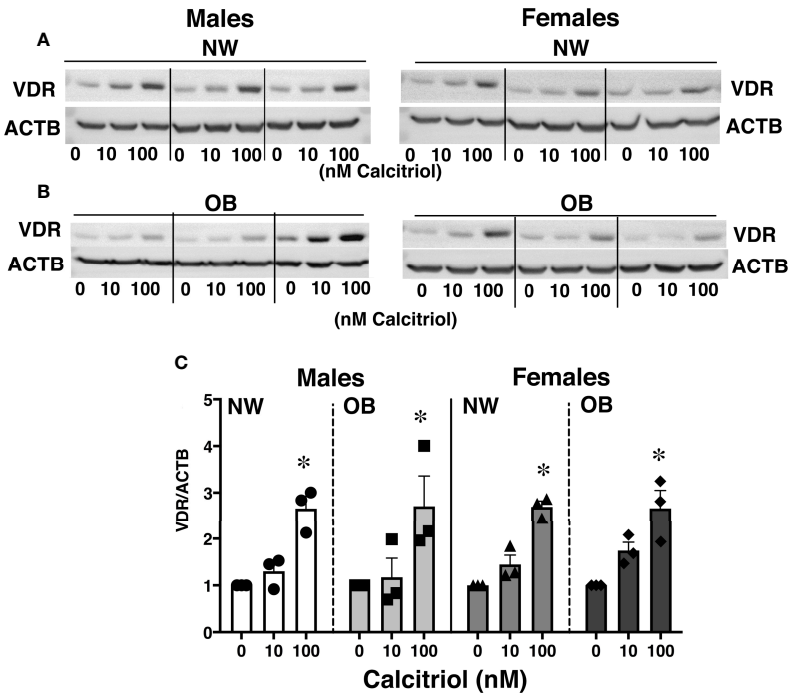


FIGURE 3 | Effect of 24-hour treatment with calcitriol, an active form of Vitamin D, on expression of VDR in primary trophoblasts isolated from placentae of NW and OB women. Representative Western blots **(A, B)** and quantification data **(C)** demonstrating a dose-dependent response to treatment. Data were normalized to β-actin (ACTB) and expressed as fold-change relative to untreated cells. *, $p < 0.05$. N=3-5/dose/group/fetal sex.

trophoblasts. Previous studies have shown that people with obesity have less circulating VitD than normal-weight individuals (43). Vitamin D deficiency during pregnancy has been linked to adverse health outcomes including preeclampsia (44), gestational diabetes mellitus (36), increased risk for a cesarean section (45), and preterm birth (46). Maternal VitD deficiency has also been linked to fetal growth restriction (47), congenital heart defects (48), type 1 diabetes mellitus (49), schizophrenia (50), and weak bones in offspring (51). The offspring of mothers who had low circulating VitD concentrations during late pregnancy have been reported to have reduced bone mass at nine years of age (51). Vitamin D has been also shown to play an important role in regulating immune responses during gestation (52).

Vitamin D in Maternal and Cord Plasma

The only source of Vitamin D for a fetus is the mother, who transfers it across the placenta (53). Maternal 25-hydroxyvitamin concentrations are higher than fetal concentrations, and this metabolite crosses the placenta in relatively large quantities. In agreement with previous studies (54), we found a strong positive correlation between maternal and cord plasma VitD concentrations in both male and female offspring. Bodnar et al. (44) have previously reported a two-fold increase in maternal and neonatal VitD deficiency as maternal BMI increases from 22 to 34 kg/m^2; we also observed a reduction in maternal plasma VitD levels with increased maternal adiposity, but only in the group of women with BMI higher than 30. The reason for high within-group variability in VitD levels could be that plasma VitD concentrations show seasonal variation, being significantly higher in samples collected during warmer months (April-September) than in winter (55). Due to the smaller sample size in this study, we were unable to factor seasonal periodicity into our data analysis. Another reason could be confounding from VitD supplementation, as maternal plasma concentrations are known to be significantly higher in mothers who receive VitD with their prenatal vitamins.

Our data indicate that in both male and female offspring, there is a significant decrease in cord blood levels of calcidiol with increased maternal BMI. While we observed no relationship between maternal or fetal VitD levels and birth weights (not shown), we found that cord blood VitD deficiency in obese women was correlated with decreased ratio between fetal and placental weights, suggesting placental insufficiency. These findings are in agreement with previously published data showing placental insufficiency in two different mouse models of gestational VitD deficiency (56).

VDR Expression in the Placenta

The physiologically-active Vitamin D metabolite, 1a,25$(OH)_2D_3$ or calcitriol, does not readily cross the placenta; this is addressed through placental expression of the enzyme CYP27B1, which hydroxylates the inactive form that does cross, 25$(OH)D_3$ or calcidiol, to the active form (54). In a study undertaken in a small

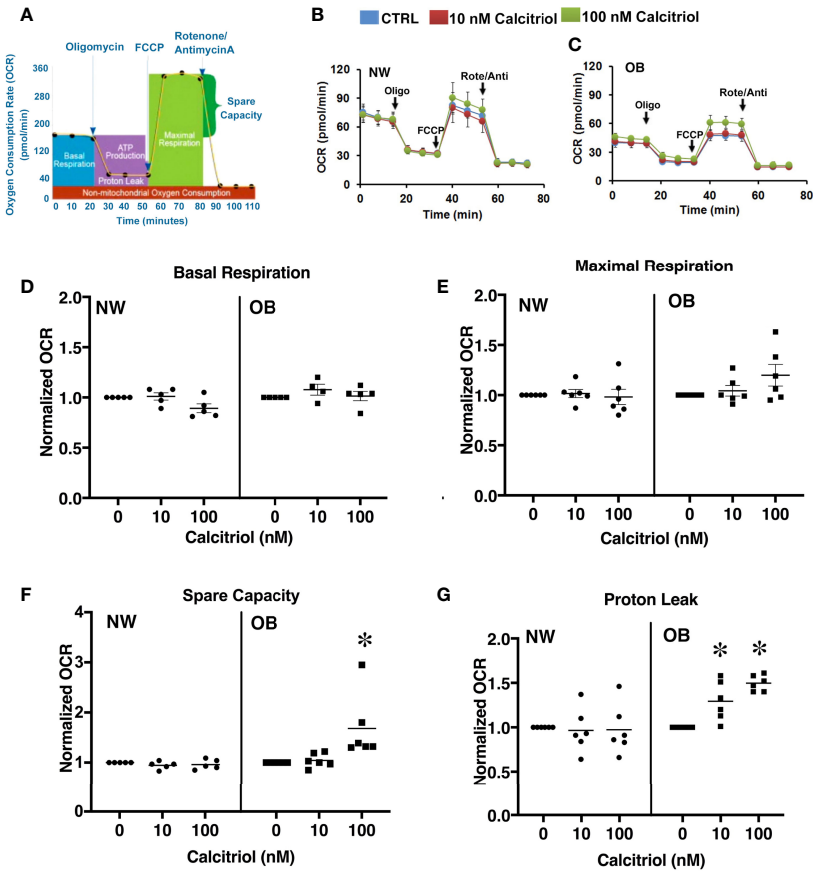


FIGURE 4 | Dose-dependent effect of 24-hour treatment with calcitriol on mitochondrial function in cytotrophoblasts isolated from placentae of NW and OB women. Data from males and females were combined. **(A)** Flowchart of the Seahorse XF Cell Mito Stress test; **(B, C)** Representative curves. **(D)** Basal respiration. **(E)** Maximal respiration. **(F)** Spare capacity. **(G)** Proton leak. *, $p < 0.05$, N=6-7.

cohort of 70 pregnant adolescents (<18 years of age) with normal BMI and their term neonates, O'Brien et al. showed a significant correlation between maternal calcidiol and placental expression of CYP27B1, suggesting a link between substrate availability and placental production of calcitriol (57). We, in contrast, found no difference in placental CYP27B1 expression between normal-weight and obese women. This could be explained by differences in clinical characteristics of participants including maternal age (adolescent vs. adult), and maternal pre-pregnancy BMI (all lean vs. lean and obese).

Calcitriol is the major active ligand of the Vitamin D receptor (VDR), a nuclear steroid hormone receptor that acts as a transcriptional activator (58) but can also exert rapid non-genomic effects that influence processes such as cell proliferation and differentiation and apoptosis; these are probably realized *via* VDRs located within the plasma membrane (59). Placentae from obese mothers have lower levels of VDR than those from normal-weight mothers, which means that less active VitD can bind to and be utilized by the organ. Vitamin D deficiency in the placenta has previously been associated with adverse health outcomes including preeclampsia, gestational diabetes, increased risk of having a C-section delivery, and bacterial vaginosis (59). However, in our study, no differences in VDR expression were observed in maternal BMI-matched placentae, whether from normal pregnancies or complicated by preeclampsia or gestational diabetes. This potentially suggests that maternal adiposity is a key determinant in dysregulation of placental VitD metabolism.

Treatment of CTBs With Vitamin D

Our data show that treatment of cytotrophoblasts with calcitriol increases VDR expression independent of maternal adiposity and fetal sex. We observed a dose-dependent response in trophoblast VDR concentration after short-term treatment with calcitriol, indicating a relationship between VitD levels and *de novo* translation or reduced degradation of VDR; the mechanism underlying this relationship is not yet understood. While the increased presence of VDR in CTBs upon treatment with the active form of VitD may conceptually seem beneficial to overall placental health, it has also been shown that high concentrations of VitD can induce apoptosis (60). Therefore, more research must be done regarding what concentration of

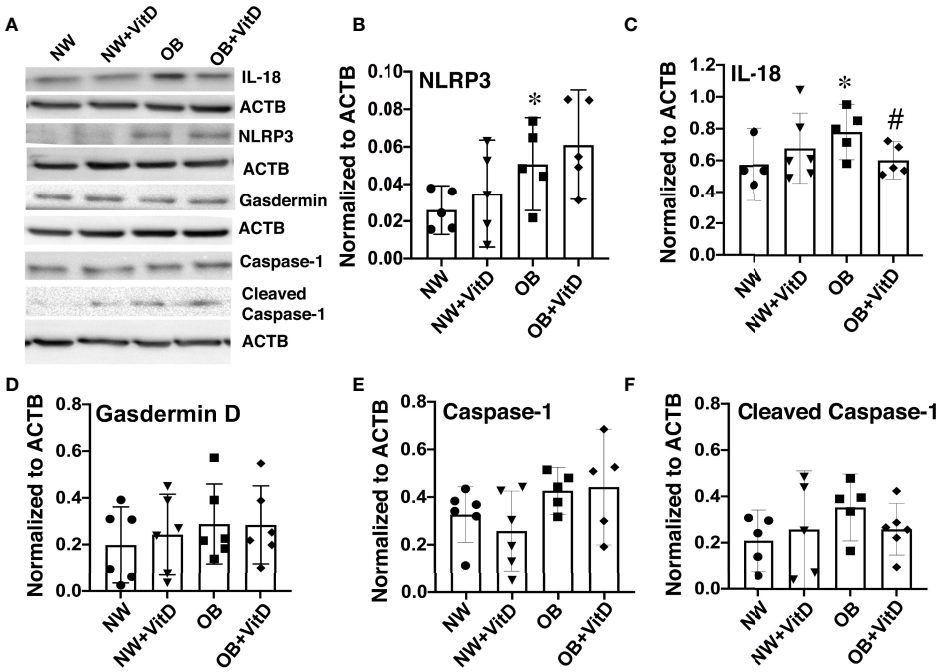


FIGURE 5 | Effect of 24-hour calcitriol treatment on protein expression of NLRP3 inflammasome and the downstream inflammasome activation and pyroptosis factors IL-18, gasdermin D, and caspase-1 in trophoblasts isolated from placentae of normal-weight and obese women. Data from males and females were combined. **(A)** Representative Western blots. **(B)** NLRP3. **(C)** IL-18. **(D)** Gasdermin **(D, E)** Total caspase-1. **(F)** Cleaved p20 caspase-1. Data were normalized to β-actin (ACTB) and expressed as fold-change relative to untreated cells. *, $p < 0.05$. N=6-7. #, p<0.05 vitamin D treated vs. untreated cells.

prenatal VitD supplementation is optimal to reduce deficiency and increase VDR production while avoiding harm to maternal and fetal cells.

Mitochondrial Respiration in CTBs Treated With Vitamin D

We have previously reported reduced placental mitochondrial respiration in pregnancies complicated by maternal obesity (16). Since a growing body of evidence suggests that VitD supplementation in deficient individuals improves measures of mitochondrial function (61, 62), we investigated the effects of calcitriol on mitochondrial respiration in trophoblasts. No clear responses of trophoblast mitochondrial respiration to VitD supplementation were seen in either female or male offspring of normal-weight mothers. In contrast, calcitriol-treated trophoblasts from placentae of obese women showed increased spare capacity and proton leak.

In fact, recent studies have confirmed that Vitamin D regulates oxidative capacity through binding of calcitriol to VDRs in skeletal muscle (63). Furthermore, mitochondrial ATP production has been shown to be significantly reduced in VDR-deficient C2C12 myoblasts. These results were recapitulated by an *in vivo* experiment in VitD-deficient mice, which exhibited decreased maximum oxidative capacity (63). Ryan et al. (64) explored the effect of VitD supplementation on human skeletal muscle cells and found that calcitriol administration increases the oxygen consumption rate. Meanwhile, a mouse study similarly looking at the effect of VitD supplementation on mitochondrial function found that treatment with calcitriol leads to inhibition of oxygen consumption, maximal respiration, and proton leak in brown adipocytes (65). Given these disparate findings, future research will reveal potential crosstalk between tissue-specific VDR expression, different VitD doses, and mitochondrial respiration. In our study, the isolation and purification of cytotrophoblasts from term placentae was performed using media with 25 mM glucose, consistent with previous reports (66–68). Further studies are needed to determine the effect of culture conditions, and particularly glucose levels, on the trophoblasts' response to Vitamin D supplementation.

Vitamin D Supplementation and Trophoblast Inflammation

Vitamin D is thought to play a role in reducing inflammation and infection in the placenta (69), and has previously been shown to reduce lipopolysaccharide-induced inflammation in the placenta by suppressing placental translocation of the NFκB subunit from cytoplasm to nucleus (70). A mouse model of VitD deficiency revealed immune challenge to elicit a large inflammatory response in the placenta, further underscoring the importance of VitD in placental immune function (52). Inflammasomes are large protein complexes that assemble in the cytosol after activation by pathogen-associated and danger-associated molecular patterns (71). Both direct and indirect interactions have been reported between VitD and the NLRP3 inflammasome. Using immunoprecipitation,

Huang et al. demonstrated that VDR forms complexes with NLRP3 in nuclear extracts (26). Rao et al. further demonstrated that binding of the VDR to NLRP3 appears to attenuate deubiquitination of the latter, which is a critical step in inflammasome activation (27). Studies have also shown that calcitriol is capable of inhibiting NLRP3 inflammasome activation and its downstream cytokine signaling in mouse models of liver injury and fibrosis (72), ulcerative colitis (73), and diabetic retinopathy (74). In our study, calcitriol-treated trophoblasts showed no change in NLRP3 expression, but exhibited significantly reduced expression of IL-18. Interestingly, a recent study in COVID-19 patients observed a strong inverse correlation between VitD levels and cytokine production, suggesting a potential role of VitD in reducing complications attributed to the cytokine storm and unregulated inflammation (75).

In summary, receiving adequate amounts of Vitamin D is highly important for maintaining normal placental function in the setting of maternal obesity. We observed beneficial effects of VitD supplementation on VDR expression, mitochondrial respiration, and inflammation in trophoblasts from placentae of obese women. It is unclear whether or not maternal VitD deficiency in obese women is directly responsible for placental dysfunction, but work is underway to evaluate this potentially important phenomenon. Several published reports suggest that VitD controls about 3% of the human genome (76–79), and maternal and fetal deficiencies in VitD could potentially lead to genetic and metabolic abnormalities that emerge later in offspring life. If this is the case, future studies will need to address the important question of when in gestation supplementation with Vitamin D is particularly beneficial in improving placental function, and thus offspring health.

DATA AVAILABILITY STATEMENT

The original contributions presented in the study are included in the article/**Supplementary Material**. Further inquiries can be directed to the corresponding author.

ETHICS STATEMENT

The studies involving human participants were reviewed and approved by Institutional Review Board of Oregon Health & Science University. The patients/participants provided their written informed consent to participate in this study.

AUTHOR CONTRIBUTIONS

EP, NH, MB and AM conceived and planned the experiments; EP, NH, and MB, carried out the experiments; MB and EP collected and processed human samples; NH and AM wrote the manuscript. All authors provided critical feedback and helped shape the research, analysis and manuscript. All authors contributed to the article and approved the submitted version.

FUNDING

This work was funded by M. J. Murdock Charitable Trust (to NH), and NIH/NICHD grants HD097398, HD076259A, American Heart Association GRNT29960007 (to AM).

ACKNOWLEDGMENTS

We are grateful for the placental donations from mothers delivering at Oregon Health & Science University Hospital who enable us to conduct this study. We also thank Kim R. Montaniel for technical assistance.

SUPPLEMENTARY MATERIAL

The Supplementary Material for this article can be found online at: https://www.frontiersin.org/articles/10.3389/fendo.2022.893848/full#supplementary-material

REFERENCES

1. Pereira-Santos M, Costa PR, Santos CA, Santos DB, Assis AM. Obesity and Vitamin D Deficiency: Is There an Association? *Obes Rev* (2016) 17(5):484. doi: 10.1111/obr.12393
2. Gallagher JC, Riggs BL, Eisman J, Hamstra A, Arnaud SB, DeLuca HF. Intestinal Calcium Absorption and Serum Vitamin D Metabolites in Normal Subjects and Osteoporotic Patients: Effect of Age and Dietary Calcium. *J Clin Invest* (1979) 64(3):729–36. doi: 10.1172/JCI109516
3. Gombart AF. The Vitamin D-antimicrobial Peptide Pathway and its Role in Protection Against Infection. *Future Microbiol* (2009) 4(9):1151–65. doi: 10.2217/fmb.09.87
4. Bui L, Zhu Z, Hawkins S, Cortez-Resendiz A, Bellon A. Vitamin D Regulation of the Immune System and its Implications for COVID-19: A Mini Review. *SAGE Open Med* (2021) 9:20503121211014073. doi: 10.1177/20503121211014073
5. Danik JS, Manson JE. Vitamin D and Cardiovascular Disease. *Curr Treat Options Cardiovasc Med* (2012) 14(4):414–24. doi: 10.1007/s11936-012-0183-8
6. Larqué E, Morales E, Leis R, Blanco-Carnero JE. Maternal and Foetal Health Implications of Vitamin D Status During Pregnancy. *Ann Nutr Metab* (2018) 72(3):179–92. doi: 10.1159/000487370
7. Hales CM, Carroll MD, Fryar CD, Ogden CL. Prevalence of Obesity and Severe Obesity Among Adults: United State-2018. *NCHS Data Brief* (2020) 360):1–8.
8. Zhu MJ, Du M, Nathanielsz PW, Ford SP. Maternal Obesity Up-Regulates Inflammatory Signaling Pathways and Enhances Cytokine Expression in the Mid-Gestation Sheep Placenta. *Placenta* (2010) 31(5):387–91. doi: 10.1016/j.placenta.2010.02.002
9. Catalano PM, Huston L, Amini SB, Kalhan SC. Longitudinal Changes in Glucose Metabolism During Pregnancy in Obese Women With Normal Glucose Tolerance and Gestational Diabetes Mellitus. *Am J Obstet Gynecol* (1999) 180(4):903–16. doi: 10.1016/S0002-9378(99)70662-9
10. Yogev Y, Catalano PM. Pregnancy and Obesity. *Obstet Gynecol Clin North Am* (2009) 36(2):285–300. doi: 10.1016/j.ogc.2009.03.003
11. Maloyan A, Muralimanoharan S, Huffman S, Cox LA, Nathanielsz PW, Myatt L, et al. Identification and Comparative Analyses of Myocardial miRNAs Involved in the Fetal Response to Maternal Obesity. *Physiol Genomics* (2013) 45(19):889–900. doi: 10.1152/physiolgenomics.00050.2013
12. Bucher M, Montaniel KRC, Myatt L, Weintraub S, Tavori H, Maloyan A. Dyslipidemia, Insulin Resistance, and Impairment of Placental Metabolism in the Offspring of Obese Mothers. *J Dev Orig Health Dis* (2021) 12(5):738–47. doi: 10.1017/S2040174420001026

13. Montaniel KRC, Bucher M, Phillips EA, Li C, Sullivan EL, Kievit P, et al. Dipeptidyl Peptidase IV Inhibition Delays Developmental Programming of Obesity and Metabolic Disease in Male Offspring of Obese Mothers. *J Dev Orig Health Dis* (2022) 1-14. doi: 10.1017/S2040174422000010
14. Segovia SA, Vickers MH, Gray C, Reynolds CM. Maternal Obesity, Inflammation, and Developmental Programming. *BioMed Res Int* (2014) 2014:418975. doi: 10.1155/2014/418975
15. Burton GJ, Fowden AL. Review: The Placenta and Developmental Programming: Balancing Fetal Nutrient Demands With Maternal Resource Allocation. *Placenta* (2012) 33 Suppl:S23–27. doi: 10.1016/j.placenta.2011.11.013
16. Mele J, Muralimanoharan S, Maloyan A, Myatt L. Impaired Mitochondrial Function in Human Placenta With Increased Maternal Adiposity. *Am J Physiol Endocrinol Metab* (2014) 307(5):E419–425. doi: 10.1152/ajpendo.00025.2014
17. Muralimanoharan S, Gao X, Weintraub S, Myatt L, Maloyan A. Sexual Dimorphism in Activation of Placental Autophagy in Obese Women With Evidence for Fetal Programming From a Placenta-Specific Mouse Model. *Autophagy* (2016) 12(5):752–69. doi: 10.1080/15548627.2016.1156822
18. Bucher M, Montaniel KRC, Myatt L, Weintraub S, Tavori H, Maloyan A. Dyslipidemia, Insulin Resistance, and Impairment of Placental Metabolism in the Offspring of Obese Mothers. *J Dev Orig Health Dis* (2020) 738–47. doi: 10.1017/S2040174420001026
19. Challier JC, Basu S, Bintein T, Minium J, Hotmire K, Catalano PM, et al. Obesity in Pregnancy Stimulates Macrophage Accumulation and Inflammation in the Placenta. *Placenta* (2008) 29(3):274–81. doi: 10.1016/j.placenta.2007.12.010
20. Muralimanoharan S, Guo C, Myatt L, Maloyan A. Sexual Dimorphism in miR-210 Expression and Mitochondrial Dysfunction in the Placenta With Maternal Obesity. *Int J Obes (Lond)* (2015) 39(8):1274–81. doi: 10.1038/ijo.2015.45
21. Agarwal P, Morriseau TS, Kereliuk SM, Doucette CA, Wicklow BA, Dolinsky VW. Maternal Obesity, Diabetes During Pregnancy and Epigenetic Mechanisms That Influence the Developmental Origins of Cardiometabolic Disease in the Offspring. *Crit Rev Clin Lab Sci* (2018) 55(2):71–101. doi: 10.1080/10408363.2017.1422109
22. Aye ILMH, Lager S, Powell TL. The Role of Placental Inflammasomes in Linking the Adverse Effects of Maternal Obesity on Fetal Development. In: E Ferrazzi, B Sears, editors. *Metabolic Syndrome and Complications of Pregnancy: The Potential Preventive Role of Nutrition*. Cham: Springer International Publishing (2015). p. 77–90.
23. Kayagaki N, Stowe IB, Lee BL, O'Rourke K, Anderson K, Warming S, et al. Caspase-11 Cleaves Gasdermin D for non-Canonical Inflammasome Signalling. *Nature* (2015) 526(7575):666–71. doi: 10.1038/nature15541
24. Ye Z, Ting JP. NLR, the Nucleotide-Binding Domain Leucine-Rich Repeat Containing Gene Family. *Curr Opin Immunol* (2008) 20(1):3–9. doi: 10.1016/j.coi.2008.01.003
25. Hotamisligil GS, Erbay E. Nutrient Sensing and Inflammation in Metabolic Diseases. *Nat Rev Immunol* (2008) 8(12):923–34. doi: 10.1038/nri2449
26. Huang H, Hong JY, Wu YJ, Wang EY, Liu ZQ, Cheng BH, et al. Vitamin D Receptor Interacts With NLRP3 to Restrict the Allergic Response. *Clin Exp Immunol* (2018) 194(1):17–26. doi: 10.1111/cei.13164
27. Rao Z, Chen X, Wu J, Xiao M, Zhang J, Wang B, et al. Vitamin D Receptor Inhibits Nlrp3 Activation by Impeding its BRCC3-Mediated Deubiquitination. *Front Immunol* (2019) 10(2783). doi: 10.3389/fimmu.2019.02783
28. Cindrova-Davies T, Yung HW, Johns J, Spasic-Boskovic O, Korolchuk S, Jauniaux E, et al. Oxidative Stress, Gene Expression, and Protein Changes Induced in the Human Placenta During Labor. *Am J Pathol* (2007) 171(4):1168–79. doi: 10.2353/ajpath.2007.070528
29. Lager S, Aye ILMH, Gaccioli F, Ramirez VI, Jansson T, Powell TL. Labor Inhibits Placental Mechanistic Target of Rapamycin Complex 1 Signaling. *Placenta* (2014) 35(12):1007–12. doi: 10.1016/j.placenta.2014.10.006
30. Simon B, Bucher M, Maloyan A. A Primary Human Trophoblast Model to Study the Effect of Inflammation Associated With Maternal Obesity on Regulation of Autophagy in the Placenta. *J Vis Exp* (2017) 127:56484. doi: 10.3791/56484
31. Christakos S, Li S, De La Cruz J, Bikle DD. New Developments in Our Understanding of Vitamin D Metabolism, Action and Treatment. *Metabolism* (2019) 98:112–20. doi: 10.1016/j.metabol.2019.06.010
32. Pourshahidi LK. Vitamin D and Obesity: Current Perspectives and Future Directions. *Proc Nutr Soc* (2015) 74(2):115–24. doi: 10.1017/S0029665114001578
33. Carlberg C, Seuter S, Heikkinen S. The First Genome-Wide View of Vitamin D Receptor Locations and Their Mechanistic Implications. *Anticancer Res* (2012) 32(1):271–82.
34. Hossein-nezhad A, Spira A, Holick MF. Influence of Vitamin D Status and Vitamin D3 Supplementation on Genome Wide Expression of White Blood Cells: A Randomized Double-Blind Clinical Trial. *PloS One* (2013) 8(3):e58725. doi: 10.1371/journal.pone.0058725
35. Lewis S, Lucas RM, Halliday J, Ponsonby AL. Vitamin D Deficiency and Pregnancy: From Preconception to Birth. *Mol Nutr Food Res* (2010) 54(8):1092–102. doi: 10.1002/mnfr.201000044
36. Soheilykhah S, Mojibian M, Rashidi M, Rahimi-Saghand S, Jafari F. Maternal Vitamin D Status in Gestational Diabetes Mellitus. *Nutr Clin Pract* (2010) 25(5):524–7. doi: 10.1177/0884533610379851
37. Bodnar LM, Simhan HN, Catov JM, Roberts JM, Platt RW, Diesel JC, et al. Maternal Vitamin D Status and the Risk of Mild and Severe Preeclampsia. *Epidemiology* (2014) 25(2):207–14. doi: 10.1097/EDE.0000000000000039
38. Holick MF, Chen TC. Vitamin D Deficiency: A Worldwide Problem With Health Consequences. *Am J Clin Nutr* (2008) 87(4):1080s–6s. doi: 10.1093/ajcn/87.4.1080S
39. Rigby WF, Shen L, Ball ED, Guyre PM, Fanger MW. Differentiation of a Human Monocytic Cell Line by 1,25-Dihydroxyvitamin D3 (Calcitriol): A Morphologic, Phenotypic, and Functional Analysis. *Blood* (1984) 64(5):1110–5. doi: 10.1182/blood.V64.5.1110.1110
40. Barrera D, Avila E, Hernández G, Méndez I, González L, Halhali A, et al. Calcitriol Affects hCG Gene Transcription in Cultured Human Syncytiotrophoblasts. *Reprod Biol Endocrinol* (2008) 6(1):3. doi: 10.1186/1477-7827-6-3
41. Abboud M, Rybchyn MS, Ning YJ, Brennan-Speranza TC, Girgis CM, Gunton JE, et al. 1,25-Dihydroxycholecalciferol (Calcitriol) Modifies Uptake and Release of 25-Hydroxycholecalciferol in Skeletal Muscle Cells in Culture. *J Steroid Biochem Mol Biol* (2018) 177:109–15. doi: 10.1016/j.jsbmb.2017.10.018
42. Ricca C, Aillon A, Bergandi L, Alotto D, Castagnoli C, Silvagno F. Vitamin D Receptor Is Necessary for Mitochondrial Function and Cell Health. *Int J Mol Sci* (2018) 19(6):1672. doi: 10.3390/ijms19061672
43. Cipriani C, Pepe J, Piemonte S, Colangelo L, Cilli M, Minisola S. Vitamin D and its Relationship With Obesity and Muscle. *Int J Endocrinol* (2014) 2014:841248. doi: 10.1155/2014/841248
44. Bodnar LM, Catov JM, Roberts JM, Simhan HN. Prepregnancy Obesity Predicts Poor Vitamin D Status in Mothers and Their Neonates. *J Nutr* (2007) 137(11):2437–42. doi: 10.1093/jn/137.11.2437
45. Merewood A, Mehta SD, Chen TC, Bauchner H, Holick MF. Association Between Vitamin D Deficiency and Primary Cesarean Section. *J Clin Endocrinol Metab* (2009) 94(3):940–5. doi: 10.1210/jc.2008-1217
46. Bodnar LM, Platt RW, Simhan HN. Early-Pregnancy Vitamin D Deficiency and Risk of Preterm Birth Subtypes. *Obstet Gynecol* (2015) 125(2):439–47. doi: 10.1097/AOG.0000000000000621
47. Scholl TO, Chen X. Vitamin D Intake During Pregnancy: Association With Maternal Characteristics and Infant Birth Weight. *Early Hum Dev* (2009) 85(4):231–4. doi: 10.1016/j.earlhumdev.2008.10.006
48. Koster MPH, van Duijn L, Krul-Poel YHM, Laven JS, Helbing WA, Simsek S, et al. A Compromised Maternal Vitamin D Status is Associated With Congenital Heart Defects in Offspring. *Early Hum Dev* (2018) 117:50–6. doi: 10.1016/j.earlhumdev.2017.12.011
49. Stene LC, Ulriksen J, Magnus P, Joner G. Use of Cod Liver Oil During Pregnancy Associated With Lower Risk of Type I Diabetes in the Offspring. *Diabetologia* (2000) 43(9):1093–8. doi: 10.1007/s001250051499
50. Kinney DK, Teixeira P, Hsu D, Napoleon SC, Crowley DJ, Miller A, et al. Relation of Schizophrenia Prevalence to Latitude, Climate, Fish Consumption, Infant Mortality, and Skin Color: A Role for Prenatal Vitamin D Deficiency and Infections? *Schizophr Bull* (2009) 35(3):582–95. doi: 10.1093/schbul/sbp023
51. Javaid MK, Crozier SR, Harvey NC, Gale CR, Dennison EM, Boucher BJ, et al. Maternal Vitamin D Status During Pregnancy and Childhood Bone Mass at Age 9 Years: A Longitudinal Study. *Lancet* (2006) 367(9504):36–43. doi: 10.1016/S0140-6736(06)67922-1

52. Liu NQ, Kaplan AT, Lagishetty V, Ouyang YB, Ouyang Y, Simmons CF, et al. Vitamin D and the Regulation of Placental Inflammation. *J Immunol* (2011) 186(10):5968–74. doi: 10.4049/jimmunol.1003332
53. Markestad T, Aksnes L, Ulstein M, Aarskog D. 25-Hydroxyvitamin D and 1,25-Dihydroxyvitamin D of D2 and D3 Origin in Maternal and Umbilical Cord Serum After Vitamin D2 Supplementation in Human Pregnancy. *Am J Clin Nutr* (1984) 40(5):1057–63. doi: 10.1093/ajcn/40.5.1057
54. Greer FR. 25-Hydroxyvitamin D: Functional Outcomes in Infants and Young Children. *Am J Clin Nutr* (2008) 88(2):529s–33s. doi: 10.1093/ajcn/88.2.529S
55. Cockburn F, Belton NR, Purvis RJ, Giles MM, Brown JK, Turner TL, et al. Maternal Vitamin D Intake and Mineral Metabolism in Mothers and Their Newborn Infants. *Br Med J* (1980) 281(6232):11–4. doi: 10.1136/bmj.281.6232.11
56. Chen YH, Liu ZB, Ma L, Zhang ZC, Fu L, Yu Z, et al. Gestational Vitamin D Deficiency Causes Placental Insufficiency and Fetal Intrauterine Growth Restriction Partially Through Inducing Placental Inflammation. *J Steroid Biochem Mol Biol* (2020) 203:105733. doi: 10.1016/j.jsbmb.2020.105733
57. O'Brien KO, Li S, Cao C, Kent T, Young BV, Queenan RA, et al. Placental CYP27B1 and CYP24A1 Expression in Human Placental Tissue and Their Association With Maternal and Neonatal Calcitropic Hormones. *J Clin Endocrinol Metab* (2014) 99(4):1348–56. doi: 10.1210/jc.2013-1366
58. Palomer X, González-Clemente JM, Blanco-Vaca F, Mauricio D. Role of Vitamin D in the Pathogenesis of Type 2 Diabetes Mellitus. *Diabetes Obes Metab* (2008) 10(3):185–97. doi: 10.1111/j.1463-1326.2007.00710.x
59. Shin JS, Choi MY, Longtine MS, Nelson DM. Vitamin D Effects on Pregnancy and the Placenta. *Placenta* (2010) 31(12):1027–34. doi: 10.1016/j.placenta.2010.08.015
60. Welsh J. Induction of Apoptosis in Breast Cancer Cells in Response to Vitamin D and Antiestrogens. *Biochem Cell Biol* (1994) 72(11-12):537–45. doi: 10.1139/o94-072
61. Sinha A, Hollingsworth KG, Ball S, Cheetham T. Improving the Vitamin D Status of Vitamin D Deficient Adults is Associated With Improved Mitochondrial Oxidative Function in Skeletal Muscle. *J Clin Endocrinol Metab* (2013) 98(3):E509–513. doi: 10.1210/jc.2012-3592
62. Latham CM, Brightwell CR, Keeble AR, Munson BD, Thomas NT, Zagzoog AM, et al. Vitamin D Promotes Skeletal Muscle Regeneration and Mitochondrial Health. *Front Physiol* (2021) 12(463). doi: 10.3389/fphys.2021.660498
63. Ashcroft SP, Bass JJ, Kazi AA, Atherton PJ, Philp A. The Vitamin D Receptor Regulates Mitochondrial Function in C2C12 Myoblasts. *Am J Physiol Cell Physiol* (2020) 318(3):C536–c541. doi: 10.1152/ajpcell.00568.2019
64. Ryan ZC, Craig TA, Folmes CD, Wang X, Lanza IR, Schaible NS, et al. 1α,25-Dihydroxyvitamin D3 Regulates Mitochondrial Oxygen Consumption and Dynamics in Human Skeletal Muscle Cells. *J Biol Chem* (2016) 291(3):1514–28. doi: 10.1074/jbc.M115.684399
65. Ricciardi CJ, Bae J, Esposito D, Komarnytsky S, Hu P, Chen J, et al. 1,25-Dihydroxyvitamin D3/Vitamin D Receptor Suppresses Brown Adipocyte Differentiation and Mitochondrial Respiration. *Eur J Nutr* (2015) 54 (6):1001–12. doi: 10.1007/s00394-014-0778-9
66. Kliman HJ, Nestler JE, Sermasi E, Sanger JM, Strauss JF3rd. Purification, Characterization, and In Vitro Differentiation of Cytotrophoblasts From Human Term Placentae. *Endocrinology* (1986) 118(4):1567–82. doi: 10.1210/endo-118-4-1567
67. Wang Y, Bucher M, Myatt L. Use of Glucose, Glutamine and Fatty Acids for Trophoblast Respiration in Lean, Obese and Gestational Diabetic Women. *J Clin Endocrinol Metab* (2019) 104(9):4176–87. doi: 10.1210/jc.2019-00166
68. Nursalim YNS, Blenkiron C, Groom KM, Chamley LW. Growing Human Trophoblasts *In Vitro*: A Review of the Media Commonly Used in Trophoblast Cell Culture. *Reproduction* (2020) 160(6):R119–28. doi: 10.1530/REP-19-0605
69. Liu N, Kaplan AT, Low J, Nguyen L, Liu GY, Equils O, et al. Vitamin D Induces Innate Antibacterial Responses in Human Trophoblasts *Via* an Intracrine Pathway. *Biol Reprod* (2009) 80(3):398–406. doi: 10.1095/biolreprod.108.073577
70. Chen YH, Yu Z, Fu L, Wang H, Chen X, Zhang C, et al. "Vitamin D3 Inhibits Lipopolysaccharide-Induced Placental Inflammation Through Reinforcing Interaction Between Vitamin D Receptor and Nuclear Factor Kappa B p65 Subunit". *Sci Rep* (2015) 5:10871. doi: 10.1038/srep10871
71. Guo H, Callaway JB, Ting JP. Inflammasomes: Mechanism of Action, Role in Disease, and Therapeutics. *Nat Med* (2015) 21(7):677–87. doi: 10.1038/nm.3893
72. Wang X, Wang G, Qu J, Yuan Z, Pan R, Li K. Calcipotriol Inhibits Nlrp3 Signal Through YAP1 Activation to Alleviate Cholestatic Liver Injury and Fibrosis. *Front Pharmacol* (2020) 11:200. doi: 10.3389/fphar.2020.00200
73. Cao R, Ma Y, Li S, Shen D, Yang S, Wang X, et al. 1,25(Oh)(2) D(3) Alleviates DSS-induced Ulcerative Colitis *Via* Inhibiting NLRP3 Inflammasome Activation. *J Leukoc Biol* (2020) 108(1):283–95. doi: 10.1002/JLB.3MA0320-406RR
74. Lu L, Lu Q, Chen W, Li J, Li C, Zheng Z. Vitamin D(3) Protects Against Diabetic Retinopathy by Inhibiting High-Glucose-Induced Activation of the ROS/TXNIP/NLRP3 Inflammasome Pathway. *J Diabetes Res* (2018) 74:8193523. doi: 10.1155/2018/8193523
75. Daneshkhah A, Agrawal V, Eshein A, Subramanian H, Roy HK, Backman V. Evidence for Possible Association of Vitamin D Status With Cytokine Storm and Unregulated Inflammation in COVID-19 Patients. *Aging Clin Exp Res* (2020) 32(10):2141–58. doi: 10.1007/s40520-020-01677-y
76. Wang T-T, Tavera-Mendoza LE, Laperriere D, Libby E, Burton MacLeod N, Nagai Y, et al. Large-Scale in Silico and Microarray-Based Identification of Direct 1,25-Dihydroxyvitamin D3 Target Genes. *Mol Endocrinol* (2005) 19 (11):2685–95. doi: 10.1210/me.2005-0106
77. Kriebitzsch C, Verlinden L, Eelen G, Tan BK, Van Camp M, Bouillon R, et al. The Impact of 1,25(OH)2D3 and its Structural Analogs on Gene Expression in Cancer Cells–a Microarray Approach. *Anticancer Res* (2009) 29(9):3471–83.
78. Ramagopalan SV, Heger A, Berlanga AJ, Maugeri NJ, Lincoln MR, Burrell A, et al. A ChIP-seq Defined Genome-Wide Map of Vitamin D Receptor Binding: Associations With Disease and Evolution. *Genome Res* (2010) 20 (10):1352–60. doi: 10.1101/gr.107920.110
79. Heikkinen S, Väisänen S, Pehkonen P, Seuter S, Benes V, Carlberg C. Nuclear Hormone 1α,25-Dihydroxyvitamin D3 Elicits a Genome-Wide Shift in the Locations of VDR Chromatin Occupancy. *Nucleic Acids Res* (2011) 39 (21):9181–93. doi: 10.1093/nar/gkr654

Conflict of Interest: The authors declare that the research was conducted in the absence of any commercial or financial relationships that could be construed as a potential conflict of interest.

Publisher's Note: All claims expressed in this article are solely those of the authors and do not necessarily represent those of their affiliated organizations, or those of the publisher, the editors and the reviewers. Any product that may be evaluated in this article, or claim that may be made by its manufacturer, is not guaranteed or endorsed by the publisher.

Copyright © 2022 Phillips, Hendricks, Bucher and Maloyan. This is an open-access article distributed under the terms of the Creative Commons Attribution License (CC BY). The use, distribution or reproduction in other forums is permitted, provided the original author(s) and the copyright owner(s) are credited and that the original publication in this journal is cited, in accordance with accepted academic practice. No use, distribution or reproduction is permitted which does not comply with these terms.

frontiers | Frontiers in Endocrinology

ORIGINAL RESEARCH
published: 20 July 2022
doi: 10.3389/fendo.2022.945736

Detection of Shiga Toxin-Producing *Escherichia coli* (STEC) in the Endocervix of Asymptomatic Pregnant Women. Can STEC Be a Risk Factor for Adverse Pregnancy Outcomes?

María Luján Scalise[1], *Nicolás Garimano*[1], *Marcelo Sanz*[2], *Nora Lia Padola*[2], *Patricia Leonino*[3], *Adriana Pereyra*[3], *Roberto Casale*[3], *María Marta Amaral*[1], *Flavia Sacerdoti*[1†*] *and Cristina Ibarra*[1†*]

[1] *Laboratorio de Fisiopatogenia, Instituto de Fisiología y Biofísica, IFIBIO-Houssay (UBA-CONICET), Departamento de Ciencias Fisiológicas, Facultad de Medicina, Universidad de Buenos Aires, Buenos Aires, Argentina,* [2] *CIVETAN-Centro de Investigación Veterinaria Tandil (CONICET, CICPBA), Facultad de Ciencias Veterinarias, Tandil, Argentina,* [3] *Departamento de Obstetricia, Hospital Nacional "Prof. A. Posadas", Buenos Aires, Argentina*

The presence of *Escherichia coli* in the vaginal microbiome has been associated with pregnancy complications. In previous works, we demonstrated that Shiga toxin-producing *Escherichia coli* (STEC) can produce abortion and premature delivery in rats and that Shiga toxin type 2 (Stx2) can impair human trophoblast cell lines. The hypothesis of this work was that STEC may colonize the lower female reproductive tract and be responsible for adverse pregnancy outcomes. Thus, the aim of this work was to evaluate the presence and prevalence of virulence factor genes from STEC in the endocervix of asymptomatic pregnant women. For that purpose, endocervical swabs were collected from pregnant women during their prenatal examination. Swab samples were enriched in a differential medium to select *Enterobacteria*. Then, positive samples were analyzed by PCR to detect genes characteristic of *Escherichia* sp. (such as *uidA* and *yaiO*), genes specific for portions of the *rfb* (O-antigen-encoding) regions of STEC O157 (rfb_{O157}), and STEC virulence factor genes (such as *stx1*, *stx2*, *eae*, $lpfA_{O113}$, *hcpA*, *iha*, *sab, subAB*). The cytotoxic effects of stx2-positive supernatants from *E. coli* recovered from the endocervix were evaluated in Vero cells. Our results showed that 11.7% of the endocervical samples were positive for *E. coli*. Additionally, we found samples positive for *stx2* and other virulence factors for STEC. The bacterial supernatant from an isolate identified as *E. coli* O113:NT, carrying the *stx2* gene, exhibited cytotoxic activity in Vero, Swan 71 and Hela cells. Our results open a new perspective regarding the presence of STEC during pregnancy.

Keywords: Endocervical microbiota, pregnancy, STEC, virulence factors, Stx2

OPEN ACCESS

Edited by:
Mariana Farina, CONICET Centro de Estudios Farmacológicos y Botánicos (CEFYBO), Argentina

Reviewed by:
Mohammad Yousef Alikhani, Hamadan University of Medical Sciences, Iran
Reggie Garcia-Robles, Pontifical Javeriana University, Colombia

***Correspondence:**
Cristina Ibarra
ibarra@fmed.uba.ar
Flavia Sacerdoti
fsacerdoti@fmed.uba.ar

†These authors have contributed equally to this work

Specialty section:
This article was submitted to Developmental Endocrinology, a section of the journal Frontiers in Endocrinology

Received: *16 May 2022*
Accepted: *14 June 2022*
Published: *20 July 2022*

Citation:
Scalise ML, Garimano N, Sanz M, Padola NL, Leonino P, Pereyra A, Casale R, Amaral MM, Sacerdoti F and Ibarra C (2022) Detection of Shiga Toxin-Producing Escherichia coli (STEC) in the Endocervix of Asymptomatic Pregnant Women. Can STEC Be a Risk Factor for Adverse Pregnancy Outcomes?. Front. Endocrinol. 13:945736. doi: 10.3389/fendo.2022.945736

INTRODUCTION

Shiga toxin-producing *Escherichia coli* (STEC), a bacterium that belongs to the family *Enterobacteriaceae*, can cause severe foodborne diseases. The main reservoir for STEC is the intestinal tract of cattle, and the bacterium can survive for months in soil, water, or organic material (1). The main route of transmission is through contaminated food, mainly minced meat (undercooked meat below 71°C), unpasteurized food, contaminated vegetables and person-to-person contact by the fecal-oral route (2, 3).

STEC comprises strains producing two Shiga toxins: Stx type 1 (Stx1) and Stx type 2 (Stx2) (4) and its variants, Stx1 (a – c) and Stx2 (a – k) (5–7). Not all Stx subtypes have been associated with severe illness (8). In this sense, it has been described that Stx2a and Stx2c are clinically more related with severe cases of hemolytic uremic syndrome (HUS), and that STEC O157 strains carrying stx2a predominate in human infections, causing more severe disease symptoms than those carrying stx2c (9, 10).

Stx is the main virulence factor of STEC and, in combination with other virulence factors, contributes to the pathogenic potential of STEC strains. In this sense, intimin (*eae* gene) plays an essential role in the intimate attachment and colonization of intestinal cells of STEC O157:H7, although many STEC isolates lacking the *eae* gene are also able to efficiently colonize the human gut (11). Many other proteins, such as the long polar fimbriae (Lpf) (12), the hemorrhagic *coli* pilus (Hcp) (13), the IrgA homolog adhesin (IhA) (14), and the STEC autotransporter contributing to biofilm formation (Sab) (15), are also involved in the adherence of O157 and non-O157 STEC strains. Non-O157 STEC strains also produce Subtilase cytotoxin (SubAB), able to cause cytotoxic effects in epithelial cells (16).

It is currently known that *E. coli* strains can colonize the vagina, usually asymptomatically, although epidemiological studies have shown that the presence of these bacteria in the female reproductive tract may be a risk factor for pregnancy (17). Some studies developed in Argentina and other countries have shown a high prevalence of *E. coli* in vaginal microbiota of adult women (17, 18). However, to our knowledge, there are no reports about the effects of STEC infection on human pregnancy, although some reports have indicated that STEC transmission from the mother to the child during delivery can cause neonatal HUS (19) or STEC-mediated HUS during pregnancy (20). In Argentina, the most common STEC serotype is O157:H7 (21, 22). Nevertheless, the appearance of non-O157 STEC strains is a clear evidence of the dynamic genome of these *E. coli* pathogens and their ability to transfer or acquire important virulence factors (23, 24). Since there are no epidemiological studies regarding STEC infections during pregnancy, it is difficult to know their impact on reproductive health.

Previous works in our laboratory have demonstrated that Stx2 injection in pregnant rats in early and late pregnancy causes premature delivery, miscarriage and impairments in placental development (25, 26). Also, we have shown that the immunization of rats against Stx2 can prevent the detrimental effects of the toxin during pregnancy (27). Taking these previous findings into account, we hypothesized that STEC can colonize the endocervix and may be responsible for complications in pregnancy. The main goal of this work was to evaluate the presence and prevalence of virulence factor genes from STEC in the endocervix from asymptomatic pregnant women and to better understand the possible clinical relevance of this pathogen during human pregnancy.

MATERIALS AND METHODS

Endocervical Samples

Asymptomatic pregnant women (from 17 to 37 years old) with gestational age from 12 to 34 weeks were enrolled (n=103) during their prenatal examination in the Obstetrics Service of the Maternal and Child Department of the Prof. A. Posadas National Hospital (Buenos Aires, Argentina) between January and March 2019. Endocervical swab samples were collected under direct visualization during a speculum examination. Swabs were transported in sterile tubes containing Cary Blair transport medium (Britania, Argentina) and stored at 4-8°C until used.

Selection of *Enterobacteria* From Endocervical Samples

Endocervical swabs were enriched in 3 mL of Tryptic Soy Broth (Oxoid, UK) overnight (ON) at 37°C and shaken at 150 rpm. Then, cultures were streaked into Sorbitol MacConkey (SMAC) agar (Oxoid, UK) and incubated ON at 37°C. SMAC agar was used for a preliminary selection of *Enterobacteria* based on a differential sorbitol and lactose fermentation profile. SMAC agar is recommended as a selective and differential medium for the detection of STEC O157:H7. *Enterobacteria* capable of fermenting sorbitol form pink colonies on SMAC agar, while non-sorbitol fermenting bacteria, such as STEC O157:H7, form white/colorless colonies.

Detection of *E. Coli* and STEC O157:H7 in Enriched Endocervical Samples by PCR

Total genomic DNA from colonies grown in SMAC agar was obtained to detect the presence of *E. coli* by PCR. DNA was purified using PURO bacteria Kit (PB-L products, Bio-Logicos, Argentina) according to the manufacturer's instructions and quantified by Nanodrop One (Thermo Fisher Scientific, USA). Specific genes encoding for the enzyme beta-glucuronidase (*uidA* gene) (28) and external membrane protein of *E. coli* (*yaiO* gene) (29), and genes specific for portions of the *rfb* (O-antigen-encoding) regions of STEC O157 ($rfbO_{157}$ gene) (11) were detected by PCR using specific primers (**Table 1**).

PCRs were performed in a total volume of 20 µL: 6 µL H_2O, 3 µL DNA, 0.5 µL of each forward and reverse primer (10 µM) and 10 µL Master Mix 2X Kit (M024, Inbio Highway, Argentina). The thermocycler (Thermo Fisher Scientific, USA) program used consisted of one cycle at 95°C for 10 min followed by 35 cycles of

TABLE 1 | Primers used.

Gene	primers	Sequence (5´-3´)	Amplicon size (bp)
uidA	*uidA for*	*TGGTAATTACCGACGAAAACGGC*	162
	uidA rev	*ACGCGTGGTTACAGTCTTGCG*	
yaiO	*yaiO for*	*TGATTTCCGTGCGTCTGAATG*	116
	yaiO rev	*ATGCTGCCGTAGCGTGTTTC*	
$rfbO_{157}$	$rfbO_{157}$ *for*	*CGGACATCCATGTGATATGG*	259
	$rfbO_{157}$ *rev*	*TTGCCTATGTACAGCTAATCC*	

94°C for 40 s, 58°C for 30 s, and 72°C for 60 s, ending with one cycle of 72°C for 2 min. A total of 10 µL of each PCR reaction product was loaded into an agarose gel to confirm the presence and size of the corresponding amplicon.

Samples positive for *yaiO* were analyzed for *rfbO157* as well as for the presence of other STEC virulence factor genes, including: *stx1*, *stx2*, *stx2a*, *stx2c* (4), *subAB* (30), *eae* (31), $lpfAO_{113}$ (12), *hcp* (13), *iha* (32) and *sab* (15) by PCR (**Table 2**).

Cell Line Cultures

The Vero cell line (Vero), derived from African green monkey kidney, was purchased from the American Type Culture Collection (ATCC-CCL-81, Manassas, VA, USA). The HeLa cell line (ATCC-CCL-2), derived from a human cervix adenocarcinoma, was used as a human endocervical model. The Swan 71 cell line, derived by telomerase-mediated transformation of a 7-week cytotrophoblast isolate, was kindly provided by Dr. Gil Mor, Yale University, New Haven, CT, USA (33).

All cell lines were cultured in Dulbecco's Modified Eagle Medium/Nutrient Mixture F-12 (DMEM-F12 medium, Sigma Aldrich, USA) supplemented with 10% Fetal Bovine Serum (FBS, Internegocios S.A., Argentina), 100 U/mL penicillin/streptomycin, and 2 mM L-glutamine (GIBCO, USA), and grown at 37°C in a humidified 5% CO_2 incubator. For growth-arrested conditions, the medium was used without FBS.

Evaluation of the Cytotoxic Effects of Bacterial Supernatants From Bacteria Isolated From the Endocervical Samples

Endocervical samples that were positive for *stx2* by PCR were grown ON in Luria-Bertani Broth (LB) (Sigma Aldrich, USA) at 37°C with shaking at 150 rpm. Then, the cultures were diluted (1:20) in DMEM-F12 medium (Sigma Aldrich, USA), supplemented with 1 mM of HEPES buffer solution (4-(2-Hydroxyethyl)piperazine-1-ethanesulfonic acid, N-(2-Hydroxyethyl)piperazine-N′-(2-ethanesulfonic acid)) (GIBCO, USA) and grown until exponential phase (OD_{600} = 0.4-0.5) at 37°C with shaking at 150 rpm. Subsequently, bacterial supernatants were collected after centrifugation at 10,000 x *g* for 5 min and filtered (0.22-µm pore-size filter; Millipore, USA). In some experiments, to induce Stx2 production, mitomycin-C (1 µg/mL) was added at the exponential phase and the bacterial culture was grown for additional 3 h (34).

Cell Viability Assays

Cell viability assays were performed as previously described (35). Briefly, 15x 10^3 cells/well (Vero, Swan 71, and HeLa) were seeded in 96-well plates and grown at 80% of confluence. Then, cells were exposed for 72 h to different concentrations ($1x10^{-6}$ – 0.1 µg/mL) of purified Stx2 (Phoenix Laboratory, Tufts Medical Center, Boston, USA) or to serial dilutions of bacterial supernatant (10^{-1}-10^{-6}) in growth-arrested conditions.

TABLE 2 | Evaluation of STEC virulence factors, primer sequences and size of amplicons .

Virulence factor	primers	Sequence (5´-3´)	Amplicon size (bp)
Shiga toxin type 1	*stx1 for*	*ATGTCATTCGCTCTGCAATAGGTAC*	1020
	stx1 rev	*GAAGAAGAGACTGAAGATTCCATCTG*	
Shiga toxin type 2	*stx2 for*	*GGCACTGTCTGAAACTGCTCCTGT*	627
	stx2 rev	*ATTAAACTGCACTTCAGCAAATCC*	
Shiga toxin type 2a	*stx2a for*	*GCGATACTGRGBACTGTGGCC*	349
	stx2a rev	*CCGKCAACCTTCACTGTAAATGTG*	
Shiga toxin type 2c	*stx2c for*	*GAAAGTCACAGTTTTTATATACAACGGGTA*	177
	stx2c rev	*CCGGCCACYTTTACTGTGAATGTA*	
Subtilase	*subAB for*	*TATGGCTTCCCTCATTGCC*	556
	subAB rev	*TATAGCTGTTGCTTCTGACG*	
Intimin	*eae for*	*GGAACGGCAGAGGTTAATCTGCAG*	346
	eae rev	*GGCGCTCATCATAGTCTTTC*	
Long polar fimbriae A_{O113}	$lpfA_{O113}$ *for*	*ATGAAGCGTAATATTATAG*	573
	$lpfA_{O113}$ *rev*	*TTATTTCTTATATTCGAC*	
Hemorragic *coli* pilus	*hcp for*	*TCGCTAGTTGCTGACAGATTT*	868
	hcp rev	*AATGTCTGTTGTGTGCGACTG*	
IhA adhesion	*iha for*	*CAGTTCAGTTTCGCATTCACC*	1305
	iha rev	*GTATGGCTCTGATGCGATG*	
Sab (STEC AT) mediating biofilm formation	*sab for*	*GGTGGATACAGCAGGTAATG*	163
	sab rev	*TATCTCACCACCTGCTATCG*	

After treatment, cells were incubated with a neutral red solution (50 μg/mL) at 37°C for 1 h in 5% CO_2. Then, cells were washed and fixed with 1% $CaCl_2$-1% formaldehyde and finally lysed with 1% acetic acid in 50% ethanol solution to solubilize the neutral red uptake by cells. Absorbance in each well was read at 540 nm in an automated plate spectrophotometer (RT-6000, Rayto Life and Analytical Sciences Co. Ltd., China). Results are expressed as percentage of cell viability, where 100% represents control cells without toxin or supernatant treatment. The 50% cytotoxic dose (CD_{50}) of Stx2 and the bacterial supernatant corresponded to the dilution required to kill 50% of cells.

Stx2-Neutralization Assay

For the neutralization assay, bacterial supernatant in a dilution required to kill 50% of Vero cells (CD_{50}) was co-incubated with 25 μg/mL of the mouse monoclonal antibody 2E11 against the A-subunit of Stx2 (anti-Stx2 mAb) at 37°C for 1 h (36). The mixture was added to a 96-well culture plate containing Vero cells grown at 80% of confluence and then incubated for 72 h. The cytotoxicity was analyzed by neutral red uptake as previously described. The CD_{50} of purified Stx2 (1 ng/mL) was used as control.

Isolation and Characterization of STEC Samples From the Endocervix

The enriched bacterial culture from endocervical samples carrying the *stx2* gene and showing cytotoxic effects on Vero was streaked onto LB agar plates and incubated ON at 37°C. Grown colonies were picked and added in 96-well plates and grown in LB medium ON at 37°C with agitation at 150 rpm. The next day, wells of each column were pooled and the DNA was purified to test the presence of the *stx2* gene. Afterward, individual colonies grown in each well of stx2-positive columns were directly picked and confirmed to be STEC by testing the presence of the *stx2* gene by PCR and by Vero cell assays. Isolates were then sub-cultured for further genetic or phenotypic typing.

Determination of the Serotypes of STEC Isolates

The serotypes (O and H) of STEC isolates were determined by microagglutination, as described by Blanco etal. (37).

Ethical Approval

This study had the approval of the Human Research Ethics Committee of the Prof. A. Posadas National Hospital, Buenos Aires, Argentina (Ref # 423 EMnPeSe/20), in accordance with the Argentine Good Clinical Practice Guidelines. All pregnant women were thoroughly informed about the purpose of the study and provided a written informed consent. The exclusion criteria were: women with genital papilloma virus infection (HPV), human immunodeficiency virus (HIV), pelvic inflammatory disease (PID) and sexually transmitted diseases such as chlamydia, gonorrhea, and genital herpes.

Statistical Analysis

Data were plotted and statistically analyzed using Graph Pad Prism 5.0 (San Diego, CA, USA). Cytotoxicity curves were fitted using a four-parameter logarithmic regression. Statistical significance for all experiments was assessed using analysis of variance (ANOVA) with Tukey's multiple comparison test as a *posteriori* test. In all cases, statistical significance was set at $^*p < 0.05$.

RESULTS

Detection and Identification of *E. coli* From Endocervical Swab Samples

Sixteen out of the 103 endocervical swab samples developed colonies on SMAC agar. Only non-sorbitol fermenting colonies were observed. Fifteen out of those sixteen samples had the *uidA* gene and 12 out of the 16 had the *yaiO* gene (**Table 3**). Considering that the *yaiO* gene is more specific than the *uidA* gene for the identification of *E. coli*, only those containing the *yaiO* gene were considered positive for *E. coli* (29). One sample (S12) was negative for both genes (**Table 3**). Therefore, 12 out of the 103 endocervical samples recruited for this study (11.7%) were considered positive for *E. coli* spp. in the endocervical microbiota. The absence of sorbitol-fermenting colonies (characteristic of O157:H7 *E. coli*) on SMAC agar was confirmed by PCR (none of the samples evaluated were positive for the rfb_{O157} gene) (**Table 3**).

Detection of STEC Virulence Genes in Bacterial Isolates Obtained From Endocervical Swab Samples

The presence of STEC virulence factors was analyzed in the 12 endocervical samples that developed colonies on SMAC agar and were confirmed positive for *E. coli* by the presence of the *yaiO* gene. Seven out of the 12 samples (58.3%) amplified for the *stx2* gene, 5 out of the 12 (41.7%) for the lpf_{AO113} gene, 8 out of the 12

TABLE 3 | Genotypic characterization of *E. coli* in endocervical samples grown on SMAC agar.

Endocervical samples SMAC agar POS	*uidA*	*yaiO*	$rfbO_{157}$
S1	POS	POS	–
S2	POS	POS	–
S3	POS	POS	–
S4	POS	POS	–
S5	POS	–	–
S6	POS	POS	–
S7	POS	–	–
S8	POS	POS	–
S9	POS	POS	–
S10	POS	–	–
S11	POS	POS	–
S12	–	–	–
S13	POS	POS	–
S14	POS	POS	–
S15	POS	POS	–
S16	POS	POS	–

(-): NEGATIVE (POS): POSITIVE

(66.7%) for the *hcpA* gene and 3 out of the 12 (25%) for the *iha* gene (**Table 4**). None of them were positive for the *eae*, *stx1* or *sab* genes.

Evaluation of the Cytotoxic Activity of Bacterial Supernatants Obtained From Endocervical Swab Samples Positive for the *Stx2* Gene

The cytotoxic activity of filter-sterilized bacterial supernatants obtained from endocervical samples positive for *E. coli* carrying the *stx2* gene was evaluated in Vero cells (**Figure 1**).

Incubation of Vero cells for 72 h with serial dilutions of the bacterial supernatant corresponding to sample 14 (S14-SN) caused a significant cytotoxicity in a dose-dependent manner, reaching a CD_{50} at $2x10^{-4}$ dilution. The CD_{50} of Stx2 in S14-SN was equivalent to that elicited by approximately 5 μg/mL of purified Stx2 (**Figure 1**). In contrast, the other filter-sterilized bacterial supernatants showed no cytotoxic effects on the viability of Vero cells, even if previously grown with mitomycin-C, an inductor of *stx2* phages (data not shown).

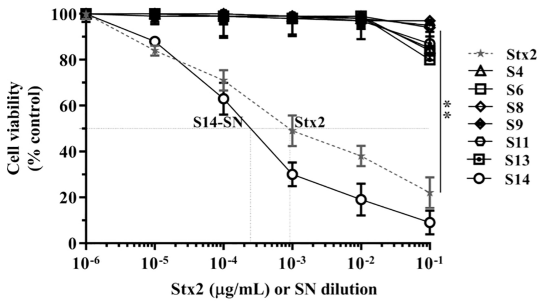


FIGURE 1 | Cytotoxicity of *E. coli*-positive endocervical samples carrying the *stx2* gene on the viability of Vero cells. Vero cells were exposed to serial dilutions of bacterial supernatants (SN) from endocervical samples carrying the *stx2* gene or different concentrations of purified Stx2 under growth-arrested conditions. Cell viability was determined by neutral red uptake after 72 h of incubation, and 100% represents cells incubated under identical conditions but without treatment. Data are shown as means ± S.D from at least three independent experiments performed in triplicate. $^{**}p < 0.01$.

Neutralization of Stx2 Cytotoxicity of Bacterial Supernatants From Endocervical Samples

Neutralization studies were used to confirm that the significant decrease in Vero cell viability caused by S14-SN was due to the cytotoxic action of Stx2. The results showed that S14-SN cytotoxicity was prevented by preincubation of the bacterial S14-SN (1:5000) with the anti-Stx2 mAb (25 μg/mL) at 37°C for 1 h. Neutralization of purified Stx2 was used as control (**Figure 2**).

Cytotoxic Effects of STEC-Positive Endocervical Samples on the Viability of Human Endocervical and Extravillous Trophoblast Cells

A significant cytotoxic effect was observed when monolayers of human endocervical (HeLa) cells were exposed to different concentrations of Stx2 or serial dilutions of the filter-sterilized bacterial supernatants or bacteria isolated from endocervical sample S14 (S14-SN) for 72 h. The CD_{50} was obtained with 10 ng/mL of purified Stx2 and with a $5x10^{-3}$ dilution of S14-SN. In agreement with the results described above, cytotoxicity was also observed with purified Stx2 on monolayers of extravillous trophoblasts (Swan 71 cells). The CD_{50} after 72 h of incubation with purified Stx2 was obtained at 100 ng/mL and with a dilution of approximately $2x10^{-2}$ of S14-SN (**Figure 3**). These results indicate that filter-sterilized bacterial supernatants from the STEC-positive endocervical microbiota can impair endocervical and trophoblast cell viabilities mediated by Stx2.

Genotypic Characterization of STEC Isolated From an Endocervical Sample

The bacterial isolate from endocervical sample S14, named STEC 123/21, was subtyped for *stx2* by PCR, using specific primers for the *stx2a* and *stx2c* genes (**Table 2**). **Figure 4** shows a representative gel of the STEC isolate subjected to PCR assay. Results showed PCR products of the expected sizes, consistent with the presence of the *stx2a* gene (**Figure 4**) and the absence of the *subAB* gene (S14 in **Table 3**).

TABLE 4 | Genotypic identification of STEC virulence factors in *E. coli*-positive samples .

Endocervical sample *E. coli* POS	*stx1*	*stx2*	*subAB*	*eae*	$lpfA_{O113}$	*hcpA*	*iha*	*sab*
S1	–	–	–	–	POS	–	–	–
S2	–	–	–	–	POS	POS	–	–
S3	–	–	–	–	POS	POS	–	–
S4	–	POS	–	–	–	POS	–	–
S6	–	POS	–	–	POS	POS	POS	–
S8	–	POS	–	–	–	–	–	–
S9	–	POS	–	–	–	POS	–	–
S11	–	POS	–	–	–	POS	POS	–
S13	–	POS	–	–	–			–
S14	–	POS	–	–	POS	POS	POS	–
S15	–	–	–	–	–	–	–	–
S16	–	–	–	–	–	POS	–	–

(-): NEGATIVE: (POS): POSITIVE

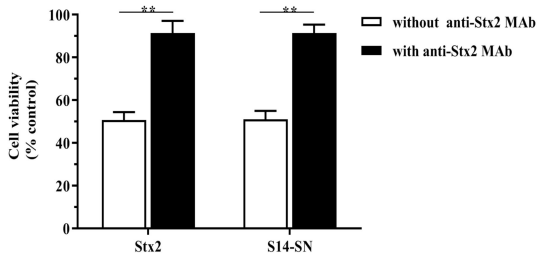


FIGURE 2 | Neutralization of the Stx2 cytotoxicity of bacterial supernatants isolated from endocervical samples on the viability of Vero cells. The bacterial supernatant from the endocervical sample 14 (S14-SN, dilution 1:5000) was preincubated with the mouse monoclonal antibody 2E11 against the A-subunit of Stx2 (anti-Stx2 mAb, 25 µg/mL) at 37°C for 1 h. The mixture was then added to a 96-well culture plate containing Vero cells and incubated for 72 h. The CD_{50} of purified Stx2 (1 ng/mL) incubated with anti-Stx2 mAb was used as control. Cell viability was analyzed by neutral red uptake. Data are shown as mean ± S.D from at least three independent experiments performed in triplicate. $^{**}p < 0.01$, n=3.

Serotypification of STEC Strain 123/21

STEC strain 123/21 belonged to the O113 type, but the H type could not be determined (nondetermined, NT). The analysis of the supernatant from STEC O113:NT demonstrated that it was able to induce a marked decrease in cell viability. The cytotoxicity of the supernatant of this STEC isolate was similar to that obtained from the initial endocervical sample S14 containing other bacteria (SN-S14) (**Figure 5**).

DISCUSSION

The vaginal microbiota is a complex ecosystem consisting of around 200 species of microorganisms, being *Lactobacillus crispatus*, *L. jensenii* and *L. gasseri* the most represented species. Several studies have shown that around 70% of the vaginal microbiota in pregnant and non-pregnant women is

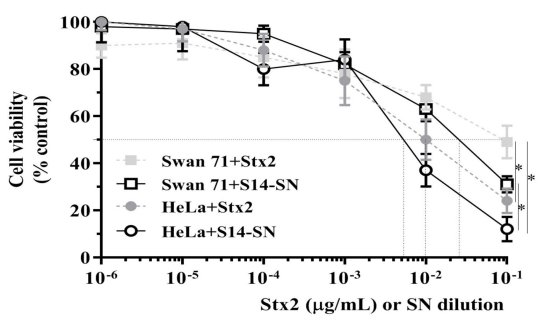


FIGURE 3 | Cytotoxic effects of STEC-positive endocervical samples on the viability of Swan 71 and HeLa cell lines. Cells were exposed to purified Stx2 or serial dilutions of the supernatant from endocervical sample S14 (S14-SN) for 72 h. Cell viability was analyzed by neutral red uptake. Data are shown as mean ± S.D from at least three independent experiments performed in triplicate. $^{*}p < 0.05$, n=3.

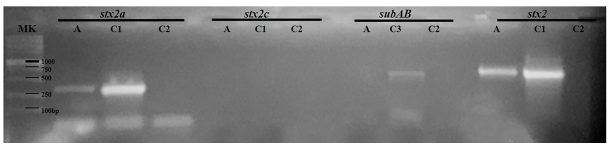


FIGURE 4 | Characterization of a STEC strain isolated from an endocervical sample by PCR assays. The STEC strain named 123/21 was subtyped for the stx2 gene. The amplicons were seeded on 1.5% agarose gel for 30 min at 80 Volts. A: STEC strain 123/21. C1: *E. coli* O157:H7 strain 125/99 (stx2a + 349 bp; stx2 627 bp), C2: negative control of PCR; C3: *E. coli* O113:H21 (subAB; 556 bp); DNA size marker (MK).

composed of *Lactobacillus* (38–40). The substitution of *Lactobacillus* by pathogenic or opportunistic microorganisms is associated with the development of bacterial vaginosis and lower urinary tract infections, and the presence of non-*Lactobacillus* species has been associated with poor reproductive health and/or complications in pregnancy (41–44). In this regard, the presence of *E. coli* in the female reproductive tract has been found to be a risk factor for the progression of pregnancy (17, 45, 47).

The results of this work demonstrate the prevalence of *E. coli* in the endocervical microbiota in 11.7% of asymptomatic pregnant women. Previous studies performed in Argentina (18) and other countries of South America, Europe and North America (17) have reported an incidence similar to that found in this work. *E. coli* are commensal bacteria of the intestine of humans and animals, and some pathogenic strains, such as STEC, can cause moderate to severe gastrointestinal disease in humans. However, the risk of spontaneous abortion or preterm delivery in humans associated with STEC infection or its main virulence factor, Stx2, has not yet been evaluated.

Our results showed that 7 out of the 12 endocervical samples positive for *E. coli* carried the *stx2* gene, although only one of them (1/12, 8.3%) caused significant cytotoxicity in Vero cells due to the presence of Stx2 in the bacterial culture supernatant. The isolated STEC was identified as O113:NT Stx2a-positive.

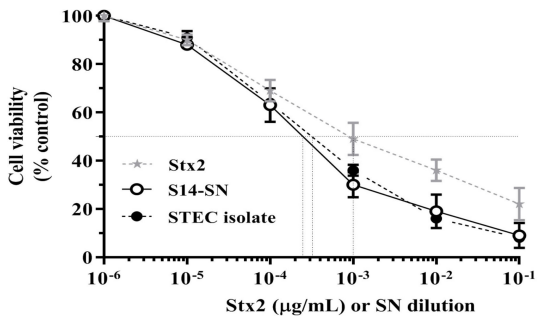


FIGURE 5 | Cytotoxic effects of the STEC isolate O113:NT obtained from an endocervical sample on the viability of Vero cells. Cells were exposed to purified Stx2 or serial dilutions of supernatants from STEC O113:NT or sample S14 for 72 h. Cell viability was analyzed by neutral red uptake. Data are shown as mean ± S.D from at least three independent experiments performed in triplicate. $^{*}p < 0.05$.

The Stx2 cytotoxicity evaluated by neutral red uptake method in the remaining stx2-positive *E. coli* samples was undetectable. We hypothesized that the composition of the endocervical gram-negative microbiota may be negatively regulating Stx2 expression and/or STEC growth, as previously described (46, 47). Moreover, the relationship between induction of Stx2-encoding phages and toxin production in STEC (48) may vary considerably in response to the microenvironment (49).

An interesting finding was the detection of $lpfA_{O113}$ and *hcpA* in our samples, considering that lpf_{AO113}-positive STEC strains are associated with the appearance of small outbreaks of intestinal and extra-intestinal diseases in humans (50) and that the *hcpA* gene is associated with the pathogenicity of non-O157 STEC (51).

The fact that the microbiological selection by SMAC was negative for O157:H7, together with the absence of amplification for the *eae* gene that encodes for *Locus of Enterocyte Effacement* (LEE), led us to study the expression of the *iha* gene, which encodes an outer membrane adhesin protein. This adhesin was detected in 25% (3/12) of the endocervical samples also positive for *E. coli*, which is an interesting finding because previous studies have demonstrated the positivity of the *iha* gene in non-STEC uropathogenic *E. coli* (52). LEE-negative STEC strains have been found to be associated with clinical cases of HUS (53, 54). In the present work, we also studied the *sab* gene, which encodes an adhesin that promotes adherence to human epithelial cells, mediates the formation of biofilm, and is involved in intestinal colonization of LEE-negative STEC strains (15), but found no positive samples.

It is known that non-O157 STEC expressing Stx2 can affect the adult population, as observed in the outbreak that occurred in Germany in 2011, which produced approximately 3,500 cases of infection, 810 cases of HUS, and 39 deaths (55). Detailed studies of this outbreak demonstrated that the stx2-encoding phage can insert into the genome of non-O157 STEC strains and cause serious disease in the adult population, mostly women (56), although details on complications of pregnant vs non-pregnant women were not reported.

In summary, our results show the presence of a STEC O113:NT strain with Stx2a production in the endocervix of an asymptomatic woman during the first trimester of pregnancy. The patient (sample S14) received cephalexin, a broad-spectrum antibiotic, during the second trimester of gestation (20 weeks) to treat uterine inflammation and urinary infection. Probably antibiotic administration is the reason for no longer presence of the STEC strain in subsequent analysis of the endocervical samples during the second and third trimester as well as urine and fecal sample during the third trimester. At birth, the newborn presented a good general condition, and subsequent clinical checks of the mother and baby were normal. Therefore, the contributions of this study encourage us about the importance of the detection of *E. coli* during prenatal studies to prevent possible complications in pregnancy. Epidemiological studies related to the presence of vaginal STEC may establish its association with possible risks for the reproductive health of women.

DATA AVAILABILITY STATEMENT

The raw data supporting the conclusions of this article will be made available by the authors, without undue reservation.

ETHICS STATEMENT

The studies involving human participants were reviewed and approved by Human Research Ethics Committee of the Prof. A. Posadas National Hospital, Buenos Aires, Argentina (Ref # 423 EMnPeSe/20). The patients/participants provided their written informed consent to participate in this study. Written informed consent was obtained from the individual(s) for the publication of any potentially identifiable images or data included in this article.

AUTHOR CONTRIBUTIONS

The authors contributions are as follows: Conceived and designed the experiments: SML, GN, CR, MA, SF, IC. Performed the experiments: SML, GN, SM, PN, MA, SF. Analyzed the data: SML, GN, SM, PN, MA, SF, IC. Contributed reagents/materials/analysis tools: SML, LP, PA, CR, MA, SF, IC. Wrote the paper: SML, GN, SF, IC. All authors contributed to the article and approved the submitted version.

ACKNOWLEDGMENTS

We are grateful to Roxane M. F. Piazza from the Laboratorio de Bacteriología, Instituto Butantan, São Paulo, Brazil, for kindly providing mAb 2E11 directed against the A-subunit of Stx2.

REFERENCES

1. Sapountzis P, Segura A, Desvaux M, Forano E. An Overview of the Elusive Passenger in the Gastrointestinal Tract of Cattle: The Shiga Toxin Producing. *Microorganisms* (2020) 8(6):877. doi: 10.3390/microorganisms8060877
2. Rivas M, Chinen I, Miliwebsky E, Masana M. Risk Factors for Shiga Toxin-Producing *Escherichia coli*-Associated Human Diseases. *Microbiol Spectr* (2014) 2(5):1–14. doi: 10.1128/microbiolspec.ehec-0002-2013
3. Alconcher LF, Rivas M, Lucarelli LI, Galavotti J, Rizzo M. Shiga Toxin-Producing *Escherichia coli* in Household Members of Children With Hemolytic Uremic Syndrome. *Eur J Clin Microbiol Infect Dis* (2020) 39 (3):427–32. doi: 10.1007/s10096-019-03738-1
4. Scheutz F, Teel LD, Beutin L, Piérard D, Buvens G, Karch H, et al. Multicenter Evaluation of a Sequence-Based Protocol for Subtyping Shiga Toxins and Standardizing Stx Nomenclature. *J Clin Microbiol* (2012) 50(9):2951–63. doi: 10.1128/JCM.00860-12

5. Bai X, Fu S, Zhang J, Fan R, Xu Y, Sun H, et al. Identification and Pathogenomic Analysis of an *Escherichia coli* Strain Producing a Novel Shiga Toxin 2 Subtype. *Sci Rep* (2018) 8(1):1–11. doi: 10.1038/s41598-018-25233-x
6. Yang X, Bai X, Zhang J, Sun H, Fu S, Fan R, et al. *Escherichia coli* Strains Producing a Novel Shiga Toxin 2 Subtype Circulate in China. *Int J Med Microbiol* (2020) 310(1):151377. doi: 10.1016/j.ijmm.2019.151377
7. Hughes AC, Zhang Y, Bai X, Xiong Y, Wang Y, Yang X, et al. Structural and Functional Characterization of Stx2k, a New Subtype of Shiga Toxin 2. *Microorganisms* (2020) 8(1):1–18. doi: 10.3390/microorganisms8010004
8. Hofer E, Cernela N, Stephan R. Shiga Toxin Subtypes Associated With Shiga Toxin-Producing *Escherichia coli* Strains Isolated From Red Deer, Roe Deer, Chamois, and Ibex. *Foodborne Pathog Dis* (2012) 9(9):792–5. doi: 10.1089/fpd.2012.1156
9. Orth D, Grif K, Khan AB, Naim A, Dierich MP, Würzner R. The Shiga Toxin Genotype Rather Than the Amount of Shiga Toxin or the Cytotoxicity of Shiga Toxin *In Vitro* Correlates With the Appearance of the Hemolytic Uremic Syndrome. *Diagn Microbiol Infect Dis* (2007) 59(3):235–42. doi: 10.1016/j.diagmicrobio.2007.04.013
10. Pianciola L, D'Astek BA, Mazzeo M, Chinen L, Masana M, Rivas M. Genetic Features of Human and Bovine *Escherichia coli* O157: H7 Strains Isolated in Argentina. *Int J Med Microbiol* (2016) 306:123–30. doi: 10.1016/j.ijmm.2016.02.005
11. Paton JC, Paton AW. Pathogenesis and Diagnosis of Shiga Toxin-Producing *Escherichia coli* Infections. *Clin Microbiol Rev* (1998) 11(3):450–79. doi: 10.1128/cmr.11.3.450
12. Doughty S, Sloan J, Bennett-Wood V, Robertson M, Robins-Browne RM, Hartland EL. Identification of a Novel Fimbrial Gene Cluster Related to Long Polar Fimbriae in Locus of Enterocyte Effacement-Negative Strains of Enterohemorrhagic *Escherichia coli*. *Infect Immun* (2002). doi: 10.1128/IAI.70.12.6761-6769.2002
13. Xicohtencatl-Cortes J, Monteiro-Neto V, Ledesma MA, Jordan DM, Francetic O, Kaper JB, et al. Intestinal Adherence Associated With Type IV Pili of Enterohemorrhagic *Escherichia coli* O157:H7. *J Clin Invest* (2007) 117 (11):3519–29. doi: 10.1172/JCI30727
14. Tarr PI, Bilge SS, Vary JC, Jelacic S, Habeeb RL, Ward TR, et al. Iha: A Novel *Escherichia coli* O157:H7 Adherence-Conferring Molecule Encoded on a Recently Acquired Chromosomal Island of Conserved Structure. *Infect Immun* (2000) 68(3):1400–7. doi: 10.1128/IAI.68.3.1400-1407.2000
15. Herold S, Paton JC, Paton AW. Sab, a Novel Autotransporter of Locus of Enterocyte Effacement-Negative Shiga-Toxigenic *Escherichia coli* O113:H21, Contributes to Adherence and Biofilm Formation. *Infect Immun* (2009) 77 (8):3234–43. doi: 10.1128/IAI.00031-09
16. Paton A, Srimanote P, Talbot U, Wang H, Paton J. A New Family of Potent AB(5) Cytotoxins Produced by Shiga Toxigenic *Escherichia coli*. *J Exp Med* (2004) 200(1):35–46. doi: 10.1084/jem.20040392
17. Cools P. The Role of *Escherichia coli* in Reproductive Health: State of the Art. *Res Microbiol* (2017) 168(9-10):892–901. doi: 10.1016/j.resmic.2017.02.002
18. Villar HE, Aubert V, Baserni MN, Jugo MB. Maternal Carriage of Extended-Spectrum Beta-Lactamase-Producing *Escherichia coli* Isolates in Argentina. *J Chemother* (2013) 25(6):324–7. doi: 10.1179/1973947813Y.0000000081
19. Ulinski T, Lervat C, Ranchin B, Gillet Y, Floret D, Cochat P. Neonatal Hemolytic Uremic Syndrome After Mother-to-Child Transmission of *Escherichia coli* O157. *Pediatr Nephrol* (2005) 20(9):1334–5. doi: 10.1007/s00467-005-1871-3
20. Chart H, Perry NT, Cheasty T, Wright PA. The Kinetics of Antibody Production to Antigens of *Escherichia coli* O157 in a Pregnant Woman With Haemolytic Uraemic Syndrome. *J Med Microbiol* (2002) 51(6):522–5. doi: 10.1099/0022-1317-51-6-522
21. Carbonari CC, Fittipaldi N, Teatero S, Athey TBT, Pianciola L, Masana M, et al. Whole-Genome Sequencing Applied to the Molecular Epidemiology of Shiga Toxin-Producing *Escherichia coli* O157:H7 in Argentina. *Genome Announc* (2016) 4(6):4–5. doi: 10.1128/genomeA.01341-16
22. Pianciola L, Rivas M. Genotypic Features of Clinical and Bovine *Escherichia coli* O157 Strains Isolated in Countries With Different Associated-Disease Incidences. *Microorganisms* (2018) 6(2):36. doi: 10.3390/microorganisms6020036
23. Oderiz S, Leotta GA, Galli L. Detection and Characterization of Shiga Toxin-Producing *Escherichia coli* in Children Treated at an Inter-Zonal Pediatric Hospital in the City of La Plata. *Rev Argent Microbiol* (2018) 50(4):341–50. doi: 10.1016/j.ram.2017.08.008
24. Cundon C, Carbonari CC, Zolezzi G, Rivas M, Bentancor A. Putative Virulence Factors and Clonal Relationship of O174 Shiga Toxin-Producing *Escherichia coli* Isolated From Human, Food and Animal Sources. *Vet Microbiol* (2018) 215(11):29–34. doi: 10.1016/j.vetmic.2017.12.006
25. Burdet J, Zotta E, Franchi A, Ibarra C. Intraperitoneal Administration of Shiga Toxin Type 2 in Rats in the Late Stage of Pregnancy Produces Premature Delivery of Dead Fetuses. *Placenta* (2009) 30(6):491–6. doi: 10.1016/j.placenta.2009.03.012
26. Sacerdoti F, Amaral MM, Zotta E, Franchi AM, Ibarra C. Effects of Shiga Toxin Type 2 on Maternal and Fetal Status in Rats in the Early Stage of Pregnancy. *BioMed Res Int* (2014) 2014:384645. doi: 10.1155/2014/384645
27. Sacerdoti F, Mejías MP, Bruballa AC, Alvarez RS, Amaral MM, Palermo MS, et al. Immunization With BLS-Stx2B Chimera Totally Protects Dams From Early Pregnancy Loss Induced by Shiga Toxin Type 2 (Stx2) and Confers Anti-Stx2 Immunity to the Offspring. *Vaccine* (2016) 34(39):4732–7. doi: 10.1016/j.vaccine.2016.07.049
28. Tantawiwat S, Tansuphasiri U, Wongwit W, Wongchotigul V, Kitayaporn D. Development of Multiplex PCR for the Detection of Total Coliform Bacteria for *Escherichia coli* and *Clostridium perfringens* in Drinking Water. *Southeast Asian J Trop Med Public Health* (2005) 36(1):162–9.
29. Molina F, López-Acedo E, Tabla R, Roa I, Gómez A, Rebollo JE. Improved Detection of *Escherichia coli* and Coliform Bacteria by Multiplex PCR. *BMC Biotechnol* (2015) 15(1):1–9. doi: 10.1186/s12896-015-0168-2
30. Paton A, Paton J. Multiplex PCR for Direct Detection of Shiga Toxigenic *Escherichia coli* Strains Producing the Novel Subtilase Cytotoxin. *J Clin Microbiol* (2005) 43(6):2944–7. doi: 10.1128/JCM.43.6.2944-2947.2005
31. Blanco M, Blanco JE, Mora A, Dahbi G, Alonso MP, Gonza EA, et al. Serotypes, Virulence Genes, and Intimin Types of Shiga Toxin (Verotoxin)-Producing *Escherichia coli* Isolates From Cattle in Spain and Identification 427 of a New Intimin Variant Gene (Eae-Xi). *J Clin Microbiol* (2004) 42(2):645–51. doi: 10.1128/JCM.42.2.645-651.2004
32. Schmidt H, Beutin L, Karch H. Molecular Analysis of the Plasmid-Encoded Hemolysin of *Escherichia coli* O157:H7 Strain EDL 933. *Infect Immun* (1995) 63(3):1055–61. doi: 10.1128/iai.63.3.1055-1061.1995
33. Straszewski-Chavez SL, Abrahams VM, Alvero AB, Aldo PB, Ma Y, Guller S, et al. The Isolation and Characterization of a Novel Telomerase Immortalized First Trimester Trophoblast Cell Line, Swan 71. *Placenta* (2009). doi: 10.1016/j.placenta.2009.08.007
34. Thuraisamy T, Lodato PB. Influence of RNase E Deficiency on the Production of Stx2-Bearing Phages and Shiga Toxin in an RNase E-Inducible Strain of Enterohaemorrhagic *Escherichia coli* (EHEC) O157:H7. *J Med Microbiol* (2018) 67(5):724–32. doi: 10.1099/jmm.0.000728
35. Creydt VP, Silberstein C, Zotta E, Ibarra C. Cytotoxic Effect of Shiga Toxin-2 Holotoxin and Its B Subunit on Human Renal Tubular Epithelial Cells. *Microbes Infect* (2006) 8(2):410–9. doi: 10.1016/j.micinf.2005.07.005
36. Rocha LB, Luz DE, Moraes CTP, Caravelli A, Fernandes I, Guth BEC, et al. Interaction Between Shiga Toxin and Monoclonal Antibodies: Binding Characteristics and *In Vitro* Neutralizing Abilities. *Toxins* (2012) 4(9):729–47. doi: 10.3390/toxins4090729
37. Blanco J, Blanco M, Alonso MP, Blanco JE, Garabal J, González EA. Serogroups of *Escherichia coli* Strains Producing Cytotoxic Necrotizing Factors CNF1 and CNF2. *FEMS Microbiol Lett* (1992) 96(2–3):155–9. doi: 10.1016/0378-1097(92)90396-6
38. Romero R, Hassan SS, Gajer P, Tarca AL, Fadrosh DW, Nikita L, et al. The Composition and Stability of the Vaginal Microbiota of Normal Pregnant Women Is Different From That of Non-Pregnant Women. *Microbiome* (2014) 2(1):1–19. doi: 10.1186/2049-2618-2-4
39. Chen X, Lu Y, Chen T, Li R. The Female Vaginal Microbiome in Health and Bacterial Vaginosis. *Front Cell Infect Microbiol* (2021) 11:631972. doi: 10.3389/fcimb.2021.631972
40. Juliana NCA, Suiters MJM, Al-Nasiry S, Morré SA, Peters RPH, Ambrosino E. The Association Between Vaginal Microbiota Dysbiosis, Bacterial Vaginosis, and Aerobic Vaginitis, and Adverse Pregnancy Outcomes of Women Living in Sub-Saharan Africa: A Systematic Review. *Front Public Health* (2020) 8:567885(12). doi: 10.3389/fpubh.2020.567885
41. Moreno I, Codoñer FM, Vilella F, Valbuena D, Martinez-Blanch JF, Jimenez-Almazán J, et al. Evidence That the Endometrial Microbiota has an Effect on

Implantation Success or Failure. *Am J Obstet Gynecol* (2016) 215(6):684–703. doi: 10.1016/j.ajog.2016.09.075
42. Smith SB, Ravel J. The Vaginal Microbiota, Host Defense and Reproductive Physiology. *J Physiol* (2017) 595(2):451–63. doi: 10.1113/JP271694
43. Han C, Li H, Han L, Wang C, Yan Y, Qi W, et al. Aerobic Vaginitis in Late Pregnancy and Outcomes of Pregnancy. *Eur J Clin Microbiol Infect Dis* (2019) 38(2):233–9. doi: 10.1007/s10096-018-3416-2
44. Riganelli L, Iebba V, Piccioni M, Illuminati I, Bonfiglio G, Neroni B, et al. Structural Variations of Vaginal and Endometrial Microbiota: Hints on Female Infertility. *Front Cell Infect Microbiol* (2020) 10:350(7). doi: 10.3389/fcimb.2020.00350
45. Sáez-López E, Guiral E, Fernández-Orth D, Villanueva S, Goncé A, López M, et al. Vaginal Versus Obstetric Infection *Escherichia coli* Isolates Among Pregnant Women: Antimicrobial Resistance and Genetic Virulence Profile. *PloS One* (2016) 11(1):1–11. doi: 10.1371/journal.pone.0146531
46. Krüger A, Lucchesi PMA. Shiga Toxins and Stx Phages: Highly Diverse Entities. *Microbiol (United Kingdom)* (2015) 161(3):1–12. doi: 10.1099/mic.0.000003
47. Liu TH, Wang HP, Cho FN, Wang JL, Hung CH, Chiou YH, et al. Rectovaginal Colonization With Pathogenic Escherichia coli During Pregnancy and Neonatal Outcomes. *Infect Drug Resist* (2019) 12:3103–12. doi: 10.2147/IDR.S207857
48. Muniesa M, Blanco JE, de Simón M, Serra-Moreno R, Blanch AR, Jofre J. Diversity of Stx2 Converting Bacteriophages Induced From Shiga-Toxin-Producing Escherichia coli Strains Isolated From Cattle. *Microbiology* (2004) 150(9):2959–71. doi: 10.1099/mic.0.27188-0
49. Berger M, Aijaz I, Berger P, Dobrindt U, Koudelka G. Transcriptional and Translational Inhibitors Block SOS Response and Shiga Toxin Expression in Enterohemorrhagic Escherichia coli. *Sci Rep* (2019) 9(1):1–9. doi: 10.1038/s41598-019-55332-2
50. Dos Santos LF, Gonçalves EM, Vaz TMI, Irino K, Guth BEC. Distinct Pathotypes of O113 *Escherichia coli* Strains Isolated From Humans and Animals in Brazil. *J Clin Microbiol* (2007) 45(6):2028–30. doi: 10.1128/JCM.00340-07
51. Cadona JS, Bustamante AV, Parma AE, Lucchesi PMA, Sanso AM. Distribution of Additional Virulence Factors Related to Adhesion and Toxicity in Shiga Toxin-Producing *Escherichia coli* Isolated From Raw Products in Argentina. *Lett Appl Microbiol* (2013) 56(6):449–55. doi: 10.1111/lam.12067
52. Colello R, Krüger A, Velez MV, Del Canto F, Etcheverría AI, Vidal R, et al. Identification and Detection of Iha Subtypes in LEE-Negative Shiga Toxin-Producing *Escherichia coli* (STEC) Strains Isolated From Humans, Cattle and Food. *Heliyon* (2019) 5(12):1–6. doi: 10.1016/j.heliyon.2019.e03015
53. Hauser E, Mellmann A, Semmler T, Stoeber H, Wieler LH, Karch H, et al. Phylogenetic and Molecular Analysis of Food-Borne Shiga Toxin-Producing *Escherichia coli*. *Appl Environ Microbiol* (2013) 79(8):2731–40. doi: 10.1128/AEM.03552-12
54. Galli L, Miliwebsky E, Irino K, Leotta G, Rivas M. Virulence Profile Comparison Between LEE-Negative Shiga Toxin-Producing *Escherichia coli* (STEC) Strains Isolated From Cattle and Humans. *Vet Microbiol* (2010) 143 (2–4):307–13. doi: 10.1016/j.vetmic.2009.11.028
55. Frank C, Werber D, Cramer J, Askar M, Faber M, An der Heiden M, et al. Epidemic Profile of Shiga-Toxin–Producing. *N Engl J Med* (2011) 365 (19):1771–80. doi: 10.1056/NEJMoa1106483
56. Bielaszewska M, Mellmann A, Zhang W, Köck R, Fruth A, Bauwens A, et al. Characterisation of the Escherichia coli Strain Associated With an Outbreak of Haemolytic Uraemic Syndrome in Germany, 2011: A Microbiological Study. *Lancet Infect Dis* (2011) 11(9):671–6. doi: 10.1016/S1473-3099(11)70165-7

Conflict of Interest: The authors declare that the research was conducted in the absence of any commercial or financial relationships that could be construed as a potential conflict of interest.

Publisher's Note: All claims expressed in this article are solely those of the authors and do not necessarily represent those of their affiliated organizations, or those of the publisher, the editors and the reviewers. Any product that may be evaluated in this article, or claim that may be made by its manufacturer, is not guaranteed or endorsed by the publisher.

Copyright © 2022 Scalise, Garimano, Sanz, Padola, Leonino, Pereyra, Casale, Amaral, Sacerdoti and Ibarra. This is an open-access article distributed under the terms of the Creative Commons Attribution License (CC BY). The use, distribution or reproduction in other forums is permitted, provided the original author(s) and the copyright owner(s) are credited and that the original publication in this journal is cited, in accordance with accepted academic practice. No use, distribution or reproduction is permitted which does not comply with these terms.

frontiers | Frontiers in Endocrinology

TYPE Systematic Review
PUBLISHED 22 July 2022
DOI 10.3389/fendo.2022.945543

Check for updates

OPEN ACCESS

EDITED BY
Reinaldo Marín,
Instituto Venezolano de Investigaciones Científicas (IVIC), Venezuela

REVIEWED BY
Chloe A. Brady,
The University of Manchester, United Kingdom
Marta Cohen,
Sheffield Children's Hospital, United Kingdom

*CORRESPONDENCE
Panicos Shangaris
panicos.shangaris@kcl.ac.uk

†These authors share first authorship

SPECIALTY SECTION
This article was submitted to Developmental Endocrinology, a section of the journal Frontiers in Endocrinology

RECEIVED 16 May 2022
ACCEPTED 29 June 2022
PUBLISHED 22 July 2022

CITATION
Moar L, Simela C, Nanda S, Marnerides A, Al-Adnani M, Nelson-Piercy C, Nicolaides KH and Shangaris P (2022) Chronic histiocytic intervillositis (CHI): current treatments and perinatal outcomes, a systematic review and a meta-analysis. *Front. Endocrinol.* 13:945543. doi: 10.3389/fendo.2022.945543

COPYRIGHT
© 2022 Moar, Simela, Nanda, Marnerides, Al-Adnani, Nelson-Piercy, Nicolaides and Shangaris. This is an open-access article distributed under the terms of the Creative Commons Attribution License (CC BY). The use, distribution or reproduction in other forums is permitted, provided the original author(s) and the copyright owner(s) are credited and that the original publication in this journal is cited, in accordance with accepted academic practice. No use, distribution or reproduction is permitted which does not comply with these terms.

Chronic histiocytic intervillositis (CHI): current treatments and perinatal outcomes, a systematic review and a meta-analysis

Laurel Moar[1†], Chloe Simela[1†], Surabhi Nanda[1,2], Andreas Marnerides[3], Mudher Al-Adnani[3], Catherine Nelson-Piercy[1,2], Kypros H. Nicolaides[1,4] and Panicos Shangaris[1,2,5*]

[1]School of Life Course and Population Sciences, King's College London, London, United Kingdom, [2]Department of Women and Children, Guy's and St. Thomas' NHS Foundation Trust, London, United Kingdom, [3]Department of Histopathology, St. Thomas Hospital, Westminster Bridge Road, London, United Kingdom, [4]Harris Birthright Research Centre for Fetal Medicine, King's College London, London, United Kingdom, [5]Peter Gorer Department of Immunobiology, School of Immunology and Microbial Sciences, Faculty of Life Sciences and Medicine, King's College London, London, United Kingdom

Background: Chronic histiocytic intervillositis (CHI) is a rare placental lesion with a high recurrence rate and poor perinatal outcomes. There are currently limited guidelines regarding the diagnosis of this condition in the index pregnancy and treatment where recurrence is suspected.

Objective: The primary objective of this systematic review and meta-analysis was to determine the perinatal outcomes of pregnancies affected by chronic histiocytic intervillositis and to what extent they can be improved with treatment. The secondary objective was to assess the relationship between CHI lesion severity and pregnancy loss.

Methods: A systematic search of Ovid Embase, Web of Science, Science Direct, PubMed, Ovid Medline, Google Scholar and CINAHL was carried out. Case reports, cohort, case-control and randomised controlled trials (RCT) detailing the perinatal outcomes of CHI pregnancies, both treated and untreated, were included.

Results: No RCTs were identified. However, in a review population of 659 pregnancies, with additional 7 in case reports, CHI treatments included aspirin, prednisone, prednisolone, low molecular weight heparin (LMWH), hydroxychloroquine and adalimumab. A descriptive synthesis of data found mixed results for treatments in relation to live birth, miscarriage and fetal growth restriction outcomes. Furthermore, quantitative synthesis of 38 pregnancies revealed a non-significant improvement in live birth rate with CHI targeted treatment (OR 1.79 [95% CI 0.33-9.61] (p=0.50), while meta-

analysis of CHI severity in line with pregnancy loss, in a sample of 231 pregnancies, revealed lower odds of pregnancy loss with less severe lesions (OR: 0.17 [0.03-0.80], p=0.03).

Conclusions: This systematic review and meta-analysis reinforce notions surrounding the insufficient evidence for CHI treatment. It also strengthens previous hypotheses detailing the positive association between CHI lesion severity and odds of pregnancy loss. Aspirin, LMWH, prednisolone, hydroxychloroquine and adalimumab are candidates with varying levels of weak to moderate evidence supporting their use. Further prospective research is required to obtain robust evidence pertaining to treatment safety and efficacy and optimal drug regimes.

Systematic Review Registration: [website], identifier CRD42021237604

KEYWORDS

CHI, recurrent miscarriage, intervillositis, stillbirth, small gestation age (SGA)

Introduction

Chronic histiocytic intervillositis (CHI) (also referred as CHIV) is a rare but severe placental condition characterised by the presence of an inflammatory mononuclear infiltrate in the intervillous space. CHI has been estimated to affect 6 in every 10 000 pregnancies that reach 12 weeks gestation (1, 2) and the term was first introduced by Labarrere and Mullen in 1987 as massive chronic intervillositis (3). This pathology has since been referred to by several names across the literature, including chronic intervillositis of unknown aetiology (CIUE), massive chronic intervillositis, massive perivillous histiocytosis and shortened forms - chronic intervillositis or intervillitis. Diagnostic understanding has also grown in differentiating CHI from other placental lesions through its non-infectious origin and minimal involvement of the villi or basal plate (1). Although the lesion is well described in the placental pathology literature, there is no agreed standardised diagnostic criteria or grading system for the severity of this lesion (4–7). However, the paucity of knowledge surrounding CHI biomarkers only permits retrospective diagnosis following examination of the placenta postpartum.

Furthermore, while the aetiology of CHI remains undetermined, the pathology's high recurrence rate, reported to lie between 70 and 100% (8), highlights the need for effective treatment in future pregnancies. Some evidence of pathogenic immune mechanisms has been proposed, including an absence of the usual Th1 to Th2 immune response shift observed in normal pregnancy (1, 9–13). This raises the question of possible therapeutic benefits for immunologically based CHI treatments, with steroids and other immunosuppressants having been used in some cases.

Objectives

This systematic review summarises the available research on treatment approaches for gravid women diagnosed with CHI in a previous pregnancy, including antithrombotic and immunosuppressive drug combinations. Primary objectives include quantifying the effectiveness of these therapies in improving perinatal outcomes compared to baseline data without treatment. Moreover, further analysis was undertaken to determine how CHI severity impacts perinatal outcomes.

Methods

Search strategy

PROSPERO registration for the review was fulfilled following the completion of the protocol form (CRD42021237604).

The literature search was carried out by the two reviewers, CS and LM, across seven databases: PubMed, OVID MEDLINE, Google Scholar, OVID EMBASE, Web of Science, Science Direct and CENTRAL (Cochrane Central Register of Controlled Trials) between 15th February and 16th February 2021. Each reviewer used the search strategy (1) comprising all known terms for CHI and a period spanning from Jan 1990 to December 2020, in three databases. CENTRAL was searched by both reviewers. Formatting adjustments were made to the search terms to optimise the strategy for each database, and email alerts were put in place to notify the reviewers of new results after the search period (**Table 1**). The two reviewers screened the search results

TABLE 1 Search strategy for database.

No.	Science Direct, Ovid Embase, Web of Science search strategy
1	(((chronic histiocytic intervill*) OR (chronic intervill*)) OR (chronic intervill* of unknown?etiology)) OR (massive chronic intervill*)) OR (massive perivillous histiocyt*)
2	"chronic histiocytic intervillositis" [All Fields] OR "chronic histiocytic intervillositis chi" [All Fields] OR "chronic histiocytosis" [All Fields] OR "chronic histiocytosis x" [All Fields]
3	Search 1 OR 2

independently, and discussions were held at both screening stages to resolve any disagreements before the final papers were decided.

Study selection

Selection criteria were based on the following predetermined characteristics from the protocol, starting with the population in question being identified as pregnant women of any age diagnosed with CHI in a previous pregnancy. CHI was defined as an idiopathic inflammatory lesion in the intervillous space in line with the criteria devised by Bos and colleagues (4). All other similar but distinct placental lesions were excluded, including villitis, even if in co-occurrence with CHI. Interventions described included varying doses of drug-based mono or combination therapy for CHI. However, studies without interventions were also included for comparison. Outcomes assessing the efficacy of treatment and impact of disease severity included, but were not limited to, quantitative measures such as live birth rate and birth weight. Only randomised controlled trials, cohort, case-control studies and case reports were included, with abstracts excluded. While there were no geographical limits, time constraints enforced excluding texts not in English.

Data extraction

A modified Cochrane Public Health Group (CPHG) data extraction form was used to collect population, intervention and outcome data from the chosen papers independently by both reviewers (C.S and L.M). Additionally, each structure underwent a data checking process against the original article to detect and minimise human error. The specific information collected for each study included authors, publication year; study design, location; the number of women, number of CHI pregnancies, and number undergoing treatment. Authors were contacted to confirm information regarding population data where clarification was needed (14, 15).

Outcome measures

Outcome measures reported in the systematic review included growth restriction and preterm birth, while those of interest in the meta-analysis were live birth rate and pregnancy loss. The preterm birth rate was defined as a live birth before 37 + 0 weeks gestation. Fetal growth restriction (FGR) or intrauterine growth restriction (IUGR) was defined as a birth weight below the 10^{th} percentile (16).

Several terms were used when determining rates of pregnancy loss in CHI. In this paper, pregnancy loss data were divided into early miscarriage (before 14 + 0 weeks gestation), late miscarriages (14 + 1 to 24 + 0 weeks gestation) and stillbirths (intrauterine death after 24 + 0 weeks gestation). Some studies also included neonatal deaths as an outcome, where this term described the loss of an infant within seven days of birth (17).

In some cases (such as with FGR), there was variation in how outcomes were classified (e.g., birth weight below 10^{th} percentile versus 3^{rd} percentile, stillbirth including pregnancy loss as early as 20 weeks versus after 24 weeks) in different studies. Such instances of outcome measure variation are indicated in the review.

The measure of CHI lesion severity

The extent of intervillous space involvement defined CHI lesion severity as a quantifiable and standard measure. In this case, low to moderate grading referred to infiltrate occupying less than 50% of the intervillous space, and severe grading infiltrate more than 50% of the intervillous space [Parant (18), Simula (6), Sauvestre (15) but not Marchaudon (19)].

Risk of bias and quality assessment

The risk of bias and quality of included studies was assessed independently by both reviewers using adapted versions of the Newcastle-Ottawa scale (20) and Critical Appraisal Skills Programme (CASP) checklist (21).

The 7-point system of the Newcastle Ottawa scale contained domains of selection, comparability, and outcome, while the CASP checklist aimed to detect instances of selection, measurement, classification or reporting bias. Additional consideration was given to the lack of accountability for confounding factors.

Analysis and data synthesis

The Cohen kappa coefficient was used to assess agreement between the two reviewers at the full-text eligibility stage before

generating a narrative synthesis of the findings. A high ratio indicated a reasonable level of agreement between the reviewers.

Inclusion in the meta-analysis component depended on cohort studies with a suitable differentiation of outcomes according to the presence of treatment or severity of lesions. The chosen effect measures for the meta-analyses were relative risk (RR) of pregnancy loss in moderate vs severe CHI and odds ratios (OR) for live births in treated vs untreated pregnancies, each with a 95% confidence interval and calculated based on the number of pregnancies and events. All analyses herein were carried out using RevMan (Review Manager (RevMan) Version 5.4.1, The Cochrane Collaboration 2020). Heterogeneity was measured using the I^2 statistic, with an I^2 >50% indicating significant heterogeneity, not due to chance. As recommended, random-effects models were used to determine the summary effect estimate where considerable heterogeneity was detected (I^2>30%) (22).

Due to the small meta-analysis population, no additional sensitivity, subgroup, or meta-regression analyses were undertaken.

Results

Study selection

Figure 1 summarises (23) the study selection process and its outcomes. In total, 805 papers were found, and of these, 384 remained for the title and abstract screening once duplicates were removed. Titles and abstracts were excluded for review format, language limitation and lack of relevance leading to 66 full texts, which were narrowed down to the final 20 for systematic review inclusion. Reasons for exclusion included irrelevance, language limitation, conference abstract, poster or thesis format, full-text unavailability, and data insufficiency.

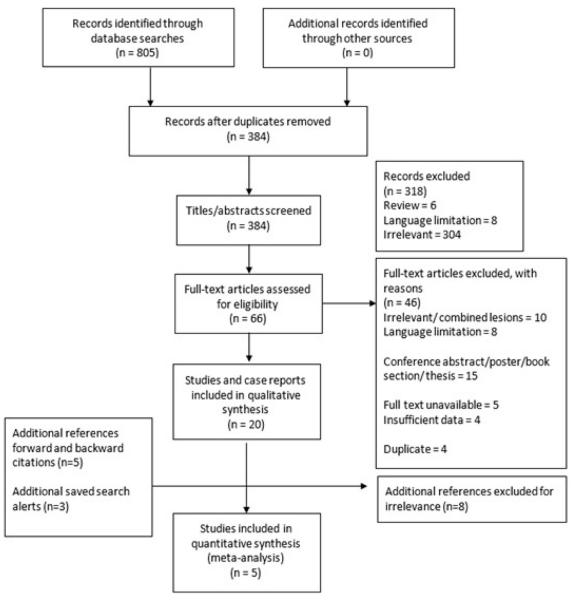


FIGURE 1
Study selection process of the systematic review and meta-analysis into outcomes of pregnancies affected by CHI.

The Cohen kappa coefficient for full-text screening between the two reviewers was 0.81, indicating almost perfect agreement at this stage of study selection.

Study characteristics

The final twenty papers comprised 12 cohort studies and 8 case reports as no RCTs were identified. The characteristics of these mainly retrospective studies and case reports are summarised in Table 2. Five of the twelve cohort studies were selected for inclusion in either meta-analysis. The limited number of studies selected for meta-analysis was due to treated vs untreated outcomes being unavailable for pooling in the other seven studies.

Excluding case reports and series, the review population included the outcomes of 527 pregnancies affected by CHI in 439 women with a mean age of approximately 31.9 years. Fifty-eight of these cohort study pregnancies were treated, and sample size ranged from 6 to 122 pregnancies. A further 6 instances of treatment were reported in case reports and series. In total, 64 pregnancies were treated out of 554 across cohort studies, case reports and case series.

Email correspondence with authors confirmed a shared cohort between two papers, and this is highlighted in all subsequent results tables to avoid duplication and reporting errors. For review population totals, these cohorts have been counted as one (14, 15).

Risk of bias of included studies

The risk of bias scores for each case-control and cohort study can be seen in Table 3. Following a judgement by both reviewers, the risk of bias was considered generally low, with an average bias score of 1.83 out of 4 across the twelve studies.

Selection bias was reported in four of the twelve studies due to how participants were selected from a pathology database (15, 18, 37, 39). Furthermore, in other cases, selection bias was detected because of limited search terms comprising only of 'CIUE and chronic intervillositis' in one study and 'intervillositis' in another (15, 39).

Seven studies indicated measurement/classification bias in diagnosis and grading of CHI, whereby pathologists were aware of and not blinded to the previous CHI diagnosis.

Reporting bias was undetected. However, ten out of twelve studies did not state accountability for confounding variables.

Study quality assessment outcomes are shown in Table 4. High scores were obtained in the selection domain, with participants seen

10.3389/fendo.2022.945543

TABLE 2 Characteristics of studies included.

Study	Location	Study design	Duration	N women	N CHI pregnancies	Mean age	Ethnicity	BMI	n/N pregnancies treated
Doss 1995 (9)	USA	Case report	1974-1994	1	4	36	NR	NR	1/4
Parant 2009 (18)*σ	France	retrospective cohort	2000-2006	10	14	30 (24-39)	99% white	21 (19-27)	6/14
Marchaudon 2011 (19)σ	France	retrospective	1997-2006	50	69	31 (16-43)	NR	NR	NONE
Reus 2013 (11)	Netherlands	retrospective cohort study	2000-2010	22	30	31.8 (22-45)	NR	NR	NONE
Ramya 2014 (24)	India	Case report	2014	1	1	22	NR	NR	NR
Mekinian 2015 (25)σ	France	multi-centre prospective	2011-2013	24	24	34	46% white	26	NONE
Crawford 2016 (26)	Australia	Case report	2016	1	4	28	NR	NR	NONE
Nowak 2016 (27)	France	retrospective cohort	1998-2010	NR	24	NR	NR	NR	NONE
Sabra 2016 (28)	Spain	retrospective	2012-2016	6	6	34.83 (32-39)	83.3% European 16.7% Latinx	NR	NONE
Ozawa 2017 (29)	Japan	Case report	2010-2017	1	3	29	NR	NR	1/1
Vardi 2017 (30)	New Zealand	Case report	2003-2013	1	6	31	NR	NR	1
Koby 2018 (31)	Canada	retrospective observational	2001-2014	29	33	Median 31 (IQR 28.5-34.5)	45.5% white, 42.4% African, 12.1% Asian	median 29.8 (26-31.7)	NONE
Mekinian 2019 (32)	France	Case report	2019	2	3	38.5 (33–36)	NR	NR	2/2
Bos 2020 (37)	Netherlands	Observational cohort	2000-2015	38	38	34 (24-43)	NR	NR	NONE
Homatter 2020 (38)	France	retrospective case-control	2000-2016	111	111	30.8	72.1% white	NR	21/111
Mattuizzi 2020 (14) †	France	retrospective	1997-2018	102	122	Median 32 (IQR 28-36)	61.6% white, 2% Asian 19.2% North African, 15.2% South African, 2% Hispanic	median 22	21/24
Nohr 2020 (33)	Canada	Case report	2020	1	2	34	NR	NR	1/1
Sauvestre 2020 (15)σ†	France	multi-centre retrospective	1997-2018	102	122	31.7	NR	23.1	NONE
Simula 2020 (39)σ	Canada	retrospective cohort	2006-2019	47	56	33.2	NR	25.9	10/56
Traeder 2010 (40)	Germany	case series	1994-2008	4	4	34 (30-40)	NR	NR	NONE

N CHI pregnancies – only includes pregnancies diagnosed with CHI, NR – not reported, * - pregnancies with villitis excluded, all ages are means with range included in brackets if reported, ** - median and IQR used where mean and range not available, σ included in either one or both of the meta-analyses, † studies share same cohort.

as broadly representative of the population in question. The area in which numerous studies were deficient was comparability and outcome measures. Lack of differentiation between early and late miscarriage outcomes and methods that did not describe the assessment of lesion severity as a possible mediator of perinatal outcome was also suboptimal. Furthermore, lack of information on population comorbidities or medication also led to lower quality scores in the outcome domain.

Treatment combinations

None of the cohorts included in the systematic review was fully treated. The proportion of the four cohorts receiving targeted treatment for CHI ranged from 18-88%, and the other eight cohorts were labelled as untreated. **Table 5** summarises the treatment combination details in the treated pregnancies.

10.3389/fendo.2022.945543

TABLE 3 Risk of bias.

Study	selection bias	measurement/classification bias	reporting bias	confounding not accounted for (no regression model)	score*
Parant 2009 (18)	✓	× No mention of blinding	✓	×	2
Reus 2013 (11)	✓	✓	✓	×	1
Mekinian 2015 (25)	✓		✓	✓	1
Nowak 2016 (27)	✓	× No mention of blinding	✓	×	2
Sabra 2016 (28)	✓	× No blinding mentioned	✓	×	2
Koby 2018 (31)	✓	× Investigator was aware of diagnosis no mention of blinding	✓	×	2
Marchaudon 2011 (19)	✓	× Histology in conjunction with fetal autopsy so outcome known	✓	×	2
Bos 2020 (37)	✓	× No mention of blinding when pathologist reviewed slides	✓	✓	1
Homatter 2020 (38)	✓	× Only CHI positive cases assessed histologically	✓	×	2
Mattuizzi 2020 (14)	✓	× No blinding to CHI diagnosis	✓	×	2
Sauvestre 2020 (15)	× Only database search term was 'intervillositis'	✓ All 3 pathologists blinded to diagnosis	✓	×	2
Simula 2020 (39)	× Database search was for CIUE and chronic intervillositis	×	✓	×	3

*Risk of bias score is out of a total of 4.
✓ Low risk of bias.
× High risk of bias.

There was a variation of gestational ranges when the treatment was commenced. Those containing aspirin were the most common of the treatment regimes, followed by low molecular weight heparin (LMWH) and finally corticosteroid regimes (prednisone/corticoid), either alone or in combination.

Outcomes

Table 6 summarises the perinatal outcomes of these studies. Continuous variables are reported as means followed by the standard deviation and range in brackets if available.

Live births

The live birth rate varied considerably between studies, ranging from 30.4% to 100%. Interestingly, neither of the cohorts displaying results at these extremes were indicated as receiving target CHI treatment (19, 40). There was also variance within similar populations, as several of the papers were based within the same countries yet yielded different live birth rates for example the study by Bos et al., 2020 reported a live birth rate more than twice as high as that reported by Reus et al., 2013 (11, 37). Comparable live birth rates of 67% and 70% were observed in two studies with a similar cohort size despite 88% of one cohort receiving targeted treatment (25) versus none of the other (27). Overall, the average live birth rate for cohorts in which no treatment was stated was 58.3% versus 40.9% in cohorts with a partial treatment.

Birth weight

Data on average live birth weight were available in seven studies, three of which had a proportion receiving treatment. In most cases, this outcome rarely reached 2500g however, the highest mean birth weight of 2493g was achieved in one study in which 88% of the cohort received treatment (25). Furthermore, a low average birth weight of 995g was reported by Traeder and

10.3389/fendo.2022.945543

TABLE 4 Quality assessment using Newcastle-Ottawa scoring system.

Study	year	Study design	Selection (3)	Comparability (2)	Outcome (2)	total (7)	Comment
Parant 2009 (18)	2009	retrospective cohort	3	2	1	6	No details of whether pathologists were blinded
Marchaudon 2011 (19)	2011	retrospective	3	1	1	5	Pathologists carried out histological analysis in conjunction with autopsy - no blinding, no mention of medications
Reus 2013 (11)	2013	retrospective	3	1	2	6	
Mekinian 2015 (25)	2015	prospective	3	2	2	7	
Nowak 2016 (27)	2016	retrospective cohort	3	2	1	6	
Sabra 2016 (28)	2016	retrospective	2	1	1	4	No blinding mentioned, and only 6 patients
Koby 2018 (31)	2018	retrospective observational	3	1	1	5	Pathologist was aware of diagnosis, no details on medication
Bos 2020 (37)	2020	observational cohort	3	1	1	5	No comment on whether pathologists were blinded to prior diagnosis.
Homatter 2020 (38)	2020	retrospective case-control	2	1	2	5	Early miscarriage excluded
Mattuizzi 2020 (14)	2020	retrospective	3	1	1	5	No comments on anyon any blinding
Sauvestre 2020 (15)	2020	retrospective	2	1	1	4	Only histological database search term was 'intervillositis', live birth outcomes unclear in table, 10 placentas missing
Simula 2020 (39)	2020	retrospective cohort	3	2	1	6	No comment on whether pathologist was blinded

TABLE 5 Treatment combinations used in case pregnancies affected by CHI.

Author/Year	Intervention details		
	N	Untreated	Treatment details
Parant 2009 (18)	14	8	aspirin (n=4) aspirin + corticoid (n=2)
Traeder 2010 (40)	4	4	NONE
Marchaudon 2011 (19)	69	69	NONE
A. Reus 2013 (11)	30	30	NONE
Mekinian 2015 (25)	24	3	aspirin/LMWH (n=4) aspirin + prednisone (n=6) aspirin+ prednisone+ LMWH (n=5) aspirin +prednisone+ LMWH+ hydroxychloroquine (n=6)
Nowak 2016 (27)	24	24	NONE
Sabra 2016 (28)	6	6	NONE
Koby 2018 (31)	33	33	NONE
Bos 2020 (37)	38	38	NONE
Homatter 2020* (38)	111	90	aspirin (n=18) LMWH (n=7) corticosteroids(n=6)
Mattuizzi 2020 (14)	122	122	NONE
N.K Simula 2020 (39)	56	37	aspirin 81mg +dalteparin 7500 IU+ hydroxychloroquine 400mg (n=2) aspirin 81mg (n=3) dalteparin (n=1) prednisone (n=1) aspirin + dalteparin (n=3)
Sauvestre 2020 (15)	122	122	NONE

* in combination but assessed separately.

10.3389/fendo.2022.945543

TABLE 6 Perinatal outcomes for CHI pregnancy cohorts.

Study	Year	n/N pregnancies treated	Live Birth Rate	Avg. Live Birth weight (g)	Gestational age at delivery (weeks)	Spontaneous preterm live birth	FGR (<10th centile) live or not	Miscarriage < 14 weeks	Miscarriage 14 -24 weeks	Still birth IUD > 24 weeks
Parant 2009 (18)	2009	6/14	5/14	1550 (590-2760)	34.6 (27.5-37)	10/10	8/11	2/14	1/14	2/14
Traeder 2010 (40)	2010	NONE	4/4	995 (495-1640)	31.2 (27-35.6)	4/4	3/4 (<10th percentile) 2/4 (<3rd percentile)	NO	NO	NO
Marchaudon 2011 (19)	2011	NONE	21/69	1780 ± 590 (920-2830)	35.0 ± 2.5 (30.6-39.0)	13/21	24/69 (<3rd percentile)	21/69 (<12 weeks)	9/69 (12-22 weeks)	18/69 (>22 weeks)
Reus 2013 (11)	2013	NONE	10/30	NR	NR	6/10	NR	4/30 (<12 weeks)	2/30 (12-16 weeks)	NR
Mekinian 2015 (25)	2015	21/24	16/24	2493 ± 678	38 ± 1.6	5/16	3/24	4/24 (<10 weeks)	4/24 (>10 weeks)	NR
Nowak 2016 (27)	2016	NONE	17/24	1634 (610-2875)	34.3± 3.7	11/17	14/21	/1/24	2/24	2/24
Sabra 2016 (28)	2016	NONE	2/6	1695 (1290-2100)	35.5 (33-38)	1/2	2/6	4/6	NO	NO
Koby 2018 (31)	2018	NONE	20/33	NR	NR	16/20	23/33 (<10th percentile), 15/33 (<3rd percentile)	2/33 (<20 weeks)	NR	11/31 (>20 weeks)
Bos 2020 (37)	2020	NONE	31/38	NR	NR	21/31	16/38 (<3rd percentile)	NR	1/38	3/38
Homatter 2020 (38)	2020	21/111	62/111	1500 ± 885	33.6 ± 4.7	4/62	62/111 (<3rd percentile)	NR	6/111 (14-21 weeks)	22/111 (22-42 weeks)
Mattuizzi 2020 (14)	2020	NONE	70/122	NR	NR	38/70	81/122	17/122	17/122	NR
Simula 2020 (39)	2020	10/56	3/56	NR	NR	1/6	7/15 at 20 weeks	29/56 (<12 weeks)	13/56 (12-22 weeks)	6/56 (>23 weeks)
Sauvestre 2020 (15)	2020	NONE	70/122	NR	NR	5/70	46/70 (alive)	17/122	1/122	16/122
Total		58	336/659	1679.68	34.47	135/336	289/424	101	56	80

Live birth rate is as a fraction over total CHI pregnancies in each study, * pregnancies with villitis excluded, NR – not reported, average birth weight and gestational age at delivery with standard deviation if reported and range in parentheses. Parentheses in miscarriage and FGR indicate differing classification criteria.

colleagues (40) across a case series of four untreated pregnancies. However, this positive treatment effect was not always reflected, with higher birth weight observed in untreated cohorts (19, 27, 28) compared to partially treated cohorts (18, 38).

Preterm birth

In five out of six studies, a low average birth weight was accompanied by an average gestational age at delivery <37+0 weeks. The general trend towards high preterm birth in both untreated and treated CHI pregnancies is also evident in a preterm birth rate of 40.2% across the twelve studies. Interestingly, the study by Mekinian and colleagues in which the largest proportion of the cohort was treated (88%) had a lower preterm birth rate of 31.25% (25). However, this was not the case for all partially treated cohorts, which, for the most part, had a lower mean gestational age at delivery (38) and higher preterm live birth rate than the untreated cohort (19, 27, 28).

Fetal growth restriction

Many infants were small for gestational age. Studies reported fetal growth restriction of below 10th centile (with some even below 3rd centile) in both live and stillborn or neonatal death groups.

Similar prevalence of FGR < 10th centiles was reported in two studies (66.7% and 69.7%, respectively), both of which had entirely untreated cohorts (27, 31). In treated cohorts, this same variable ranged from 12.5% (25) to 72.7% (18)[19] with treated proportions being 88% and 42.8%, respectively.

Severe FGR, <3rd centile, was only reported as an outcome in 5 studies (19, 31, 37, 40). Of these, one study had an 18.9% treated cohort with a severe FGR prevalence of 55.9% (38). Four untreated study cohorts have reported an occurrence rate of severe FGR as 69.7%, 42.1%, 34.8% and 50% (19, 31, 37, 40) respectively.

Miscarriage, stillbirth and neonatal death

Overall, miscarriage rates ranged between 2.63% and 20% in untreated cohorts (11, 37). The miscarriage rate was much wider in treated cohorts (range between 5.4% and 75%). In some cases, miscarriage timing was before 14 weeks rather than after 14 weeks, but this was only in five out of the twelve cohorts (11, 15, 18, 28, 39).

Stillbirth rates varied between 10.7% and 19.8% in treated pregnancies (38, 39). Like miscarriage rates, this was comparatively higher than the untreated cohort range of 7.9% to 13.1% (15, 22). Interestingly, there were also instances of no reported stillbirths in untreated populations with small sample sizes (28, 40).

Neonatal death

Neonatal death was not widely reported as an outcome and ranged from 1.11% up to 23.3% across four studies (11, 14, 15, 38). There are no reported cases in both partially treated and untreated cohorts (18, 27).

Individual pregnancy outcomes

As shown in **Table 7**, individual patient outcomes were available from seven case reports, one case series, and two retrospective cohort studies that reported individual patient details. 21 of the 31 case pregnancies were treated, and 9 of these resulted in a live birth, of which 4 were at term. This is compared to 6 out of 10 untreated pregnancies resulting in live births and 1 of these 6 occurring at term.

Meta-analysis

Meta-analysis of live birth outcomes in two studies in which treated and untreated data was available revealed a non-significant improvement in live birth rates with treatment (Odds Ratio: 1.79 [0.33-9.61], p=0.50) (**Figure 2**). The pooled population included 27 treated and 11 untreated pregnancies. Heterogeneity (I^2) was estimated to be 6%, using fixed effect model.

Meta-analysis of pregnancy loss in relation to CHI severity across four studies with a pooled population of 174 low to moderate severity cases and 84 severe cases indicated significantly lower odds of pregnancy loss in cases with less severe lesions vs those with increased severity (Odds Ratio: 0.17 [0.03-0.80], p=0.03) (**Figure 3**). Largely homogenous grading criteria in all four studies permitted low to moderate lesions to be defined as <50% intervillous infiltrate involvement and >50% leading to a severe classification (supplementary data file).

Discussion

Principle findings

The primary objective of this systematic review and meta-analysis was to identify and quantify the effectiveness of current treatment regimens for pregnant women diagnosed with CHI following a previous pregnancy. Effectiveness was quantified by comparing perinatal outcomes, including live birth, miscarriage, stillbirth rates and neonatal death in treated and untreated pregnancies, birth weight (normal, IUGR), as well as preterm birth rate, with a positive effect in such measures indicating effective treatment.

The commonly used treatment regimens for CHI, either as standalone or as combination therapy include aspirin, prednisone, low molecular weight heparin, biological agents most commonly adalimumab and hydroxychloroquine (**Table 8**). The partially treated cohorts often performed equally or even worse in the outcome domains of live birth rates, preterm birth, fetal growth restriction, miscarriage and stillbirth rates. Indeed, the pooled treatment effect for live birth rates in treated vs untreated pregnancies produced an odds ratio of 1.79 [95% CI 0.33-9.61] (p=0.50). This converts to a risk ratio of 1.4 [95% CI 0.48-4.05] (p=0.54), which reveals the likelihood of live births in the treated group was 1.4 times that in the untreated, although this was not statistically significant. Taken collectively, this suggests that antithrombotic and immunosuppressive treatment for CHI cannot be significantly effective in improving perinatal outcomes in affected pregnancies. However, classifying these results as clinically insignificant due to exceeding the arbitrary cut off p=0.05 would be misleading as such a small, pooled population of 27 treated and 11 untreated pregnancies suggests a degree of imprecision. Consequently, we can conclude that these findings are inconclusive, and there is insufficient evidence of a treatment effect, as opposed to proof of no treatment effect (34).

The secondary objective of this review was to determine the extent to which CHI severity – measured as a percentage of intervillous space occupied by infiltrate- impacts perinatal

TABLE 7 Individual patient outcomes in pregnancies affected by CHI.

Author/ Year	Maternal Age	G	P	No. previous CHI pregnancies	Case Pregnancy Treatment	Treatment duration	Case Pregnancy Outcome
Doss 1995 (9)	36	13	2	4/12	Prednisone	NR	Live birth, 2170g
Parant 2009 (18) a	35	8	5	NR	None listed	–	Miscarriage 14 weeks
Parant 2009 (18) b	25	5	0	NR	Aspirin/corticoid (prednisone 20mg)	Full gestation	Miscarriage 8 weeks
Parant 2009 (18) c	29	2	1	NR	None listed	-	Live birth, 2310g, 34 weeks
Parant 2009 (18) d	31	2	1	NR	None listed	-	IUFD (Intrauterine fetal death), 180g, 23 weeks severe IUGR
Parant 2009 (18) e	31	2	1	NR	None listed	-	TOP, 190g fetal weight, 22 weeks, severe IUGR
Parant 2009 (18) f	29	1	0	NR	None listed	-	Live birth, 2080g, 37 weeks, severe IUGR
Parant 2009 (18) g	24	4	0	NR	Aspirin	Full gestation	Miscarriage 10 weeks
Parant 2009 (18) h	25	2	0	NR	Aspirin	Full gestation	IUFD, 330g, 26.5 weeks FGR
Parant 2009 (18) i	31	3	1	NR	Aspirin/corticoid (prednisone 5mg)	Full gestation	TOP, 215g, 22.5 weeks, FGR
Parant 2009 (18) j	28	3	2	NR	Aspirin	Full gestation	Live birth, 2760g, 37 weeks
Parant 2009 (18) k	27	2	1	NR	Aspirin	Full gestation	Live birth, 2320g, 37.5 weeks, IUGR
Parant 2009 (18) l	33	3	2	NR	None listed	-	TOP, 392g fetal weight, 26 weeks, FGR
Parant 2009 (18) m	25	3	0	NR	None listed	–	Live birth, 590g, 27.5 weeks, FGR
Parant 2009 (18) n	31	2	0	NR	None listed	-	IUFD, 160g, 28.5 weeks, FGR
Traeder 2010 (40) a	30	2	2	NR	NONE	NONE	Live birth, 1640g, 32 weeks
Traeder 2010 (40) b	40	4	1	NR	NONE	NONE	Live birth FGR, 1440g, 35 weeks
Traeder 2010 (40) c	30	1	1	NR	NONE	NONE	Live birth FGR, 405g, 29 weeks

(Continued)

TABLE 7 Continued

Author/ Year	Maternal Age	G	P	No. previous CHI pregnancies	Case Pregnancy Treatment	Treatment duration	Case Pregnancy Outcome
Traeder 2010 (40) d	36	1	1	NR	NONE	NONE	Live birth FGR, 495g, 27 weeks
Ramya 2014 (24)	22	1	0	NR	None listed	–	IUD 460g, 24 weeks
Crawford 2016 (26)	28	5	1	3/4	None listed	-	TOP 21 weeks
Ozawa 2017 (29)	29	7	0	2/6 **	Prednisolone 20mg + LDA	4 - 29 weeks	Live birth, 2051g, 35 weeks
Vardi 2017 (30)	31	6	0	3/5	20mg oral prednisone OD, 40mg LMWH (enoxaparin) subcutaneously OD, aspirin 100mg OD	Prednisone conception-20weeks and decreasing dose to 28 weeks; LMWH 6 weeks onwards	Live birth, 2200g, 34 weeks
Mekinian 2019 (32) a	37	13	1	NR	Adalimumab + aspirin 100mg/day + prednisone 10mg/day	2 months preconception - 9 weeks gestation	Live birth, 2960g 38 weeks
Mekinian 2019 (32) b	40	NR	NR	NR	Adalimumab 40mg every 2 weeks subcutaneously	2 months prior to oocyte donation - 9 weeks gestation	Live birth, - g, 39 weeks
NK Simula 2020 (39) a	NR	6	1	5/5*	Aspirin 81mg daily, dalteparin 7500 IU daily, hydroxychloroquine	From positive pregnancy test - delivery	Live birth, -g, - weeks
NK Simula 2020 (39) b	NR	NR	NR	NR	Aspirin 81mg daily	From positive pregnancy test - delivery	Live birth at term, - g
NK Simula 2020 (39) c	NR	NR	NR	NR	Aspirin 81mg daily	From positive pregnancy test - delivery	Pregnancy loss
NK Simula 2020 (39) d	NR	NR	NR	NR	Aspirin 81mg daily	From positive pregnancy test - delivery	Pregnancy loss
NK Simula 2020 (39) e	NR	NR	NR	NR	Dalteparin 5000-7500 IU daily	From positive pregnancy test - delivery	Pregnancy loss
NK Simula 2020 (39) f	NR	NR	NR	NR	Prednisone	From positive pregnancy test - delivery	Pregnancy loss
NK Simula 2020 (39) g	NR	NR	NR	NR	Aspirin 81mg daily, dalteparin 5000-7500 IU daily	From positive pregnancy test - delivery	Pregnancy loss
NK Simula 2020 (39) h	NR	NR	NR	NR	Aspirin 81mg daily, dalteparin 5000-7500 IU daily	From positive pregnancy test - delivery	Pregnancy loss
NK Simula 2020 (39) i	NR	NR	NR	NR	Aspirin 81mg daily, dalteparin 5000-7500 IU daily	From positive pregnancy test - delivery	Pregnancy loss
NK Simula	NR	NR	NR	NR	Aspirin 81mg daily, dalteparin 7500 IU daily, hydroxychloroquine	From positive pregnancy test - delivery	Ongoing?

(Continued)

TABLE 7 Continued

Author/ Year	Maternal Age	G	P	No. previous CHI pregnancies	Case Pregnancy Treatment	Treatment duration	Case Pregnancy Outcome
2020 (39) **j**							
Nohr 2020 (33)	34	4	1	2/3	IVIg therapy, prednisone, LMWH, Aspirin	NR	IUGR, IUFD 25 weeks

Live birth rate as a fraction over total CHI pregnancies in study, * 3/5 treated with Aspirin 81mg daily, dalteparin 5000-7500 IU daily, prednisone 10-40mg daily; 1/5 treated with aspirin 81mg daily, dalteparin 7500 IU daily, hydroxychloroquine 400mg daily.** pregnancy 5 treated with aspirin 81mg/ day resulted in IUD and IUGR 210g at 17 weeks; pregnancy 6 treated with aspirin 81mg/day, heparin 10 000-15 000IU/day IUGR 33 weeks 1032g.

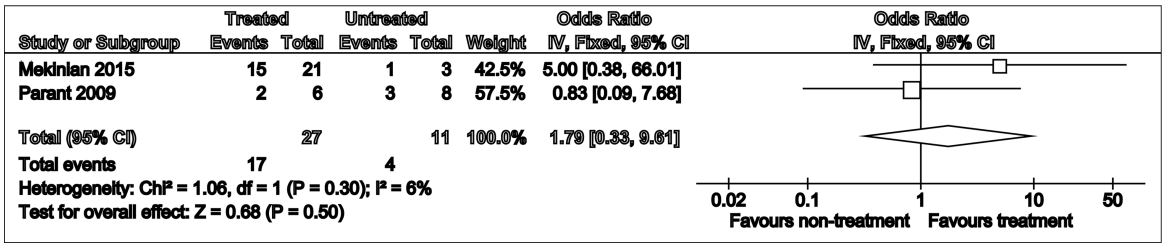


FIGURE 2
Forest plot summarising odds of live birth rates in treated vs untreated pregnancies.

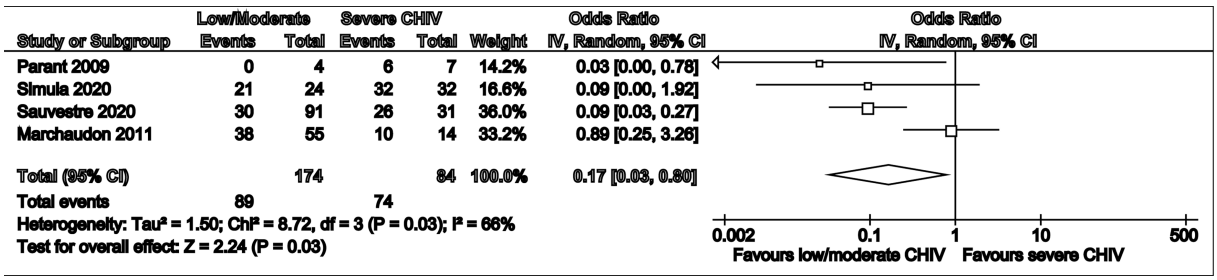


FIGURE 3
Forest plot summarising risk ratios of pregnancy loss in low/moderate vs severe CHI.

TABLE 8 Summary of CHI treatments, their indication in mild, moderate, or severe cases and the strength of evidence surrounding each.

Treatment	Dose	Indication	Strength of Evidence
Aspirin	75-100mg	Low, moderate, severe	Moderate
Dalteparin	———	Low, moderate, severe	Moderate
Enoxaparin	———	Low, moderate, severe	Moderate
Prednisone/Prednisolone	10-20mg	Low, moderate, severe	Moderate
Adalimumab	———	Moderate to severe	Weak
Hydroxychloroquine	———	Moderate to severe	Weak
Tacrolimus	———	Moderate to severe	Weak

10.3389/fendo.2022.945543

TABLE 9 Different diagnostic criteria for CHI among included studies in which it was stated.

	Doss 1995 (9)	Parant 2009 (18)	Traeder 2010 (40)	Marchaudon 2011 (19)	Reus 2013 (11)	Ramya 2014 (24)	Mekinian 2015 (25)	Nowak 2016 (27)	Sabra 2016 (28)	Vardi 2017 (30)	Koby 2018 (31)	Bos 2020 (37)	Homatter 2020 (38)	Matuizzi 2020 (14)	Simula 2020 (39)	Nohr 2020 (33)	Sauvestre 2020 (15)
Inclusion																	
Infiltrate in intervillous space	+	+	+	+	+	+	+	+	+		+	+	+	+	+	+	+
Mononuclear infiltrate	+	+		+	+	+	+	+	+		+	+	+	+	+	+	+
Histiocytic CD68+ marker			+			+	+		+								+
Massive/ diffuse infiltrate				+			+						+				
Fibrin deposits	+	+			+								+/-				
Trophoblastic necrosis	+																
Maternal origin of infiltrate																	
Exclusion																	
Signs of infection						+	+		+			+		+	+		+
Villitis																	
Presence of other placental lesions			+														
Malaria						+	+		+								

outcomes. It was anticipated that establishing a relationship between progression of placental pathology, in subsequent pregnancies, and extent of adverse outcomes would improve understanding of treatment potential as seen by the effect of treatment (monotherapy or combination therapy) on the placental tissue. This in turn would help to explore if improvements in lesions (with or without complete remission) positively correlate with more favourable perinatal outcomes. Results demonstrate a small severity effect in relation to pregnancy loss (Odds Ratio: 0.17 [0.03-0.80], (p=0.03). The larger pooled population of 174 low or moderately affected pregnancies and 84 pregnancies affected with severe CHI infers a more reliable evidence that any improvement in the severity of lesions correlates to a reduction (albeit small) in the odds of miscarriage or stillbirth.

The proposed hypothesis around the effect of treatment regimens is the reduction in the severity of lesions through targeted anti-inflammatory, immunosuppressive and anti-thrombotic mechanisms, which in turn would help improve the perinatal outcome.

The discrepancies in severity classification systems between papers cannot be ignored. It is known that CHI can exist with or without fibrin deposition and so while it is not necessary for diagnosis, the role of fibrin in severity classification systems is interesting. While in some, fibrin was acknowledged, this was not the case in studies with methods that did not call for fibrin to be noted (19, 39). **Table 9** illustrates the varying inclusion and exclusion criteria for CHI classification in all the studies included.

In retrospective studies, it was not possible for all placentas in the database to be examined for CHI. Therefore, many relied on the assumption that CHI placentas had accurately been documented as such and the search terms used to recover them were adequate (38).

Furthermore, there was an invariable absence of adjustment for confounders known to increase risk of adverse perinatal outcomes such as maternal BMI and smoking which at times, were not measured during the process of data gathering in some cases or noted in many of the case reports.

Comparison with existing literature

Overall, the findings of this review were consistent with those previously available evidence. For instance, the strong association between FGR, miscarriage, and stillbirth reflected in **Table 6** (2). FGR frequency <10th percentile, was estimated at

61% across nine studies in our review population compared to 48% in a previous meta-analysis (35). The total population in our review did not confirm a higher prevalence of early miscarriage compared to late, as was seen by Rota and colleagues (5), however it was found that there was a higher rate of intrauterine deaths in the remit of early miscarriage rather than stillbirth or late miscarriage. Nevertheless, the relatively high incidence of either early or late pregnancy loss emphasises the impact of placental insufficiency without maternal vascular malperfusion on increased adverse pregnancy outcomes.

Interestingly, our conclusion that increased CHI lesion severity correlates with increased risk of pregnancy loss disagrees with the findings of the most prominent prospective study in the area (25) which states that maintenance of visible CHI pathology is not always indicative of adverse outcomes. However, this study did find that the absence of these lesions was linked to more positive outcomes. Further investigation may be required to find a more definitive answer. It is worth acknowledging here that there has previously been a lack of international consensus on indications for sending placental pathology (and for reporting by perinatal pathologists), following an adverse pregnancy outcome, and therefore CHI itself may be under-reported. However, there has been a reform in this area more recently due to the creation of the international Amsterdam consensus criteria in 2016 (36).

The lack of significant treatment effects in CHI, though cautiously interpreted by our review, was also highlighted by Contro et al (41). This 2010 review on CHI concluded that treatments investigated at the time had no significant, and even a detrimental, effect on perinatal outcome. Our review provides evidence supporting this conclusion, despite numerous novel studies conducted in the 10-years since the last systematic review (41). However, one of the explanations for this may be a lack of consensus about the case selection for treatment, gestation of commencing treatment (and stopping), and treatment regimens (monotherapy or combination therapy). Further explanation for individual worse outcomes in combination therapy pregnancies has been highlighted by Mekinian et al., pertaining to confounding by indication and severity – whereby pregnancies with worse prognoses (maternal history of previous IUD) are targeted with combination treatment, while those with prognostically better outcomes are not (25).

Historically, there has been a lack of evidence around the generic use of immunosuppressive therapies in the management of recurrent pregnancy loss (42). A previous study, albeit with suboptimal case selection and design, highlighted a possible association between first-trimester prednisone exposure and cleft lips and palates in infants (43). This has since been disputed (44), and there is considerable experience in the use of oral steroids for many a condition in pregnancy, including lupus, transplants, severe asthma, etc. Nevertheless, long term use of steroids has been linked with increased preterm delivery rates (secondary to preterm prelabour rupture of membranes), neonatal intensive care admission and low birth weights in the neonates, and increased chance of maternal dependence on steroids and steroid induced diabetes (and its associated complications) (45–47). While it is not clear whether any of these adverse outcomes were documented as a result of oral steroids like prednisone in our review studies, its use in the management of pregnancies previously affected by CHI as a part of off-label treatment regimes in the UK, in order to optimise pregnancy outcome (improve live birth rate, and prolong gestation at delivery), is still surrounded by controversy (48).

Antithrombotic therapy is relatively effective in treating pregnancy loss, particularly in those with associated antiphospholipid syndrome (42, 46). A recent Cochrane review concluded that combined treatment of aspirin with heparin is more likely to lead to higher birth rates in women with recurrent pregnancy loss associated with antiphospholipid antibodies, compared to aspirin alone (49). Though still yet to be confirmed, this offers a potential means of treating the proposed antibody mediated and pro-inflammatory pathophysiology of CHI. A recent review drew upon the application of immunomodulatory drugs in autoimmune conditions during pregnancy to emphasise the safety and merit of hydroxychloroquine in CHI (50).

Additionally, CHI has been associated with maternal hypertensive disorders in some studies but evaluating this was outside the remit of this paper (8). Antithrombotic therapy such as aspirin is also cited by The American College of Obstetricians and Gynaecologists as appropriate in the prevention of fetal growth restriction, which in some cases is due to placental insufficiency (16, 51). Hence, despite further research being warranted, the practice of the use of aspirin and heparin in the management of pregnancies affected by CHI, is not discordant with current practice. Anti-thrombotic drugs such as unfractionated and low molecular weight heparin, adjunctive low dose aspirin (with or without other immunosuppressive agents such as hydroxychloroquine, azathioprine, adalimumab, tacrolimus) currently form the basis of off-label CHI treatment in the UK (48). A 2021 study by Brady and colleagues has however offered some promising results in the application of hydroxychloroquine and prednisolone (in conjunction with mainstay aspirin and heparin) in improving CHI lesion severity and bringing about a 62.3% reduction in subsequent pregnancy loss (52). The study reported lower FGR, preterm, stillbirth and neonatal death rates in treated pregnancies although statistical significance was restricted by the small sample size (52).

Co-occurrence of placental lesions was encountered as frequently as 30% in one study and 25% in another (5, 18). While these cases were beyond the scope of the review, the reality of coexisting pathology is worth recognising (50). In one study, combined lesions formed a considerable proportion of placental samples (35%). Although these were excluded from

our data, the debate on viewing combined lesions as separate entities continues (27). The application of aspirin and corticosteroids in a pregnancy affected by both villitis and CHI was documented as having a positive outcome in one case report (53). It is questionable whether the same treatment effect would be observed in pregnancies affected by other placental lesions adjunct to CHI, and further research into this should be encouraged. We stress the value of a multidisciplinary discussion involving perinatal pathologists in such cases, where there are such services available, to have a case-based consensus of treatment regimes (36).

Strengths and limitations

This is a rare condition. As discussed above, there is a lack of consensus and guidance on indications for placental pathology following pregnancy loss or adverse pregnancy outcomes. Not all placental pathology is assessed by perinatal pathologists. Therefore, it can be acknowledged that the actual incidence of CHI is underreported. There is only a small amount of literature on CHI, and it is unlikely that any relevant studies were omitted through the search strategy. It has been noted that observational study titles can be misleading and require full-text screening for relevance (22). The manageable number of search results enabled manual screening and several checking processes to be carried out to ensure that no relevant studies were missed. Saved search alerts permitted new papers released after the search period to be identified and screened equally.

However, it must be acknowledged that there was an enforcement of an English-language criterion due to time constraints, and it is possible that this introduced a level of selection bias to this systematic review and meta-analysis.

Lastly, not all relevant data, i.e., treated vs untreated outcomes, appeared to be included in studies, and although raw data were requested through email correspondence, this was not available. As a result, only 38 untreated and treated cases across two studies could be included in the meta-analysis for treatment effect concerning live birth rates specifically, and while data from individual studies appeared to favour untreated cohorts, pooled data in the meta-analysis revealed a non-significant improvement in treated outcomes may suggest publication bias. This is likely due to the exclusion of multiple studies from the meta-analysis. There was a lack of data distinguishing treated vs untreated outcomes in all these other partially treated cohorts (18, 25).

Associated maternal outcomes like hypertensive disorders in pregnancy and treatment-related adverse effects like steroid-induced diabetes have been noted in case reports and from experience with our group. However, evaluating this was outside the remit of this review (54).

Conclusion

This review examined the outcomes of 554 pregnancies, 64 of which were treated by either aspirin, prednisolone or LMWH alone or in conjunction. Additional therapies included hydroxychloroquine and adalimumab. Based on efficacy being defined as significantly reducing the prevalence of adverse perinatal outcomes in affected pregnancies, the findings have further strengthened the available evidence that there is no known effective treatment for CHI in pregnancy. The paucity of research using comparison groups in a case-control design has led to challenging analysis and equivocal results. Gaining a deeper insight into novel, effective therapeutics will require international collaboration due to the rare nature of this pathology.

Current therapies for the general treatment of recurrent pregnancy loss form a basis for building these next steps for CHI treatment. Existing recommendations support the use of antithrombotic therapies more than immunosuppressants. The likely need for combination therapy in the event of previous IUFD has been highlighted (25), and this review showed the general value of combination therapy in current practice. Novel therapies not previously reviewed, such as adalimumab and hydroxychloroquine, warrant further research as uncertainty surrounding their efficacy and safety has led to their application only informally recommended in moderate to severe cases.

Compared to other lesions, the high recurrence rate and more severe perinatal outcomes associated with CHI underscore the value of a precise differential diagnosis. Further research may permit a stepwise approach utilising aspirin, heparin, and hydroxychloroquine to form the basis of individualised treatment plans with cost/benefit analysis in line with the previous pregnancy outcomes and multidisciplinary treatment counselling.

Fundamentally, research needs to address the aetiology of CHI to gain a complete understanding of possible ways to treat it. Once this is achieved, observational studies are of value, and even if still retrospective, augmentation of database results with additional hospital data will help account for confounding. Our review only identified one complete and one ongoing prospective multi-centre study. A prospective registry of women with pregnancies previously affected by CHI, involving non-profit organisations like CHI support (48), who may provide ongoing support to these families, may help with a holistic multidisciplinary approach to the management of these pregnancies and improve our understanding of this rare pathology. Equally, a prospective multi-centre design should be the objective model of future studies with additional outcome measures such as Apgar Scores and NICU admissions and later achievement of neurodevelopmental milestones.

Interventions should include, but not be limited to, aspirin, prednisone, and heparin, with or without other immunosuppressive agents such as hydroxychloroquine, azathioprine, adalimumab, tacrolimus). Researchers should be attentive to side effects caused by therapies and their comparative effectiveness in combination or alone. This will help develop future guidelines for CHI treatment, and hopefully, long-term follow-up data regarding childhood outcomes in untreated versus treated CHI pregnancies will also become available.

The best effort to improve pregnancy outcomes in pregnancies associated with CHI is surveillance and identification of screening tools in the index pregnancy, where CHI is suspected. Equally, where CHI has been previously identified, screening tools may help increase surveillance and tailor treatment modalities and regimens. Use of first-trimester markers (55, 56) like placental growth factor or second-trimester markers like alkaline phosphatase, ultrasound markers like increased uterine artery pulsatility index and reduction in amniotic fluid in the third trimester, and use of fetal placental MRI using diffusion imaging have all been reported either alone or in conjunction with each other. Although a single sufficiently specific biomarker is yet to be identified (31), further research into these potential prognostic biomarkers would be invaluable (54) in reducing the prevalence of adverse perinatal outcomes in this pathology by permitting earlier intervention and better treatment.

Author contributions

PS, LM and CS conceptualized the topic and structure of the systematic review. LM and CS drafted and revised the manuscript. SN, AM, MA-A, CN-P, KN and PS provided expert opinion, edited, and approved the final manuscript. All authors contributed to the article and approved the submitted version.

Funding

PS is funded by an NIHR Clinical Lectureship (CL-2018-17-002). This study was funded by the Fetal Medicine Foundation (KHN) (registered charity 1037116), National Institute for Health Research (NIHR) Biomedical Research Centre at Guy's and St Thomas' National Health Service Foundation Trust and King's College London (IS-BRC-1215–20006). The views expressed in this Article are those of the authors and not necessarily those of the National Health Service, the NIHR, or the Department of Health.

Conflict of interest

The authors declare that the research was conducted in the absence of any commercial or financial relationships that could be construed as a potential conflict of interest.

Publisher's note

All claims expressed in this article are solely those of the authors and do not necessarily represent those of their affiliated organizations, or those of the publisher, the editors and the reviewers. Any product that may be evaluated in this article, or claim that may be made by its manufacturer, is not guaranteed or endorsed by the publisher.

Supplementary material

The Supplementary Material for this article can be found online at: https://www.frontiersin.org/articles/10.3389/fendo.2022.945543/full#supplementary-material

References

1. Boyd TK, Redline RW. Chronic histiocytic intervillositis: A placental lesion associated with recurrent reproductive loss. *Hum Pathol* (2000) 31:1389–96. doi: 10.1016/S0046-8177(00)80009-X

2. Brady CA, Williams C, Sharps MC, Shelleh A, Batra G, Heazell AEPP, et al. Chronic histiocytic intervillositis: A breakdown in immune tolerance comparable to allograft rejection? *Am J Reprod Immunol* (2021) 85:e13373. doi: 10.1111/aji.13373

3. Labarrere C, Mullen E. Fibrinoid and trophoblastic necrosis with massive chronic intervillositis: An extreme variant of villitis of unknown etiology. *Am J Reprod Immunol Microbiol* (1987) 15:85–91. doi: 10.1111/j.1600-0897.1987.tb00162.x

4. Bos M, Nikkels PGJ, Cohen D, Schoones JW, Bloemenkamp KWM, Bruijn JA, et al. Towards standardized criteria for diagnosing chronic intervillositis of unknown etiology: A systematic review. *Placenta* (2018) 61:80–8. doi: 10.1016/j.placenta.2017.11.012

5. Rota C, Carles D, Schaeffer V, Guyon F, Saura R, Horovitz J. Pronostic périnatal des grossesses compliquées d'intervillites chroniques placentaires. *J Gynécologie Obs Biol la Reprod* (2006) 35:711–9. doi: 10.1016/S0368-2315(06)76468-7

6. Simula NK, Terry J, Kent NE, Robertson J, Purkiss S, Bedaiwy MA. Chronic intervillositis of unknown etiology (CIUE): a cause for reproductive failure. *Fertil Steril* (2019) 112:e402. doi: 10.1016/j.fertnstert.2019.07.1144

7. Ongaro D, Terry J. Reproducibility of grading in chronic intervillositis of unknown etiology. *Pediatr Dev Pathol* (2020) 23:210–4. doi: 10.1177/1093526619882522

8. Lee AX, Tan BRY, Kho CL, Tan KT. Chronic histiocytic intervillositis (CHI): an under-recognised condition with potential serious sequelae in pregnancy. *BMJ Case Rep* (2021) 14:e241637. doi: 10.1136/bcr-2021-241637

9. Doss BJ, Greene MF, Hill J, Heffner LJ, Bieber FR, Genest DR. Massive chronic intervillositis associated with recurrent abortions. *Hum Pathol* (1995) 26:1245–51. doi: 10.1016/0046-8177(95)90201-5

10. Salafia C, Cowchock F. Placental pathology and antiphospholipid antibodies: A descriptive study. *Am J Perinatol* (1997) 14:435–41. doi: 10.1055/s-2007-994176

11. Reus AD, van Besouw NM, Molenaar NM, Steegers EAP, Visser W, de Kuiper RP, et al. An immunological basis for chronic histiocytic intervillositis in recurrent fetal loss. *Am J Reprod Immunol* (2013) 70:230–7. doi: 10.1111/aji.12125

12. Labarrere CA, Bammerlin E, Hardin JW, DiCarlo HL. Intercellular adhesion molecule-1 expression in massive chronic intervillositis: Implications for the invasion of maternal cells into fetal tissues. *Placenta* (2014) 35:311–7. doi: 10.1016/j.placenta.2014.02.006

13. Bendon RW, Coventry S, Thompson M, Rudzinski ER, Williams EM, Oron AP. Significance of C4d immunostaining in placental chronic intervillositis. *Pediatr Dev Pathol* (2015) 18:362–8. doi: 10.2350/14-12-1582-OA.1

14. Mattuizzi A, Sauvestre F, André G, Poingt M, Camberlein C, Carles D, et al. Adverse perinatal outcomes of chronic intervillositis of unknown etiology: an observational retrospective study of 122 cases. *Sci Rep* (2020) 10:12611. doi: 10.1038/s41598-020-69191-9

15. Sauvestre F, Mattuizzi A, Sentilhes L, Poingt M, Blanco P, Houssin C, et al. Chronic intervillositis of unknown etiology. *Am J Surg Pathol* (2020) 44:1367–73. doi: 10.1097/PAS.0000000000001549

16. Suhag A, Berghella V. Intrauterine growth restriction (IUGR): Etiology and diagnosis. *Curr Obstet Gynecol Rep* (2013) 2:102–11. doi: 10.1007/s13669-013-0041-z

17. MacGregor B, Shakespeare J, Kotnis R, Knight M, Hillman S. MBRRACE 2021: preventing maternal deaths — we are all part of the solution. *Br J Gen Pract* (2022) 72:148–9. doi: 10.3399/bjgp22X718829

18. Parant O, Capdet J, Kessler S, Aziza J, Berrebi A. Chronic intervillositis of unknown etiology (CIUE): Relation between placental lesions and perinatal outcome. *Eur J Obstet Gynecol Reprod Biol* (2009) 143:9–13. doi: 10.1016/j.ejogrb.2008.06.012

19. Marchaudon V, Devisme L, Petit S, Ansart-Franquet H, Vaast P, Subtil D. Chronic histiocytic intervillositis of unknown etiology: Clinical features in a consecutive series of 69 cases. *Placenta* (2011) 32:140–5. doi: 10.1016/j.placenta.2010.11.021

20. Luchini C, Stubbs B, Solmi M, Veronese N. Assessing the quality of studies in meta-analyses: Advantages and limitations of the Newcastle Ottawa scale. *World J Meta Analysis* (2017) 5:80. doi: 10.13105/wjma.v5.i4.80

21. Long HA, French DP, Brooks JM. Optimising the value of the critical appraisal skills programme (CASP) tool for quality appraisal in qualitative evidence synthesis. *Res Methods Med Heal Sci* (2020) 1:31–42. doi: 10.1177/2632084320947559

22. Lefebvre C, Glanville J BS, et al. *Cochrane handbook for systematic reviews of interventions version 6.2. cochrane; 2021* (2021). Available at: https://training.cochrane.org/handbook.

23. Page MJ, McKenzie JE, Bossuyt PM, Boutron I, Hoffmann TC, Mulrow CD, et al. The PRISMA 2020 statement: an updated guideline for reporting systematic reviews. *BMJ* (2021) 372:n71. doi: 10.1136/bmj.n71

24. Ramya T, Chaitra V UG. Chronic histiocytic intervillositis- a rare placental cause of poor obstetric outcome: a clinicopathological study and literature review. *Int J Reprod Contraception Obstet Gynecol* (2014) 3:1146. doi: 10.5455/2320-1770.ijrcog20141258

25. Mekinian A, Costedoat-Chalumeau N, Masseau A, Botta A, Chudzinski A, Theulin A, et al. Chronic histiocytic intervillositis: Outcome, associated diseases and treatment in a multicenter prospective study. *Autoimmunity* (2015) 48:40–5. doi: 10.3109/08916934.2014.939267

26. Crawford A, Moore L, Bennett G, Savarirayan R, Manton N, Khong Y, et al. Recurrent chronic histiocytic intervillositis with intrauterine growth restriction, osteopenia, and fractures. *Am J Med Genet Part A* (2016) 170:2960–4. doi: 10.1002/ajmg.a.37856

27. Nowak C, Joubert M, Jossic F, Masseau A, Hamidou M, Philippe H-JJ, et al. Perinatal prognosis of pregnancies complicated by placental chronic villitis or intervillositis of unknown etiology and combined lesions: About a series of 178 cases. *Placenta* (2016) 44:104–8. doi: 10.1016/j.placenta.2016.04.017

28. Sabra S, Zurriaga CR, Saborit A, Gómez Roig MD. A series of rare chronic histiocytic intervillositis cases and its association with fetal growth restriction. *Gynecol Obstet Res - Open J* (2016) 3:26–31. doi: 10.17140/GOROJ-3-133

29. Ozawa N, Yamaguchi K, Shibata M, Sugibayashi R, Yagi H, Sago H, et al. Chronic histiocytic intervillositis in three consecutive pregnancies in a single patient: Differing clinical results and pathology according to treatment used. *J Obstet Gynaecol Res* (2017) 43:1504–8. doi: 10.1111/jog.13404

30. Vardi L, Paterson H, Hung NA. Successful pregnancy following treatment of recurrent chronic histiocytic intervillositis. *BMJ Case Rep* (2017) 2017: bcr2016217886. doi: 10.1136/bcr-2016-217886

31. Koby L, Keating S, Malinowski AK, D'Souza R. Chronic histiocytic intervillositis - clinical, biochemical and radiological findings: An observational study. *Placenta* (2018) 64:1–6. doi: 10.1016/j.placenta.2018.02.002

32. Mekinian A, Houfflin-Debarge V, Kolanska K, Cohen J, Abisror N, Bornes M, et al. Antagonists of TNFalpha for recurrent miscarriages: 2 illustrative cases. *Eur J Obstet Gynecol Reprod Biol* (2019) 236:263–4. doi: 10.1016/j.ejogrb.2019.02.036

33. Nohr EW, Wright JRJ EWN, Wright JR. Diffuse subamniotic calcification: A novel pattern of placental calcification. *Pediatr Dev Pathol* (2020) 23:438–42. doi: 10.1177/1093526620957843

34. Alderson P. Research pointers: Survey of claims of no effect in abstracts of cochrane reviews. *BMJ* (2003) 326:475–5. doi: 10.1136/bmj.326.7387.475

35. Mekinian A, Costedoat-Chalumeau N, Carbillon L, Coulomb-L'Hermine A, Le Guern V, Masseau A, et al. Intervillites chroniques histiocytaires : bilan et prise en charge. *La Rev Médecine Interne* (2018) 39:117–21. doi: 10.1016/j.revmed.2017.10.422

36. Khong TY, Mooney EE, Ariel I, Balmus NCM, Boyd TK, Brundler M-A, et al. Sampling and definitions of placental lesions: Amsterdam placental workshop group consensus statement. *Arch Pathol Lab Med* (2016) 140:698–713. doi: 10.5858/arpa.2015-0225-CC

37. Bos M, Harris-Mostert ETMSTMS, van der Meeren LEE, Baelde JJJ, Williams DJJ, Nikkels PGJGJ, et al. Clinical outcomes in chronic intervillositis of unknown etiology. *Placenta* (2020) 91:19–23. doi: 10.1016/j.placenta.2020.01.001

38. Homatter C, Stichelbout M, Devisme L, Chudzinski A, Debarge V, Garabedian C, et al. Is chronic histiocytic intervillositis a severe placental disease? a case-control study. *Placenta* (2020) 91:31–6. doi: 10.1016/j.placenta.2019.12.020

39. Simula NK, Terry J, Kent NE, Robertson J, Purkiss S, Bloomenthal D, et al. Chronic intervillositis of unknown etiology (CIUE): Prevalence, patterns and reproductive outcomes at a tertiary referral institution. *Placenta* (2020) 100:60–5. doi: 10.1016/j.placenta.2020.07.032

40. Traeder J, Jonigk D, Feist H, Bröcker V, Länger F, Kreipe H, et al. Pathological characteristics of a series of rare chronic histiocytic intervillositis of the placenta. *Placenta* (2010) 31:1116–9. doi: 10.1016/j.placenta.2010.09.012

41. Contro E, DeSouza R, Bhide A. Chronic intervillositis of the placenta: A systematic review. *Placenta* (2010) 31:1106–10. doi: 10.1016/j.placenta.2010.10.005

42. Gynaecologists RC of O. The investigation and treatment of couples with recurrent first-trimester and second-trimester miscarriage. In: *RCOG green-top guidel no 17*. London: Royal College of Obstetricians and Gynaecologists (2011). p. 1–18.

43. Carmichael SL, Shaw GM, Ma C, Werler MM, Rasmussen SA, Lammer EJ. Maternal corticosteroid use and orofacial clefts. *Am J Obstet Gynecol* (2007) 197:585.e1–7. doi: 10.1016/j.ajog.2007.05.046

44. Skuladottir H, Wilcox AJ, Ma C, Lammer EJ, Rasmussen SA, Werler MM, et al. Corticosteroid use and risk of orofacial clefts. *Birth Defects Res Part A Clin Mol Teratol* (2014) 100:499–506. doi: 10.1002/bdra.23248

45. Empson MB, Lassere M, Craig JC, Scott JR. Prevention of recurrent miscarriage for women with antiphospholipid antibody or lupus anticoagulant. *Cochrane Database Syst Rev* (2005) 2012:CD002859. doi: 10.1002/14651858.CD002859.pub2

46. Bender Atik R, Christiansen OB, Elson J, Kolte AM, Lewis S, Middeldorp S, et al. ESHRE guideline: recurrent pregnancy loss. *Hum Reprod Open* (2018) 2018:1–12. doi: 10.1093/hropen/hoy004

47. Laskin CA, Bombardier C, Hannah ME, Mandel FP, Ritchie K, Farewell V, et al. Prednisone and aspirin in women with autoantibodies and unexplained recurrent fetal loss. *N Engl J Med* (1997) 337:148–54. doi: 10.1056/nejm199707173370302

48. Belardo CAA. *Summary of suggested treatments for chronic histiocytic intervillositis (CHI)* (2019). Available at: https://chisupport.org/wp-content/uploads/2019/01/Summary-of-suggested-treatments-for-Chronic-Histiocytic-Intervillositis.docx-Google-Docs.pdf.

49. Hamulyák EN, Scheres LJJJ, Marijnen MC, Goddijn M, Middeldorp S. Aspirin or heparin or both for improving pregnancy outcomes in women with persistent antiphospholipid antibodies and recurrent pregnancy loss. *Cochrane Database Syst Rev* (2020) 2020:CD012852. doi: 10.1002/14651858.CD012852.pub2

50. Bouariu A, Gică N, Ciobanu AM, Scutelnicu AM, Popescu MR, Panaitescu AM. The potential benefit of hydroxychloroquine in chronic placental inflammation of unknown etiology associated with adverse pregnancy outcomes. *Healthcare* (2022) 10:168. doi: 10.3390/healthcare10010168

51. Berghella V. Prevention of recurrent fetal growth restriction. *Obstet Gynecol* (2007) 110:904–12. doi: 10.1097/01.AOG.0000267203.55718.aa

52. Brady CA, Williams C, Batra G, Church E, Tower CL, Crocker IP, et al. Immunomodulatory therapy reduces the severity of placental lesions in chronic histiocytic intervillositis. *Front Med* (2021) 8:753220. doi: 10.3389/fmed.2021.753220

53. Boog G, Le Vaillant C, Alnoukari F, Jossic F, Barrier J, Muller J-YY, et al. Combining corticosteroid and aspirin for the prevention of recurrent villitis or intervillositis of unknown etiology. *J Gynecol Obstet Biol la Reprod* (2006) 35:396–404. doi: 10.1016/s0368-2315%2806%2976411-0

54. Cornish EF, McDonnell T, Williams DJ. Chronic inflammatory placental disorders associated with recurrent adverse pregnancy outcome. *Front Immunol* (2022) 13:825075. doi: 10.3389/fimmu.2022.825075

55. Tan MY, Syngelaki A, Poon LC, Rolnik DL, O'Gorman N, Delgado JL, et al. Screening for pre-eclampsia by maternal factors and biomarkers at 11-13 weeks' gestation. *Ultrasound Obstet Gynecol* (2018) 52:186–95. doi: 10.1002/uog.19112

56. Chaemsaithong P, Sahota DS, Poon LC. First trimester preeclampsia screening and prediction. *Am J Obstet Gynecol* (2020) 226:S1071-97.e2. doi: 10.1016/j.ajog.2020.07.020

frontiers | Frontiers in Endocrinology

TYPE Original Research
PUBLISHED 28 July 2022
DOI 10.3389/fendo.2022.908240

Check for updates

OPEN ACCESS

EDITED BY
Reinaldo Marín,
Instituto Venezolano de Investigaciones Científicas (IVIC), Venezuela

REVIEWED BY
Jorge Lopez-Tello,
University of Cambridge, United Kingdom
Tania M. Ortiga-Carvalho,
Federal University of Rio de Janeiro, Brazil

*CORRESPONDENCE
Juneo Freitas Silva
jfsilva@uesc.br

SPECIALTY SECTION
This article was submitted to Developmental Endocrinology, a section of the journal Frontiers in Endocrinology

RECEIVED 30 March 2022
ACCEPTED 04 July 2022
PUBLISHED 28 July 2022

CITATION
Santos BR, dos Anjos Cordeiro JM, Santos LC, Barbosa EM, Mendonça LD, Santos EO, de Macedo IO, de Lavor MSL, Szawka RE, Serakides R and Silva JF (2022) Kisspeptin treatment improves fetal-placental development and blocks placental oxidative damage caused by maternal hypothyroidism in an experimental rat model. *Front. Endocrinol.* 13:908240. doi: 10.3389/fendo.2022.908240

COPYRIGHT
© 2022 Santos, dos Anjos Cordeiro, Santos, Barbosa, Mendonça, Santos, de Macedo, de Lavor, Szawka, Serakides and Silva. This is an open-access article distributed under the terms of the Creative Commons Attribution License (CC BY). The use, distribution or reproduction in other forums is permitted, provided the original author(s) and the copyright owner(s) are credited and that the original publication in this journal is cited, in accordance with accepted academic practice. No use, distribution or reproduction is permitted which does not comply with these terms.

Kisspeptin treatment improves fetal-placental development and blocks placental oxidative damage caused by maternal hypothyroidism in an experimental rat model

Bianca Reis Santos[1], Jeane Martinha dos Anjos Cordeiro[1], Luciano Cardoso Santos[1], Erikles Macedo Barbosa[1], Letícia Dias Mendonça[1], Emilly Oliveira Santos[1], Isabella Oliveira de Macedo[1], Mário Sergio Lima de Lavor[1], Raphael Escorsim Szawka[2], Rogeria Serakides[3] and Juneo Freitas Silva[1]*

[1]Centro de Microscopia Eletronica, Departamento de Ciencias Biologicas, Universidade Estadual de Santa Cruz, Campus Soane Nazare de Andrade, Ilheus, Brazil, [2]Departamento de Fisiologia e Biofísica, Instituto de Ciencias Biologicas, Universidade Federal de Minas Gerais, Belo Horizonte, Brazil, [3]Departamento de Clinica e Cirurgia Veterinarias, Escola de Veterinaria, Universidade Federal de Minas Gerais, Belo Horizonte, Brazil

Maternal hypothyroidism is associated with fetal growth restriction, placental dysfunction, and reduced kisspeptin/Kiss1R at the maternal-fetal interface. Kisspeptin affects trophoblastic migration and has antioxidant and immunomodulatory activities. This study aimed to evaluate the therapeutic potential of kisspeptin in the fetal-placental dysfunction of hypothyroid Wistar rats. Hypothyroidism was induced by daily administration of propylthiouracil. Kisspeptin-10 (Kp-10) treatment was performed every other day or daily beginning on day 8 of gestation. Feto-placental development, placental histomorphometry, and expression levels of growth factors (VEGF, PLGF, IGF1, IGF2, and GLUT1), hormonal (Dio2) and inflammatory mediators (TNFα, IL10, and IL6), markers of hypoxia (HIF1α) and oxidative damage (8-OHdG), antioxidant enzymes (SOD1, Cat, and GPx1), and endoplasmic reticulum stress mediators (ATF4, GRP78, and CHOP) were evaluated on day 18 of gestation. Daily treatment with Kp-10 increased free T3 and T4 levels and improved fetal weight. Both treatments reestablished the glycogen cell population in the junctional zone. Daily treatment with Kp-10 increased the gene expression levels of *Plgf*, *Igf1*, and *Glut1* in the placenta of hypothyroid animals, in addition to blocking the increase in 8-OHdG and increasing protein and/or mRNA expression levels of SOD1, Cat, and GPx1. Daily treatment with Kp-10 did not alter the higher protein expression levels of VEGF, HIF1α, IL10, GRP78, and CHOP caused by hypothyroidism in the junctional zone compared to control, nor the lower expression of *Dio2* caused by hypothyroidism. However, in the

labyrinth zone, this treatment restored the expression of VEGF and IL10 and reduced the GRP78 and CHOP immunostaining. These findings demonstrate that daily treatment with Kp-10 improves fetal development and placental morphology in hypothyroid rats, blocks placental oxidative damage, and increases the expression of growth factors and antioxidant enzymes in the placenta.

KEYWORDS

kisspeptin, trophoblast, thyroid, cell stress, inflammation, fetal development, rat

Introduction

Kisspeptin, encoded by the gene *Kiss1*, was first purified from human placenta (1, 2). Soon after kisspeptin was discovered, it was recognized as essential for fertility, as it regulates gonadotropin-releasing hormone (GnRH) secretion by the hypothalamus through the G protein-coupled receptor GPR54 (Kiss1R). Therefore, failures in the kisspeptin/Kiss1R signaling system result in hypogonadotropic hypogonadism (3, 4). In addition to its hypothalamic action, however, the kisspeptin/Kiss1R system is expressed in a variety of tissues, including the placenta (5, 6), although studies on the action of kisspeptin on the placenta are still scarce (7–9).

In humans, circulating levels of kisspeptin are low in most physiological conditions, except in the final third of gestation, when these levels increase almost 10, 000 times, after which they quickly return to basal level after delivery (10–12). This suggests that the placenta is one of the main sources of systemic kisspeptin. Studies have shown that kisspeptin influences the adhesion and implantation of blastocysts and the decidualization and migration of trophoblasts, and regulates the immunological profile and uterine natural killer cells (uNKs) (5, 7–9, 11–17), suggesting that faults in its expression in the maternal-fetal interface may be involved in placental disorders (12, 18).

Gestational diseases such as preeclampsia, gestational hypertension, miscarriage, gestational diabetes, and obesity have altered plasma and/or placental levels of kisspeptin (17–30). Therefore, its plasma profile can be assessed to predict gestational success (12, 18). We have recently demonstrated that rats with maternal hypothyroidism, another important gestational disease, also exhibit decidual and placental reduction of the kisspeptin/Kiss1R system (31).

Women with maternal hypothyroidism are more likely to suffer miscarriage and intrauterine growth restriction (Silva et al., 2012; Silva, Ocarino, and Serakides, 2018). Moreover, plasma levels of triiodothyronine (T3) and thyroxine (T4) are low in patients with preeclampsia (32, 33). Studies in rats have also shown that hypothyroidism reduces intrauterine trophoblast migration and proliferation, increases placental apoptosis, compromises placental morphogenesis and vascularization, causes oxidative and reticular stress, and alters the immune profile and uNK cell population at the maternal-fetal interface (34–40). However, the role of kisspeptin in these placental changes is still unknown.

Although T4 replacement is the first choice in patients with hypothyroidism, some patients are refractory to T4 replacement (41) and need other therapeutic alternatives when they need to treat a medical condition, such as infertility problems. In this sense, exogenous kisspeptin has been shown to restore ovarian function in hypothyroid rats (42). Furthermore, studies have shown that kisspeptin administration has an immunomodulatory effect on gestation (15) and an antioxidative effect on the ovary (43), liver (44), and testicle (45), and blocks the occurrence of reticular stress in hypothalamic GT1-7 cell line (46). Therefore, this study aimed to evaluate the therapeutic potential of kisspeptin in placental dysfunction caused by maternal hypothyroidism. We demonstrate that daily kisspeptin treatment improves development of the fetus and placenta in hypothyroid rats, increases the expression of growth factors and antioxidant enzymes by the placenta, and positively modulates oxidative stress, reticular stress and immune mediators, thus characterizing the therapeutic potential of kisspeptin in a gestational disease for the first time.

Materials and methods

Animal management and induced hypothyroidism

Adult Wistar rats (200-250 grams) were kept in plastic boxes with controlled temperature (22 ± 2°C) and brightness (12 h light/12 h dark), and water and feed *ad libitum*. The animals were equally distributed into euthyroid (control) (n=13), hypothyroid (n=15), and hypothyroid groups treated with kisspeptin-10 (Kp10) every other day (KpT1; n=15) or every

day (KpT2; n=15). Hypothyroidism was induced by administering 6-propyl-2-thiouracil (PTU) (4 mg/Kg/day) through an orogastric tube every day, starting five days before mating, while the control group received water as a placebo (35, 36). All experimental procedures were approved by the Ethics Committee on the Use of Animals of Santa Cruz State University (UESC) (Protocol 036/16).

Five days after the start of treatment with PTU, five animals from each group were euthanized by decapitation for blood collection and dosage of free T4 to confirm the induction of hypothyroidism (Control, 1.20 ± 0.05 µg/dL; Hypothyroid, 0.47 ± 0.09 µg/dL; KpT1, 0.52 ± 0.06 µg/dL; KpT2, 0,42 ± 0.08 µg/dL ($P<0.01$)). Vaginal cytology was performed in the remaining rats, and the animals in proestrus were housed with fertile adult males for mating. The presence of spermatozoa in the vaginal cytology the next morning confirmed copulation and was defined as day 0 of gestation (0 GD). All animals from control group were mated and became pregnant, while from hypothyroid groups (Hypothyoid; KpT1; KpT2) around 86.6% of the females became pregnant.

Treatment with kisspeptin-10

The hypothyroid animals treated with Kp10 were distributed into two groups, one treated every other day (KpT1) and one treated daily with Kp10 (KpT2). Treatment was initiated on the 8th GD (8 µg/Kg/day) (Cat. No. 4243, Tocris Bioscience, Bristol, UK), intraperitoneally, and was maintained until the day of euthanasia. Kp10 treatment was initiated on the 8th GD so that it would not influence embryo implantation. The animals in the control and hypothyroid groups received sterile water as a placebo.

Euthanasia and material collection

The animals were euthanized by decapitation on the 18th GD and blood was collected from the neck into tubes with heparin for dosage of free T3 and T4. The blood was centrifuged at 3000 rpm for 20 min and the plasma was obtained and stored at -20°C.

At necropsy, the entire genital system was collected. Subsequently, the uterus containing the placenta and fetuses, and the uterus with placenta were weighed, as were the fetuses, individually. Hysterectometric (maternal weight without the gravid uterus) maternal weight gain was also evaluated. The weight of amniotic fluid was estimated by subtracting the weight of the uterus and placenta with the fetuses from the weight of the fetuses and the weight of the uterus and placenta without the fetuses. The number of fetuses and the number of sites with resorption or fetal death were also counted. Fragments of the central region of the placenta measuring 2 mm in diameter were dissected and removed from two placental sites/animal and separately immersed in TRIzol®, followed by freezing in liquid nitrogen and storing at -80°C for quantitative real-time reverse transcriptase-polymerase chain reaction (qRT-PCR) analyses. The remaining discs (placenta+basal decidua+metrial gland) were fixed in 4% paraformaldehyde at 4°C for 24 hours and processed using the paraffin embedding technique for histomorphometry and immunohistochemistry analysis. The tissues were dehydrated in a serial solution of 70% to 100% alcohol, with subsequent xylene diaphanization and paraffin impregnation and embedding. Microtomy on histological slides was used to obtain 4-µm tissue sections for histomorphometry evaluation. Silane-coated polarized slides (StarFrost Polycat, Germany) were used for immunohistochemistry.

Hormone analysis

Dosage of Free T3 and T4 was performed using enzyme-linked immunosorbent assay (ELISA) kits according to the manufacturer's instructions (IMMULITE, Siemens Medical Solutions Diagnostics, Malvern, PA, USA).

Evaluation of fetal development

The brain, heart, liver, lungs, and kidneys of each fetus were dissected and weighed, and the relative weight of the organs in relation to fetal weight was obtained. After weighing the fetal organs, the brain to liver ratio, an indicator of asymmetric fetal growth restriction, was calculated (47).

For analysis of fetal weight distribution and risk of fetal growth restriction, fetal weight histograms were constructed for each group with the individual fetal weight and non-linear regression was performed according to Dilworth et al. (48). The 5th percentile weight was calculated as: (-Z score x SD) + mean, assuming that Z score = 1.645, SD = standard deviation, mean = mean of control group.

Histomorphometry analysis

Histomorphometry analysis of the placenta was performed on 4 µm histological sections stained with hematoxylin and eosin. All evaluations were performed blindly by two evaluators and without knowledge of the experimental groups. The quantitative evaluation was performed on 7-8 placental discs/group, and a histological section/placental disc was obtained from the center of the tissue with maternal central blood vessel to ensure the histological sections were uniform. Images of each placental disc were captured using a Leica S9i stereo microscope, and the thickness of each placental layer (junctional zone and labyrinth zone) was assessed in 10 random regions and averaged

per placental site. The analyses were performed using Image Pro Plus® version 4.5 software and the values were transformed into millimeters using a micrometer scale.

In the junctional zone, the proportion of area occupied by glycogen cells, spongiotrophoblasts, and trophoblastic giant cells per field was evaluated by selecting 5 random fields with the 20x lens. In the labyrinth zone, the proportion of area occupied by maternal vascular sinus, fetal capillaries, and fetal mesenchyme/trophoblastic cells per field was evaluated by selecting 10 random fields of the labyrinth with the 40x lens. The images were captured on a Leica DM2500 photon microscope and quantification was performed using a graticule of 99 (junctional zone) and 100 (labyrinth zone) points with Image Pro Plus® software version 4.5 (35).

Immunohistochemistry

Histological sections of the placental discs were submitted to immunohistochemistry analysis using the antibodies anti-8-OHdG (sc-393871), anti-HIF1α (sc-13515), anti-SOD1 (sc-101523), anti-catalase (sc-271803), anti-GPx 1/2 (sc-133160), anti-GRP78 (sc-13539), anti-CHOP (sc-71136), anti-ATF4 (sc-390063), anti-TNFα (sc-52746), anti-IL-10 (sc-365858), and anti-VEGF (sc-152), from Santa Cruz Biotechnology, CA, USA. All antibodies used in this study were validated by the manufacturer.

The streptavidin-biotin-peroxidase staining technique (Novolink Polymer Detection Systems, Leica Biosystems Inc., Buffalo Grove, IL, USA) was used and antigen retrieval was performed with heat in a water bath at 98°C using citric acid solution at pH 6.0. The slides were incubated in a humid chamber for 18 or 40 hours with the primary antibody (Supplementary Figure 1) and for 30 minutes in the blocking stages of endogenous peroxidase, serum blocking, and streptavidin peroxidase. The chromogen was diaminobenzidine (EnVision FLEX DAB+ Chromogen, Agilent Technologies, Inc., Santa Clara, CA. USA). The sections were counterstained with Harris hematoxylin. The negative control was obtained by replacing the primary antibody with phosphate buffered saline (PBS) (36).

A descriptive and quantitative evaluation of the immunohistochemistry expression of HIF1α, 8-OHdG, SOD1, Catalase, GPx1/2, GRP78, CHOP, ATF4, VEGF, TNFα, and IL-10 was performed in the junctional zone and labyrinth zone layers of the placenta. A quantitative evaluation was performed randomly on six placental discs/group. Images of 5 random fields in each region of the placental disc were obtained with a Leica DMI 300B photon microscope (Leica Microsystems, Germany) with the 40x lens. The immunolabeling area was determined using WCIF ImageJ® software (Media Cybernetics Manufacturing, Rockville, MD, USA). The images were subjected to color deconvolution and thresholding. Data from each placental disc were archived, analyzed, and expressed as immunolabeling area in pixels (36).

qRT-PCR

For the qRT-PCR technique, total RNA from the placenta was extracted using TRIzol® according to the manufacturer's instructions (Invitrogen, Life Technologies, Carlsbad, CA, USA). Subsequently, 1 μg of RNA was used for the reverse transcription reactions with the GoTaq® qPCR and RT-qPCR Systems kit (A6010, PROMEGA). The transcripts of the target genes were quantified by qPCR using SYBR Green in the Applied Biosystems® 7500 Real-Time PCR System. For the reactions, 1.5 μL of cDNA, 100 nM of each primer, and 12.5 μL of the GoTaq® qPCR Master Mix 2X reagent was used in a final volume of 20 μL of reaction. As a negative control, the DNA amplification mix was used, in which the cDNA sample was replaced by water. The amplifications were performed under the following conditions: enzyme activation at 95°C for 2 min, 40 cycles of denaturation at 95°C for 15 s, and annealing/extension at 60°C for 60 s. To evaluate the linearity and efficiency of qPCR amplification, standard curves of all transcripts were generated using serial dilutions of the cDNA, followed by an evaluation of the melting curve of the amplification products. The primers for *Sod1*, *Catalase*, *Gpx1*, *Hif1α*, *Grp78*, *Chop*, *Il-10*, *Tnf*, *Il-6*, *Dio2*, *Igf1*, *Igf2*, *Glut1*, *Vegf*, and *Plgf* were delineated based on *Rattus norvegicus* mRNA sequence (Table 1). Gene expression was calculated by the $2^{-\Delta\Delta CT}$ method, where the results obtained for each group were quantitatively compared after normalization based on the expression of *Polr2a Rattus norvegicus* (36, 49).

Statistical analysis

The differences of means among of the groups were determined by performing ANOVA followed by the Student-Newman-Keuls (SNK) test. The data were tested for normality (Shapiro-Wilk) and homoscedasticity (Brown-Forsythe) of the residuals, and for those that did not meet the assumptions, even after logarithmic transformation, the non-parametric Kruskal-Wallis test followed by Dunn's test were used. Generalized linear mixed-model analysis followed by the Tukey test was used to evaluate the fetal and fetal organs' weight and liver/brain ratio (50). Parametric data were represented by mean ± standard error of the mean (SEM), while non-parametric data were represented by median and interquartile range. The analyses were performed using GraphPad Prism 9.0.0 and R version 4.2.0 software, and differences where $P<0.05$ were considered significant.

TABLE 1 List of genes and nucleotide sequences for qPCR primers.

Gene	Sequence (5'->3')	Accession number
Sod1	F: GAAAGGACGGTGTGGCCAATR: CTCGTGGACCACCATAGTACG	NM_017050.1
Hifα	F: AGCAATTCTCCAAGCCCTCCR: TTCATCAGTGGTGGCAGTTG	NM_024359.1
Catalase	F: CTGACTGACGCGATTGCCTAR: GTGGTCAGGACATCGGGTTT	NM_012520.2 R
Gpx1	F: GCGCTACAGCGGATTTTTGAR: GAAGGCATACACGGTGGACT	NM_030826.4
Grp78	F: TGAAGGGGAGCGTCTGATTGR: TCATTCCAAGTGCGTCCGAT	NM_013083.2
Chop	F: TGGCACAGCTTGCTGAAGAGR: TCAGGCGCTCGATTTCCT	NM_001109986.1
Il10	F: GGCCATTCCATCCGGGGTGAR: AAGGCAGCCCTCAGCTCTCG	NM_012854.2
Tnfα	F: AGCCCGTAGCCCACGTCGTAR: CGGTGTGGGTGAGGAGCACG	NM_012675.3
Il6	F: GACTTCCAGCCAGTTGCCTTR: AAGTCTCCTCTCCGGACTTGT	NM_053595.2
Vegf	F: GCCCAGACGGGGTGGAGAGTR: AGGGTTGGCCAGGCTGGGAA	NM_001110336.1
Plgf	F: CCGGCCCTGGCTGCATTGAAR: CAGGCAAAGCCCACAGGCGA	NM_053595.2
Igf 1	F: ACCCGGGACGTACCAAAATGR: CGAGCTGGTAAAGGTGAGCA	NM_178866.4
Igf 2	F: CATCATGTCCCACACTAAGGR: GTGCCAATTGGGTTGTTTAG	XM_008760074.2
Dio2	F: TGCAGTCTCATAGGTGCCTGGAAAR: ACCACTCCCAGCAACAACAACAAC	NM_031720.5
Glut1 (Slc2a1)	F: CAATCAAACATGGAACCACCGR: CGATTGATGAGCAGGAAGCG	NM_138827.1
Polr2a	F: GCTGGACCTACTGGCATGTTR: ACCATAGGCTGGAGTTGCAC	XM_001079162.5

Results

Daily kisspeptin treatment improves fetal restricted growth and plasma free T3 and T4 levels in hypothyroid rats

Because fetal growth restriction in hypothyroid rats is associated with reduced Kiss1 and Kiss1R expression at the maternal-fetal interface (31), the effect of two treatment protocols with Kp-10 was evaluated every other day (KpT1) and daily (KpT2), starting on the 8th GD, on the maternal and fetal parameters of hypothyroid rats. The evaluation of maternal and placental parameters revealed that daily treatment with Kp-10 increased hysterectometric maternal weight gain during gestation when compared to the hypothyroid and KpT1 groups (Figure 1A; $P<0.05$), which had lower gestational weight gain compared to the control ($P<0.001$). No significant difference was observed between the hypothyroid and KpT1 groups for hysterectometric maternal weight gain ($P>0.05$). Interestingly, there was an increase in plasma free T3 and T4 levels in the group treated daily with Kp10 compared to the hypothyroid and KpT1 groups (Figures 1B, C; $P<0.0001$; $P<0.05$) which had lower free T3 and T4 levels compared to the control ($P<0.001$). Furthermore, the KpT1 and KpT2 treatments did not increase the uteroplacental weight or the amniotic fluid of the hypothyroid animals ($P>0.05$), which showed a reduction compared to the control group ($P<0.05$) (Figures 1E, F).

In the evaluation of fetal parameters, although a significant difference was not observed in the number of viable fetuses between the experimental groups (Figure 1G), the KpT1 and KpT2 treatments did not present any differences in the percentage of fetal death when compared to the hypothyroid group ($P>0.05$), which showed a higher percentage of fetal death when compared to the control (Figure 1H; $P<0.05$). The KpT1 and KpT2 treatments were also unable of restore the reduction of fetal weight cause by hypothyroidism when compared to the control (Figures 1D, I; $P<0.001$; $P<0.05$). However, in assessing the relative frequency of fetal weight distribution, both the KpT2 (87.30%) and control (95.05%) groups had a greater distribution than 5th percentile (1.278g) (dashed line), while most fetuses in the hypothyroid (61.49%) and KpT1 (78.58%) groups was below the 5th, with a shift to the left of the distribution curve (Figure 1J).

The KpT2 treatment did not restore the lower heart and lung weights exhibited by the fetuses of hypothyroid animals ($P>0.05$), which had reduced weights when compared to the control (Figure 1K; $P<0.001$; $P<0.01$). However, the fetuses in the KpT1 group had lower liver weight when compared to the control and KpT2 groups ($P<0.001$), as well as lower heart and lung weight in relation to the control and hypothyroid groups. Regarding kidney weight, the fetuses of the KpT1 group also showed a reduction compared to the control ($P<0.01$), hypothyroid ($P<0.001$), and KpT2 ($P<0.01$) groups. No significant difference was observed for fetal brain weight and the brain/liver ratio between the experimental groups (Figures 1K, L; $P>0.05$). Together, these data demonstrate that daily treatment with Kp10 was not able to increase fetal weight, but improved the "growth restricted" condition demonstrated by the fetal weight distribution curve. This was unlike the KpT1 treatment, which did not increase fetal weight, kept the greater part of the fetal weight below the 5th percentile of the control group, and had negative effects on fetal organogenesis.

10.3389/fendo.2022.908240

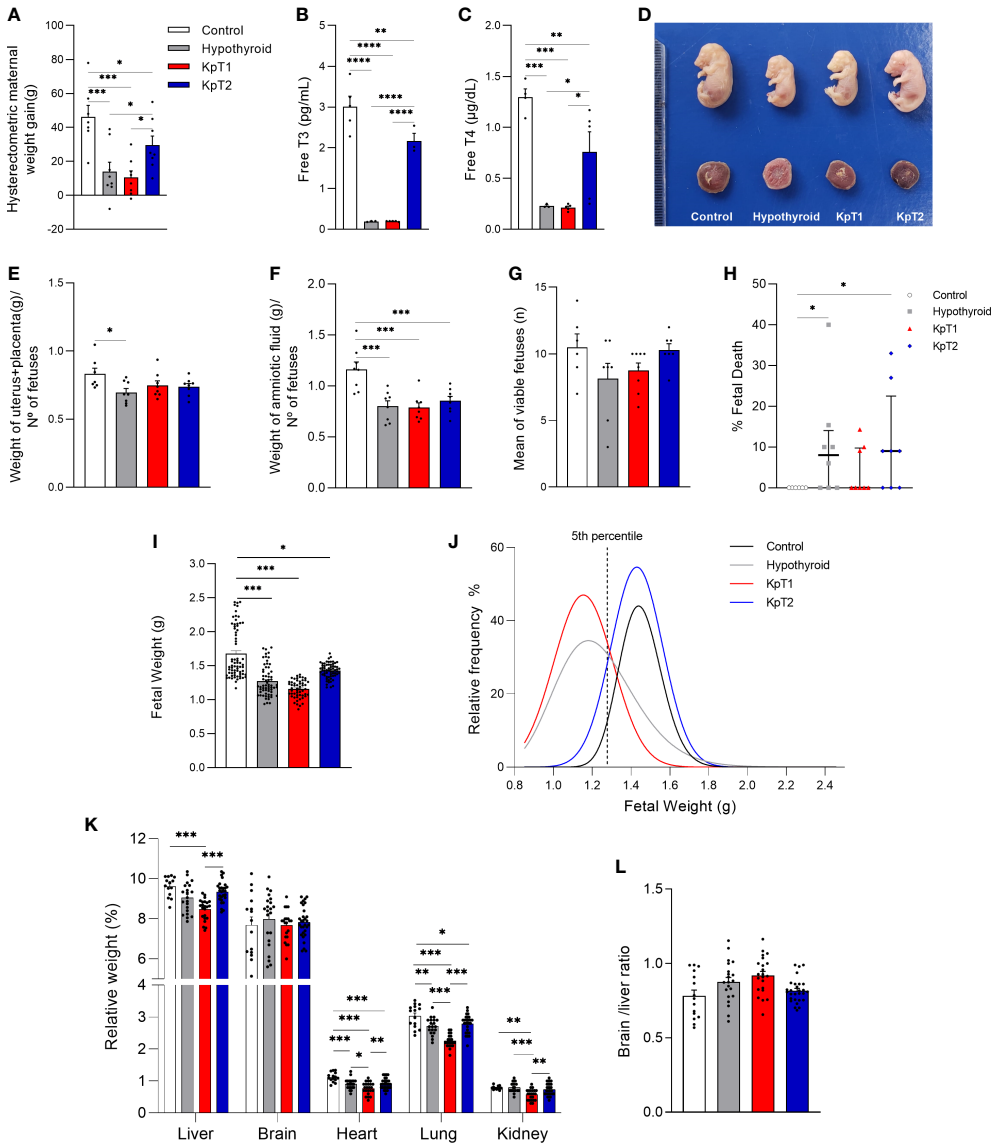


FIGURE 1
Maternal and fetal parameters of control, hypothyroid, and kisspeptin-10-treated rats on the 18th GD. **(A)** Hysterectometric maternal weight gain (mean ± SEM; n = 8). **(B)** Free T3 (mean ± SEM; n = 4-5). **(C)** Free T4 (mean ± SEM; n = 4-5). **(D)** Representative image of fetuses and placentas from each experimental group ... **(E–F)** Uteroplacental **(E)** and amniotic fluid **(F)** weight (mean ± SEM; n = 8). **(G)** Number of viable fetuses/litter (mean ± SEM; n = 8). **(H)** Percentage of fetal death (median, interquatile range; n = 8). **(I)** Fetal weight (mean ± SEM; n = 63-76). **(J)** Relative frequency distribution curve of fetal weight. **(K)** Weight of fetal organs (liver, brain, heart, lung, kidney) (mean ± SEM; n = 15-30). **(L)** Brain/liver ratio (mean ± SEM; n = 15-30). Significant differences were determined by ANOVA *post hoc* SNK except for fetal weight and fetal organs' weight, which were determined by Generalized linear mixed-model analysis followed by the Tukey test, and fetal death which was determined by Dunn's *post hoc* Kruskal-Wallis test, *P<0.05, **P<0.01, ***P<0.001, ****P<0.0001. KpT1, yes/no day treatment with Kp10; KpT2, daily treatment with Kp10; GD, gestational day.

Kisspeptin treatment improves placental development in hypothyroid rats

After observing that daily treatment with Kp-10 improved fetal development in hypothyroid rats, it was necessary to assess whether this effect could result from improved placental morphology (Figures 2A–D). No difference was observed in the thickness of the junctional zone between the experimental groups, while the hypothyroid and KpT1 groups showed reduced thickness of the labyrinth zone when compared to the control group (Figure 2E; P<0.05). In the cellularity evaluation of the junctional zone, the placenta of hypothyroid animals had a higher percentage of area

10.3389/fendo.2022.908240

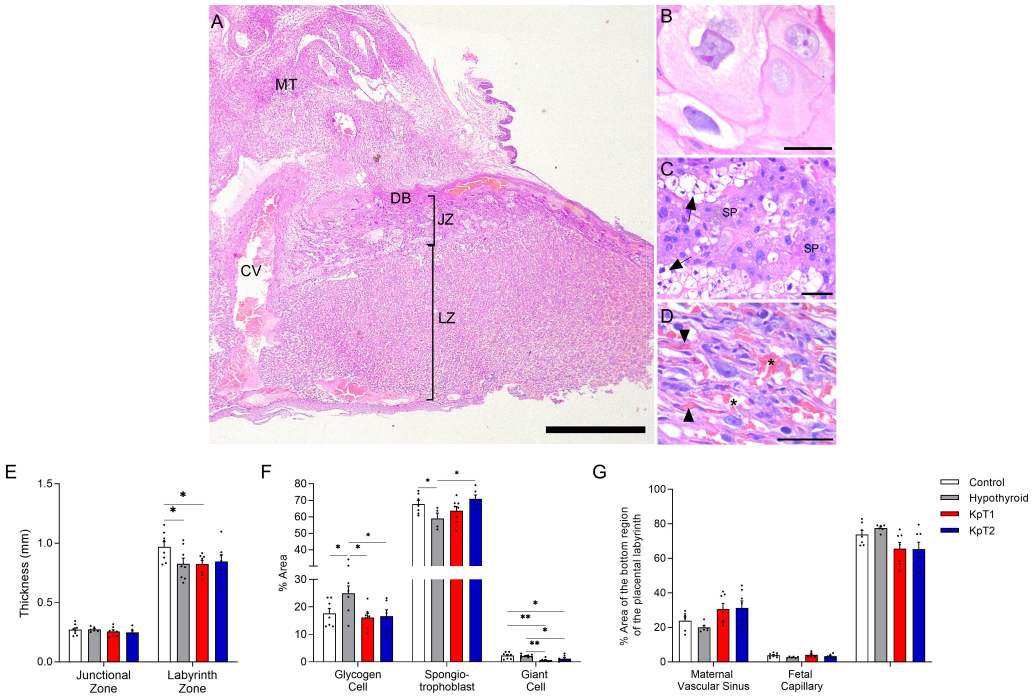


FIGURE 2
Histomorphometry evaluation of the placenta of control, hypothyroid, and kisspeptin-10 treated-rats on the 18th GD. **(A–D)** Illustrative photomicrographs of the maternal-fetal interface **(A)** and placental layers **(B)**, giant cells; **(C)**, spongiotrophoblast; **(D)**, labyrinth zone) (Hematoxylin and eosin staining; Bar = 500µm **(A)**; 50µm **(B–D)**. **(E)** Thickness of the junctional zone (giant cells+spongiotrophoblast) and labyrinth zone (mean ± SEM; n = 8). **(F)** Percentage of area occupied by glycogen cells, spongiotrophoblasts, and giant cells in the junctional zone (mean ± SEM; n = 8). **(G)** Percentage of area occupied by maternal vascular sinus, fetal capillaries, and fetal mesenchyme/trophoblast in the labyrinth zone (mean ± SEM; n = 8). Significant differences were determined by ANOVA *post hoc* SNK, *P<0.05, **P<0.01. MT, mesometrial triangle; BD, basal decidua; JZ, junctional zone; LZ, labyrinth zone; CV, central vessel; SP, spongiotrophoblast; Arrow, glycogen cells; Arrowhead, fetal capillaries; Asterisks, maternal vascular sinus; KpT1, yes/no day treatment with Kp-10; KpT2, daily treatment with Kp-10; GD, gestational day.

occupied by glycogen cells and fewer spongiotrophoblasts when compared to the control group (P<0.05). The treatments with KpT1 and KpT2 were able to restore the population of glycogen cells and/or spongiotrophoblasts in the placenta of hypothyroid animals, resembling that of the control animals (Figure 2F; P>0.05). A significant reduction was also observed in the giant cells from junctional zone in the KpT1 and KpT2 groups compared to the control (P<0.01;P<0.05) and to the hypothyroid group (Figure 2F; P<0.01;P<0.05). In the evaluation of the labyrinth zone, no significant difference was observed in the regions evaluated (fetal capillary, maternal vascular sinus and fetal mesenchyme/trophoblastic cells) between the groups (Figure 2G; P>0.05).

Kisspeptin treatment increases placental gene expression of growth (*Plgf*, *Igf1*) and transport (*Glut1*) factors in rats with hypothyroidism

The macroscopic evaluations of fetal-placental development and histological evaluations of the placenta showed that daily treatment with Kp10 had a better effect on fetal and placental development of hypothyroid rats, particularly by improving fetal weight distribution and junctional zone cellularity, while the group KpT1 presented negative effects on fetal organogenesis. For this reason, the placental expression of growth (VEGF, PLGF, IGF1, IGF2) and hormonal (Dio2) factors, and transporters (GLUT1) was evaluated in the KpT2 group in relation to the control and hypothyroid groups, as the altered expression of these factors is associated with altered fetal-placental growth (51–54).

Immunolabeling for VEGF was cytoplasmic and heterogeneous in trophoblasts in the junctional and labyrinth zones, regardless of the experimental group. However, the analysis of the labeled area revealed that the hypothyroid and KpT2 groups had higher expression of VEGF in the junctional zone when compared to the control group (Figures 3A–C, G). This was also observed in the placental gene transcript expression for *Vegf*, which had higher expression in the hypothyroid and KpT2 groups compared to the control group (Figure 3H; P<0.05). In the labyrinth zone, on the other hand, KpT2 treatment reduced VEGF immunolabeling compared to the hypothyroid group (P<0.001), equaling the

10.3389/fendo.2022.908240

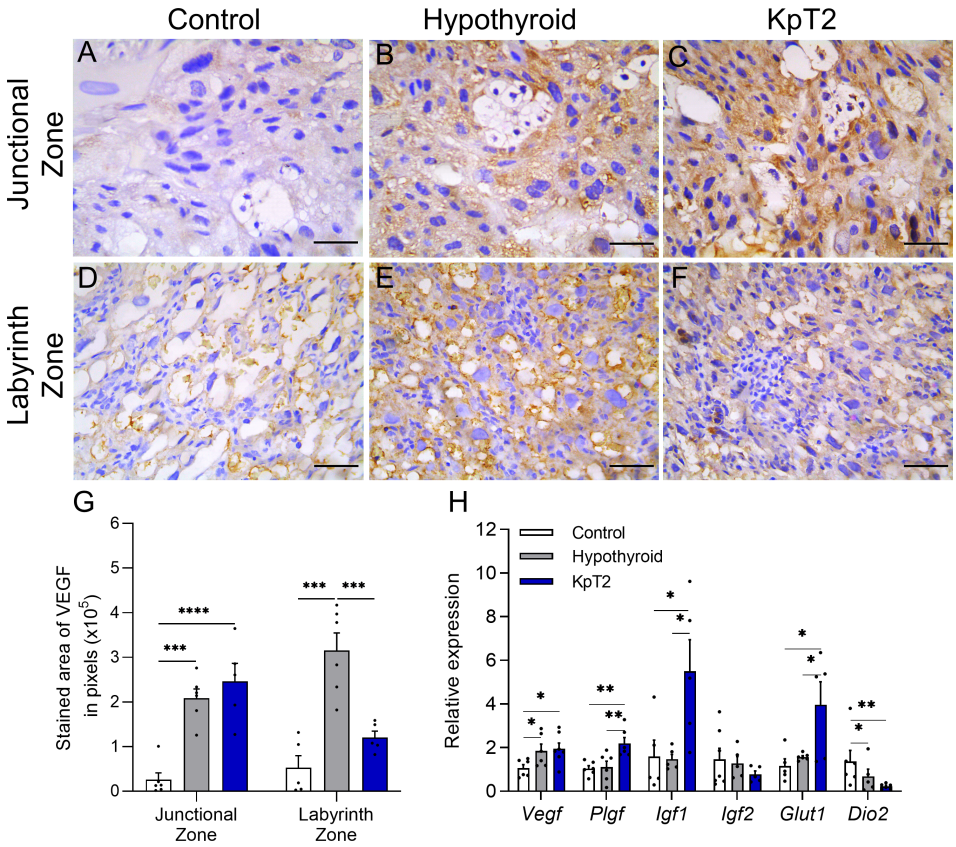


FIGURE 3
Expression of VEGF, PIGF, IGF1, IGF2, GLUT1 and DIO2 in the placenta of control, hypothyroid, and kisspeptin-10-treated rats on the 18th GD. **(A–F)** Photomicrographs of immunohistochemical expression of VEGF in the junctional zone **(A–C)** and labyrinth zone **(D–F)** (Streptavidin-biotin-peroxidase; Harris hematoxylin; Bar = 50 µm). **(G)** Immunolabeling area, in pixels, of VEGF expression in the junctional zone and labyrinth zone on the 18 GD (mean ± SEM; n = 8). **(H)** Relative gene expression of *Vegf, Pigf, Igf1, Igf2, Glut1, and Dio2* in the placenta (mean ± SEM; n = 8). Significant differences were determined ANOVA post hoc SNK, *P<0.05, **P<0.01, ***P<0.001, ****P<0.0001. KpT2, daily treatment with Kp10; GD, gestational day.

control group (Figures 3D–G; P>0.05). Regarding the other placental growth and transport factors, daily treatment with Kp10 significantly increased mRNA expression for *Plgf, Igf1*, and *Glut1* in the placenta when compared to the control and hypothyroid groups (Figure 3H; P<0.05; P<0.01). For *Igf2*, no difference was observed between the groups (P>0.05), while *Dio2* had lower expression in the hypothyroid and KpT2 groups compared to the control group (Figure 3H; P<0.01; P<0.01).

Kisspeptin treatment alters placental IL10 and TNFα expression in rats with hypothyroidism

Since fetal-placental development is influenced by immune mediators produced by the placenta, and considering that previous studies have shown that maternal hypothyroidism affects placental TNFα, MIF, and NOS2 expression in rats (36), the effect of daily treatment with Kp-10 on placental TNFα, IL-10, and IL-6 expression was evaluated in hypothyroid rats. TNFα and IL-10 immunolabeling was cytoplasmic in trophoblastic cells of the junctional and labyrinth zones, and was heterogeneous for TNFα and homogeneous for IL-10 (Figures 4A, C). Immunolabeling for TNFα was more intense in the junctional zone of the Kp10 group than in the control and hypothyroid groups (Figure 4A), as confirmed by the immunolabeling area analysis (Figure 4B; P<0.05). In the labyrinth zone, hypothyroid rats showed higher TNFα expression compared to the control (P<0.05), while the Kp10 treatment was similar to the hypothyroid group (P>0.05). No significant differences in mRNA expression for *Tnf* were observed between the groups (Figure 4E; P>0.05).

For IL-10, both the hypothyroid and KpT2 groups showed higher immunolabeling in the junctional zone compared to the

10.3389/fendo.2022.908240

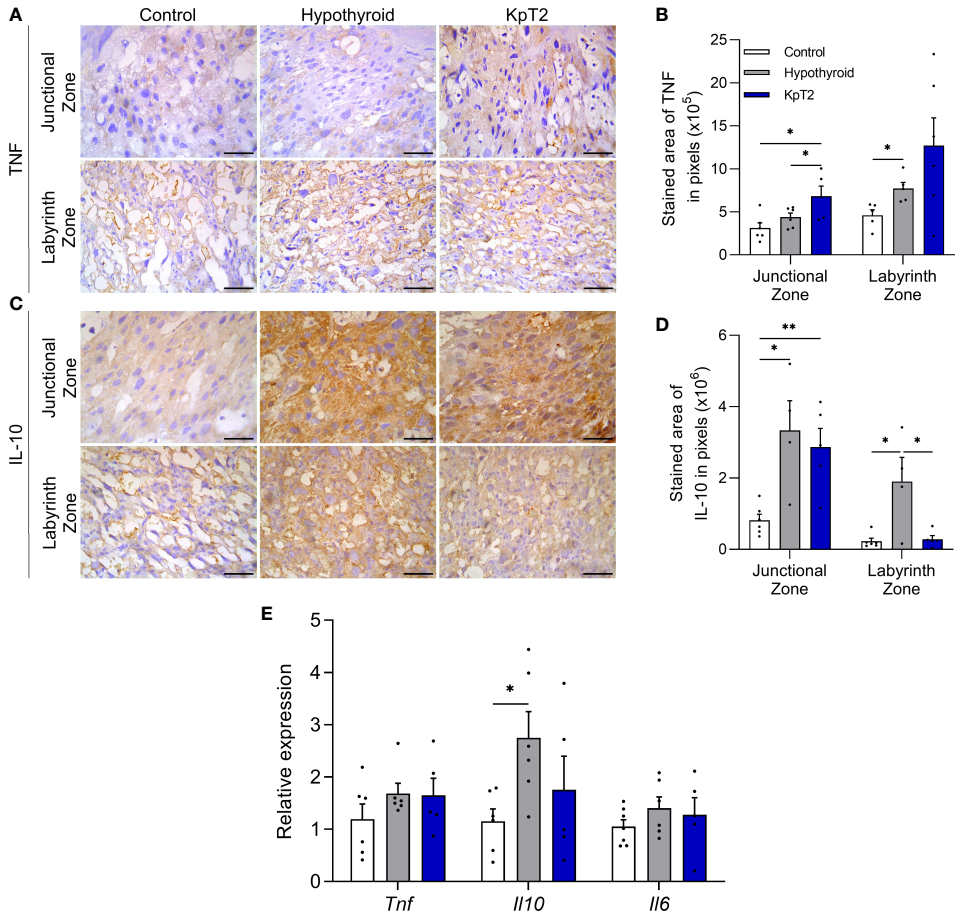


FIGURE 4
Expression of TNFα, IL-10, and IL-6 in the placenta of control, hypothyroid, and kisspeptin-10-treated rats on the 18th GD. **(A)** Photomicrographs of immunohistochemical expression of TNFα in the junctional zone and labyrinth zone (Streptavidin-biotin-peroxidase; Harris hematoxylin; Bar = 50 μm). **(B)** Immunolabeling area, in pixels, of TNFα expression in the junctional zone and labyrinth zone (mean ± SEM; n = 8). **(C)** Photomicrographs of immunohistochemical expression of IL-10 in the junctional zone and labyrinth zone (Streptavidin-biotin-peroxidase; Harris hematoxylin; Bar = 50 μm). **(D)** Immunolabeling area, in pixels, of IL-10 expression in the junctional zone and labyrinth zone (mean ± SEM; n = 8). **(E)** Relative gene expression of *Tnf*, *Il10*, and *Il6* in the placenta (mean ± SEM; n = 8). Significant differences were determined by ANOVA *post hoc* SNK, *P<0.05, **P<0.01. KpT2, daily treatment with Kp10; GD, gestational day.

control (Figure 4C), as confirmed by the immunolabeling area analysis (Figure 4D; P<0.05; P<0.01). In the labyrinth zone, however, while hypothyroidism also increased the IL-10 labeling area when compared to the control (P<0.05), Kp10 treatment reduced IL-10 immunolabeling, matching it to that of the control group (Figure 4D; P>0.05). As observed in the immunohistochemistry, hypothyroidism increased mRNA expression for *Il10* compared to the control (P<0.05), while daily treatment with Kp10 showed no significant differences compared to the control and hypothyroid groups (Figure 4E; P>0.05). There was no difference in the mRNA expression for *Il6* between the groups (Figure 4E).

Kisspeptin treatment blocks oxidative damage in the junctional zone of hypothyroid rats

Since oxidative stress is associated with placental dysfunction (55–57), and maternal hypothyroidism has been recently reported to cause oxidative damage in rat placenta (40), it was important to evaluate whether daily treatment with Kp10 can reverse or reduce this oxidative stress caused by hypothyroidism. To this end, the gene and/or protein expression profile of HIF1α and 8-Hydroxy-2′-deoxyguanosine (8-OHdG), biomarkers of hypoxia and oxidative DNA damage, respectively (58–60), were analyzed.

10.3389/fendo.2022.908240

HIF1α and 8-OHdG immunolabeling were cytoplasmic and heterogeneous in trophoblastic cells of the junctional and labyrinth zones, regardless of the experimental group (Figures 5A, B). In the HIF1α immunolabeling analysis, both the hypothyroid and Kp10-treated groups showed a larger immunolabeling area in the junctional zone when compared to the control (Figures 5C, P<0.05). In the labyrinth zone, in contrast, no significant differences in immunolabeling were observed between the groups (P>0.05). However, in gene evaluation, similar to the result of junctional zone immunolabeling, the hypothyroid and Kp10-treated groups showed higher placental mRNA expression of *Hif1α* compared to the control (Figure 5E; P<0.05).

Regarding 8-OHdG immunolabeling, Kp10 treatment reduced the greater immunolabeling in the junctional zone caused by hypothyroidism (P<0.05), equaling the control (Figure 5D; P >0.05). No difference was observed in 8-OHdG expression in the labyrinth zone between the groups (P>0.05).

Kisspeptin treatment increases placental expression of antioxidant enzymes in hypothyroid rats

Since studies have already demonstrated that exogenous administration of kisspeptin exhibits antioxidant action in the

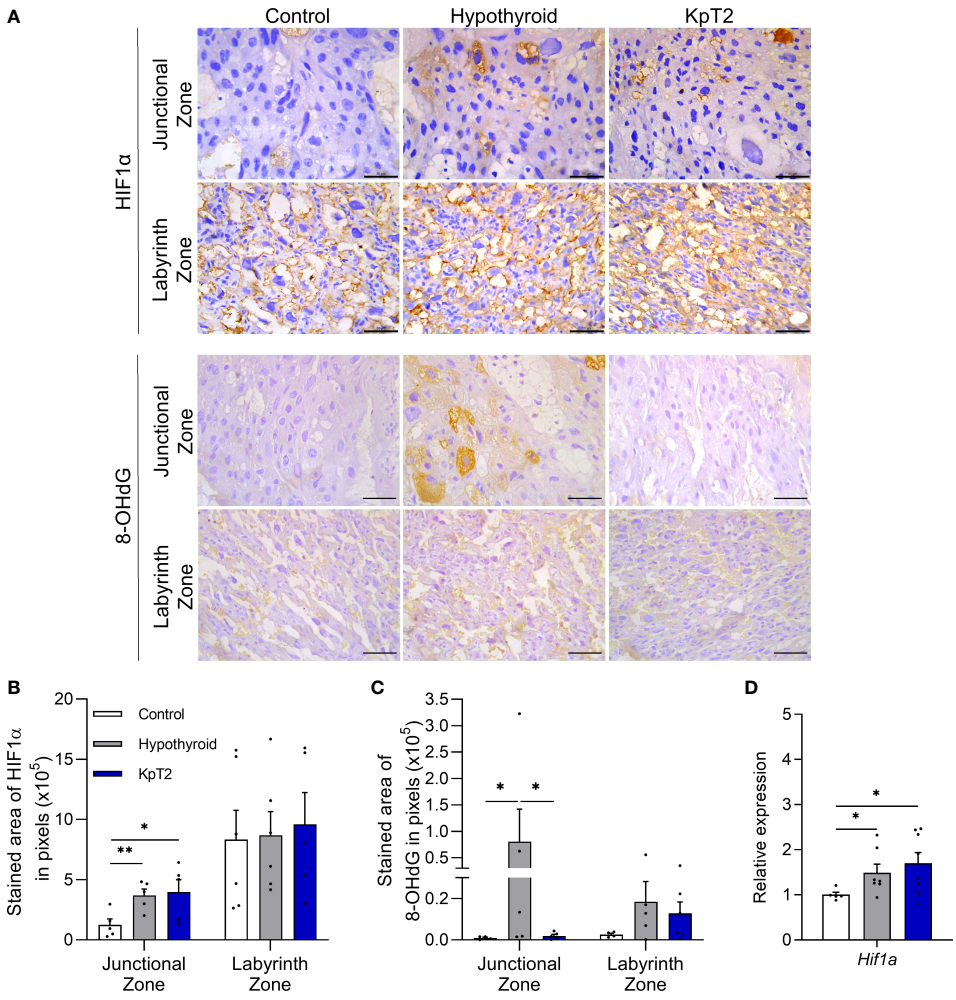


FIGURE 5
Expression of HIF1α and 8-OHdG in the placenta of control, hypothyroid, and kisspeptin-10-treated rats on the 18th GD. **(A)** Photomicrographs of immunohistochemical expression of HIF1α in the junctional zone and labyrinth zone (Streptavidin-biotin-peroxidase; Harris hematoxylin; Bar = 50 μm). **(B)** Immunolabeling area, in pixels, of HIF1α expression in the junctional zone and labyrinth zone (mean ± SEM; n = 8). **(C)** Immunolabeling area, in pixels, of HIF1α expression in the junctional zone and labyrinth zone (mean ± SEM; n = 8). **(D)** Relative gene expression of *Hif1α* in the placenta (mean ± SEM; n = 8). Significant differences were determined by ANOVA *post hoc* SNK, *P<0.05, **P<0.01. KpT2, daily treatment with Kp10; GD, gestational day.

10.3389/fendo.2022.908240

ovary (43), liver (44), and testicle (45), the placental profile of SOD1, catalase, and GPx1/2 was evaluated for the animals in the present study. The immunostaining of SOD1, catalase, and GPx1/2 was cytoplasmic and heterogeneous in trophoblast cells of the junctional and labyrinth zones, and the expression of catalase was weaker in the junctional zone when compared to that of SOD1 and GPx1/2 (Figures 6A, C and E). Treatment with Kp10 significantly increased the expression of SOD1 and catalase in the junctional zone when compared to the control and hypothyroid groups (Figures 6B, D; P<0.01, P<0.0001). In the labyrinth zone, while the KpT2 group showed reduced SOD1 immunolabeling compared to the control (P<0.05), Kp10

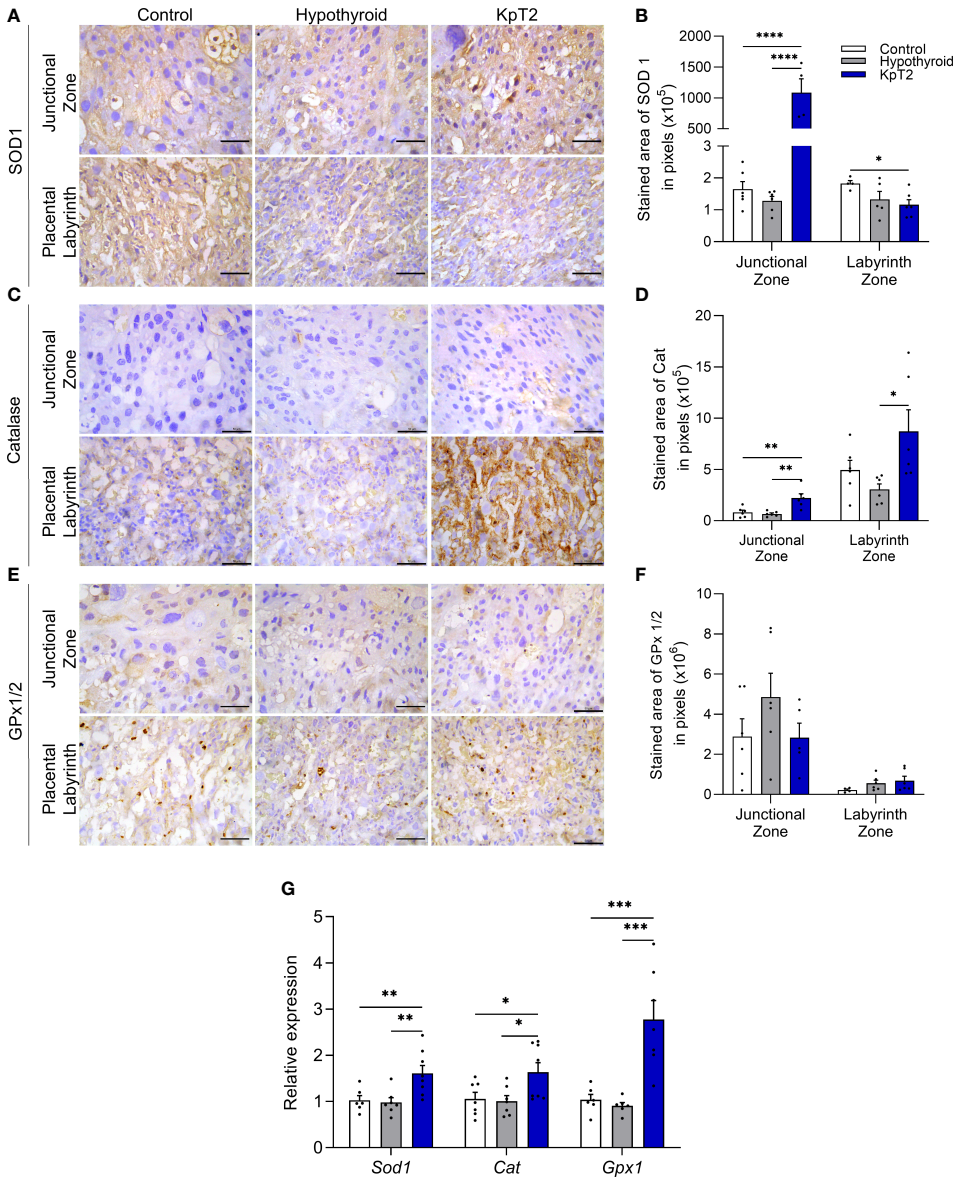


FIGURE 6
Expression of SOD1, catalase, and GPx1/2 in the placenta of control, hypothyroid, and kisspeptin-10-treated rats on the 18th GD. **(A)** Photomicrographs of immunohistochemical expression of SOD1 in the junctional zone and labyrinth zone (Streptavidin-biotin-peroxidase; Harris hematoxylin; Bar = 50 µm). **(B)** Immunolabeling area, in pixels, of SOD1 expression in the junctional zone and labyrinth zone (mean ± SEM; n = 8). **(C)** Photomicrographs of immunohistochemical expression of catalase in the junctional zone and labyrinth zone (Streptavidin-biotin-peroxidase; Harris hematoxylin; Bar = 50 µm). **(D)** Immunolabeling area, in pixels, of catalase expression in the junctional zone and labyrinth zone (mean ± SEM; n = 8). **(E)** Photomicrographs of the immunohistochemical expression of GPx1/2 in the junctional zone and labyrinth zone (Streptavidin-biotin-peroxidase; Harris hematoxylin; Bar = 50 µm). **(F)** Immunolabeling area, in pixels, of GPx1/2 expression in the junctional zone and labyrinth zone (mean ± SEM; n = 8). **(G)** Relative gene expression of *Sod1*, *catalase*, and *Gpx1* in the placenta (mean ± SEM; n = 8). Significant differences were determined by ANOVA *post hoc* SNK, *P<0.05, **P<0.01, ***P<0.001, ****P<0.0001. KpT2, daily treatment with Kp10; GD, gestational day.

treatment increased catalase expression when compared to the hypothyroid group (Figures 6B, D; P<0.05). No significant difference was observed in the GPx1/2 immunolabeling between groups in both the junctional zone and labyrinth zone (Figure 6F; P>0.05). However, in the gene transcript expression analysis, *Gpx1*, *Sod1*, and *Cat* showed higher mRNA expression in the Kp10-treated group when compared to the control and hypothyroid groups (Figure 6G).

Kisspeptin treatment affects the expression of reticular stress mediators in the placenta of hypothyroid rats

Since maternal hypothyroidism causes reticular stress in rat placenta (40), and *in vitro* and *in vivo* studies have demonstrated that Kp-10 administration blocks the occurrence of reticular stress in hypothalamic neuronal cells exposed to androgen (46), it was evaluated whether Kp-10 treatment would affect the expression of GRP78, CHOP and ATF4 in the placenta of rats with hypothyroidism. Immunolabeling of these three mediators was cytoplasmic and heterogeneous in the junctional and labyrinth zones, and expression in the junctional zone was usually in isolated spongiotrophoblast cells or in glycogen cells (Figures 7A, C and E). According to the immunolabeling area analysis, the hypothyroid group showed higher immunolabeling of GRP78 and CHOP in the junctional zone when compared to the control (Figures 7B, D; P<0.05), while the KpT2 group showed no significant difference compared to the hypothyroid group for CHOP. However, with respect to GRP78, Kp-10 treatment increased immunolabeling in the junctional zone when compared to the control and hypothyroid groups (Figure 7B; P<0.05; P<0.01). In contrast, in the labyrinth zone, KpT2 treatment reduced the immunolabeled area of both GRP78 and CHOP relative to the hypothyroid group (Figures 7B, D; P<0.05; P<0.01). For ATF4, no differences in the immunolabeling area were observed between the groups (Figures 7F; P>0.05).

In the gene transcript analysis, treatment with Kp-10 increased the placental expression of *Grp78* compared to the control and hypothyroid groups (P<0.0001), as observed in junctional zone immunolabeling, while an increase in *Chop* gene expression was also observed relative to the hypothyroid group (Figure 7G; P<0.05). Taken together, these results demonstrate that daily treatment with Kp10 differentially affects the expression of reticular stress mediators in the placenta of hypothyroid rats since it maintains high expression in the junctional zone and reduces immunolabeling in the labyrinth zone.

Discussion

Although the kisspeptin/Kiss1R system is mainly known for its action on the hypothalamic-pituitary-gonadal axis, stimulating the secretion of GnRH/LH, studies have shown that kisspeptin has peripheral action in the genital tract (5, 6). and gestational dysfunctions such as preeclampsia, spontaneous abortion, gestational diabetes, obesity, and even maternal hypothyroidism, are associated with alterations in the serum and/or placental profile of kisspeptin (12, 17, 20, 26–28, 30, 31). The results of the present study demonstrated that daily kisspeptin treatment was able to improve fetal development and placental morphology in hypothyroid rats. This improvement in fetal-placental development was associated with both increased expression of growth and transport factors in the placenta *(Plgf*, *Igf1*, and *Glut1*), and with blockage of placental oxidative damage and increased antioxidant enzymes (SOD1, catalase, GPx1).

Daily treatment with Kp-10 from the 8th GD not only increased maternal weight gain and plasma free T3 and T4 levels of hypothyroid rats, but also improved fetal weight distribution, which was not observed in the treatment performed every other day. These results reaffirm the need for precise control of kisspeptin plasma levels during pregnancy, since only daily treatment with Kp-10 had a positive effect on maternal weight gain, fetal weight distribution and on free T3 and T4 levels. This is the first *in vivo* study to demonstrate that kisspeptin can modulate the Corroborating our study, Radwańska and Kosior-Korzecka (61) demonstrated that *in vitro* treatment of ovine pituitary cells with 10^{-11} to 10^{-8} M of Kp10 increased TSH secretion. However, despite the increase in plasma levels of free T3 and T4 caused by the daily treatment with Kp-10, it is suggested that the local availability of T3 in the placenta has not changed, since the treatment with Kp-10 did not change the lower placental expression of *Dio2* caused by hypothyroidism, the enzyme responsible for the intracellular availability of T3 (62). This reduction of *Dio2* in the placenta of the hypothyroid rats may be associated with fetoplacental dysfunction presented by these animals, since *Dio2* is involved in proliferation, differentiation and trophoblastic migration and low placental expression was associated early recurrent miscarriage (54).

The increase in the maternal weight gain and improviment fetal weight distribution of hypothyroid rats may be associated not only with increased levels of free T3 and T4 but also with the action of kisspeptin on maternal pancreatic function, as exogenous kisspeptin increases *in vivo* and *in vitro* insulin secretion by pancreatic β-cells in rats, mice, humans, and non-human primates (63–67), and pharmacological blockade or *in vivo* genetic ablation of the Kiss1R receptor in β-cells of pregnant mice results in glucose intolerance and impaired insulin secretion (68).

For fetal weight distribution, most fetuses (61.49%) of the hypothyroid group were below the 5th percentile of the control group, indicating the growth restriction (48, 50, 69, 70). Once the reduced body weight was accompanied by reduced fetal organ weight (heart and lung), prioritizing the brain

10.3389/fendo.2022.908240

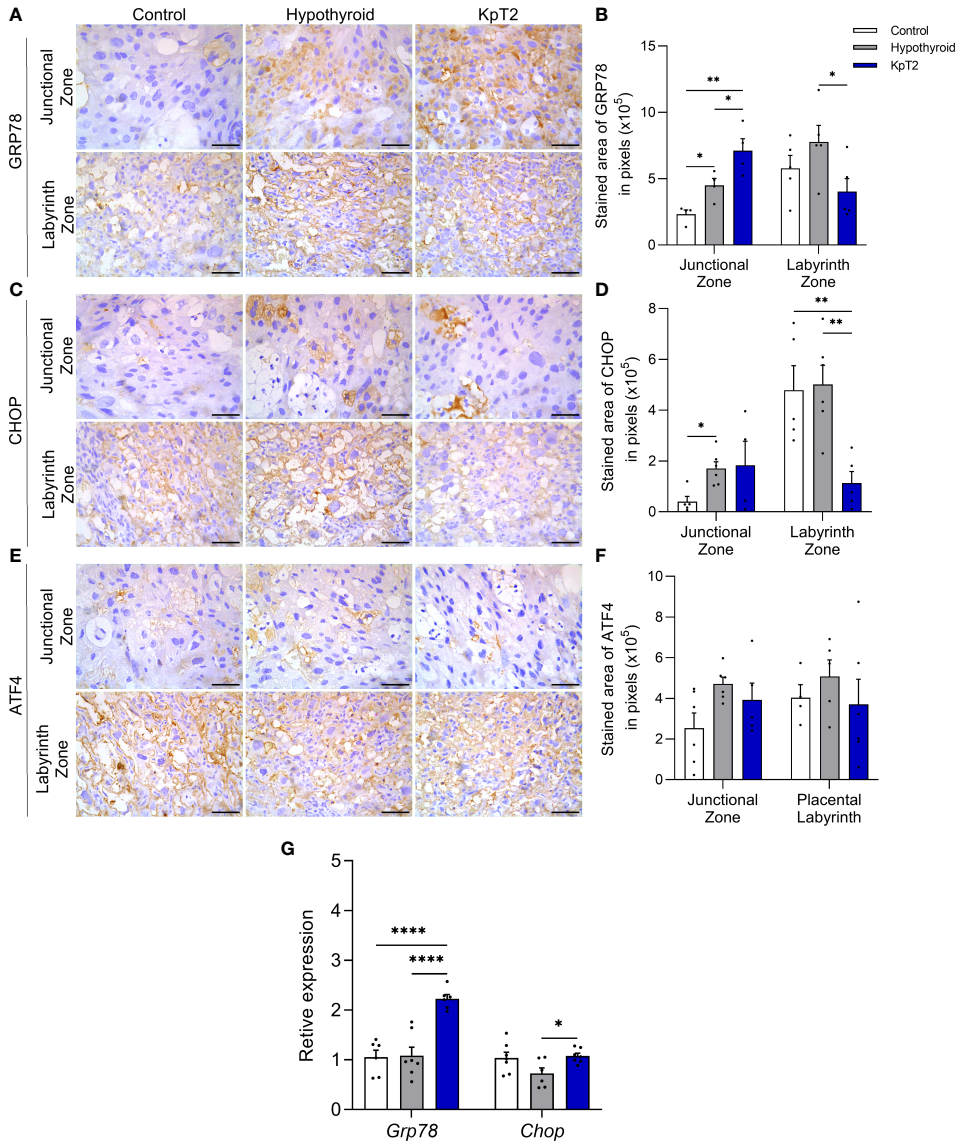


FIGURE 7
Expression of GRP78, CHOP, and ATF4 in the placenta of control, hypothyroid, and kisspeptin-10-treated rats on the 18th GD. **(A)** Photomicrographs of immunohistochemical expression of GRP78 in the junctional zone and labyrinth zone (Streptavidin-biotin-peroxidase; Harris hematoxylin; Bar = 50 µm). **(B)** Immunolabeling area, in pixels, of GRP78 expression in the junctional zone and labyrinth zone (mean ± SEM; n = 8). **(C)** Photomicrographs of immunohistochemical expression of CHOP in the junctional zone and labyrinth zone (Streptavidin-biotin-peroxidase; Harris hematoxylin; Bar = 50 µm). **(D)** Immunolabeling area, in pixels, of CHOP expression in the junctional zone and labyrinth zone (mean ± SEM; n = 8). **(E)** Photomicrographs of immunohistochemical expression of ATF4 in the junctional zone and labyrinth zone (Streptavidin-biotin-peroxidase; Harris hematoxylin; Bar = 50 µm). **(F)** Immunolabeling area, in pixels, of ATF4 expression in the junctional zone and labyrinth zone (mean ± SEM; n = 8). **(G)** Relative gene expression of *Grp78* and *Chop* in the placenta (mean ± SEM; n = 8). Significant differences were determined by ANOVA *post hoc* SNK, *P<0.05, **P<0.01, ****P<0.0001. KpT2, daily treatment with Kp10; GD, gestational day.

development, we suggest the growth restriction caused by hypothyroidism was asymmetric, even though was no difference in the liver/brain ratio (48, 50, 71). Daily treatment with Kp-10 improved fetal weight distribution once most of the fetal weight (87.30%) were above the 5th percentile of the control group. This outcome in terms of fetal development is very important, as fetal growth restriction is associated with an increased risk of cardiovascular and metabolic diseases in postnatal life (51, 72).

However, optimal fetal development depends not only on maternal and fetal metabolism but also on adequate placental function (32). In the present study, daily treatment with Kp10 also improved the placental morphology of hypothyroid rats by restoring the proportion of trophoblastic cells forming the

junctional zone. Previous studies have also demonstrated altered trophoblast population in the junctional zone of hypothyroid rats (35). The cells in the junctional zone are mainly responsible for the synthesis and secretion of peptides and hormones by the placenta, which are fundamental for controlling maternal and fetal metabolism (73).

In addition to improving placental morphology, daily treatment with Kp-10 increased mRNA expression for *Plgf, Igf1*, and *Glut1* in the placenta. These factors are decisive for proper fetal growth and placental development (32, 51, 74, 75). PLGF is responsible for placental vascular bed maturation (76), and low plasma PLGF levels are associated with fetal growth restriction, HELLP syndrome, preeclampsia, and gestational hypertension (74). Therefore, plasma PLGF is considered an important predictor of fetal development (74). Reduced placental expression of IGF1 also compromises fetal and placental development (75), while GLUT1 is an important placental glucose transporter. The expression of GLUT1 is reduced when the placental expression of IGF1 fails (77, 78).Therefore, in the present study, restored fetal weight distribution caused by Kp-10 treatment may have also resulted from increased placental IGF1/GLUT1 signaling, as kisspeptin stimulates the release of insulin (63–68).

However, in relation to VEGF, treatment with Kp-10 did not reverse the increase in placental gene and protein expression caused by hypothyroidism, particularly in the junctional zone. In addition to the critical role of VEGF in the process of placental angiogenesis, especially in early to mid-gestation (79), it is an indicator of hypoxia since low oxygen levels stimulate its expression (80). In this sense, higher gene expression of VEGF in the placenta of hypothyroid and Kp-10-treated animals, and the higher immunolabeling in the junctional zone, suggest a low oxygen tension environment in the junctional zone of these animals. This hypothesis is supported by the higher gene and protein expression of HIF1α, especially in the junctional zone, observed in the hypothyroid and Kp-10-treated animals. HIF1α is expressed under hypoxic conditions and performs its functions in vascular permeability and cell survival by signaling *via* VEGF (81). Furthermore, studies have already demonstrated increased expression of HIF1α and VEGF in preeclamptic placentas, which are known to present a hypoxic environment (81–83). However, when evaluating the labyrinth zone, Kp10 treatment reduced the increase in VEGF immunolabeling caused by hypothyroidism, matching its expression to that of the control animals. These data reinforce the importance of immunohistochemistry analysis to discriminate and adequately evaluate the protein expression profile of the mediators evaluated in each region of the placenta.

Regarding TNFα, Kp10 treatment increased immunolabeling in the junctional zone, while in the labyrinth zone, hypothyroid animals showed higher expression compared to the control animals. *In vitro* studies have shown that TNFα secreted by decidual macrophages is recognized by TNF-R1 receptors in the trophoblasts and activates the extrinsic apoptosis pathway (84), while, according to a recent study, kisspeptin increases cell apoptosis (85). Therefore, Kp-10 treatment may have increased activation of placental apoptosis *via* TNFα signaling, although studies are needed to confirm this hypothesis. However, increased TNFα also occurs with increasing insulin resistance (86). Thus, another possibility to explain its higher expression in the junctional zone of Kp-10-treated animals may be the increase in insulin that occurs after kisspeptin administration (63–68).

As observed for TNFα, IL-10 showed higher expression in the junctional zone of hypothyroid and Kp-10-treated animals compared to the control, as well as higher gene expression in the placenta of hypothyroid animals. This increase in IL-10 may be a reflection of increased TNFα expression, as IL-10 attenuates the effects of pro-inflammatory cytokines at the maternal-fetal interface (38, 87) and TNFα stimulates the *in vitro* secretion of IL-10 in first-trimester trophoblastic villi (88). However, Kp-10 treatment reduced the higher IL-10 immunolabeling in the labyrinth zone caused by hypothyroidism, matching it to that of the control. Further studies are needed to elucidate the reduction of IL10 and VEGF in the labyrinth zone of the hypothyroid rats caused by Kp10 treatment.

As previously described, the increased mRNA and immunolabeling of HIF1α in the junctional zone of hypothyroid and Kp-10-treated animals signals low oxygen tension and suggests the occurrence of oxidative stress in the placenta of hypothyroid rats, which was recently confirmed in a previous study (40). Activation of HIF1α in the placenta of rats also favors the reduction of labyrinth zone thickness (89), thus corroborating the histomorphometry results of the present study. Moreover, Kp-10 treatment blocked the increase in placental immunolabeling of 8-OHdG caused by hypothyroidism. 8-OHdG is a biomarker of oxidative stress that signals DNA damage resulting from oxidative stress and lipid peroxidation (90), and studies have shown increased placental expression in preeclampsia, gestational diabetes mellitus, and maternal smoking (60, 90, 91). Thus, the results of the present study suggest that although Kp-10 treatment was not able to protect against placental hypoxia caused by maternal hypothyroidism, it was effective in protecting against the occurrence of placental oxidative damage.

Daily treatment with Kp-10 also increased the gene and/or protein expression of SOD1, catalase, and GPx1 in the placenta of hypothyroid rats. This suggests an antioxidant function of kisspeptin at the maternal-fetal interface. These results are in line with those of previous studies conducted on the ovary (43), liver (44), and testicle (45), that demonstrated increased antioxidant enzymes after kisspeptin treatment. Thus, together, these data suggest that in the condition of placental oxidative stress caused by hypothyroidism, treatment with Kp-10 can improve placental antioxidant defenses, inhibit oxidative damage, and, consequently, improve fetus and placenta development.

Furthermore, hypothyroidism increased immunolabeling in the junctional zone of endoplasmic reticulum stress mediators, GRP78, and CHOP, another pathophysiological process involved in placental dysfunction in preeclamptic women (92–94) and that has been recently demonstrated in the placenta of hypothyroid rats (40). Interestingly, although treatment with Kp-10 was not able to reverse the expression of these mediators in the junctional zone of hypothyroid rats, including with increased placental gene expression of *Grp78* and *Chop* when compared to the hypothyroid group, Kp-10 treatment reduced GRP78 and CHOP immunolabeling in the labyrinth zone of hypothyroid animals. This suggests attenuation of reticular stress in this placental layer after Kp-10 treatment. Furthermore, a recent study demonstrated *in vitro* in hypothalamic GT1-7 cells, that silencing of *Kiss1* or inhibition of *Kiss1r* with the antagonist Kp234 resulted in endoplasmic reticulum stress, while treatment with Kp-10 blocked its activation (46). Since maternal hypothyroidism in rats reduces placental and decidual expression of the Kiss/Kiss1r system (31), this may also be one of the reasons for the activation of reticular stress in the placenta of these animals (40).

The findings of this study demonstrated that daily treatment with Kp-10 in hypothyroid pregnant rats was able to improve fetus and placenta development and the plasma free T3 and T4 levels. This improvement was associated with not only increased expression of placental growth factors and antioxidant enzymes, but also with blockage of oxidative damage and positive modulation of reticular stress mediators, IL-10, and VEGF in the labyrinth zone. This is the first study to use kisspeptin as a therapeutic tool in a gestational disease.

Data availability statement

The raw data supporting the conclusions of this article will be made available by the authors, without undue reservation.

Ethics statement

The animal study was reviewed and approved by Ethics Committee on the Use of Animals of Santa Cruz State University (UESC) (Protocol 036/16).

Author contributions

BS and JS conceived and designed the study. BS, JA, EB, and LS conducted sample collection. BS and EB conducted the evaluation of maternal and fetus data. BS conducted histopathological preparation and analysis. BS, JA, LS, ES, LM, IM, and JS performed immunohistochemistry analysis. BS, JA, LS, and JS performed qRT-PCR. BS and JS analyzed data. JS, ML, RES, and RS provided reagents. BS and JS wrote the paper. All authors read and approved the manuscript. All authors contributed to the article and approved the submitted version.

Funding

This work was supported by Conselho Nacional de Desenvolvimento Cientifico e Tecnologico (CNPq), Universidade Estadual de Santa Cruz (UESC) and Coordenaçao de Aperfeiçoamento de Pessoal de Nivel Superior (Capes).

Acknowledgments

The authors thank Ivo Arouca (*Universidade Estadual de Santa Cruz, Ilheus, Brazil*) by the technical support provided.

Conflict of interest

The authors declare that the research was conducted in the absence of any commercial or financial relationships that could be construed as a potential conflict of interest.

Publisher's note

All claims expressed in this article are solely those of the authors and do not necessarily represent those of their affiliated organizations, or those of the publisher, the editors and the reviewers. Any product that may be evaluated in this article, or claim that may be made by its manufacturer, is not guaranteed or endorsed by the publisher.

Supplementary material

The Supplementary Material for this article can be found online at: https://www.frontiersin.org/articles/10.3389/fendo.2022.908240/full#supplementary-material

SUPPLEMENTARY FIGURE 1
Immunohistochemistry. **(A–B)** Representative images of the junctional zone **(A)** and the labyrinth zone **(B)** in the negative control. **(C)** Antibodies used with their respective dilutions and incubation and revelation times.

References

1. Kotani M, Detheux M, Vandenbogaerde A, Communi D, Vanderwinden J-M, Le Poul E, et al. The metastasis suppressor gene KiSS-1 encodes kisspeptins, the natural ligands of the orphan G protein-coupled receptor GPR54. *Cell Mol Life Sci* (2019) 76:3479–96. doi: 10.1074/jbc.M104847200

2. Ohtaki T, Shintani Y, Honda S, Matsumoto H, Hori A, Kanehashi K, et al. Metastasis suppressor gene KiSS-1 encodes peptide ligand of a G-protein-coupled receptor. *Nature* (2001) 411:613–7. doi: 10.1038/35079135

3. de Roux N, Genin E, Carel J-C, Matsuda F, Chaussain J-L, Milgrom E. Hypogonadotropic hypogonadism due to loss of function of the KiSS1-derived peptide receptor GPR54. *Proc Natl Acad Sci* (2003) 100:10972–6. doi: 10.1073/pnas.1834399100

4. Seminara SB, Messager S, Chatzidaki EE, Thresher RR, Acierno JS, Shagoury JK, et al. The GPR54 gene as a regulator of puberty. *N Engl J Med* (2003) 349:1614–27. doi: 10.1056/NEJMoa035322

5. Cao Y, Li Z, Jiang W, Ling Y, Kuang H. Reproductive functions of Kisspeptin/KISS1R systems in the periphery. *Reprod Biol Endocrinol* (2019) 17:1–9. doi: 10.1186/s12958-019-0511-x

6. D'Occhio MJ, Campanile G, Baruselli PS, D'Occhio MJ, Campanile G, Baruselli PS. Peripheral action of kisspeptin at reproductive tissues–role in ovarian function and embryo implantation and relevance to assisted reproductive technology in livestock: a review. *Biol Reprod* (2020) 103:1157–70. doi: 10.1093/biolre/ioaa135

7. Hu K-LL, Chang H-MM, Zhao H-CC, Yu Y, Li R, Qiao J. Potential roles for the kisspeptin/kisspeptin receptor system in implantation and placentation. *Hum Reprod Update* (2019) 25:326–43. doi: 10.1093/humupd/dmy046

8. Fang L, Gao Y, Wang Z, Li Y, Yan Y, Wu Z, et al. EGF stimulates human trophoblast cell invasion by downregulating ID3-mediated KISS1 expression. *Cell Commun Signal* (2021) 19:1–13. doi: 10.1186/s12964-021-00783-2

9. Fang L, Yan Y, Gao Y, Wu Z, Wang Z, Yang S, et al. TGF-β1 inhibits human trophoblast cell invasion by upregulating kisspeptin expression through ERK1 / 2 but not SMAD signaling pathway. *Reprod Biol Endocrinol* (2022) 20:1–12. doi: 10.1186/s12958-022-00902-9

10. Harter CJLL, Kavanagh GS, Smith JT. The role of kisspeptin neurons in reproduction and metabolism. *J Endocrinol* (2018) 238:R173–83. doi: 10.1530/JOE-18-0108

11. Hiden U, Bilban M, Knöfler M, Desoye G. Kisspeptins and the placenta: Regulation of trophoblast invasion. *Rev Endocr Metab Disord* (2007) 8:31–9. doi: 10.1007/s11154-007-9030-8

12. Hu K-LL, Zhao H, Yu Y, Li R. Kisspeptin as a potential biomarker throughout pregnancy. *Eur J Obstet Gynecol Reprod Biol* (2019) 240:261–6. doi: 10.1016/j.ejogrb.2019.07.016

13. Bilban M, Ghaffari-Tabrizi N, Hintermann E, Bauer S, Molzer S, Zoratti C, et al. Kisspeptin-10, a KiSS-1/metastin-derived decapeptide, is a physiological invasion inhibitor of primary human trophoblasts. *J Cell Sci* (2004) 117:1319–28. doi: 10.1242/jcs.00971

14. Fayazi M, Calder M, Bhattacharya M, Vilos GA, Power S, Babwah AV. The pregnant mouse uterus exhibits a functional kisspeptin/KISS1R signaling system on the day of embryo implantation. *Reprod Biol Endocrinol* (2015) 13:1–6. doi: 10.1186/s12958-015-0105-1

15. Gorbunova OL, Shirshev SV. The role of kisspeptin in immune tolerance formation during pregnancy. *Dokl Biol Sci* (2014) 457:258–60. doi: 10.1134/S0012496614040085

16. Zhang P, Tang M, Zhong T, Lin Y, Zong T, Zhong C, et al. Expression and function of kisspeptin during mouse decidualization. *PloS One* (2014) 9:1–8. doi: 10.1371/journal.pone.0097647

17. Park DW, Lee SK, Hong SR, Han AR, Kwak-Kim J, Yang KM. Expression of kisspeptin and its receptor GPR54 in the first trimester trophoblast of women with recurrent pregnancy loss. *Am J Reprod Immunol* (2012) 67:132–9. doi: 10.1111/j.1600-0897.2011.01073.x

18. Sullivan-Pyke C, Haisenleder DJ, Senapati S, Nicolais O, Eisenberg E, Sammel MD, et al. Kisspeptin as a new serum biomarker to discriminate miscarriage from viable intrauterine pregnancy. *Fertil Steril* (2018) 109:137–141.e2. doi: 10.1016/j.fertnstert.2017.09.029

19. Wu S, Zhang H, Tian J, Liu L, Dong Y, Mao T. Expression of kisspeptin/GPR54 and PIBF/PR in the first trimester trophoblast and decidua of women with recurrent spontaneous abortion. *Pathol Res Pract* (2014) 210:47–54. doi: 10.1016/j.prp.2013.09.017

20. Logie JJ, Denison FC, Riley SC, Ramaesh T, Forbes S, Norman JE, et al. Evaluation of kisspeptin levels in obese pregnancy as a biomarker for pre-eclampsia. *Clin Endocrinol (Oxf)* (2012) 76:887–93. doi: 10.1111/j.1365-2265.2011.04317.x

21. Kołodziejski PA, Pruszyńska-Oszmałek E, Korek E, Sassek M, Szczepankiewicz D, Kaczmarek P, et al. Serum levels of spexin and kisspeptin negatively correlate with obesity and insulin resistance in women. *Physiol Res* (2018) 67:45–56. doi: 10.33549/physiolres.933467

22. Pérez-López FR, López-Baena MT, Varikasuvu SR, Ruiz-Román R, Fuentes-Carrasco M, Savirón-Cornudella R. Preeclampsia and gestational hypertension are associated to low maternal circulating kisspeptin levels: a systematic review and meta-analysis. *Gynecol Endocrinol* (2021) 37:1055–62. doi: 10.1080/09513590.2021.2004396

23. Adali E, Kurdoglu Z, Kurdoglu M, Kamaci M, Kolusari A, Yildizhan R. Metastin levels in pregnancies complicated by pre-eclampsia and their relation with disease severity. *J Matern Neonatal Med* (2012) 25:2671–5. doi: 10.3109/14767058.2012.708369

24. Armstrong RA, Reynolds RM, Leask R, Shearing CH, Calder AA, Riley SC. Decreased serum levels of kisspeptin in early pregnancy are associated with intra-uterine growth restriction and pre-eclampsia. *Prenat Diagn* (2009) 29:982–5. doi: 10.1002/pd.2328

25. Cartwright JE, Williams PJ. Altered placental expression of kisspeptin and its receptor in pre-eclampsia. *J Endocrinol* (2012) 214:79–85. doi: 10.1530/JOE-12-0091

26. Ćetković A, Miljic D, Ljubić A, Patterson M, Ghatei M, Stamenkovi J, et al. Plasma kisspeptin levels in pregnancies with diabetes and hypertensive disease as a potential marker of placental dysfunction and adverse perinatal outcome. *Endocr Res* (2012) 37:78–88. doi: 10.3109/07435800.2011.639319

27. Colak E, Ozcimen EE, Erinanç OH, Tohma YA, Ceran MU. Is placental KISS-1 expression associated with first trimester abortion spontaneous? *Obstet Gynecol Sci* (2020) 63:490–6. doi: 10.5468/OGS.19242

28. Kapustin RV, Drobintseva AO, Alekseenkova EN, Onopriychuk AR, Arzhanova ON, Polyakova VO, et al. Placental protein expression of kisspeptin-1 (KISS1) and the kisspeptin-1 receptor (KISS1R) in pregnancy complicated by diabetes mellitus or preeclampsia. *Arch Gynecol Obstet* (2020) 301:437–45. doi: 10.1007/s00404-019-05408-1

29. Li L, Tian J, Zhou L, Wu S, Zhang S, Qi L, et al. Role of kisspeptin/GPR54 in the first trimester trophoblast of women with a history of recurrent spontaneous abortion. *Int J Clin Exp Pathol* (2017) 10:8161–73.

30. Matjila M, Millar R, van der Spuy Z, Katz A. Elevated placental expression at the maternal-fetal interface but diminished maternal circulatory kisspeptin in preeclamptic pregnancies. *Pregnancy Hypertens* (2016) 6:79–87. doi: 10.1016/j.preghy.2015.11.001

31. Santos BR, dos Anjos Cordeiro JM, Santos LC, de Oliveira LS, Mendonça LD, Santos EO, et al. Maternal hypothyroidism reduces the expression of the kisspeptin/Kiss1r system in the maternal-fetal interface of rats. *Reprod Biol* (2022) 22:16–20. doi: 10.1016/j.repbio.2022.100615

32. Newbern D, Freemark M. Placental hormones and the control of maternal metabolism and fetal growth. *Curr Opin Endocrinol Diabetes Obes* (2011) 18:409–16. doi: 10.1097/MED.0b013e32834c800d

33. Kurlak LO, Mistry HD, Kaptein E, Visser TJ, Broughton Pipkin F. Thyroid hormones and their placental deiodination in normal and pre-eclamptic pregnancy. *Placenta* (2013) 34:395–400. doi: 10.1016/j.placenta.2013.02.009

34. Silva JF, Ocarino NM, Serakides R. Thyroid hormones and female reproduction†. *Biol Reprod* (2018) 99:907–21. doi: 10.1093/biolre/ioy115

35. Silva JF, Vidigal PN, Galvão DD, Boeloni JN, Nunes PP, Ocarino NM, et al. Fetal growth restriction in hypothyroidism is associated with changes in proliferative activity, apoptosis and vascularisation of the placenta. *Reprod Fertil Dev* (2012) 24:923. doi: 10.1071/RD11219

36. Silva JF, Ocarino NM, Serakides R. Maternal thyroid dysfunction affects placental profile of inflammatory mediators and the intrauterine trophoblast migration kinetics. *Reproduction* (2014) 147:803–16. doi: 10.1530/REP-13-0374

37. Silva JF, Ocarino NM, Serakides R. Placental angiogenic and hormonal factors are affected by thyroid hormones in rats. *Pathol Res Pract* (2015) 211:226–34. doi: 10.1016/j.prp.2014.11.003

38. Silva JF, Ocarino NM, Serakides R. Spatiotemporal expression profile of proteases and immunological, angiogenic, hormonal and apoptotic mediators in rat placenta before and during intrauterine trophoblast migration. *Reprod Fertil Dev* (2017) 29:1774–86. doi: 10.1071/RD16280

39. Souza CA, Silva JF, Ocarino NM, Silva CLR, Gomes LA, Assunção GSM, et al. Efeito do hipotireoidismo materno na expressão espaço-temporal de mediadores imunológicos e população de células natural killers na decídua e na glândula metrial de ratas. *Arq Bras Med Veterinária e Zootec* (2020) 72:177–90. doi: 10.1590/1678-4162-10697

40. dos A Cordeiro JM, Santos BR, Santos LC, Santos EO, de Oliveira LS, Barbosa EM, et al. "Manganese porphyrin-based treatment blocks placental stress caused by maternal hypothyroidism and improves placental morphogenesis and fetal development in a rat experimental model.,". In: MD Bronstein, editor. *Archives of archives of and metabolism*. São Paulo: Brazilian Society of Endocrinology and Metabolism (2021). p. S11.

41. Centanni M, Benvenga S, Sachmechi I. Diagnosis and management of treatment-refractory hypothyroidism: an expert consensus report. *J Endocrinol Invest* (2017) 40:1289–301. doi: 10.1007/s40618-017-0706-y

42. de Oliveira LS, da Silva TQM, Barbosa EM, dos A Cordeiro JM, Santos LC, Henriques PC, et al. "Kisspeptin treatment restores ovarian function in hypothyroid rats.,". In: ALC Armani and EJ de A Araújo, editors. *Annals of the III international symposium of experimental pathology*. Londrina: UEL (2021). p. 42.

43. Aslan M, Erkanli Senturk G, Akkaya H, Sahin S, Yılmaz B. The effect of oxytocin and kisspeptin-10 in ovary and uterus of ischemia-reperfusion injured rats. *Taiwan J Obstet Gynecol* (2017) 56:456–62. doi: 10.1016/j.tjog.2016.12.018

44. Aydin M, Oktar S, Yonden Z, Ozturk OH, Yilmaz B. Direct and indirect effects of kisspeptin on liver oxidant and antioxidant systems in young male rats. *Cell Biochem Funct* (2010) 28:293–9. doi: 10.1002/cbf.1656

45. Akkaya H, Eyuboglu S, Erkanlı Senturk G, Yilmaz B. Investigation of the effects of kisspeptin-10 in methionine-induced lipid peroxidation in testicle tissue of young rats. *J Biochem Mol Toxicol* (2017) 31:1–7. doi: 10.1002/jbt.21881

46. Yuan C, Huang WQ, Guo JH, Liu XY, Yang JZ, Chen JJ, et al. Involvement of kisspeptin in androgen-induced hypothalamic endoplasmic reticulum stress and its rescuing effect in PCOS rats. *Biochim Biophys Acta - Mol Basis Dis* (2021) 1867:166242. doi: 10.1016/j.bbadis.2021.166242

47. Napso T, Hung Y-P, Davidge ST, Care AS, Sferruzzi-Perri AN. Advanced maternal age compromises fetal growth and induces sex-specific changes in placental phenotype in rats. *Sci Rep* (2019) 9:16916. doi: 10.1038/s41598-019-53199-x

48. Dilworth MR, Kusinski LC, Baker BC, Renshall LJ, Greenwood SL, Sibley CP, et al. Defining fetal growth restriction in mice: A standardized and clinically relevant approach. *Placenta* (2011) 32:914–6. doi: 10.1016/j.placenta.2011.08.007

49. Solano ME, Thiele K, Kowal MK, Arck PC. Identification of suitable reference genes in the mouse placenta. *Placenta* (2016) 39:7–15. doi: 10.1016/j.placenta.2015.12.017

50. Charnock JC, Dilworth MR, Aplin JD, Sibley CP, Westwood M, Crocker IP. The impact of a human IGF-II analog ([Leu27]IGF-II) on fetal growth in a mouse model of fetal growth restriction. *Am J Physiol - Endocrinol Metab* (2015) 310:E24–31. doi: 10.1152/ajpendo.00379.2015

51. Fowden AL, Forhead AJ, Coan PM, Burton GJ. The placenta and intrauterine programming. *J Neuroendocrinol* (2008) 20:439–50. doi: 10.1111/j.1365-2826.2008.01663.x

52. Vrachnis N, Kalampokas E, Sifakis S, Vitoratos N, Kalampokas T, Botsis D, et al. Placental growth factor (PlGF): A key to optimizing fetal growth. *J Matern Neonatal Med* (2013) 26:995–1002. doi: 10.3109/14767058.2013.766694

53. Balachandiran M, Bobby Z, Dorairajan G, Gladwin V, Vinayagam V, Packirisamy RM. Decreased maternal serum adiponectin and increased insulin-like growth factor-1 levels along with increased placental glucose transporter-1 expression in gestational diabetes mellitus: Possible role in fetal overgrowth: Regulation of placental GLUT-1 expr. *Placenta* (2021) 104:71–80. doi: 10.1016/j.placenta.2020.11.008

54. Adu-Gyamfi EA, Lamptey J, Chen X-M, Li F-F, Li C, Ruan L-L, et al. Iodothyronine deiodinase 2 (DiO2) regulates trophoblast cell line cycle, invasion and apoptosis; and its downregulation is associated with early recurrent miscarriage. *Placenta* (2021) 111:54–68. doi: 10.1016/j.placenta.2021.06.004

55. Burton GJ, Yung HW, Cindrova-Davies T, Charnock-Jones DS. Placental endoplasmic reticulum stress and oxidative stress in the pathophysiology of unexplained intrauterine growth restriction and early onset preeclampsia. *Placenta* (2009) 30:43–8. doi: 10.1016/j.placenta.2008.11.003

56. Yung HW, Hemberger M, Watson ED, Senner CE, Jones CP, Kaufman RJ, et al. Endoplasmic reticulum stress disrupts placental morphogenesis: Implications for human intrauterine growth restriction. *J Pathol* (2012) 228:554–64. doi: 10.1002/path.4068

57. Yung HW, Atkinson D, Campion-Smith T, Olovsson M, Charnock-Jones DS, Burton GJ. Differential activation of placental unfolded protein response pathways implies heterogeneity in causation of early- and late-onset pre-eclampsia. *J Pathol* (2014) 234:262–76. doi: 10.1002/path.4394

58. Rosario GX, Konno T, Soares MJ. Maternal hypoxia activates endovascular trophoblast cell invasion. *Dev Biol* (2008) 314:362–75. doi: 10.1016/j.ydbio.2007.12.007

59. Soares MJ, Iqbal K, Kozai K. Hypoxia and placental development. *Birth defects Res* (2017) 109:1309–29. doi: 10.1002/bdr2.1135

60. Urbaniak SK, Boguszewska K, Szewczuk M, Kázmierczak-Barańska J, Karwowski BT. 8-Oxo-7,8-dihydro-2′-deoxyguanosine (8-oxodG) and 8-hydroxy-2′-deoxyguanosine (8-OHdG) as a potential biomarker for gestational diabetes mellitus (GDM) development. *Molecules* (2020) 25:202. doi: 10.3390/molecules25010202

61. Radwańska P, Kosior-Korzecka U. Relationships between leptin, KiSS-1/GPR54 expression and TSH secretion from pituitary cells of pubertal ewes *in vitro*. *Res Vet Sci* (2016) 105:180–7. doi: 10.1016/j.rvsc.2016.02.014

62. Adu-Gyamfi EA, Wang Y-X, Ding Y-B. The interplay between thyroid hormones and the placenta: a comprehensive review†. *Biol Reprod* (2020) 102:8–17. doi: 10.1093/biolre/ioz182

63. Bowe JE, King AJ, Kinsey-Jones JS, Foot VL, Li XF, O'Byrne KT, et al. Kisspeptin stimulation of insulin secretion: Mechanisms of action in mouse islets and rats. *Diabetologia* (2009) 52:855–62. doi: 10.1007/s00125-009-1283-1

64. Bowe JE, Foot VL, Amiel SA, Huang GC, Lamb M, Lakey J, et al. GPR54 peptide agonists stimulate insulin secretion from murine, porcine and human islets. *Islets* (2012) 4:20–3. doi: 10.4161/isl.18261

65. Izzi-Engbeaya C, Comninos AN, Clarke SA, Jomard A, Yang L, Jones S, et al. The effects of kisspeptin on β-cell function, serum metabolites and appetite in humans. *Diabetes Obes Metab* (2018) 20:2800–10. doi: 10.1111/dom.13460

66. Schwetz TA, Reissaus CA, Piston DW. Differential stimulation of insulin secretion by glp-1 and kisspeptin-10. *PLoS One* (2014) 9:1–10. doi: 10.1371/journal.pone.0113020

67. Wahab F, Riaz T, Shahab M. Study on the effect of peripheral kisspeptin administration on basal and glucose-induced insulin secretion under fed and fasting conditions in the adult male rhesus monkey (Macaca mulatta). *Horm Metab Res* (2011) 43:37–42. doi: 10.1055/s-0030-1268458

68. Bowe JE, Hill TG, Hunt KF, Smith LIF, Simpson SJS, Amiel SA, et al. A role for placental kisspeptin in β cell adaptation to pregnancy. *JCI Insight* (2019) 4:e124540. doi: 10.1172/jci.insight.124540

69. Kusinski LC, Stanley JL, Dilworth MR, Hirt CJ, Andersson IJ, Renshall LJ, et al. eNOS knockout mouse as a model of fetal growth restriction with an impaired uterine artery function and placental transport phenotype. *Am J Physiol - Regul Integr Comp Physiol* (2012) 303:R86–93. doi: 10.1152/ajpregu.00600.2011

70. Renshall LJ, Morgan HL, Moens H, Cansfield D, Finn-Sell SL, Tropea T, et al. Melatonin increases fetal weight in wild-type mice but not in mouse models of fetal growth restriction. *Front Physiol* (2018) 9:1141. doi: 10.3389/fphys.2018.01141

71. Shrivastava D, Master A. Fetal growth restriction. *J Obstet Gynecol India* (2020) 70:103–10. doi: 10.1007/s13224-019-01278-4

72. Burton GJ, Fowden AL, Thornburg KL. Placental origins of chronic disease. *Physiol Rev* (2016) 96:1509–65. doi: 10.1152/physrev.00029.2015

73. Silva JF, Serakides R. Intrauterine trophoblast migration: A comparative view of humans and rodents. *Cell Adh Migr* (2016) 10:88–110. doi: 10.1080/19336918.2015.1120397

74. Cowans NJ, Stamatopoulou A, Matwejew E, von Kaisenberg CS, Spencer K. First-trimester placental growth factor as a marker for hypertensive disorders and SGA. *Prenat Diagn* (2010) 30:565–70. doi: 10.1002/pd.2525

75. Sferruzzi-Perri AN, Sandovici I, Constancia M, Fowden AL. Placental phenotype and the insulin-like growth factors: resource allocation to fetal growth. *J Physiol* (2017) 595:5057–93. doi: 10.1113/JP273330

76. Torry DS, Ahn H, Barnes EL, Torry RJ. Placenta growth factor: Potential role in pregnancy. *Am J Reprod Immunol* (1999) 41:79–85. doi: 10.1111/j.1600-0897.1999.tb00078.x

77. Desoye G, Gauster M, Wadsack C. Placental transport in pregnancy pathologies. *Am J Clin Nutr* (2011) 94:1896–902. doi: 10.3945/ajcn.110.000851

78. Lüscher BP, Marini C, Joerger-Messerli MS, Huang X, Hediger MA, Albrecht C, et al. Placental glucose transporter (GLUT)-1 is down-regulated in preeclampsia. *Placenta* (2017) 55:94–9. doi: 10.1016/j.placenta.2017.04.023

79. Ahmed A, Dunk C, Ahmad S, Khaliq A. Regulation of placental vascular endothelial growth factor (VEGF) and placenta growth factor (PIGF) and soluble flt-1 by oxygen–a review. *Placenta* (2000) 21 Suppl:A:S16–24. doi: 10.1053/plac.1999.0524

80. Ferrara N. Vascular endothelial growth factor: Basic science and clinical progress. *Endocr Rev* (2004) 25:581–611. doi: 10.1210/er.2003-0027

81. Kaelin WG, Ratcliffe PJ. Oxygen sensing by metazoans: The central role of the HIF hydroxylase pathway. *Mol Cell* (2008) 30:393–402. doi: 10.1016/j.molcel.2008.04.009

82. Ali LE, Salih MM, Elhassan EM, Mohmmed AA, Adam I. Placental growth factor, vascular endothelial growth factor, and hypoxia-inducible factor-1α in the placentas of women with pre-eclampsia. *J Matern Neonatal Med* (2019) 32:2628–32. doi: 10.1080/14767058.2018.1443066

83. Sezer SD, Küçük M, Döger FK, Yüksel H, Odabaşı AR, Türkmen MK, et al. VEGF, PIGF and HIF-1α in placentas of early- and late-onset pre-eclamptic patients. *Gynecol Endocrinol* (2013) 29:797–800. doi: 10.3109/09513590.2013.801437

84. Kaufmann P, Black S, Huppertz B. Endovascular trophoblast invasion: Implications for the pathogenesis of intrauterine growth retardation and preeclampsia. *Biol Reprod* (2003) 69:1–7. doi: 10.1095/biolreprod.102.014977

85. Gorbunova OL, Shirshev SV. Role of kisspeptin in regulation of reproductive and immune reactions. *Biochem* (2020) 85:839–53. doi: 10.1134/S0006297920080015

86. Borst SE. The role of TNF-α in insulin resistance. *Endocrine* (2004) 23:177–82. doi: 10.1385/ENDO:23:2-3:177

87. Thaxton JE, Sharma S. Interleukin-10: A multi-faceted agent of pregnancy. *Am J Reprod Immunol* (2010) 63:482–91. doi: 10.1111/j.1600-0897.2010.00810.x

88. Siwetz M, Blaschitz A, El-Heliebi A, Hiden U, Desoye G, Huppertz B, et al. TNF-α alters the inflammatory secretion profile of human first trimester placenta. *Lab Investig* (2016) 96:428–38. doi: 10.1038/labinvest.2015.159

89. Soares MJ, Chakraborty D, Kubota K, Renaud SJ, Karim Rumi MA, Rumi MAK. Adaptive mechanisms controlling uterine spiral artery remodeling during the establishment of pregnancy. *Int J Dev Biol* (2014) 58:247–59. doi: 10.1387/ijdb.140083ms

90. Fukushima K, Murata M, Tsukimori K, Eisuke K, Wake N. 8-Hydroxy-2-deoxyguanosine staining in placenta is associated with maternal serum uric acid levels and gestational age at diagnosis in pre-eclampsia. *Am J Hypertens* (2011) 24:829–34. doi: 10.1038/ajh.2011.40

91. Kumar SN, Bastia B, Borgohain D, Agrawal U, Raisuddin S, Jain AK. Structural changes, increased hypoxia, and oxidative DNA damage in placenta due to maternal smokeless tobacco use. *Birth Defects Res* (2021) 113:1198–214. doi: 10.1002/bdr2.1941

92. Walter P, Ron D. The unfolded protein response: From stress pathway to homeostatic regulation. *Science* (2011) 334:1081–6. doi: 10.1126/science.1209038

93. wa Yung H, Alnæs-Katjavivi P, Jones CJPP, El-Bacha T, Golic M, Staff A-CC, et al. Placental endoplasmic reticulum stress in gestational diabetes: the potential for therapeutic intervention with chemical chaperones and antioxidants. *Diabetologia* (2016) 59:2240–50. doi: 10.1007/s00125-016-4040-2

94. Yung HW, Calabrese S, Hynx D, Hemmings BA, Cetin I, Charnock-Jones DS, et al. Evidence of placental translation inhibition and endoplasmic reticulum stress in the etiology of human intrauterine growth restriction. *Am J Pathol* (2008) 173:451–62. doi: 10.2353/ajpath.2008.071193

frontiers | Frontiers in Endocrinology

TYPE Original Research
PUBLISHED 10 November 2022
DOI 10.3389/fendo.2022.1031013

Check for updates

OPEN ACCESS

EDITED BY
Reinaldo Marín,
Instituto Venezolano de Investigaciones Científicas (IVIC), Venezuela

REVIEWED BY
Xuntian Jiang,
Washington University in St. Louis, United States
Alison Ondrus,
California Institute of Technology, United States

*CORRESPONDENCE
William J. Griffiths
w.j.griffiths@swansea.ac.uk

SPECIALTY SECTION
This article was submitted to Developmental Endocrinology, a section of the journal Frontiers in Endocrinology

RECEIVED 29 August 2022
ACCEPTED 18 October 2022
PUBLISHED 10 November 2022

CITATION
Dickson AL, Yutuc E, Thornton CA, Wang Y and Griffiths WJ (2022) Identification of unusual oxysterols biosynthesised in human pregnancy by charge-tagging and liquid chromatography - mass spectrometry. *Front. Endocrinol.* 13:1031013. doi: 10.3389/fendo.2022.1031013

COPYRIGHT
© 2022 Dickson, Yutuc, Thornton, Wang and Griffiths. This is an open-access article distributed under the terms of the Creative Commons Attribution License (CC BY). The use, distribution or reproduction in other forums is permitted, provided the original author(s) and the copyright owner(s) are credited and that the original publication in this journal is cited, in accordance with accepted academic practice. No use, distribution or reproduction is permitted which does not comply with these terms.

Identification of unusual oxysterols biosynthesised in human pregnancy by charge-tagging and liquid chromatography - mass spectrometry

Alison L. Dickson, Eylan Yutuc, Catherine A. Thornton, Yuqin Wang and William J. Griffiths*

Swansea University Medical School, Swansea, Wales, United Kingdom

The aim of this study was to identify oxysterols and any down-stream metabolites in placenta, umbilical cord blood plasma, maternal plasma and amniotic fluid to enhance our knowledge of the involvement of these molecules in pregnancy. We confirm the identification of 20S-hydroxycholesterol in human placenta, previously reported in a single publication, and propose a pathway from 22R-hydroxycholesterol to a C_{27} bile acid of probable structure 3β,20R,22R-trihydroxycholest-5-en-(25R)26-oic acid. The pathway is evident not only in placenta, but pathway intermediates are also found in umbilical cord plasma, maternal plasma and amniotic fluid but not non-pregnant women.

KEYWORDS

sterol, oxysterol, bile acids, CYP11A1, LC-MS, CYP27A1

1 Introduction

Amongst other functions, the placenta plays a key role in the transport of cholesterol from the mother to the fetus (1). The placenta is rich in cholesterol metabolising enzymes, particularly those involved in progesterone and estrogen synthesis (2). Hence, it should also be a site for oxysterol synthesis and further metabolism. Cytochrome P450 (CYP) 11A1 (also known as $P450_{SCC}$) is the enzyme that generates pregnenolone from cholesterol *via* consecutive 22R- and 20R-hydroxylations followed by side-chain cleavage (3). Progesterone is then formed from pregnenolone by oxidation at C-3 and Δ^5 – Δ^4 isomerisation by hydroxysteroid dehydrogenase (HSD) 3B1 (See Figure 1). Although 22R-hydroxycholesterol (22R-HC) and 20R,22R-dihydroxycholesterol (20R,22R-diHC)

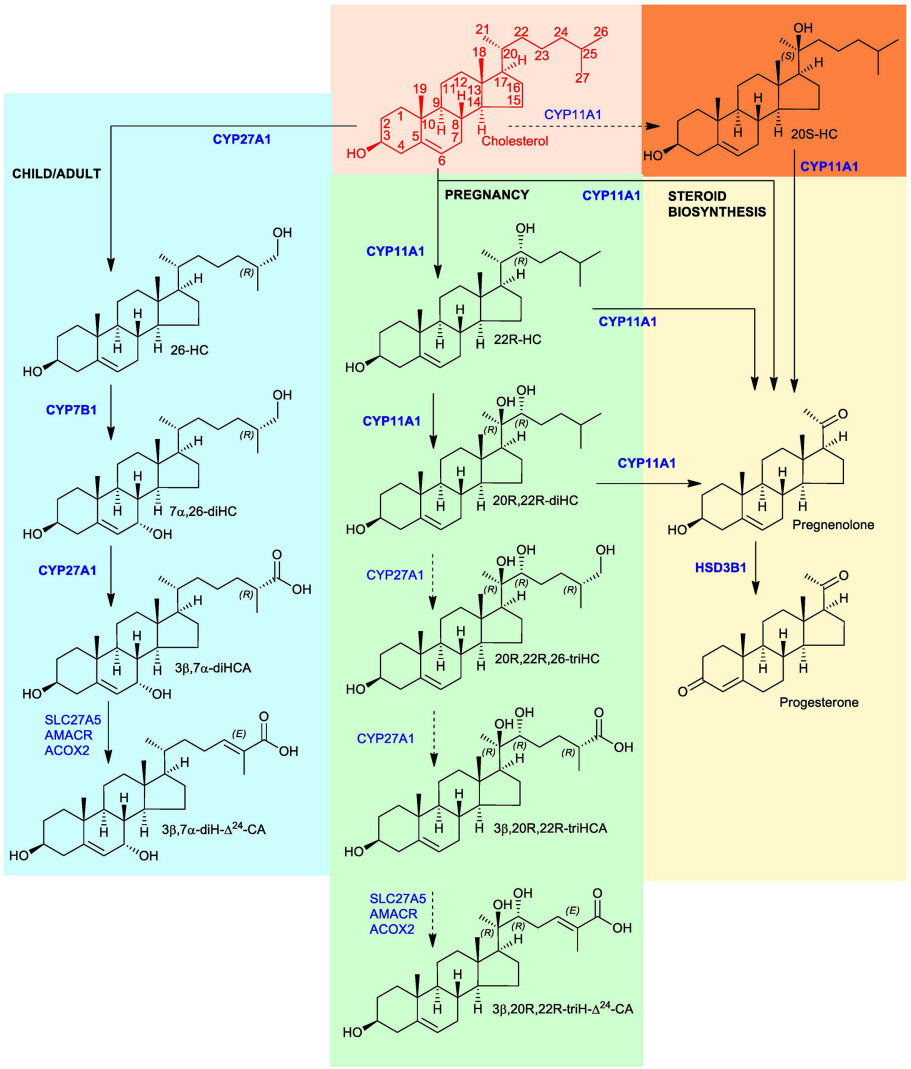


FIGURE 1
Proposed metabolism of cholesterol to the C_{27} bile acid 3β,20R,22R-triH-Δ^{24}-CA (green background). For comparison the acidic pathway to the C_{27} bile acid 3β,7α-diH-Δ^{24}-CA is shown (blue background) as is the pathway to progesterone (yellow background). Enzymes are indicated in blue. When shown in bold the enzymatic reactions can be found in the literature, when shown in normal typeface and with a broken arrow they are postulated. Cholesterol is shown in red with full stereochemistry and numbering system on a salmon background. For simplicity the 3β,20R,22R-triH-Δ^{24}-CA and 3β,7α-diH-Δ^{24}-CA are shown as the acids rather than the CoA-thioester products of SLC27A5 (bile acid CoA ligase). 20S-HC is shown on an orange background, although the enzyme responsible for its formation is unproven, it can be converted to 20R,22R-diHC by CYP11A1. Note the stereochemistry of metabolites down-stream of 20R,22R-diHC towards and including 3β,20R,22R-triH-Δ^{24}-CA are assumed based on biosynthetic considerations.

are known intermediates in CYP11A1-mediated side-chain cleavage of cholesterol to give pregnenolone (4), few studies have explored the oxysterol profile of placenta (5, 6). One important, but until now not replicated, finding made in the early 2000's was the presence of 20S-hydroxycholesterol (20S-HC) in human placenta (7). 20S-HC is an enigmatic oxysterol with many biological properties, but seldom reported in mammalian systems (8). Note, the actual stereochemical location of the 20S-hydroxy group in 20S-HC is the same as that of the 20R-hydroxy group in 20R,22R-diHC (see structures in Figure 1), but they are named 20S and 20R, respectively, according to rules of chemical priority. Similar to the situation with placenta, there are few reports of the oxysterol profiles of umbilical cord blood (5), i.e. blood of fetal origin that remains in the placenta and in the attached umbilical cord after childbirth, or of amniotic fluid, the fluid that acts as a cushion for the growing fetus and serves to facilitate the exchange of biochemicals between mother and fetus. Interestingly, however, oxysterols have been found as their sulphate esters in meconium, the earliest stool of a mammalian infant, including

20,22-diHC, 22-HC, 23-hydroxycholesterol (23-HC) and 24-hydroxycholesterol (24-HC) (9, 10).

Here we report liquid chromatography (LC) – mass spectrometry (MS)-based methods for the identification of oxysterols in full term placenta, plasma derived from cord blood and pregnant female blood (maternal blood) and in mid-gestation amniotic fluid. The methods are based on high mass resolution MS with multistage fragmentation (MS^n) exploiting charge-tagging to enhance analyte signal (Supplemental Figure S1A).

2 Materials and methods

2.1 Human material

Maternal blood was taken 24 - 48 hr prior to elective caesarean section at 37+ weeks of gestation for reasons that did not include maternal or fetal anomaly. Umbilical cord blood was collected at delivery of the baby. Control plasma was from non-pregnant females. Amniotic fluid was obtained at 16 – 18 weeks of pregnancy during diagnostic amniocentesis; only samples with no fetal chromosomal abnormality were used. All samples were collected with approval from an appropriate Health Research Authority Research Ethics Committee. All participants provided informed consent and the study adhered to the principles of the Declaration of Helsinki.

2.2 Sterol and oxysterol standards

Isotope-labelled standards [25,26,26,26,27,27,27-$^2H_7$]24R/S-hydroxycholesterol ([$^2H_7$]24R/S-HC), [25,26,26,26,27,27,27-$^2H_7$]22R-hydroxycholesterol ([$^2H_7$]22R-HC), [25,26,26,26,27,27,27-$^2H_7$]22S-hydroxycholesterol ([$^2H_7$]22S-HC), [25,26,26,26,27,27,27-$^2H_7$]7α-hydroxycholesterol ([$^2H_7$]7α-HC), [26,26,26,27,27,27-$^2H_6$]7α,25-dihydroxycholesterol ([$^2H_6$]7α,25-diHC) were from Avanti Polar Lipids, Alabaster, AL. [25,26,26,26,27,27,27-$^2H_7$]20S-Hydroxycholesterol ([$^2H_7$]20S-HC) was purchased from Toronto Research Chemicals (TCI, Toronto, Canada). [$^2H_7$]22R-Hydroxycholest-4-en-3-one ([$^2H_7$]22R-HCO) was prepared from [$^2H_7$]22R-HC by treatment with cholesterol oxidase enzyme (*Streptomyces* sp., Merck, Dorset, UK) (11).

2.3 Sterol and oxysterol extraction

2.3.1 Placenta

Sterols and oxysterols were extracted from placental tissue using a modified protocol previously used to extract oxysterols from brain and liver tissue (12, 13). Approximately 400 mg of tissue was cut from the maternal side of fresh placenta, weighed and washed three times in PBS to remove blood. The tissue was then transferred to a gentleMACS™ C tube (Miltenyi Biotec, Woking, UK) followed by 4.2 mL of absolute ethanol containing 50 ng of [$^2H_7$]24R/S-HC and 50 ng of [$^2H_7$]22R-HCO. The tissue was homogenised for 2 min. The homogenate was transferred to a 15 mL corning tube and sonicated for 15 min. Whilst sonicating, 1.8 mL of HPLC grade water was added dropwise to give 6 mL of homogenate at 70% ethanol. The homogenate was then centrifuged for 1 hr at 4,000 x *g*. The supernatant was transferred to a fresh 15 mL corning tube and the remaining pellet re-suspended in a further 4.2 mL ethanol containing 50 ng of [$^2H_7$]24R/S-HC and 50 ng of [$^2H_7$]22R-HCO. The suspension was vortex mixed and transferred back into the original gentleMACS™ C tube where it was then homogenised for a further 2 min. The homogenate was removed and sonicated for 15 min, then 1.8 mL of water added to give 6 mL of 70% ethanol. The supernatants from the two extractions were combined to yield 12 mL in 70% ethanol. This was mixed by vortex and sonicated for a further 10 min followed by centrifugation for 1 hr at 4,000 x *g*. Ten % (1.2 mL) of the total supernatant was added to 300 µL of 70% ethanol under sonication. The 1.5 mL of sample was subjected to solid phase extraction (SPE) by a procedure modified from an earlier protocol (12, 13) to allow the collection of C_{21} steroids besides sterols and oxysterols including sterol acids.

The sample from above was loaded onto a Certified Sep-Pak C_{18}, 200 mg (3 cm^3, Waters Inc. Elstree, UK) reversed-phase SPE column previously conditioned with ethanol (4 mL) followed by 70% ethanol (6 mL). The sample flow-through (1.5 mL) was combined with a column wash of 70% ethanol (5.5 mL) resulting in SPE1-Fr1 (7 mL) which contained oxysterols, sterol acids and C_{21} steroids. A second fraction was obtained by further washing with 70% ethanol (4 mL) and collected as SPE1-Fr2. Cholesterol and other sterols of similar hydrophobicity were eluted from the SPE column with absolute ethanol (2 mL) to give SPE1-Fr3. A final fourth fraction was eluted with a further 2 mL of absolute ethanol (SPE1-Fr4). Each of the four fractions was divided equally into A and B sub-fractions and dried overnight under vacuum by centrifugal evaporation (ScanLaf ScanSpeed vacuum concentrator, Lynge, Denmark).

Each lyophilised sample was reconstituted in propan-2-ol (100 µL) and mixed thoroughly by vortex. To fractions (A), 50 mM K_2HPO_4 buffer, pH 7 (1 mL) containing cholesterol oxidase solution (3.0 µL, 2 mg/mL in water, 44 units/mg of protein) was added. The samples were mixed by vortex and incubated at 37°C for 1 hr in a water bath. The reaction was then quenched by the addition of methanol (2 mL). Fractions (B) were treated in parallel in an identical fashion to fractions (A) but in the absence of cholesterol oxidase. Glacial acetic acid (150 µL) was added to fractions (A) and (B) and mixed by vortex. [$^2H_5$]Girard P (GP) reagent (11) (190 mg, bromide salt) was added to fractions (A) and [$^2H_0$]GP reagent (150 mg, chloride salt, TCI Europe, Oxford UK) was added to fractions (B). The samples were mixed by vortex until the derivatising reagent had dissolved. The reaction

was left to proceed overnight at room temperature protected from light.

An OASIS HLB 60 mg (3 cm^3) SPE cartridge was washed with methanol (6 mL), 5% methanol (6 mL) and conditioned with 70% methanol (4 mL). Sample from above (3.25 mL, 69% organic) was loaded onto the column and the flow-through collected. The sample tube was rinsed with 70% methanol (1 mL) which was then loaded onto the SPE column, and the eluent combined with the earlier flow-through. The column was re-conditioned with 35% methanol (1 mL) and the eluent combined with the earlier collection. The total eluent (~5 mL) was diluted with 4 mL of water to give ~9 mL of 35% methanol. The 9 mL sample solution was loaded onto the column and the flow-through collected. The sorbent was re-conditioned with 17.5% methanol (1 mL) and the eluent combined with earlier flow-through. To the combined 10 mL, water (9 mL) was added to give a 19 mL of 17.5% methanol. This solution was loaded onto the column and the flow-through collected once more. The sorbent was re-conditioned with 8.75% methanol (1 mL) and the flow-through combined with the earlier collection. The total combined eluent of 20 mL was diluted with 19 mL of water to give 39 mL 8.75% methanol. The solution was loaded onto the column and the flow-through discarded. A 5% methanol solution (6 mL) was used to wash the column before the analytes were eluted. The samples were eluted into four separate 1.5 mL microcentrifuge tubes using 3 x 1 mL methanol followed by 1 mL ethanol to give SPE2-FR1, -Fr2, -Fr3, -Fr4. Oxysterols originating from SPE1-Fr1 elute across SPE2-Fr1 and SPE2-Fr2, cholesterol originating from SPE1-Fr3 elutes across SPE2-Fr1,-Fr2, Fr-3. Here we report data only for oxysterols and more polar metabolites.

Immediately prior to LC-MS analysis of oxysterols, equal volumes of SPE2-Fr1A and SPE2-Fr2A were combined with equal aliquots of SPE2-Fr1B and SPE2-Fr2B and diluted with water to form a solvent composition of 60% methanol.

2.3.2 Plasma

The extraction protocol for sterols and oxysterols was essentially that described previously (11, 13, 14), with minor modification to allow for extraction of C_{21} steroids. 100 µL of plasma was added dropwise to a solution of acetonitrile (1.05 mL) containing 20 ng of [$^2H_7$]24R/S-HC and 20 ng of [$^2H_7$]22R-HCO in an ultrasonic bath with sonication. After a further 5 min of sonication, 350 µL of water was added. The sample (1.5 mL), now in 70% acetonitrile, was sonicated for a further 5 minutes and centrifuged at 17,000 x *g* at 4°C for 30 min. The sample was subjected to SPE and prepared for LC-MS analysis exactly as for the placental extract with the following modification: SPE1, Certified Sep-Pak C_{18}, 200 mg, was conditioned with 70% acetonitrile rather than 70% ethanol.

2.3.3 Amniotic fluid

The protocol for extraction of sterols and oxysterols from amniotic fluid was exactly as that described for plasma except the internal standards were 7 ng of [$^2H_7$]24R/S-HC and 7 ng of [$^2H_7$]22R-HCO.

2.4 LC-MS(MS^n)

Analysis was performed on a Dionex Ultimate 3000 UHPLC system (Dionex, now Thermo Fisher Scientific, Hemel Hempstead, UK) interfaced *via* an electrospray ionisation (ESI) probe to an Orbitrap Elite MS (Thermo Fisher Scientific). Chromatographic separation was carried out on a Hypersil Gold reversed phase C_{18} column (1.9 µm particle size, 50 x 2.1 mm, Thermo Fisher Scientific, UK). Details of the mobile phase and gradients employed are given in Supplemental Materials and Methods. MS analysis on the Orbitrap Elite was performed in the positive-ion mode with five scan events, one high resolution (120,000 full width at half maximum height at *m/z* 400) scan over the *m/z* range 400 – 610 in the Orbitrap and four MS^3 scans performed in parallel in the linear ion trap (LIT). Mass accuracy in the Orbitrap was typically < 5 ppm. More details of the scan events are provided in Supplemental Materials and Methods. Injection volumes were 35 µL for plasma extracts and at 90 µL for amniotic fluid and placental extracts.

3 Results

The aim of this study was to identify oxysterols and any downstream metabolites in placenta, cord plasma, maternal plasma and amniotic fluid to enhance our knowledge of the involvement of these molecules in pregnancy. For side-chain oxysterols expected to be present quantitative measurements were possible by reference to an isotope-labelled standard, for unexpected metabolites only semi-quantitative data was obtained, however, this could be used for relative quantification between sample sets (Table 1).

3.1 Identification of oxysterols in placenta

The placenta is a blood-rich organ. The maternal side contains less vascular tissue than the fetal side and was selected for analysis. During sample preparation tissue was washed three times with PBS to remove blood.

3.1.1 Monohydroxycholesterols:- 20S-HC, 22R-HC, 22S-HC, 24S-HC, 26-HC, 7α-HC and 7β-HC

Shown in Figure 2A (upper panel) is the LC-MS reconstructed ion chromatogram (RIC) for monohydroxycholesterols (HC, *m/z* 539.4368 ± 5ppm) found in placenta following derivatisation with [$^2H_5$]GP reagent. At first glance, the chromatogram shows some similarity to that of adult plasma (Figure 2A central panel) except

TABLE 1 Oxysterols in placenta, cord plasma, maternal plasma and amniotic fluid.

m/z	Compound	Placenta[1]	Cord Plasma	Maternal Plasma	Control Female Plasma	Amniotic Fluid	Quantification	Characteristic ion
$[^2H_5]$GP or $[^2H_0]$GP	Abbreviation	ng/g (SD) n=3	ng/mL (SD) n=14	ng/mL (SD) n=10	ng/mL (SD) n=5	ng/mL (SD) n=5		
539.4368	**7α-HC**	D/NM	31.46 (32.45)	57.27 (35.00)	46.08 (39.70)[2]	D/NM	Semi-quantitative[3]	151 (*b_1-12), 231 (*c_2-H_2O+2H)
534.4054	**7α-HCO**	D/NM	0.65 (0.74)	12.51 (9.34)	1.33 (2.97)[2]	D/NM	Semi-quantitative[3]	151 (*b_1-12), 231 (*c_2-H_2O+2H)
539.4368	**7β-HC**	D/NM	33.87 (38.68)	77.26 (61.09)	70.77 (74.37)[2]	D/NM	Semi-quantitative[3]	151 (*b_1-12), 231 (*c_2-H_2O+2H)
539.4368	**20S-HC**	D/NM	ND	ND	ND	ND	Not quantified[4]	151 (*b_1-12), 163 (*b_3-28), 327 (*e')
539.4368	**22R-HC**	210.3 (16.1)	6.19 (3.01)	2.55 (1.18)	ND	0.31 (0.34)	Quantitative[5]	151 (*b_1-12), 163 (*b_3-28), 273 (*d_1-12), 353 ('*f), 355 (*f')
539.4368	**22S-HC**	D/NM	ND	ND	ND	ND	Not quantified	151 (*b_1-12), 163 (*b_3-28), 273 (*d_1-12), 353 ('*f), 355 (*f')
539.4368	**24S-HC**	D/NM	7.34 (2.38)	14.99 (4.28)	14.48 (3.33)	D/NM	Quantitative[5]	151 (*b_1-12), 163 (*b_3-28), 353 ('*f)
539.4368	**26-HC**	41.5 (3.20)	7.23 (2.88)	21.61 (5.63)	25.67 (2.30)	D/NM	Quantitative[5]	151 (*b_1-12), 163 (*b_3-28), 427 (M-Py-CO) > 437 (M-Py-H_2O)
555.4317	**7α,26-diHC**	D/NM[6]	0.49 (0.23)	1.03 (0.54)	1.08 (0.55)	0.04 (0.03)	Semi-quantitative[3]	151 (*b_1-12), 231 (*c_2-H_2O+2H), 410 (M-Py-H_2O-CO-NH)
550.4003	**7α,26-diHCO**	D/NM[6]	3.24 (1.26)	3.89 (1.19)	4.13 (1.23)	0.19 (0.13)	Semi-quantitative[3]	151 (*b_1-12), 231 (*c_2-H_2O+2H), 410 (M-Py-H_2O-CO-NH)
555.4317	**20R,22R-diHC**	D/NM	49.74 (23.97)	13.23 (6.79)	ND	3.02 (1.63)	Quantitative[5]	151 (*b_1-12), 163 (*b_3-28), 325 ('*e), 327 (*e'), 353 ('*f-16), 355 (*f'-16)
555.4317	**22,23-diHC** [7]	D/NM	ND	ND	ND	ND	Semi-quatitative[7]	151 (*b_1-12), 163 (*b_3-28), 327 (*e'), 353 ('*f), 367 ('*g-16)
571.4266	**20R,22R,23-triHC** [7]	D/NM	D/NM	ND	ND	ND	Not quantified	151 (*b_1-12), 163 (*b_3-28), 325 ('*e), 327 (*e'), 353 ('*f-16), 355 (*f'-16), 383 ('*g-16)
571.4266	**20R,22R,24-triHC** [7]	D/NM	D/NM	ND	ND	ND	Not quantified	151 (*b_1-12), 163 (*b_3-28), 325 ('*e), 327 (*e'), 353 ('*f-16), 383 ('*g-16), 397 ('*h-16)
571.4266	**20R,22R,26-triHC** [7]	D/NM	0.30 (0.23)	0.06 (0.06)	ND	0.04 (0.03)	Semi-quantitative[7,8]	151 (*b_1-12), 163 (*b_3-28), 325 ('*e), 327 (*e'), 353 ('*f-16), 355 (*f'-16)
553.4161	**3β-HCA**	4.14 (0.48)	10.56 (4.71)	43.64 (13.71)	90.02 (21.40)	0.73 (0.46)	Quantitative[5]	151 (*b_1-12), 163 (*b_3-28), 423 ('*j), 426 (M-Py-CO-NH)
583.3902	**3β,20R,22R-triH-Δ^{24}-CA** [7]	D/NM	D/NM	ND	ND	D/NM	Not quantified	151 (*b_1-12), 163 (*b_3-28), 325 ('*e), 327 (*e'), 353 ('*f-16), 369 ('*f), 371 (*f'), 417 ('*j-36), 435 ('*j-18)
585.4059	**3β,20R,22R-triHCA** [7]	D/NM	9.32 (4.93)	0.48 (0.38)	ND	0.64 (0.43)	Semi-quantitative[7]	151 (*b_1-12), 163 (*b_3-28), 325 ('*e), 327 (*e'), 353 ('*f-16), 355 (*f'-16), 419 ('*j-36), 437 ('*j-18)
585.4059	**isomer of triHCA** [7]	D/NM	ND	D/NM	ND	ND	Not quantified	163 (*b_3-28), 385, 397, 415, 453, 471

D/NM, detected but not measured. ND, not detected. Authentic standards are available for each metabolite unless otherwise noted. An asterisk preceding a fragment describing letter indicates that the fragment-ion has lost the pyridine ring. A prime before the fragment describing letter indicates that the fragment-ion is deficient in a hydrogen atom compared to a similar fragment formed by a homolytic cleavage, A prime after the fragment describing letter indicates that the fragment-ion has gained a hydrogen atom compared to a similar fragment formed by homolytic cleavage. See Supplemental Figure S1C for examples.

[1]Extraction of oxysterols was performed according to methods designed primarily for brain and liver without further validation.

[2]Single outlier removed.

[3]Ring-oxysterols were not the focus of this study, and their measurement is only semi-quantitative.

[4]20S-HC and 24S-HC give chromatographic peaks that were not completely resolved so were not quantified.

[5]Previous studies have shown $[^2H_7]$24R/S-HC to be a satisfactory internal standard for the quantification of side-chain oxysterols and steroid-acids [Yutuc E, et al., 2021, Anal Chim Acta 1154: 338259].

[6]7α,26-diHC and 7α,26-diHCO were not differentiated.

[7]Presumptive identification, no authentic standard available.

[8]Quantification at the MS^3 level.

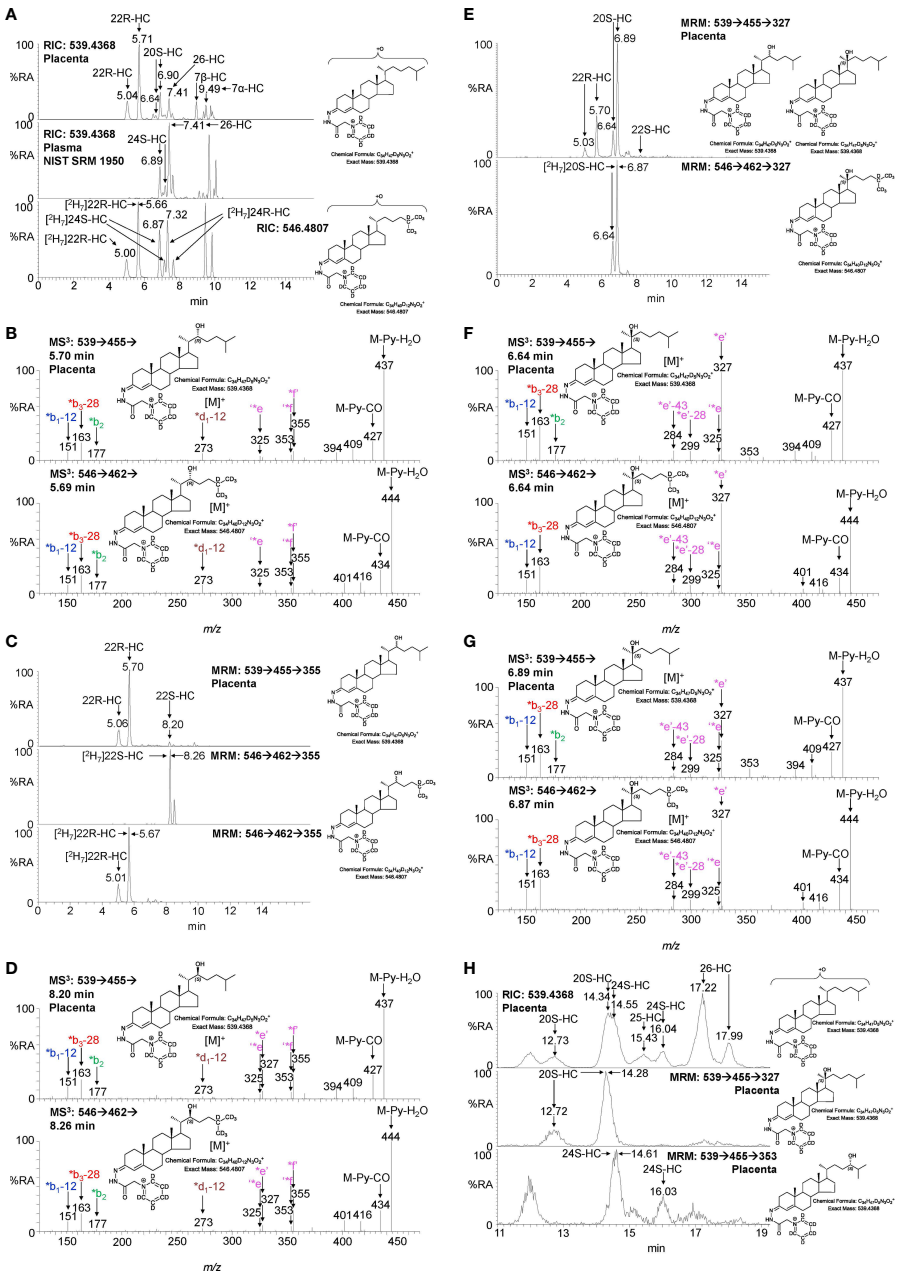


FIGURE 2
LC-MS(MS^n) analysis of GP-derivatised monohydroxycholesterols (HC) in placenta and NIST SRM 1950 plasma. **(A)** Reconstructed ion chromatograms (RICs) for monohydroxycholesterols (HC, *m/z* 539.4368 ± 5 ppm) in placenta (upper panel), NIST SRM 1950 plasma (15) (central panel), and of [$^2H_7$]-labelled standards (546.4807 ± 5 ppm, lower panel). GP-derivatised oxysterols give *syn* and *anti* conformers about the CN double bond which may or may not be resolved. **(B)** MS^3 ([M]$^+$ ➔[M-Py]$^+$ ➔) spectra of 22R-HC identified in placenta (upper panel) and [$^2H_7$] 22R-HC reference standard (lower panel). **(C)** Multiple reaction monitoring-like (MRM) chromatograms targeting 22-HC isomers ([M]$^+$ ➔[M-Py]$^+$ ➔355) found in placental (upper panel), and authentic standards of [$^2H_7$]22S-HC (central panel) and [$^2H_7$]22R-HC (lower panel). **(D)** MS^3 ([M]$^+$ ➔ [M-Py]$^+$ ➔) spectra of 22S-HC identified in placenta (upper panel) and [$^2H_7$]22S-HC reference standard (lower panel). **(E)** MRM-like chromatograms targeting 20S-HC ([M]$^+$ ➔[M-Py]$^+$ ➔327) in placenta (upper panel) and [$^2H_7$]20S-HC authentic standard (lower panel). **(F, G)** MS^3 ([M]$^+$ ➔[M-Py]$^+$ ➔) spectra of *syn* and *anti* conformers of 20S-HC identified in placenta (upper panels) and of [$^2H_7$]20S-HC reference standard (lower panels). **(H)** 20S-HC and 24S-HC can be resolved *via* MRM but not by chromatography alone even when using an extended chromatographic gradient (37 min). Peaks corresponding to 20S-HC and 24S-HC coalesce in the RIC for their [M]$^+$ ions (upper panel), but are resolved by their specific MRMs, i.e. 20S-HC ([M]$^+$ ➔[M-Py] ➔327, central panel) and 24S-HC ([M]$^+$ ➔[M-Py]$^+$ ➔353, lower panel). See Supplemental Figure S3 for MS^3 spectra of 24S-HC. As data was collected during different sessions, 17 min gradient chromatograms **(A, C, E)**, have been aligned to the peak corresponding to 26-HC in NIST SRM 1950 plasma.

for the additional presence an intense pair of peaks corresponding to the *syn* and *anti* conformers of [$^2H_5$]GP-derivatised 22R-HC in the placental sample. Note *syn* and *anti* conformers are a consequence of GP-derivatisation at C-3 of the sterol A-ring (see Supplemental Figure S1B). 22R-HC is usually only a minor oxysterol in adult plasma/serum (14, 16) and is essentially absent in the NIST SRM 1950 plasma sample (representative of the adult population of the USA) illustrated here (15). The observation of 22R-HC in placenta is not surprising as CYP11A1, the enzyme which generates this oxysterol in the pathway from cholesterol to pregnenolone, is abundant in placenta (2, 17). The identity of the two early eluting peaks was confirmed by reference to [$^2H_7$]22R-HC authentic standard which co-elutes and gives an identical MS^3 ($[M]^+ \rightarrow [M\text{-}Py]^+ \rightarrow$, where Py is pyridine) fragmentation pattern (Figures 2A, B). A major advantage of the GP-derivatisation method is that unlike the un-derivatised $[M+H]^+$, $[M+NH_4]^+$ or $[M-(H_2O)_n+H]^+$ ion, the $[M]^+$ ion of the GP-derivative gives a structurally informative MS^3 spectrum. The fragmentation of GP-derivatised oxysterols has been described in detail elsewhere (18, 19). In brief, a 3β-hydroxy-5-ene function in the parent structure, with no additional substitutions on the ring system, gives following cholesterol oxidase treatment, GP derivatisation and MS^3, a pattern of low-*m/z* fragment ions at 151.1 (*b_1-12), 163.1 (*b_3-28) and 177.1 (*b_2) and a mid-*m/z* fragment ion at 325.2 ('*e, Supplemental Figure S1C). A characteristic, but not unique, fragment ion of 22R-HC is at *m/z* 355.3 (*f', Figure 2B and Supplemental Figure S2A), this appears alongside a satellite peak at *m/z* 353.3 ('*f). By generating a multiple reaction monitoring (MRM)-like chromatogram $[M]^+ \rightarrow [M\text{-}Py]^+ \rightarrow$355.3 the 22R-HC peaks in placenta are highlighted (Figure 2C upper panel). A minor unknown pair of peaks were also observed eluting much later in the MRM chromatogram. Their MS^3 spectra suggests that these correspond to the 22S-epimer (Figure 2D). This was confirmed by analysis of [$^2H_7$]22S-HC which gave an identical MS^3 fragmentation pattern and co-eluted with the endogenous molecule.

In many LC-MS/MS studies oxysterols are identified by MRM where the transition is often non-specific (16, 20). This provides high sensitivity but relies on chromatographic separation of isomers and co-elution with isotopic labelled standards (21). In an initial interpretation of the data presented in Figure 2A (upper panel), the peak at 6.90 min was assumed to be 24S-HC, presumably from contaminating blood. However, closer scrutiny of the chromatogram and relevant MS^3 spectra suggested that the earlier eluting peak 6.64 min was one of the *syn* or *anti* conformers of 20S-HC. 20S-HC has a characteristic MS^3 fragmentation spectrum with a major fragment ion at 327.2 (*e', Figure 2F and Supplemental Figure S2B). By generating a MRM chromatogram for $[M]^+ \rightarrow [M\text{-}Py]^+ \rightarrow$327.2, two peaks corresponding to the *syn* and *anti* conformers of 20S-HC are revealed (Figure 2E). The second peak co-elutes with 24S-HC, of which minor quantities are present as revealed by the 24S-HC characteristic fragment ion at *m/z* 353.3 ('*f, Figure 2G upper panel & Supplemental Figure S1D). However, by extending the chromatographic gradient and by exploiting the specific MRM chromatograms i.e. $[M]^+ \rightarrow [M\text{-}Py]^+ \rightarrow$327.2 for 20-HC and $[M]^+ \rightarrow [M\text{-}Py]^+ \rightarrow$353.3 for 24-HC, the two isomers can be partially resolved (Figure 2H, see Supplemental Figure S3 for the MS^3 spectrum of 24S-HC). Fortuitously, as both 20S-HC and 24S-HC give *syn* and *anti* conformers following GP-derivatisation, the first peak of 20S-HC (12.73 min) is completely resolved from both peaks of 24S-HC and it is only the second peak of 20S-HC and the first peak of 24S-HC that partially co-elute, leaving the second peak of 24S-HC (16.04 min) completely resolved from 20S-HC.

As is evident from Figures 2A, H, other monohydroxycholesterols were also observed in placenta including (25R)26-hydroxycholesterol (26-HC, also known by the non-systematic name 27-hydroxycholesterol, 27-HC) and 7α-hydroxycholesterol (7α-HC). MS^3 spectra are shown in Supplemental Figure S3. 7β-Hydroxycholesterol (7β-HC) was also observed, this like 7α-HC may be endogenous, but can also be formed during sample preparation by *ex vivo* oxidation (22). In placenta minor quantities of (25R)26-hydroxycholest-4-en-3-one and 22R-hydroxycholest-4-en-3-one, the natural 3-oxo-4-ene relatives of 26-HC and 22R-HC, respectively, were also observed, but are the subject of a separate report (23).

3.1.2 Dihydroxycholesterols, trihydroxycholesterols, pregnenolone and progesterone

The second step in the conversion of cholesterol to pregnenolone by CYP11A1 is the generation of 20R,22R-diHC from 22R-HC (Figure 1). The RIC (*m/z* 555.4317 ± 5 ppm) for dihydroxycholesterols reveals two major peaks which appear at retention times, and give identical MS^3 ($[M]^+ \rightarrow [M\text{-}Py]^+ \rightarrow$) spectra, to the authentic standard of 20R,22R-diHC and are identified as the *syn* and *anti* conformers of the GP-derivative (Figures 3A, B). The MS^3 fragmentation pattern shows features of both 20-HC (*e', *m/z* 327.2, Supplemental Figure S2C) and 22-HC (*f-16, *m/z* 355.3, Supplemental Figure S2D) and to search for possible epimers of 20R,22R-diHC, MRM-like chromatograms were constructed for the transitions $[M]^+ \rightarrow [M\text{-}Py]^+ \rightarrow$327.2 and $[M]^+ \rightarrow [M\text{-}Py]^+ \rightarrow$355.3 (Figure 3A). A minor peak was observed at 5.04 min, but the MS^3 fragmentation pattern corresponded to a different isomer (x,y-diHC), possibly 22,23-dihydroxycholesterol (22,23-diHC, Figures 3C upper panel, and Supplemental Figure S2E). Unsurprisingly, when a search was made for pregnenolone by constructing the appropriate RIC (*m/z* 450.3115) this steroid was evident as was progesterone (*m/z* 448.2959), its HSD3B1 oxidised metabolite, in the fraction not treated with cholesterol oxidase i.e. fraction B (Figures 3D, E). Besides 20R,22R-diHC and the presumptively identified 22,23-diHC, low levels of 7α,(25R)26-dihydroxycholesterol (7α,26-diHC) were also found in placenta (Figures 3A, C).

20R,22R-diHC extracted from placenta gives intense signals in LC-MS and based on this and on the additional presumptive

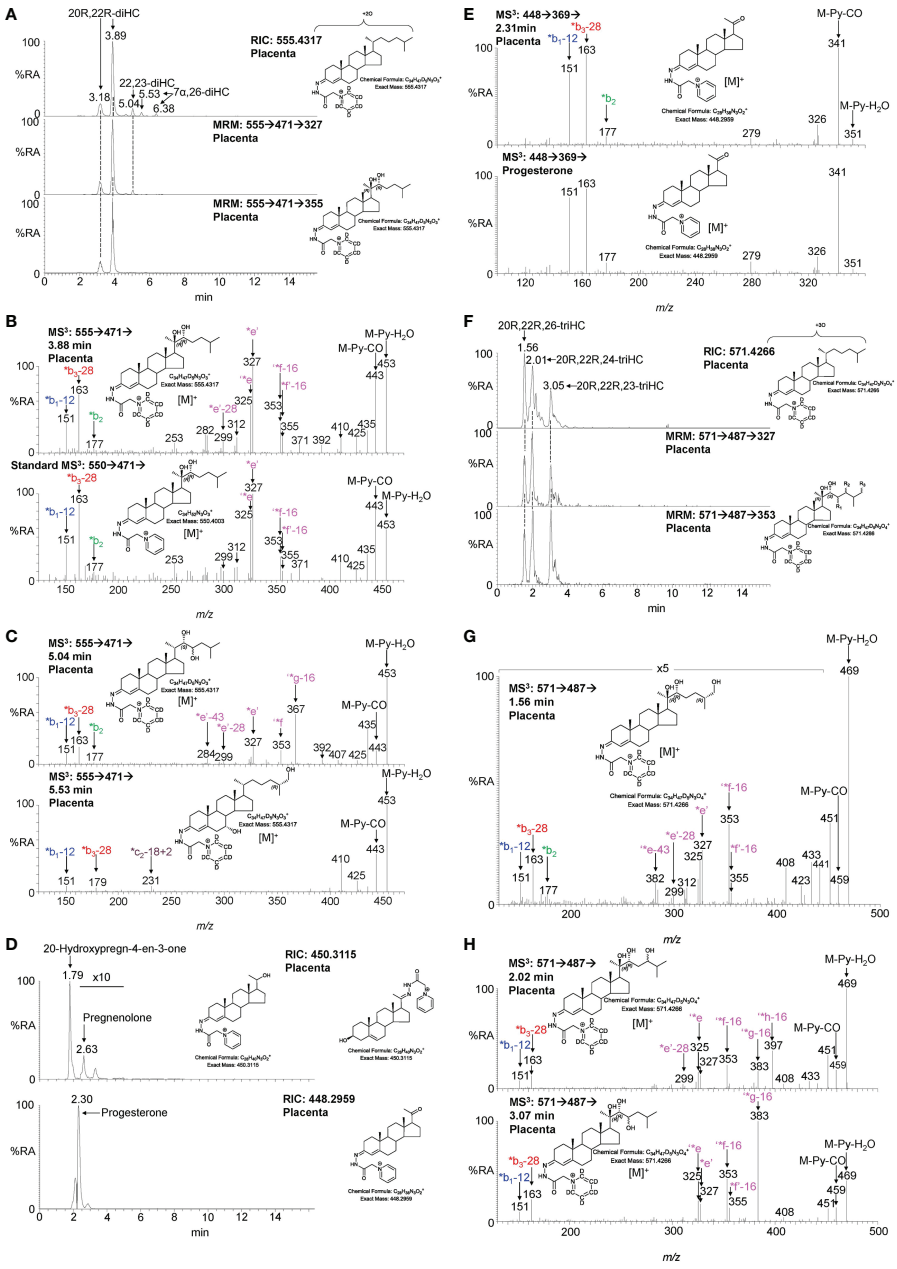


FIGURE 3
LC-MS(MS^n) analysis of GP-derivatised 20R,22R-diHC and its metabolites in placenta. **(A)** RIC (*m/z* 555.4317 ± 5 ppm) corresponding to the $[M]^+$ ion of dihydroxycholesterols (diHC, upper panel). MRM-like chromatograms targeting 20R,22R-diHC ($[M]^+$ ➔$[M\text{-}Py]^+$ ➔327, central panel) and ($[M]^+$ ➔$[M\text{-}Py]^+$ ➔355, lower panel). **(B)** MS^3 ($[M]^+$ ➔$[M\text{-}Py]^+$ ➔) spectra of 20R,22R-diHC from placenta (upper panel) and of an authentic standard (lower panel). **(C)** MS^3 ($[M]^+$ ➔$[M\text{-}Py]^+$ ➔) spectra of other dihydroxycholesterols found in placenta, possibly 22,23-diHC (upper panel) and 7α,26-diHC (lower panel). **(D)** RICs (*m/z* 450.3115) corresponding to pregnenolone (upper panel) and *m/z* 448.2959 corresponding to progesterone. **(E)** MS^3 ($[M]^+$ ➔$[M\text{-}Py]^+$ ➔) spectra of progesterone from placenta (upper panel) and of the reference standard (lower panel). **(F)** RIC (*m/z* 571.4266 ± 5 ppm) corresponding to the $[M]^+$ ion of trihydroxycholesterols (triHC, upper panel). MRM-like chromatograms targeting 20R,22R,x-triHC ($[M]^+$ ➔$[M\text{-}Py]^+$ ➔327, central panel) and ($[M]^+$ ➔$[M\text{-}Py]^+$ ➔353, lower panel). In the structure shown in the lower panel, one of R_1, R_2 or R_3 is a hydroxy group, the other two are hydrogens. **(G)** MS^3 ($[M]^+$ ➔$[M\text{-}Py]^+$ ➔) spectrum of the trihydroxycholesterol found in placenta and commensurate with the 20R,22R,26-triHC structure. **(H)** MS^3 ($[M]^+$ ➔$[M\text{-}Py]^+$ ➔) spectra of other trihydroxycholesterols with possible structures of 20R,22R,24-triHC (upper panel) and 20R,22R,23-triHC. In the absence of authentic standards 20R,22R stereochemistry is assumed on the presumption that the triHCs are derived from 20R,22R-diHC.

identification of 22,23-diHC, it is likely that other hydroxylase activities are present in placenta besides those normally associated with CYP11A1, potentially resulting in the formation of trihydroxycholesterols (triHC). The RIC for triHC (*m/z* 571.4266 ± 5 ppm) reveals three major peaks (Figure 3F upper panel). To tighten the search for hydroxylated metabolites of 20R,22R-diHC, MRM-like chromatograms were generated for the major side-chain cleavage fragment ions associated with the 20R,22R-diHC structure i.e. $[M]^+$ ➔$[M\text{-}Py]^+$ ➔327.2, $[M]^+$ ➔$[M\text{-}Py]^+$ ➔353.3 (cf. Figure 3B). Again, three major peaks were evident in these chromatograms. Interrogation of the respective MS^3 spectra suggested isomers of 20,22,x-triHC, where x is the location of an additional hydroxy group on the side-chain. Considering the spectrum of the last eluting isomer at 3.05 min (Figures 3F, H lower panel), besides pairs of fragment ions at *m/z* 325/327 ('*e/*e'), *m/z* 353/355 ('*f-16/*f-16) a dominating fragment ion is observed at *m/z* 383 ('*g-16), this pattern is consistent with a 20R,22R,23-triHC isomer (Supplemental Figure S2F cf. S2C). Considering the isomer eluting second at 2.01 min (Figure 3F), the MS^3 spectrum shows an additional fragment ion at *m/z* 397 ('*h-16, Figure 3H upper panel); the structure that explains this fragment ion formation most easily is 20R,22R,24-triHC (Supplemental Figure S2G, cf. S2C & S2D). The MS^3 spectrum of the first eluting peak at 1.56 min (Figure 3G) does not show the fragment-ions at *m/z* 383 or 397 (Figure 3H), suggesting that the extra hydroxy group does not encourage additional side-chain fragmentation. The most likely structures for this isomer are 20R,22R,26-triHC or perhaps 20R,22R,25-triHC (Supplemental Figure S2H, I, cf. S2C & S2D). Note, authentic standards are not available for the 20,22,x-triHC isomers and stereochemical assignments are made based on biosynthetic considerations. As was the situation with 22R-HCO, a minor proportion of 20R,22R-dihydroxysterols are found as the 3-oxo-4-ene, i.e. 20R,22R-dihydroxycholest-4-en-3-one (20R,22R-diHCO) (23).

3.1.3 Cholestenoic acids

Sterol 27-hydroxylase (CYP27A1) is the enzyme that introduces both (25R)26-hydroxy and (25R)26-carboxy groups to sterols (Figure 1) (24), it is expressed in trophoblast cells of the placenta (25). We identify 26-HC (Figures 2A, H; Supplemental Figure S3D) and 3β-hydroxycholest-5-en-(25R)26-oic acid (3β-HCA, Supplemental Figure S4) in placenta, and there is the possibility that 20R,22R-diHC may be a substrate for CYP27A1 and be metabolised *via* 20R,22R,26-triHC to the C_{27} bile acid 3β,20R,22R-trihydroxycholest-5-en-(25R)26-oic acid (3β,20R,22R-triHCA) in placenta (Figure 1). The RIC appropriate for 3β,20R,22R-triHCA (*m/z* 585.4059 ± 5ppm) reveals two major and a minor peak (Figure 4A) of which only the first gives an MS^3 spectrum compatible with a 3β,20R,22R-triHCA structure (Figure 4B & Supplemental Figure S2J & K, cf. Supplemental Figure S2H, I). The similarity between the MS^3 spectra of 20R,22R-diHC, and the presumptively identified 20R,22R,26-triHC and 3β,20R,22R-triHCA can be visualised in Figure 4C where the low-middle *m/z* range of the three spectra are shown on the same *m/z* scale. While the low-middle *m/z* range provides evidence for the 20,22-dihydroxy structural motif (presumably 20R,22R-) the high *m/z* range (Figure 4B) is indicative of a C-26 acid. Sterol acids show characteristic neutral losses from the $[M\text{-}Py]^+$ ion corresponding to the net loss of H_2CO_2 + n(H_2O), where n is the number of OH groups on the sterol beyond that derivatised at C-3 (19). In Figure 4B we see such losses giving fragments at *m/z* 437 (M-Py-H_2O-H_2CO_2 i.e. '*j-18) and *m/z* 419 (M-Py-2H_2O-H_2CO_2 i.e. '*j-36). These fragment ions are associated with satellite peaks at *m/z* 440 ($[M\text{-}Py\text{-}61]^+$ and 422 ($[M\text{-}Py\text{-}79]^+$) providing a pattern characteristic of a trihydroxycholestenoic acid (See Supplemental Figure S2L). Note, the third hydroxy group is the site of derivatisation. The other two chromatographic peaks give almost identical MS^3 spectra (Figure 4D) presumably *syn* and *anti* conformers of a second isomer whose structure is not obvious from the MS^3 spectra, although fragment-ions at *m/z* 385, 397 and 471 are probably structurally significant.

Cholestenoic acids are intermediates in bile acid biosynthesis pathways (26–28). In the route towards C_{24} acids, C_{27} acids become converted to their CoA-thioesters by bile acid CoA-synthetase (BACS, SLC27A5), stereochemistry at C-25 is inverted by α-methylacyl-CoA racemase (AMACR) and a double bond introduced at Δ^{24} with *trans* geometry by acyl-CoA oxidase 2 (ACOX2, see Figure 1) (27). The next steps are catalysed by D-bifunctional protein (DBP, HSD17B4) and lead to a C-24 oxo group. Beta-oxidation by sterol carrier protein 2 (SCP2) then gives a C_{24} CoA-thioester which is finally amidated with glycine or taurine or hydrated to give the C_{24} acid (27). In bioanalysis, intermediates are almost always observed as the carboxylic acids rather than the thioesters (28). Following this pathway, the CoA-thioester of 3β,20R,22R-triHCA would be isomerised from the 25R-epimer to one with 25S-stereochemistry which would then be oxidised to the CoA-thioester of 3β,20R,22R-trihydoxycholest-5,24-dienoic acid (3β,20R,22R-triH-Δ^{24}-CA, Figure 1). Shown in Figure 4E is the RIC (*m/z* 583.3902 ± 5 ppm) appropriate to the $[M]^+$ ion of 3β,20R,22R-triH-Δ^{24}-CA, along with MRM-like chromatograms characteristic of sterols with 20- and 22-hydroxylation of the side-chain. One major chromatographic peak is evident at 2.20 min, and the MS^3 ($[M]^+$ ➔$[M\text{-}Py]^+$ ➔) spectrum associated with this peak (Figure 4F) resembles, in the low to middle *m/z* range, that of 3β,20R,22R-triHCA (Figure 4B), however, the fragment-ion observed at *m/z* 355 (*f-16) in spectrum of 3β,20R,22R-triHCA is replaced by one at *m/z* 371 (*f) in the spectrum shown Figure 4F. This spectrum is compatible with the 3β,20R,22R-triH-Δ^{24}-CA structure (see Supplemental Figures S2M–O). Further evidence for the MS^3 spectrum presented in Figure 4F corresponding to 3β,20R,22R-triH-Δ^{24}-CA is the presence of fragment ions characteristic of sterol acids, '*j-18 (M-Py-H_2O-H_2CO_2) at *m/z* 435 and '*j-36 (M-Py-2H_2O-H_2CO_2) at *m/z* 417. These fragment ions are associated with satellite peaks at *m/z* 438 ($[M\text{-}Py\text{-}61]^+$ and 420

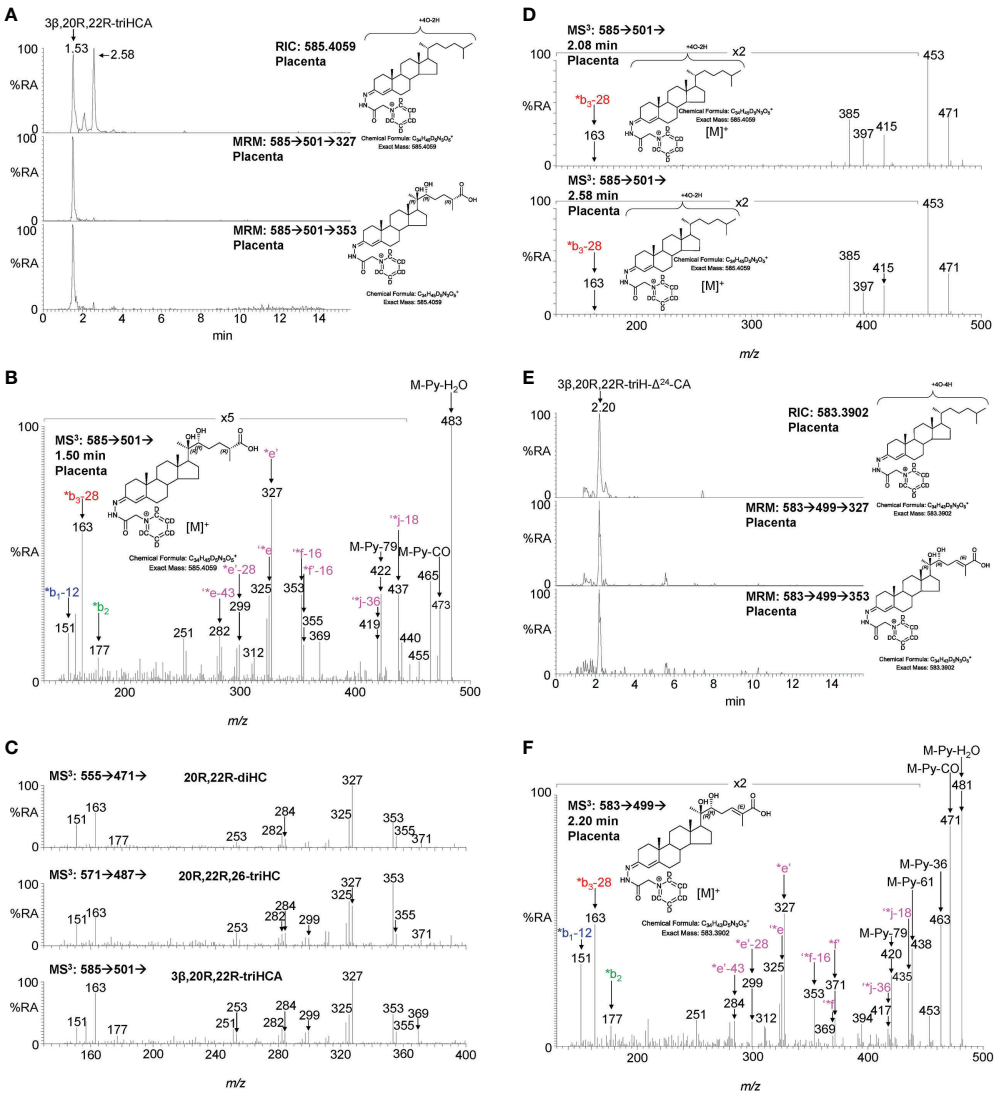


FIGURE 4
LC-MS(MS^n) analysis of GP-derivatised 3β,20R,22R-triHCA, its isomers and of 3β,20R,22R-triH-Δ^{24}-CA in placenta. **(A)** RIC (*m/z* 585.4059 ± 5 ppm) corresponding to the $[M]^+$ ion of trihydroxycholestenoic acids (upper panel). MRM-like chromatograms targeting 3β,20R,22R-triHCA ($[M]^+$ ➔$[M\text{-}Py]^+$ ➔327, central panel) and ($[M]^+$ ➔$[M\text{-}Py]^+$ ➔353, lower panel). **(B)** MS^3 ($[M]^+$ ➔$[M\text{-}Py]^+$ ➔) spectrum postulated to correspond to 3β,20R,22R-triHCA. **(C)** Comparison of MS^3 ($[M]^+$ ➔$[M\text{-}Py]^+$ ➔) spectra of 20R,22R-diHC (upper panel) with spectra postulated to correspond to 20R,22R,26-triHC (central panel) and 3β,20R,22R-triHCA (lower panel) over the *m/z* range 130 – 400. **(D)** MS^3 spectra of two other isomers but the spectra do not appear to be of cholestenoic acids. **(E)** RIC (*m/z* 583.3902 ± 5 ppm) corresponding to the $[M]^+$ ion of a trihydroxycholestadienoic acid (upper panel). MRM-like chromatograms targeting 3β,20R,22R-triH-Δ^{24}-CA ($[M]^+$ ➔$[M\text{-}Py]^+$ ➔327, central panel) and ($[M]^+$ ➔$[M\text{-}Py]^+$ ➔353, lower panel). **(F)** MS^3 ($[M]^+$ ➔$[M\text{-}Py]^+$ ➔) spectrum postulated to correspond to 3β,20R,22R-triH-Δ^{24}-CA. As was the case with 20R,22R,26-triHC in Figure 3, the 20R,22R-stereochemistry is assumed in 3β,20R,22R-triHCA and 3β,20R,22R-triH-Δ^{24}-CA.

($[M\text{-}Py\text{-}79]^+$, see Supplemental Figure S2N). However, as is the case with other postulated structures definitive identification awaits synthesis of the authentic standard. Again, as was the case with 20R,22R,26-triHC, the 20R,22R-stereochemistry is assumed in 3β,20R,22R-triHCA and 3β,20R,22R-triH-Δ^{24}-CA. Note the ultimate C_{24} bile acid 3β,20R,22R-trihydroxychol-5-enoic acid was not observed, perhaps due to low expression of HSD17B4 or SCP2 in placenta.

3.2 Identification of oxysterols in cord and maternal plasma

To investigate if the placental oxysterols are transported to the fetus, umbilical cord plasma derived from umbilical cord blood was analysed for oxysterols. The data was compared to the oxysterol profiles in plasma from maternal blood, taken 1 - 2 day before elective caesarean section and plasma from “control”

non-pregnant females. As might be expected, the oxysterol profile of cord plasma resembles that of non-pregnant females, but with the additional presence of CYP11A1-derived oxysterols. 22R-HC is present in both cord and maternal plasma but is absent from controls (Figures 5A, B, 6A–C; Table 1). If present, 20S-HC is at levels in cord, maternal and control plasma samples below the limit of detection (0.1 ng/mL). The dihydroxycholesterol 20R,22R-diHC is the dominant oxysterol in cord plasma, it is also a major oxysterol in maternal plasma but is absent from control plasma (Figures 5C, D, 6D–F). Presumptively identified 20R,22R,26-triHC was near the limit of quantification in both cord and maternal plasma but was absent from controls (Figures 5E, F, 6G, H). The presumptively identified C_{27} bile acid 3β,20R,22R-triHCA was evident in cord plasma and just detected in maternal plasma but was absent from control plasma (Figures 5G, H, 7A–C). Presumptively identified 3β,20R,22R-triH-Δ^{24}-CA was only detected in cord plasma (Supplemental Figures S5A, B).

Besides the oxysterols discussed above, the profile of cord and maternal plasma was investigated for other oxysterols and sterol acids routinely found in adult plasma, this data is included in Table 1. While it was possible to make quantitative measurements for mono- and di-hydroxycholesterols thanks to the availability of authentic standards, the absence of standards for 20R,22R,26-triHC and 3β,20R,22R-triHCA means that the values determined for these metabolites are semi-quantitative, but by using the same internal standard for quantification across samples should give reliable measurements for relative quantification across the sample groups.

In cord plasma, but not plasma from pregnant and non-pregnant females, 22R-HCO was found but at a much lower level than 22R-HC. 20R,22R-diHCO was found in both cord plasma and plasma from pregnant females, but not non-pregnant females. Further details are reported elsewhere (23).

3.3 Identification of oxysterols in amniotic fluid

Amniotic fluid is derived from maternal plasma but also contains progressively more fetal urine as pregnancy continues. One of its functions is to facilitate the exchange of biochemicals between mother and fetus. Based on the data from analysis of placenta and cord plasma, it is reasonable to expect to find 22R-HC and its down-stream metabolites in amniotic fluid. As in cord and maternal blood 22R-HC (Figures 6A–C), 20R,22R-diHC (Figures 6D–F), 20R,22R,26-triHC (Figures 6G, H) and 3β,20R,22R-triHCA (Figures 7A–C) were identified and quantified in amniotic fluid (Table 1). Presumptively identified 3β,20R,22R-triH-Δ^{24}-CA was also detected but not quantified (Supplemental Figures S5C, D).

3.4 Relative quantification between samples groups

As mentioned above although the measurement of some of the metabolites of 22R-HC is only semi-quantitative, relative values are likely to be accurate (Table 1). Shown in Figure 8 are plots displaying the quantities determined in the different samples for 22R-HC and its dominant metabolites. With respect to these metabolites, cord plasma is very different to control plasma from non-pregnant females with statistical differences also observed between cord and maternal plasma for 20R,22R-diHC and 3β,20R,22R-triHCA.

3.5 Quantification of other oxysterols

Besides the oxysterols discussed in the previous section, other oxysterols typically measured by the charge-tagging approach were also measured and are presented in Table 1 (11, 14, 19). Note the values for the oxysterols and sterol acids for which there is no authentic standard were quantified against [$^2H_7$]24R/S-HC and are only semi-quantitative values.

4 Discussion

In the current study we have investigated the oxysterol profile of placenta, cord plasma, maternal plasma, non-pregnant female plasma (control plasma) and amniotic fluid. In each of the pregnancy samples we identify metabolites derived from CYP11A1 which are essentially absent from non-pregnant females (Figure 8; Table 1). There are two significant findings from the current study. Firstly, the rediscovery of 20S-HC and the discovery of 22S-HC in human placenta (7), and secondly the uncovering of a shunt pathway for 22R-HC metabolism to C_{27} bile acids.

20S-HC is a controversial oxysterol as it has been detected in very few analytical studies (7, 8, 29, 30) despite being biologically active *in vitro*. 20S-HC, like 22R-HC, is a ligand to the liver X receptors α and β (LXRα, LXRβ) (31) and to the retinoic acid receptor-related orphan receptor γ (RORγ) (32), but unlike 22R-HC, activates the G protein-coupled receptor (GPCR) Smoothened (SMO), a key protein in the hedgehog signalling pathway, required for proper cell differentiation in the embryo (33, 34). 20S-HC also inhibits the processing of SREBP-2 (sterol regulatory element-binding protein 2) to its active form as the master transcription factor regulating cholesterol biosynthesis (35, 36), presumably by binding to INSIG (insulin induced gene) in a manner similar to other side-chain hydroxycholesterols (37). Recently, 20S-HC has been identified as a ligand to the sigma 2 (σ2) receptor (38), also known as transmembrane

10.3389/fendo.2022.1031013

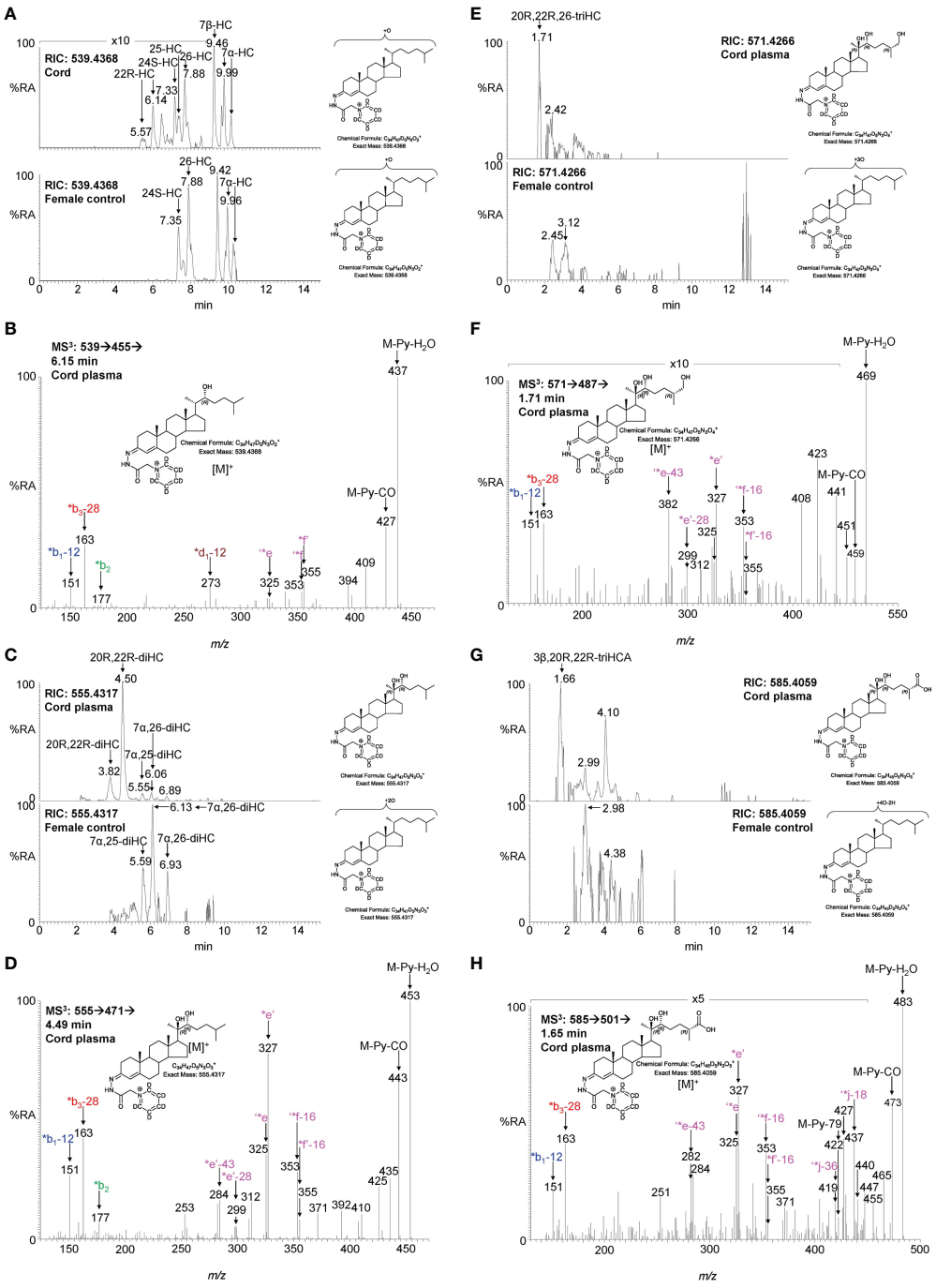


FIGURE 5
LC-MS(MS^n) analysis of GP-derivatised oxysterols in umbilical cord plasma. **(A)** RICs for monohydroxycholesterols (*m/z* 539.4368 ± 5 ppm) in cord (upper panel) and control non-pregnant female plasma (lower panel). **(B)** MS^3 ([M]$^+$ ➔[M-Py]$^+$ ➔) spectrum of 22R-HC from cord plasma. **(C)** RICs for dihydroxycholesterols (*m/z* 555.4317 ± 5 ppm) in cord (upper panel) and control female plasma (lower panel). **(D)** MS^3 ([M]$^+$ ➔[M-Py]$^+$ ➔) spectrum of 20R,22R-diHC from cord plasma. **(E)** RICs for trihydroxycholesterols (*m/z* 571.4266 ± 5 ppm) in cord (upper panel) and control female plasma (lower panel). **(F)** MS^3 ([M]$^+$ ➔[M-Py]$^+$ ➔) spectrum postulated to correspond to 20R,22R,26-triHC. **(G)** RIC (*m/z* 585.4059 ± 5 ppm) corresponding to the [M]$^+$ ion of trihydroxycholestenoic acids in cord plasma (upper panel) and control female plasma. **(H)** MS^3 ([M]$^+$ ➔[M-Py]$^+$ ➔) spectrum postulated to correspond to 3β,20R,22R-triHCA. Note, cord and control female plasma were analysed using a different LC column (same type, different batch) to placenta.

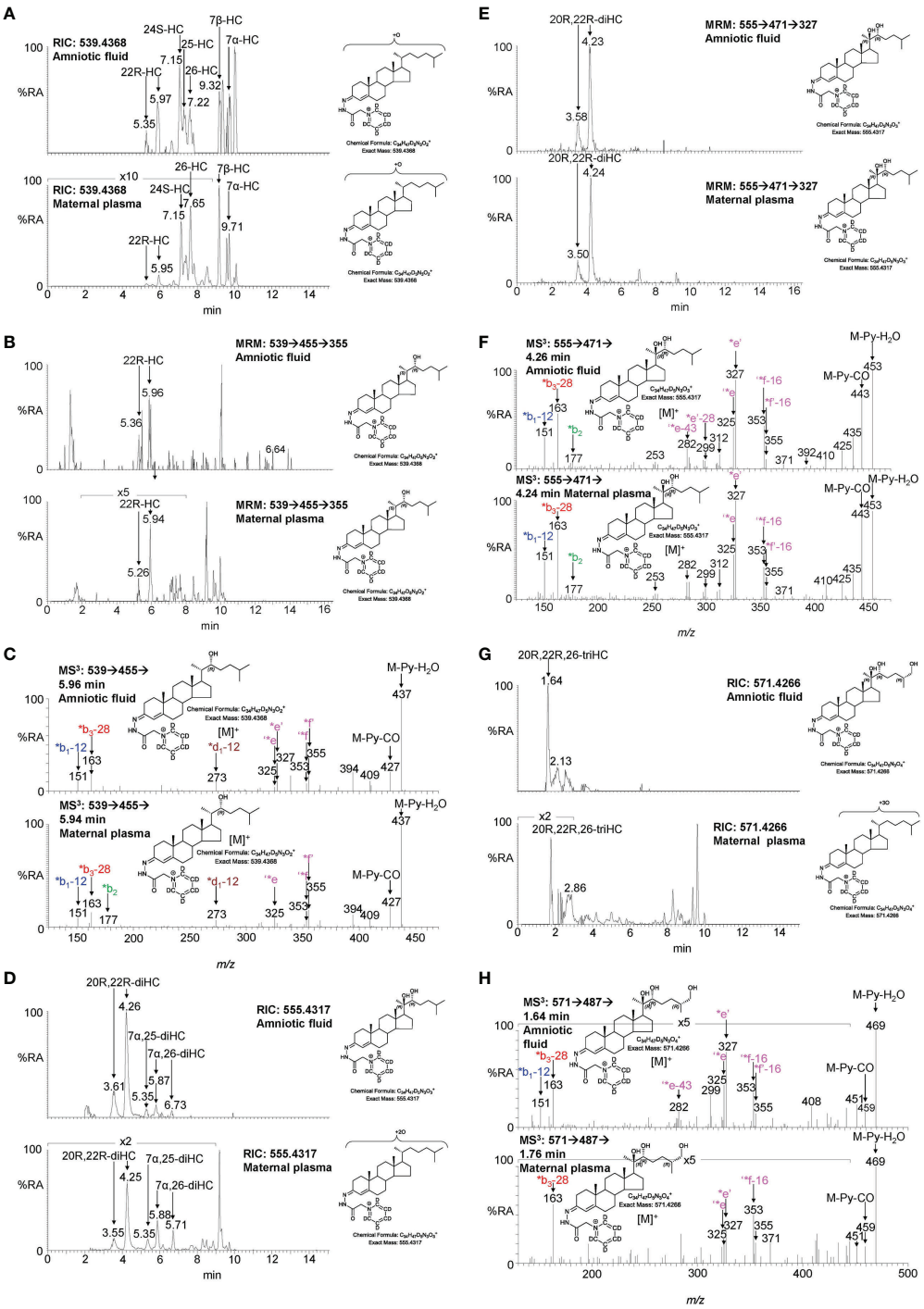


FIGURE 6
LC-MS(MS^n) analysis of GP-derivatised oxysterols in amniotic fluid and plasma from pregnant females (maternal plasma). **(A)** RICs for monohydroxycholesterols (*m/z* 539.4368 ± 5 ppm) in amniotic fluid (upper panel), and in plasma from pregnant females (lower panel). **(B)** MRM-like ($[M]^+$ ➔$[M\text{-}Py]^+$ ➔355) chromatograms targeting 22-HC in amniotic fluid (upper panel) and in plasma from pregnant females (lower panel). **(C)** MS^3 ($[M]^+$ ➔$[M\text{-}Py]^+$ ➔) spectra of 22R-HC identified in amniotic fluid (upper panel) and in plasma from pregnant females (lower panel). **(D)** RIC (*m/z* 555.4317 ± 5 ppm) corresponding to the $[M]^+$ ion of dihydroxycholesterols identified in amniotic fluid (upper panel) and in plasma from pregnant females (lower panel). **(E)** MRM-like chromatograms targeting 20R,22R-diHC ($[M]^+$ ➔$[M\text{-}Py]^+$ ➔327) in amniotic fluid (upper panel) and in plasma from pregnant females (lower panel). **(F)** MS^3 ($[M]^+$ ➔$[M\text{-}Py]^+$ ➔) spectra of 20R,22R-diHC in amniotic fluid (upper panel) and in plasma from pregnant females (lower panel). **(G)** RICs for trihydroxycholesterols (*m/z* 571.4266 ± 5 ppm) in amniotic fluid (upper panel) and in plasma from pregnant females (lower panel). **(H)** MS^3 ($[M]^+$ ➔$[M\text{-}Py]^+$ ➔) spectra of the trihydroxycholesterols found in amniotic fluid (upper panel) and in plasma from pregnant females (lower panel) commensurate with the 20R,22R,26-triHC structure.

10.3389/fendo.2022.1031013

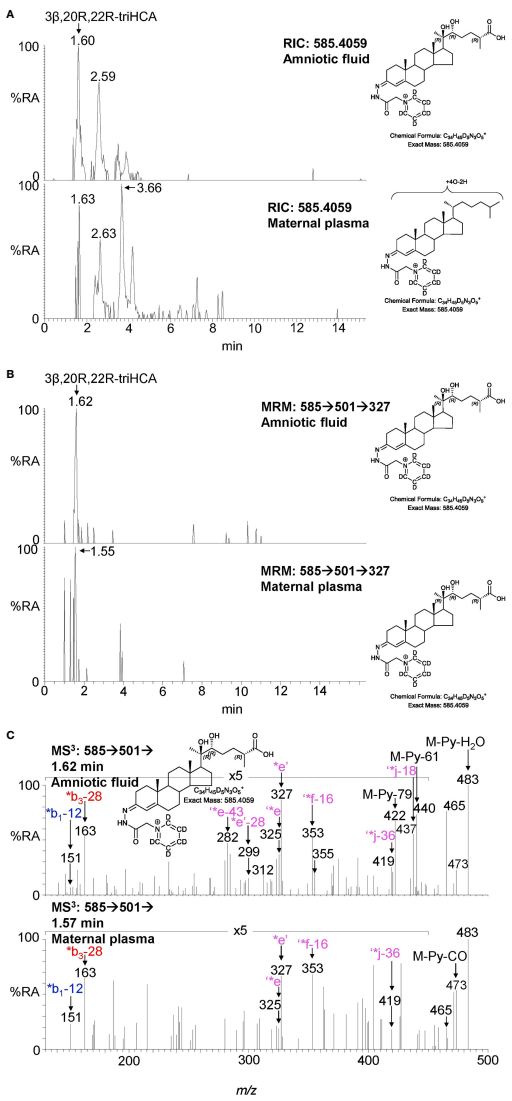


FIGURE 7
LC-MS(MS^n) analysis of GP-derivatised trihydroxycholestenoic acids found in amniotic fluid and plasma from pregnant females (maternal plasma). **(A)** RICs (*m/z* 585.4059 ± 5 ppm) corresponding to the $[M]^+$ ion of trihydroxycholestenoic acids found in amniotic fluid (upper panel) and in plasma from pregnant females (lower panel). **(B)** MRM-like ($[M]^+$ ➔$[M\text{-}Py]^+$ ➔327) chromatograms targeting 3β,20R,22R-triHCA in amniotic fluid (upper panel) and in plasma from pregnant females (lower panel). **(C)** MS^3 ($[M]^+$ ➔$[M\text{-}Py]^+$ ➔) spectra postulated to correspond to 3β,20R,22R-tiHCA in amniotic fluid (upper panel) and in plasma from pregnant females (lower panel).

protein 97 (Tmem97), which is expressed in the central nervous system (39), and has been suggested to be a chaperone protein for NPC1 (Niemann Pick C1), the lysosomal cholesterol transport protein (38). The enzyme required to biosynthesise 20S-HC has not been identified, although CYP11A1 has been reported to generate both 20-hydroxyvitamin D_3 and 20,22-dihydroxyvitamin D_3 or 20,23-dihydroxyvitamin D_3 from vitamin D_3 (40, 41). The high level of CYP11A1 in placenta (17), makes this a good candidate enzyme for biosynthesis of 20S-HC. Like 20S-HC, there are few reports of the detection of 22S-HC in biological systems (30), however, 22S-HC has been identified as the sulphate ester in human meconium (10), the earliest stool of a mammalian infant, and in the human cell lines HCT-15 and HCT-116 (42). Unlike 20S-HC and most other side-chain oxysterols, 22S-HC is not an LXR agonist (43), behaving more like an antagonist (44), neither does it activate the Hh signalling pathway through SMO (33).

22R-HC and 20R,22R-diHC are abundant oxysterols in cord plasma and placenta. 20R,22R-diHC, like 22R-HC and 20S-HC, is an LXR ligand and all three appears to have similar activating capacity (45). Although the primary function of the LXRs is considered to be the regulation of cellular cholesterol (46), LXRs

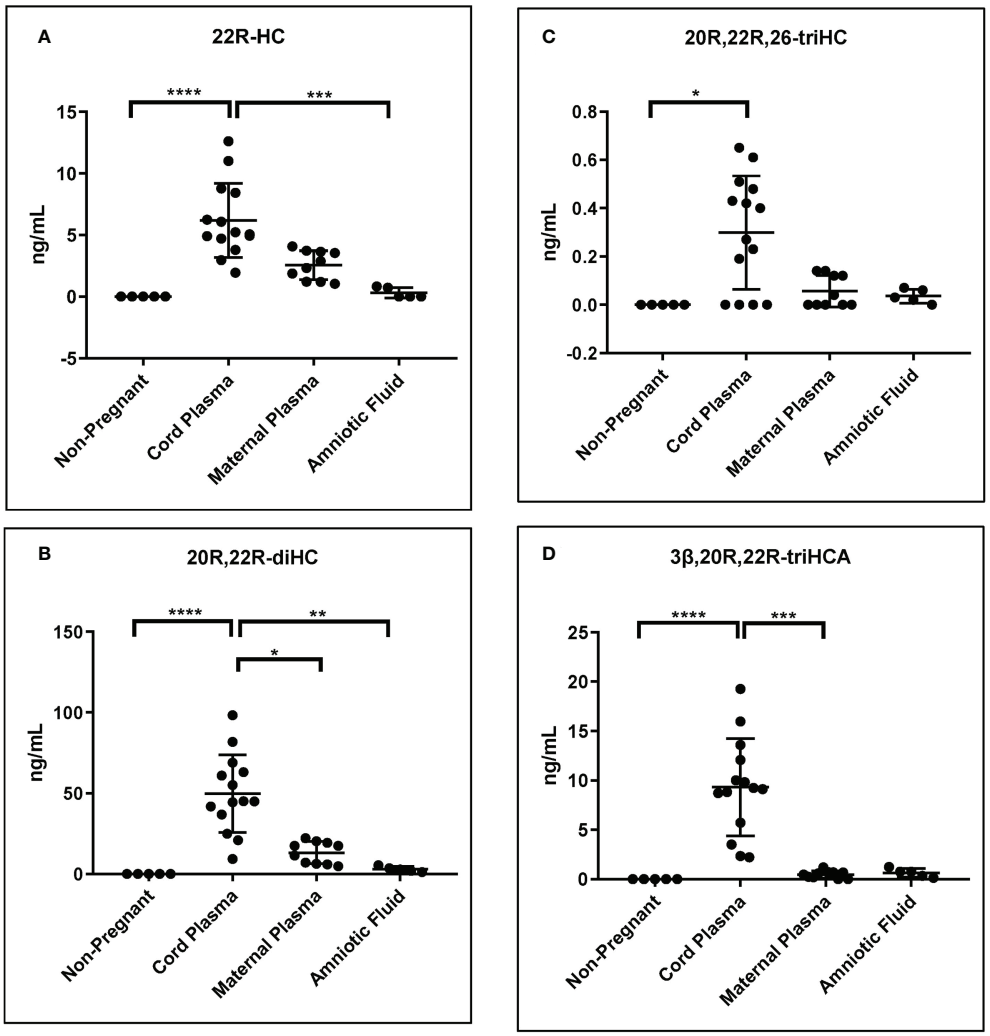


FIGURE 8
Concentration of 22R-HC and downstream metabolites. For each sample type: Control non-pregnant female plasma (plasma, n = 5); cord plasma (n = 14); maternal (pregnant female) plasma (n = 10); and amniotic fluid (n = 5). Concentrations of **(A)** 22R-HC, **(B)** 20R,22R-diHC, **(C)** 20R,22R,26-triHC and **(D)** 3β,20R,22R-triHCA were determined by LC-MS exploiting charge-tagging utilising GP derivatisation. Vales in **(A)** and **(B)** are quantitative (authentic standards available), those in **(C)** and **(D)** are semi-quantitative (authentic standards not available). The band represents the median where the whiskers extend to the most extreme upper and lower data points which are no more than 1.5 times the range between the first and third quartile. Non-parametric Kruskal-Wallis multiple comparisons test was used for comparison of data. *P < 0.05; **P < 0.01, ***P < 0.001 ****P < 0.0001.

also appear to have developmental functions, being required for the development of dopaminergic neurons in midbrain (47). In fact, LXRβ also appears to have a protective role towards dopaminergic neurons, as the synthetic agonist GW3965 protects against the loss of dopaminergic neurons in a Parkinson's disease mouse model (48).

CYP11A1 is an inner mitochondrial membrane protein and catalyses the side-chain cleavage of cholesterol to pregnenolone. The intermediates in this reaction scheme i.e. 22R-HC and 20R,22R-diHC, bind more tightly to CYP11A1 and are converted to pregnenolone at a greater rate than cholesterol (49). It is generally considered that 22R-HC and 20R,22R-diHC remain in the active site until all three oxidation steps are complete (3), however, the abundance of 22R-HC, and the observation of 20R,22R-diHC, in cord plasma, maternal plasma and placenta in this study would argue that this is not always the case.

Pregnenolone is converted to progesterone by HSD3B1 which is localised in both mitochondria and the endoplasmic reticulum (50, 51), and is highly expressed in placenta (52). Progesterone has many roles associated with the establishment and maintenance of pregnancy, including ovulation, uterine and mammary gland development and the onset of labour (53). Progesterone

suppresses spontaneous uterine contractility during pregnancy and, in most mammals, a fall in systemic progesterone is required for the initiation of labour at term. However, in humans, labour occurs in the presence of elevated circulating levels of progesterone. Despite this, disruption of progesterone signalling by the progesterone receptor (PR) antagonist RU486 at any stage of pregnancy results in myometrial contractions and labour, strongly suggesting that reduced progesterone signalling is responsible for labour in women (54). In the current study we have uncovered a shunt pathway that operates in parallel to pregnenolone/progesterone biosynthesis in the placenta (Figure 1). Beyond 20R,22R-diHC we identified three trihydroxycholesterol isomers, one of which gives an MS^3 fragmentation pattern consistent with 20R,22R,26-triHC, and two dihydroxycholestenoic acid isomers one of which gives a fragmentation pattern we assign to 3β,20R,22R-triHCA. A downstream metabolite 3β,20R,22R-triH-Δ^{24}-CA was also presumptively identified. Here we assign stereochemistry based on the assumption of 20R,22R-diHC being the precursor, but we await the chemical synthesis of these metabolites to definitively confirm their identification, this will be required whether LC-MS/MS or gas chromatography - MS is the identification method. However, their presence during pregnancy would define a new pathway of C_{27} bile acid biosynthesis (Figure 1). Most of the metabolites of this pathway are also observed in cord plasma, maternal plasma and amniotic fluid (Table 1). Notably, the amniotic fluid samples were from 16 – 18 weeks of gestation and the other pregnancy samples 37 + weeks indicating a pathway operational throughout pregnancy. CYP27A1 is the likely sterol hydroxylase which will convert 20R,22R-diHC to 20R,22R,26-triHC and on to 3β,20R,22R-triHCA. Like CYP11A1, CYP27A1 is an inner mitochondrial membrane enzyme and is expressed in placenta (6, 25). Although the C_{27} bile acid 3β,20R,22R-triHCA has not previously been identified, a C_{27} bile acid with 22R-hydroxylation has been identified in a patient with Zellweger's syndrome (55). It should be noted that 20S-HC will also act as a substrate for pregnenolone formation *via* a CYP11A1 catalysed reaction (30), presumably *via* 20R,22R-diHC (56). Thus, a potential route for 20S-HC metabolism is through 20R,22R-diHC and on to C_{27} bile acids.

How important is the 20R,22R-diHC shunt pathway? At present we can only speculate, but the LXR-activating capacity of 22R-HC and 20R,22R-diHC and the expression of both LXRα and β during mammalian development makes it tempting to speculate that 20R-HC, 20R,22R-diHC and also 20S-HC by activating LXR, and in the case of 20S-HC by binding to Smo and Tmem97, are important for development of the embryo (Figure 9). Interestingly Tmem97 is a SREBP target gene (57), meaning that 20S-HC is both a Tmem97 ligand and a regulator of its synthesis. Tmem97 is associated with NPC1 in the endosomal-lysosomal compartment linking it to cholesterol transport. Little is known about the biological activities of trihydroxycholesterols and trihydroxycholestenoic acids and it is unknown whether 20R,22R,26-triHC, 3β,20R,22R-triHCA

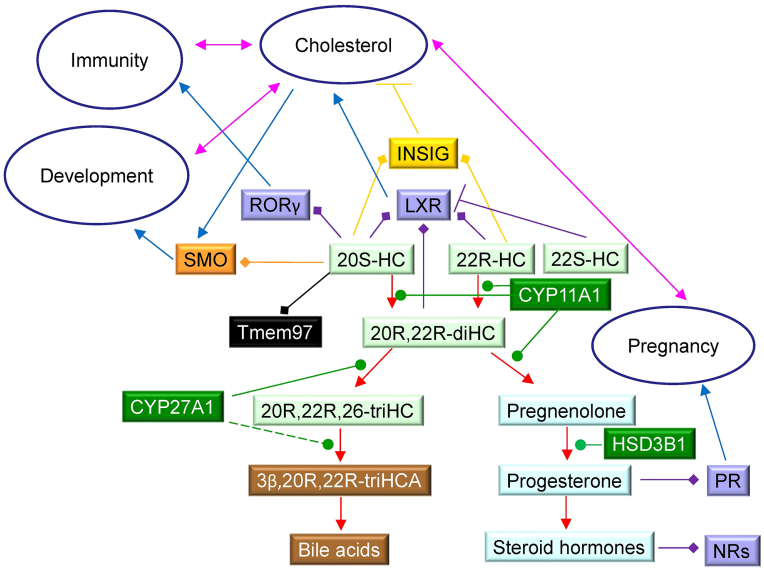


FIGURE 9
Schematic showing some cholesterol metabolites identified in placenta and their interactions with protein receptors. 22R-HC, 22S-HC and 20S-HC are formed from cholesterol, 22R-HC by CYP11A1 which may also be the enzyme that catalyses the formation of 20S-HC. Oxysterols are shown on a light green background, steroids on a light blue background, bile acids on a brown background and enzymes on a dark green background. Nuclear receptors are shown on a purple background, GPCR on an orange background, sigma-2 receptor on a black background and INSIG on a mustard background. Blue arrows indicate a "process", red arrows a chemical reaction, T signifies inhibition of a process, arrows with a diamond arrowhead indicate activation of a receptor, and green oval arrowheads indicate catalysis. Pink double headed arrows link processes.

and 3β,20R,22R-triH-Δ^{24}-CA are simply inactive intermediates on the road to bile acids or biologically active molecules themselves. A final point of note, during the course of this study we found evidence that HSD3B1 can oxidise sterols as well as steroids. Further details are reported elsewhere (23).

Data availability statement

The original contributions presented in the study are included in the article/Supplementary Material. Further inquiries can be directed to the corresponding author. Datasets generated during this study are available in the Open Science Framework repository.

Ethics statement

The studies involving human participants were reviewed and approved by Local ethics committee at Swansea University Medical School. The patients/participants provided their written informed consent to participate in this study.

Author contributions

AD wrote the first draft of the manuscript, acquired, analysed and interpreted the data. EY analysed data and contributed to writing the manuscript by revising it critically for important intellectual content. CT provided essential materials and contributed to writing the manuscript by revising it critically for important intellectual content. YW conceived and designed the work, interpreted the data and contributed to writing the manuscript by revising it critically for important intellectual content. WG conceived and designed the work, interpreted the data and wrote the manuscript. All authors contributed to writing of the manuscript and approved the final version.

Funding

This work was supported by the Biotechnology and Biological Sciences Research Council (BBSRC, grant numbers BB/I001735/1, BB/N015932/1 and BB/S019588/1 to WG, BB/L001942/1 to YW), the European Union through European Structural Funds (ESF), as part of the Welsh Government funded Academic Expertise for Business project (to WG and YW). AD was supported *via* a KESS2 award in association with Markes International from the Welsh Government and the European Social Fund.

Acknowledgments

Dr Peter Grosshans and Steve Smith of Markes International are thanked for helpful discussions. Members of the European Network for Oxysterol Research (ENOR, https://www.oxysterols.net/) are thanked for informative discussions.

Conflict of interest

WG and YW are listed as inventors on the patent "Kit and method for quantitative detection of steroids" US9851368B2. WG, EY, and YW are shareholders in CholesteniX Ltd.

The remaining authors declare that the research was conducted in the absence of any commercial or financial relationships that could be construed as a potential conflict of interest.

Publisher's note

All claims expressed in this article are solely those of the authors and do not necessarily represent those of their affiliated organizations, or those of the publisher, the editors and the reviewers. Any product that may be evaluated in this article, or claim that may be made by its manufacturer, is not guaranteed or endorsed by the publisher.

Supplementary material

The Supplementary Material for this article can be found online at: https://www.frontiersin.org/articles/10.3389/fendo.2022.1031013/full#supplementary-material

References

1. Woollett LA. Where does fetal and embryonic cholesterol originate and what does it do? *Annu Rev Nutr* (2008) 28:97–114. doi: 10.1146/annurev.nutr.26.061505.111311

2. Chatuphonprasert W, Jarukamjorn K, Ellinger I. Physiology and pathophysiology of steroid biosynthesis, transport and metabolism in the human placenta. *Front Pharmacol* (2018) 91027. doi: 10.3389/fphar.2018.01027

3. Mast N, Annalora AJ, Lodowski DT, Palczewski K, Stout CD, Pikuleva IA. Structural basis for three-step sequential catalysis by the cholesterol side chain cleavage enzyme CYP11A1. *J Biol Chem* (2011) 286:5607–13. doi: 10.1074/jbc.M110.188433

4. Tuckey RC, Cameron KJ. Catalytic properties of cytochrome p-450scc purified from the human placenta: comparison to bovine cytochrome p-450scc. *Biochim Biophys Acta* (1993) 1163:185–94. doi: 10.1016/0167-4838(93)90180-Y

5. Sun Y, Kopp S, Strutz J, Gali CC, Zandl-Lang M, Fanaee-Danesh E, et al. Gestational diabetes mellitus modulates cholesterol homeostasis in human fetoplacental endothelium. *Biochim Biophys Acta Mol Cell Biol Lipids* (2018) 1863:968–79. doi: 10.1016/j.bbalip.2018.05.005

6. Mistry HD, Kurlak LO, Mansour YT, Zurkinden L, Mohaupt MG, Escher G. Increased maternal and fetal cholesterol efflux capacity and placental CYP27A1 expression in preeclampsia. *J Lipid Res* (2017) 58:1186–95. doi: 10.1194/jlr.M071985

7. Lin YY, Welch M, Lieberman S. The detection of 20S-hydroxycholesterol in extracts of rat brains and human placenta by a gas chromatograph/mass spectrometry technique. *J Steroid Biochem Mol Biol* (2003) 85:57–61. doi: 10.1016/S0960-0760(03)00137-7

8. Roberg-Larsen H, Strand MF, Krauss S, Wilson SR. Metabolites in vertebrate hedgehog signaling. *Biochem Biophys Res Commun* (2014) 446:669–74. doi: 10.1016/j.bbrc.2014.01.087

9. Gustafsson JA, Eneroth P. Steroids in meconium and faeces from newborn infants. *Proc R Soc Lond B Biol Sci* (1972) 180:179–86. doi: 10.1098/rspb.1972.0013

10. Eneroth P, Gustafsson J. Steroids in newborns and infants. hydroxylated cholesterol derivatives in the steroid monosulphate fraction from meconium. *FEBS Lett* (1969) 3:129–32. doi: 10.1016/0014-5793(69)80115-8

11. Crick PJ, William Bentley T, Abdel-Khalik J, Matthews I, Clayton PT, Morris AA, et al. Quantitative charge-tags for sterol and oxysterol analysis. *Clin Chem* (2015) 61:400–11. doi: 10.1373/clinchem.2014.231332

12. Raselli T, Hearn T, Wyss A, Atrott K, Peter A, Frey-Wagner I, et al. Elevated oxysterol levels in human and mouse livers reflect nonalcoholic steatohepatitis. *J Lipid Res* (2019) 60:1270–83. doi: 10.1194/jlr.M093229

13. Griffiths WJ, Crick PJ, Meljon A, Theofilopoulos S, Abdel-Khalik J, Yutuc E, et al. Additional pathways of sterol metabolism: Evidence from analysis of Cyp27a1-/- mouse brain and plasma. *Biochim Biophys Acta Mol Cell Biol Lipids* (2019) 1864:191–211. doi: 10.1016/j.bbalip.2018.11.006

14. Abdel-Khalik J, Yutuc E, Crick PJ, Gustafsson JA, Warner M, Roman G, et al. Defective cholesterol metabolism in amyotrophic lateral sclerosis. *J Lipid Res* (2017) 58:267–78. doi: 10.1194/jlr.P071639

15. Phinney KW, Ballihaut G, Bedner M, Benford BS, Camara JE, Christopher SJ, et al. Development of a standard reference material for metabolomics research. *Anal Chem* (2013) 85:11732–8. doi: 10.1021/ac402689t

16. Quehenberger O, Armando AM, Brown AH, Milne SB, Myers DS, Merrill AH, et al. Lipidomics reveals a remarkable diversity of lipids in human plasma. *J Lipid Res* (2010) 51:3299–305. doi: 10.1194/jlr.M009449

17. Chung BC, Matteson KJ, Voutilainen R, Mohandas TK, Miller WL. Human cholesterol side-chain cleavage enzyme, P450scc: cDNA cloning, assignment of the gene to chromosome 15, and expression in the placenta. *Proc Natl Acad Sci U.S.A.* (1986) 83:8962–6. doi: 10.1073/pnas.83.23.8962

18. Griffiths WJ, Hearn T, Crick PJ, Abdel-Khalik J, Dickson A, Yutuc E, et al. Charge-tagging liquid chromatography-mass spectrometry methodology targeting oxysterol diastereoisomers. *Chem Phys Lipids* (2017) 207:69–80. doi: 10.1016/j.chemphyslip.2017.04.004

19. Yutuc E, Dickson AL, Pacciarini M, Griffiths L, Baker PRS, Connell L, et al. Deep mining of oxysterols and cholestenoic acids in human plasma and cerebrospinal fluid: Quantification using isotope dilution mass spectrometry. *Anal Chim Acta* (2021) 1154:338259. doi: 10.1016/j.aca.2021.338259

20. Sidhu R, Jiang H, Farhat NY, Carrillo-Carrasco N, Woolery M, Ottinger E, et al. A validated LC-MS/MS assay for quantification of 24(S)-hydroxycholesterol in plasma and cerebrospinal fluid. *J Lipid Res* (2015) 56:1222–33. doi: 10.1194/jlr.D058487

21. Stiles AR, Kozlitina J, Thompson BM, McDonald JG, King KS, Russell DW. Genetic, anatomic, and clinical determinants of human serum sterol and vitamin d levels. *Proc Natl Acad Sci U.S.A.* (2014) 111:E4006–4014. doi: 10.1073/pnas.1413561111

22. Griffiths WJ, Yutuc E, Abdel-Khalik J, Crick PJ, Hearn T, Dickson A, et al. Metabolism of non-enzymatically derived oxysterols: Clues from sterol metabolic disorders. *Free Radic Biol Med* (2019) 144:124–33. doi: 10.1016/j.freeradbiomed.2019.04.020

23. Dickson A, Yutuc E, Thornton CA, Dunford JE, Oppermann U, Wang Y, et al. HSD3B1 is an oxysterol 3β-hydroxysteroid dehydrogenase in human placenta. *bioRxiv* (2022) 2004.2001:486576. doi: 10.1101/2022.04.01.486576

24. Cali JJ, Russell DW. Characterization of human sterol 27-hydroxylase. A mitochondrial cytochrome p-450 that catalyzes multiple oxidation reaction in bile acid biosynthesis. *J Biol Chem* (1991) 266:7774–8. doi: 10.1016/S0021-9258(20)89517-9

25. Uhlen M, Fagerberg L, Hallstrom BM, Lindskog C, Oksvold P, Mardinoglu A, et al. Proteomics. tissue-based map of the human proteome. *Science* (2015) 347:1260419. doi: 10.1126/science.1260419

26. Axelson M, Sjovall J. Potential bile acid precursors in plasma–possible indicators of biosynthetic pathways to cholic and chenodeoxycholic acids in man. *J Steroid Biochem* (1990) 36:631–40. doi: 10.1016/0022-4731(90)90182-R

27. Russell DW. The enzymes, regulation, and genetics of bile acid synthesis. *Annu Rev Biochem* (2003) 72:137–74. doi: 10.1146/annurev.biochem.72.121801.161712

28. Griffiths WJ, Wang Y. Oxysterols as lipid mediators: Their biosynthetic genes, enzymes and metabolites. *Prostaglandins Other Lipid Mediat* (2020) 147:106381. doi: 10.1016/j.prostaglandins.2019.106381

29. Yutuc E, Angelini R, Baumert M, Mast N, Pikuleva I, Newton J, et al. Localization of sterols and oxysterols in mouse brain reveals distinct spatial cholesterol metabolism. *Proc Natl Acad Sci U.S.A.* (2020) 117:5749–60. doi: 10.1073/pnas.1917421117

30. Schroepfer GJJr. Oxysterols: modulators of cholesterol metabolism and other processes. *Physiol Rev* (2000) 80:361–554. doi: 10.1152/physrev.2000.80.1.361

31. Lehmann JM, Kliewer SA, Moore LB, Smith-Oliver TA, Oliver BB, Su JL, et al. Activation of the nuclear receptor LXR by oxysterols defines a new hormone response pathway. *J Biol Chem* (1997) 272:3137–40. doi: 10.1074/jbc.272.6.3137

32. Jin L, Martynowski D, Zheng S, Wada T, Xie W, Li Y. Structural basis for hydroxycholesterols as natural ligands of orphan nuclear receptor RORgamma. *Mol Endocrinol* (2010) 24:923–9. doi: 10.1210/me.2009-0507

33. Nachtergaele S, Mydock LK, Krishnan K, Rammohan J, Schlesinger PH, Covey DF, et al. Oxysterols are allosteric activators of the oncoprotein smoothened. *Nat Chem Biol* (2012) 8:211–20. doi: 10.1038/nchembio.765

34. Nachtergaele S, Whalen DM, Mydock LK, Zhao Z, Malinauskas T, Krishnan K, et al. Structure and function of the smoothened extracellular domain in vertebrate hedgehog signaling. *Elife* (2013) 2:e01340. doi: 10.7554/eLife.01340

35. Goldstein JL, DeBose-Boyd RA, Brown MS. Protein sensors for membrane sterols. *Cell* (2006) 124:35–46. doi: 10.1016/j.cell.2005.12.022

36. Abrams ME, Johnson KA, Perelman SS, Zhang LS, Endapally S, Mar KB, et al. Oxysterols provide innate immunity to bacterial infection by mobilizing cell surface accessible cholesterol. *Nat Microbiol* (2020) 5:929–42. doi: 10.1038/s41564-020-0701-5

37. Radhakrishnan A, Ikeda Y, Kwon HJ, Brown MS, Goldstein JL. Sterol-regulated transport of SREBPs from endoplasmic reticulum to golgi: oxysterols block transport by binding to insig. *Proc Natl Acad Sci U.S.A.* (2007) 104:6511–8. doi: 10.1073/pnas.0700899104

38. Cheng Y-S, Zhang T, Ma X, Pratuangtham S, Zhang GC, Ondrus AA, et al. A proteome-wide map of 20(S)-hydroxycholesterol interactors in cell membranes. *Nat Chem Biol* (2021) 17:1271–80. doi: 10.1038/s41589-021-00907-2

39. Yu W, Baskin JM. There is a lock for every key. *Nat Chem Biol* (2021) 17:1214–6. doi: 10.1038/s41589-021-00908-1

40. Guryev O, Carvalho RA, Usanov S, Gilep A, Estabrook RW. A pathway for the metabolism of vitamin D3: Unique hydroxylated metabolites formed during catalysis with cytochrome P450scc (CYP11A1). *Proc Natl Acad Sci* (2003) 100:14754–9. doi: 10.1073/pnas.2336107100

41. Tuckey RC, Li W, Zjawiony JK, Zmijewski MA, Nguyen MN, Sweatman T, et al. Pathways and products for the metabolism of vitamin D3 by cytochrome P450scc. *FEBS J* (2008) 275:2585–96. doi: 10.1111/j.1742-4658.2008.06406.x

42. Roberg-Larsen H, Strand MF, Grimsmo A, Olsen PA, Dembinski JL, Rise F, et al. High sensitivity measurements of active oxysterols with automated filtration/filter backflush-solid phase extraction-liquid chromatography-mass spectrometry. *J Chromatogr A* (2012) 1255:291–7. doi: 10.1016/j.chroma.2012.02.002

43. Spencer TA, Li D, Russel JS, Collins JL, Bledsoe RK, Consler TG, et al. Pharmacophore analysis of the nuclear oxysterol receptor LXRα. *J Medicinal Chem* (2001) 44:886–97. doi: 10.1021/jm0004749

44. Tranheim Kase E, Andersen B, Nebb HI, Rustan AC, Hege Thoresen G. 22-hydroxycholesterols regulate lipid metabolism differently than T0901317 in human myotubes. *Biochim Biophys Acta (BBA) - Mol Cell Biol Lipids* (2006) 1761:1515–22. doi: 10.1016/j.bbalip.2006.09.010

45. Forman BM, Ruan B, Chen J, Schroepfer GJ, Evans RM. The orphan nuclear receptor LXRα is positively and negatively regulated by distinct products of mevalonate metabolism. *Proc Natl Acad Sci* (1997) 94:10588–93. doi: 10.1073/pnas.94.20.10588

46. Korach-André M, Gustafsson J. Liver X receptors as regulators of metabolism. *Biomol Concepts* (2015) 6:177–90. doi: 10.1515/bmc-2015-0007

47. Sacchetti P, Sousa KM, Hall AC, Liste I, Steffensen KR, Theofilopoulos S, et al. Liver X receptors and oxysterols promote ventral midbrain neurogenesis *in vivo* and in human embryonic stem cells. *Cell Stem Cell* (2009) 5:409–19. doi: 10.1016/j.stem.2009.08.019

48. Dai Y-b, Tan X-j, Wu W-f, Warner M, Gustafsson. J.-Å. Liver X receptor β protects dopaminergic neurons in a mouse model of Parkinson disease. *Proc Natl Acad Sci* (2012) 109:13112–7. doi: 10.1073/pnas.1210833109

49. Tuckey RC, Cameron KJ. Side-chain specificities of human and bovine cytochromes p-450scc. *Eur J Biochem* (1993) 217:209–15. doi: 10.1111/j.1432-1033.1993.tb18235.x

50. Thomas JL, Myers RP, Strickler RC. Human placental 3 beta-hydroxy-5-ene-steroid dehydrogenase and steroid 5--4-ene-isomerase: purification from mitochondria and kinetic profiles, biophysical characterization of the purified mitochondrial and microsomal enzymes. *J Steroid Biochem* (1989) 33:209–17. doi: 10.1016/0022-4731(89)90296-3

51. Chapman JC, Polanco JR, Min S, Michael SD. Mitochondrial 3 beta-hydroxysteroid dehydrogenase (HSD) is essential for the synthesis of progesterone by corpora lutea: An hypothesis. *Reprod Biol Endocrinol* (2005) 3:11. doi: 10.1186/1477-7827-3-11

52. Simard J, Ricketts ML, Gingras S, Soucy P, Feltus FA, Melner MH. Molecular biology of the 3beta-hydroxysteroid dehydrogenase/delta5-delta4 isomerase gene family. *Endocr Rev* (2005) 26:525–82. doi: 10.1210/er.2002-0050

53. Astle S, Slater DM, Thornton S. The involvement of progesterone in the onset of human labour. *Eur J Obstet Gynecol Reprod Biol* (2003) 108:177–81. doi: 10.1016/S0301-2115(02)00422-0

54. Nadeem L, Shynlova O, Matysiak-Zablocki E, Mesiano S, Dong X, Lye S. Molecular evidence of functional progesterone withdrawal in human myometrium. *Nat Commun* (2016) 7:11565. doi: 10.1038/ncomms11565

55. Une M, Tsujimura K, Kihira K, Hoshita T. Identification of (22R)-3 alpha,7 alpha,12 alpha,22- and (23R)-3 alpha,7 alpha,12 alpha,23-tetrahydroxy-5 beta-cholestanoic acids in urine from a patient with zellweger's syndrome. *J Lipid Res* (1989) 30:541–7. doi: 10.1016/S0022-2275(20)38346-2

56. Lambeth JD, Kitchen SE, Farooqui AA, Tuckey R, Kamin H. Cytochrome p-450scc-substrate interactions. studies of binding and catalytic activity using hydroxycholesterols. *J Biol Chem* (1982) 257:1876–84. doi: 10.1016/S0021-9258(19)68119-6

57. Bartz F, Kern L, Erz D, Zhu M, Gilbert D, Meinhof T, et al. Identification of cholesterol-regulating genes by targeted RNAi screening. *Cell Metab* (2009) 10:63–75. doi: 10.1016/j.cmet.2009.05.009

frontiers | Frontiers in Endocrinology

TYPE Original Research
PUBLISHED 01 December 2022
DOI 10.3389/fendo.2022.1032499

Check for updates

OPEN ACCESS

EDITED BY
Cilia Abad,
Charles University, Czechia

REVIEWED BY
Camille Fung,
The University of Utah, United States
Chad Slawson,
University of Kansas Medical Center Research Institute, United States

*CORRESPONDENCE
Rinaldo Rodrigues dos Passos Junior
rinaldo_passos@discente.ufg.br

SPECIALTY SECTION
This article was submitted to Developmental Endocrinology, a section of the journal Frontiers in Endocrinology

RECEIVED 30 August 2022
ACCEPTED 18 November 2022
PUBLISHED 01 December 2022

CITATION
dos Passos Junior RR, de Freitas RA, Dela Justina V, San Martín S, Lima VV and Giachini FR (2022) Protein *O*-GlcNAcylation as a nutrient sensor signaling placental dysfunction in hypertensive pregnancy. *Front. Endocrinol.* 13:1032499. doi: 10.3389/fendo.2022.1032499

COPYRIGHT
© 2022 dos Passos Junior, de Freitas, Dela Justina, San Martín, Lima and Giachini. This is an open-access article distributed under the terms of the Creative Commons Attribution License (CC BY). The use, distribution or reproduction in other forums is permitted, provided the original author(s) and the copyright owner(s) are credited and that the original publication in this journal is cited, in accordance with accepted academic practice. No use, distribution or reproduction is permitted which does not comply with these terms.

Protein *O*-GlcNAcylation as a nutrient sensor signaling placental dysfunction in hypertensive pregnancy

Rinaldo Rodrigues dos Passos Junior[1]*, Raiany Alves de Freitas[1], Vanessa Dela Justina[2], Sebastián San Martín[3], Victor Vitorino Lima[2] and Fernanda Regina Giachini[1,2]

[1]Graduate Program in Biological Sciences, Federal University of Goiás, Goiânia, Brazil, [2]Institute of Biological and Health Sciences, Federal University of Mato Grosso, Barra do Garças, Brazil, [3]Biomedical Research Center, School of Medicine, Universidad de Valparaíso, Valparaíso, Chile

Introduction: During pregnancy, arterial hypertension may impair placental function, which is critical for a healthy baby's growth. Important proteins during placentation are known to be targets for O-linked β-N-acetylglucosamine modification (O-GlcNAcylation), and abnormal protein O-GlcNAcylation has been linked to pathological conditions such as hypertension. However, it is unclear how protein O-GlcNAcylation affects placental function and fetal growth throughout pregnancy during hypertension.

Methods: To investigate this question, female Wistar and spontaneously hypertensive rats (SHR) were mated with male Wistar rats, and after pregnancy confirmation by vaginal smear, rats were divided into groups of 14, 17, and 20 days of pregnancy (DOPs). On the 14th, 17th, and 20th DOP, rats were euthanized, fetal parameters were measured, and placentas were collected for western blot, immunohistochemical, and morphological analyses.

Results: SHR presented a higher blood pressure than the Wistar rats ($p=0.001$). Across all DOPs, SHR showed reduced fetal weight and an increase in small-for-gestational-age fetuses. While near-term placentas were heavier in SHR ($p=0.006$), placental efficiency decreased at 17 ($p=0.01$) and 20 DOPs ($p<0.0001$) in this group. Morphological analysis revealed reduced junctional zone area and labyrinth vasculature changes on SHR placentas in all DOPs. O-GlcNAc protein expression was lower in placentas from SHR compared with Wistar at 14, 17, and 20 DOPs. Decreased expression of O-GlcNAc transferase ($p=0.01$) and O-GlcNAcase ($p=0.002$) enzymes was found at 14 DOPs in SHR. Immunohistochemistry showed reduced placental O-GlcNAc content in both the junctional zone and labyrinth of the placentas from SHR. Periodic acid-Schiff analysis showed decreased glycogen cell content in the placentas from SHR at 14, 17, and 20 DOPs. Moreover, glucose transporter 1 expression was decreased in placentas from SHR in all DOPs.

10.3389/fendo.2022.1032499

Conclusions: These findings suggest that decreased protein O-GlcNAcylation caused by insufficient placental nutritional apport contributes to placental dysfunction during hypertensive pregnancy, impairing fetal growth.

KEYWORDS

hypertension, placenta, *O*-GlcNac, glycosylation, glucose uptake, fetal growth restriction

Introduction

Hypertensive disorders of pregnancy (HDPs) are a worldwide health problem that complicate up to 10% of all pregnancies and are among the leading causes of pregnancy-related mortality and morbidity, with an estimated 14% of global pregnancy deaths (1, 2). Therefore, the term HDP is commonly used to describe a wide spectrum of patients, including those with mildly elevated blood pressure, as well as those with severe hypertension, with or without organ dysfunction (3). Although many pregnancies affected by hypertension usually progress well and have normal outcomes, there is an increased risk of complications such as preeclampsia, fetal growth restriction, and perinatal death (4). Despite various etiopathologies, HDPs are characterized by structural and functional alterations of the placenta (5, 6).

The placenta is undoubtedly known to be vital during pregnancy because it helps to establish the pregnant state, protect the embryo, and promote the exchange of nutrients, gasses, and waste products so that the embryo can survive and develop in the intrauterine environment (7). During the multiple events of placental development, several signaling pathways are triggered to coordinate these processes, and specific proteins that regulate placental function are known to be targets for post-translational modification involving glycans (8).

O-linked β-N-acetylglucosamine modification (*O*-GlcNAcylation) is a dynamic and reversible process that regulates protein stability, activity, and localization, and therefore cellular response, by the addition of a single saccharide to the serine, threonine, and tyrosine sites of nuclear, cytosolic, and mitochondrial proteins (9). The cycling of *O*-GlcNAcylation is tightly controlled by two unique and essential enzymes: *O*-GlcNAc transferase (OGT) and *O*-GlcNAcase (OGA), which catalyze the addition and removal of *O*-GlcNAc, respectively (10). The substrate for *O*-GlcNAcylation requires glucose conjugation with amino acids, lipids, and nucleic acids to produce uridine diphosphate-N-acetylglucosamine (UDP-GlcNAc) through the hexosamine biosynthetic pathway (HBP) (11). Therefore, HBP and *O*-GlcNAcylation are considered to be major nutrient-sensitive pathways (12, 13) and aberrant *O*-GlcNAcylation has been associated with metabolic disruption and pathological conditions, such as diabetes and arterial hypertension (14, 15).

The growth and development of a healthy baby require the transport of essential nutrients through the placenta, such as glucose and amino acids. Glucose reaches the growing fetus *via* numerous glucose transporters (GLUT) present in the placenta, where GLUT1 and GLUT3 isoforms are known to be major contributors to placental glucose transport (16, 17). Moreover, nutrient uptake in response to fetal demand is tightly coordinated by an array of signaling pathways, and *O*-GlcNacylation is known to be a nutrient-sensing pathway involved in glucose utilization (12, 13). Interestingly, arterial hypertension during pregnancy has been associated with impaired fetal growth and small-term babies. However, the involvement of the *O*-GlcNacylation pathway on placental nutritional apport and fetal development in this condition remains unknown.

Therefore, in the present study, we investigated how hypertension affects *O*-GlcNacylation of proteins, availability of glucose in the placenta, and fetal growth during pregnancy in hypertensive rats.

Materials and methods

Ethics statement

All the procedures and animal handling and maintenance were carried out according to the guidelines provided by the Brazilian College of Animal Experimentation upon approval by the Ethics Committee on the Use of Animals of the Federal University of Mato Grosso (CEUA-Araguaia; #23108.038471/2019-14).

Animals

Female Wistar and Spontaneously Hypertensive Rats (SHR) (12-14 weeks old, 180-200 g) obtained from the Laboratory of Vascular Biology and Histopathology of the Institute of Biological

and Health Sciences at the Federal University of Mato Grosso were used in this study. The rats were maintained in the animal facility room, at 23 ± 2°C, with 12-hour light/dark cycles, fed a standard commercial diet, and received free water intake. The blood pressure was measured by tail-cuff plethysmography after three days of adaptation to the device, before mating.

Mating and pregnancy determination

For mating, females were housed with males of the same species during the night (of ±4 females for each male). By the morning of the following day, the rats were separated, and vaginal smears were taken to observe the presence of sperm and keratinized cells from the estrous cycle. If positive for the presence of spermatozoa, this was designated gestational day 0.

Experimental design

Pregnant SHR and Wistar rats were separated into hypertensive and normotensive groups, respectively, and divided into 14, 17, and 20 days of pregnancy (DOP) subgroups (n = 6, for each group). On the 14^{th}, 17^{th}, and 20^{th} DOP, rats were anesthetized with 3% sodium pentobarbital (50 mg/kg body weight, i.p.) and submitted to laparotomies for removal of the placentas and fetuses. The placentas were cleaned of connective tissue, cut in half, and stored at -80°C or immersed in a fixative solution for the histological experiments. The living fetuses were individually weighted and classified according to the mean values of fetal weights in the normotensive group as small for gestational age [(SGA) fetal weight < Wistar mean - SD x 1.7]; appropriate for gestational age [(AGA) fetal weight within Wistar mean ± SD x 1.7]; and large for gestational age [(LGA) fetal weight > Wistar mean +SD x 1.7] (18), demised fetuses were not included. Posteriorly, rats were killed by pneumothorax, and fetuses were killed by placement in a CO_2 chamber.

Western blotting

Placentas were immersed in liquid nitrogen and mechanically macerated to obtain total cell lysate by incubating samples with lysis buffer containing protease inhibitors. Protein concentration was determined using the Bradford Assay Kit (Sigma-Aldrich). Extracted proteins (60 µg per lane) were loaded and separated on a polyacrylamide gel (8-10%) by electrophoresis and transferred to a nitrocellulose membrane (Sigma-Aldrich). The success of protein transfer was further detected by Ponceau S staining. Non-specific binding sites were blocked with 5% skimmed dry milk in Tris-buffered saline solution with Tween-20 (TBS-T, pH 7.6) for 1 hour, at room temperature. Membranes were rinsed and incubated with primary antibodies overnight at 4°C under constant agitation. The following antibodies were used: anti-*O*-GlcNAc (Sigma-Aldrich Cat# O7764, RRID : AB_1079524, 1:500), anti-OGT (Abcam Cat# ab50273, RRID : AB_881784, 1:1000), anti-OGA (Sigma-Aldrich Cat# SAB4200311, RRID : AB_10898726, 1:500), anti-GLUT1 (Abcam Cat# ab115730, RRID : AB_10903230, 1:8000), anti-β-actin (Abcam Cat# ab8227, RRID : AB_2305186, 1:3000). Thereafter, membranes were removed from primary antibodies and washed with TBS-T. Membranes were treated with the respective secondary antibodies for 1 hour at room temperature. Protein bands were detected using the ECL Plus Western Blotting Detection System (GE Healthcare) and then quantified using an image-analysis software program. The protein expressions were normalized to the intensity of β-actin protein and were further expressed as arbitrary units.

Histological procedures

Placentas were fixed in methacarn solution (60% methanol, 30% chloroform, and 10% acetic acid), for 3 hours, at 4 °C, under constant agitation. Then, the placentas were dehydrated in successive alcohol dilutions, clarified in xylene, and subsequently infiltrated with paraffin. Sections of 4 µm thickness were made using a microtome, stretched in a floating bath at 50°C, and adhered to glass slides previously treated with poly-*L*-lysine 0.1% (Sigma) for better adhesion of the sections.

Hematoxylin and eosin staining

For morphological analysis, hematoxylin-eosin staining was performed. Sections were deparaffinized and rehydrated, and the slides were immersed in hematoxylin for 1 minute, rinsed in running water and in distilled water, and subsequently counterstained with aqueous eosin for 30 seconds.

Periodic Acid-Schiff (PAS) staining

Sections were deparaffinized and rehydrated. Slides were dipped in a periodic acid solution and rinsed in distilled water. Subsequently, slides were placed in Schiff's solution (basic fuchsin, sodium bisulfite, hydrochloric acid, and distilled water) at room temperature and rinsed in sulfuric water. Finally, the histological sections were counterstained with Harris hematoxylin to fully recognize PAS-positive staining and rinsed well in distilled water.

10.3389/fendo.2022.1032499

Immunohistochemistry

Immunohistochemistry was performed according to a previously established protocol (19). Sections were deparaffinized and rehydrated. Each of the following steps was followed by rinses in 0.1M phosphate buffer solution (PBS) – pH 7.2-7.4. Antigenic epitope retrieval was performed by immersing slides in citrate buffer (pH 6.0) at 95°C for 25 minutes. Then, sections were incubated in a hydrogen peroxide solution (3% H_2O_2 (v/v) in PBS) to block endogenous peroxidase activity. To reduce nonspecific antigenic sites (background), the slides were incubated with Cas-Block solution (ThermoFisher Scientific), for 30 minutes. The incubation of the primary antibody was preceded by a series of standardizations, and the antibody dilutions were previously determined. The slides were subsequently incubated with the anti-*O*-GlcNAc primary antibody (Cell Signaling Technology Cat# 9875, RRID : AB_10950973), diluted 1:50 in PBS containing 0.3% (v/v) Tween 20, overnight at 4°C in a humid chamber. After extensive rinsing in PBS, all sections were incubated with biotin-conjugated goat anti-mouse IgG (Sigma-Aldrich Cat# A9044, RRID : AB_258431) diluted 1:250 in PBS for 1 h, at room temperature. The peroxidase reaction was visualized using the NovaRED® kit (Vector). A slight counter-stain was performed with Harris hematoxylin to provide a contrast to the chromogen. The secondary antibody specificity was tested by omitting the primary antibody. The specificity of the primary antibody was tested in experiments with positive control tissues, already described in the literature (19).

Histochemical, morphological, and morphometric analysis

Sections were examined in a Nikon Eclipse microscope, and the images were captured using a digital camera (Opton) and TCapture software. For morphometric analyses, the areas of the junctional zone and the labyrinth were measured in (mm^2) using the Image-Pro-Plus software (Media Cybernetics, Silver Spring, MD, USA). PAS stain-positive cells were counted for each captured field and normalized by the area (mm^2) of the junctional zone. They were expressed as the number of cells per mm^2 of the junctional zone. Protein expression of immunohistochemistry staining was determined by semi-quantitative analysis using ImageJ Fiji (WS Rasband, National Institute of Health, Bethesda, MD) and was expressed as the percentage of staining intensity normalized by the nuclei number, as described previously (20).

Statistical analysis

Data were presented as mean ± standard error of the mean (SEM), and "n" represents the number of animals used in the experiment. Statistical analysis was performed using the Prisma program (GraphPad Prism 5.0, GraphPad Software Incorporated, CA) (GraphPad Software Inc.), with Student t test, compared to the respective normotensive group. For analysis between three or more groups, a one-way analysis of variance (One-Way ANOVA) followed by the Tukey post-test was used. For percentage analysis, Fisher's exact test was used in the SPSS program (IBM SPSS Statistics 20). P values <0.05 were considered statistically significant.

Results

Reduced placental *O*-GlcNac, OGT, and OGA expression in SHR

Systolic blood pressure (SBP) was higher in SHR when compared to Wistar rats [(mmHg) 181 ± 3 vs. 128 ± 5 Wistar; $p < 0.001$] (Figure 1A). We accessed the *O*-GlcNac protein expression on placentas from SHR and Wistar rats at 14, 17, and 20 DOP. Placentas from SHR presented reduced *O*-GlcNac protein expression at 14, 17, and 20 DOP when compared to those from Wistar rats (Figure 1B). Moreover, reduced expression of OGT (0.5 ± 0.01 vs. 0.9 ± 0.1 Wistar; $p = 0.01$) and OGA (0.4 ± 0.01 vs. 1 ± 0.1 Wistar; $p = 0.002$) enzymes was found on 14 DOP in SHR (Figures 1C, D), but not in 17 or 20 DOP.

Reduced fetal weight and increased percentage of small for gestational age (SGA) fetuses in SHR

Fetal parameters from pregnant SHR and Wistar rats at 14, 17, and 20 DOP are shown in Table 1. SHR presented increased pre-implantation losses. Reduced fetal weight with an increased number of small for gestational age (SGA) fetuses was found on SHR at 14, 17, and 20 DOP when compared to Wistar. The percentage of SGA fetuses increased throughout pregnancy in SHR, and near term, 100% of all the fetuses were found to be SGA in this group.

Placental structural and functional alterations in SHR

Once the fetal weight was decreased and the fetuses were smaller in SHR, we investigated the placenta (Table 2). Placental weight was found to increase throughout pregnancy, and near-term placentas from SHR were found to be significantly heavier when compared to those from Wistar rats [(g) 0.6 ± 0.02 vs. 0.4 ± 0.02 Wistar; $p = 0.006$]. On the other hand, placental efficiency, indicated by the fetal/placental weight ratio, decreased in SHR at 17 (1.7 ± 0.1 vs. 2.3 ± 0.1 Wistar; p=0.01) and 20 DOP (6 ± 0.2 vs. 10 ± 0.2 Wistar; p<0.0001).

10.3389/fendo.2022.1032499

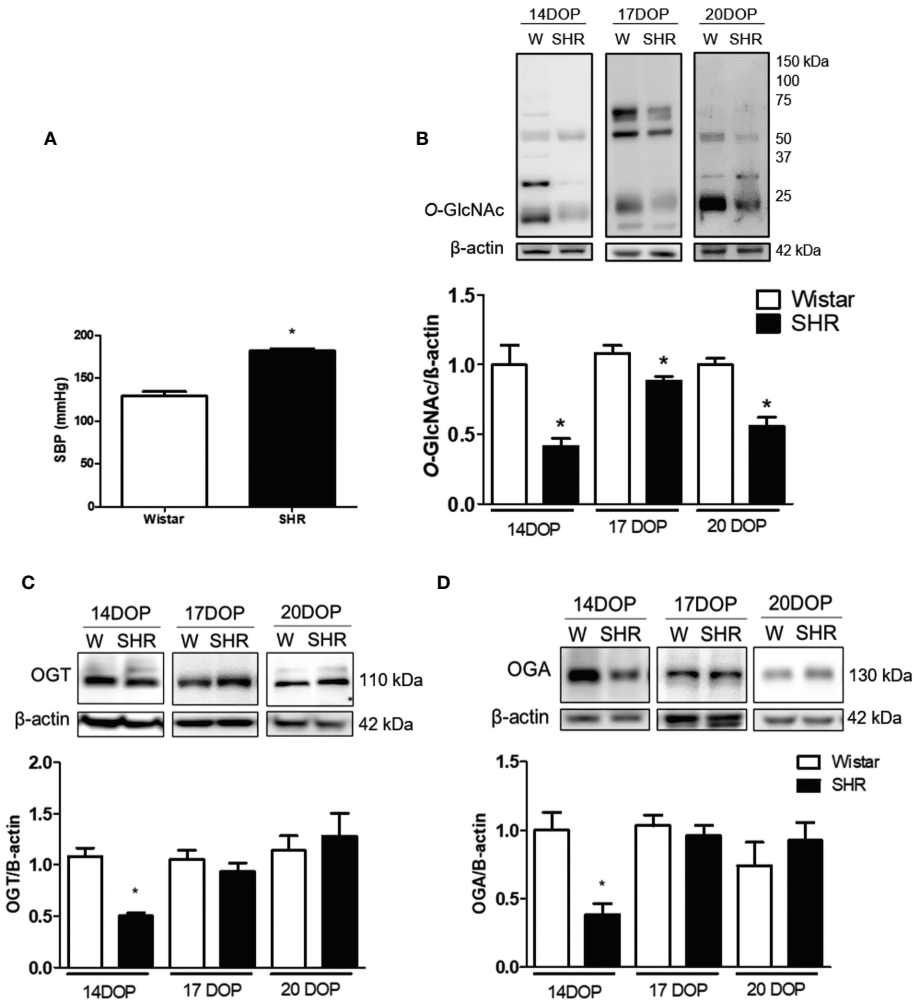


FIGURE 1
Reduced placental *O*-GlcNAc, OGT and OGA expression in SHR. **(A)** Bar graph showing SBP (mmHg) in Wistar and SHR; n = 6 each group. **(B)** Upper representative picture of western blot membrane of placental *O*-Glcnac expression in Wistar and SHR at 14, 17 and 20 DOP. Bar graph showing the *O*-Glcnac expression in Wistar and SHR at 14, 17 and 20 DOP; n = 6 each group. **(C)** Upper representative picture of western blot membrane of placental OGT expression in Wistar and SHR at 14, 17 and 20 DOP. Bar graph showing the OGT expression in Wistar and SHR at 14, 17 and 20 DOP, n = 6 each group. **(D)** Upper representative picture of western blot membrane of placental OGA expression in Wistar and SHR at 14, 17 and 20 DOP. Bar graph showing the OGA expression in Wistar and SHR at 14, 17 and 20 DOP, n = 6 each group. Values are presented as means ± SEM, and data were analyzed by one-way ANOVA, followed by Tukey post-test. *p < 0.05 vs Wistar at respective DOP. Protein expression was individually determined and corrected by β–actin expression.

TABLE 1 Fetal parameters from Wistar and SHR at 14, 17 and 20 DOP.

	14 DOP		17 DOP		20 DOP	
	Wistar	SHR	Wistar	SHR	Wistar	SHR
Pre-implantation loss	1.2 ± 0.4	4 ± 0.7*	1 ± 0.6	4 ± 0.8*	0.5 ± 0.2	4 ± 1.7*
Fetal weight (g)	0.15 ± 0.004	0.13 ± 0.007*	0.9 ± 0.03	0.7 ± 0.03*	4.9 ± 0.1	3.4 ± 0.04*
SGA (%)	3.40	27.60*	1.60	43.50*	1.50	100.0*
AGA (%)	96.60	72.40*	91.80	56.50*	97.0	0.0*
LGA (%)	0.0	0.0	6.60	0.0	1.5	0.0

SGA, small for gestational age; AGA, appropriate for gestational age; LGA, large for gestational age. *p<0.05 vs Wistar. Student unpaired t-test and Fisher exact test (%).

10.3389/fendo.2022.1032499

TABLE 2 Placental parameters from Wistar and SHR, at 14, 17 and 20 DOP.

	14 DOP		17 DOP		20 DOP	
	Wistar	SHR	Wistar	SHR	Wistar	SHR
Placental weight (g)	0.16 ± 0.01	0.17 ± 0.01	0.37 ± 0.03	0.42 ± 0.02	0.45 ± 0.007	0.55 ± 0.02*
fetal/placental weight ratio	0.98 ± 0.09	0.78 ± 0.06	2.33 ± 0.1	1.78 ± 0.1*	10.43 ± 0.2	6.1 ± 0.2*

*p<0.05 vs Wistar. Student unpaired t-test.

Morphometric analysis showed that the junctional zone (Jz) increases throughout pregnancy, reaching a higher peak area on day 17 of pregnancy in both Wistar and SHR. However, placentas from SHR presented decreased Jz area on all DOP analyzed, compared to the respective Wistar group (Figures 2A–C). Although no alterations were found in the labyrinth zone (Lz) between groups (Figure 2B), the placental Lz from SHR presented a compacted area with thicker wall vessels and vascular congestion (Figure 2C).

Reduced protein *O*-GlcNAcylation on both Jz and Lz of the placentas from SHR

We performed immunohistochemistry to characterize the localization of the *O*-GlcNAc protein profile in placental tissue. Immunohistochemistry analysis showed reduced *O*-GlcNAc deposition on both Jz and Lz of the placentas from SHR when compared to Wistar rats (Figures 3A, B). In these zones, proteins from both endothelial and trophoblast cells were the most frequent targets for *O*-GlcNAcylation (Figure 3C).

Reduced glucose storage and GLUT1 expression on placentas from SHR

Thus, we decided to investigate placental glucose uptake and storage. PAS analysis evidenced the presence of islets of glycogen cells in the Jz of placentas from both groups, with a greater amount of glycogen cells at 17 DOP when compared to the other gestational time points. We observed a decreased glycogen cell content in placental tissue from SHR at 14, 17, and 20 DOP when compared to Wistar (Figures 4A–D).

Moreover, GLUT1 expression was found to be decreased in placentas from SHR at 14, 17, and 20 DOP when compared to Wistar rats (Figure 5).

Discussion

In this study, we sought to investigate the relationship between protein *O*-GlcNAcylation, placental glucose availability, and fetal growth throughout the pregnancy affected by hypertension. Our findings showed that hypertension interestingly promotes alterations in the protein *O*-GlcNAc profile throughout pregnancy that are associated with placental structure-function alterations and impaired fetal growth, due to decreased placental glucose availability in SHR.

In the present study, SHR presented decreased fetal weight at 14, 17, and 20 DOP with an increasing percentage of SGA fetuses. Near-term, 100% of all the fetuses from SHR were SGA, indicating intrauterine growth retardation. The growth of a healthy baby relies on a healthy placenta, and functional or structural defects of the placenta impact fetal growth (21). In this study, the placental weight increased throughout pregnancy, and near-term placentas from SHR were found to be significantly heavier, compared to Wistar. A bigger placenta could indicate a compensatory mechanism to ensure proper nutrient supply to the growing fetus due to uteroplacental hypoperfusion resulting from increased blood pressure (22). Moreover, the fetal/placental weight ratio was found to be decreased in SHR at 17 and 20 DOP, indicating a loss of placental efficiency from the 17th DOP until term. In rodents, placental efficiency can be estimated by the grams of fetus produced per gram of placenta (23), and a reduced fetal/placental weight ratio may indicate a dysfunctional placenta because fetuses do not grow properly despite an enlarged placenta. These findings are in accordance with previous studies that already described fetal and placental parameters in this animal model (24–26). However, the previous reports did not show the relation between *O*-GlcNAc, placental development, and fetal growth, as reported here.

O-GlcNAcylation is known to regulate the function of more than 4000 proteins, therefore contributing to the appropriate modulation of cellular responses and adaptation to cellular stress (27). Several stages of embryonic development during pregnancy have been shown to depend on the *O*-GlcNAc cycling, including placentation (28). Protein *O*-GlcNAcylation has been implicated in embryonic development once the OGT enzyme was determined to be essential for embryonic stem cell viability and OGT depletion was related to embryonic lethality (29, 30). Lately, *O*-GlcNAc was found to promote trophectoderm differentiation into invasive trophoblast, a pattern required during embryo implantation (31). These data could relate to our findings once SHR presented an increased number of pre-implantation losses along with reduced placental *O*-GlcNAc expression since 14 DOP. We speculate that protein *O*-

10.3389/fendo.2022.1032499

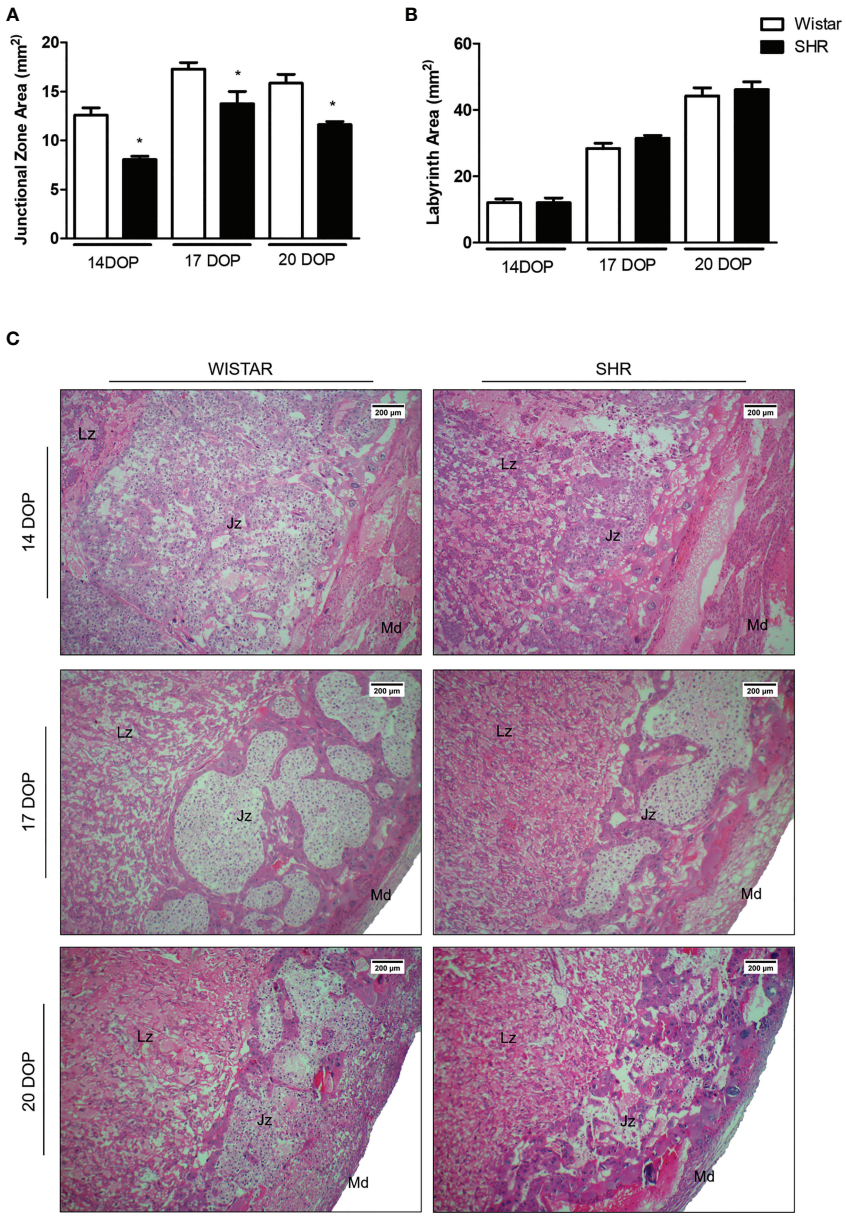


FIGURE 2
Morphometric and morphological alterations in placentas from SHR. **(A)** Bar graph showing the Jz area (mm^2) of placentas from Wistar and SHR at 14, 17 and 20 DOP; n = 5-6 each group. **(B)** Bar graph showing the Lz (mm^2) area of placentas from Wistar and SHR at 14, 17 and 20 DOP; n = 5-6 each group. **(C)** Hematoxylin & eosin-stained placentas (40X) from SHR and Wistar at 14, 17 and 20 DOP; Overall view of the labyrinth (Lz) region, junctional zone (Jz) and maternal decidua (Md). Values are presented as means ± SEM, and data were analyzed by Student unpaired t-test. *$p < 0.05$ vs Wistar at respective DOP.

GlcNAcylation may be reduced in the early stages of embryonic development as a consequence of hypertension in these animals.

To better understand the importance of *O*-GlcNAc in placental tissue, a recent study documented approximately 750 *O*-GlcNAcylated proteins in trophoblast and fetal capillaries within the villous of the human placenta (32). Here, we show structural alterations of the placenta in SHR at 14, 17, and 20 DOP. A reduced Jz area of the placenta was found on all DOPs analyzed, and the Lz showed a compacted area with thicker wall vessels and vascular congestion. Interestingly, immunohistochemistry showed reduced protein *O*-GlcNAcylation on both Jz and Lz of the placentas from SHR. The Jz contains three main cell types (spongiotrophoblast cells, trophoblast giant cells, and glycogen cells), and constitutes the main endocrine compartment of the placenta (33). The Lz

10.3389/fendo.2022.1032499

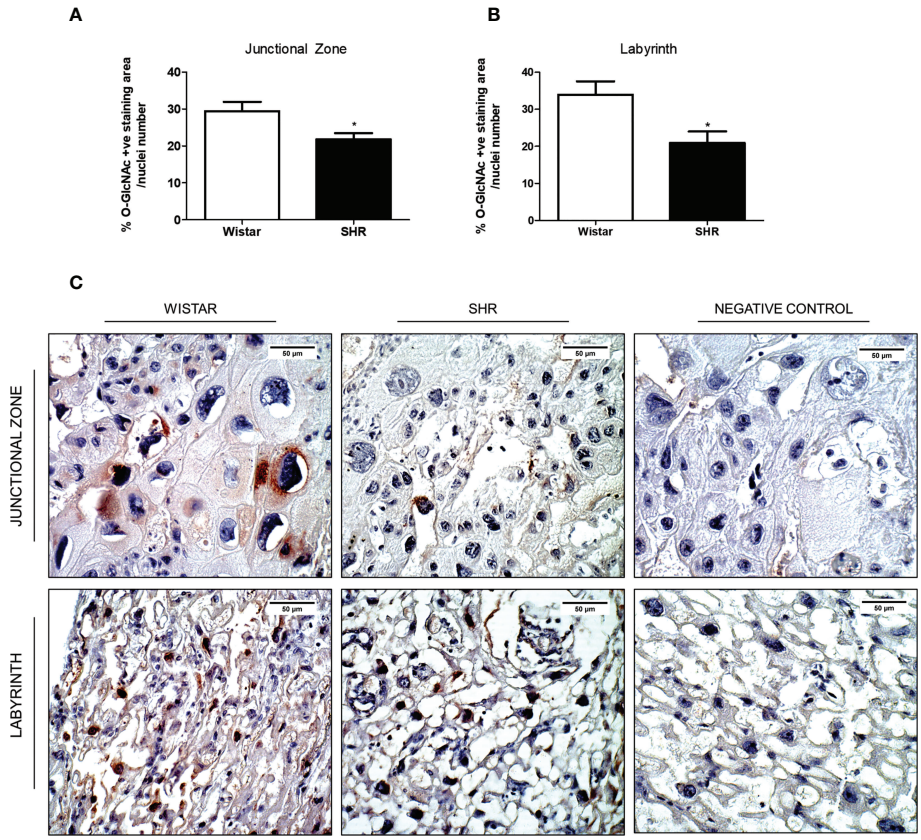


FIGURE 3
Reduced *O*-GlcNAc protein expression on both Jz and Lz of the placentas from SHR. **(A)** Bar graph showing the % of *O*-GlcNAc protein expression on the Jz of the placentas from Wistar and SHR; n = 4 each group. **(B)** Bar graph showing the % of *O*-GlcNAc protein expression on the Lz of the placentas from Wistar and SHR; n = 4 each group. **(C)** Immunoreaction on the Jz and Lz of the placentas from Wistar and SHR. After antigen retrieval, sections were treated with anti-*O*-GlcNAc (1:50) and biotin-conjugated goat anti-mouse IgG (1:250). Negative control sections were incubated with PBS or with the secondary antibody (omitting the primary antibody). Values are presented as means ± SEM, and data were analyzed by Student unpaired t-test. *$p < 0.05$ vs Wistar.

comprises the entire placental exchange area and is responsible for transport in which maternal and fetal blood circulations come into close contact without mixing (34). Structural defects in both Jz and Lz during placentation impair fetal development (35, 36). In this regard, a few proteins and transcription factors that are important for the development of the placental tissue were found to be *O*-GlcNAcylated. For example, the hypoxia-inducible factor-1 alpha (HIF-1α), essential for placental vascular development, is a target for the *O*-GlcNAc cycling enzymes OGA and OGT, playing a critical role in HIF-1α stabilization (37). Another example is the histone H2A, which is highly expressed in the early mouse placenta (38), where its *O*-GlcNAcylation was found to be important for trophoblast differentiation and placental development (39). Finally, the specific protein 1 (SP1), a transcription factor involved in placental trophoblast invasion and migration, is also a target for *O*-GlcNAc (40).

As mentioned before, HBP and *O*-GlcNAcylation have been established as nutrient sensor signaling pathways (10). Therefore, *O*-GlcNAc pathway regulation is critical for growth signaling of the human placenta, and OGT has been elicited as a primary nutrient sensing protein, involved in glucose and amino acid utilization, and as a biomarker of cellular stress (11, 41). Hypertension in pregnancy is known to be associated with placental hypoperfusion (42, 43) and hypoxia was shown to decrease *O*-GlcNAcylation. Here, we observed reduced placental protein *O*-GlcNAcylation in all DOP analyzed concomitantly with reduced OGT and OGA expression in 14 DOP in SHR. These data, combined with the reduced PAS stain, could indicate nutrient stress in the early placenta as a consequence of decreased placental glucose uptake during chronic hypertension. In fact, disruption in this nutrient-sensing pathway is related to placental insufficiency and fetal growth restriction. Moreover, we believe that the decreased OGA expression observed here may be a compensatory mechanism to raise protein *O*-GlcNAc levels. Furthermore, while maternal nutrition influences significant placental changes that affect fetal

10.3389/fendo.2022.1032499

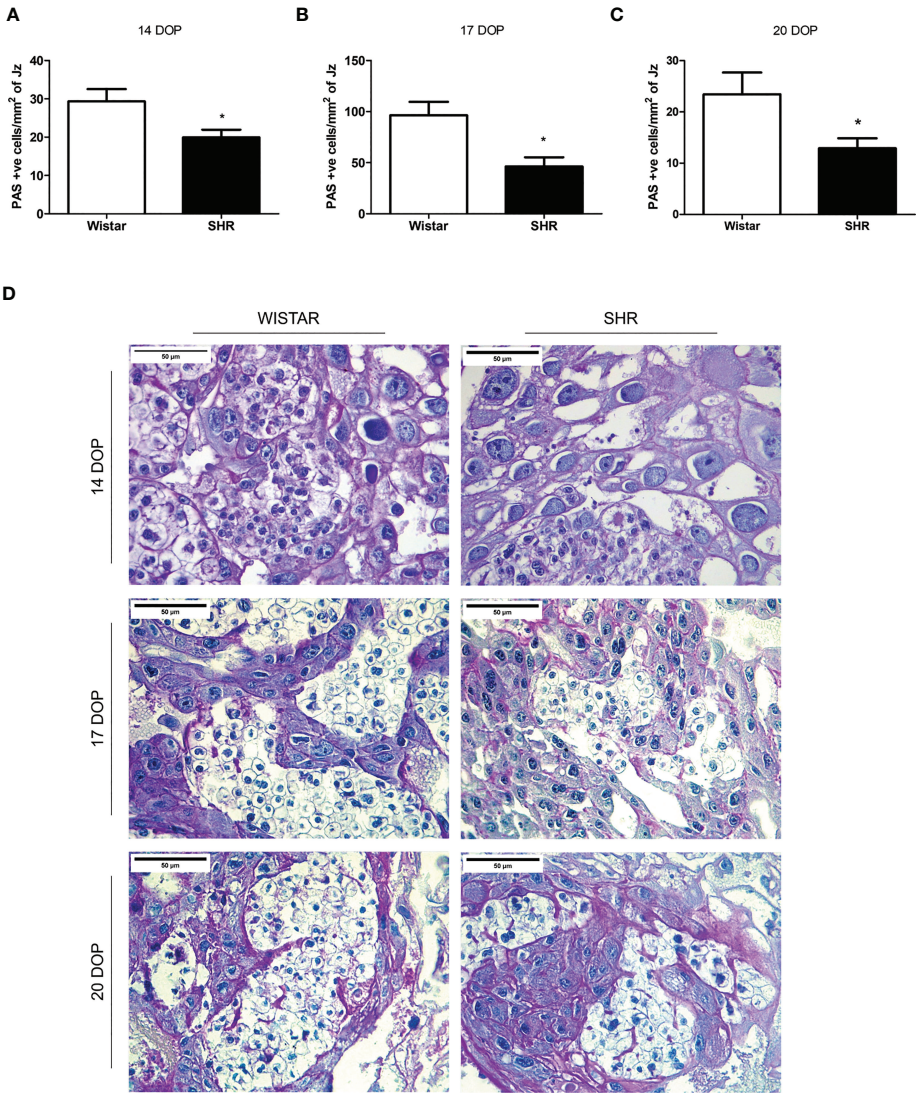


FIGURE 4
Reduced glycogen cells content in placentas from SHR at 14, 17 and 20 DOP. **(A-C)** Bar graph showing the placental amount of glycogen cells per mm2 of Jz in Wistar and SHR at 14, 17 and 20 DOP, respectively. **(D)** Representative placental tissue sections showing PAS positive stained glycogen cells in Wistar and SHR at 14, 17 and 20 DOP. Values are presented as means ± SEM, and data were analyzed by Student unpaired t-test. *$p < 0.05$ vs Wistar at respective DOP.

growth, the majority of cases of fetal growth restriction result from changes in placenta function that result in the dysfunctional transport of nutrients, especially glucose and amino acids, which have been linked to OGT sensing pathways (44, 45).

Thus, we decided to investigate glucose transport availability in the placentas of hypertensive rats. In rodents, glucose is stored in the form of glycogen cells grouped in clusters in the Jz of the placenta. PAS analysis showed a reduced number of glycogen cells per mm^2 of Jz in placentas from SHR at 14, 17, and 20 DOP when compared to Wistar rats. On day 17, a substantial amount of glycogen cells was found in both SHR and Wistar placentas when compared to the other days. This indicates that glycogen storage peaks at this period. Previous studies have also shown a peak in placental glycogen stores between 15.5 and 18.5 days (46, 47). Moreover, reduced glycogen stores in placentas of stroke-prone SHR have been described previously at 18 DOP, compared to the Wistar-Kyoto strain (48) and this was associated with inadequate uterine artery remodeling and uteroplacental blood flow in these animals.

Fetal growth and development require glucose as the primary nutrient, which is transported across the placenta through facilitated diffusion by the glucose transporter family. GLUT1 was described as the principal glucose transporter in the

10.3389/fendo.2022.1032499

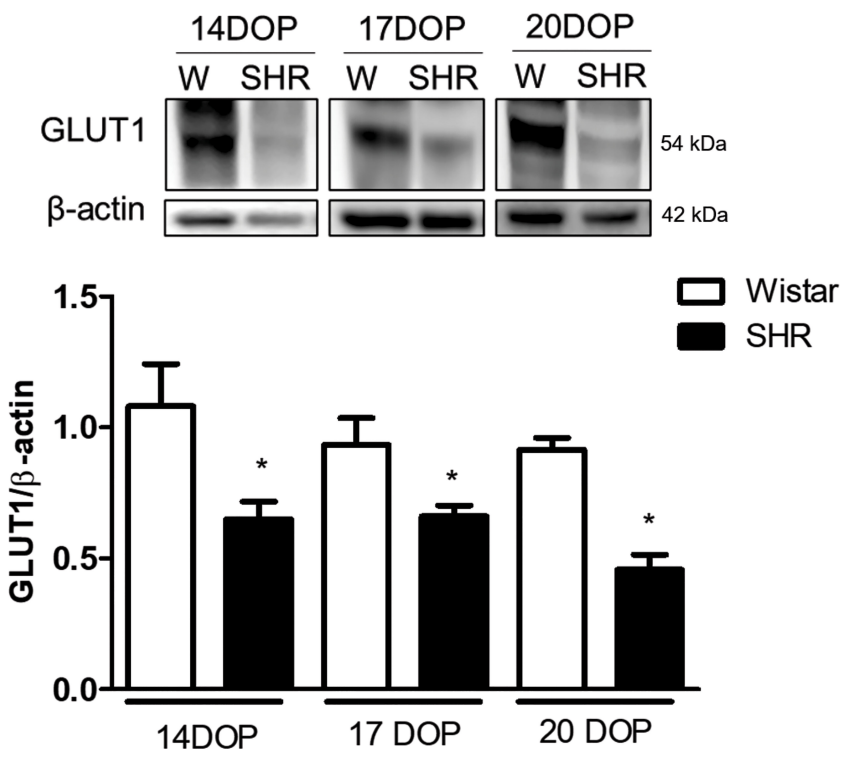


FIGURE 5
Reduced placental GLUT1 expression in SHR at 14, 17 and 20 DOP. Upper representative picture of western blot membrane of placental GLUT1 expression in Wistar and SHR at 14, 17 and 20 DOP. Bar graph showing the GLUT1 expression in Wistar and SHR at 14, 17 and 20 DOP; n=6 each group. Values are presented as means ± SEM, and data were analyzed by one-way ANOVA, followed by Tukey post-test. *p < 0.05 vs Wistar at respective DOP. Protein expression was individually determined and corrected by β–actin expression.

placenta (49), and its expression was found to increase throughout gestation in humans (45). In this study, placentas from SHR presented decreased GLUT1 expression at 14, 17, and 20 DOP when compared to Wistar. Thus, nutrient flux from glucose, fatty acid, and nucleotide metabolism in the placenta is expected to impact OGT's enzymatic activity in the placenta. Less is known about the role of OGT regulation of nutrients in fetal growth restriction. However, OGT-deficient placentas and those from growth-restricted fetuses contain diminished levels of GLUT1 receptors (50). GLUT1 protein expression was found to be down-regulated, and glucose transport activity was decreased in placentas from pregnancies affected by preeclampsia (51). Recently, a study showed that in addition to reduced GLUT1 in the decidua of patients with severe preeclampsia, GLUT1 deficiency may trigger aberrant glycolysis, thereby leading to poor decidualization and subsequent impaired placental development (52). Furthermore, a recent study showed that *O*-GlcNAcylation mediates the regulation of the water channel aquaporin 3 (AQP3) and that both elevated *O*-GlcNAcylation and AQP3 increase glucose uptake *via* GLUT1 (53). Interestingly, we have previously described that SHR presents a lack of placental AQP3 expression and that AQP3 is important for trophoblast cell migration, a crucial step during placentation (54). Curiously, loss of AQP3 in the placentas was shown to induce growth restriction in mice (55). *O*-GlcNAcylation was found to regulate GLUT1 through c-Myc (56) and AQP3 through SP1 (53). Together, our findings make a significant contribution to our understanding of how protein *O*-GlcNAcylation affects fetal growth and placental function during hypertension.

Finally, the data we presented establish protein *O*-GlcNAcylation cycling as a nutrient sense signaling and cellular stress biomarker of placental dysfunction and impaired fetal growth during hypertension in pregnancy. Moreover, we showed reduced *O*-GlcNAc in the two main functional parts of the placenta, which could be related to structural and functional derangements of the placenta in SHR.

Data availability statement

The original contributions presented in the study are included in the article/supplementary material. Further inquiries can be directed to the corresponding author.

Ethics statement

The animal study was reviewed and approved by Ethics Committee on the Use of Animals of the Federal University of Mato Grosso (CEUA-Araguaia).

Author contributions

RRPJ: designed the hypothesis, performed research and analyzed data, and wrote the manuscript. RAF: performed research and data curation. VDJ: performed research and data curation. SSM: supervision, data curation, and revision of the manuscript. VVL: supervision, data curation, and revision of the manuscript. FG: designed the hypothesis, supervision, project administration, revision of the manuscript, and funding acquisition. All authors contributed to the article and approved the submitted version.

Funding

This work was supported by the Fundação de Amparo à Pesquisa do Estado de Mato Grosso (FAPEMAT, 443/2022 to FG); Conselho Nacional de Desenvolvimento Científico e Tecnológico (CNPq, 406974/2021-7 to FG, and 141502/2020-7 Scholarship to RRPJ).

Acknowledgments

The authors thank the Biomedical Research Center, School of Medicine, Universidad de Valparaíso, Valparaíso, Chile, and the Laboratory of Vascular Biology and Histopathology of the Federal University of Mato Grosso, Barra do Garças, Brazil.

Conflict of interest

The authors declare that the research was conducted in the absence of any commercial or financial relationships that could be construed as a potential conflict of interest.

Publisher's note

All claims expressed in this article are solely those of the authors and do not necessarily represent those of their affiliated organizations, or those of the publisher, the editors and the reviewers. Any product that may be evaluated in this article, or claim that may be made by its manufacturer, is not guaranteed or endorsed by the publisher.

References

1. Say L, Chou D, Gemmill A, Tuncalp O, Moller AB, Daniels J, et al. Global causes of maternal death: A who systematic analysis. *Lancet Glob Health* (2014) 2 (6):e323–33. doi: 10.1016/S2214-109X(14)70227-X

2. Hunley TE, Desai N, Jones DP. Hypertension in the pregnant teenager. In: Flynn JT, Ingelfinger JR, Redwine KM, editors. *Pediatric hypertension*. Cham: Springer International Publishing (2018). p. 581–603.

3. Lindheimer MD, Taler SJ, Cunningham FG. Hypertension in pregnancy. *J Am Soc Hypertens* (2010) 4(2):68–78. doi: 10.1016/j.jash.2010.03.002

4. ACOG Practice Bulletin No. 203: Chronic Hypertension in Pregnancy. *Obstet Gynecol* (2019) 133(1):e26–50. doi: 10.1097/aog.0000000000003020

5. Correa RR, Gilio DB, Cavellani CL, Paschoini MC, Oliveira FA, Peres LC, et al. Placental morphometrical and histopathology changes in the different clinical presentations of hypertensive syndromes in pregnancy. *Arch Gynecol Obstet* (2008) 277(3):201–6. doi: 10.1007/s00404-007-0452-z

6. Jain K, Kavi V, Raghuveer CV, Sinha R. Placental pathology in pregnancy-induced hypertension (Pih) with or without intrauterine growth retardation. *Indian J Pathol Microbiol* (2007) 50(3):533–7.

7. Burton GJ, Fowden AL, Thornburg KL. Placental origins of chronic disease. *Physiol Rev* (2016) 96(4):1509–65. doi: 10.1152/physrev.00029.2015

8. Borowski S, Tirado-Gonzalez I, Freitag N, Garcia MG, Barrientos G, Blois SM. Altered glycosylation contributes to placental dysfunction upon early disruption of the nk cell-dc dynamics. *Front Immunol* (2020) 11:1316. doi: 10.3389/fimmu.2020.01316

9. Chatham JC, Zhang J, Wende AR. Role of O-linked n-acetylglucosamine protein modification in cellular (Patho)Physiology. *Physiol Rev* (2021) 101(2):427–93. doi: 10.1152/physrev.00043.2019

10. Hart GW. Nutrient regulation of signaling and transcription. *J Biol Chem* (2019) 294(7):2211–31. doi: 10.1074/jbc.AW119.003226

11. Hanover JA, Krause MW, Love DC. The hexosamine signaling pathway: O-glcnac cycling in feast or famine. *Biochim Biophys Acta* (2010) 1800(2):80–95. doi: 10.1016/j.bbagen.2009.07.017

12. Hart GW. Three decades of research on O-glcnacylation - a major nutrient sensor that regulates signaling, transcription and cellular metabolism. *Front Endocrinol (Lausanne)* (2014) 5:183. doi: 10.3389/fendo.2014.00183

13. Mannino MP, Hart GW. The beginner's guide to O-glcnac: From nutrient sensitive pathway regulation to its impact on the immune system. *Front Immunol* (2022) 13:828648. doi: 10.3389/fimmu.2022.828648

14. Dos Passos Junior RR, Bomfim GF, Giachini FR, Tostes RC, Lima VV. O-Linked beta-N-Acetylglucosamine modification: Linking hypertension and the immune system. *Front Immunol* (2022) 13:852115. doi: 10.3389/fimmu.2022.852115

15. Peterson SB, Hart GW. New insights: A role for O-glcnacylation in diabetic complications. *Crit Rev Biochem Mol Biol* (2016) 51(3):150–61. doi: 10.3109/10409238.2015.1135102

16. Brown K, Heller DS, Zamudio S, Illsley NP. Glucose transporter 3 (Glut3) protein expression in human placenta across gestation. *Placenta* (2011) 32 (12):1041–9. doi: 10.1016/j.placenta.2011.09.014

17. Illsley NP. Glucose transporters in the human placenta. *Placenta* (2000) 21 (1):14–22. doi: 10.1053/plac.1999.0448

18. Damasceno DC, Silva HP, Vaz GF, Vasques-Silva FA, Calderon IM, Rudge MV, et al. Diabetic rats exercised prior to and during pregnancy: Maternal reproductive outcome, biochemical profile, and frequency of fetal anomalies. *Reprod Sci* (2013) 20(7):730–8. doi: 10.1177/1933719112461186

19. Dela Justina V, Dos Passos Junior RR, Bressan AF, Tostes RC, Carneiro FS, Soares TS, et al. O-Linked n-Acetyl-Glucosamine deposition in placental proteins varies according to maternal glycemic levels. *Life Sci* (2018) 205:18–25. doi: 10.1016/j.lfs.2018.05.013

20. Crowe AR, Yue W. Semi-quantitative determination of protein expression using immunohistochemistry staining and analysis: An integrated protocol. *Bio Protoc* (2019) 9(24):e3465. doi: 10.21769/BioProtoc.3465

21. Sharma D, Shastri S, Sharma P. Intrauterine growth restriction: Antenatal and postnatal aspects. *Clin Med Insights Pediatr* (2016) 10:67–83. doi: 10.4137/CMPed.S40070

22. Granger JP, Alexander BT, Llinas MT, Bennett WA, Khalil RA. Pathophysiology of hypertension during preeclampsia linking placental ischemia with endothelial dysfunction. *Hypertension* (2001) 38(3 Pt 2):718–22. doi: 10.1161/01.hyp.38.3.718

23. Fowden AL, Sferruzzi-Perri AN, Coan PM, Constancia M, Burton GJ. Placental efficiency and adaptation: Endocrine regulation. *J Physiol* (2009) 587(Pt 14):3459–72. doi: 10.1113/jphysiol.2009.173013

24. Lewis RM, Vickers MH, Batchelor DC, Bassett NS, Johnston BM, Skinner SJ. Effects of maternal captopril treatment on growth, blood glucose and plasma insulin in the fetal spontaneously hypertensive rat. *Reprod Fertil Dev* (1999) 11(7-8):403–8. doi: 10.1071/rd99081

25. Wlodek ME, Koutsis K, Westcott KT, Ho PW, Di Nicolantonio R, Moseley JM. The spontaneously hypertensive rat fetus, not the mother, is responsible for the reduced amniotic fluid pthrp concentrations and growth restriction. *Placenta* (2001) 22(7):646–51. doi: 10.1053/plac.2001.0699

26. Johnston BM. Fetal growth retardation and increased placental weight in the spontaneously hypertensive rat. *Reprod Fertil Dev* (1995) 7(3):639–45. doi: 10.1071/rd9950639

27. Martinez MR, Dias TB, Natov PS, Zachara NE. Stress-induced O-glcnacylation: An adaptive process of injured cells. *Biochem Soc Trans* (2017) 45 (1):237–49. doi: 10.1042/BST20160153

28. Lima VV, Dela Justina V, Dos Passos RRJr., Volpato GT, Souto PCS, San Martin S, et al. O-Glcnac modification during pregnancy: Focus on placental environment. *Front Physiol* (2018) 9:1263. doi: 10.3389/fphys.2018.01263

29. Shi FT, Kim H, Lu W, He Q, Liu D, Goodell MA, et al. Ten-eleven translocation 1 (Tet1) is regulated by O-linked n-acetylglucosamine transferase (Ogt) for target gene repression in mouse embryonic stem cells. *J Biol Chem* (2013) 288(29):20776–84. doi: 10.1074/jbc.M113.460386

30. Shafi R, Iyer SP, Ellies LG, O'Donnell N, Marek KW, Chui D, et al. The O-glcnac transferase gene resides on the X chromosome and is essential for embryonic stem cell viability and mouse ontogeny. *Proc Natl Acad Sci U.S.A.* (2000) 97(11):5735–9. doi: 10.1073/pnas.100471497

31. Ruane PT, Tan CMJ, Adlam DJ, Kimber SJ, Brison DR, Aplin JD, et al. Protein O-glcnacylation promotes trophoblast differentiation at implantation. *Cells* (2020) 9(10):2246. doi: 10.3390/cells9102246

32. Palin V, Russell M, Graham R, Aplin JD, Westwood M. Altered protein O-glcnacylation in placentas from mothers with diabetes causes aberrant endocytosis in placental trophoblast cells. *Sci Rep* (2021) 11(1):20705. doi: 10.1038/s41598-021-00045-8

33. Simmons DG, Fortier AL, Cross JC. Diverse subtypes and developmental origins of trophoblast giant cells in the mouse placenta. *Dev Biol* (2007) 304 (2):567–78. doi: 10.1016/j.ydbio.2007.01.009

34. Georgiades P, Ferguson-Smith AC, Burton GJ. Comparative developmental anatomy of the murine and human definitive placentae. *Placenta* (2002) 23(1):3–19. doi: 10.1053/plac.2001.0738

35. Tunster SJ, Van de Pette M, John RM. Impact of genetic background on placental glycogen storage in mice. *Placenta* (2012) 33(2):124–7. doi: 10.1016/j.placenta.2011.11.011

36. Perez-Garcia V, Fineberg E, Wilson R, Murray A, Mazzeo CI, Tudor C, et al. Placentation defects are highly prevalent in embryonic lethal mouse mutants. *Nature* (2018) 555(7697):463–8. doi: 10.1038/nature26002

37. Yang YR, Jang HJ, Lee YH, Kim IS, Lee H, Ryu SH, et al. O-Glcnac cycling enzymes control vascular development of the placenta by modulating the levels of hif-1alpha. *Placenta* (2015) 36(10):1063–8. doi: 10.1016/j.placenta.2015.08.001

38. Kafer GR, Carlton PM, Lehnert SA. The histone variant H2a.Z is dynamically expressed in the developing mouse placenta and in differentiating trophoblast stem cells. *Placenta* (2015) 36(11):1325–8. doi: 10.1016/j.placenta.2015.08.018

39. Hirosawa M, Hayakawa K, Yoneda C, Arai D, Shiota H, Suzuki T, et al. Novel O-glcnacylation on Ser(40) of canonical H2a isoforms specific to viviparity. *Sci Rep* (2016) 6:31785. doi: 10.1038/srep31785

40. Roos MD, Su K, Baker JR, Kudlow JE. O Glycosylation of an Sp1-derived peptide blocks known Sp1 protein interactions. *Mol Cell Biol* (1997) 17(11):6472–80. doi: 10.1128/MCB.17.11.6472

41. Diaz P, Powell TL, Jansson T. The role of placental nutrient sensing in maternal-fetal resource allocation. *Biol Reprod* (2014) 91(4):82. doi: 10.1095/biolreprod.114.121798

42. Phoswa WN, Khaliq OP. The role of oxidative stress in hypertensive disorders of pregnancy (Preeclampsia, gestational hypertension) and metabolic disorder of pregnancy (Gestational diabetes mellitus). *Oxid Med Cell Longev* (2021) 2021:5581570. doi: 10.1155/2021/5581570

43. Mary S, Small H, Herse F, Carrick E, Flynn A, Mullen W, et al. Preexisting hypertension and pregnancy-induced hypertension reveal molecular differences in placental proteome in rodents. *Physiol Genomics* (2021) 53(6):259–68. doi: 10.1152/physiolgenomics.00160.2020

44. Brett KE, Ferraro ZM, Yockell-Lelievre J, Gruslin A, Adamo KB. Maternal-fetal nutrient transport in pregnancy pathologies: The role of the placenta. *Int J Mol Sci* (2014) 15(9):16153–85. doi: 10.3390/ijms150916153

45. Hart B, Morgan E, Alejandro EU. Nutrient sensor signaling pathways and cellular stress in fetal growth restriction. *J Mol Endocrinol* (2019) 62(2):R155–R65. doi: 10.1530/JME-18-0059

46. Coan PM, Conroy N, Burton GJ, Ferguson-Smith AC. Origin and characteristics of glycogen cells in the developing murine placenta. *Dev Dyn* (2006) 235(12):3280–94. doi: 10.1002/dvdy.20981

47. Lopez MF, Dikkes P, Zurakowski D, Villa-Komaroff L. Insulin-like growth factor ii affects the appearance and glycogen content of glycogen cells in the murine placenta. *Endocrinology* (1996) 137(5):2100–8. doi: 10.1210/endo.137.5.8612553

48. Small HY, Morgan H, Beattie E, Griffin S, Indahl M, Delles C, et al. Abnormal uterine artery remodelling in the stroke prone spontaneously hypertensive rat. *Placenta* (2016) 37:34–44. doi: 10.1016/j.placenta.2015.10.022

49. Baumann MU, Schneider H, Malek A, Palta V, Surbek DV, Sager R, et al. Regulation of human trophoblast Glut1 glucose transporter by insulin-like growth factor I (Igf-I). *PloS One* (2014) 9(8):e106037. doi: 10.1371/journal.pone.0106037

50. Stanirowski PJ, Szukiewicz D, Majewska A, Watroba M, Pyzlak M, Bomba-Opon D, et al. Differential expression of glucose transporter proteins glut-1, glut-3, glut-8 and glut-12 in the placenta of macrosomic, small-for-Gestational-Age and growth-restricted foetuses. *J Clin Med* (2021) 10(24):5833. doi: 10.3390/jcm10245833

51. Luscher BP, Marini C, Joerger-Messerli MS, Huang X, Hediger MA, Albrecht C, et al. Placental glucose transporter (Glut)-1 is down-regulated in preeclampsia. *Placenta* (2017) 55:94–9. doi: 10.1016/j.placenta.2017.04.023

52. Yang M, Li H, Rong M, Zhang H, Hou L, Zhang C. Dysregulated Glut1 may be involved in the pathogenesis of preeclampsia by impairing decidualization. *Mol Cell Endocrinol* (2022) 540:111509. doi: 10.1016/j.mce.2021.111509

53. Zhang H, Qi J, Pei J, Zhang M, Shang Y, Li Z, et al. O-Glcnac modification mediates aquaporin 3 to coordinate endometrial cell glycolysis and affects embryo implantation. *J Adv Res* (2022) 37:119–31. doi: 10.1016/j.jare.2021.06.022

54. Dos Passos Junior RR, de Freitas RA, Reppetti J, Medina Y, Dela Justina V, Bach CW, et al. High levels of tumor necrosis factor-alpha reduce placental aquaporin 3 expression and impair in vitro trophoblastic cell migration. *Front Physiol* (2021) 12:696495. doi: 10.3389/fphys.2021.696495

55. Seo MJ, Lim JH, Kim DH, Bae HR. Loss of aquaporin-3 in placenta and fetal membranes induces growth restriction in mice. *Dev Reprod* (2018) 22(3):263–73. doi: 10.12717/DR.2018.22.3.263

56. Wang Y, Liu J, Jin X, Zhang D, Li D, Hao F, et al. O-Glcnacylation destabilizes the active tetrameric Pkm2 to promote the warburg effect. *Proc Natl Acad Sci USA* (2017) 114(52):13732–7. doi: 10.1073/pnas.1704145115

frontiers | Frontiers in Endocrinology

TYPE Review
PUBLISHED 01 December 2022
DOI 10.3389/fendo.2022.1061317

Check for updates

OPEN ACCESS

EDITED BY
Alicia E. Damiano,
Faculty of Pharmacy and Biochemistry,
University of Buenos Aires, Argentina

REVIEWED BY
Gendie Lash,
Guangzhou Medical University, China
Fernanda Regina Giachini,
Federal University of Mato Grosso,
Brazil

*CORRESPONDENCE
Jasminka Štefulj
jasminka.stefulj@irb.hr

†These authors have contributed equally to this work and share first authorship

SPECIALTY SECTION
This article was submitted to Developmental Endocrinology, a section of the journal Frontiers in Endocrinology

RECEIVED 04 October 2022
ACCEPTED 10 November 2022
PUBLISHED 01 December 2022

CITATION
Perić M, Bečeheli I, Čičin-Šain L, Desoye G and Štefulj J (2022) Serotonin system in the human placenta – the knowns and unknowns. *Front. Endocrinol.* 13:1061317. doi: 10.3389/fendo.2022.1061317

COPYRIGHT
© 2022 Perić, Bečeheli, Čičin-Šain, Desoye and Štefulj. This is an open-access article distributed under the terms of the Creative Commons Attribution License (CC BY). The use, distribution or reproduction in other forums is permitted, provided the original author(s) and the copyright owner(s) are credited and that the original publication in this journal is cited, in accordance with accepted academic practice. No use, distribution or reproduction is permitted which does not comply with these terms.

Serotonin system in the human placenta – the knowns and unknowns

Maja Perić[1†], Ivona Bečeheli[1†], Lipa Čičin-Šain[1], Gernot Desoye[2] and Jasminka Štefulj[1*]

[1]Laboratory of Neurochemistry and Molecular Neurobiology, Division of Molecular Biology, Ruđer Bošković Institute, Zagreb, Croatia, [2]Department of Obstetrics and Gynecology, Medical University of Graz, Graz, Austria

The biogenic monoamine serotonin (5-hydroxytryptamine, 5-HT) is a chemical messenger widely distributed in the brain and various other organs. Its homeostasis is maintained by the coordinated activity of a variety of proteins, including enzymes of serotonin metabolism, transmembrane transporters of serotonin, and serotonin receptors. The serotonin system has been identified also in the placenta in rodent models as a key component of placental physiology. However, serotonin pathways in the human placenta are far from well understood. Their alterations may have long-lasting consequences for the fetus that can manifest later in life. In this review, we summarize information on the location of the components of the serotonin system in the human placenta, their regulation, function, and alterations in pathological pregnancies. We highlight current controversies and discuss important topics for future research.

KEYWORDS

human placenta, pregnancy, serotonin, serotonin receptors, serotonin transporters, MAO, TPH, fetal sex

1 Introduction

The placenta is a temporary fetal organ that develops early in pregnancy. It acts as a barrier/facilitator for transport of gases, nutrients, and waste between maternal and fetal blood. In addition, the placenta produces and secretes a variety of hormones, cytokines, and growth factors that are essential for proper placental and fetal development and for facilitating maternal adaptation to and maintenance of pregnancy (1). Human placental development begins shortly after the blastocyst implants into the uterine wall, when cytotrophoblast cells begin to proliferate and fuse into a multinucleate syncytiotrophoblast. During the first trimester of pregnancy, as the cytotrophoblasts continue to invade the uterine wall, protrusions and fetal vessels form, eventually giving rise to chorionic villi. At the end of the first trimester, flow of fully oxygenated maternal blood is established enabling

maternal blood to fill the lacunae formed within the syncytiotrophoblast (2). At the sites where the chorionic villi anchor into the maternal decidua (anchoring villi), a subpopulation of trophoblasts, the extravillous cytotrophoblasts, remodels the maternal spiral arteries by transiently partially replacing the endothelial cells lining the arteries and colonizing the inner layers of the myometrium (1, 3). Finally, the placental barrier formed consists of feto-placental endothelial cells lining the fetal capillaries, a mesenchymal core (Hofbauer cells, fibroblasts, and collagenous stroma), and cytotrophoblast cells overlaid by a continuous layer of syncytiotrophoblast (4). Although essential to the life of the fetus, the placenta is in many aspects still a rather mysterious organ.

Primary biogenic monoamines, such as dopamine, epinephrine, norepinephrine and serotonin, are widely used chemical messengers that act as neurotransmitters, hormones and autacoids. As low weight molecules with an amino group attached to an aromatic ring, all are synthesized from aromatic L-amino acids and inactivated by removal of the amino group. They play various regulatory roles in the nervous system and other organ systems. Serotonin not only regulates functions in the mature organism, but also acts as a significant growth factor during development and regulates various developmental processes, including nervous system development. Homeostasis of serotonin signaling during both development and adulthood is maintained by the coordinated activity of a variety of serotonin-regulating proteins, including its metabolic enzymes, membrane transporters and receptors. These proteins are widely distributed in the brain and various other organs, including the placenta.

Available evidence from clinical and animal studies suggests that placental serotonin system regulates placental development and functions and plays a role in proper embryo/fetal development. Its alterations may have long-lasting consequences for the fetus, which may manifest later in life like reverberations of the original effect. Despite the emerging evidence of the important role of serotonin for the feto-placental unit, its pathways in the human placenta are still far from being understood.

Here, we summarize the current data on the presence, regulation and function of serotonin system components in the human placenta, as well as on their putative role in normal and pathological pregnancy. We also highlight gaps and controversies in current knowledge and discuss directions for future research.

Abbreviations: 5-HIAA, 5-hydroxyindoleacetic acid; 5-HT, 5-hydroxytryptamine; 5-HTP, 5-hydroxytryptophan; 5-HTR, 5-hydroxytryptamine receptor; BH4, tetrahydrobiopterin; FGR, fetal growth restriction; GDM, gestational diabetes mellitus; IHC, immunohistochemistry; L-trp, L-tryptophan; MAO A/B, monoamine oxidase A/B; PE, pre-eclampsia; OCT 1/2/3, organic cation transporter 1/2/3; PMAT, plasma membrane monoamine transporter; VMAT 1/2, vesicular monoamine transporter 1/2; SERT, serotonin transporter; TPH1/2, tryptophan hydroxylase 1/2.

2 Serotonin system and its components in general

Serotonin (5-hydroxytryptamine, 5-HT), originally called enteramine, is a biogenic monoamine first isolated in 1937 from enterochromaffin cells of the intestine, and shown to induce intestinal contractions (5). In the 1940s, the same substance was identified as a "tone-modifier" present in serum and therefore named serotonin (6). Soon thereafter, its synthesis was discovered in the brain and more recently in several other peripheral sites (cf. below).

Today, serotonin is best known for its neurotransmitter role in the brain, but it acts also as a hormone and autocrine/paracrine messenger in various other organs (7). Many of its roles are highly conserved in a variety of animal species (8). In vertebrates, it modulates brain functions such as mood, emotion, cognition, sleep/wake rhythm, appetite, sexual behavior, pain perception, and response to stress (9). In addition, it regulates and fine tunes numerous other physiological processes, including hemostasis and vascular tone, gastrointestinal functions, immune response, reproductive functions, bone remodeling, and energy balance (7, 10, 11). Moreover, it contributes to regulating organ development and regeneration, by controlling basic cellular processes such as proliferation, differentiation, and migration (12, 13). In the developing fetal brain, it acts as a neurotrophic factor for various neuronal populations and also regulates the maturation of its own neurons (14, 15). Less well known are the antioxidant effects of serotonin in scavenging reactive oxygen species and inhibiting lipid peroxidation (16).

The effects of serotonin are primarily mediated by its interaction with plasma membrane receptors. In humans, 14 different serotonin receptor subtypes were identified and classified into 7 families (HTR1 to HTR7) based on structural, pharmacological, and signal transduction properties. With the exception of HTR3, a ligand-gated cation channel, all other subtypes are G protein-coupled receptors that activate various intracellular signaling pathways (17, 18). Serotonin receptors are widely distributed in the brain and various peripheral organs. During development, several serotonin receptor subtypes emerge in the developing brain prior to enzymes for serotonin synthesis, suggesting an extra-embryonic source of serotonin in the early stages of neurodevelopment (19).

Serotonin can also act in a receptor-independent manner by covalently binding to glutamine residues of various extracellular, cytoplasmic or nuclear proteins, in a process known as serotonylation. Serotonylation has been implicated in the regulation of platelet functions (20, 21), insulin secretion (22) and gene expression regulation (23).

Most of serotonin in the human body is produced and stored in the gastrointestinal tract. Some of the intestine-derived serotonin is secreted into the blood, where it is rapidly internalized in platelets and only a tiny fraction (< 1%) remains

10.3389/fendo.2022.1061317

free in plasma (24). There are other niches of local serotonin synthesis in the human body, including serotonergic neurons, pinealocytes, pulmonary artery endothelial cells, mammary epithelial cells, mast cells, pancreatic beta cells, adipocytes, hepatocytes, osteoclasts, melanocytes, keratinocytes, and fibroblasts (25–27).

Serotonin biosynthesis uses essential amino acid L-tryptophan (L-trp) as precursor and involves two enzymatic steps (Figure 1). The first step, conversion of L-trp to 5-hydroxytryptophan (5-HTP), is catalyzed by rate-limiting tryptophan hydroxylase (TPH) and subsequent decarboxylation of 5-hydroxytryptophan to serotonin, is catalyzed by aromatic acid decarboxylase. There are two TPH isoforms, TPH1 and TPH2, encoded by genes located on human chromosome 11 and 12, respectively. The two TPH isoforms have different tissue expression – TPH1 (peripheral) is abundant in enterochromaffin cells of the intestine and in other peripheral tissues, whereas TPH2 (neuronal) is found mainly in serotonergic neurons of the brain (28).

Serotonin is catabolized mainly to the final metabolite 5-hydroxyindoleacetic acid (5-HIAA), which can be excreted by the kidneys. The first step in this catabolic pathway, oxidative deamination, is catalyzed by the outer mitochondrial membrane enzyme monoamine oxidase (MAO). Its two isoforms, MAOA and MAOB, are encoded by distinct genes on the human X chromosome (29). Both isoforms catalyze oxidative deamination of serotonin and various other endogenous and dietary monoamines, with MAOA having preferential affinity for 5-HT over other substrates (30). Serotonin can also be converted into melatonin *via* two enzymatic steps.

As a hydrophilic substance, serotonin cannot freely pass through the phospholipid bilayer of the plasma membranes but is transported by specialized transmembrane proteins. These plasma membrane transporters mediate the uptake of extracellular serotonin into cells, which is the key mechanism responsible for terminating receptor-mediated serotonin signaling. There are two plasma membrane transport systems for serotonin, with fundamentally different kinetic properties:

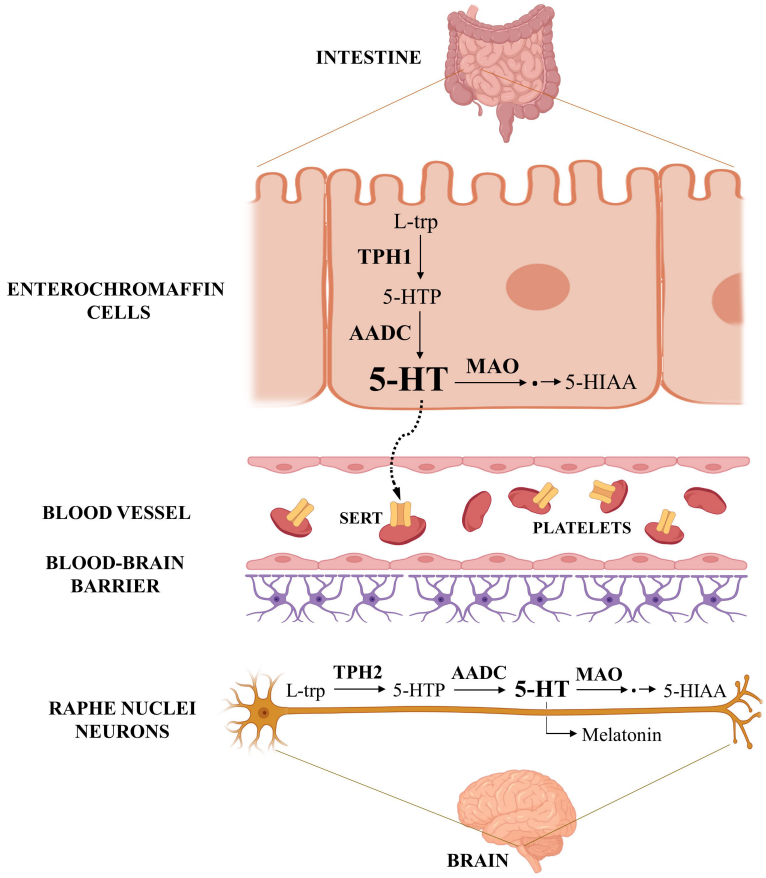


FIGURE 1
Serotonin metabolism. The figure shows the serotonin pathways in the gastrointestinal tract and in the central nervous system, the main sites of its synthesis in the human body. Serotonin synthesized in the enterochromaffin cells of the intestine is released into the portal circulation, taken up into platelets, and distributed to various other organs. Created with BioRender.com.

the high-affinity/low capacity (uptake-1) system and the low-affinity/high capacity (uptake-2) system. The uptake-1 system is represented by the serotonin transporter (SERT, also known as 5-HTT) (31), whereas the uptake-2 system includes the plasma membrane monoamine transporter (PMAT) and organic cation transporters (OCTs) 1, 2 and 3 (32). SERT is highly selective for serotonin while PMAT and OCTs can transport both serotonin and other monoamines.

Once inside the cell, another group of transmembrane transporters, the vesicular monoamine transporters (VMATs), mediate the transfer of cytosolic serotonin into secretory/storage organelles such as dense granules in platelets, synaptic vesicles in neurons, and secretory granules in enterochromaffin cells, pancreatic beta cells, mastocytes, and adipocytes (33–35). The storage of serotonin in intracellular organelles protects it from degradation by MAO and enables its release *via* exocytosis. There are two closely related VMATs, VMAT1 and VMAT2, with different pharmacological properties and tissue distribution (36).

Export of serotonin from cells storing the amine in secretory/storage organelles occurs *via* calcium-stimulated exocytosis (37–39). The export mechanism(s) from cells where it is not stored in intracellular vesicles are much less well understood. One possible efflux pathway could be *via* OCT2 (40) or OCT3 (41), which transport organic cations in both directions across the plasma membrane. It has been observed that SERT also reverses the direction of transport in the presence of some exogenous substrates (42), but it is unknown whether this phenomenon occurs under physiological conditions. Serotonin "leakage" *via* passive diffusion is generally considered insignificant because of its hydrophilic properties, but ability of serotonin to bind to lipid membranes (43) suggests that this may be more important than assumed. Nevertheless, a thorough investigation of more efficient and regulated, carrier-mediated efflux mechanisms for serotonin is warranted.

The activity of serotonin metabolizing enzymes, receptors, and transmembrane transporters is regulated by multiple mechanisms. In general, transcription of serotonin-related genes is modulated by genetic (44, 45) and epigenetic factors (45–47) and transcripts are further processed by prominent, tissue-specific alternative splicing and RNA editing (48, 49). In addition, the activity of serotonin-related proteins is controlled by post-translational modifications such as palmitoylation, phosphorylation, glycosylation, serotonylation, and disulfide bond formation, as well as by membrane trafficking, cell-surface localization and interactions with other proteins (50–55).

An interesting feature of the serotonin system, observed in both rodents and humans, is the presence of sex differences in some of its components resulting in functional differences between males and females. In humans, sex differences have been found in the concentration of serotonin and its metabolite 5-HIAA (56, 57) and in the rate of serotonin synthesis (58) in the central nervous system. The function/density of SERT and certain serotonin receptors in the human brain also differs between men and women (59, 60). In rodent models, pharmacological (61, 62) or genetic (63) manipulation of the serotonergic system causes sex-dependent behavioral and biochemical changes.

Sex differences in the serotonin system occur early in development. Studies in animal models have shown that the developing serotonergic system of males and females is differentially affected by various prenatal and perinatal factors including the microbiome (64), maternal overnutrition (65), and traumatic experiences such as parental separation (66). In humans, prenatal exposure to selective serotonin reuptake inhibitor (SSRI) antidepressants had sex-dependent effects on neonatal brain microstructure (67). Sexually dimorphic features of the human serotonergic system during the prenatal period were also evidenced by a positive correlation between placental and brain serotonin levels found only in male but not female human fetuses (65).

3 Serotonin system and its components in the human placenta

3.1 Localization of serotonin system components in the human placenta

The human placenta expresses many components of the serotonin system, including multiple serotonin receptor subtypes and several other proteins responsible for handling serotonin (Figure 2). The results of studies that examined the expression and/or localization of serotonin-related genes in human placenta are shown in Table 1 (studies in placental tissue homogenates), Table 2 (studies in placental tissue sections) and Table 3 (studies in isolated placental cells). Several studies have also compared the expression of serotonin-related genes in the human placenta between different stages of pregnancy (Table 4).

3.1.1 Serotonin

Evidence on the presence of serotonin itself in the human placental cells is yet inconclusive. An early immunohistochemical (IHC) study of the human term placenta reported the presence of serotonin in syncytiotrophoblast, stromal cells, and capillary endothelium (86). However, recent IHC study of the human term placenta detected serotonin only in platelets in the chorionic villus vessels and maternal intervillous space, but not in untreated syncytiotrophoblast and cytotrophoblasts (82). Similarly, in the human first and second trimester placentas, platelets were strongly stained for serotonin, while only traces of serotonin were seen in untreated trophoblast cells (82). In the presence of exogenously added serotonin, both cytoplasmic and nuclear compartments of the cytotrophoblast stained for

10.3389/fendo.2022.1061317

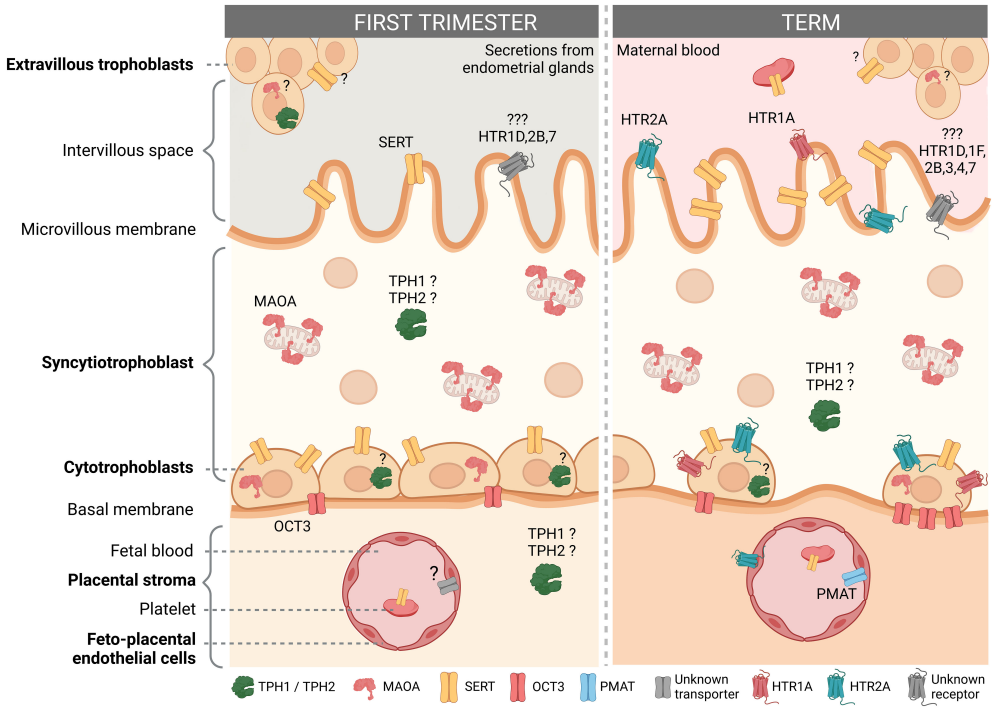


FIGURE 2
Localization of the serotonin system components in the human placenta according to gestational age. The figure shows the presence and localization of the components of the serotonin system in the human first trimester and term placenta according to the available literature. For details see main text. Components for which the results of different studies do not agree or which are reported only at the mRNA level are indicated with a question mark (?). Cell types not studied to date, such as mast cells, Hofbauer cells and other stromal cells are not shown. Created with BioRender.com.

TABLE 1 Presence of components of the serotonin system in homogenates of human placental tissue.

	Gestational period	mRNA	Protein	Activity	Study
Enzymes					
TPH1	First trimester	+ [a]	*n.a.*	+ [g]	(68)
	Term	+ [a]	*n.a.*	+ [g]	(68)
	First trimester	+ [b]	(+) [e]	+ [g]	(69)
	Term	(+) [b]	+ [e]	+ [g]	(69)
	Term	(+)/– [a]	*n.a.*	*n.a.*	(70)
TPH2	First trimester	– [a]	*n.a.*	+ [g]	(68)
	Term	+ [a]	*n.a.*	+ [g]	(68)
	First trimester	(+) [b]	*n.a.*	+ [g]	(69)
	Term	(+) [b]	*n.a.*	+ [g]	(69)
	Term	(+)/– [a]	*n.a.*	*n.a.*	(70)
MAOA	First trimester	+ [b]	+ [e]	+	(69)
	Term	+ [b]	+ [e]	+	(69)
	Term	+ [b]	+ [f]	+	(71)
	Term	+ [b]	*n.a.*	*n.a.*	(72)
	Term	*n.a.*	+ [h]	+	(73)
MAOB	Term	*n.a.*	– [h]	–	(73)
	Term	+ [b]	*n.a.*	*n.a.*	(71)

(Continued)

TABLE 1 Continued

	Gestational period	mRNA	Protein	Activity	Study
	Term	+ [b]	*n.a.*	*n.a.*	(72)
Transporters					
OCT1	First trimester	+ [a]	*n.a.*	*n.a.*	(74)
(SLC22A1)	Term	+ [a]	*n.a.*	*n.a.*	(74)
	Term	(+) [a]	*n.a.*	*n.a.*	(75)
	Term	– [a]	*n.a.*	*n.a.*	(76)
	Term	– [b]	*n.a.*	*n.a.*	(77)
OCT2	First trimester	+ [a]	*n.a.*	*n.a.*	(74)
(SLC22A2)	Term	(+) [a]	*n.a.*	*n.a.*	(74)
	Term	(+) [a]	*n.a.*	*n.a.*	(75)
	Term	– [a]	*n.a.*	*n.a.*	(76)
	Term	– [b]	*n.a.*	*n.a.*	(77)
OCT3	First trimester	+ [a]	*n.a.*	*n.a.*	(74)
(SLC22A3)	First trimester	(+) [a]	(+) [d]	*n.a.*	(75)
	Second trimester	+ [a]	+ [d]	*n.a.*	(75)
	Term	(+) [a]	*n.a.*	*n.a.*	(74)
	Term	+ [a]	+ [d]	*n.a.*	(75)
	Term	+ [a]	*n.a.*	*n.a.*	(76)
	Term	+ [b]	*n.a.*	*n.a.*	(77)
PMAT (SLC29A4)	Term	(+) [a]	*n.a.*	*n.a.*	(75)
VMAT2 (SLC18A2)	Term	(+) [b]	*n.a.*	*n.a.*	(78)
Receptors					
HTR2A	Term	+ [b]	+ [e]	*n.a*	(79)
	Term	+ [b]	+ [e]	*n.a*	(80)
HTR2B	Term	+ [a]	*n.a.*	*n.a.*	(81)
HTR1D	Term	+ [a]	*n.a.*	*n.a.*	(68)
HTR1E	Term	+ [a]	*n.a.*	*n.a.*	(68)
HTR5A	Term	+ [a]	*n.a.*	*n.a.*	(68)
HTR5B	Term	+ [a]	*n.a.*	*n.a.*	(68)

[a]RT–qPCR (quantitative reverse transcriptase–polymerase chain reaction).
[b]RT–PCR (reverse transcription–end point PCR).
[c]ddPCR (digital droplet PCR).
[d]LC–MS/MS (liquid chromatography coupled with tandem mass spectrometry).
[e]Western blot.
[f]ELISA (enzyme-linked immunosorbent assay).
[g]The activity assay used does not distinguish between the activity of TPH1 and TPH2.
[h]Binding studies with isoform-specific inhibitors.
n.a.: not analysed; +: detected; –: not detected; (+): low levels detected; (+)/–: low levels detected or below detection limit.

TABLE 2 Results on the localization of mRNAs and proteins of serotonin-related genes in human placenta obtained by *in situ* hybridization (ISH) and by immunohistochemical analysis (ISH), respectively.

	Gestational period	Location	mRNA/protein	Finding	Study
Enzymes					
TPH1	Weeks 7 to 39	All placental cells	protein	–	(82)
	First trimester	Syncytiotrophoblast	protein	+	(68, 83)
	First trimester	Cytotrophoblasts	protein	+	(68, 83)
	First trimester	Extravillous cytotrophoblasts	protein	+	(68, 83)
	First trimester	Villous stromal cells	protein	+	(68, 83)
	Term	Syncytiotrophoblast	protein	+	(68, 83)

(Continued)

TABLE 2 Continued

	Gestational period	Location	mRNA/protein	Finding	Study
	Term	Cytotrophoblasts	protein	+	(68, 83)
TPH2	First trimester	Syncytiotrophoblast	protein	+	(68, 83)
	First trimester	Cytotrophoblasts	protein	+	(68, 83)
	First trimester	Extravillous trophoblast	protein	+	(68, 83)
	First trimester	Villous stromal cells	protein	+	(68, 83)
	Term	Syncytiotrophoblast	protein	+	(68, 83)
	Term	Cytotrophoblasts	protein	+	(68, 83)
MAOA	Weeks 8, 12, 40	Syncytiotrophoblast	protein	+	(82)
	Weeks 8, 12, 40	Cytotrophoblasts	protein	–	(82)
	Term	Syncytiotrophoblast	protein	+	(84)
	Term	Syncytiotrophoblast	protein	+	(71)
	Term	Syncytiotrophoblast	mRNA	+	(72)
	Term	Cytotrophoblasts	mRNA	(+)	(72)
	Term	Vascular smooth muscle and endothelial cells	mRNA	(+)	(72)
MAOB	Term	Syncytiotrophoblast	protein	–	(71)
	Term	Syncytiotrophoblast	mRNA	+	(72)
	Term	Cytotrophoblasts	mRNA	+	(72)
	Term	Vascular smooth muscle and endothelial cells	mRNA	+	(72)
Transporters					
SERT (SLC6A4)	Weeks 7 to 41	Syncytiotrophoblast	protein	+	(82)
	Weeks 7 to 41	Cytotrophoblasts	protein	+	(82)
	Term	Syncytiotrophoblast	protein	+	(80)
	Term	Cytotrophoblasts	protein	+	(80)
	Term	Feto–placental endothelial cells	protein	+	(80)
OCT1 (SLC22A1)	Term	Intima layer of some placental vessels	mRNA	–/+	(78)
OCT2 (SLC22A2)	Term	Intima layer of some placental vessels	mRNA	–/+	(78)
OCT3 (SLC22A3)	Term	Adventitial cells of placental vessels	mRNA	–/+	(78)
	Term	Syncytiotrophoblast	protein	+	(85)
	Term	Feto-placental endothelial cells	protein	+	(85)
	Weeks 7 to 39	Syncytiotrophoblast	protein	–	(82)
	Weeks 7 to 39	Cytotrophoblasts	protein	+	(82)
	Weeks 7 to 39	Mesenchymal cells	protein	+	(82)
VMAT2 (SLC18A2)	Term	Extravillous cytotrophoblasts	mRNA	–/+	(78)
Receptors					
HTR2A	Term	Syncytiotrophoblast	protein	+	(80)
	Term	Cytotrophoblasts	protein	+	(80)
	Term	Feto–placental endothelial cells	protein	+	(80)
HTR1A	Term	Syncytiotrophoblast	mRNA	+	(86)
	Term	Cytotrophoblasts	mRNA	+	(86)
	Term	Syncytiotrophoblast	protein	+	(86)
	Term	Cytotrophoblasts	protein	+	(86)

+: detected; –: not detected; –/+: sporadically detected weak signal.

serotonin, but only nuclei in the syncytiotrophoblast stained for serotonin, whereas cytoplasmic serotonin staining in the syncytiotrophoblast was observed only after pharmacological blockade of serotonin catabolism (82). This suggests that serotonin levels in the syncytiotrophoblast are tightly controlled by rapid enzymatic degradation.

3.1.2 Serotonin-synthesizing enzymes

Studies also disagree about the presence of serotonin synthesis and expression of serotonin-synthesizing enzymes in the placenta. It has long been assumed that all serotonin affecting peripheral organ functions is synthesized in the intestine and distributed throughout the body by circulating platelets

TABLE 3 Results on the presence of components of the serotonin system in human primary cell cultures (PCC) or single cells (SC).

	Gestational period	Cell type	PCC/SC	mRNA	Protein	Activity	Study
Enzymes							
TPH1	First trimester	Syncytiotrophoblast	PCC	+ [a]	*n.a.*	*n.a.*	(83)
	First trimester	Cytotrophoblasts	PCC	+ [a]	*n.a.*	*n.a.*	(83)
	First trimester	Extravillous cytotrophoblasts	PCC	+ [a]	*n.a.*	*n.a.*	(83)
	Term	Syncytiotrophoblast	PCC	+ [a]	+ [e]	*n.a.*	(83)
	Term	Cytotrophoblasts	PCC	+ [a]	+ [e]	*n.a.*	(83)
	Term	Syncytiotrophoblast	SC	– [b]	*n.a.*	*n.a.*	(87)
	Term	Cytotrophoblasts	SC	– [b]	*n.a.*	*n.a.*	(87)
	Term	Extravillous cytotrophoblasts	SC	– [b]	*n.a.*	*n.a.*	(87)
	Term	Trophoblasts	PCC	*n.a.*	*n.a.*	+ [g]	(68)
TPH2	First trimester	Syncytiotrophoblast	PCC	+ [a]	*n.a.*	*n.a.*	(83)
	First trimester	Cytotrophoblasts	PCC	+ [a]	*n.a.*	*n.a.*	(83)
	First trimester	Extravillous cytotrophoblasts	PCC	+ [a]	*n.a.*	*n.a.*	(83)
	Term	Syncytiotrophoblast	PCC	+ [a]	+ [e]	*n.a.*	(83)
	Term	Cytotrophoblasts	PCC	+ [a]	+ [e]	*n.a.*	(83)
	Term	Syncytiotrophoblast	SC	– [b]	*n.a.*	*n.a.*	(87)
	Term	Cytotrophoblasts	SC	(+) [b]	*n.a.*	*n.a.*	(87)
	Term	Extravillous cytotrophoblasts	SC	– [b]	*n.a.*	*n.a.*	(87)
MAOA	First trimester	Syncytiotrophoblast	SC	+ [b]	*n.a.*	*n.a.*	(88)
	First trimester	Cytotrophoblasts	SC	+ [b]	*n.a.*	*n.a.*	(88)
	First trimester	Extravillous cytotrophoblasts	SC	+ [b]	*n.a.*	*n.a.*	(88)
	Term	Syncytiotrophoblast	SC	+ [b]	*n.a.*	*n.a.*	(87)
	Term	Cytotrophoblasts	SC	+ [b]	*n.a.*	*n.a.*	(87)
	Term	Extravillous cytotrophoblasts	SC	+ [b]	*n.a.*	*n.a.*	(87)
	Term	Trophoblasts	PCC	+ [a]	*n.a.*	*n.a.*	(89)
	Term	Feto-placental endothelial cells	PCC	+ [a]	*n.a.*	*n.a.*	(89)
MAOB	First trimester	Syncytiotrophoblast	SC	– [b]	*n.a.*	*n.a.*	(88)
	First trimester	Cytotrophoblasts	SC	– [b]	*n.a.*	*n.a.*	(88)
	First trimester	Extravillous cytotrophoblasts	SC	– [b]	*n.a.*	*n.a.*	(88)
	Term	Syncytiotrophoblast	SC	– [b]	*n.a.*	*n.a.*	(87)
	Term	Cytotrophoblasts	SC	– [b]	*n.a.*	*n.a.*	(87)
	Term	Extravillous cytotrophoblasts	SC	– [b]	*n.a.*	*n.a.*	(87)
Transporters							
SERT	First trimester	Syncytiotrophoblast	SC	+ [b]	*n.a.*	*n.a.*	(88)
(SLC6A4)	First trimester	Cytotrophoblasts	SC	+ [b]	*n.a.*	*n.a.*	(88)
	First trimester	Extravillous cytotrophoblasts	SC	(+) [b]	*n.a.*	*n.a.*	(88)
	Term	Syncytiotrophoblast	SC	+ [b]	*n.a.*	*n.a.*	(87)
	Term	Cytotrophoblasts	SC	+ [b]	*n.a.*	*n.a.*	(87)
	Term	Extravillous cytotrophoblasts	SC	+ [b]	*n.a.*	*n.a.*	(87)
	Term	Syncytiotrophoblast	PCC	+ [c]	+ [e]	*n.a.*	(80)
	Term	Cytotrophoblasts	PCC	+ [c]	+ [e]	*n.a.*	(80)
	Term	Feto-placental endothelial cells	PCC	(+) [a]	*n.a.*	–	(89)
OCT1	Term	Trophoblasts	PCC	(+) [a]	*n.a.*	*n.a.*	(89)
(SLC22A1)	Term	Feto-placental endothelial cells	PCC	(+)/– [a]	*n.a.*	*n.a.*	(89)
OCT2	Term	Trophoblasts	PCC	– [a]	*n.a.*	*n.a.*	(89)
(SLC22A2)	Term	Feto-placental endothelial cells	PCC	– [a]	*n.a.*	*n.a.*	(89)
OCT3	First trimester	Syncytiotrophoblast	SC	+ [b]	*n.a.*	*n.a.*	(88)
(SLC22A3)	First trimester	Cytotrophoblasts	SC	+ [b]	*n.a.*	*n.a.*	(88)

(Continued)

TABLE 3 Continued

	Gestational period	Cell type	PCC/SC	mRNA	Protein	Activity	Study
	First trimester	Extravillous cytotrophoblasts	SC	+ [b]	*n.a.*	*n.a.*	(88)
	Term	Syncytiotrophoblast	SC	+ [b]	*n.a.*	*n.a.*	(87)
	Term	Cytotrophoblasts	SC	– [b]	*n.a.*	*n.a.*	(87)
	Term	Extravillous cytotrophoblasts	SC	– [b]	*n.a.*	*n.a.*	(87)
	Term	Trophoblasts	PCC	(+)/– [a]	*n.a.*	*n.a.*	(89)
	Term	Feto-placental endothelial cells	PCC	(+)/– [a]	*n.a.*	*n.a.*	(89)
PMAT	First trimester	Syncytiotrophoblast	SC	– [b]	*n.a.*	*n.a.*	(88)
(SLC29A4)	First trimester	Cytotrophoblasts	SC	– [b]	*n.a.*	*n.a.*	(88)
	First trimester	Extravillous cytotrophoblasts	SC	– [b]	*n.a.*	*n.a.*	(88)
	Term	Syncytiotrophoblast	SC	– [b]	*n.a.*	*n.a.*	(87)
	Term	Cytotrophoblasts	SC	– [b]	*n.a.*	*n.a.*	(87)
	Term	Extravillous cytotrophoblasts	SC	– [b]	*n.a.*	*n.a.*	(87)
	Term	Trophoblasts	PCC	– [a]	*n.a.*	–	(89)
	Term	Feto-placental endothelial cells	PCC	+ [a]	*n.a.*	+	(89)
VMAT1	First trimester	Syncytiotrophoblast	SC	– [b]	*n.a.*	*n.a.*	(88)
(SLC18A1)	First trimester	Cytotrophoblasts	SC	– [b]	*n.a.*	*n.a.*	(88)
	First trimester	Extravillous cytotrophoblasts	SC	– [b]	*n.a.*	*n.a.*	(88)
	Term	Syncytiotrophoblast	SC	– [b]	*n.a.*	*n.a.*	(87)
	Term	Cytotrophoblasts	SC	– [b]	*n.a.*	*n.a.*	(87)
	Term	Extravillous cytotrophoblasts	SC	– [b]	*n.a.*	*n.a.*	(87)
VMAT2	Term	Trophoblasts	PCC	– [d]	*n.a.*	–	(90)
(SLC18A2)	Term	Syncytiotrophoblast	SC	(+) [b]	*n.a.*	*n.a.*	(87)
	Term	Cytotrophoblasts	SC	(+) [b]	*n.a.*	*n.a.*	(87)
	Term	Extravillous cytotrophoblasts	SC	+ [b]	*n.a.*	*n.a.*	(87)
Receptors							
HTR2A	Term	Cytrophoblasts	PCC	+ [c]	+ [e]	*n.a.*	(80)
	Term	Syncytiotrophoblast	PCC	+ [c]	+ [e]	*n.a.*	(80)
	Term	Cytotrophoblasts	SC	(+) [b]	*n.a.*	*n.a.*	(87)
	Term	Syncytiotrophoblast	SC	– [b]	*n.a.*	*n.a.*	(87)
	Term	Extravillous cytotrophoblasts	SC	– [b]	*n.a.*	*n.a.*	(87)
	Term	Trophoblasts	PCC	*n.a.*	+ [f]	*n.a.*	(91)
HTR2B	First trimester	Cytotrophoblasts	SC	+ [b]	*n.a.*	*n.a.*	(88)
	First trimester	Syncytiotrophoblast	SC	– [b]	*n.a.*	*n.a.*	(88)
	First trimester	Extravillous cytotrophoblasts	SC	– [b]	*n.a.*	*n.a.*	(88)
	Term	Cytotrophoblasts	SC	+ [b]	*n.a.*	*n.a.*	(87)
	Term	Syncytiotrophoblast	SC	+ [b]	*n.a.*	*n.a.*	(87)
	Term	Extravillous cytotrophoblasts	SC	– [b]	*n.a.*	*n.a.*	(87)
HTR1D	Term	Syncytotrophoblast	SC	(+) [b]	*n.a.*	*n.a.*	(87)
HTR1F	Term	Syncytotrophoblast	SC	(+) [b]	*n.a.*	*n.a.*	(87)
HTR3 (A)	Term	Cytotrophoblasts	SC	(+) [b]	*n.a.*	*n.a.*	(87)
HTR4	Term	Cytotrophoblasts	SC	(+) [b]	*n.a.*	*n.a.*	(87)
HTR7	First trimester	Cytotrophoblasts	SC	+ [b]	*n.a.*	*n.a.*	(88)

[a]RT–qPCR (quantitative reverse transcriptase–polymerase chain reaction.
[b]RNA-sequencing.
[c]RT–PCR (reverse transcription–end point PCR).
[d]Northern blot.
[e]Western blot.
[f]Receptor binding studies.
[g]The activity assay used does not distinguish between the activity of TPH1 and TPH2.
n.a.: not analysed; +: detected; –: not detected; (+): low levels detected; (+)/–: low levels detected or below detection limit.

TABLE 4 Changes in the expression of serotonin components in human placenta in the third trimester compared with the first trimester of pregnancy.

Gene	Location	mRNA/protein	First trimester	Term	Change*	Study
Enzymes						
TPH1	Tissue homogenate	mRNA	y	y	↓	(69)
	Tissue homogenate	protein	y	y	=	(69)
	Tissue homogenate	activity	y	y	=	(69)
TPH2	Tissue homogenate	mRNA	y	y	=	(69)
	Tissue homogenate	mRNA	n	y	↑	(68)
MAOA	Tissue homogenate	mRNA	y	y	↓	(69)
	Tissue homogenate	protein	y	y	=	(69)
	Tissue homogenate	activity	y	y	↑	(69)
	Syncytiotrophoblast	protein	y	y	=	(82)
MAOB	Cytotrophoblasts	mRNA	n	y	↑	(87, 88)
Transporters						
SERT	Tissue homogenate	mRNA	y	y	↓	(69)
(SLC6A4)		protein	y	y	↑	(69)
OCT1	Tissue homogenate	mRNA	y	y	=	(74)
(SLC22A1)						
OCT2	Tissue homogenate	mRNA	y	y	↓	(74)
(SLC22A2)						
OCT3	Tissue homogenate	mRNA	y	y	=	(69, 75)
(SLC22A3)	Tissue homogenate	protein	y	y	↑	(69, 75)
	Tissue homogenate	mRNA	y	y	↓	(74)
	Cytotrophoblasts	mRNA	y	n	↓	(87, 88)
	Extravillous cytotrophoblasts	mRNA	y	n	↓	(87, 88)
PMAT	Cytotrophoblasts	mRNA	y	n	↓	(87, 88)
(SLC29A4)						
Receptors						
HTR1D	Cytotrophoblasts	mRNA	y	n	↓	(87, 88)
	Syncytiotrophoblast	mRNA	n	y	↑	(87, 88)
	Extravillous cytotrophoblasts	mRNA	y	n	↓	(87, 88)
HTR2A	Cytotrophoblasts	mRNA	n	y	↑	(87, 88)
HTR2B	Syncytiotrophoblast	mRNA	n	y	↑	(87, 88)
HTR7	Cytotrophoblasts	mRNA	y	n	↓	(87, 88)

y: detected, n: not detected.
* ↑, up-regulated; ↓, down-regulated; =, no change at term of pregnancy compared to first trimester.

(Figure 1). This classical view of serotonin as a gut-derived hormone has been extended by the discovery of local sources of serotonin in various organs expressing TPH1, a peripheral isoform of the rate-limiting enzyme in serotonin synthesis (26). As for the placenta, an initial study demonstrated a lack of serotonin synthesis in the mouse placenta (92). However, Bonnin et al. (93) found evidence for serotonin synthesis in both mouse and human placenta. They demonstrated that levels of both serotonin and its immediate precursor (5-HTP) increase in homogenates of human first trimester placenta incubated with L-tryptophan (L-trp) and tetrahydrobiopterin (BH4, cofactor for TPH1 and TPH2 activity) (93). Conversion of L-trp to 5-HTP or serotonin in homogenates of human first trimester placenta has been replicated in independent studies and has also been demonstrated in homogenates of human term placenta (68, 69) and in cultured human term syncytiotrophoblast (83).

In addition, the presence of *TPH1* and *TPH2* mRNAs (encoding the peripheral and neuronal isoforms, respectively, of the rate-limiting enzyme of serotonin synthesis) and the presence of TPH1 and TPH2 proteins was demonstrated in primary syncytiotrophoblast and cytotrophoblasts isolated from human first trimester and term placentas (83). Studies in human placental homogenates reported that *TPH1* mRNA was the predominant isoform throughout pregnancy (69) or the only one detected in the first trimester (68). In IHC analysis, TPH1 and TPH2 proteins were localized in syncytiotrophoblast, cytotrophoblasts, and some stromal cells of human first trimester and term placentas (68, 83).

In contrast to the above results, another IHC study failed to find TPH1 protein in human placentas from the first and second trimesters of pregnancy, while rare TPH1 signals were observed in human term placentas, differing from strong signals in human appendix (82). In addition, single-cell transcriptome analysis by RNA-sequencing (RNA-seq) did not detect *TPH1* mRNAs in human term syncytiotrophoblast and cytotrophoblasts, whereas *TPH2* mRNAs were detected only in term cytotrophoblasts, but at very low levels (87).

3.1.3 Serotonin-catabolizing enzymes

Serotonin catabolizing isoenzyme MAOA is abundant in the human placenta throughout pregnancy, as demonstrated by IHC (82) and enzyme activity studies (69). Known sites of *MAOA* expression in human placenta appear to be syncytiotrophoblast (29, 72, 82, 84), cytotrophoblasts (72, 87, 88) and feto-placental endothelial cells (89). Single cell transcriptomic data show that syncytiotrophoblast as compared with cytotrophoblasts contain much higher levels of *MAOA* mRNA (about 10-fold higher in the first trimester, and about 2-fold higher at term) (87, 88). mRNA encoding MAOB, MAO isoform with a lower affinity for serotonin, was detected at very low levels in term placenta (70, 87) and was absent in first trimester placenta (88).

3.1.4 Serotonin receptors

Ten serotonin receptor subtypes (HTR1A, HTR1D, HTR1E, HTR1F, HTR2A, HTR2B, HTR3 (subunit HTR3A), HTR4, HTR5A and HTR5B) have been reported to be expressed in the human term placenta (68, 79–81, 86, 87, 91). HTR2A has been localized in syncytiotrophoblast, cytotrophoblasts and fetal capillary endothelium of human term placentas (80). HTR2B, the most abundant subtype according to single cell transcriptomic analyses, is also expressed in both syncytiotrophoblast and cytotrophoblasts (81, 87). In contrast, *HTR1D* and *HTR1F* mRNAs were detected only in syncytiotrophoblast, whereas *HTR3A* and *HTR4* mRNAs were found at low levels only in cytotrophoblasts (87) of human term placentas. So far, only *HTR1D*, *HTR2B* and *HTR7* mRNAs have been detected in human first trimester placentas (specifically in cytotrophoblasts) (88).

However, it should be emphasized that the expression of most serotonin receptor subtypes in human placenta (with the exception of HTR2A (79, 80, 91) and HTR1A (86)) has been detected only at the mRNA level, so the presence and location of their proteins and their functions in human placenta require further investigation.

3.1.5 Vesicular transporters

Transcripts encoding VMAT2 were not detected in cultured human term trophoblasts by Northern blot analysis, and functional analysis demonstrated the absence of VMAT activity in the human trophoblast cell line JAR (90). Furthermore, *in situ* hybridization (ISH) did not detect *VMAT2* mRNA in human villous trophoblasts, while only a weak signal was occasionally seen in extravillous trophoblasts within the uterine wall; very low levels were detected in placental homogenates by the more sensitive RT-PCR analysis (78), which may also have targeted platelet mRNA content. Single-cell transcriptome (RNA-seq) analyses reported that *VMAT1* mRNA was not found in trophoblasts throughout pregnancy, while only very low levels of *VMAT2* mRNA were detected in term trophoblasts (87, 88). Taken together, these results indicate that serotonin in trophoblasts is not stored in intracellular vesicles.

3.1.6 Plasma membrane transporters

Human placenta expresses several plasma membrane transporters for serotonin. Activity of the high-affinity SERT has been shown in plasma membrane vesicles (70, 94) and primary trophoblasts (89) isolated from human term placenta. *SERT* mRNA levels were lower in term compared to first trimester placentas, while the opposite was found for SERT protein levels (69). IHC analyses localized SERT protein to both syncytiotrophoblast and cytotrophoblasts (80, 82). Single-cell transcriptome analyses showed lower *SERT* mRNA levels in syncytiotrophoblast and cytotrophoblasts, both in the first trimester (88) and at term (87). On the other hand, recent study found that *SERT* mRNA levels were upregulated during spontaneous syncytialization of human primary trophoblasts, but SERT protein and activity levels were downregulated by syncytialization (95). Low levels of *SERT* mRNA and SERT protein were also detected in feto-placental endothelial cells (80, 82, 89), but functional analysis did not support significant SERT activity in these cells (89).

Low-affinity, polyspecific transporters OCT1 and OCT2 have been reported to be absent (77) or expressed at very low levels (74–76, 78, 89) in human first trimester and term placentas. This is consistent with the absence of their mRNAs in single cell transcriptome analyses (87, 88).

OCT3 is the most prominent member of OCT family and abundant in the human placenta throughout pregnancy (76, 77), with slightly lower mRNA and protein levels found in the first trimester than at term (69, 75). OCT3 protein and activity were detected in membrane vesicles isolated from the fetus-facing (basal) side, but not from the maternal-facing (microvillous) side of the human term placenta (70, 77). However, the exact cell type(s) harboring this transporter are not entirely clear. Thus, in one IHC study, prominent OCT3 staining was found on basolateral surface and in cytoplasm of cytotrophoblasts, while it was absent in syncytiotrophoblast in all three trimesters of pregnancy (82). This is consistent with OCT3 protein levels being down-regulated during spontaneous syncytialization of human term primary trophoblasts (95). However, in another study, OCT3 was localized to the basal (fetal-facing), but not the apical (maternal-facing) membrane of term syncytiotrophoblast (85). Weak OCT3 staining was occasionally observed in fetal capillaries (82, 85), but *OCT3*

mRNA was not detected in primary feto-placental endothelial cells (89). Single-cell transcriptome analysis by RNA-Seq demonstrated weak *OCT3* mRNA signal in all types of first trimester trophoblasts (88), while at the end of pregnancy, *OCT3* transcripts were detected only in syncytiotrophoblast (87).

Low levels of *PMAT* mRNA, encoding another low-affinity serotonin transporter, were detected in human term placental tissue (75). *PMAT* mRNA was absent in human first trimester (88) and term trophoblasts (87, 89), but was detected in human term feto-placental endothelial cells (89). In addition, efficient low-affinity serotonin uptake activity was detected in feto-placental endothelial cells, most likely mediated by PMAT (89).

3.2 Functions of serotonin system components in the human placenta

Serotonin is a potent vasoactive agent. Therefore, it was recognized early on that the placental serotonin system may contribute to the regulation of umbilico-placental blood flow. Serotonin induced a strong contractile effect on human umbilical and placental arteries and veins in tissue explants (96–98). Ketanserin, a known antagonist of the HTR2A receptor, significantly decreased the contractile response to serotonin in chorionic artery and vein segments from human placentas, suggesting that HTR2A is likely the receptor subtype mediating the vasoconstrictive effects of serotonin (98). At the cellular level, several studies have aimed to understanding the function and regulation of the serotonin system in the human placenta using cell culture models. Some of these studies have been performed on the human trophoblast-like cell lines such as BeWo, JEG-3 and JAR. These choriocarcinoma-derived cells are commonly used *in vitro* models in human placenta research (99). Recently, however, concerns have been raised about their suitability for studying serotonin pathways (70, 89, 95). Suitable *in vitro* models for future studies would be primary trophoblasts, placental explants, and organoid trophoblast cultures (100), as well as primary feto-placental endothelial cells, Hofbauer cells, and other cell types. Also, *in vitro* studies should preferably be conducted at physiological oxygen tension as *TPH1* and *SERT* have been shown to be oxygen-regulated in pulmonary endothelial and smooth muscle cells, respectively (101, 102).

Thus, serotonin has been shown to stimulate proliferation of human placental trophoblast-like cell lines (BeWo, JEG-3) through activation of the HTR2A receptor and subsequent activation of a downstream signaling cascade involving both the ERK1/2 and STAT3 signaling pathways (79, 103, 104). Based on the known roles of the ERK1/2 and STAT3 signaling pathways, it has been proposed that serotonin regulates placental development and structure by controlling cell viability, differentiation, migration and invasion (103, 104). *In vivo*, the role of serotonin in regulating placental development is supported by a study in a knock-out mouse model showing that altered serotonin levels in placental intervillous space impair trophoblast survival and disrupt normal placental structure (105).

One more role assigned to the HTR2A receptor in the human placenta relates to the regulation of placental estrogen production. Specifically, studies in human primary trophoblasts (106) as well as trophoblast-like cell lines (BeWo, JEG-3) (107) have shown that serotonin induces the expression and activity of aromatase CYP19, a key enzyme in placental estrogen synthesis, *via* activation of the HTR2A receptor. The observed increase in aromatase activity was induced by HTR2A-mediated stimulation of the protein kinase C pathway (107) and possibly the JAK2/STAT3 pathway (104).

The expression of various serotonin receptor subtypes (cf. 3.1.4), coupled to different intracellular signaling pathways, suggests diverse and as yet unknown roles for serotonin in the human placenta. For example, some of the serotonin receptor subtypes expressed in the human term placenta (i.e., HTR1F, HTR3, and HTR4) have been shown to regulate mitochondrial function and homeostasis in different mouse organs (108, 109). It would be interesting to investigate whether serotonin plays a similar role in the human placenta during late pregnancy.

3.3 Regulation of serotonin system components in the human placenta

The mechanisms that regulate components of the serotonin system in the human placenta are largely unexplored, with studies to date focusing on SERT and MAOA.

Expression of the *SERT* is regulated by two distinct variable number tandem repeat polymorphisms in the promoter and intron 2 region (5HTTLPR and STin2, respectively), as well as by several single nucleotide polymorphisms (SNPs) in the promoter region, including rs25531 and rs25532 (110). In addition to genetic variants, epigenetic mechanisms play an important role in the regulation of *SERT* expression. *SERT* promoter contains a region enriched in CpG dinucleotides (CpG island), a sequence context in which cytosine is frequently methylated. Increased methylation of this region correlates with decreased *SERT* mRNA expression (111). We have found that *SERT* mRNA levels in the human term placenta are predominantly determined by *SERT* methylation in this region and not by *SERT* genetic variants (45). Studies in the trophoblast-like cell line JAR suggest that small noncoding RNAs, namely miR-15a and miR-16, also play an important role in the epigenetic regulation of *SERT* expression in the human placenta (46).

Expression and activity of the *SERT* in JAR cells is modulated by cytokines. Interleukin-1 upregulated *SERT* expression in JAR cells *via* cyclic adenosine monophosphate-independent signaling pathways (112), whereas interleukin-6 downregulated its expression and activity *via* a STAT3-dependent signaling pathway (113).

SERT activity in placental cells is regulated also by hormones such as insulin and estrogen. Insulin upregulates SERT activity in primary human trophoblast by enhancing dissociation of SERT protein from the endoplasmic reticulum chaperone ERp44, thereby enabling its maturation and translocation to the cell surface (55). Estrogen (17β-estradiol) decreased the activity of SERT in trophoblast-like BeWo cells, but increased the level of SERT protein and had no effect on the level of *SERT* mRNA (114). A discrepancy between the levels of *SERT* mRNA and SERT protein in human placenta was also observed in relation to the effects of gestational age (69) and trophoblast differentiation (95), indicating the presence of important regulatory mechanisms acting at the translational level.

The increasing use of SERT-targeting antidepressants (115–117) and psychostimulants (118) during pregnancy has led to investigations into the potential of these drugs to alter SERT activity in the placenta. We have shown that many common antidepressants at therapeutic plasma concentrations effectively inhibit the activity of SERT in primary trophoblasts isolated from human term placentas (89). This finding and studies in other placental models (82, 94, 119–121) highlight that antidepressant therapy in pregnancy may affect serotonin homeostasis in the placenta.

Expression of the *MAOA* gene is regulated by a variable number tandem repeat polymorphism located upstream of the *MAOA* coding region (MAOA-uVNTR), consisting of a 30-bp sequence present in 2, 3, 3.5, 4 or 5 copies (122). In trophoblast-like JAR cells, alleles with 3.5 and 4 repeats were transcribed more efficiently than those with 3 or 5 repeats (122), suggesting that alleles with 3.5 and 4 repeats correspond to the optimal length of this regulatory region. Consistent with this, the 4-repeat allele was associated with higher levels of *MAOA* mRNA in human term placenta than the 3-repeat allele (123). The *MAOA* promoter also contains two CpG islands (124), but their role in regulating *MAOA* transcription in the placenta has not yet been studied.

3.4 Changes of placental serotonin system components in pregnancy pathologies

It has long been known that serotonin signaling plays a role in the pathogenesis of pre-eclampsia (PE), a hypertensive pregnancy disorder characterized by multiple organ dysfunction. As suggested recently (125), dysregulation of serotonin signaling may underlie several features of PE, including excessive platelet aggregation, vascular hyporeactivity, and pro-inflammation. The placentas of pregnancies complicated with PE show decreased MAOA activity (71, 126), which may lead to decreased serotonin catabolism and contribute to the elevated circulating serotonin levels observed in women with PE. On the other hand, placental SERT activity is unchanged in PE (126). Decreased vascular reactivity of placental and umbilical vessels to serotonin has also been noted in PE (96, 98), possibly contributing to decreased umbilico-placental blood flow (127).

Changes in placental serotonin system have been found also in gestational diabetes mellitus (GDM), with most studies focusing on SERT. An initial study in a small cohort found decreased *SERT* mRNA and protein levels in placentas from GDM pregnancies (80). However, later studies with larger and better defined samples reported increased *SERT* mRNA levels in GDM placentas (45, 128). In contrast, primary trophoblasts isolated from GDM placentas showed decreased activity of SERT, which was attributed to decreased localization of the SERT protein to the plasma membrane (55). Interestingly, trophoblasts isolated from GDM placentas also showed an attenuated response to *in vitro* insulin treatment in terms of dissociation of SERT from the endoplasmic reticulum chaperone ERp44, suggesting that defects in insulin signaling are responsible for the impaired functional expression of SERT on the cell surface in GDM trophoblasts (55). In addition to increased expression of *SERT*, GDM placentas exhibited decreased methylation of the *SERT* promoter region (45). It may be speculated that epigenetic mechanisms increase *SERT* transcription to counteract the impact of defective insulin signaling on the activity of SERT in GDM placentas. It has also been reported that expression of serotonin receptor HTR2A is decreased in GDM placentas (80). Interestingly, DNA methylation of the placental *HTR2A* gene was associated with maternal overweight/obesity and GDM only in female, but not in male placentas (129).

Maternal mental health in pregnancy was also associated with alterations in placental serotonin homeostasis. As with PE, downregulation of *MAOA* expression in the placenta has been associated with increased symptoms of maternal depression during pregnancy (130). Maternal alcohol consumption during pregnancy was associated with decreased *SERT* mRNA levels and increased *TPH1* mRNA levels in the placenta (131).

Recent evidence links alterations in the placental serotonin system to fetal growth restriction (FGR) (68) and preterm birth (132), serious pregnancy conditions accounting for significant perinatal morbidity and mortality. Thus, increased TPH activity and altered expression of *SERT*, *TPH2*, *HTR1D*, and *HTR5A* genes were found in third-trimester placentas from FGR pregnancies compared with gestational age-matched control pregnancies (68). In placentas from spontaneous preterm births, expression of both *SERT* and *OCT3* transporters was upregulated compared with placentas from term births (132).

In summary, changes of serotonin system in the human placenta have been associated with several pregnancy-related medical conditions, including PE, GDM, maternal overweight/obesity, maternal mental health in pregnancy, FGR, and preterm birth. Whether the observed changes are causally involved in the pathogenesis of the above pathologies or are their consequence,

or both, requires further investigation. Further studies are also needed to validate these findings in independent samples and to investigate the mechanisms underlying the observed changes.

4 Outlook - future perspectives

4.1 Does the human placenta provide serotonin to the fetus?

An important role attributed to the placental serotonin system in animal studies is to provide the embryo/fetus with an exogenous source of serotonin needed for proper brain and other organ development (93, 133, 134). However, studies disagree on the exact source of serotonin delivered to the fetus *via* the placenta, supporting either its maternal origin (133) or its synthesis in the placenta (93). In humans, it is generally believed that the placenta supplies maternal and/or placental serotonin to the developing fetal brain until the late first/early second trimester of pregnancy, when serotonergic neurons organize in the raphe nuclei and synthesis begins *in situ* (19, 135). This is supported by a recent discovery of a (male-specific) correlation between serotonin levels in the human fetal brain and the placenta (65).

As mentioned earlier (cf. 3.1.2), most studies to date support the ability of the human placenta to synthesize serotonin during both early and late pregnancy (68, 69, 83, 93). However, it should be noted that none of these studies examined the time and substrate concentration dependence of 5-HTP or serotonin production, or applied pharmacological approaches to demonstrate the involvement of TPH1/2 enzyme(s) (68, 69, 83, 93). In addition, the TPH activity assays used relatively high concentrations of L-trp (200 or 250 μM) compared with the Michaelis-Menten constant of human TPH for L-trp (7.5 μM) (136). Thus, convincing evidence for serotonin synthesis in the human placenta is still lacking. This is also supported by contrasting results obtained with a combination of immunohistochemical and pharmacological experiments on human placental tissue sections and placental explants (82). These argue that serotonin synthesis does not occur in the human placenta at any stage of pregnancy. Rather, the results suggest that serotonin released from maternal platelets into the intervillous space may be taken up into the syncytiotrophoblast *via* SERT and subsequently transferred to the fetal blood *via* a putative pathway involving several other proteins such as gap junction connexin-43 and OCT3 (82).

Placental perfusion is a method allowing studies into potential transfer of substances from the maternal to the fetal side of the placenta or in the opposite direction. The possible release of substances synthesized in the placenta into the maternal or fetal circulation can also be studied by this method. The only perfusion study performed to date on the human placenta suggests that serotonin is not transferred in appreciable amounts from the maternal to the fetal side at term pregnancy (137). This is consistent with results showing that serotonin taken up in the human term syncytiotrophoblast is rapidly catabolized by MAOA (70). Perfusion studies investigating the transfer of maternal/placental serotonin into fetal blood during early human pregnancy have not yet been performed.

In conclusion, current evidence does not support transplacental transfer of maternal serotonin into the fetal circulation at the end of human pregnancy. Further studies are needed to determine whether this might be different at earlier stages of pregnancy and to clarify whether the human placenta is capable of synthesizing serotonin under physiological conditions.

4.2 Epigenetic regulation of serotonin system components and epigenetic effects of serotonin

Epigenetic mechanisms are central to gene regulation and gene-environment interactions and are therefore of particular importance to the biology of the placenta as an organ that responds to changes in the intrauterine environment (138). The regulation of placental serotonin homeostasis by epigenetic mechanisms remains largely unexplored – so far, only two studies have addressed the role of DNA methylation (45) and noncoding RNAs (46) in the regulation of serotonin-related genes in the human placenta. Further studies on the role of DNA methylation, histone modifications, and noncoding RNAs and how they are modulated by various factors are warranted. In addition, further important studies should encompass the interaction of epigenetic mechanisms with functionally relevant genetic polymorphisms and post-translational regulatory mechanisms.

In addition to investigating the epigenetic regulation of genes involved in serotonin signaling, also the possible role of serotonin as a regulator of placental gene expression warrants studies. Recently, serotonylation of glutamine 5 on histone H3 (H3Q5ser) was identified as an epigenetic mechanism involved in the regulation of genes important for neuronal cell differentiation (23). The H3Q5ser modification was found in both neuronal and non-neuronal brain cells as well as in heart, colon, and blood samples. Its presence in the placenta has not been examined. However, findings on the presence of serotonin in the nuclei of various human placental cells (82) encourage future research on its presence and role in the human placenta.

4.3 Role of placental serotonin system in the developmental origins of health and disease

Animal studies show that changes in maternal and placental serotonin homeostasis not only impact the developing fetal brain

but also have lasting neurochemical and neurobehavioral consequences (113, 114, 116, 117). In humans, changes in serotonin levels in maternal blood have been linked to an increased risk of neurodevelopmental disorders in the offspring, such as attention deficit/hyperactivity disorder (139) and autism (140). As for the human placenta, methylation of the placental *HTR2A* gene has been linked to key behavioral measures of neurodevelopment (quality of movement and attention) in human newborns (141), and placental expression of the *SERT* gene has been linked to regulatory behaviors in infants at two weeks of age (142). Furthermore, placental expression of the *SERT* and *HTR2B* genes has been associated with the incidence of febrile seizure in children (81), while placental expression of the *MAOA* gene has been identified as a biological mediator of the association between prenatal stress and child temperament at 12 months of age (143). Further longitudinal studies in human cohorts are needed to better understand the consequences of altered placental serotonin homeostasis in the developmental origins of health and disease. As mentioned earlier, changes in placental serotonin homeostasis have been associated with various pregnancy disorders (cf. 3.4). It is, therefore, of utmost importance to clarify whether they are innocent bystanders or play a role in the development of the disorder or in mediating the consequences for fetal health outcomes. This could easily open up new therapeutic opportunities, as there are already many approved drugs available that modulate the activity of various serotonin system components (144–146).

4.4 The importance of fetal sex

A well-established feature of the serotonin system in the brain of both humans and rodents is sexual dimorphism (cf. 2). Studies in rodents showing that serotonin uptake into placental membrane vesicles differs between female and male fetuses (70) suggest a sexual dimorphism also in placental handling of serotonin. The sexually dimorphic nature of the serotonin system in the human placenta is supported by the male-specific correlation of serotonin levels in placenta and fetal brain (65). In addition, methylation of the *HTR2A* gene in human placenta has been shown to be associated with maternal overweight/obesity only in female placentas (129), suggesting that fetal sex modulates the sensitivity of the placental serotonin system to the intrauterine environment. Furthermore, studies in animals and humans suggest an interaction between sex hormones and the serotonin system. For example, estrogens modulate the synthesis, uptake and catabolism of serotonin (147), while changes in serotonin signaling have been reported to affect estrogen production (106, 148). Overall, the influence of fetal sex needs to be considered in future studies of the function, regulation, and pathology-related changes of the serotonin system in the human placenta.

5 Final comments

Phylogenetically, serotonin is an ancient molecule. However, it has taken a long while until the components of the complex system regulating activity of serotonin have been identified in general. Only in the past decade, the serotonin system has received attention for its potential role in reproduction and development. Studies into serotonin's involvement in the maternal-fetal interplay to ultimately contribute to fetal development through its actions on and within the placenta have been hampered for a variety of reasons. These include, but are not limited to, availability of proper experimental systems that fully capture the complexity of cellular interplay in the placenta, the difficulty in separating potential effects of maternal from those of fetal serotonin and by the temporal changes of placental cellular composition and function throughout pregnancy.

In this review we have not only summarized the current knowledge in this emerging field, but also provided suggestions for further studies. We hope that new molecular and cellular data can be integrated into a larger framework to better understand the role of serotonin system for placental and fetal development and its potential dysregulation in pathological pregnancy conditions.

Author contributions

JŠ and GD conceived and designed the article. MP, IB and JŠ wrote the first draft. MP and IB prepared the figures and tables. LČ-Š, GD, and JŠ critically revised the manuscript. All authors read and approved the final version.

Funding

This work was funded by Croatian Science Foundation grant IP-2018-01-6547 to JŠ. MP is supported by Croatian Science Foundation grant DOK-2018-09-7794.

Conflict of interest

The authors declare that the research was conducted in the absence of any commercial or financial relationships that could be construed as a potential conflict of interest.

Publisher's note

All claims expressed in this article are solely those of the authors and do not necessarily represent those of their affiliated organizations, or those of the publisher, the editors and the reviewers. Any product that may be evaluated in this article, or claim that may be made by its manufacturer, is not guaranteed or endorsed by the publisher.

References

1. Burton GJ, Fowden AL. The placenta: A multifaceted, transient organ. *Philos Trans R Soc Lond B Biol Sci* (2015) 370:20140066. doi: 10.1098/rstb.2014.0066

2. Jaremek A, Jeyarajah MJ, Jaju Bhattad G, Renaud SJ. Omics approaches to study formation and function of human placental syncytiotrophoblast. *Front Cell Dev Biol* (2021) 9:674162. doi: 10.3389/fcell.2021.674162

3. Bulmer JN, Innes BA, Robson SC, Lash GE. Transient loss of endothelial cells in human spiral artery remodelling during early pregnancy: Challenging the dogma. *Placenta* (2020) 101:230–3. doi: 10.1016/j.placenta.2020.10.003

4. Jones CJ, Fox H. Ultrastructure of the normal human placenta. *Electron Microsc Rev* (1991) 4:129–78. doi: 10.1016/0892-0354(91)90019-9

5. Vialli M, Erspamer V. Ricerche sul secreto delle cellule enterocromaffini. *Z fur Zellforschung und Mikrosk Anat* (1937) 27:81–99. doi: 10.1007/bf00391792

6. Rapport MM, ArdaAlden G, Page IH. Serum vasoconstrictor (Serotonin). *J Biol Chem* (1948) 176:1243–51. doi: 10.1016/s0021-9258(18)57137-4

7. Berger M, Gray JA, Roth BL. The expanded biology of serotonin. *Annu Rev Med* (2009) 60:355–66. doi: 10.1146/annurev.med.60.042307.110802

8. Azmitia EC. *Evolution of serotonin: Sunlight to suicide*. Amsterdam, Netherlands: Elsevier B.V (2010). doi: 10.1016/s1569-7339(10)70069-2

9. Jacobs BL, Azmitia EC. Structure and function of the brain serotonin system. *Physiol Rev* (1992) 72:165–229. doi: 10.1152/physrev.1992.72.1.165

10. Yabut JM, Crane JD, Green AE, Keating DJ, Khan WI, Steinberg GR. Emerging roles for serotonin in regulating metabolism: New implications for an ancient molecule. *Endocr Rev* (2019) 40:1092–107. doi: 10.1210/er.2018-00283

11. Lv J, Liu F. *The role of serotonin beyond the central nervous system during embryogenesis. frontiers in cellular neuroscience* (2017) (Accessed September 12, 2022).

12. Whitaker-Azmitia PM, Druse M, Walker P, Lauder JM. Serotonin as a developmental signal. *Behav Brain Res* (1996) 73:19–29. doi: 10.1016/0166-4328(96)00071-x

13. Papadimas GK, Tzirogiannis KN, Mykoniatis MG, Grypioti AD, Manta GA, Panoutsopoulos GI. The emerging role of serotonin in liver regeneration. *Swiss Med Weekly* (2012) 142:1–6. doi: 10.4414/smw.2012.13548

14. Gaspar P, Cases O, Maroteaux L. The developmental role of serotonin: News from mouse molecular genetics. *Nat Rev Neurosci* (2003) 4:1002–12. doi: 10.1038/nrn1256

15. Sodhi MSK, Sanders-Bush E. Serotonin and brain development. *Int Rev Neurobiol* (2004) 59:111–74. doi: 10.1016/S0074-7742(04)59006-2

16. Azouzi S, Santuz H, Morandat S, Pereira C, Côté F, Hermine O, et al. Antioxidant and membrane binding properties of serotonin protect lipids from oxidation. *Biophys J* (2016) 112:1863–73. doi: 10.1016/j.bpj.2017.03.037

17. Sharp T, Barnes NM. Central 5-HT receptors and their function; present and future. *Neuropharmacology* (2020) 177:108155. doi: 10.1016/j.neuropharm.2020.108155

18. Celli J, Rappold G, Niesler B. The human serotonin type 3 receptor gene (HTR3A-e) allelic variant database. *Hum Mutat* (2017) 38:137–47. doi: 10.1002/humu.23136

19. Bonnin A, Levitt P. Fetal, maternal and placental sources of serotonin and new implications for developmental programming of the brain. *Neuroscience* (2011) 197:1–7. doi: 10.1016/j.neuroscience.2011.10.005

20. Dale GL. Coated-platelets: An emerging component of the procoagulant response. *J Thromb Haemost* (2005) 3:2185–92. doi: 10.1111/j.1538-7836.2005.01274.x

21. Walther DJ, Peter J-U, Winter S, Höltje M, Paulmann N, Grohmann M, et al. Serotonylation of small GTPases is a signal transduction pathway that triggers platelet alpha-granule release. *Cell* (2003) 115:851–62. doi: 10.1016/s0092-8674(03)01014-6

22. Paulmann N, Grohmann M, Voigt JP, Bert B, Vowinckel J, Bader M, et al. Intracellular serotonin modulates insulin secretion from pancreatic β-cells by protein serotonylation. *PloS Biol* (2009) 7:1–10. doi: 10.1371/journal.pbio.1000229

23. Farrelly LA, Thompson RE, Zhao S, Lepack AE, Lyu Y, Bhanu NV, et al. Histone serotonylation is a permissive modification that enhances TFIID binding to H3K4me3. *Nature* (2019) 567:535–9. doi: 10.1038/s41586-019-1024-7

24. Lechin F, van der Dijs B, Orozco B, Lechin M, Lechin AE. Increased levels of free serotonin in plasma of symptomatic asthmatic patients. *Ann Allergy Asthma Immunol* (1996) 77:245–53. doi: 10.1016/S1081-1206(10)63263-2

25. Slominski AT, Zmijewski MA, Cezary S, Zbytek B, Slominski RM, Steketee JD. Sensing the environment: Regulation of local and globalhomeostasis by the skin neuroendocrine system. *Adv Anat Embryol Cell Biol* (2012) 212:1–98. doi: 10.1007/978-3-642-19683-6_1

26. Spohn SN, Mawe GM. Non-conventional features of peripheral serotonin signalling-the gut and beyond. *Nat Rev Gastroenterol Hepatol* (2017) 14:412–20. doi: 10.1038/nrgastro.2017.51

27. Yabut JM, Desjardins EM, Chan EJ, Day EA, Leroux JM, Wang B, et al. Genetic deletion of mast cell serotonin synthesis prevents the development of obesity and insulin resistance. *Nat Commun* (2020) 11:463. doi: 10.1038/s41467-019-14080-7

28. Walther DJ, Peter J-U, Bashammakh S, Hörtnagl H, Voits M, Fink H, et al. Synthesis of serotonin by a second tryptophan hydroxylase isoform. *Science* (2003) 299:76. doi: 10.1126/science.1078197

29. Sivasubramaniam SD, Finch CC, Rodriguez MJ, Mahy N, Billett EE. A comparative study of the expression of monoamine oxidase-a and -b mRNA and protein in non-CNS human tissues. *Cell Tissue Res* (2003) 313:291–300. doi: 10.1007/s00441-003-0765-6

30. Ramsay RR, Albreht A. Kinetics, mechanism, and inhibition of monoamine oxidase. *J Neural Transm* (2018) 125:1659–83. doi: 10.1007/s00702-018-1861-9

31. Ramamoorthy S, Giovanetti E, Qian Y, Blakely RD. Phosphorylation and regulation of antidepressant-sensitive serotonin transporters. *J Biol Chem* (1998) 273:2458–66. doi: 10.1074/jbc.273.4.2458

32. Duan H, Wang J. Selective transport of monoamine neurotransmitters by human plasma membrane monoamine transporter and organic cation transporter 3. *J Pharmacol Exp Ther* (2010) 335:743–53. doi: 10.1124/jpet.110.170142

33. Ahmad MF, Ferland D, Ayala-Lopez N, Contreras GA, Darios E, Thompson J, et al. Perivascular adipocytes store norepinephrine by vesicular transport. *Arterioscler Thromb Vasc Biol* (2019) 39:188–99. doi: 10.1161/ATVBAHA.118.311720

34. Almaça J, Molina J, Menegaz D, Pronin AN, Tamayo A, Slepak V, et al. Human beta cells produce and release serotonin to inhibit glucagon secretion from alpha cells. *Cell Rep* (2016) 17:3281–91. doi: 10.1016/j.celrep.2016.11.072

35. Takeuchi T, Harada Y, Moriyama S, Furuta K, Tanaka S, Miyaji T, et al. Vesicular polyamine transporter mediates vesicular storage and release of polyamine from mast cells. *J Biol Chem* (2017) 292:3909–18. doi: 10.1074/jbc.M116.756197

36. Wimalasena K. Vesicular monoamine transporters: Structure-function, pharmacology and meidcinal chemistry. *Med Res Rev* (2011) 31:483–519. doi: 10.1002/med.20187

37. De-Miguel FF, Trueta C. Synaptic and extrasynaptic secretion of serotonin. *Cell Mol Neurobiol* (2005) 25:297–312. doi: 10.1007/s10571-005-3061-z

38. Leon-Pinzon C, Cercós MG, Noguez P, Trueta C, De-Miguel FF. Exocytosis of serotonin from the neuronal soma is sustained by a serotonin and calcium-dependent feedback loop. *Front Cell Neurosci* (2014) 8:169. doi: 10.3389/fncel.2014.00169

39. Reed GL, Fitzgerald ML, Polgár J. Molecular mechanisms of platelet exocytosis: insights into the "secrete" life of thrombocytes. *Blood* (2000) 96:3334–42. doi: 10.1182/blood.V96.10.3334

40. Busch AE, Karbach U, Miska D, Gorboulev V, Akhoundova A, Volk C, et al. Human neurons express the polyspecific cation transporter hOCT2, which translocates monoamine neurotransmitters, amantadine, and memantine. *Mol Pharmacol* (1998) 54:342–52. doi: 10.1124/mol.54.2.342

41. Kekuda R, Prasad PD, Wu X, Wang H, Fei YJ, Leibach FH, et al. Cloning and functional characterization of a potential-sensitive, polyspecific organic cation

transporter (OCT3) most abundantly expressed in placenta. *J Biol Chem* (1998) 273:15971–9. doi: 10.1074/jbc.273.26.15971

42. Hilber B, Scholze P, Dorostkar MM, Sandtner W, Holy M, Boehm S, et al. Serotonin-transporter mediated efflux: A pharmacological analysis of amphetamines and non-amphetamines. *Neuropharmacology* (2005) 49:811–9. doi: 10.1016/j.neuropharm.2005.08.008

43. Peters GH, Wang C, Cruys-Bagger N, Velardez GF, Madsen JJ, Westh P. Binding of serotonin to lipid membranes. *J Am Chem Soc* (2013) 135:2164–71. doi: 10.1021/ja306681d

44. Manca M, Pessoa V, Lopez AI, Harrison PT, Miyajima F, Sharp H, et al. The regulation of monoamine oxidase a gene expression by distinct variable number tandem repeats. *J Mol Neurosci* (2018) 64:459–70. doi: 10.1007/s12031-018-1044-z

45. Blazevic S, Horvaticek M, Kesic M, Zill P, Hranilovic D, Ivanisevic M, et al. Epigenetic adaptation of the placental serotonin transporter gene (SLC6A4) to gestational diabetes mellitus. *PloS One* (2017) 12:e0179934. doi: 10.1371/journal.pone.0179934

46. Moya PR, Wendland JR, Salemme J, Fried RL, Murphy DL. miR-15a and miR-16 regulate serotonin transporter expression in human placental and rat brain raphe cells. *Int J Neuropsychopharmacol* (2013) 16:621–9. doi: 10.1017/S1461145712000454

47. Ruble CL, Smith RM, Calley J, Munsie L, Airey DC, Gao Y, et al. Genomic structure and expression of the human serotonin 2A receptor gene (HTR2A) locus: Identification of novel HTR2A and antisense (HTR2A-AS1) exons. *BMC Genet* (2016) 17:1–15. doi: 10.1186/s12863-015-0325-6

48. Grohmann M, Hammer P, Walther M, Paulmann N, Büttner A, Eisenmenger W, et al. Alternative splicing and extensive RNA editing of human TPH2 transcripts. *PloS One* (2010) 5:e8956. doi: 10.1371/journal.pone.0008956

49. Ozsarac N, Santha E, Hoffman BJ. Alternative non-coding exons support serotonin transporter mRNA expression in the brain and gut. *J Neurochem* (2002) 82:336–44. doi: 10.1046/j.1471-4159.2002.00964.x

50. Woehler A, Wlodarczyk J, Ponimaskin EG. Specific oligomerization of the 5-HT1A receptor in the plasma membrane. *Glycoconj J* (2009) 26:749–56. doi: 10.1007/s10719-008-9187-8

51. Tate CG, Blakely RD. The effect of n-linked glycosylation on activity of the na+- and cl– dependent serotonin transporter expressed using recombinant baculovirus in insect cells. *J Biol Chem* (1994) 269:26303–10. doi: 10.1016/s0021-9258(18)47194-3

52. Xia Z, Gray JA, Compton-Toth BA, Roth BL. A direct interaction of PSD-95 with 5-HT2A serotonin receptors regulates receptor trafficking and signal transduction. *J Biol Chem* (2003) 278:21901–8. doi: 10.1074/jbc.M301905200

53. Gorinski N, Bijata M, Prasad S, Wirth A, Abdel Galil D, Zeug A, et al. Attenuated palmitoylation of serotonin receptor 5-HT1A affects receptor function and contributes to depression-like behaviors. *Nat Commun* (2019) 10:3924. doi: 10.1038/s41467-019-11876-5

54. Cooper A, Woulfe D, Kilic F. Post-translational modifications of serotonin transporter. *Pharmacol Res* (2019) 140:7–13. doi: 10.1016/j.phrs.2018.10.018

55. Li Y, Hadden C, Singh P, Mercado CP, Murphy P, Dajani NK, et al. GDM-associated insulin deficiency hinders the dissociation of SERT from ERp44 and down-regulates placental 5-HT uptake. *Proc Natl Acad Sci United States America* (2014) 111:E5697–705. doi: 10.1073/pnas.1416675112

56. Gottfries CG, Roos BE, Winblad B. Determination of 5-hydroxytryptamine, 5-hydroxyindoleacetic acid and homovanillic acid in brain tissue from an autopsy material. *Acta Psychiatr Scand* (1974) 50:496–507. doi: 10.1111/j.1600-0447.1974.tb09711.x

57. Young SN, Gauthier S, Anderson GM, Purdy WC. Tryptophan, 5-hydroxyindoleacetic acid and indoleacetic acid in human cerebrospinal fluid: Interrelationships and the influence of age, sex, epilepsy and anticonvulsant drugs. *J Neurol Neurosurg Psychiatry* (1980) 43:438–45. doi: 10.1136/jnnp.43.5.438

58. Nishizawa S, Benkelfat C, Young SN, Leyton M, Mzengeza S, De Montigny C, et al. Differences between males and females in rates of serotonin synthesis in human brain. *Proc Natl Acad Sci United States America* (1997) 94:5308–13. doi: 10.1073/pnas.94.10.5308

59. Biver F, Lotstra F, Monclus M, Wiklera D, Damhaut P, Mendlewicz J, et al. Sex difference in 5HT 2 receptor in the living human brain. *Neurosci Lett* (1996) 204:25–8. doi: 10.1016/0304-3940(96)12307-7

60. Jovanovic H, Lundberg J, Karlsson P, Cerin Å, Saijo T, Varrone A, et al. Sex differences in the serotonin 1A receptor and serotonin transporter binding in the human brain measured by PET. *NeuroImage* (2008) 39:1408–19. doi: 10.1016/j.neuroimage.2007.10.016

61. Carlsson M, Svensson K, Eriksson E, Carlsson A. Rat brain serotonin: Biochemical and functional evidence for a sex difference. *J Neural Transm* (1985) 63:297–313. doi: 10.1007/BF01252033

62. Dickinson SL, Curzon G. 5-hydroxytryptamine-mediated behaviour in male and female rats. *Neuropharmacology* (1986) 25:771–6. doi: 10.1016/0028-3908(86)90094-8

63. Jones MD, Lucki I. Sex differences in the regulation of serotonergic transmission and behavior in 5-HT receptor knockout mice. *Neuropsychopharmacology* (2005) 30:1039–47. doi: 10.1038/sj.npp.1300664

64. Clarke G, Grenham S, Scully P, Fitzgerald P, Moloney RD, Shanahan F, et al. The microbiome-gut-brain axis during early life regulates the hippocampal serotonergic system in a sex-dependent manner. *Mol Psychiatry* (2013) 18:666–73. doi: 10.1038/mp.2012.77

65. Ceasrine AM, Devlin BA, Bolton JL, Jo YC, Patrick B, Washington K, et al. Maternal diet disrupts the placenta-brain axis in a sex-specific manner. *bioRxiv* (2022) doi: 10.1101/2021.11.12.468408

66. Llorente R, O'Shea E, Gutierrez-Lopez MD, Llorente-Berzal A, Colado MI, Viveros M-P. Sex-dependent maternal deprivation effects on brain monoamine content in adolescent rats. *Neurosci Lett* (2010) 479:112–7. doi: 10.1016/j.neulet.2010.05.039

67. Campbell KSJ, Williams LJ, Bjornson BH, Weik E, Brain U, Grunau RE, et al. Prenatal antidepressant exposure and sex differences in neonatal corpus callosum microstructure. *Dev Psychobiol* (2021) 63:1–15. doi: 10.1002/dev.22125

68. Ranzil S, Ellery S, Walker DW, Vaillancourt C, Alfaidy N, Bonnin A, et al. Disrupted placental serotonin synthetic pathway and increased placental serotonin: Potential implications in the pathogenesis of human fetal growth restriction. *Placenta* (2019) 84:74–83. doi: 10.1016/j.placenta.2019.05.012

69. Karahoda R, Abad C, Horackova H, Kastner P, Zaugg J, Cerveny L, et al. Dynamics of tryptophan metabolic pathways in human placenta and placental-derived cells: Effect of gestation age and trophoblast differentiation. *Front Cell Dev Biol* (2020) 8:574034. doi: 10.3389/fcell.2020.574034

70. Karahoda R, Horackova H, Kastner P, Matthios A, Cerveny L, Kucera R, et al. Serotonin homeostasis in the materno-foetal interface at term: Role of transporters (SERT/SLC6A4 and OCT3/SLC22A3) and monoamine oxidase a (MAO-a) in uptake and degradation of serotonin by human and rat term placenta. *Acta Physiol* (2020) 229:e13478. doi: 10.1111/apha.13478

71. Sivasubramaniam SD, Finch CC, Billett MA, Baker PN, Billett EE. Monoamine oxidase expression and activity in human placentae from pre-eclamptic and normotensive pregnancies. *Placenta* (2002) 23:163–71. doi: 10.1053/plac.2001.0770

72. Auda GR, Kirk SH, Billett MA, Billett EE. Localization of monoamine oxidase mRNA in human placenta. *J Histochem Cytochem* (1998) 46:1393–400. doi: 10.1177/002215549804601208

73. O'Carroll AM, Anderson MC, Tobbia I, Phillips JP, Tipton KF. Determination of the absolute concentrations of monoamine oxidase a and b in human tissues. *Biochem Pharmacol* (1989) 38:901–5. doi: 10.1016/0006-2952(89)90278-5

74. Ahmadimoghaddam D, Zemankova L, Nachtigal P, Dolezelova E, Neumanova Z, Cerveny L, et al. Organic cation transporter 3 (OCT3/SLC22A3) and multidrug and toxin extrusion 1 (MATE1/SLC47A1) transporter in the placenta and fetal tissues: expression profile and fetus protective role at different stages of gestation. *Biol Reprod* (2013) 88:55. doi: 10.1095/biolreprod.112.105064

75. Lee N, Hebert MF, Prasad B, Easterling TR, Kelly EJ, Unadkat JD, et al. Effect of gestational age on mRNA and protein expression of polyspecific organic cation transporters during pregnancy. *Drug Metab Dispos* (2013) 41:2225–32. doi: 10.1124/dmd.113.054072

76. Hasegawa N, Furugen A, Ono K, Koishikawa M, Miyazawa Y, Nishimura A, et al. Cellular uptake properties of lamotrigine in human placental cell lines: Investigation of involvement of organic cation transporters (SLC22A1–5). *Drug Metab Pharmacokinet* (2020) 35:266–73. doi: 10.1016/j.dmpk.2020.01.005

77. Sata R, Ohtani H, Tsujimoto M, Murakami H, Koyabu N, Nakamura T, et al. Functional analysis of organic cation transporter 3 expressed in human placenta. *J Pharmacol Exp Ther* (2005) 315:888–95. doi: 10.1124/jpet.105.086827

78. Bottalico B, Larsson I, Brodszki J, Hernandez-Andrade E, Casslén B, Marsál K, et al. Norepinephrine transporter (NET), serotonin transporter (SERT), vesicular monoamine transporter (VMAT2) and organic cation transporters (OCT1, 2 and EMT) in human placenta from pre-eclamptic and normotensive pregnancies. *Placenta* (2004) 25:518–29. doi: 10.1016/j.placenta.2003.10.017

79. Sonier B, Lavigne C, Arseneault M, Ouellette R, Vaillancourt C. Expression of the 5-HT2A serotoninergic receptor in human placenta and choriocarcinoma cells: mitogenic implications of serotonin. *Placenta* (2005) 26:484–90. doi: 10.1016/j.placenta.2004.08.003

80. Viau M, Lafond J, Vaillancourt C. Expression of placental serotonin transporter and 5-HT 2A receptor in normal and gestational diabetes mellitus pregnancies. *Reprod BioMed Online* (2009) 19:207–15. doi: 10.1016/s1472-6483(10)60074-0

81. Thébault-Dagher F, Robles M, Herba CM, St-Pierre J, Brochen C, Muckle G, et al. Febrile seizure incidence and age at first occurrence are associated with changes in placental normalized gene expression: the "3D" pregnancy cohort study. *J Neuroendocrinol* (2021) 33:e13046. doi: 10.1111/jne.13046

82. Kliman HJ, Quaratella SB, Setaro AC, Siegman EC, Subha ZT, Tal R, et al. Pathway of maternal serotonin to the human embryo and fetus. *Endocrinology* (2018) 159:1609–29. doi: 10.1210/en.2017-03025

83. Laurent L, Deroy K, St-Pierre J, Côté F, Sanderson JT, Vaillancourt C. Human placenta expresses both peripheral and neuronal isoform of tryptophan hydroxylase. *Biochimie* (2017) 140:159–65. doi: 10.1016/j.biochi.2017.07.008

84. Gujrati VR, Shanker K, Vrat S, Chandravati, Parmar SS. Novel appearance of placental nuclear monoamine oxidase: Biochemical and histochemical evidence for hyperserotonomic state in preeclampsia-eclampsia. *Am J Obstet Gynecol* (1996) 175:1543–50. doi: 10.1016/S0002-9378(96)70104-7

85. Lee N, Hebert MF, Wagner DJ, Easterling TR, Liang CJ, Rice K, et al. Organic cation transporter 3 facilitates fetal exposure to metformin during pregnancy. *Mol Pharmacol* (2018) 94:1125–31. doi: 10.1124/mol.118.112482

86. Huang WQ, Zhang CL, Di XY, Zhang RQ. Studies on the localization of 5-hydroxytryptamine and its receptors in human placenta. *Placenta* (1998) 19:655–61. doi: 10.1016/s0143-4004(98)90027-3

87. Pavličev M, Wagner GP, Chavan AR, Owens K, Maziarz J, Dunn-Fletcher C, et al. Single-cell transcriptomics of the human placenta: inferring the cell communication network of the maternal-fetal interface. *Genome Res* (2017) 27:349–61. doi: 10.1101/gr.207597.116

88. Suryawanshi H, Morozov P, Straus A, Sahasrabudhe N, Max KEA, Garzia A, et al. A single-cell survey of the human first-trimester placenta and decidua. *Sci Adv* (2018) 4:eaau4788. doi: 10.1126/sciadv.aau4788

89. Baković P, Kesić M, Perić M, Bečeheli I, Horvatiček M, George M, et al. Differential serotonin uptake mechanisms at the human maternal–fetal interface. *Int J Mol Sci* (2021) 22:7807. doi: 10.3390/ijms22157807

90. Prasad PD, Hoffmans BJ, Moe AJ, Smith CH, Leibach FH, Ganapathy V. Functional expression of the plasma membrane serotonin transporter but not the vesicular monoamine transporter in human placental trophoblasts and choriocarcinoma cells. *Placenta* (1996) 17:201–7. doi: 10.1016/s0143-4004(96)90039-9

91. Vaillancourt C, Petit A, Gallo-Payet N, Bellabarba D, Lehoux JG, Bélisle S. Labelling of D2-dopaminergic and 5-HT2-serotonergic binding sites in human trophoblastic cells using [3H]-spiperone. *J Recept Res* (1994) 14:11–22. doi: 10.3109/10799899409066993

92. Yavarone MS, Shuey DL, Sadler TW, Lauder JM. Serotonin uptake in the ectoplacental cone and placenta of the mouse. *Placenta* (1993) 14:149–61. doi: 10.1016/s0143-4004(05)80257-7

93. Bonnin A, Goeden N, Chen K, Wilson ML, King J, Shih JC, et al. A transient placental source of serotonin for the fetal forebrain. *Nature* (2011) 472:347–50. doi: 10.1038/nature09972

94. Balkovetz DF, Tiruppathi C, Leibach FH, Mahesh VB, Ganapathy V. Evidence for an imipramine-sensitive serotonin transporter in human placental brush-border membranes. *J Biol Chem* (1989) 264:2195–8. doi: 10.1016/S0021-9258(18)94161-X

95. Vachalova V, Karahoda R, Ottaviani M, Anandam KY, Abad C, Albrecht C, et al. Functional reorganization of monoamine transport systems during villous trophoblast differentiation: evidence of distinct differences between primary human trophoblasts and BeWo cells. *Reprod Biol Endocrinol* (2022) 20:112. doi: 10.1186/s12958-022-00981-8

96. Bertrand C, St-Louis J. Reactivities to serotonin and histamine in umbilical and placental vessels during the third trimester after normotensive pregnancies and pregnancies complicated by preeclampsia. *Am J Obstet Gynecol* (1999) 180:650–9. doi: 10.1016/s0002-9378(99)70268-1

97. Reviriego J, Fernandez-Alfonso MS, Marín J. Actions of vasoactive drugs on human placental vascular smooth muscle. *Gen Pharmacol* (1990) 21:719–27. doi: 10.1016/0306-3623(90)91024-l

98. Ugun-Klusek A, Tamang A, Loughna P, Billett E, Buckley G, Sivasubramaniam S. Reduced placental vascular reactivity to 5-hydroxytryptamine in pre-eclampsia and the status of 5HT(2A) receptors. *Vascul Pharmacol* (2011) 55:157–62. doi: 10.1016/j.vph.2011.07.006

99. Rothbauer M, Patel N, Gondola H, Siwetz M, Huppertz B, Ertl P. A comparative study of five physiological key parameters between four different human trophoblast-derived cell lines. *Sci Rep* (2017) 7:5892. doi: 10.1038/s41598-017-06364-z

100. Sheridan MA, Fernando RC, Gardner L, Hollinshead MS, Burton GJ, Moffett A, et al. Establishment and differentiation of long-term trophoblast organoid cultures from the human placenta. *Nat Protoc* (2020) 15:3441–63. doi: 10.1038/s41596-020-0381-x

101. Ciuclan L, Hussey MJ, Burton V, Good R, Duggan N, Beach S, et al. Imatinib attenuates hypoxia-induced pulmonary arterial hypertension pathology *via* reduction in 5-hydroxytryptamine through inhibition of tryptophan hydroxylase 1 expression. *Am J Respir Crit Care Med* (2013) 187:78–89. doi: 10.1164/rccm.201206-1028OC

102. Eddahibi S, Fabre V, Boni C, Martres MP, Raffestin B, Hamon M, et al. Induction of serotonin transporter by hypoxia in pulmonary vascular smooth muscle cells. *Relatsh Mitogenic Action Serotonin Circ Res* (1999) 84:329–36. doi: 10.1161/01.res.84.3.329

103. Oufkir T, Arseneault M, Sanderson JT, Vaillancourt C. The 5-HT2A serotonin receptor enhances cell viability, affects cell cycle progression and activates MEK–ERK1/2 and JAK2–STAT3 signalling pathways in human choriocarcinoma cell lines. *Placenta* (2010) 31:439–47. doi: 10.1016/j.placenta.2010.02.019

104. Oufkir T, Vaillancourt C. Phosphorylation of JAK2 by serotonin 5-HT (2A) receptor activates both STAT3 and ERK1/2 pathways and increases growth of JEG-3 human placental choriocarcinoma cell. *Placenta* (2011) 32:1033–40. doi: 10.1016/j.placenta.2011.09.005

105. Hadden C, Fahmi T, Cooper A, Savenka AV, Lupashin VV, Roberts DJ, et al. Serotonin transporter protects the placental cells against apoptosis in caspase 3-independent pathway. *J Cell Physiol* (2017) 232:3520–9. doi: 10.1002/jcp.25812

106. Hudon Thibeault A-A, de Los Santos YL, Doucet N, Sanderson JT, Vaillancourt C. Serotonin and serotonin reuptake inhibitors alter placental aromatase. *J Steroid Biochem Mol Biol* (2019) 195:105470. doi: 10.1016/j.jsbmb.2019.105470

107. Klempan T, Hudon-Thibeault A-A, Oufkir T, Vaillancourt C, Sanderson JT. Stimulation of serotonergic 5-HT2A receptor signaling increases placental aromatase (CYP19) activity and expression in BeWo and JEG-3 human choriocarcinoma cells. *Placenta* (2011) 32:651–6. doi: 10.1016/j.placenta.2011.06.003

108. Gibbs WS, Collier JB, Morris M, Beeson CC, Megyesi J, Schnellmann RG. 5-HT1F receptor regulates mitochondrial homeostasis and its loss potentiates acute kidney injury and impairs renal recovery. *Am J Physiol Renal Physiol* (2018) 315:F1119–28. doi: 10.1152/ajprenal.00077.2018

109. Wang Q, Zhang H, Xu H, Guo D, Shi H, Li Y, et al. 5-HTR3 and 5-HTR4 located on the mitochondrial membrane and functionally regulated mitochondrial functions. *Sci Rep* (2016) 6:37336. doi: 10.1038/srep37336

110. Murphy DL, Moya PR. Human serotonin transporter gene (SLC6A4) variants: their contributions to understanding pharmacogenomic and other functional G×G and G×E differences in health and disease. *Curr Opin Pharmacol* (2011) 11:3–10. doi: 10.1016/j.coph.2011.02.008

111. Philibert R, Madan A, Andersen A, Cadoret R, Packer H, Sandhu H. Serotonin transporter mRNA levels are associated with the methylation of an upstream CpG island. *Am J Med Genet Part B: Neuropsychiatr Genet* (2007) 144B:101–5. doi: 10.1002/ajmg.b.30414

112. Ramamoorthy S, Ramamoorthy JD, Prasad PD, Bhat GK, Mahesh VB, Leibach FH, et al. Regulation of the human serotonin transporter by interleukin-1 beta. *Biochem Biophys Res Commun* (1995) 216:560–7. doi: 10.1006/bbrc.1995.2659

113. Kong E, Sucic S, Monje FJ, Savalli G, Diao W, Khan D, et al. STAT3 controls IL6-dependent regulation of serotonin transporter function and depression-like behavior. *Sci Rep* (2015) 5:9009. doi: 10.1038/srep09009

114. Hudon Thibeault A-A, Laurent L, Vo Duy S, Sauvé S, Caron P, Guillemette C, et al. Fluoxetine and its active metabolite norfluoxetine disrupt estrogen synthesis in a co-culture model of the feto-placental unit. *Mol Cell Endocrinol* (2017) 442:32–9. doi: 10.1016/j.mce.2016.11.021

115. Andrade SE, Raebel MA, Brown J, Lane K, Livingston J, Boudreau D, et al. Use of antidepressant medications during pregnancy: a multisite study. *Am J Obstet Gynecol* (2008) 198:e1–5:194. doi: 10.1016/j.ajog.2007.07.036

116. Bakker MK, Kölling P, van den Berg PB, de Walle HEK, de Jong vdBLTW. Increase in use of selective serotonin reuptake inhibitors in pregnancy during the last decade, a population-based cohort study from the Netherlands. *Br J Clin Pharmacol* (2008) 65:600–6. doi: 10.1111/j.1365-2125.2007.03048.x

117. Cooper WO, Willy ME, Pont SJ, Ray WA. Increasing use of antidepressants in pregnancy. *Am J Obstet Gynecol* (2007) 196:544.e1–5. doi: 10.1016/j.ajog.2007.01.033

118. Smid MC, Metz TD, Gordon AJ. Stimulant use in pregnancy: An under-recognized epidemic among pregnant women. *Clin Obstet Gynecol* (2019) 62:168–84. doi: 10.1097/GRF.0000000000000418

119. Cool DR, Leibach FH, Bhalla VK, Mahesh VB, Ganapathy V. Expression and cyclic AMP-dependent regulation of a high affinity serotonin transporter in the human placental choriocarcinoma cell line (JAR). *J Biol Chem* (1991) 266:15750–7. doi: 10.1016/S0021-9258(18)98473-5

120. Cool DR, Leibach FH, Ganapathy V. High-affinity paroxetine binding to the human placental serotonin transporter. *Am J Physiol* (1990) 259:C196–204. doi: 10.1152/ajpcell.1990.259.2.C196

121. Cool DR, Liebach FH, Ganapathy V. Interaction of fluoxetine with the human placental serotonin transporter. *Biochem Pharmacol* (1990) 40:2161–7. doi: 10.1016/0006-2952(90)90249-k

122. Sabol SZ, Hu S, Hamer D. A functional polymorphism in the monoamine oxidase a gene promoter. *Hum Genet* (1998) 103:273–9. doi: 10.1007/s004390050816

123. Zhang H, Smith GN, Liu X, Holden JJA. Association of MAOA, 5-HTT, and NET promoter polymorphisms with gene expression and protein activity in human placentas. *Physiol Genomics* (2010) 42:85–92. doi: 10.1152/physiolgenomics.00220.2009

124. Shumay E, Fowler JS. Identification and characterization of putative methylation targets in the MAOA locus using bioinformatic approaches. *Epigenetics* (2010) 5:325–42. doi: 10.4161/epi.5.4.11719

125. Gumusoglu S, Scroggins S, Vignato J, Santillan D, Santillan M. The serotonin-immune axis in preeclampsia. *Curr Hypertens Rep* (2021) 23:37. doi: 10.1007/s11906-021-01155-4

126. Carrasco G, Cruz MA, Dominguez A, Gallardo V, Miguel P, González C. The expression and activity of monoamine oxidase a, but not of the serotonin transporter, is decreased in human placenta from pre-eclamptic pregnancies. *Life Sci* (2000) 67:2961–9. doi: 10.1016/S0024-3205(00)00883-3

127. Pinter SZ, Kripfgans OD, Treadwell MC, Kneitel AW, Fowlkes JB, Rubin JM. Evaluation of umbilical vein blood volume flow in preeclampsia by angle-independent 3D sonography. *J Ultrasound Med* (2018) 37:1633–40. doi: 10.1002/jum.14507

128. Murthi P, Vaillancourt C. Placental serotonin systems in pregnancy metabolic complications associated with maternal obesity and gestational diabetes mellitus. *Biochim Biophys Acta - Mol Basis Dis* (2020) 1866:165391. doi: 10.1016/j.bbadis.2019.01.017

129. Horvatiček M, Perić M, Bečeheli I, Klasić M, Žutić M, Kesić M, et al. Maternal metabolic state and fetal sex and genotype modulate methylation of the serotonin receptor type 2A gene (HTR2A) in the human placenta. *Biomedicines* (2022) 10:467. doi: 10.3390/biomedicines10020467

130. Blakeley PM, Capron LE, Jensen AB, O'Donnell KJ, Glover V. Maternal prenatal symptoms of depression and down regulation of placental monoamine oxidase a expression. *J Psychosom Res* (2013) 75:341–5. doi: 10.1016/j.jpsychores.2013.07.002

131. Ruyak SL, Noor S, DiDomenico J, Sun MS, Fernandez Oropeza AK, Rodriguez DE, et al. Effects of prenatal opioid and alcohol exposures on immune and serotonin factors in human placenta. *Exp Neurol* (2022) 353:114057. doi: 10.1016/j.expneurol.2022.114057

132. Karahoda R, Robles M, Marushka J, Stranik J, Abad C, Horackova H, et al. Prenatal inflammation as a link between placental expression signature of tryptophan metabolism and preterm birth. *Hum Mol Genet* (2021) 30:2053–67. doi: 10.1093/hmg/ddab169

133. Côté F, Fligny C, Bayard E, Launay J-M, Gershon MD, Mallet J, et al. Maternal serotonin is crucial for murine embryonic development. *Proc Natl Acad Sci U.S.A.* (2007) 104:329–34. doi: 10.1073/pnas.0606722104

134. Fligny C, Fromes Y, Bonnin P, Darmon M, Bayard E, Launay J-M, et al. Maternal serotonin influences cardiac function in adult offspring. *FASEB J* (2008) 22:2340–9. doi: 10.1096/fj.07-100743

135. Takahashi H, Nakashima S, Ohama E, Takeda S, Ikuta F. Distribution of serotonin-containing cell bodies in the brainstem of the human fetus determined with immunohistochemistry using antiserotonin serum. *Brain Dev* (1986) 8:355–65. doi: 10.1016/s0387-7604(86)80055-9

136. McKinney J, Knappskog PM, Pereira J, Ekern T, Toska K, Kuitert BB, et al. Expression and purification of human tryptophan hydroxylase from escherichia coli and pichia pastoris. *Protein Expression Purification* (2004) 33:185–94. doi: 10.1016/j.pep.2003.09.014

137. Mathiesen L, Bay-Richter C, Wegener G, Liebenberg N, Knudsen LE. Maternal stress and placental function; ex vivo placental perfusion studying cortisol, cortisone, tryptophan and serotonin. *PloS One* (2020) 15:e0233979. doi: 10.1371/journal.pone.0233979

138. Hjort L, Novakovic B, Cvitic S, Saffery R, Damm P, Desoye G. Placental DNA methylation in pregnancies complicated by maternal diabetes and/or obesity: State of the art and research gaps. *Epigenetics* (2022) 17:1–21. doi: 10.1080/15592294.2022.2111755

139. Halmøy A, Johansson S, Winge I, McKinney JA, Knappskog PM, Haavik J. Attention-deficit/hyperactivity disorder symptoms in offspring of mothers with impaired serotonin production. *Arch Gen Psychiatry* (2010) 67:1033–43. doi: 10.1001/archgenpsychiatry.2010.124

140. Leboyer M, Philippe A, Bouvard M, Guilloud-Bataille M, Bondoux D, Tabuteau F, et al. Whole blood serotonin and plasma beta-endorphin in autistic probands and their first-degree relatives. *Biol Psychiatry* (1999) 45:158–63. doi: 10.1016/s0006-3223(97)00532-5

141. Paquette AG, Lesseur C, Armstrong DA, Koestler DC, Appleton AA, Lester BM, et al. Placental HTR2A methylation is associated with infant neurobehavioral outcomes. *Epigenetics* (2013) 8:796–801. doi: 10.4161/epi.25358

142. Räikkönen K, Pesonen A-K, O'Reilly JR, Tuovinen S, Lahti M, Kajantie E, et al. Maternal depressive symptoms during pregnancy, placental expression of genes regulating glucocorticoid and serotonin function and infant regulatory behaviors. *Psychol Med* (2015) 45:3217–26. doi: 10.1017/S003329171500121X

143. Pehme PM, Zhang W, Finik J, Pritchett A, Buthmann J, Dana K, et al. Placental MAOA expression mediates prenatal stress effects on temperament in 12-month-olds. *Infant Child Dev* (2018) 27:e2094. doi: 10.1002/icd.2094

144. Köhler S, Cierpinsky K, Kronenberg G, Adli M. The serotonergic system in the neurobiology of depression: Relevance for novel antidepressants. *J Psychopharmacol* (2016) 30:13–22. doi: 10.1177/0269881115609072

145. Garfield AS, Heisler LK. Pharmacological targeting of the serotonergic system for the treatment of obesity. *J Physiol* (2009) 587:49–60. doi: 10.1113/jphysiol.2008.164152

146. Beattie D, Smith J. Serotonin pharmacology in the gastrointestianl tract: a review. *Naunyn-Schmiedeberg's Arch Pharmacol* (2008) 377:181–203. doi: 10.1007/s00210-008-0276-9

147. Hernández-Hernández OT, Martínez-Mota L, Herrera-Pérez JJ, Jiménez-Rubio G. Role of estradiol in the expression of genes involved in serotonin neurotransmission: Implications for female depression. *Curr Neuropharmacol* (2019) 17:459–71. doi: 10.2174/1570159X16666180628165107

148. Zha W, Ho HTB, Hu T, Hebert MF, Wang J. Serotonin transporter deficiency drives estrogen-dependent obesity and glucose intolerance. *Sci Rep* (2017) 7:1137. doi: 10.1038/s41598-017-01291-5

frontiers | Frontiers in Endocrinology

TYPE Original Research
PUBLISHED 20 January 2023
DOI 10.3389/fendo.2022.951388

Check for updates

OPEN ACCESS

EDITED BY
Alicia E. Damiano,
University of Buenos Aires, Argentina

REVIEWED BY
Jia Chen,
Icahn School of Medicine at Mount Sinai, United States
Marcelo González,
University of Concepcion, Chile

*CORRESPONDENCE
Yuping Wang
yuping.wang@lsuhs.edu

SPECIALTY SECTION
This article was submitted to Developmental Endocrinology, a section of the journal Frontiers in Endocrinology

RECEIVED 23 May 2022
ACCEPTED 20 December 2022
PUBLISHED 20 January 2023

CITATION
Wang Y, Gu Y, Lewis DF, Gu X, Brown K, Lachute C, Hankins M, Scott RS, Busada C, Cooper DB, McCathran CE and Barrilleaux P (2023) Cell-type specific distribution and activation of type I IFN pathway molecules at the placental maternal-fetal interface in response to COVID-19 infection. *Front. Endocrinol.* 13:951388. doi: 10.3389/fendo.2022.951388

COPYRIGHT
© 2023 Wang, Gu, Lewis, Gu, Brown, Lachute, Hankins, Scott, Busada, Cooper, McCathran and Barrilleaux. This is an open-access article distributed under the terms of the Creative Commons Attribution License (CC BY). The use, distribution or reproduction in other forums is permitted, provided the original author(s) and the copyright owner(s) are credited and that the original publication in this journal is cited, in accordance with accepted academic practice. No use, distribution or reproduction is permitted which does not comply with these terms.

Cell-type specific distribution and activation of type I IFN pathway molecules at the placental maternal-fetal interface in response to COVID-19 infection

Yuping Wang [1*], Yang Gu [1], David F. Lewis [1], Xin Gu [2], Karisa Brown [1], Courtney Lachute [1], Miriam Hankins [1], Rona S. Scott [3], Caitlin Busada [1], Danielle B. Cooper [1], Charles E. McCathran [1] and Perry Barrilleaux [1]

[1]Department of Obstetrics and Gynecology, Louisiana State University Health Sciences Center - Shreveport, Shreveport, LA, United States, [2]Department of Pathology, Louisiana State University Health Sciences Center - Shreveport, Shreveport, LA, United States, [3]Department of Immunology and Microbiology, Louisiana State University Health Sciences Center - Shreveport, Shreveport, LA, United States

Background and objective: COVID-19 infection in pregnancy significantly increases risks of adverse pregnancy outcomes. However, little is known how the innate immunity at the placental maternal-fetal interface responds to COVID-19 infection. Type I IFN cytokines are recognized as a key component of the innate immune response against viral infection. In this study, we specifically evaluated expression of IFN antiviral signaling molecules in placentas from women infected with COVID-19 during pregnancy.

Methods: Expression of IFN activation signaling pathway molecules, including cyclic GMP–AMP synthase (cGAS), stimulator of interferon genes (STING), interferon regulatory factor 3 (IRF3), Toll-like receptor 7 (TLR7), mitochondrial antiviral-signaling protein (MAVS), and IFNβ were determined in formalin-fixed paraffin embedded (FFPE) placental tissue sections (villous and fetal membrane) by immunostaining. A total of 20 placentas were examined, 12 from COVID-19 patients and 8 from non-COVID-19 controls. Patient demographics, clinical data, and placental pathology report were acquired *via* EPIC medical record review.

Results: Except BMI and placental weight, there was no statistical difference between COVID and non-COVID groups in maternal age, gestational age at delivery, gravity/parity, delivery mode, and newborn gender and weight. In COVID-exposed group, the main pathological characteristics in the placental disc are maternal and fetal vascular malperfusion and chronic inflammation. Compared to non-COVID controls, expression of IFN activation pathway

molecules were all upregulated with distinct cell-type specific distribution in COVID-exposed placentas: STING in villous and decidual stromal cells; IRF3 in cytotrophoblasts (CTs) and extra-villous trophoblasts (EVTs); and TLR7 and MAVS in syncytiotrophoblasts (STs), CTs, and EVTs. Upregulation of STING, MAVS and TLR7 was also seen in fetal endothelial cells.

Conclusions: STING, IRF3, TLR7, and MAVS are key viral sensing molecules that regulate type I IFN production. Type I IFNs are potent antiviral cytokines to impair and eradicate viral replication in infected cells. The finding of cell-type specific distribution and activation of these innate antiviral molecules at the placental maternal-fetal interface provide plausible evidence that type I IFN pathway molecules may play critical roles against SARS-CoV-2 infection in the placenta. Our findings also suggest that placental maternal-fetal interface has a well-defined antiviral defense system to protect the developing fetus from SARS-CoV-2 infection.

KEYWORDS

COVID-19, STING, IRF3, TLR7, MAVS, type I IFNs, pregnancy, placental maternal-fetal interface

Introduction

The pandemic coronavirus disease 2019 (COVID-19) caused by severe acute respiratory syndrome coronavirus 2 (SARS-CoV-2) has significantly impacted public health worldwide. Women infected with COVID-19 during pregnancy results in higher rate of adverse maternal and fetal outcomes, including preterm birth, preeclampsia, stillbirth, gestational diabetes, and low birth weight, than those were not (1–3). Furthermore, emerging studies of placenta, embryos, and cerebral organoids also suggest that fetal organs, such as the brain, could be vulnerable to COVID-19 infection (4). Although newborns delivered to women infected with COVID-19 was reported (5–7), vertical transmission of the virus is rare. However, the findings of detection of SARS-CoV-2 spike protein, nucleocapsid protein, and viral nucleic acids in the placenta from women with COVID-19 infection during pregnancy demonstrated that SARS-CoV-2 can infect placenta (8–11).

Placenta controls oxygen and metabolite exchange, produces growth factors and hormones, and transfers nutrients to support fetal development and growth. Placenta is also an important structural and immunological barrier to prevent pathogen transmission to fetus during pregnancy. In terms of the immune barrier, there are at least 3 boundaries at the maternal-fetal interface: A) intervillous space: where syncytiotrophoblasts (STs) overlay villous tissue and are in direct contact with maternal blood. STs are highly resistant to infection to pathogens (12–14); B) the implantation site or decidua basalis: where the invading extra-villous trophoblasts (EVTs) are in direct contact with maternal decidual cells; and C) fetal membrane, which contains EVTs and maternal decidual cells, is in direct contact with the uterine cavity. Although the placental cells express high levels of antimicrobial defense molecules (15) such as antimicrobial peptides defensins and pattern recognition receptors (PRRs), it remains unclear how the placental defense system functions against SARS-CoV-2 infection at the maternal-fetal interface.

Abnormal vascular development and increased inflammatory response have been characterized in placentas from women infected with COVID-19 during pregnancy as evidenced by substantial maternal vascular malperfusion (MVM) in decidua and fetal vascular malperfusion (FVM) in villous tissue, along with increased focal fibrin deposition and increased lymphocyte and macrophage infiltration, etc. (14–16). These findings indicate that aberrant vascular development and hyper-inflammatory status in the placenta are associated with maternal COVID-19 infection. However, despite fast-tracked intensive research on many aspects of COVID-19, the impact of the viral infection in the placenta and the immune response of the placental defense mechanism(s) are poorly explored.

Interferon (IFN) cytokines are key molecules modulating immune responses and type I IFNs are considered to play crucial roles in protection of pregnancy *via* their antiviral and immune modulatory properties (17–19). The baseline expression

of type I IFN is very low in most tissues and could be rapidly triggered by viral attack and bacterial infections. It was reported that SARS-CoV-2 infection in pregnancy is associated with robust inflammatory response at the maternal-fetal interface, with increased activation of natural killer (NK) and T cells and increased expression of interferon-related genes, such as ISG15, an interferon-induced protein (20). In this study, we investigated if type I IFN pathway molecules are differentially activated at the maternal-fetal interface in placentas from women infected with COVID-19 during pregnancy. We specifically evaluated several key molecules that are involved in type I IFN activation, including 1) cyclic GMP–AMP synthase (cGAS); 2) stimulator of interferon genes (STING); 3) interferon regulatory factor 3 (IRF3); The cGAS-STING-IRF3 pathway plays critical roles in the induction of type I IFN activation in cells encountered viral infection (21, 22). We also examined Toll-like receptor 7 (TLR7) and mitochondrial antiviral-signaling protein (MAVS) expression. TLR7 is an endosomal innate immune sensor capable of recognizing single-stranded RNA (ssRNA) of virus infection (23, 24). MAVS is an essential adaptor protein of antiviral immunity in mitochondria, which could activate IRF3 and subsequently induce type I IFN expression (22). We also assessed IFNβ expression, a key type I IFN cytokine. These type I IFN activation markers were examined in both villous tissue and fetal membrane of placentas from women infected with COVID-19 during pregnancy.

Materials and methods

Study subjects and placenta specimen

This study was approved by the Institutional Review Board (IRB) at Louisiana State University Health Sciences Center-Shreveport (LSUHSC-S). Formalin-fixed paraffin embedded (FFPE) placental tissue sections, including villous tissue and fetal membrane, were obtained from Pathology archives at LSUHSC-S. A total of 20 placentas were examined, 12 from women infected with COVID-19 during pregnancy and 8 controls from women never infected with COVID-19 before and during pregnancy. Patients diagnosed with COVID-19 infection were detected by polymerase chain reaction (PCR) of SARS-CoV-2 RNA in nasopharyngeal swab specimens. Patients classified as asymptomatic, mild to moderate, or severe were based on their symptoms and clinical findings as defined by the NIH COVID-19 guidelines (25). Demographic and clinical information was obtained by chart review *via* EPIC medical record system. As showed in Table 1, BMI was significantly higher in the COVID-19 than in the control group. There were no statistical differences between control and COVID-19 groups in maternal age, gestational age at delivery, gravity/parity, racial status, delivery mode, and newborn gender and weight. However, placental weight was significantly less in the COVID-19 than in the control group.

TABLE 1 Demographic data of pregnant women with or without COVID-19 infection from whom placenta was studied.

Characteristics	Non-COVID Control	COVID-19 Infection	*P* value
	n = 8	n = 12	
Maternal age	29 ± 9	26 ± 7	0.4387
Racial status*, AA/Caucasian	5/3	12/0	0.0491
Gestational age (weeks^{+days})	$38^{+5} \pm 1^{+0}$	$36^{+3} \pm 4^{+1}$	0.1308
Singleton/Twins*	8/0	11/1	1.0000
Nulliparous*, n (%)	2 (25%)	3 (25%)	1.0000
BMI	31.7 ± 6.5	38.6 ± 6.7	0.0345
Delivery mode*, Vaginaldelivery/C-section	4/4	7/5	1.0000
Placental weight (gram)	615 ± 124	441 ± 134	0.0078
Newborn gender* (male/female)	4/4	7/6	1.0000
Newborn weight (gram)	3405 ± 365	2702 ± 992	0.0711

Data are expressed as mean ± SD. Statistics was calculated by un-paired test; *Statistics on racial status, singleton/twin, nulliparous, delivery mode, and newborn gender were done by Fisher's exact test. AA, African American; BMI, body mass index.

Immunohistochemical (IHC) staining

IHC was performed to evaluate expression and distribution of cGAS, STING, IRF3, TLR7, MAVS, and IFNβ in villous and fetal membrane tissue sections from all study subjects. Expression of vimentin (a marker of mesenchymal stromal cells) and CD68 and CD16 (markers of macrophage) were also determined. Villous tissue section contains STs, cytotrophoblasts (CTs), mesenchymal stromal cells (MSCs), Hofbauer cells (placental macrophages), and fetal endothelial cells. Fetal membrane contains amnionic epithelial cells, EVTs, and maternal decidual cells and MSCs. Supplemental Figure S1 shows a sagittal plan of a placenta and hematoxylin and eosin (H&E) and cytokeratin 5/8 (a marker of trophoblasts) staining in villous and fetal membrane tissue sections, which provide a general overview of villous and fetal membrane structure to show the typical layout and cell distribution of the tissue sections.

A standard immunohistochemistry staining procedure was performed. Briefly, a series of deparaffinization was carried out with xylene and ethanol alcohol. Antigen retrieval was performed by boiling tissue slides with 0.01mol/L citric buffer. Hydrogen peroxide was used to quench the endogenous peroxidase activity. After blocking, tissue sections were incubated with primary antibody overnight at 4°C. Corresponding biotinylate-conjugated secondary antibodies and ABC staining system (Santa Cruz Biotechnology) were used subsequently according to the manufacturer's instruction. Stained slides were counterstained with Gill's formulation hematoxylin. Tissue sections stained with isotype IgG or secondary antibody only were used as controls. Stained slides were reviewed under an Olympus microscope (Olympus IX71, Tokyo, Japan). In general, 3-4 images were randomly captured by a digital camera and recorded into a microscope-linked PC computer. The source of antibodies used in the study and antibody dilution factors are present in Supplemental Table S1.

For semi-quantification analysis of villous tissue immunostaining, STING and IRF3 positive cells were analyzed using Image J Plugins IHC profiler as described by Seyed Jafari and Hunger (26) with modification. Percentage contribution of high positive and percentage contribution of positive were combined as relative positive cell accounts. The intensity of TLR7, MAVS, and IFNβ staining in villous tissue sections was analyzed using semi-quantitative H-score as described by Lockwood et al. (27). Categories 1-4 were assigned: 1 (negative staining); 2 (detectable but weak staining); 3 (moderate or distinct staining), and 4 (intensive staining). The mean of H-score was generated as relative intensity immunostaining in each specimen. Semi-quantification was not done in fetal membrane staining since cell types and staining intensity can be easily differentiated.

Statistical analysis

Comparisons of clinical demographic data were performed with un-paired t-test or Chi-square test and data are presented as mean ± SD. Data for villous immunostaining were analyzed with un-paired t-test and expressed as mean ± SE. Computer software Prism 9 (GraphPad Software, Inc. La Jolla, CA) was used. A probability level less than 0.05 was considered statistically significant.

Results

Clinical data and placental pathology of COVID-19 subjects

Clinical characteristics of women infected with COVID-19 in pregnancy, including gestational age at COVID-19 infection and delivery, and maternal and newborn complications and outcomes are presented in Table 2. There were 2 cases (cases 5 and 6) infected with COVID-19 in the first trimester, 4 cases (cases 7-11) in the second trimester, and 5 cases (cases 1-4 and 12) in the third trimester. Among them, except case 11, who was complicated with antiphospholipid syndrome (APS) and delivered at 26 weeks of gestation, and case 12, a twin pregnancy complicated with severe preeclampsia and asthma, with severe COVID-19 complication of acute respiratory distress syndrome (ARDS) delivered at 30 weeks of gestation, cases 1-10 were all delivered at term or closed to term (Table 2). The two preterm cases could impact the relatively lower mean newborn weight in the COVID-19 group. None of the newborns was infected with COVID-19. It was noted that placental weight was significantly less in the COVID group than in the control group, Table 1. If excluding cases 11 and 12 (the two preterm births in the COVID group), the mean placental weight was still significantly less in the COVID group than in the control group, 501 ± 77 grams vs. 615 ± 124 grams, p = 0.0289. Supplemental Figure S2 shows the correlation of newborn weight with placental weight in the control and COVID groups.

Characteristics of placental microscopic pathology for COVID-19 patients were extracted from pathology report, re-evaluated by pathologist at LSUHSC-S, and presented in Table 3. The main pathological characteristics in placental disc are maternal and fetal vascular malperfusion and chronic inflammation. The main features of maternal vascular malperfusion include infarct, intervillous thrombus, and peri-villous fibrin deposition. The main features of fetal vascular malperfusion include avascular villi, vascular thrombi (infarction), and perivascular fibrin deposition. Chronic deciduitis is the major inflammatory pathology highlighted in the placental disc. For fetal membrane, 6 out of the 12 cases showed acute or chronic chorioamnionitis and/or chronic

TABLE 2 Clinical characteristics of women infected with COVID-19 in pregnancy.

Case#	Maternal Age	Racial Status	Parity	BMI	GA at COVID (+)	GA at Delivery	COVID test at Delivery	COVID-19 Symptoms	Maternal Outcomes	Newborn Outcomes	Newborn COVID Test
1	22	AA	G4P1	36.2	39^{+3}	39^{+3}	Pos	Asymptomatic	Severe PE	Singleton, M/3260g NICU 3days, Sepsis evaluation	Neg
2	35	AA	G7P5	41.2	37^{+0}	39^{+1}	Pos	Asymptomatic	Type-2 DM	Singleton, M/3282g, NICU 3days, COVID/glucose monitoring	Neg
3	26	AA	G3P2	36.8	37^{+1}	37^{+1}	Pos	Mild	Type-2 DM	Singleton, F/3280g NICU 3days, RDS, COVID monitoring	Neg
4	20	AA	G2P0	41.2	35^{+4}	38^{+1}	NT	Mild	SIPE, CHTN, Syphilis, Marijuana abuse	Singleton, M/3,250g NICU 11days Congenital syphilis	NT
5	20	AA	G1P0	24	8^{+3}	40^{+0}	Neg	N/A	GBS (+)	Singleton, M/3315g Meconium	NT
6	35	AA	G7P2	41.7	4^{+2}	35^{+3}	Neg	Mild	PE	Singleton, M/2,500g Extra digit on both hands	NT
7	19	AA	G3P2	30.1	14^{+1}	39^{+0}	Neg	Mild	GBS (+), Cannabis abuse	Singleton, F/3,670g NICU 1day, Sepsis evaluation	NT
8	39	AA	G8P0	44.5	14^{+3}	37^{+4}	Neg	Mild	Severe PE, Type I Diabetes	Singleton, F/3,450g	NT
9	20	AA	G1P0	46.5	16^{+4}	37^{+2}	Neg	N/A	Type-2 DM, Hodgkin Lymphoma	Singleton, F/3,200g	NT
10	33	AA	G6P1	43.8	20^{+0}	37^{+5}	Neg	Mild	CHTN, GBS(+), Oligohydramnios, Cigarette smoking	Singleton, M/2,770g Abnormal quad screen	NT
11	23	AA	G3P0	33.3	18^{+0}	26^{+1}	Neg	Asymptomatic	APS, GPS(+), Syphilis, Oligohydramnios	Singleton, F/730g NICU 59 days, Prematurity	NT
12	27	AA	G5P4	43.5	28^{+1}	30^{+1}	Pos	Severe	ARDS, Severe PE, Asthma, Di/Di Twins, Thrombocytosis, Leukocytosis, Hypokalemia	Twins, M/F. 1,320g/1,100g, Prematurity Sepsis, BPD, RDS, NICU 78/79days	Neg/Neg

AA, African American; GA, gestational age; BMI, body mass index; PE, preeclampsia; SIPE, superimposed preeclampsia; CHTN, chronic hypertension; GBS, Group B Streptococcus; APS, antiphospholipid syndrome; ADRS, acute respiratory distress syndrome; NICU, neonatal intensive care unit; BPD, bronchopulmonary dysplasia; RDS, respiratory distress syndrome. Pos, Positive; Neg, negative; NT, not tested; N/A, information is not available.

10.3389/fendo.2022.951388

10.3389/fendo.2022.951388

TABLE 3 Placental microscopic pathology of COVID-19 subjects.

Case# Placenta	Weight (grams)	Placental Disc	Fetal Membrane
1	556	intervillous thrombus, infarction, dystrophic calcification	acute chorioamnionitis
2	538	focal infarct, subchorionic hematoma	no histopathological abnormality
3	451	peri-villous fibrin deposition	no significant pathology finding
4	570	fibrin deposition, villous congestion	acute chorionitis
5	430	fibrin deposition	necrotic changes
6	394	fibrin deposition, focal infarction	no significant pathology finding
7	568	fibrin deposition, calcification, focal chorangiomatosis	chorioamnionitis
8	487	focal infarction, fibrin deposition	no significant pathology finding
9	409	decidual vasculopathy	acute chorioamnionitis
10	608	villous congestion, subchorionic hematoma	no histopathological abnormality
11	194	acute chorioamnionitis chorionic plate vasculitis	acute chorioamnionitis
12	526* dichorionic, diamnionic twins	A: lymphoplasmacytic infiltration chronic deciduitis B: lymphoplasmacytic infiltration chronic deciduitis	Chronic deciduitis lymphoplascytic infiltration chronic deciduitis lymphoplasmacytic infiltration

*Total placental weight.

deciduitis. These placental vascular abnormalities and inflammatory marks found in our study are consistent with what were reported previously (8, 11, 13, 14). Figure 1A shows representative H&E staining in control (a) and COVID placentas (b and c). H&E staining in COVID-exposed placentas clearly shows the features of fetal vascular malperfusion including avascular villi, vascular thrombi, and perivascular fibrin deposition in villous tissue from COVID-19 exposed placentas.

Detection of STING and IFNβ expression in villous tissue and fetal membrane

To determine if type I IFN pathway is activated in placentas exposed to maternal COVID-19 infection, we first examined cGAS, STING, and IFNβ expression. Our results showed that cGAS expression was neither detected in villous nor fetal membrane tissue sections in placentas with or without exposure to COVID-19 in pregnancy (data not shown). Surprisingly, abundant STING positive cells were detected in villous stroma in all placentas in the COVID group (Figure 1B, a). Stromal cells in chorionic mesoderm (CM) and decidual layer in fetal membrane also showed positive STING staining (Figure 1B, a1). STING expression was not detected in trophoblasts, including STs, CTs, and EVTs, in COVID-19-exposed placentas. Interestingly, strong IFNβ expression was detected in villous trophoblasts (STs, CTs) (Figure 1B, b) in COVID-19-exposed placentas. IFNβ signal was also detected in fetal membrane cells, including amnion epithelial cells, EVTs, stromal cells in chorionic mesoderm (CM) and decidual layer (Figure 1B, b1). These results suggest that STING and IFNβ expressing cells are cell type-specific at the placental maternal-fetal interface in response to maternal COVID-19 infection.

Hofbauer cells (placental macrophages) locate in villous stroma. To determine if the STING positive cells are Hofbauer cells, expression of CD68, CD16, and vimentin were determined in villous tissue sections. CD68 and CD16 are markers of macrophages, and vimentin is a marker of stromal mesenchymal cells. Figure 2 shows representative STING, CD68, CD16, and vimentin expression in villous tissue sections from active infection and COVID-19 recovered cases, and non-infected controls. Active infection was the placenta from pregnant women with positive detection of SARS-CoV-2 RNA in nasopharyngeal swab specimen when admitted to hospital for delivery. COVID-19 recovered was the placenta from women infected with COVID-19 during first or second trimester with negative detection of SARS-CoV-2 RNA when admitted to hospital for delivery. Non-infected control was a placenta from women never infected with COVID-19 before and during pregnancy. Abundant STING expressing cells are seen in villous stroma in placentas from COVID-19 infected cases (Figure 2, a1, b1), but not in non-COVID controls (Figure 2, c1). For CD68 and CD16 expression, only a few positive cells were detected in villous tissue sections from COVID-19-exposed and non-COVID placentas, CD68: Figure 2, a2, b2, and c2 and CD16: a3, b3, and c3, respectively. However, abundant vimentin positive cells were detected in villous stroma in all specimens

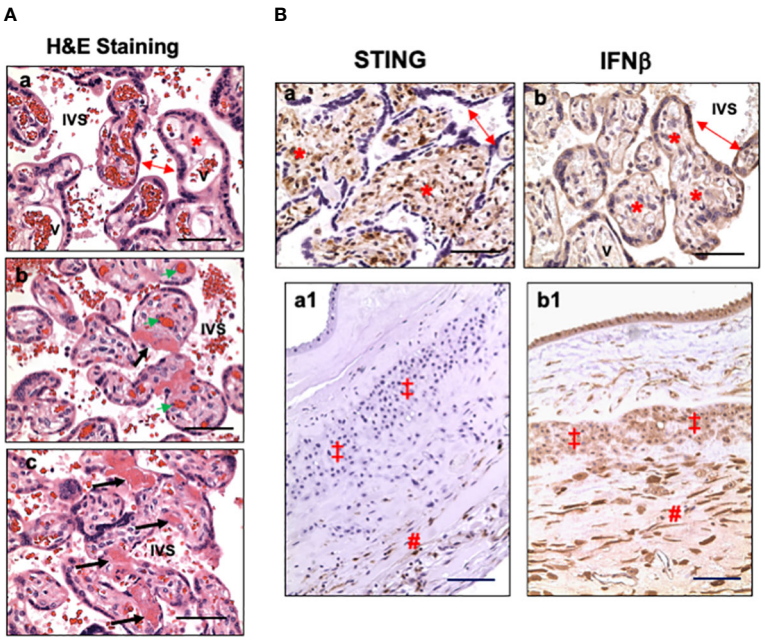


FIGURE 1
Representative villous tissue H&E staining and expression of STING and IFNβ in villous tissue and fetal membrane in placentas exposed to maternal COVID-19 infection. **(A)** Representative villous tissue H&E staining in COVID-exposed (b and c) placentas compared to non-COVID control (a) showing features of fetal vascular malperfusion including avascular villi, vascular thrombi, and perivascular fibrin deposition in villous tissue from COVID-19 exposed placentas. IVS: intervillous space; double arrow: STs; *: villous stroma; bold arrows: avascular villi and perivascular fibrin deposition; green arrow: fetal vessel thrombi. Bar = 50μm. **(B)** STING and IFNβ expression in villous tissue and fetal membrane in placentas exposed to maternal COVID-19 infection. a and b: villous tissue; a1 and b1: fetal membrane; a and a1: STING; and b and b1: IFNβ. In villous tissue: double arrow: STs; *: villous stroma. In fetal membrane: ‡: EVTs; #: decidua. Bar = 50μm in a and b; Bar = 100μm in a1 and b1.

regardless of COVID-19 infection status, Figure 2, a4, b4, and c4. These results demonstrate that STING positive cells may not be macrophages, but MSCs. These results also suggest that placental villous MSCs are activated in response to maternal COVID-19 infection.

Differential activation of type I IFN pathway molecules in villous tissue cells in placentas from women infected with COVID-19 in pregnancy

Figure 3A shows representative images of STING, IRF3, TLR7, MAVS, and IFNβ expression in villous tissue sections from COVID-19 exposed placentas compared to non-COVID controls. Again, abundant STING positive cells were detected in stromal cells and fetal endothelial cells in COVID-19 exposed placentas (Figure 3A, f and f1) vs. non-COVID controls (Figure 3A, a and a1). Interestingly, increased IRF3 expression was detected in CTs in COVID-19 exposed placentas (Figure 3A, g and g1) compared to that in non-COVID controls (Figure 3A, b and b1). STING and IRF3 expression were not detected in STs in COVID-19 exposed placentas. In contrast to STING and IRF3 expression, upregulation of TLR7 was seen in both STs, and CTs in COVID-19 exposed placentas (Figure 3A, h and h1) compared to non-COVID controls (Figure 3A, c and c1). Upregulation of TLR7 expression was also seen in stromal cells and fetal endothelial cells in COVID-19 exposed placentas (Figure 3A, h and h1). STING, IRF3, and TLR7 are all viral sensing molecules in type I IFN pathway. The findings of STING, IRF3, and TLR7 upregulation in different cell-types in villous tissue of COVID-19 exposed placentas suggest that cells at the placental maternal-fetal interface react differently in response to maternal COVID-19 infection.

MAVS plays a major role in antiviral defense mechanisms by coordinating and activating IFN pathway signaling. Our results showed that MAVS was expressed in STs and fetal endothelial cells in villous tissue of non-COVID control placentas (Figure 3A, d and d1). However, MAVS expression was robustly upregulated in all villous cells, including STs, CTs, stromal cells, and fetal endothelial cells in COVID-exposed placentas (Figure 3A, i and i1) compared to the controls (Figure 3A, d and d1). The observation of MAVS upregulation in all villous cells provides further evidence that mitochondria act as a platform and are actively involved in antiviral immunity against SARS-CoV-2 infection in cells at the maternal-fetal interface. Compared to non-COVID controls (Figure 3, e and e1), strong IFNβ expression was

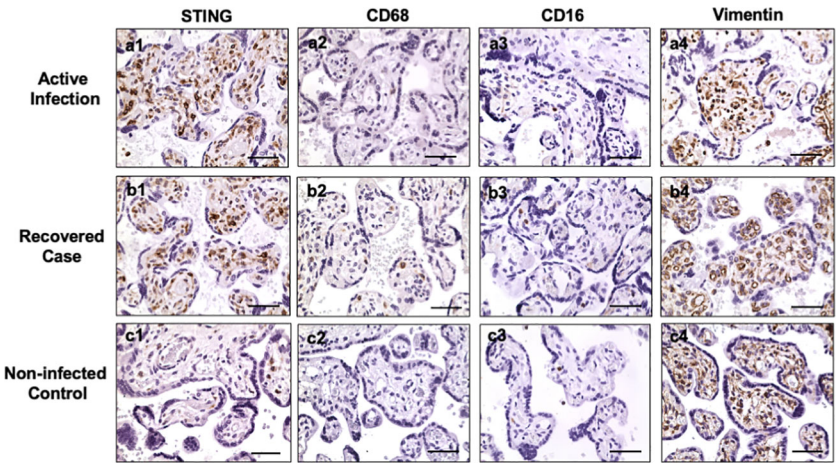


FIGURE 2
STING, CD68, CD16, and vimentin expression in villous tissue of placentas with or without exposure to maternal COVID-19 infection. Active infection: from placentas delivered by women with positive detection of SARS-COV-2 RNA when admitted to Labor and Delivery. Recovered case: from placentas delivered by women with positive detection of SARS-COV-2 RNA at second trimester and negative detection of SARS-COV-2 RNA when the patient was admitted to hospital for delivery. Non-infected control: from placenta delivered by women who was never infected with COVID-19 before and during pregnancy. STING is strongly expressed in villous stromal cells in both active infection (a1) and recovered (b1) cases, but only a few positive cells were seen in villous stromal in non-infected control (c1) placentas. Both CD68 and CD16 are markers for macrophages. Only a few positive CD68 and CD16 cells were detected in villous stromal in active (a2, a3), recovered (b2, b3), and control (c2, c3) placentas. Vimentin is a marker of mesenchymal cells. Vimentin positive cells were detected in villous stroma in all villous tissue examined: active infection (a4), recovered (b4), and non-COVID control (c4) placentas. These results indicate that STING positive cells are villous mesenchymal stromal cells (MSCs), not Hofbauer cells (macrophages), in placentas exposed to COVID infection. Bar = 50μm.

detected in placental STs and fetal endothelial cells in villous tissue in COVID-19 exposed placentas (Figure 3, j and j1), respectively.

Figure 3B shows relative expression of STING, IRF3, TLR7, MAVS, and IFNβ in villous sections from COVID-19 exposed placentas compared to non-COVID controls. Significant upregulation of STING, IRF3, TLR7, MAVS, and IFNβ expression was found in COVID-19 exposed placentas vs. controls ($p<0.01$ for STING, TLR7, MAVS, and IFNβ, and $p<0.05$ for IRF3).

Differential activation of type I IFN pathway molecules in fetal membrane cells in placentas from women infected with COVID-19 in pregnancy

We also examined STING, IRF3, TLR7, MAVS, and IFNβ expression in fetal membrane from non-COVID and COVID-exposed placentas. We found that differential upregulation of these antiviral molecules in fetal membrane cells are also present in COVID-exposed placentas. Figure 4 shows representative images of STING, IRF3, TLR7, MAVS, and IFNβ expression in non-COVID controls (Figure 4, a to e) and in COVID-exposed (Figure 4, f to j) fetal membranes, respectively. Compared to non-COVID controls, increased STING expression in chorionic mesoderm and decidual stromal cells, and upregulation of IRF3 in EVTs were observed in fetal membranes in COVID-exposed placentas. TLR7 expression was also upregulated in EVTs and decidual cells in COVID-exposed placentas. Although, MAVS expression did not show different in fetal membrane cells between non-COVID control and COVID-exposed placentas, upregulation of IFNβ expression was detected in EVTs and decidual cells in COVID-exposed in comparison to non-COVID control placentas.

Discussion

In the present study, we specifically examined expression of antiviral sensing molecules associated with activation of type I IFNs in placentas with or without maternal COVID-19 infection. Strikingly, we found that compared to non-COVID controls, antiviral sensing molecules including STING, IRF3, and TLR7 that link to type I IFN production are substantially upregulated with distinct cell type specific distribution at the maternal-fetal interface in COVID-exposed placentas, i.e., STING in villous and decidual MSCs; IRF3 in CTs and EVTs; and TLR7 in almost all three types of trophoblasts, fetal vessel endothelial cells, and decidual stromal cells.

STING activation in villous MSCs in COVID-19-exposed placentas is a novel finding in our study. Demonstration that STING expressing cells are MSCs, but not Hofbauer cells, is supported by the pattern of vimentin expressing cells in the villous stroma with no differences in CD68 and CD16 positive cells in both COVID-19 infected and non-infected placentas.

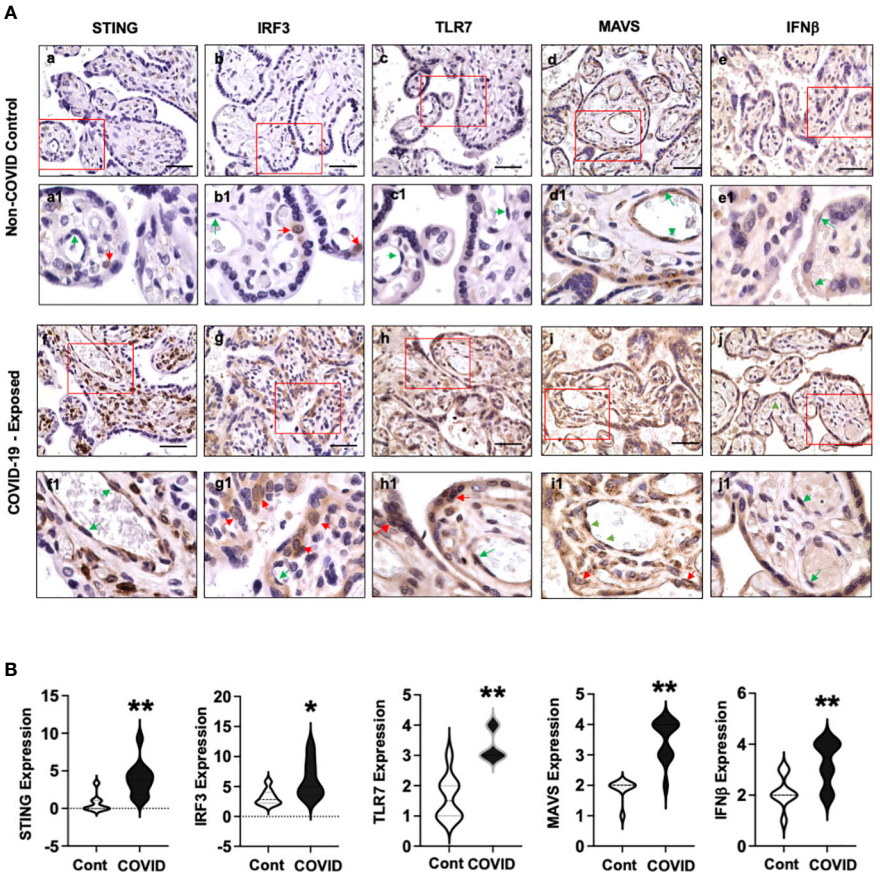


FIGURE 3
STING, IRF3, TLR7, MAVS, and IFNβ expression in villous tissue of placentas with or without exposure to maternal COVID-19 infection. **(A)** STING, IRF3, TLR7, MAVS, and IFNβ expression in villous tissues from placentas with or without exposure to maternal COVID-19 infection. Images a to e are representative images of STING, IRF3, TLR7, MAVS, and IFNβ expression in villous tissue sections in non-COVID control placentas, and images a1 to e1 show zoom of enlarged rectangle area in a to e of each, respectively. Images f to j are representative images of STING, IRF3, TLR7, MAVS, and IFNβ expression in villous tissue sections in COVID-exposed placentas, and images f1 to j1 show zoom of enlarged rectangle area in f to j of each, respectively. Bar = 50μm. Activation or upregulation of STING, IRF3, TLR7, MAVS, and IFNβ expression were found in different cell-types in COVID-exposed placental villous tissue compared to non-COVID controls: 1) strong STING expression signal in stromal cells and fetal endothelial cells; 2) activation of IRF3 in CTs; and 3) increased TLR7 expression in STs, CTs, and fetal endothelial cells; 4) upregulation of MAVS expression in STs, CTs, stromal cells, and fetal endothelial cells; and 5) increased IFNβ expression in STCs and fetal endothelial cells, respectively. Red arrow: CTs; Green arrow: fetal endothelial cells. **(B)** Violin graphs show that relative expression for STING, IRF3, TLR7, MAVS, and IFNβ in villous tissue sections are significantly increased in COVID-exposed placental villous tissue (COVID) vs. non-COVID controls (Cont), * $p<0.05$ and ** $p<0.01$, respectively.

There are number of biomarkers for macrophages, including CD14, CD16, CD64, CD68, CD71, and CD163, etc. Using CD68 as the marker for placental Hofbauer cells, Rebutini et al. studied the correlation of COVID-19 severity in pregnant women with placental morphologic features. Their results showed no difference in CD68 account in placentas between control and COVID-19 cases (13), which was consistent with ours. While using CD163 as the marker for macrophages, Sharps et al. did find increased CD163 positive cells in villous tissue following maternal COVID-19 infection (16). Increased placental macrophages was also reported in severe preeclampsia complicated by HELLP syndrome (28). It is possible that different subset of macrophages might be activated in the placenta in response to maternal COVID-19 infection and in placentas from various pregnancy complications, which warrant further investigation.

STING is an endoplasmic reticulum-associated membrane protein and can be activated by cGAS when cGAS recognizes cellular DNA in cytosol. cGAS-STING pathway plays critical roles in inducing type I IFN production and activating innate immune defense system in response to both DNA and RNA viral infection (21). Our results of undetectable cGAS expression in villous tissue and fetal membrane from COVID-19 placentas suggest that STING activation in villous and decidual stromal cells is cGAS-independent. In fact, cGAS-independent STING activation has been reported and considered as non-canonical activation of STING in cells after DNA damage (29). Stromal cells possess diverse immune regulatory capacities (30).

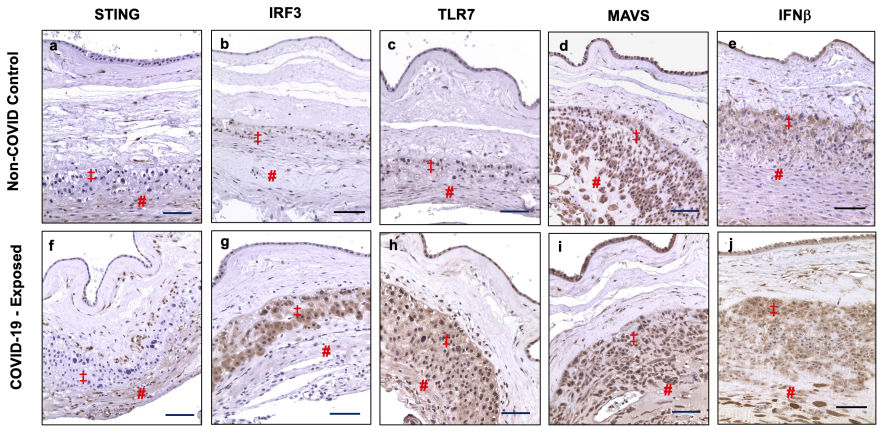


FIGURE 4
STING, IRF3, TLR7, MAVS, and IFNβ expression in fetal membrane of placentas with or without exposure to maternal COVID-19 infection. Images **a–e** show STING, IRF3, TLR7, MAVS, and IFNβ expression in fetal membrane from non-COVID control placentas, and images **f–j** show STING, IRF3, TLR7, MAVS, and IFNβ expression in fetal membrane from COVID-exposed placentas. Upregulation of IRF3 in EVTs, and increased STING, TLR7, and IFNβ expression in chorionic mesoderm and decidual stromal cells were detected in fetal membrane of COVID-exposed vs. non-COVID control placentas. Increased IFNβ expression was also noticed in EVTs in fetal membrane of COVID-exposed placentas. ‡: EVTs and # decidual cells. Bar = 100μm.

Although villous stromal cells do not directly contact to maternal components that circulate in placental intervillous space, the finding of STING activation in villous stromal cells suggests that these cells are activated in response to maternal SARS-CoV-2 infection, which could be a feature of antiviral defense network at the placental maternal-fetal interface.

Another important finding is increased IRF3 levels in villous CTs and chorion EVTs in COVID-19 exposed placentas. IRF3 is a member of the interferon regulatory transcription factor (IRF) family. IRF3 activation could lead to type I IFN production in cells respond to viral infection (31). EVTs or invasive trophoblasts are trophoblasts residing outside of villi, which can be found in chorion, cell columns, basal plate, and decidua basalis. These cells directly contact maternal cells, including decidual cells, macrophages, dendritic cells, and T cells, etc. Currently, little is known about specific immune function of EVTs in viral infection, the finding of IRF3 activation in chorion EVTs suggests that EVTs may play vital roles at the boundary of EVTs and maternal decidual cells against COVID infection. Further study is needed to define the function of EVTs in the host innate immune system.

Elevated TLR7 positivity was noticed almost in all types of cells in villous tissue and fetal membrane, including STs, CTs, EVTs, fetal endothelial cells, amnion epithelial cells, and maternal decidual cells. It is known that among the TLR family members, TLR7 and TLR8 are recognized as sensors to ssRNA viruses (32) and SARS-CoV-2 genome contains a large number of fragments that can be recognized by TLR7/8 (24). TLR7/8 are X-linked genes. It was reported that X-linked recessive TLR7 deficiency was a highly penetrant genetic etiology of critical COVID-19 pneumonia (33, 34) and deficient TLR7 gene was associated with severity of SARS-CoV-2 infection in young male patients (35). Further study needs to determine if TLR7 gene deficiency in placenta or fetus is associated with vertical transmission of SARS-CoV-2 in pregnancy. It is worth to note that upregulation of TLR7 expression was also observed in villous core fetal endothelial cells in COVID-exposed placentas. Activation of TLR receptors has been linked to endothelial dysfunction in various cardiovascular diseases, such as atherosclerosis, hypertension, and ischemic injury (36). Although endothelial cells are not considered as classical immune cells, they are actively involved in inflammatory responses to various stimuli. Increased TLR7 expression seen in fetal endothelial cells could be a sign of fetal vascular response to maternal COVID infection. Whether TLR7 upregulation contributes to fetal endothelial cell dysfunction warrants further investigation. Nonetheless, upregulation of TLR7 expression in cells at the maternal-fetal interface indicates that TLR7 plays an important role in response to maternal COVID-19 infection.

MAVS is an adaptor protein that locates in multiple intracellular membranous compartments including mitochondria, peroxisomes, and endoplasmic reticulum (37). MAVS is also known as IFN-β promoter stimulator I (IPS-1) or virus induced signaling adaptor (VISA) (38). It is activated when pattern recognition receptors, such as retinoic acid-inducible gene I (RIG-I)-like receptors and melanoma differentiation-associated gene 5 (MDA5), detect the presence of viruses within cells. Aggregated MAVS activates a series of cellular responses which directly induce type I IFN production. Upregulation of MAVS expression in villous STs in COVID-exposed placentas indicates that MAVS could be a key antiviral

sensing molecule in STs. Moreover, the finding of strong MAVS signals in fetal membrane cells in both control and COVID-exposed placentas also suggests that MAVS may play a dominant antiviral role in EVTs at the maternal decidual boundary.

Increased STING, IRF3, TLR7, and MAVS expression directly link to IFN activation in cells at the maternal-fetal interface in COVID-exposed placentas. This notion is supported by the finding of strong IFNβ (a type I IFN) expression in villous STs and in EVTs and maternal decidual cells in fetal membrane in COVID-exposed placentas. IFN response is considered a first line of defense against viral infection because it promotes virus clearance, induces tissue repair, and triggers a prolonged adaptive immune response against viruses (39). Type I IFN family has several members, including IFNα, IFNβ, IFNε, IFNω, and IFNv. IFNα and IFNβ are major type I IFNs. Humans produce 13 IFNα and 2 IFNβ. We evaluated IFNβ1 expression, and our results showed that IFNβ1 expression was robustly upregulated especially in STs and maternal decidual cells in COVID-exposed placentas, which indicates activation of IFNβ1 in cells at the maternal-fetal interface. IFN signaling is a main driver of the antiviral defense. Therefore, our findings support the notion that activation of type I IFN signaling pathway is a pivotal antiviral defense mechanism at the maternal-fetal interface against SARS-CoV-2 infection.

In addition, we did notice that placental weight was significantly less in the COVID group than in the control group (Table 1). Our data also showed that newborn weight was correlated with placental weight (Supplemental Figure 2). As mentioned early that abnormal vascular development and hyper-inflammatory status in the placenta are associated with maternal COVID-19 infection. There is no doubt that COVID-19 infection during pregnancy has significant impact on placental vascular development, which may account to low birth weight in COVID cases. Whether type I IFN upregulation plays a role in aberrant placental vasculature development warrants further investigation.

There are some limitations in our study. This is a retrospective specimen analysis using archived placental tissues. All placentas in the COVID-19 group are from Africa American women. This disproportionate COVID-19 infection population represents the demographic and ethnic disparities in the Shreveport community. Although the sample size is small and the intensity of immunostaining in fetal membrane is not quantified, the staining results are consistent showing distinct cell-type specific upregulation of the markers tested in the COVID group. Since SARS-CoV-2 antibody test was not the standard of care and no maternal and fetal blood specimen were preserved, viral load and maternal/fetal antibody (IgG and IgM) levels were not available to these subjects. Therefore, whether activation of antiviral IFN signaling pathway at the maternal-fetal interface correlates with maternal antibody levels or transplacental antibody transfer are not known. It is also unknown if maternal type I IFN levels affect IFN signaling pathway activation at the maternal-fetal interface in placentas exposed to CIVID-19 infection.

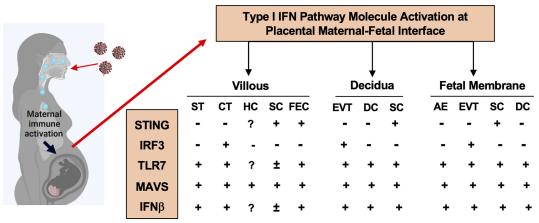


FIGURE 5
A summary of type I IFN pathway molecule activation in different cell types at the maternal-fetal interface in placentas from women infected with COVID-19 in pregnancy. ST, Syncytiotrophoblasts; CT, cytotrophoblasts; HC, Hofbauer cells; SC, stromal cells; FEC, fetal endothelial cells; DC, decidual cells; AE, amnion epithelial cells; EVT, extra-villous trophoblasts, respectively.

Conclusion

In the present study, we identified distinct cell-type specific sensing and activation of type I IFN pathway molecules at the maternal-fetal interface in placentas exposed to maternal COVID-19 infection. As summarized in Figure 5, STING in villous and decidual MSCs; IRF3 in CTs and EVTs; and MAVS, and TLR7 in STs. Upregulation of MAVS and TLR7 was also seen in fetal endothelial cells. These findings highlight that type I IFN signaling pathway is an important antiviral defense network at the maternal-fetal interface in the course of SARS-CoV-2 infection in pregnancy. Our data also suggest that the placenta has a well-defined innate antiviral defense system to limit and eradicate SARS-CoV-2 infection, which could, in part, explain why vertical transmission of SARS-CoV-2 is rare in pregnancy.

Data availability statement

The original contributions presented in the study are included in the article/Supplementary Material. Further inquiries can be directed to the corresponding author.

Ethics statement

The studies involving human participants were reviewed and approved by Institutional Review Board (IRB) at Louisiana State University Health Sciences Center - Shreveport approved the

study entitled "Effects of SARS-CoV-2 infection in women during pregnancy on maternal and fetal outcomes and placental pathology" on 04/30/2021. The IRB ID number is STUDY00001744. Written informed consent for participation was not required for this study in accordance with the national legislation and the institutional requirements.

Author contributions

YW, YG, DL, XG: study design. YW, YG, XG, KB, CL, MH, CB, DC: specimen process, analysis, data interpretation. YW, DL, RS, CM, PB: drafting and revising manuscript. All authors contributed to the article and approved the submitted version.

Funding

This study was supported in part by COVID-19 Intramural funding - LSUHSC Grant-in-Aid Award and National Institute of Health R21 AI169392-01 to YW.

Conflict of interest

The authors declare that the research was conducted in the absence of any commercial or financial relationships that could be construed as a potential conflict of interest.

Publisher's note

All claims expressed in this article are solely those of the authors and do not necessarily represent those of their affiliated organizations, or those of the publisher, the editors and the reviewers. Any product that may be evaluated in this article, or claim that may be made by its manufacturer, is not guaranteed or endorsed by the publisher.

Supplementary material

The Supplementary Material for this article can be found online at: https://www.frontiersin.org/articles/10.3389/fendo.2022.951388/full#supplementary-material

References

1. Villar J, Ariff S, Gunier RB, Thiruvengadam R, Rauch S, Kholin A, et al. Maternal and neonatal morbidity and mortality among pregnant women with and without COVID-19 infection: The INTERCOVID multinational cohort study. *JAMA Pediatr* (2021) 175(8):817–26. doi: 10.1001/jamapediatrics.2021.1050

2. Narang K, Enninga EAL, Gunaratne MDSK, Ibirogba ER, Trad ATA, Elrefaei A, et al. SARS-CoV-2 infection and COVID-19 during pregnancy: A multidisciplinary review. *Mayo Clin Proc* (2020) 95:1750–65. doi: 10.1016/j.mayocp.2020.05.011

3. Wei SQ, Bilodeau-Bertrand M, Liu S, Auger N. The impact of COVID-19 on pregnancy outcomes: A systematic review and meta-analysis. *CMAJ* (2021) 193: E540–48. doi: 10.1503/cmaj.202604

4. Varma P, Lybrand ZR, Antopia MC, Hsieh J. Novel targets of SARS-CoV-2 spike protein in human fetal brain development suggest early pregnancy vulnerability. *Front Neurosci* (2021) 14:614680. doi: 10.3389/fnins.2020.614680

5. Alzamora MC, Paredes T, Caceres D, Webb CM, Valdez LM, La Rosa M. Severe COVID-19 during pregnancy and possible vertical transmission. *Am J Perinatol* (2020) 37:861–5. doi: 10.1055/s-0040-1710050

6. Dong L, Tian J, He S, Zhu C, Wang J, Liu C, et al. Possible vertical transmission of SARS-CoV-2 from an infected mother to her newborn. *JAMA* (2020) 323:1846–8. doi: 10.1001/jama.2020.4621

7. Fenizia C, Biasin M, Cetin I, Vergani P, Mileto D, Spinillo A, et al. Analysis of SARS-CoV-2 vertical transmission during pregnancy. *Nat Commun* (2020) 11:5128. doi: 10.1038/s41467-020-18933-4

8. Hosier H, Farhadian SF, Morotti RA, Deshmukh U, Lu-Culligan A, Campbell KH, et al. SARS-CoV-2 infection of the placenta. *J Clin Invest* (2020) 130:4947–53. doi: 10.1172/JCI139569

9. Facchetti F, Bugatti M, Drera E, Tripodo C, Sartori E, Cancila V, et al. SARS-CoV2 vertical transmission with adverse effects on the newborn revealed through integrated immunohistochemical, electron microscopy and molecular analyses of placenta. *EBioMedicine* (2020) 59:102951. doi: 10.1016/j.ebiom.2020.102951

10. Hsu AL, Guan M, Johannesen E, Stephens AJ, Khaleel N, Kagan N, et al. Placental SARS-CoV-2 in a pregnant woman with mild COVID-19 disease. *J Med Virol* (2021) 93:1038–44. doi: 10.1002/jmv.26386

11. Hecht JL, Quade B, Deshpande V, Mino-Kenudson M, Ting DT, Desai N, et al. SARS-CoV-2 can infect the placenta and is not associated with specific placental histopathology: A series of 19 placentas from COVID-19-positive mothers. *Mod Pathol* (2020) 33:2092–103. doi: 10.1038/s41379-020-0639-4

12. Sharps MC, Hayes DJL, Lee S, Zou Z, Brady CA, Almoghrabi Y, et al. A structured review of placental morphology and histopathological lesions associated with SARS-CoV-2 infection. *Placenta* (2020) 101:13–29. doi: 10.1016/j.placenta.2020.08.018

13. Rebutini PZ, Zanchettin AC, Stonoga ETS, Prá DMM, de Oliveira ALP, Dezidério FDS, et al. Association between COVID-19 pregnant women symptoms severity and placental morphologic features. *Front Immunol* (2021) 12:685919. doi: 10.3389/fimmu.2021.685919

14. Shanes ED, Mithal LB, Otero S, Azad HA, Miller ES, Goldstein JA. Placental pathology in COVID-19. *Am J Clin Pathol* (2020) 154:23–32. doi: 10.1093/ajcp/aqaa089

15. Arora N, Sadovsky Y, Dermody TS, Coyne CB. Microbial Vertical Transmission during Human Pregnancy. *Cell Host Microbe*. (2017) 21:561–7. doi: 10.1016/j.chom.2017.04.007

16. Sharps MC, Garrod A, Aneni E, Jones CJP, Batra G, Heazell AEP. Placental macrophages following maternal SARS-CoV-2 infection in relation to placental pathology. *Front Virol* (2022) 2:813312. doi: 10.3389/fviro.2022.813312

17. Sadler AJ, Williams BR. Interferon-inducible antiviral effectors. *Nat Rev Immunol* (2008) 8:559–68. doi: 10.1038/nri2314

18. Hadjadj J, Yatim N, Barnabei L, Corneau A, Boussier J, Smith N, et al. Impaired type I interferon activity and inflammatory responses in severe COVID-19 patients. *Science* (2020) 369:718–24. doi: 10.1126/science.abc6027

19. Zhang Q, Bastard P, Liu Z, Le Pen J, Moncada-Velez M, Chen J, et al. Inborn errors of type I IFN immunity in patients with life-threatening COVID-19. *Science* (2020) 370:eabd4570. doi: 10.1126/science.abd4570

20. Lu-Culligan A, Chavan AR, Vijayakumar P, Irshaid L, Courchaine EM, Milano KM, et al. Maternal respiratory SARS-CoV-2 infection in pregnancy is associated with a robust inflammatory response at the maternal-fetal interface. *Med (N Y)* (2021) 2:591–610.e510. doi: 10.1016/j.medj.2021.04.016

21. Ishikawa H, Barber GN. STING is an endoplasmic reticulum adaptor that facilitates innate immune signalling. *Nature* (2008) 455:674–8. doi: 10.1038/nature07317

22. Liu S, Cai X, Wu J, Cong Q, Chen X, Li T, et al. Phosphorylation of innate immune adaptor proteins MAVS, STING, and TRIF induces IRF3 activation. *Science* (2015) 347:aaa2630. doi: 10.1126/science.aaa2630

23. Diebold SS, Kaisho T, Hemmi H, Akira S, Reis e Sousa C. Innate antiviral responses by means of TLR7-mediated recognition of single-stranded RNA. *Science* (2004) 303:1529–31. doi: 10.1126/science.1093616

24. Moreno-Eutimio MA, López-Macías C, Pastelin-Palacios R. Bioinformatic analysis and identification of single-stranded RNA sequences recognized by TLR7/8 in the SARS-CoV-2, SARS-CoV, and MERS-CoV genomes. *Microbes Infect* (2020) 22:226–9. doi: 10.1016/j.micinf.2020.04.009

25. *Clinical spectrum of SARS-CoV-2 infection. NIH COVID-19 treatment guidelines* (2021). Available at: https://www.covid19treatmentguidelines.nih.gov/overview/clinical-spectrum/.

26. Seyed Jafari SM, Hunger RE. IHC optical density score: A new practical method for quantitative immunohistochemistry image analysis. *Appl Immunohistochem Mol Morphol* (2017) 25:e12–3. doi: 10.1097/PAI.0000000000000370

27. Lockwood CJ, Yen CF, Basar M, Kayisli UA, Martel M, Buhimschi I, et al. Preeclampsia-related inflammatory cytokines regulate interleukin-6 expression in human decidual cells. *Am J Pathol* (2008) 172:1571–9. doi: 10.2353/ajpath.2008.070629

28. Evsen MS, Kalkanli S, Deveci E, Sak ME, Ozler A, Baran O, et al. Human placental macrophages (Hofbauer cells) in severe preeclampsia complicated by HELLP syndrome: Immunohistochemistry of chorionic villi. *Anal Quant Cytopathol Histpathol* (2013) 35:283–8.

29. Unterholzner L, Dunphy G. cGAS-independent STING activation in response to DNA damage. *Mol Cell Oncol* (2019) 6:1558682. doi: 10.1080/23723556.2018.1558682

30. Hoogduijin MJ. Are mesenchymal stromal cells immune cells? *Arthritis Res Ther* (2015) 17:88. doi: 10.1186/s13075-015-0596-3

31. Collins SE, Noyce RS, Mossman KL. Innate cellular response to virus particle entry requires IRF3 but not virus replication. *J Virol* (2004) 78:1706–17. doi: 10.1128/jvi.78.4.1706-1717.2004

32. Crozat K, Beutler B. TLR7: A new sensor of viral infection. *Proc Natl Acad Sci U.S.A.* (2004) 101:6835–6. doi: 10.1073/pnas.0401347101

33. Asano T, Boisson B, Onodi F, Matuozzo D, Moncada-Velez M, Maglorius Renkilaraj MRL, et al. X-Linked recessive TLR7 deficiency in ~1% of men under 60 years old with life-threatening COVID-19. *Sci Immunol* (2021) 6:eabl4348. doi: 10.1126/sciimmunol.abl4348

34. Fallerini C, Daga S, Mantovani S, Benetti E, Picchiotti N, Francisci D, et al. Association of toll-like receptor 7 variants with life-threatening COVID-19 disease in males: Findings from a nested case-control study. *Elife* (2021) 10:e67569. doi: 10.7554/eLife.67569

35. van der Made CI, Simons A, Schuurs-Hoeijmakers J, van den Heuvel G, Mantere T, Kersten S, et al. Presence of genetic variants among young men with severe COVID-19. *JAMA* (2020) 324:663–73. doi: 10.1001/jama.2020.13719

36. Salvador B, Arranz A, Francisco S Córdoba L, Punzón C, Llamas MÁ, Fresno M. Modulation of endothelial function by toll like receptors. *Pharmacol Res* (2016) 108:46–56. doi: 10.1016/j.phrs.2016.03.038

37. Vazquez C, Beachboard DC, Horner SM. Methods to visualize MAVS subcellular localization. *Methods Mol Biol* (2017) 1656:131–42. doi: 10.1007/978-1-4939-7237-1_7

38. Vazquez C, Horner SM. MAVS coordination of antiviral innate immunity. *J Virol* (2015) 89:6974–7. doi: 10.1128/JVI.01918-14

39. Ribero MS, Jouvenet N, Dreux M, Nisole S. Interplay between SARS-CoV-2 and the type I interferon response. *PloS Pathog* (2020) 16:e1008737. doi: 10.1371/journal.ppat.1008737

frontiers | Frontiers in Endocrinology

TYPE Review
PUBLISHED 31 January 2023
DOI 10.3389/fendo.2023.1107182

Check for updates

OPEN ACCESS

EDITED BY
Mariana Farina,
Centro de Estudios Farmacológicos y Botánicos (CEFYBO) (CONICET), Argentina

REVIEWED BY
Julieta Aisemberg,
Centro de Estudios Farmacológicos y Botánicos (CEFYBO) (CONICET), Argentina
Felipe Vadillo-Ortega,
Faculty of Medicine, National Autonomous University of Mexico, Mexico

*CORRESPONDENCE
Songying Zhang
zhangsongying@zju.edu.cn
Haiyan Zhu
haiyan@zju.edu.cn

SPECIALTY SECTION
This article was submitted to Developmental Endocrinology, a section of the journal Frontiers in Endocrinology

RECEIVED 24 November 2022
ACCEPTED 20 January 2023
PUBLISHED 31 January 2023

CITATION
Zhou H, Zhao C, Wang P, Yang W, Zhu H and Zhang S (2023) Regulators involved in trophoblast syncytialization in the placenta of intrauterine growth restriction. *Front. Endocrinol.* 14:1107182. doi: 10.3389/fendo.2023.1107182

COPYRIGHT
© 2023 Zhou, Zhao, Wang, Yang, Zhu and Zhang. This is an open-access article distributed under the terms of the Creative Commons Attribution License (CC BY). The use, distribution or reproduction in other forums is permitted, provided the original author(s) and the copyright owner(s) are credited and that the original publication in this journal is cited, in accordance with accepted academic practice. No use, distribution or reproduction is permitted which does not comply with these terms.

Regulators involved in trophoblast syncytialization in the placenta of intrauterine growth restriction

Hanjing Zhou[1,2], Chenqiong Zhao[1,2], Peixin Wang[1,2], Weijie Yang[1,2], Haiyan Zhu[1,2]* and Songying Zhang[1,2]*

[1]Assisted Reproduction Unit, Department of Obstetrics and Gynecology, Sir Run Run Shaw Hospital, School of Medicine, Zhejiang University, Hangzhou, China, [2]Key Laboratory of Reproductive Dysfunction Management of Zhejiang Province, Hangzhou, China

Placental dysfunction refers to the insufficiency of placental perfusion and chronic hypoxia during early pregnancy, which impairs placental function and causes inadequate supply of oxygen and nutrients to the fetus, affecting fetal development and health. Fetal intrauterine growth restriction, one of the most common outcomes of pregnancy-induced hypertensions, can be caused by placental dysfunction, resulting from deficient trophoblast syncytialization, inadequate trophoblast invasion and impaired vascular remodeling. During placental development, cytotrophoblasts fuse to form a multinucleated syncytia barrier, which supplies oxygen and nutrients to meet the metabolic demands for fetal growth. A reduction in the cell fusion index and the number of nuclei in the syncytiotrophoblast are found in the placentas of pregnancies complicated by IUGR, suggesting that the occurrence of IUGR may be related to inadequate trophoblast syncytialization. During the multiple processes of trophoblasts syncytialization, specific proteins and several signaling pathways are involved in coordinating these events and regulating placental function. In addition, epigenetic modifications, cell metabolism, senescence, and autophagy are also involved. Study findings have indicated several abnormally expressed syncytialization-related proteins and signaling pathways in the placentas of pregnancies complicated by IUGR, suggesting that these elements may play a crucial role in the occurrence of IUGR. In this review, we discuss the regulators of trophoblast syncytialization and their abnormal expression in the placentas of pregnancies complicated by IUGR.

KEYWORDS

intrauterine growth restriction, trophoblast, syncytialization, signaling pathway, epigenetic modification, metabolism, senescence, autophagy

Introduction

Small for gestational age (SGA) refers to new-borns whose birth weight is below the 10th percentile for gestational age (1). A pregnancy in which an SGA fetus that cannot reach its genetically determined growth potential at any gestational age is diagnosed with IUGR (2). According to the literature, fetal IUGR occurs in 4% to 7% of global live births each year and occurs either alone or accompanied by pre-eclampsia (PE) or syndrome hemolytic anemia (HELLP) (3, 4). IUGR is the second leading cause of perinatal mortality (5). IUGR not only increases the incidence of fetal distress, premature delivery, and stillbirth, but also significantly increases the risk of various neurological and respiratory diseases in newborns (6, 7). Moreover, the incidence of cognitive impairment in childhood and the risk of heart disease, hypertension, and type 2 diabetes in adulthood are also increased (8–10).

Fetal growth is a continuous process in which cells, tissues, and organs differentiate and undergo maturation. During this process, the transport of primary nutrients, such as glucose, amino acids, and lipids, is essential for the development of a healthy baby (11). The placenta not only maintains the pregnant state and protects the embryo from infection, but also promotes the exchange of nutrients, gases, and waste products so that the embryo can safely survive and grow in a healthy intrauterine environment (12). In pregnancies complicated by placental dysfunction, oxygen and nutrient supply is inadequate to meet the metabolic demand of the growing fetus. This condition may lead to fetal growth restriction and fetal hypoxia, and in severe cases, irreversible ischemic organ damage and intrauterine fetal death may occur (13). Recent study findings suggested that insufficient placental nutrition transport during hypertensive pregnancy impairs fetal growth by decreasing placental protein O-GlcNAcylation (11). The proper functioning of the placenta depends on the integrity of its structure, which involves trophoblasts, immune cells and other placental cells proliferating, differentiating, and undergoing apoptosis at proper rates and in a balanced state. Unlike other placental cells, cytotrophoblasts (CTBs) have a tendency to fuse during pregnancy, which promotes the form of a multinucleated syncytial barrier that constitutes the interface between the maternal and fetal circulation and has the main function of transporting gases, nutrients and wastes between the fetus and the mother. On the other hand, extravillous trophoblasts (EVTs) invade the decidua and arterial vessels to participate in vascular remodeling. In hypertensive pregnancies, dysfunctional placentas showed a deregulation of cell fusion in the formation of the syncytiotrophoblast (STB) and increased apoptosis (14). In addition, the shallow invasion of trophoblasts and incomplete remodeling of the uterine arteries reduced vessel pulsatility, preventing placentas from achieving a steady blood flow to ensure the perfusion of the intervillous space and adequate transit time for exchange (15). In humans, placental tissues from pregnancies complicated by PE showed a lower STB/CTB ratio than normal placentas (16). Similarly, placental tissues from pregnancies complicated by IUGR showed evidence of placental underdevelopment, including villous hypermaturity and distal villous hypoplasia (17). Moreover, primary CTBs isolated from placentas of PE and IUGR pregnancies showed evidence of impaired syncytialization compared to those from normal pregnancies (18). During the multiple processes of trophoblast syncytialization, specific proteins and several signaling pathways are involved in coordinating these events and regulating placental function. It has been reported that cytokines and growth factors act on different signaling pathways to produce a series of cascade effects and to induce the expression of downstream molecules to regulate the syncytialization of trophoblasts (19). In this article, we discuss the relationships between abnormal trophoblast syncytialization and IUGR caused by placental dysfunction.

The etiology of IUGR

IUGR and PE are two different but clinically relevant pregnancy disorders attributed to an inadequate depth of trophoblast invasion into the maternal endometrium (20). At present, the causes of approximately one-third of IUGR cases including genetic factors, placental dysfunction and maternal influences. The remaining cases of IUGR are classified as idiopathic (21, 22). Although the causes are ambiguous, most of them are frequently associated with placental perfusion insufficiency. In patients with idiopathic IUGR, the placentas are smaller in size, the proliferation of trophoblasts is reduced, and the structures of placental villi are shortened. Interestingly, pathological results show that these small placentas are ischemic, indicating inadequate invasion of trophoblasts into the placental bed and deficient remodeling of the uterine spiral arteries, which eventually leads to chronic placental hypoxia (23, 24).

The development of the placenta depends on the balance of trophoblast proliferation, differentiation, and apoptosis. As with tumor cells, trophoblasts also have the ability to migrate into and invade the endometrium with strict biological regulation (25). On the 12th day after fertilization, CTBs invade STB columns to form primary villi. Approximately 10 days later, the chorionic trophoblasts in contact with maternal decidua differentiate into interstitial cytotrophoblasts (iCTBs) and endovascular cytotrophoblasts (eCTBs). iCTBs then invade the decidual matrix to control the depth of placental implantation and establish contact with decidual matrix cells, giant cells, and uterine natural killer (uNK) cells to accelerate the apoptosis of smooth muscle cells and the degradation of elastin (26–28). The latter passes through arterial walls and replaces vascular endothelial cells to participate in uterine spiral artery remodeling (26). This process changes the state of placental blood vessels from a high-resistance and low-flow state in early pregnancy to a low-resistance and high-volume state in subsequent pregnancy stages, thus improving placental perfusion and promoting villous microvascular formation to ensure sufficient material exchange between the mother and fetus (29). Although the existence of a low oxygen environment in the first trimester of pregnancy is essential to protect the fetus from injury due to excessive oxidative stress, persistently low perfusion with hypoxia can result in the development of pregnancy complications (30). Doppler ultrasound detected increased resistance of uterine spiral arteries in placentas from pregnancies complicated by PE or IUGR (31, 32). Interestingly, the clinical outcomes depend on the number of arteries involved and the extent of arterial involvement in remodeling in these pregnancies (33, 34).

To date, most scholars believe that the reduced migration and survivability of trophoblasts may be a key feature leading to IUGR. However, changes in other trophoblast cell behaviors can also lead to IUGR. In early pregnancy, placental CTBs proliferate and fuse to form a multinucleated syncytial barrier that mediates immune tolerance, steroid and peptide hormone synthesis, nutrient and gas exchange, and waste product removal between the mother and fetus. Apoptosis occurs throughout placental development, which causes senescent

trophoblasts or damaged syncytia to be continuously released into the maternal circulation in the form of fragments or vesicles; this process is called syncytial deportation (35). In normal placentas, the formation and deportation of the syncytial barrier are in equilibrium. Nevertheless, as fetal growth is closely correlated with the nutrient supply mediated by the syncytium, the imbalance between trophoblast syncytialization and syncytial deportation could lead to nutrient deficiency and eventually cause pathologies such as PE, fetal IUGR, and embryonic death (36, 37). It has been reported that placentas from patients with pregnancies complicated by IUGR showed a reduced fusion index, which was calculated as "the ratio of the number of nuclei in the syncytia divided by the total number of nuclei", where the syncytium was defined as at least three nuclei surrounded by a cell membrane (38, 39). In addition, studies have also shown that the proportion of syncytial deportation to the maternal circulation increased, while the expression of the fusion protein syncytin-1, which mediates syncytia formation, was reduced in placentas from pregnancies complicated by PE and IUGR (35). Furthermore, cultured CTBs from pregnancies complicated by PE and HELLP-associated IUGR were correlated with a pronounced lower cell fusion index, human chorionic gonadotropin beta (β-hCG) secretion, *syncytin* gene expression, and a significantly higher apoptosis rate (14). The above findings suggest that the occurrence of IUGR may be related to insufficient syncytialization of trophoblasts (14, 40).

Trophoblast syncytialization

Cell fusion processes occurring in a variety of biological contexts share many steps that are tightly regulated in space and time. Trophoblast cell fusion is mainly divided into three steps, in which a variety of proteins are involved and function in a space- and time-regulated manner (41, 42). For example, the first stage (competence stage) involves cell morphological changes with proliferative activity loss. The second stage (commitment stage) is characterized by cell adhesion and communication processes that lead to the activation, expression, exposure or assembly of the fusogenic machinery. In this stage, adherens junctions, tight junctions and gap junctions trigger the commitment of primary cells, followed by their fusion (39). The final stage (cell-cell fusion stage) is defined by the merging of two plasma membranes and the mixing of cellular contents (43) (see Figure 1).

In placentas, the process in which CTBs break down cell boundaries, and gradually fuse into a multinucleated STB layer is called trophoblast syncytialization (44). Under the physiological conditions of pregnancy, syncytialization is divided into two stages. The first stage begins on the 7th day and lasts until the 11th day after fertilization. During this phase, trophoblasts make contact with the maternal endometrium and begin to differentiate into STB. Then, STB fuse and lose their cell boundaries to form a multinucleated structure called the primitive syncytium, which facilitates the implantation of the embryo into the maternal endometrium (39, 45). After blastocysts are completely implanted, the fusion between STB ceases, while the proliferation of CTBs continues (39). The second stage begins on the 12th day after fertilization. As the pregnancy progresses, the surface area of the villi is expanded and regenerated, which depends on the continuous fusion of CTBs. This stage continues until delivery (45). These two syncytialization stages involve two different types of trophoblasts, and the processes involved in these two stages may be regulated by different mechanisms (45). The first stage of syncytialization occurs after early apoptosis. A series of apoptotic cascades cause negatively charged phosphatidylserines to accumulate in the outside of the cell membrane, which is a prerequisite for the

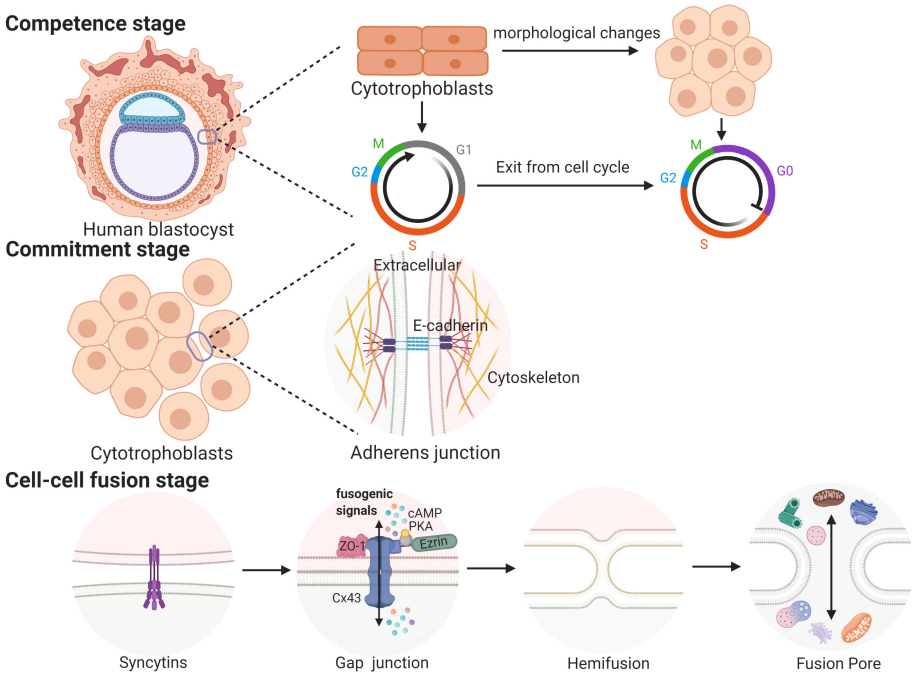


FIGURE 1
The three stages of trophoblast syncytialization.

fusion of trophoblasts (46, 47). However, it is not clear whether these processes of apoptosis or differentiation are the same prior to cell fusion because the initial stages of these two processes depend on the same molecular mechanism (48, 49). During the second stage of syncytialization, when the CTBs begin to fuse into the STB layer, the apoptotic cascade is immediately suppressed by high levels of apoptosis suppressors, such as MCL-1 and BCL-2. After the fusion is completed, the apoptotic cascade is restarted; this induces syncytial knots to be released into the maternal circulation (48). The result of syncytialization is the creation of a complete epithelial-like barrier covering the surface of all villi. The STB layer is supplied by the mother's blood and transports oxygen and nutrients to the developing fetus. As a barrier between the mother and the fetus, the STB layer protects the fetus from attack by pathogens and the mother's immune system. In addition, the STB can also secrete a large number of hormones, including β-hCG; the presence of this hormone provides the basis of one of the diagnostic criteria used to confirm early pregnancy (45).

Syncytialization-related proteins

A multitude of proteins are strictly regulated to participate in cell fusion *via* appropriate mechanisms at the correct place at the right time [reviewed in (39)]. For example, the first stage involves hCG, which has the capacity to induce cell differentiation and the formation of the syncytia. The second stage involves certain gap junction proteins, including connexins, that enhance cellular communication by forming intercellular channels (50). In addition, the expression levels of several cell adhesion molecules, including cadherins and zonula occludens-1 (ZO-1), are altered during the trophoblast syncytialization process. In the final stage, fusogenic proteins (syncytin-1 and syncytin-2), along with their transcription factor (glial cell missing 1 (GCM1)), play a crucial role in trophoblast syncytialization (51). Furthermore, 11β-hydroxysteroid dehydrogenase 2 (11β-HSD2) can convert cortisol into inactive metabolites and is also regarded as a biochemical marker of syncytialization (52).

hCG

During the early stages of pregnancy, hCG is secreted by embryonic trophoblasts. In contrast, during the latter phases of pregnancy, hCG is produced by the STB layer (39). hCG is a heterodimer composed of α and β subunits and serves as the trigger for the formation of the primitive syncytium; it also promotes syncytialization *via* an autoparacrine loop (53, 54). Research has shown that hCG is vital for the production of estrogen and preventing the decline in progesterone as a result of the degradation of the corpus luteum during early pregnancy (55, 56). hCG is also involved in promoting trophoblast invasion; regulating the growth of the uterus, fetus, and placenta; and protecting the fetus from attack by the mother's immune system (56, 57). β-hCG is expressed only in the STB layer, and the level rises gradually with cell fusion; consequently, hCG is regarded as a biochemical marker of trophoblast syncytialization (58, 59). Typically, hCG increases intracellular cAMP levels *via* autocrine methods and regulates the expression of both GCM1 and syncytin-1 through the cAMP/PKA pathway to promote the syncytialization of trophoblasts (60). In addition, the abnormally low or high maternal serum levels of free β-hCG during different trimesters are closely associated with adverse pregnancy outcomes, including fetal IUGR, spontaneous abortion, and preterm birth. For this reason, free β-hCG is also regarded as a predictor of pregnancy complications (61, 62).

Cadherins

Cadherins are calcium-dependent integral member glycoproteins that not only function as cell shape and polarity stabilizers by promoting the formation of adherens junctions but also contribute to the balance of cell proliferation, migration and tissue homeostasis by interacting with the intracellular cytoskeleton (63). Cell-cell adhesion is triggered by the extracellular N-terminal domain of cadherins clustering with cadherins located on neighboring cells. E-cadherin, localized in the cell membrane of epithelial trophoblasts (cell columns and CTBs) and the inner STB, is known to be decreased after cell fusion, and is regarded as a morphological marker of cell fusion (16, 64, 65). Specific antibodies against the extracellular domain of E-cadherin have been shown to impede the human trophoblast syncytialization process by disrupting the aggregation of mononuclear CTBs, indicating that E-cadherin is directly involved in the cellular adhesion step of trophoblast syncytialization (66). It has been reported that E-cadherin is involved in regulating human trophoblast syncytialization by interacting with the β-catenin signaling complex and mediating the formation of cell junctions (67). In contrast to E-cadherin expression, cadherin-11 expression increases during trophoblast syncytialization (68). Cadherin-11 antisense treatment resulted in cellular aggregation but fusion deficiency in human trophoblasts. These data suggest that cadherins are vital for the whole process of trophoblast syncytialization, in which E-cadherin mediates mononuclear cell aggregation, while cadherin-11 is required for syncytialization.

Successful placentation relies on appropriate formation of syncytia and homing of trophoblasts to maternal spiral arteries. These processes involve a number of cell-cell adhesion molecules, the abnormal expression of which ultimately results in impaired placentation (69). In the placentas of pregnancies complicated by PE and IUGR, abnormally elevated cadherin levels may participate in the destruction of epithelial-mesenchymal transition (EMT) and the alteration of epithelial/mesenchymal balance, finally resulting in a shallower depth of trophoblast invasion into the decidua (20). Although cadherins are required for the entire trophoblast syncytialization process and change dynamically in the placentas of pregnancies complicated by IUGR and PE, until recently, there was a lack of direct evidence of abnormal cadherin expression causing fetal IUGR owing to syncytialization deficiency.

ZO-1

Tight junctions consist of transmembrane proteins such as the cytoplasmic scaffolding protein ZO-1 that regulate cell-cell adhesion and contribute to epithelial barrier function (70). ZO-1 is a 220 kDa protein that zips cells together and maintains cell polarity. In a mouse model, *ZO-1* knockout (KO) induced defects in mouse placental

development, mainly in vascular tree formation and chorioallantoic fusion (71). In humans, the involvement of ZO-1 in cell fusion and subsequent trophoblast differentiation has been established by morphological and biochemical data. ZO-1 is localized mainly in CTBs and at the intercellular boundaries between CTBs and between CTBs and STB, where its expression substantially decreases during cell fusion (72). In human primary trophoblast cultures, ZO-1 was predominant during the aggregation of CTBs and then decreased drastically with cell fusion. It has been proven that the decrease in ZO-1 induces cell fusion by establishing gap junction communication between two fusion-competent cells, where the expression of the gap junction protein connexin 43 is upregulated to initiate cell fusion (39, 72). In PE placentas, the expression levels of E-cadherin and ZO-1 were elevated compared to the controls (73). MiR-200 family members are highly relevant to PE and IUGR pregnancies. MiR-200 family impaired trophoblast invasion and altered the EMT process by stimulating the expression of the epithelial markers E-cadherin and ZO-1 (74). In contrast, Misan et al. reported that ZO-1 levels in both serum and placentas showed no significant difference between IUGR and control groups (75). Although recent study findings suggest that ZO-1 participates in the trophoblast syncytialization process, there is not sufficient evidence to prove that the occurrence of IUGR is related to the syncytialization deficiency caused by abnormal expression of ZO-1, which may be a new direction for future research.

Syncytins

Syncytins are endogenous retroviral envelope proteins containing a disulfide sequence, a furin cleavage site, a fusion peptide, and a receptor-binding domain. There are two pairs of retrovirus-derived envelope genes named *syncytin-1* and *syncytin-2* in humans and *syncytin-A* and *syncytin-B* in mice (76, 77). Both are expressed in placental trophoblasts and specifically mediate the formation of the STB layer, particularly through their fusogenic activity (78–80). In humans, syncytin-1 mediates cell fusion first by seeding its fusion peptide into the targeting membrane, then bending the cytomembrane, and finally forming fusion pores (39). During the spontaneous syncytialization process of human primary CTBs, the expression level of syncytin-1 is increased (81). It has been reported that the silencing of *syncytin-1* gene expression could significantly reduce β-hCG secretion and cell fusion (7, 51). In contrast, after transferring syncytin-1 vectors into BeWo choriocarcinoma cell lines without forskolin induction, cell-cell fusion was directly induced, suggesting that syncytin-1 may be directly involved in regulating the syncytialization of trophoblasts (51, 78). Syncytin-2 is another fusion protein expressed only in CTBs, and its receptor, major facilitator superfamily domain-containing 2 (MFSD2), is also found in CTBs (82). A previous study showed that syncytin-2 was confined to G0 cells when all trophoblasts were ready to fuse, and the overexpression of syncytin-2 resulted in the unstable fusion of cells in their S/G2/M phases (83). As syncytin-2 works on CTBs and induces the initiation of cell fusion, syncytin-2 could be regarded as a marker of the initiation of trophoblast syncytialization (84). Reduced expression of syncytin-1 and syncytin-2 was detected in IUGR placentas compared to controls (14, 38). In mice, syncytin-A disruption caused fetal IUGR and embryonic lethality by reducing glucose transport between the maternal-fetal interface (85). *Syncytin-A* gene KO changed placental morphology, resulting in low expression of neovascularization-related genes and widespread vascular abnormalities in the labyrinth, which were characterized by irregular distribution and reduced numbers of fetal vessels (86). In addition, *BCL9L*-deficient mice exhibited a striking downregulation of syncytin-A in the placenta with severe disruption of trophoblast fusion (87, 88). Moreover, *syncytin-A* null mouse embryos died between embryonic days E11.5 and E13.5 due to the failure of placental formation (89). The level of the human antiangiogenic molecule sFlt-1 was markedly increased in *syncytin-A* KO mice, which prevented spongiotrophoblast from differentiating into glycogen cells and reduced the exchange area of the labyrinth and glycogen stores, which were highly relevant to fetal IUGR (86, 90). Therefore, syncytins directly contribute to trophoblast syncytialization, and placental syncytin deficiency may be associated with the occurrence and development of fetal IUGR in both humans and mice (38).

GCM1

GCM1 is a key transcription factor that regulates placental development and is predominantly expressed in mammalian trophoblasts, regulating cell differentiation, turnover and maintenance (91, 92). GCM1 functions as a regulator of STB formation and the expression of fusogenic genes such as *syncytin-1* and *syncytin-2* (93, 94). GCM1 regulates *syncytin* gene expression by binding to two GCM1-binding sites located upstream of the 5'-long terminal repeats of the *syncytin-1* promoter region, which is essential for cell fusion (93, 95, 96). A previous study found that syncytin-A was downregulated in the placenta of *GCM1*-deficient mice (97). In humans, both reduced and increased levels of GCM1 have been described in several pregnancy complications and have been linked with altered trophoblast function *in vitro* (98–100). The expression level and transcriptional activity of GCM1 are reduced in the primary CTBs of first trimester and term pregnancies under hypoxia, along with syncytia formation deficiency (87, 101, 102). In addition, the excessive expression of syncytin-1 caused by abnormal regulation of GCM1 also leads to extensive cell fusion and cell death (103). Moreover, GCM1 promotes the transcription of syncytin-2 following interaction with the cell cycle inhibitor p21 (83). It has been reported that GCM1 is among the top scoring genes with the greatest negative association with fetal growth in human placentas from pregnancies complicated by IUGR (104). The transcription factor p45 NF-E2 (nuclear factor erythroid derived 2) has recently been found to regulate trophoblast differentiation, and its absence causes placental insufficiency and IUGR in mice (105). P45 NF-E2 negatively regulates human STB differentiation and apoptosis activation by modulating GCM1 acetylation and sumoylation, which is associated with IUGR (92). Collectively, these results suggest that the transcription factor GCM1 may play a crucial role in the trophoblast syncytialization process and that its abnormal regulation may lead to the occurrence of IUGR caused by syncytialization deficiency.

11β-HSD2

11β-HSD2 is an NAD^+-dependent oxidase that converts active cortisol to inactive cortisone and is expressed from the earliest 3 weeks after embryo implantation. The levels of 11β-HSD2 drop

intensely during the third trimester. 11β-HSD2 localizes in the STB layer, where it acts as a placental glucocorticoid barrier to protect the fetus from excessive maternal glucocorticoid disturbance (106–108). It is reported hCG upsurges 11β-HSD2 expression by activating the cAMP/PKA pathway, resulting in histones modification alteration and specificity protein 1 (Sp1) expression increase, which activates the transcription of *HSD11B2* during trophoblast syncytialization (109). In IUGR pregnancy caused by different etiologies, placental 11β-HSD2 expression is attenuated by distinct mechanisms. For examples, stress and nutritional deprivation reduce 11β-HSD2 expression by increasing its methylation, while hypoxia decrease 11β-HSD2 expression *via* alternative mechanisms rather than by methylation. A recent study revealed that the accumulation of cadmium in the placenta causes fetal IUGR by downregulating 11β-HSD2 expression *via* Sp1, which binds to GC-rich sections of the *11β-HSD2* promoter region (110, 111;). Although most of studies have shown the reduced level and activity of placental 11β-HSD2 in pregnancies complicated by PE and fetal IUGR, and the impairment of 11β-HSD2 glucocorticoid barrier is associated with fetal IUGR and the development of chronic diseases in later life (109, 112, 113). Nevertheless, increased maternal 11β-HSD2 activity was observed many weeks before the clinical manifestations of PE and preterm fetal IUGR appeared (114).

The signaling pathways involved in syncytialization

A wide range of intracellular molecules are known to participate in the regulation of trophoblast syncytialization. *In vitro*, research has identified several signaling pathways, including the cAMP/PKA, Wnt/β-Catenin, MAPK, PI3K/AKT, JAK/STAT, and TGF-β/SMAD signaling pathways, that regulate trophoblast syncytialization by targeting syncytialization-related proteins or in other ways (see Figure 2). Furthermore, abnormalities in these signaling pathways have also been reported in cases of fetal IUGR caused by placental dysfunction.

cAMP dependent signaling pathways

The cAMP signaling pathway is one of the most common signaling pathways involved in cell fusion; this pathway is strictly controlled by a range of regulators that act in a spatial and temporal manner to convey appropriate messages (115). Signaling molecules, such as hCG and forskolin, first act on their receptors to activate adenylate cyclase (AC). This, combined with ATP catalysis, results in an increase in the intracellular level of cAMP (115). As a second messenger, cAMP then activates various downstream intracellular molecules, such as cAMP-dependent protein kinase (PKA) and the exchange protein that is directly activated by cAMP1 (EPAC1) (116, 117). Both of these factors eventually target fusogenic genes, leading to cell fusion.

PKA mediates many cAMP-induced biological effects, including cell fusion (19). For example, the activation of the cAMP/PKA signaling pathway by forskolin and β-hCG has a positive impact on trophoblast fusion (60, 118). Furthermore, the inhibition of fusion arising from hypoxia can be alleviated through the activation of the PKA pathway (119). Increased levels of fusion were detected in BeWo cells following the transfer of PKA plasmids; this was associated with upregulated transcriptional activity of GCM1 and an increase in the levels of syncytin-1 protein. These studies also showed that fusion was compromised when a PKA inhibitor, such as H89, was added (120, 121). Moreover, the expression levels and distribution of type I and type II PKA showed changes during the fusion between human CTBs; this was considered to be associated with the secretion of hormones and the reorganization of the cytoskeleton (120). Research has also proven that activated cAMP/PKA phosphorylates CREB (cAMP response element-binding protein), a downstream transcription factor that binds to CBP (CREB binding protein) and P300, to

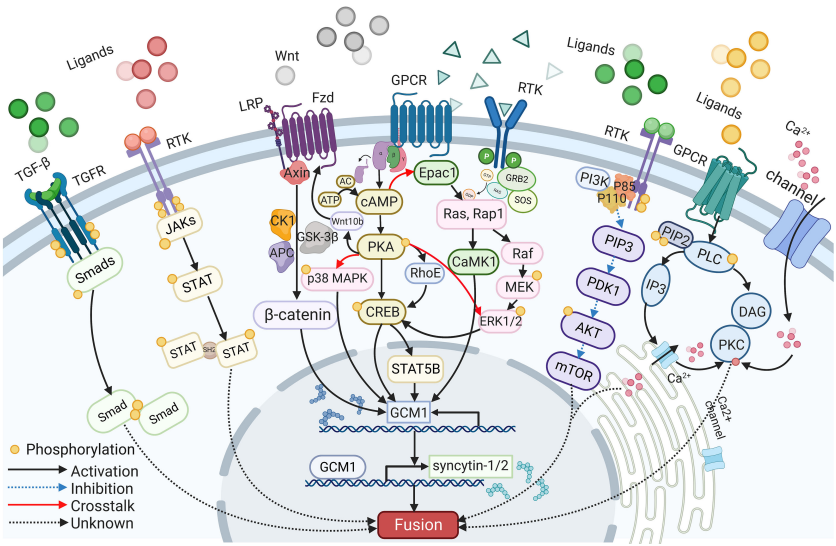


FIGURE 2
The signaling pathways participate in syncytialization.

increase the expression levels of several fusogenic genes, including *syncytins*, *hCG*, *GCM1*, and *Cx43* (39). Furthermore, cAMP, PKA, and CREB upregulate GCM1, then increase the expression levels of syncytin-2 *via* STAT5B (84). Furthermore, previous research found that cAMP can also upregulate the expression levels of the GTP-binding protein RhoE *via* cAMP and PKA, while RhoE was shown to influence the fusion of BeWo cells by activating the transcription factor GCM1 (122).

It is reported that ethanol reduces placental 11β-HSD2 expression *via* cAMP/PKA signaling, thus leads to glucocorticoids over-exposure for fetuses, which eventually induces fetal IUGR (123). Moreover, caffeine reduces placental 11β-HSD2 by decreasing intracellular level of cAMP, which is linked to fetal IUGR (124).

Wnt/β-Catenin signaling pathways

Research has shown that Wnt family members play a key role in embryonic development and tumorigenesis (125). In human cells, Wnt signaling pathways include the classic Wnt/β-catenin signaling pathway, the nonclassic Wnt/Ca^{2+} signaling pathway, and the nonclassic cell polarity pathway (126). The activation of the classic Wnt signaling pathway depends on the binding of Wnt ligands to the heterodimeric frizzled protein (FZD) or the low-density lipoprotein receptor-related protein (LRP-5/6) receptor on the cytomembrane, thereby destroying the CK1-GSK-3β-AXIN-APC phosphorylation complex; this prevents β-catenin from being degraded after undergoing phosphorylation in the cytoplasm and entering the nucleus to bind to transcription factors such as T-cell factor 4 (TCF4) and lymphocyte enhanced binding factor (LEF). Finally, target genes such as *c-Myc*, *Cyclin D1*, and *Mmp7* are activated, which causes abnormal cell proliferation and apoptosis (25).

The classic Wnt/β-Catenin signaling pathway is associated with trophoblast syncytialization. *In vitro*, silencing of TCF-4 or β-Catenin has been shown to inhibit forskolin-induced BeWo cell fusion, at least to a certain extent (88). Other studies found that GCM1 upregulates FZD5 and that elevated levels of FZD5, in combination with nuclear β-Catenin signaling, can maintain the expression of GCM1 during trophoblast differentiation and chorionic branching morphogenesis. These results indicated that Wnt/β-Catenin regulates the syncytialization of trophoblasts by directly targeting GCM1 (127). The expression levels of Wnt10b have also been shown to increase in BeWo cells during the process of forskolin-induced fusion (128). In contrast, the protein levels of Wnt10b, and the nuclear concentration of β-Catenin were both found to be decreased after the addition of a PKA inhibitor. This indicated that cAMP may upregulate Wnt10b *via* the PKA pathway. Wnt10b promoted the migration of β-Catenin into the nucleus by activating the classic Wnt/β-Catenin signaling pathway, which acts on GCM1 and finally upregulates the expression of syncytin-1 (121).

Dickkopf1 (DKK1) is a secreted glycoprotein that can block the classic Wnt/β-Catenin signaling pathway by binding to LRP5/6 (129). A previous study found that the overexpression of the transcription factor HOXB7 inhibited the differentiation of human trophoblasts by downregulating the expression of DKK1 and the transcription of Wnt1/β-Catenin in the placentas of pregnancies complicated by IUGR. This indicated that the Wnt/β-Catenin signaling pathway may play a significant role in the pathogenesis of IUGR (130). Secreted frizzled-related protein (SFRP) is another Wnt signaling pathway inhibitor. In rats, the increased expression of SFRP4 and the reduced expression of nuclear β-Catenin were related to reduced growth in certain regions of the placenta after glucocorticoid-induced growth restriction (131). Furthermore, SFRP1 and SFRP3 were reported to be highly expressed in human placentas from pregnancies complicated by IUGR (132–134).

The MAPK signaling pathway

The MAPK signaling pathway plays an important role in cell proliferation, differentiation, invasion, aging, and apoptosis (135–138). When signaling molecules act on their receptors, the signal is transmitted to the nucleus by activating a series of factors within the cascade, including MAPKKK, MAPKK, and MAPK, thereby regulating the activity of transcription factors and the expression of target genes; collectively, these actions induce a range of intracellular responses (125). The MAPK family includes four different kinases: extracellular regulated kinase (ERKs), ERK5, c-JUN N-terminal kinase (JNKs), and p38 MAPK (125, 135). ERKs are mainly activated through mitogenic signals, while JNKs and p38 MAPK respond to stress and inflammatory conditions (139).

The ERK1/2 and p38 MAPK signaling pathways regulate the differentiation and fusion of trophoblasts under the effect of various growth factors and cytokines. For example, epidermal growth factor (EGF) and leukemia inhibitory factor (LIF) both exert a positive effect on the syncytialization of trophoblasts *via* MAPK signaling pathways, while specific inhibitors of MAPKs have an opposite effect on primary trophoblast cultures (140–142). Some data have shown that the MAPK and cAMP/PKA signaling pathways communicate by crosstalk. It has been reported that ERK1/2 can be phosphorylated by either PKA or RAP1, factors that are activated by members of the Ras superfamily (143, 144). Conversely, CREB can also be activated by ERK1/2. Together, these two signaling pathways regulate the expression of fusogenic genes, such as syncytin-1 through GCM1 and collectively mediate cell fusion (145). Furthermore, cAMP/PKA and p38α can both promote the expression of syncytin-1 and hCG *via* PPARγ/RXRα during the fusion of BeWo cells and primary human trophoblasts (146).

Placental dysfunction could lead to the development of fetal IUGR; these cases were characterized by the significantly reduced expression of p38 MAPK (147). For example, the expression of both p38 and syncytin-1 was both found to be downregulated in placentas from pregnancies complicated by IUGR, while levels of the transcription factor PPARγ/RXRα remained unchanged (146). Previous research found that insulin-like growth factors (IGFs) promoted trophoblast syncytialization and proliferation *in vitro* by binding to their receptor (IGF-IR) *via* the MAPK signaling pathway (148). Moreover, marked impairment of the coordinated activation of MAPKs, with reduced p38 and JNK phosphorylation, was observed in placentas from pregnancies complicated by IUGR; these factors resulted in extensive placental apoptosis and the impairment of maternal-fetal exchange functions (149).

The PI3K/AKT signaling pathway

The PI3K/AKT signaling pathway is of great significance for regulating trophoblast proliferation, differentiation, migration, and invasion (150, 151). PI3K is a heterodimer composed of the p85 regulatory subunit and p110 catalytic subunit and has both lipid kinase activity and protein kinase activity (152, 153). When signaling molecules such as hormones and growth factors bind to their receptors on the cell surface, PI3K is activated. Then, activated PI3K phosphorylates phosphatidylinositol-4,5-bisphosphate (PIP2) to phosphatidylinositol-3,4,5-triphosphate (PIP3) (154). Subsequently, AKT is recruited and activated by PIP3 with the help of PDK1, and activated AKT then phosphorylates downstream factors such as mammalian rapamycin (mTOR) to transduce signaling messages (155).

Studies have found that in addition to increasing cAMP levels, simultaneous inhibition of the PI3K/AKT signaling pathway and reduction of intracellular calcium also result in BeWo cell fusion. Moreover, individual blockade of calcium channel function or PI3K/AKT signaling potentiate cell fusion combined with forskolin (156). The above finding suggests that the PI3K/AKT pathway may be involved in the process of trophoblast syncytialization with cAMP activation, but the mechanism of its effects on syncytialization is still unclear.

Researchers have found that some components of the PI3K/AKT signaling pathway are decreased in dysfunctional human placentas, which causes fetal IUGR. For example, defects in p110α signaling impair angiogenesis, leading to placental regional morphogenesis alteration and placental exchange deficiency, which is associated with a severe and early-onset form of IUGR (157–159). *Akt-1* KO mice have fetal growth restriction due to placental insufficiency (160). In human placentas of pregnancies complicated by IUGR, the expression level and activity of mTOR and its upstream molecule AKT are reduced, while those of AMPKα, a negative regulator of mTOR, are increased (161).

The JAK/STAT signaling pathway

Cytokines and growth factors interact with RTK on the cell membrane to activate JAK. Activated JAK subsequently phosphorylates tyrosine residues of STAT, and the latter forms dimers or multimers through its SH2 domain and is transported from the cytoplasm to the nucleus, where it combines with DNA sequences to activate gene transcription, leading to cell proliferation, differentiation, migration, and apoptosis (162–166).

A significant increase in STAT3 expression was observed during the process of forskolin-induced syncytialization of BeWo cells, and the spontaneous differentiation of primary trophoblasts was also associated with an increase in STAT3 expression (167). The above results suggest that STAT3 may participate in trophoblast syncytialization *in vitro*. In addition, the JAK/STAT signaling pathway also participates in BeWo cell fusion and β-hCG secretion mediated by LIF (142).

The study found that the expression of p-STAT3, a key molecule in the JAK/STAT signaling pathway, was decreased in human placentas from pregnancies complicated by IUGR. In addition, the expression of the JAK/STAT signaling pathway target genes *IFNAR1* and *IFNAR2* was also significantly downregulated in human IUGR placentas, suggesting that the JAK/STAT signaling pathway was inhibited (168). Moreover, the mRNA level of STAT5B is also decreased in the STB of placentas from pregnancies complicated by IUGR, which may affect syncytin-2 expression through GCM1, resulting in insufficient cell fusion (84, 167). STAT3 is located on the STB layer. The decreased level of STAT3 may lead to premature differentiation and increased apoptosis or shedding of STB (48).

The TGF-β/SMAD signaling pathway

TGF-β is a member of the transforming growth factor family, which is important for cell proliferation, differentiation, migration, apoptosis, and extracellular matrix deposition (169). TGF-β transmits signals through SMAD-dependent and non-SMAD-dependent pathways (170–172). For the SMAD-dependent pathway, TGF-β activates its type II receptors and recruits and phosphorylates type I receptors, and the activated dimeric receptor complex in turn activates SMAD transcription factors and induces them to enter the nucleus to regulate target gene transcription (173).

Expressed by STB, TGF-β negatively controls the fusion of CTBs into syncytia (174). A study revealed that after adding TGF-β1 to differentiated human primary trophoblasts, the potential for syncytialization was decreased with a reduction in hCG and human placental prolactin (hPL) secretion, suggesting that TGF-β1 signaling pathway may affect trophoblast syncytialization by generating a negative effect on the differentiation of trophoblasts, but the specific mechanism is not yet clear (175).

Aberrant activation of the TGF-β signaling pathway causes abnormal development of the placenta and induces disorders such as pregnancy-induced hypertension (PIH) (176, 177). It has been reported that TGF-β1 affects trophoblast invasion and migration abilities by suppressing EMT progression, which disrupts placental vascular remodeling, eventually inducing the occurrence and development of PE. At present, most studies have confirmed that the TGF-β1/SMAD signaling pathway is involved in the development of PE, and it is an integral part of PE treatment. For example, placenta-derived peptide regulates placental function during PE progression *via* the TGF-β1/SMAD signaling pathway (178). In addition, miR-140-5p may be involved in PIH progression by regulating the TGF-β1/SMAD signaling pathway (179). In IUGR placenta, the abnormal TGF-β signaling leads to dysregulated sphingolipoid metabolism, which may favor increased trophoblast cell death (180).

Although these signaling pathways are involved in the regulation of trophoblast syncytialization and the components of which are abnormally expressed in placentas from pregnancies complicated by IUGR, there is still a lack of direct evidence to prove that the aberrant expression of these signaling pathways leads to IUGR by impairing

trophoblast syncytialization, which may be a promising direction for further research.

Epigenetic modifications involved in syncytialization

The *syncytin-1* gene contains two long terminal repeat (LTR) regions: the 5'LTR and the 3'LTR. The U3 region of the 5'LTR overlaps with the CpG island, which extends from the proximal promoter region to the first exon, and the tissue-specific expression of *syncytin-1* is determined by the degree of DNA methylation (181). Studies have found a negative relationship between *syncytin-1* expression and gene methylation. Previous studies of both placentas from pregnancies complicated by PE and placentas from pregnancies complicated by IUGR reported the downregulation of *syncytin-1* caused by promoter hypermethylation resulting from the overexpression of DNA methyltransferase (14, 182b; 183). However, in another study, Makaroun et al. detected a marked increase in *syncytin-1* expression accompanied by reduced levels of *syncytin-1* and *syncytin-2* methylation in placentas from pregnancies complicated by IUGR (184). This concurred with the findings of Gao et al., who reported that the expression of *syncytin-1* was upregulated due to insufficient promoter methylation in the placentas of pregnancies with discordant twins that were SGA (185). One speculation is that this may represent a compensatory mechanism for fetal growth retardation caused by placental dysfunction (186). The administration of 5-AZA-2'deoxycytidine (5-AZA), a DNA demethylation agent, into a range of trophoblast-like cell lines during their fusion process led to a reduction in 5'LTR methylation and an increase in the expression levels of syncytin-1 and hCG (183).

GCM1 ubiquitination, acetylation, and sumoylation

The ubiquitin-proteasome degradation system plays an essential role in many cellular processes, including cell cycle progression, signal transduction, transcriptional regulation, receptor downregulation, and endocytosis. Studies have found that the human GCM1 (HGCM1) protein has poor stability and is degraded by the ubiquitin-proteasome degradation system under the influence of SCF-human F box protein FBW2 (hFBW2)-E3 (SCFhFBW2E3) complex ubiquitination during cell fusion, thereby permitting GCM1 to be regulated on the posttranslational level (187). Given that GCM1 regulates syncytin-1-mediated trophoblast fusion, Yang et al. speculated that the abnormal expression of hFBW2 may hinder placental development (187). In addition, the activated cAMP protects GCM1 from being degraded by FBW2-mediated ubiquitination *via* two independent pathways: the cAMP/PKA pathway or the cAMP/EPAC1/CaMK1 pathway (60, 188). Studies have already demonstrated reduced levels of HGCM1 protein in the placentas of patients with PE (189). Hypoxia is the leading cause of PE and is known to activate and recruit GSK-3β and FBW2, respectively, to trigger ubiquitination and the degradation of GCM1 *via* the PI3K/AKT signaling pathway (190). During the fusion of placental trophoblasts, histone acetyltransferases (HATs) and histone deacetylases (HDACs) play a joint role in regulating the degree of GCM1 acetylation and thus determine the transcriptional activity of GCM1 (191). It has been reported that the cAMP/PKA signaling pathway recruits CBP to mediate the acetylation of GCM1 following phosphorylation at the Ser269 and Ser275 sites (60). Moreover, the cAMP/EPAC1/CaMK1 pathway subsequently enhances the binding of GCM1 to its target genes by increasing GCM1 desumoylation (192). Collectively, these actions eventually promote cell fusion by targeting the genes downstream of GCM1, such as *syncytins*. Furthermore, increased acetylation and desumoylation of GCM1 have been observed in the placentas from pregnancies complicated by IUGR, thus indicating that the posttranslational modification of GCM1 may be involved in the occurrence of fetal IUGR (92).

Metabolism and syncytialization

Hypoxia

In the early stages of embryonic development, the uterus is a hypoxic environment. It continues until the completion of vascular remodeling and the fetal-maternal interface becomes full of blood from the mother, thus providing oxygen to the developing fetus. If vascular remodeling fails, then there is a direct influence on the fetus with respect to the source of oxygen. The failure of vascular modeling can also damage the structure and function of the placenta *via* a range of different mechanisms; this can also have indirect effects on fetal development, thus leading to IUGR.

CTBs spontaneously fused into multinucleated STB in an environment where the concentration of oxygen is 21%; when the oxygen level was reduced to 10%, the majority of trophoblasts remained mononucleated, and there was a significant reduction in the secretion of hCG and hPL (193). Research has shown that under hypoxic conditions (the concentration of oxygen is 1%), there is a reduction in the expression levels of GCM1 and syncytin-1 in primary human trophoblasts, along with reduced levels of cell fusion (87). Hypoxia-inducible factor (HIF) is a heterodimeric transcription factor, stabilized under low oxygen tension to mediate cellular responses, composed of HIFα and the arylhydrocarbon receptor nuclear translocator (ARNT/HIF1β). Studies have shown that the downregulation of GCM1 caused by hypoxia is regulated by HIF. The increased level of GCM1 in *Arnt*-null mouse trophoblast stem (TS) cells induces TS cells differentiated into chorionic trophoblasts and syncytiotrophoblasts (194). Similarly, *Arnt* KO was also shown to partially restore the secretion of hCG in primary human trophoblasts (195). Furthermore, the inhibition of STB differentiation induced by hypoxia is also related to members of the ligand-activated nuclear hormone receptor superfamily, such as peroxisome proliferator-activated receptor gamma (PPARγ). PPARγ is expressed in villous CTBs and is activated during their differentiation into STB (196). It has been reported that *PPARγ*-deficient embryos die at 10.5-11.5 dpc due to placental labyrinth deformation (197). *PPARγ*-null TS cells showed a defect in differentiation into labyrinthine trophoblasts (198). GCM1 reduction in mouse placenta leads to defective STB differentiation and gestational hypertension in later pregnancy, a phenotype resembling PE (100). A previously study showed that

the treatment of differentiating TS cells with a PPARγ agonist induced GCM1 expression. Conversely, the overexpression of PPARγ in *PPARγ*-null TS cells promoted both the expression of GCM1 and the formation of multinucleated STB *in vitro* (199). In addition, the failure to form a labyrinth and midgestation lethality were observed in both GCM1 and *PPARγ*-null gestations, suggested that PPARγ may regulate syncytiotrophoblast syncytialization *via* GCM1 (199). In another study, PPARγ agonists resulted in increased secretion of hCG and hPL and reduced expression of the apoptosis-related gene *P53* in primary human trophoblasts in a hypoxic environment (the concentration of oxygen is 1%) (200). Hypoxia can play a critical role in the induction of human IUGR by inhibiting the differentiation of STB *via* GCM1 downregulation. However, there is very little evidence to support the fact that HIF and PPARγ play a role in hypoxia-induced human fetal IUGR. Other studies have shown that hypoxia can lead to an increase in placental oxidative stress and reactive oxygen species (ROS). The latter induces placental dysfunction by increasing the levels of cellular DNA damage, apoptosis, and the peroxidation of both proteins and lipids; these factors can all cause fetal IUGR (201).

Amino acids

Taurine is the most abundant amino acid in the placenta and is expressed in STB layer. Studies have found that taurine can induce the differentiation and fusion of trophoblasts but does not increase the secretion of hCG (202); these findings demonstrated that the biochemical differentiation and morphological differentiation of trophoblasts are two independent processes (198, 203). Studies of placentas from pregnancies complicated by IUGR have identified a reduction in the activity of the taurine transporter (TauT) and syncytia formation failure; the mechanisms underlying these effects, however, remain unknown (202). However, some researchers have speculated that these effects may be related to the involvement of taurine in transducing intracellular differentiation signals or maintaining intercellular molecular exchange (204, 205). Moreover, STB showed enhanced macropinocytosis induced by mTOR signaling inhibition, which serves as an essential adaptation to amino acid shortages in the placentas from pregnancies complicated by fetal growth restriction patients (206).

Senescence and syncytialization

Cellular senescence is characterized by cell cycle arrest accompanied by morphological and metabolic changes, including a shift to a proinflammatory phenotype (207). It has a positive effect with regard to limiting injured cell replication, inhibiting tumor growth, and facilitating cell fusion. However, senescence can also induce tumorigenesis as well as a number of age-related pathologies as senescent cells begin to accumulate (208–210). Senescence is caused by oncogene activation, telomere shortening, oxidative stress, and other types of stress leading to DNA damage (211, 212). Interestingly, the fusion of cells mediated by fusogenic proteins can also induce placental senescence, which p21 is activated and the p53 pathway of senescence becomes functional; this activates the p16-pRb (retinoblastoma protein)-dependent pathway, thus inhibiting the proliferation of CTBs (213–215). Cox et al. considered that senescence involves an extension of cell volume, as it provides sufficient space for the continued formation of multinucleated STB; this would also allow the terminally differentiated syncytia to function well and sustain pregnancy (207, 216). Furthermore, senescence can exert an anti-apoptotic effect (217), thus explaining the existence of nonapoptotic yet Caspase-8-positive STB expressing decoy receptor 2 (DCR2), an anti-apoptotic marker of senescence (217, 218).

Some studies reveal that the occurrence IUGR may provide a link to accelerated placental aging, senescence and major obstetric complications, and an arrested release of syncytial knots are observed in the placentas of pregnancies complicated by IUGR (219, 220). Telomerase is an enzymatic complex that completes the replication of telomeres, genetic elements that cap and protect the ends of chromosomes (221). Suppression of telomerase activity and reduced telomere length was found in IUGR placenta with elevated expression of telomere-induced senescence biomarkers, p21, p16 and elongation factor 1 alpha (EF-1α) (219).

Autophagy and syncytialization

Autophagy protects cells from senescence by degrading and recycling senescence-related components such as misfolded proteins and damaged organelles in a lysosome-embedded manner. Autophagy can be activated under conditions of mild stress and involves two essential organelles: the mitochondria and the endoplasmic reticulum (ER) (222). Calcium can be transferred between these two organelles in a bidirectional manner by virtue of the mitochondria-associated ER membrane (MAM), which is similar to the synapses of the nervous system. The MAM features a large number of calcium transporters and ion channels and is known to play an important role in both oxidative and ER stress (223, 224). Another study showed that an important prerequisite for autophagy was the differentiation-dependent downregulation of p53 (225). Autophagy is a constitutive process, and is activated during villous CTBs syncytialization, which provides energy to cells under situations involving the moderate depletion of nutrients or oxidative stress, and is advantageous in terms of the reorganization of organelles and the degradation of cytoplasmic contents (226–228). A change in autophagy activation in response to chemical treatments or the modulation of Beclin-1 expression was shown to result in a reduction in trophoblastic syncytialization (228). Furthermore, the unfolded protein response (UPR) is activated and protects cells suffering from ER stress during syncytialization, thus inducing autophagy and apoptosis. Consequently, autophagy plays a pivotal role in cell fusion and differentiation. However, increased levels of autophagy have been reported in placentas from pregnancies complicated by IUGR with or without PE; this process provides a nutritional reserve to protect the fetus from acute deprivation (229, 230).

Conclusion

In this review, we primarily discuss the regulators of trophoblast syncytialization and their aberrant expression in placentas of pregnancies complicated by IUGR. For syncytialization-related proteins, hCG, cadherins, ZO-1, syncytins, GCM1, and 11β-HSD2 are strictly regulated to participate in cell fusion *via* appropriate

mechanisms at different fusion stages. Signaling pathways, including the cAMP/PKA, Wnt/β-Catenin, MAPK, PI3K/AKT, JAK/STAT, and TGF-β/SMAD signaling pathways, are involved in coordinating trophoblast syncytialization events and regulating placental function. The DNA methylation of *syncytin-1* and the posttranslational modifications of GCM1 are reported to affect trophoblast syncytialization and associate with fetal IUGR. In addition, metabolic mechanisms, senescence and autophagy are also vital elements involved in regulating the trophoblast syncytialization process.

Thus far, research has shown that the PI3K/AKT, JAK/STAT, and TGF-β/SMAD signaling pathways play key roles in trophoblast syncytialization *in vitro*; however, it is not yet clear how these pathways act on downstream factors and cause syncytialization. Furthermore, little is known about whether the aberrant expression of cAMP/PKA, Wnt/β-Catenin, MAPK, PI3K/AKT, JAK/STAT, and TGF-β/SMAD signaling pathways leads to IUGR by affecting other biological behaviors of trophoblasts, as the etiologies of IUGR are diverse. Thus, clarifying whether these signaling pathways participate in the pathology of IUGR caused by inadequate trophoblast syncytialization and how they act on syncytialization-related molecules is of great significance to clarify the mechanism underlying IUGR development.

This review provides us with not only a better understanding of the pathogenesis of placental dysfunction caused by insufficient trophoblast syncytialization, but also new ideas and insights to select a comprehensive approach to therapy and prevent fetal IUGR occurrence.

Author contributions

HJZ wrote the article. HJZ, CZ, PW, and WY made the figures and drafted the article. HYZ and SZ critically reviewed the article. All authors contributed to the article and approved the submitted version.

Funding

This article is supported by the National Key Research and Development Program of China (2018YFC1004800), the National Natural Science Foundation of China (81601236 and 81601308), the Natural Science Foundation of Zhejiang Province (LY19H040009 and LY22H040007).

Acknowledgments

We sincerely thanks to the help from Department of Obstetrics and Gynecology of the Sir Run Run Shaw Hospital. We thank Editage (www.editage.com) and Shannyn W. senior editor from American Journal Experts (www.aje.com) for editing the English text of a draft of this manuscript.

Conflict of interest

The authors declare that the research was conducted in the absence of any commercial or financial relationships that could be construed as a potential conflict of interest.

Publisher's note

All claims expressed in this article are solely those of the authors and do not necessarily represent those of their affiliated organizations, or those of the publisher, the editors and the reviewers. Any product that may be evaluated in this article, or claim that may be made by its manufacturer, is not guaranteed or endorsed by the publisher.

References

1. American College of OGynecologists. ACOG practice bulletin no. 204: Fetal growth restriction. *Obstet Gynecol* (2019) 133(2):e97–e109. doi: 10.1097/AOG.0000000000003070

2. Beckmann CRB, Gynecologists ACO. *Obstetrics and gynecology*. Lippincott Williams & Wilkins (2010).

3. Wilson ML, Goodwin TM, Pan VL, Ingles SA. Molecular epidemiology of preeclampsia. *Obstet Gynecol Surv* (2003) 58(1):39–66. doi: 10.1097/00006254-200301000-00022

4. Cetin I, Foidart JM, Miozzo M, Raun T, Jansson T, Tsatsaris V, et al. Fetal growth restriction: a workshop report. *Placenta* (2004) 25(8-9):753–7. doi: 10.1016/j.placenta.2004.02.004

5. Nardozza LM, Caetano AC, Zamarian AC, Mazzola JB, Silva CP, Marcal VM, et al. Fetal growth restriction: current knowledge. *Arch Gynecol Obstet* (2017) 295(5):1061–77. doi: 10.1007/s00404-017-4341-9

6. Resnik R. Intrauterine growth restriction. *Obstet Gynecol* (2002) 99(3):490–6. doi: 10.1016/s0029-7844(01)01780-x

7. Albu AR, Anca AF, Horhoianu VV, Horhoianu IA. Predictive factors for intrauterine growth restriction. *J Med Life* (2014) 7(2):165–71.

8. Barker DJ, Clark PM. Fetal undernutrition and disease in later life. *Rev Reprod* (1997) 2(2):105–12. doi: 10.1530/ror.0.0020105

9. Barker DJ. Adult consequences of fetal growth restriction. *Clin Obstet Gynecol* (2006) 49(2):270–83. doi: 10.1097/00003081-200606000-00009

10. Pallotto EK, Kilbride HW. Perinatal outcome and later implications of intrauterine growth restriction. *Clin Obstet Gynecol* (2006) 49(2):257–69. doi: 10.1097/00003081-200606000-00008

11. Dos Passos Junior RR, de Freitas RA, Dela Justina V, San Martin S, Lima VV, Giachini FR. Protein O-GlcNAcylation as a nutrient sensor signaling placental dysfunction in hypertensive pregnancy. *Front Endocrinol (Lausanne)* (2022) 13:1032499. doi: 10.3389/fendo.2022.1032499

12. Burton GJ, Fowden AL, Thornburg KL. Placental origins of chronic disease. *Physiol Rev* (2016) 96(4):1509–65. doi: 10.1152/physrev.00029.2015

13. Baadsgaard K, Hansen DN, Peters DA, Frokjaer JB, Sinding M, Sorensen A. T2* weighted fetal MRI and the correlation with placental dysfunction. *Placenta* (2022) 131:90–7. doi: 10.1016/j.placenta.2022.12.002

14. Langbein M, Strick R, Strissel PL, Vogt N, Parsch H, Beckmann MW, et al. Impaired cytotrophoblast cell-cell fusion is associated with reduced syncytin and increased apoptosis in patients with placental dysfunction. *Mol Reprod Dev* (2008) 75(1):175–83. doi: 10.1002/mrd.20729

15. Burton GJ, Woods AW, Jauniaux E, Kingdom JC. Rheological and physiological consequences of conversion of the maternal spiral arteries for uteroplacental blood flow during human pregnancy. *Placenta* (2009) 30(6):473–82. doi: 10.1016/j.placenta.2009.02.009

16. Sheridan RM, Stanek J, Khoury J, Handwerger S. Abnormal expression of transcription factor activator protein-2alpha in pathologic placentas. *Hum Pathol* (2012) 43(11):1866–74. doi: 10.1016/j.humpath.2012.01.011

17. Mifsud W, Sebire NJ. Placental pathology in early-onset and late-onset fetal growth restriction. *Fetal Diagn Ther* (2014) 36(2):117–28. doi: 10.1159/000359969

18. Newhouse SM, Davidge ST, Winkler-Lowen B, Demianczuk N, Guilbert LJ. *In vitro* differentiation of villous trophoblasts from pregnancies complicated by intrauterine growth restriction with and without pre-eclampsia. *Placenta* (2007) 28(10):999–1003. doi: 10.1016/j.placenta.2007.04.008

19. Gupta SK, Malhotra SS, Malik A, Verma S, Chaudhary P. Cell signaling pathways involved during invasion and syncytialization of trophoblast cells. *Am J Reprod Immunol* (2016) 75(3):361–71. doi: 10.1111/aji.12436

20. Kokkinos MI, Murthi P, Wafai R, Thompson EW, Newgreen DF. Cadherins in the human placenta–epithelial-mesenchymal transition (EMT) and placental development. *Placenta* (2010) 31(9):747–55. doi: 10.1016/j.placenta.2010.06.017

21. Chen CP, Bajoria R, Aplin JD. Decreased vascularization and cell proliferation in placentas of intrauterine growth-restricted fetuses with abnormal umbilical artery flow velocity waveforms. *Am J Obstet Gynecol* (2002) 187(3):764–9. doi: 10.1067/mob.2002.125243

22. Chaddha V, Viero S, Huppertz B, Kingdom J. Developmental biology of the placenta and the origins of placental insufficiency. *Semin Fetal Neonatal Med* (2004) 9 (5):357–69. doi: 10.1016/j.siny.2004.03.006

23. Burton GJ, Jauniaux E. Pathophysiology of placental-derived fetal growth restriction. *Am J Obstet Gynecol* (2018) 218(2S):S745–61. doi: 10.1016/j.ajog.2017.11.577

24. Zur RL, Kingdom JC, Parks WT, Hobson SR. The placental basis of fetal growth restriction. *Obstet Gynecol Clin North Am* (2020) 47(1):81–98. doi: 10.1016/j.ogc.2019.10.008

25. Zhang Z, Wang X, Zhang L, Shi Y, Wang J, Yan H. Wnt/beta-catenin signaling pathway in trophoblasts and abnormal activation in preeclampsia (Review). *Mol Med Rep* (2017) 16(2):1007–13. doi: 10.3892/mmr.2017.6718

26. Pijnenborg R, Dixon G, Robertson WB, Brosens I. Trophoblastic invasion of human decidua from 8 to 18 weeks of pregnancy. *Placenta* (1980) 1(1):3–19. doi: 10.1016/s0143-4004(80)80012-9

27. Hustin J, Jauniaux E, Schaaps JP. Histological study of the materno-embryonic interface in spontaneous abortion. *Placenta* (1990) 11(6):477–86. doi: 10.1016/s0143-4004(05)80193-6

28. Harris LK. IFPA gabor than award lecture: Transformation of the spiral arteries in human pregnancy: key events in the remodelling timeline. *Placenta* (2011) 32(Suppl 2): S154–158. doi: 10.1016/j.placenta.2010.11.018

29. Caniggia I, Winter JL. Adriana and luisa castellucci award lecture 2001. hypoxia inducible factor-1: oxygen regulation of trophoblast differentiation in normal and pre-eclamptic pregnancies–a review. *Placenta* (2002) 23(Suppl A):S47–57. doi: 10.1053/plac.2002.0815

30. Aouache R, Biquard L, Vaiman D, Miralles F. Oxidative stress in preeclampsia and placental diseases. *Int J Mol Sci* (2018) 19(5):1496. doi: 10.3390/ijms19051496

31. Zygmunt M. Placental circulation: Clinical significance. *Early Pregnancy* (2001) 5 (1):72–3.

32. Zygmunt M, Herr F, Munstedt K, Lang U, Liang OD. Angiogenesis and vasculogenesis in pregnancy. *Eur J Obstet Gynecol Reprod Biol* (2003) 110(Suppl 1): S10–18. doi: 10.1016/s0301-2115(03)00168-4

33. Brosens I, Puttemans P, Benagiano G. Placental bed research: I. the placental bed: from spiral arteries remodeling to the great obstetrical syndromes. *Am J Obstet Gynecol* (2019) 221(5):437–56. doi: 10.1016/j.ajog.2019.05.044

34. Turco MY, Moffett A. Development of the human placenta. *Development* (2019) 146(22):dev163428. doi: 10.1242/dev.163428

35. Mayhew TM. Turnover of human villous trophoblast in normal pregnancy: What do we know and what do we need to know? *Placenta* (2014) 35(4):229–40. doi: 10.1016/j.placenta.2014.01.011

36. Thame M, Osmond C, Bennett F, Wilks R, Forrester T. Fetal growth is directly related to maternal anthropometry and placental volume. *Eur J Clin Nutr* (2004) 58 (6):894–900. doi: 10.1038/sj.ejcn.1601909

37. Racca AC, Ridano ME, Camolotto S, Genti-Raimondi S, Panzetta-Dutari GM. A novel regulator of human villous trophoblast fusion: the kruppel-like factor 6. *Mol Hum Reprod* (2015) 21(4):347–58. doi: 10.1093/molehr/gau113

38. Ruebner M, Strissel PL, Langbein M, Fahlbusch F, Wachter DL, Faschingbauer F, et al. Impaired cell fusion and differentiation in placentae from patients with intrauterine growth restriction correlate with reduced levels of HERV envelope genes. *J Mol Med (Berl)* (2010) 88(11):1143–56. doi: 10.1007/s00109-010-0656-8

39. Gerbaud P, Pidoux G. Review: An overview of molecular events occurring in human trophoblast fusion. *Placenta* (2015) 36:S35–42. doi: 10.1016/j.placenta.2014.12.015

40. Huppertz B. Placental origins of preeclampsia: challenging the current hypothesis. *Hypertension* (2008) 51(4):970–5. doi: 10.1161/hypertensionaha.107.107607

41. Pérot P, Montgiraud C, Lavillette D, Mallet F. A comparative portrait of retroviral fusogens and syncytins. In: Larsson L-I, editor. *Cell fusions: Regulation and control*. Dordrecht: Springer Netherlands (2011). p. 63–115.

42. Aguilar PS, Baylies MK, Fleissner A, Helming L, Inoue N, Podbilewicz B, et al. Genetic basis of cell-cell fusion mechanisms. *Trends Genet* (2013) 29(7):427–37. doi: 10.1016/j.tig.2013.01.011

43. Chernomordik LV, Kozlov MM. Membrane hemifusion: Crossing a chasm in two leaps. *Cell* (2005) 123(3):375–82. doi: 10.1016/j.cell.2005.10.015

44. Gauster M, Huppertz B. Fusion of cytothrophoblast with syncytiotrophoblast in the human placenta: factors involved in syncytialization. *J für Reproduktionsmedizin und Endokrinologie-Journal Reprod Med Endocrinol* (2008) 5(2):76–82.

45. Potgens AJ, Schmitz U, Bose P, Versmold A, Kaufmann P, Frank HG. Mechanisms of syncytial fusion: a review. *Placenta* (2002) 23(Suppl A):S107–113. doi: 10.1053/plac.2002.0772

46. Lyden TW, Ng AK, Rote NS. Modulation of phosphatidylserine epitope expression by BeWo cells during forskolin treatment. *Placenta* (1993) 14(2):177–86. doi: 10.1016/s0143-4004(05)80259-0

47. Adler RR, Ng AK, Rote NS. Monoclonal antiphosphatidylserine antibody inhibits intercellular fusion of the choriocarcinoma line, JAR. *Biol Reprod* (1995) 53(4):905–10. doi: 10.1095/biolreprod53.4.905

48. Huppertz B, Frank HG, Kingdom JC, Reister F, Kaufmann P. Villous cytotrophoblast regulation of the syncytial apoptotic cascade in the human placenta. *Histochem Cell Biol* (1998) 110(5):495–508. doi: 10.1007/s004180050311

49. Bernischke K, Kaufmann P, Baergen R. *Pathology of the human placenta. 4th edition*. (New-York: Springer-Verlag) (2000).

50. Frendo JL, Cronier L, Bertin G, Guibourdenche J, Vidaud M, Evain-Brion D, et al. Involvement of connexin 43 in human trophoblast cell fusion and differentiation. *J Cell Sci* (2003) 116(16):3413–21. doi: 10.1242/jcs.00648

51. Frendo JL, Olivier D, Cheynet V, Blond JL, Bouton O, Vidaud M, et al. Direct involvement of HERV-W env glycoprotein in human trophoblast cell fusion and differentiation. *Mol Cell Biol* (2003) 23(10):3566–74. doi: 10.1128/mcb.23.10.3566-3574.2003

52. Mikelson C, Kovach MJ, Troisi J, Symes S, Adair D, Miller RK, et al. Placental 11beta-hydroxysteroid dehydrogenase type 2 expression: Correlations with birth weight and placental metal concentrations. *Placenta* (2015) 36(11):1212–7. doi: 10.1016/j.placenta.2015.09.011

53. Shi QJ, Lei ZM, Rao CV, Lin J. Novel role of human chorionic gonadotropin in differentiation of human cytotrophoblasts. *Endocrinology* (1993) 132(3):1387–95. doi: 10.1210/endo.132.3.7679981

54. Sharony R, Sharon-Weiner M, Kidron D, Sukenik-Halevy R, Biron-Shental T, Manor M, et al. The association between maternal serum first trimester free betahCG, second trimester intact hCG levels and foetal growth restriction and preeclampsia. *J Obstet Gynaecol* (2018) 38(3):363–6. doi: 10.1080/01443615.2017.1340441

55. Tulchinsky D, Hobel CJ. Plasma human chorionic gonadotropin, estrone, estradiol, estriol, progesterone, and 17 alpha-hydroxyprogesterone in human pregnancy. 3. early normal pregnancy. *Am J Obstet Gynecol* (1973) 117(7):884–93. doi: 10.1016/0002-9378(73)90057-4

56. Cole LA. Biological functions of hCG and hCG-related molecules. *Reprod Biol Endocrinol* (2010) 8:102. doi: 10.1186/1477-7827-8-102

57. Cole LA. hCG, the wonder of today's science. *Reprod Biol Endocrinol* (2012) 10:24. doi: 10.1186/1477-7827-10-24

58. Kato Y, Braunstein GD. Discordant secretion of placental protein hormones in differentiating trophoblasts *in vitro*. *J Clin Endocrinol Metab* (1989) 68(4):814–20. doi: 10.1210/jcem-68-4-814

59. Clabault H, Flipo D, Guibourdenche J, Fournier T, Sanderson JT, Vaillancourt C. Effects of selective serotonin-reuptake inhibitors (SSRIs) on human villous trophoblasts syncytialization. *Toxicol Appl Pharmacol* (2018) 349:8–20. doi: 10.1016/j.taap.2018.04.018

60. Cheong ML, Wang LJ, Chuang PY, Chang CW, Lee YS, Lo HF, et al. A positive feedback loop between glial cells missing 1 and human chorionic gonadotropin (hCG) regulates placental hCGbeta expression and cell differentiation. *Mol Cell Biol* (2016) 36 (1):197–209. doi: 10.1128/mcb.00655-15

61. Ong CY, Liao AW, Spencer K, Munim S, Nicolaides KH. First trimester maternal serum free β human chorionic gonadotrophin and pregnancy associated plasma protein a as predictors of pregnancy complications. *BJOG: Int J Obstetrics Gynaecology* (2000) 107 (10):1265–70. doi: 10.1111/j.1471-0528.2000.tb11618.x

62. Sirikunalai P, Wanapirak C, Sirichotiyakul S, Tongprasert F, Srisupundit K, Luewan S, et al. Associations between maternal serum free beta human chorionic gonadotropin (beta-hCG) levels and adverse pregnancy outcomes. *J Obstet Gynaecol* (2016) 36(2):178–82. doi: 10.3109/01443615.2015.1036400

63. Maitre JL, Heisenberg CP. Three functions of cadherins in cell adhesion. *Curr Biol* (2013) 23(14):R626–633. doi: 10.1016/j.cub.2013.06.019

64. Liu L, Wang Y, Shen C, He J, Liu X, Ding Y, et al. Benzo(a)pyrene inhibits migration and invasion of extravillous trophoblast HTR-8/SVneo cells *via* activation of the ERK and JNK pathway. *J Appl Toxicol* (2016) 36(7):946–55. doi: 10.1002/jat.3227

65. Hahn L, Meister S, Mannewitz M, Beyer S, Corradini S, Hasbargen U, et al. Gal-2 increases H3K4me(3) and H3K9ac in trophoblasts and preeclampsia. *Biomolecules* (2022) 12(5):707. doi: 10.3390/biom12050707

66. Coutifaris C, Kao LC, Sehdev HM, Chin U, Babalola GO, Blaschuk OW, et al. E-cadherin expression during the differentiation of human trophoblasts. *Development* (1991) 113(3):767–77. doi: 10.1242/dev.113.3.767

67. Getsios S, Chen GT, MacCalman CD. Alpha-, beta-, gamma-catenin, and p120 (CTN) expression during the terminal differentiation and fusion of human mononucleate cytotrophoblasts *in vitro* and *in vivo*. *Mol Reprod Dev* (2001) 59(2):168–77. doi: 10.1002/mrd.1019

68. Getsios S, MacCalman CD. Cadherin-11 modulates the terminal differentiation and fusion of human trophoblastic cells *in vitro*. *Dev Biol* (2003) 257(1):41–54. doi: 10.1016/s0012-1606(03)00041-1

69. Multhaup A, Huppertz B, Gohner C, Bohringer M, Mai M, Markert U, et al. N-cadherin knockdown leads to disruption of trophoblastic and endothelial cell interaction in a 3D cell culture model - new insights in trophoblast invasion failure. *Cell Adh Migr* (2018) 12(3):259–70. doi: 10.1080/19336918.2017.1386822

70. Leonard F, Collnot EM, Lehr CM. A three-dimensional coculture of enterocytes, monocytes and dendritic cells to model inflamed intestinal mucosa *in vitro*. *Mol Pharm* (2010) 7(6):2103–19. doi: 10.1021/mp1000795

71. Katsuno T, Umeda K, Matsui T, Hata M, Tamura A, Itoh M, et al. Deficiency of zonula occludens-1 causes embryonic lethal phenotype associated with defected yolk sac angiogenesis and apoptosis of embryonic cells. *Mol Biol Cell* (2008) 19(6):2465–75. doi: 10.1091/mbc.e07-12-1215

72. Pidoux G, Gerbaud P, Gnidehou S, Grynberg M, Geneau G, Guibourdenche J, et al. ZO-1 is involved in trophoblastic cell differentiation in human placenta. *Am J Physiol - Cell Physiol* (2010) 298(6):C1517–26. doi: 10.1152/ajpcell.00484.2008

73. Du L, Kuang L, He F, Tang W, Sun W, Chen D. Mesenchymal-to-epithelial transition in the placental tissues of patients with preeclampsia. *Hypertens Res* (2017) 40 (1):67–72. doi: 10.1038/hr.2016.97

74. Su MT, Tsai PY, Wang CY, Tsai HL, Kuo PL. Aspirin facilitates trophoblast invasion and epithelial-mesenchymal transition by regulating the miR-200-ZEB1 axis in preeclampsia. *BioMed Pharmacother* (2021) 139:111591. doi: 10.1016/j.biopha.2021.111591

75. Misan N, Michalak S, Rzymski P, Poniedzialek B, Kapska K, Osztynowicz K, et al. Molecular indicators of blood-brain barrier breakdown and neuronal injury in pregnancy complicated by fetal growth restriction. *Int J Mol Sci* (2022) 23(22):13798. doi: 10.3390/ijms232213798

76. Blaise S, de Parseval N, Heidmann T. Functional characterization of two newly identified human endogenous retrovirus coding envelope genes. *Retrovirology* (2005) 2:19. doi: 10.1186/1742-4690-2-19

77. Imakawa K, Nakagawa S, Kusama K. [Placental development and endogenous retroviruses]. *Uirusu* (2016) 66(1):1–10. doi: 10.2222/jsv.66.1

78. Mi S, Lee X, Li X, Veldman GM, Finnerty H, Racie L, et al. Syncytin is a captive retroviral envelope protein involved in human placental morphogenesis. *Nature* (2000) 403(6771):785–9. doi: 10.1038/35001608

79. Vargas A, Moreau J, Landry S, LeBellego F, Toufaily C, Rassart E, et al. Syncytin-2 plays an important role in the fusion of human trophoblast cells. *J Mol Biol* (2009) 392 (2):301–18. doi: 10.1016/j.jmb.2009.07.025

80. Dupressoir A, Vernochet C, Harper F, Guegan J, Dessen P, Pierron G, et al. A pair of co-opted retroviral envelope syncytin genes is required for formation of the two-layered murine placental syncytiotrophoblast. *Proc Natl Acad Sci U.S.A.* (2011) 108(46):E1164–1173. doi: 10.1073/pnas.1112304108

81. Leisser C, Saleh L, Haider S, Husslein H, Sonderegger S, Knofler M. Tumour necrosis factor-alpha impairs chorionic gonadotrophin beta-subunit expression and cell fusion of human villous cytotrophoblast. *Mol Hum Reprod* (2006) 12(10):601–9. doi: 10.1093/molehr/gal066

82. Hayward MD, Potgens AJ, Drewlo S, Kaufmann P, Rasko JE. Distribution of human endogenous retrovirus type W receptor in normal human villous placenta. *Pathology* (2007) 39(4):406–12. doi: 10.1080/00313020701444572

83. Lu X, Wang R, Zhu C, Wang H, Lin HY, Gu Y, et al. Fine-tuned and cell-Cycle-Restricted expression of fusogenic protein syncytin-2 maintains functional placental syncytia. *Cell Rep* (2017) 21(5):1150–9. doi: 10.1016/j.celrep.2017.10.019

84. Kusama K, Bai R, Imakawa K. Regulation of human trophoblast cell syncytialization by transcription factors STAT5B and NR4A3. *J Cell Biochem* (2018) 119(6):4918–27. doi: 10.1002/jcb.26721

85. Wang YN, Ye YX, Guo ZW, Xiong ZL, Sun QS, Zhou D, et al. Inducible knockout of syncytin-a leads to poor placental glucose transport in mice. *Placenta* (2022) 121:155–63. doi: 10.1016/j.placenta.2022.03.016

86. Qiao S, Wang F, Chen H, Jiang SW. Inducible knockout of syncytin-a gene leads to an extensive placental vasculature deficiency, implications for preeclampsia. *Clin Chim Acta* (2017) 474:137–46. doi: 10.1016/j.cca.2017.09.012

87. Wich C, Kausler S, Dotsch J, Rascher W, Knerr I. Syncytin-1 and glial cells missing a: hypoxia-induced deregulated gene expression along with disordered cell fusion in primary term human trophoblasts. *Gynecol Obstet Invest* (2009) 68(1):9–18. doi: 10.1159/000209396

88. Matsuura K, Jigami T, Taniue K, Morishita Y, Adachi S, Senda T, et al. Identification of a link between wnt/beta-catenin signalling and the cell fusion pathway. *Nat Commun* (2011) 2:548. doi: 10.1038/ncomms1551

89. Dupressoir A, Vernochet C, Bawa O, Harper F, Pierron G, Opolon P, et al. Syncytin-a knockout mice demonstrate the critical role in placentation of a fusogenic, endogenous retrovirus-derived, envelope gene. *Proc Natl Acad Sci U.S.A.* (2009) 106 (29):12127–32. doi: 10.1073/pnas.0902925106

90. Kuhnel E, Kleff V, Stojanovska V, Kaiser S, Waldschutz R, Herse F, et al. Placental-specific overexpression of sFlt-1 alters trophoblast differentiation and nutrient transporter expression in an IUGR mouse model. *J Cell Biochem* (2017) 118(6):1316–29. doi: 10.1002/jcb.25789

91. Kim J, Jones BW, Zock C, Chen Z, Wang H, Goodman CS, et al. Isolation and characterization of mammalian homologs of the drosophila gene glial cells missing. *Proc Natl Acad Sci U.S.A.* (1998) 95(21):12364–9. doi: 10.1073/pnas.95.21.12364

92. Kohli S, Hoffmann J, Lochmann F, Markmeyer P, Huebner H, Fahlbusch FB, et al. p45 NF-E2 regulates syncytiotrophoblast differentiation by post-translational GCM1 modifications in human intrauterine growth restriction. *Cell Death Dis* (2017) 8(4): e2730–0. doi: 10.1038/cddis.2017.127

93. Yu C, Shen K, Lin M, Chen P, Lin C, Chang GD, et al. GCMa regulates the syncytin-mediated trophoblastic fusion. *J Biol Chem* (2002) 277(51):50062–8. doi: 10.1074/jbc.M209316200

94. Liang CY, Wang LJ, Chen CP, Chen LF, Chen YH, Chen H. GCM1 regulation of the expression of syncytin 2 and its cognate receptor MFSD2A in human placenta. *Biol Reprod* (2010) 83(3):387–95. doi: 10.1095/biolreprod.110.083915

95. Lin C, Lin M, Chen H. Biochemical characterization of the human placental transcription factor GCMa/1. *Biochem Cell Biol* (2005) 83(2):188–95. doi: 10.1139/o05-026

96. Malassine A, Blaise S, Handschuh K, Lalucque H, Dupressoir A, Evain-Brion D, et al. Expression of the fusogenic HERV-FRD env glycoprotein (syncytin 2) in human placenta is restricted to villous cytotrophoblastic cells. *Placenta* (2007) 28(2-3):185–91. doi: 10.1016/j.placenta.2006.03.001

97. Schubert SW, Lamoureux N, Kilian K, Klein-Hitpass L, Hashemolhosseini S. Identification of integrin-alpha4, Rb1, and syncytin a as murine placental target genes of the transcription factor GCMa/Gcm1. *J Biol Chem* (2008) 283(9):5460–5. doi: 10.1074/jbc.M710110200

98. Baczyk D, Drewlo S, Proctor L, Dunk C, Lye S, Kingdom J. Glial cell missing-1 transcription factor is required for the differentiation of the human trophoblast. *Cell Death Differ* (2009) 16(5):719–27. doi: 10.1038/cdd.2009.1

99. McCaig D, Lyall F. Hypoxia upregulates GCM1 in human placenta explants. *Hypertens Pregnancy* (2009) 28(4):457–72. doi: 10.3109/10641950802629691

100. Bainbridge SA, Minhas A, Whiteley KJ, Qu D, Sled JG, Kingdom JC, et al. Effects of reduced Gcm1 expression on trophoblast morphology, fetoplacental vascularity, and pregnancy outcomes in mice. *Hypertension* (2012) 59(3):732–9. doi: 10.1161/HYPERTENSIONAHA.111.183939

101. Genbacev O, Zhou Y, Ludlow JW, Fisher SJ. Regulation of human placental development by oxygen tension. *Science* (1997) 277(5332):1669–72. doi: 10.1126/science.277.5332.1669

102. Colson A, Sonveaux P, Debieve F, Sferruzzi-Perri AN. Adaptations of the human placenta to hypoxia: opportunities for interventions in fetal growth restriction. *Hum Reprod Update* (2021) 27(3):531–69. doi: 10.1093/humupd/dmaa053

103. Knofler M, Vasicek R, Schreiber M. Key regulatory transcription factors involved in placental trophoblast development–a review. *Placenta* (2001) 22(Suppl A):S83–92. doi: 10.1053/plac.2001.0648

104. Deyssenroth MA, Li Q, Lacasana M, Nomura Y, Marsit C, Chen J. Expression of placental regulatory genes is associated with fetal growth. *J Perinat Med* (2017) 45(7):887–93. doi: 10.1515/jpm-2017-0064

105. Kashif M, Hellwig A, Kolleker A, Shahzad K, Wang H, Lang S, et al. p45NF-E2 represses Gcm1 in trophoblast cells to regulate syncytium formation, placental vascularization and embryonic growth. *Development* (2011) 138(11):2235–47. doi: 10.1242/dev.059105

106. Audette MC, Greenwood SL, Sibley CP, Jones CJP, Challis JRG, Matthews SG, et al. Dexamethasone stimulates placental system a transport and trophoblast differentiation in term villous explants. *Placenta* (2010) 31(2):97–105. doi: 10.1016/j.placenta.2009.11.016

107. Harris A, Seckl J. Glucocorticoids, prenatal stress and the programming of disease. *Horm Behav* (2011) 59(3):279–89. doi: 10.1016/j.yhbeh.2010.06.007

108. Gurugubelli Krishna R, Vishnu Bhat B. Molecular mechanisms of intrauterine growth restriction. *J Maternal-Fetal Neonatal Med* (2018) 31(19):2634–40. doi: 10.1080/14767058.2017.1347922

109. Zhu P, Wang W, Zuo R, Sun K. Mechanisms for establishment of the placental glucocorticoid barrier, a guard for life. *Cell Mol Life Sci* (2019) 76(1):13–26. doi: 10.1007/s00018-018-2918-5

110. Wu S, Chen N, Tong X, Xu X, Chen Q, Wang F. Selenium attenuates the cadmium-induced placenta glucocorticoid barrier damage by up-regulating the expression of specificity protein 1. *J Biochem Mol Toxicol* (2022) 36(7):e23056. doi: 10.1002/jbt.23056

111. Chen N, Tong X, Wu S, Xu X, Chen Q, Wang F. Cadmium induces placental glucocorticoid barrier damage by suppressing the cAMP/PKA/Sp1 pathway and the protective role of taurine. *Toxicol Appl Pharmacol* (2022) 440:115938. doi: 10.1016/j.taap.2022.115938

112. Kajantie E, Dunkel L, Turpeinen U, Stenman UH, Wood PJ, Nuutila M, et al. Placental 11 beta-hydroxysteroid dehydrogenase-2 and fetal cortisol/cortisone shuttle in small preterm infants. *J Clin Endocrinol Metab* (2003) 88(1):493–500. doi: 10.1210/jc.2002-021378

113. Cottrell EC, Seckl JR, Holmes MC, Wyrwoll CS. Foetal and placental 11beta-HSD2: a hub for developmental programming. *Acta Physiol (Oxf)* (2014) 210(2):288–95. doi: 10.1111/apha.12187

114. Jayasuriya NA, Hughes AE, Sovio U, Cook E, Charnock-Jones DS, Smith GCS. A lower maternal cortisol-to-Cortisone ratio precedes clinical diagnosis of preterm and term preeclampsia by many weeks. *J Clin Endocrinol Metab* (2019) 104(6):2355–66. doi: 10.1210/jc.2018-02312

115. Gerbaud P, Tasken K, Pidoux G. Spatiotemporal regulation of cAMP signaling controls the human trophoblast fusion. *Front Pharmacol* (2015) 6:202. doi: 10.3389/fphar.2015.00202

116. Meinkoth JL, Alberts AS, Went W, Fantozzi D, Taylor SS, Hagiwara M, et al. Signal-transduction through the camp-dependent protein-kinase. *Mol Cell Biochem* (1993) 128:179–86. doi: 10.1007/Bf01076769

117. Bos JL. Epac proteins: multi-purpose cAMP targets. *Trends Biochem Sci* (2006) 31 (12):680–6. doi: 10.1016/j.tibs.2006.10.002

118. Dubey R, Malhotra SS, Gupta SK. Forskolin-mediated BeWo cell fusion involves down-regulation of miR-92a-1-5p that targets dysferlin and protein kinase cAMP-activated catalytic subunit alpha. *Am J Reprod Immunol* (2018) 79(6):e12834. doi: 10.1111/aji.12834

119. Knerr I, Schubert SW, Wich C, Amann K, Aigner T, Vogler T, et al. Stimulation of GCMa and syncytin *via* cAMP mediated PKA signaling in human trophoblastic cells under normoxic and hypoxic conditions. *FEBS Lett* (2005) 579(18):3991–8. doi: 10.1016/j.febslet.2005.06.029

120. Keryer G, Alsat E, Tasken K, Evain-Brion D. Cyclic AMP-dependent protein kinases and human trophoblast cell differentiation *in vitro*. *J Cell Sci* (1998) 111(Pt 7):995–1004. doi: 10.1242/jcs.111.7.995

121. Malhotra SS, Banerjee P, Chaudhary P, Pal R, Gupta SK. Relevance of Wnt10b and activation of beta-catenin/GCMa/syncytin-1 pathway in BeWo cell fusion. *Am J Reprod Immunol* (2017) 78(4):e12676. doi: 10.1111/aji.12676

122. Collett GP, Goh XF, Linton EA, Redman CW, Sargent IL. RhoE is regulated by cyclic AMP and promotes fusion of human BeWo choriocarcinoma cells. *PloS One* (2012) 7(1):e30453. doi: 10.1371/journal.pone.0030453

123. Yu L, Zhou J, Zhang G, Huang W, Pei L, Lv F, et al. cAMP/PKA/EGR1 signaling mediates the molecular mechanism of ethanol-induced inhibition of placental 11beta-HSD2 expression. *Toxicol Appl Pharmacol* (2018) 352:77–86. doi: 10.1016/j.taap.2018.05.029

124. Sharmin S, Guan H, Williams AS, Yang K. Caffeine reduces 11beta-hydroxysteroid dehydrogenase type 2 expression in human trophoblast cells through the adenosine A(2B) receptor. *PloS One* (2012) 7(6):e38082. doi: 10.1371/journal.pone.0038082

125. Knofler M. Critical growth factors and signalling pathways controlling human trophoblast invasion. *Int J Dev Biol* (2010) 54(2-3):269–80. doi: 10.1387/ijdb.082769mk

126. Kestler HA, Kuhl M. From individual wnt pathways towards a wnt signalling network. *Philos Trans R Soc Lond B Biol Sci* (2008) 363(1495):1333–47. doi: 10.1098/rstb.2007.2251

127. Lu J, Zhang S, Nakano H, Simmons DG, Wang S, Kong S, et al. A positive feedback loop involving Gcm1 and Fzd5 directs chorionic branching morphogenesis in the placenta. *PloS Biol* (2013) 11(4):e1001536. doi: 10.1371/journal.pbio.1001536

128. Malhotra SS, Suman P, Gupta SK. Alpha or beta human chorionic gonadotropin knockdown decrease BeWo cell fusion by down-regulating PKA and CREB activation. *Sci Rep* (2015) 5:11210. doi: 10.1038/srep11210

129. Cselenyi CS, Lee E. Context-dependent activation or inhibition of wnt-beta-catenin signaling by kremen. *Sci Signal* (2008) 1(8):pe10. doi: 10.1126/stke.18pe10

130. Huang L, Ying H, Chen Z, Zhu YL, Gu Y, Hu L, et al. Down-regulation of DKK1 and Wnt1/beta-catenin pathway by increased homeobox B7 resulted in cell differentiation suppression of intrauterine fetal growth retardation in human placenta. *Placenta* (2019) 80:27–35. doi: 10.1016/j.placenta.2019.03.001

131. Hewitt DP, Mark PJ, Dharmarajan AM, Waddell BJ. Placental expression of secreted frizzled related protein-4 in the rat and the impact of glucocorticoid-induced fetal and placental growth restriction. *Biol Reprod* (2006) 75(1):75–81. doi: 10.1095/biolreprod.105.047647

132. Partl JZ, Fabijanovic D, Skrtic A, Vranic S, Martic TN, Serman L. Immunohistochemical expression of SFRP1 and SFRP3 proteins in normal and malignant reproductive tissues of rats and humans. *Appl Immunohistochem Mol Morphol* (2014) 22(9):681–7. doi: 10.1097/PAI.0000000000000019

133. Wang A, Zsengeller ZK, Hecht JL, Buccafusca R, Burke SD, Rajakumar A, et al. Excess placental secreted frizzled-related protein 1 in maternal smokers impairs fetal growth. *J Clin Invest* (2015) 125(11):4021–5. doi: 10.1172/JCI80457

134. Zmijanac Partl J, Karin V, Skrtic A, Nikuseva-Martic T, Serman A, Mlinarec J, et al. Negative regulators of wnt signaling pathway SFRP1 and SFRP3 expression in preterm and term pathologic placentas. *J Matern Fetal Neonatal Med* (2018) 31(22):2971–9. doi: 10.1080/14767058.2017.1359830

135. Sun Y, Liu WZ, Liu T, Feng X, Yang N, Zhou HF. Signaling pathway of MAPK/ERK in cell proliferation, differentiation, migration, senescence and apoptosis. *J Recept Signal Transduct Res* (2015) 35(6):600–4. doi: 10.3109/10799893.2015.1030412

136. Liu C, Liang X, Wang J, Zheng Q, Zhao Y, Khan MN, et al. Protein O-fucosyltransferase 1 promotes trophoblast cell proliferation through activation of MAPK and PI3K/Akt signaling pathways. *BioMed Pharmacother* (2017) 88:95–101. doi: 10.1016/j.biopha.2017.01.026

137. Ding L, Li S, Zhang Y, Gai J, Kou J. MXRA5 is decreased in preeclampsia and affects trophoblast cell invasion through the MAPK pathway. *Mol Cell Endocrinol* (2018) 461:248–55. doi: 10.1016/j.mce.2017.09.020

138. Qian S, Liu R. miR-30b facilitates preeclampsia through targeting MXRA5 to inhibit the viability, invasion and apoptosis of placental trophoblast cells. *Int J Clin Exp Pathol* (2019) 12(11):4057–65.

139. Kyriakis JM, Avruch J. Mammalian mitogen-activated protein kinase signal transduction pathways activated by stress and inflammation. *Physiol Rev* (2001) 81(2):807–69. doi: 10.1152/physrev.2001.81.2.807

140. Daoud G, Amyot M, Rassart E, Masse A, Simoneau L, Lafond J. ERK1/2 and p38 regulate trophoblasts differentiation in human term placenta. *J Physiol* (2005) 566(Pt 2):409–23. doi: 10.1113/jphysiol.2005.089326

141. Johnstone ED, Sibley CP, Lowen B, Guilbert LJ. Epidermal growth factor stimulation of trophoblast differentiation requires MAPK11/14 (p38 MAP kinase) activation. *Biol Reprod* (2005) 73(6):1282–8. doi: 10.1095/biolreprod.105.044206

142. Leduc K, Bourassa V, Asselin E, Leclerc P, Lafond J, Reyes-Moreno C. Leukemia inhibitory factor regulates differentiation of trophoblastlike BeWo cells through the activation of JAK/STAT and MAPK3/1 MAP kinase-signaling pathways. *Biol Reprod* (2012) 86(2):54. doi: 10.1095/biolreprod.111.094334

143. Lange-Carter C, Pleiman C, Gardner A, Blumer K, Johnson G. A divergence in the MAP kinase regulatory network defined by MEK kinase and raf. *Science* (1993) 260:315–9. doi: 10.1126/science.8385802

144. Kawasaki H, Springett GM, Mochizuki N, Toki S, Nakaya M, Matsuda M, et al. A family of cAMP-binding proteins that directly activate Rap1. *Science* (1998) 282(5397):2275–9. doi: 10.1126/science.282.5397.2275

145. Delidaki M, Gu M, Hein A, Vatish M, Grammatopoulos DK. Interplay of cAMP and MAPK pathways in hCG secretion and fusogenic gene expression in a trophoblast cell line. *Mol Cell Endocrinol* (2011) 332(1-2):213–20. doi: 10.1016/j.mce.2010.10.013

146. Ruebner M, Langbein M, Strissel PL, Henke C, Schmidt D, Goecke TW, et al. Regulation of the human endogenous retroviral syncytin-1 and cell-cell fusion by the nuclear hormone receptors PPARgamma/RXRalpha in placentogenesis. *J Cell Biochem* (2012) 113(7):2383–96. doi: 10.1002/jcb.24110

147. Corradetti A, Saccucci F, Emanuelli M, Vagnoni G, Cecati M, Sartini D, et al. The role of p38alpha mitogen-activated protein kinase gene in the HELLP syndrome. *Cell Stress Chaperones* (2010) 15(1):95–100. doi: 10.1007/s12192-009-0125-x

148. Sferruzzi-Perri AN, Sandovici I, Constancia M, Fowden AL. Placental phenotype and the insulin-like growth factors: resource allocation to fetal growth. *J Physiol* (2017) 595(15):5057–93. doi: 10.1113/JP273330

149. Laviola L, Perrini S, Belsanti G, Natalicchio A, Montrone C, Leonardini A, et al. Intrauterine growth restriction in humans is associated with abnormalities in placental insulin-like growth factor signaling. *Endocrinology* (2005) 146(3):1498–505. doi: 10.1210/en.2004-1332

150. Li Z, Zhou G, Jiang L, Xiang H, Cao Y. Effect of STOX1 on recurrent spontaneous abortion by regulating trophoblast cell proliferation and migration *via* the PI3K/AKT signaling pathway. *J Cell Biochem* (2018) 120(5):8291–9. doi: 10.1002/jcb.28112

151. Chen J, Yue C, Xu J, Zhan Y, Zhao H, Li Y, et al. Downregulation of receptor tyrosine kinase-like orphan receptor 1 in preeclampsia placenta inhibits human trophoblast cell proliferation, migration, and invasion by PI3K/AKT/mTOR pathway accommodation. *Placenta* (2019) 82:17–24. doi: 10.1016/j.placenta.2019.05.002

152. Walker EH, Perisic O, Ried C, Stephens L, Williams RL. Structural insights into phosphoinositide 3-kinase catalysis and signalling. *Nature* (1999) 402(6759):313–20. doi: 10.1038/46319

153. Rathinaswamy MK, Burke JE. Class I phosphoinositide 3-kinase (PI3K) regulatory subunits and their roles in signaling and disease. *Adv Biol Regul* (2020) 75:100657. doi: 10.1016/j.jbior.2019.100657

154. Li X, Wu C, Chen N, Gu H, Yen A, Cao L, et al. PI3K/Akt/mTOR signaling pathway and targeted therapy for glioblastoma. *Oncotarget* (2016) 7(22):33440–50. doi: 10.18632/oncotarget.7961

155. Sarbassov DD, Guertin DA, Ali SM, Sabatini DM. Phosphorylation and regulation of Akt/PKB by the rictor-mTOR complex. *Science* (2005) 307(5712):1098–101. doi: 10.1126/science.1106148

156. Vatish M, Tesfa L, Grammatopoulos D, Yamada E, Bastie CC, Pessin JE. Inhibition of akt activity and calcium channel function coordinately drive cell-cell fusion in the BeWO choriocarcinoma placental cell line. *PloS One* (2012) 7(1):e29353. doi: 10.1371/journal.pone.0029353

157. Anson-Cartwright L, Dawson K, Holmyard D, Fisher SJ, Lazzarini RA, Cross JC. The glial cells missing-1 protein is essential for branching morphogenesis in the chorioallantoic placenta. *Nat Genet* (2000) 25(3):311–4. doi: 10.1038/77076

158. Sferruzzi-Perri AN, Lopez-Tello J, Fowden AL, Constancia M. Maternal and fetal genomes interplay through phosphoinositol 3-kinase(PI3K)-p110alpha signaling to modify placental resource allocation. *Proc Natl Acad Sci U.S.A.* (2016) 113(40):11255–60. doi: 10.1073/pnas.1602012113

159. Lopez-Tello J, Perez-Garcia V, Khaira J, Kusinski LC, Cooper WN, Andreani A, et al. Fetal and trophoblast PI3K p110alpha have distinct roles in regulating resource supply to the growing fetus in mice. *Elife* (2019) 8:e45282. doi: 10.7554/eLife.45282

160. Yang ZZ, Tschopp O, Hemmings-Mieszczak M, Feng J, Brodbeck D, Perentes E, et al. Protein kinase b alpha/Akt1 regulates placental development and fetal growth. *J Biol Chem* (2003) 278(34):32124–31. doi: 10.1074/jbc.M302847200

161. Fahlbusch FB, Hartner A, Menendez-Castro C, Nogel SC, Marek I, Beckmann MW, et al. The placental mTOR-pathway: correlation with early growth trajectories following intrauterine growth restriction? *J Dev Orig Health Dis* (2015) 6(4):317–26. doi: 10.1017/S2040174415001154

162. Schindler C, Darnell JEJr. Transcriptional responses to polypeptide ligands: the JAK-STAT pathway. *Annu Rev Biochem* (1995) 64:621–51. doi: 10.1146/annurev.bi.64.070195.003201

163. Hoey T, Schindler U. STAT structure and function in signaling. *Curr Opin Genet Dev* (1998) 8(5):582–7. doi: 10.1016/s0959-437x(98)80015-4

164. Rawlings JS, Rosler KM, Harrison DA. The JAK/STAT signaling pathway. *J Cell Sci* (2004) 117(Pt 8):1281–3. doi: 10.1242/jcs.00963

165. Morris R, Kershaw NJ, Babon JJ. The molecular details of cytokine signaling *via* the JAK/STAT pathway. *Protein Sci* (2018) 27(12):1984–2009. doi: 10.1002/pro.3519

166. Xin P, Xu X, Deng C, Liu S, Wang Y, Zhou X, et al. The role of JAK/STAT signaling pathway and its inhibitors in diseases. *Int Immunopharmacol* (2020) 80:106210. doi: 10.1016/j.intimp.2020.106210

167. Borg AJ, Yong HE, Lappas M, Degrelle SA, Keogh RJ, Da Silva-Costa F, et al. Decreased STAT3 in human idiopathic fetal growth restriction contributes to trophoblast dysfunction. *Reproduction* (2015) 149(5):523–32. doi: 10.1530/REP-14-0622

168. Gal H, Lysenko M, Stroganov S, Vadai E, Youssef SA, Tzadikevitch-Geffen K, et al. Molecular pathways of senescence regulate placental structure and function. *EMBO J* (2019) 38(18). doi: 10.15252/embj.2018100849

169. Harradine KA, Akhurst RJ. Mutations of TGFbeta signaling molecules in human disease. *Ann Med* (2006) 38(6):403–14. doi: 10.1080/07853890600919911

170. Attisano L, Wrana JL. Signal transduction by the TGF-beta superfamily. *Science* (2002) 296(5573):1646–7. doi: 10.1126/science.1071809

171. Lu L, Wang J, Zhang F, Chai Y, Brand D, Wang X, et al. Role of SMAD and non-SMAD signals in the development of Th17 and regulatory T cells. *J Immunol* (2010) 184 (8):4295–306. doi: 10.4049/jimmunol.0903418

172. Xiong S, Cheng JC, Klausen C, Zhao J, Leung PC. TGF-beta1 stimulates migration of type II endometrial cancer cells by down-regulating PTEN *via* activation of SMAD and ERK1/2 signaling pathways. *Oncotarget* (2016) 7(38):61262–72. doi: 10.18632/oncotarget.11311

173. Shi Y, Massague J. Mechanisms of TGF-beta signaling from cell membrane to the nucleus. *Cell* (2003) 113(6):685–700. doi: 10.1016/s0092-8674(03)00432-x

174. Lysiak JJ, Hunt J, Pringle GA, Lala PK. Localization of transforming growth factor β and its natural inhibitor decorin in the human placenta and decidua throughout gestation. *Placenta* (1995) 16(3):221–31. doi: 10.1016/0143-4004(95)90110-8

175. Morrish DW, Bhardwaj D, Paras MT. Transforming growth factor beta 1 inhibits placental differentiation and human chorionic gonadotropin and human placental lactogen secretion. *Endocrinology* (1991) 129(1):22–6. doi: 10.1210/endo-129-1-22

176. Huang Z, Li S, Fan W, Ma Q. Transforming growth factor beta1 promotes invasion of human JEG-3 trophoblast cells *via* TGF-beta/Smad3 signaling pathway. *Oncotarget* (2017) 8(20):33560–70. doi: 10.18632/oncotarget.16826

177. Jia Y, Xie H, Zhang J, Ying H. Induction of TGF-beta receptor I expression in a DNA methylation-independent manner mediated by DNMT3A downregulation is involved in early-onset severe preeclampsia. *FASEB J* (2020) 34(10):13224–38. doi: 10.1096/fj.202000253RR

178. Chen T, Zhang Z, Lu Q, Ma J. Screening and functional analysis of the differential peptides from the placenta of patients with healthy pregnancy and preeclampsia using placental peptidome. *Front Genet* (2022) 13:1014836. doi: 10.3389/fgene.2022.1014836

179. Li JY, Jin Y, Cao YM, Wu GM. MiR-140-5p exerts a protective function in pregnancy-induced hypertension *via* mediating TGF-beta/Smad signaling pathway. *Hypertens Pregnancy* (2022) 41(2):116–25. doi: 10.1080/10641955.2022.2056195

180. Chauvin S, Yinon Y, Xu J, Ermini L, Sallais J, Tagliaferro A, et al. Aberrant TGFbeta signalling contributes to dysregulation of sphingolipid metabolism in intrauterine growth restriction. *J Clin Endocrinol Metab* (2015) 100(7):E986–996. doi: 10.1210/jc.2015-1288

181. Matoušková M, Blažková J, Pajer P, Pavlíček A, Hejnar J. CpG methylation suppresses transcriptional activity of human syncytin-1 in non-placental tissues. *Exp Cell Res* (2006) 312(7):1011–20. doi: 10.1016/j.yexcr.2005.12.010

182. Chen CP, Wang KG, Chen CY, Yu C, Chuang HC, Chen H. Altered placental syncytin and its receptor ASCT2 expression in placental development and pre-eclampsia. *BJOG: Int J Obstetrics Gynaecology* (2006) 113(2):152–8. doi: 10.1111/j.1471-0528.2005.00843.x

183. Ruebner M, Strissel PL, Ekici AB, Stiegler E, Dammer U, Goecke TW, et al. Reduced syncytin-1 expression levels in placental syndromes correlates with epigenetic hypermethylation of the ERVW-1 promoter region. *PloS One* (2013) 8(2):e56145. doi: 10.1371/journal.pone.0056145

184. Makaroun SP, Himes KP. Differential methylation of syncytin-1 and 2 distinguishes fetal growth restriction from physiologic small for gestational age. *AJP Rep* (2018) 8(1):e18–24. doi: 10.1055/s-0038-1627473

185. Gao Y, He Z, Wang Z, Luo Y, Sun H, Zhou Y, et al. Increased expression and altered methylation of HERVWE1 in the human placentas of smaller fetuses from monozygotic, dichorionic, discordant twins. *PloS One* (2012) 7(3):e33503. doi: 10.1371/journal.pone.0033503

186. Huang Q, Chen H, Li J, Oliver M, Ma X, Byck D, et al. Epigenetic and non-epigenetic regulation of syncytin-1 expression in human placenta and cancer tissues. *Cell Signal* (2014) 26(3):648–56. doi: 10.1016/j.cellsig.2013.11.002

187. Yang CS, Yu C, Chuang HC, Chang CW, Chang GD, Yao TP, et al. FBW2 targets GCMa to the ubiquitin-proteasome degradation system. *J Biol Chem* (2005) 280 (11):10083–90. doi: 10.1074/jbc.M413986200

188. Chang CW, Chang GD, Chen H. A novel cyclic AMP/Epac1/CaMKI signaling cascade promotes GCM1 desumoylation and placental cell fusion. *Mol Cell Biol* (2011) 31 (18):3820–31. doi: 10.1128/MCB.05582-11

189. Chen CP, Chen CY, Yang YC, Su TH, Chen H. Decreased placental GCM1 (glial cells missing) gene expression in pre-eclampsia. *Placenta* (2004) 25(5):413–21. doi: 10.1016/j.placenta.2003.10.014

190. Chiang MH, Liang FY, Chen CP, Chang CW, Cheong ML, Wang LJ, et al. Mechanism of hypoxia-induced GCM1 degradation: implications for the pathogenesis of preeclampsia. *J Biol Chem* (2009) 284(26):17411–9. doi: 10.1074/jbc.M109.016170

191. Chuang HC, Chang CW, Chang GD, Yao TP, Chen H. Histone deacetylase 3 binds to and regulates the GCMa transcription factor. *Nucleic Acids Res* (2006) 34 (5):1459–69. doi: 10.1093/nar/gkl048

192. Chou CC, Chang C, Liu JH, Chen LF, Hsiao CD, Chen H. Small ubiquitin-like modifier modification regulates the DNA binding activity of glial cell missing drosophila homolog a. *J Biol Chem* (2007) 282(37):27239–49. doi: 10.1074/jbc.M700351200

193. Alsat E, Wyplosz P, Malassine A, Guibourdenche J, Porquet D, Nessmann C, et al. Hypoxia impairs cell fusion and differentiation process in human cytotrophoblast, *in vitro*. *J Cell Physiol* (1996) 168(2):346–53. doi: 10.1002/(SICI)1097-4652(199608)168:2<346::AID-JCP13>3.0.CO;2-1

194. Maltepe E, Krampitz GW, Okazaki KM, Red-Horse K, Mak W, Simon MC, et al. Hypoxia-inducible factor-dependent histone deacetylase activity determines stem cell fate in the placenta. *Development* (2005) 132(15):3393–403. doi: 10.1242/dev.01923

195. Wakeland AK, Soncin F, Moretto-Zita M, Chang C-W, Horii M, Pizzo D, et al. Hypoxia directs human extravillous trophoblast differentiation in a hypoxia-inducible factor-dependent manner. *Am J Pathol* (2017) 187(4):767–80. doi: 10.1016/j.ajpath.2016.11.018

196. Shoaito H, Petit J, Chissey A, Auzeil N, Guibourdenche J, Gil S, et al. The role of peroxisome proliferator-activated receptor gamma (PPARgamma) in Mono(2-ethylhexyl) phthalate (MEHP)-mediated cytotrophoblast differentiation. *Environ Health Perspect* (2019) 127(2):27003. doi: 10.1289/EHP3730

197. Kadowaki T, Hara K, Kubota N, Tobe K, Terauchi Y, Yamauchi T, et al. The role of PPARgamma in high-fat diet-induced obesity and insulin resistance. *J Diabetes Complications* (2002) 16(1):41–5. doi: 10.1016/s1056-8727(01)00206-9

198. Tache V, Ciric A, Moretto-Zita M, Li Y, Peng J, Maltepe E, et al. Hypoxia and trophoblast differentiation: a key role for PPARgamma. *Stem Cells Dev* (2013) 22 (21):2815–24. doi: 10.1089/scd.2012.0596

199. Parast MM, Yu H, Ciric A, Salata MW, Davis V, Milstone DS. PPARgamma regulates trophoblast proliferation and promotes labyrinthine trilineage differentiation. *PloS One* (2009) 4(11):e8055. doi: 10.1371/journal.pone.0008055

200. Elchalal U, Humphrey RG, Smith SD, Hu C, Sadovsky Y, Nelson DM. Troglitazone attenuates hypoxia-induced injury in cultured term human trophoblasts. *Am J Obstet Gynecol* (2004) 191(6):2154–9. doi: 10.1016/j.ajog.2004.05.009

201. Aljunaidy MM, Morton JS, Cooke CM, Davidge ST. Prenatal hypoxia and placental oxidative stress: linkages to developmental origins of cardiovascular disease. *Am J Physiol Regul Integr Comp Physiol* (2017) 313(4):R395–9. doi: 10.1152/ajpregu.00245.2017

202. Desforges M, Parsons L, Westwood M, Sibley CP, Greenwood SL. Taurine transport in human placental trophoblast is important for regulation of cell differentiation and survival. *Cell Death Dis* (2013) 4:e559. doi: 10.1038/cddis.2013.81

203. Williams JL, Fyfe GK, Sibley CP, Baker PN, Greenwood SL. K+ channel inhibition modulates the biochemical and morphological differentiation of human placental cytotrophoblast cells *in vitro*. *Am J Physiol Regul Integr Comp Physiol* (2008) 295(4): R1204–1213. doi: 10.1152/ajpregu.00193.2008

204. Fukuda T, Ikejima K, Hirose M, Takei Y, Watanabe S, Sato N. Taurine preserves gap junctional intercellular communication in rat hepatocytes under oxidative stress. *J Gastroenterol* (2000) 35(5):361–8. doi: 10.1007/s005350050361

205. Park SH, Lee H, Park KK, Kim HW, Park T. Taurine-responsive genes related to signal transduction as identified by cDNA microarray analyses of HepG2 cells. *J Med Food* (2006) 9(1):33–41. doi: 10.1089/jmf.2006.9.33

206. Shao X, Cao G, Chen D, Liu J, Yu B, Liu M, et al. Placental trophoblast syncytialization potentiates macropinocytosis *via* mTOR signaling to adapt to reduced amino acid supply. *Proc Natl Acad Sci U.S.A.* (2021) 118(3):e2017092118. doi: 10.1073/pnas.2017092118

207. Cox LS, Redman C. The role of cellular senescence in ageing of the placenta. *Placenta* (2017) 52:139–45. doi: 10.1016/j.placenta.2017.01.116

208. Munoz-Espin D, Canamero M, Maraver A, Gomez-Lopez G, Contreras J, Murillo-Cuesta S, et al. Programmed cell senescence during mammalian embryonic development. *Cell* (2013) 155(5):1104–18. doi: 10.1016/j.cell.2013.10.019

209. Regulski MJ. Cellular senescence: What, why, and how. *Wounds* (2017) 29 (6):168–74.

210. Herranz N, Gil J. Mechanisms and functions of cellular senescence. *J Clin Invest* (2018) 128(4):1238–46. doi: 10.1172/JCI95148

211. Cindrova-Davies T, Fogarty NME, Jones CJP, Kingdom J, Burton GJ. Evidence of oxidative stress-induced senescence in mature, post-mature and pathological human placentas. *Placenta* (2018) 68:15–22. doi: 10.1016/j.placenta.2018.06.307

212. Manna S, McCarthy C, McCarthy FP. Placental ageing in adverse pregnancy outcomes: Telomere shortening, cell senescence, and mitochondrial dysfunction. *Oxid Med Cell Longev* (2019) 2019:3095383. doi: 10.1155/2019/3095383

213. Campisi J, d'Adda di Fagagna F. Cellular senescence: when bad things happen to good cells. *Nat Rev Mol Cell Biol* (2007) 8(9):729–40. doi: 10.1038/nrm2233

214. Kuilman T, Michaloglou C, Mooi WJ, Peeper DS. The essence of senescence. *Genes Dev* (2010) 24(22):2463–79. doi: 10.1101/gad.1971610

215. Storer M, Keyes WM. Detection of senescence markers during mammalian embryonic development. *Methods Mol Biol* (2017) 1534:199–210. doi: 10.1007/978-1-4939-6670-7_19

216. Chuprin A, Gal H, Biron-Shental T, Biran A, Amiel A, Rozenblatt S, et al. Cell fusion induced by ERVWE1 or measles virus causes cellular senescence. *Genes Dev* (2013) 27(21):2356–66. doi: 10.1101/gad.227512.113

217. Wang E, Lee MJ, Pandey S. Control of fibroblast senescence and activation of programmed cell death. *J Cell Biochem* (1994) 54(4):432–9. doi: 10.1002/jcb.240540410

218. Gauster M, Huppertz B. The paradox of caspase 8 in human villous trophoblast fusion. *Placenta* (2010) 31(2):82–8. doi: 10.1016/j.placenta.2009.12.007

219. Davy P, Nagata M, Bullard P, Fogelson NS, Allsopp R. Fetal growth restriction is associated with accelerated telomere shortening and increased expression of cell senescence markers in the placenta. *Placenta* (2009) 30(6):539–42. doi: 10.1016/j.placenta.2009.03.005

220. Goldman-Wohl D, Yagel S. United we stand not dividing: the syncytiotrophoblast and cell senescence. *Placenta* (2014) 35(6):341–4. doi: 10.1016/j.placenta.2014.03.012

221. Cech TR. Beginning to understand the end of the chromosome. *Cell* (2004) 116 (2):273–9. doi: 10.1016/s0092-8674(04)00038-8

222. Burton GJ, Yung HW, Murray AJ. Mitochondrial - endoplasmic reticulum interactions in the trophoblast: Stress and senescence. *Placenta* (2017) 52:146–55. doi: 10.1016/j.placenta.2016.04.001

223. Hayashi T, Rizzuto R, Hajnoczky G, Su TP. MAM: more than just a housekeeper. *Trends Cell Biol* (2009) 19(2):81–8. doi: 10.1016/j.tcb.2008.12.002

224. Bravo R, Gutierrez T, Paredes F, Gatica D, Rodriguez AE, Pedrozo Z, et al. Endoplasmic reticulum: ER stress regulates mitochondrial bioenergetics. *Int J Biochem Cell Biol* (2012) 44(1):16–20. doi: 10.1016/j.biocel.2011.10.012

225. Gauster M, Maninger S, Siwetz M, Deutsch A, El-Heliebi A, Kolb-Lenz D, et al. Downregulation of p53 drives autophagy during human trophoblast differentiation. *Cell Mol Life Sci* (2018) 75(10):1839–55. doi: 10.1007/s00018-017-2695-6

226. Curtis S, Jones CJ, Garrod A, Hulme CH, Heazell AE. Identification of autophagic vacuoles and regulators of autophagy in villous trophoblast from normal term pregnancies and in fetal growth restriction. *J Matern Fetal Neonatal Med* (2013) 26 (4):339–46. doi: 10.3109/14767058.2012.733764

227. Fortini P, Iorio E, Dogliotti E, Isidoro C. Coordinated metabolic changes and modulation of autophagy during myogenesis. *Front Physiol* (2016) 7:237. doi: 10.3389/fphys.2016.00237

228. Bastida-Ruiz D, Yart L, Wuillemin C, Ribaux P, Morris N, Epiney M, et al. The fine-tuning of endoplasmic reticulum stress response and autophagy activation during trophoblast syncytialization. *Cell Death Dis* (2019) 10(9):651. doi: 10.1038/s41419-019-1905-6

229. Broad KD, Keverne EB. Placental protection of the fetal brain during short-term food deprivation. *Proc Natl Acad Sci U.S.A.* (2011) 108(37):15237–41. doi: 10.1073/pnas.1106022108

230. Hung TH, Chen SF, Lo LM, Li MJ, Yeh YL, Hsieh TT. Increased autophagy in placentas of intrauterine growth-restricted pregnancies. *PloS One* (2012) 7(7):e40957. doi: 10.1371/journal.pone.0040957

frontiers | Frontiers in Endocrinology

TYPE Original Research
PUBLISHED 14 February 2023
DOI 10.3389/fendo.2023.1092024

Check for updates

OPEN ACCESS

EDITED BY
Cilia Abad,
Charles University, Czechia

REVIEWED BY
Georgina Correia-da-Silva,
University of Porto, Portugal
Frantisek Staud,
Charles University, Czechia

*CORRESPONDENCE
Christian Wadsack
christian.wadsack@medunigraz.at

SPECIALTY SECTION
This article was submitted to Developmental Endocrinology, a section of the journal Frontiers in Endocrinology

RECEIVED 07 November 2022
ACCEPTED 27 January 2023
PUBLISHED 14 February 2023

CITATION
Berger N, van der Wel T, Hirschmugl B, Baernthaler T, Gindlhuber J, Fawzy N, Eichmann T, Birner-Gruenberger R, Zimmermann R, van der Stelt M and Wadsack C (2023) Inhibition of diacylglycerol lipase β modulates lipid and endocannabinoid levels in the *ex vivo* human placenta. *Front. Endocrinol.* 14:1092024. doi: 10.3389/fendo.2023.1092024

COPYRIGHT
© 2023 Berger, van der Wel, Hirschmugl, Baernthaler, Gindlhuber, Fawzy, Eichmann, Birner-Gruenberger, Zimmermann, van der Stelt and Wadsack. This is an open-access article distributed under the terms of the Creative Commons Attribution License (CC BY). The use, distribution or reproduction in other forums is permitted, provided the original author(s) and the copyright owner(s) are credited and that the original publication in this journal is cited, in accordance with accepted academic practice. No use, distribution or reproduction is permitted which does not comply with these terms.

Inhibition of diacylglycerol lipase β modulates lipid and endocannabinoid levels in the *ex vivo* human placenta

Natascha Berger[1], Tom van der Wel[2], Birgit Hirschmugl[1,3], Thomas Baernthaler[4], Juergen Gindlhuber[5,6], Nermeen Fawzy[7], Thomas Eichmann[3,8], Ruth Birner-Gruenberger[6,9], Robert Zimmermann[3,7], Mario van der Stelt[2] and Christian Wadsack[1,3]*

[1]Department of Obstetrics and Gynecology, Medical University of Graz, Graz, Austria, [2]Department of Molecular Physiology, Leiden Institute of Chemistry, Leiden University and Oncode Institute, Leiden, Netherlands, [3]BioTechMed-Graz, Graz, Austria, [4]Otto Loewi Research Center, Division of Pharmacology, University of Graz, Graz, Austria, [5]Ludwig Boltzmann Institute for Lung Vascular Research, Graz, Austria, [6]Diagnostic and Research Center of Molecular Medicine, Diagnostic and Research Institute of Pathology, Medical University of Graz, Graz, Austria, [7]Institute of Molecular Biosciences, University of Graz, Graz, Austria, [8]Core Facility Mass Spectrometry, Center for Medical Research (ZMF), Medical University of Graz, Graz, Austria, [9]Institute of Chemical Technologies and Analytics, Vienna University of Technology, Vienna, Austria

Introduction: Lipids and fatty acids are key components in metabolic processes of the human placenta, thereby contributing to the development of the fetus. Placental dyslipidemia and aberrant activity of lipases have been linked to diverse pregnancy associated complications, such as preeclampsia and preterm birth. The serine hydrolases, diacylglycerol lipase α and β (DAGLα, DAGLβ) catalyze the degradation of diacylglycerols, leading to the formation of monoacylglycerols (MAG), including one main endocannabinoid 2-arachidonoylglycerol (2-AG). The major role of DAGL in the biosynthesis of 2-AG is evident from various studies in mice but has not been investigated in the human placenta. Here, we report the use of the small molecule inhibitor DH376, in combination with the ex vivo placental perfusion system, activity-based protein profiling (ABPP) and lipidomics, to determine the impact of acute DAGL inhibition on placental lipid networks.

Methods: DAGLα and DAGLβ mRNA expression was detected by RT-qPCR and in situ hybridization in term placentas. Immunohistochemistry staining for CK7, CD163 and VWF was applied to localize DAGLβ transcripts to different cell types of the placenta. DAGLβ activity was determined by in- gel and MS-based activity-based protein profiling (ABPP) and validated by addition of the enzyme inhibitors LEI-105 and DH376. Enzyme kinetics were measured by EnzChek™ lipase substrate assay. *Ex vivo* placental perfusion experiments were performed +/- DH376 [1 µM] and changes in tissue lipid and fatty acid profiles were measured by LC-MS. Additionally, free fatty acid levels of the maternal and fetal circulations were determined.

Results: We demonstrate that mRNA expression of DAGLβ prevails in placental tissue, compared to DAGLα ($p \leq 0.0001$) and that DAGLβ is mainly located to CK7 positive trophoblasts ($p \leq 0.0001$). Although few DAGLα transcripts were identified,

10.3389/fendo.2023.1092024

no active enzyme was detected applying in-gel or MS-based ABPP, which underlined that DAGLβ is the principal DAGL in the placenta. DAGLβ dependent substrate hydrolysis in placental membrane lysates was determined by the application of LEI-105 and DH376. *Ex vivo* pharmacological inhibition of DAGLβ by DH376 led to reduced MAG tissue levels ($p \leq 0.01$), including 2-AG ($p \leq 0.0001$). We further provide an activity landscape of serine hydrolases, showing a broad spectrum of metabolically active enzymes in the human placenta.

Discussion: Our results emphasize the role of DAGLβ activity in the human placenta by determining the biosynthesis of 2-AG. Thus, this study highlights the special importance of intra-cellular lipases in lipid network regulation. Together, the activity of these specific enzymes may contribute to the lipid signaling at the maternal-fetal interface, with implications for function of the placenta in normal and compromised pregnancies.

KEYWORDS

human placenta, lipid metabolism, endocannabinoid system, 2-arachidonoylglycerol, diacylglycerol lipase, activity-based protein profiling, chemical proteomics, *ex vivo* placental perfusion

1 Introduction

The two transmembrane enzymes diacylglycerol lipase alpha (DAGLα) and beta (DAGLβ) possess *sn-1* specific hydrolytic activity for diacylglycerols (DAG), preferably hydrolyzing DAG species with mono- or polyunsaturated fatty acids (FA) at *sn-2* position, leading to the formation of monoacylglycerols (MAG) (1). Interestingly, DAGLα/β exhibit a diverse cell-type and tissue-specific abundancy and it has been shown that specific expression patterns and regulatory mechanisms converge into distinct physiological roles of these enzymes. DAGLα is predominately expressed in the central nervous system and mainly confined to neurons (2, 3). In contrast, DAGLβ is mainly expressed in peripheral tissues where its activity is elevated in immune cells including microglia (3), macrophages (4), dendritic cells (5) and, importantly, associated with inflammatory responses. Besides the constitutive role of DAGLα/β in DAG catabolism, DAGLβ has also been proposed as polyunsaturated fatty acid-specific triacylglycerol lipase (6).

Cell membranes of the human placenta exhibit a high abundance of polyunsaturated arachidonic acid (AA) esterified phosphoglycerides (7) and quantitative analysis of placental lipid profiles revealed a high concentration of unsaturated triacylglycerol species (8). In particular, AA is essentially involved in the development of the fetal brain during the course of pregnancy (9, 10). DAGLα/β are renown as key components of the endocannabinoid system (ECS), regulating the biosynthesis of an AA-esterified monoglyceride, namely 2-arachidonoylglycerol (2-AG). 2-AG is one of the main endocannabinoids, acting as chemical messenger and full agonist for cannabinoid receptors 1 and 2. Both, 2-AG and AA serve as substrates for the synthesis of prostanoid-esters and prostanoids, respectively. These metabolites play an important role during parturition as they mediate processes like contractions of the myometrium and they are involved in a variety of pregnancy pathologies (11–13). The importance to tightly regulate bioactive lipid species is emphasized by several studies reporting aberrant lipase action linked to first trimester miscarriage (14, 15), endometrial cancer (16) and pregnancy associated disorders such as preeclampsia (17, 18). Furthermore, emerging evidence demonstrates a strong association between pregnancy disorders and dyslipidemia (19, 20). Thus, examining one of the key enzymes in lipid metabolism, contributes not only to the basic understanding of the ECS in the human placenta, but more importantly elucidates the potential role of DAGL in pregnancy pathologies.

Although many efforts have been made to describe placental hydrolases in the past decades, many functional aspects are still unknown (21–23). Furthermore, the extent to which DAGL activity may affect metabolic cellular pathways by regulating bioactive lipids in this tissue is not yet understood. Notably, animal models have major limitations to answer this question due to differences in physiology and metabolism of the human placenta compared to other species. In human cytotrophoblasts the presence of DAGLα and the main 2-AG degradative enzyme monoacylglycerol lipase (MGL) has previously been reported (24). Epithelial-like trophoblasts build up the outermost layers of the placenta and are in direct contact with the maternal blood. The multinucleated syncytiotrophoblast derives from underlying cytotrophoblasts and facilitates the exchange of nutrients, wastes and gases between the maternal and fetal circulations. In addition, it has been demonstrated that 2-AG reduced cell viability in a choriocarcinoma cell line and showed antiproliferative effects (24). In this study, we aimed to determine the

Abbreviations: 2-AG, 2-arachidonoylglycerol; AA, Arachidonic acid; ABHD6, α/β-hydrolase domain (ABHD)-containing protein 6; ABPP, Activity- based protein profiling; AEA, Anandamide; CES, Carboxylesterase; DAG, Diacylglycerol; DAGLα, Diacylglycerol lipase alpha; DAGLβ, Diacylglycerol lipase beta; ECS, Endocannabinoid system; FA, Fatty acid; FAAH, Fatty acid amide hydrolase; HSL, Hormone-sensitive lipase; LFQ, Label-free quantification; MAG, Monoacylglycerol; MGL, Monoacylglycerol lipase.

function of DAGL enzymes in bioactive lipid metabolism in the human term placenta. Furthermore, we generated a profile of catalytically active serine hydrolases in placental tissue by using activity-based protein profiling (ABPP). Lipidomics, chemical proteomics, and *ex vivo* placental perfusion were applied to comprehensively study *in vitro* and *ex vivo* the effect of acute enzyme inhibition on placental lipid homeostasis.

2 Materials and methods

2.1 Experimental model and subject characteristics

Study was performed in accordance with the protocols approved by the ethical committee of the Medical University of Graz (Vote no: 29-319 ex 16/17 and 24-529 ex 11/12). All subjects gave written informed consent. Placentas from caesarean section and vaginal delivery were used within 20 min after delivery. Important subject characteristics of this study cohort are depicted in Table 1. In order to collect tissue samples, the placenta was divided into quadrants and a cross sectioned piece of 7-10 mm diameter was scissored from each quadrant. Tissue samples were either snap frozen in liquid nitrogen and stored at −80°C for protein isolation, or formalin fixed and embedded into paraffin for immunohistochemistry.

2.2 Quantitative real-time PCR

Frozen 20-30 mg placental tissue pieces were homogenized in 700µl Qiazol lysis reagent (Qiagen, Cat# 217004) for 20 seconds 6500 revolutions per minute, by MagnaLyser (Roche, Basel, Switzerland) followed by 1 minute on ice and repeated 3 times. Next, total RNA content from cells and tissue lysates were isolated using the RNeasy®Mini Kit (Qiagen, Cat# 217004). Reverse transcription was performed using 1µg of RNA and LUNA Script RT SuperMix Kit (New England Biolabs, Cat#E3010L). For RT-qPCR analysis LUNA Universal qPCR Master Mix (New England Biolabs, Cat#M3003E) and BioRad CFX384 Touch Syllabus were used. QuantiTect Primer Assays were used for gene amplification. For 18S reference gene amplification custom DNA oligos were designed (F-(5 '-3 ') CTACCACATCCAAGGAAGCA/R-(5 '-3 ') TTTTTCGTCACTACCTCCCCG). The expression of target genes DAGLα (GeneGlobe ID - QT00038164) and DAGLβ (GeneGlobe ID - QT00074319) was normalized to reference genes 18S, RPL30 (GeneGlobe ID - QT00056651) and HPRT1 (GeneGlobe ID - QT00059066). Target and reference gene ΔCT values are corrected for respective primer efficacy.

TABLE 1 Subject characteristics. Term placentas were collected from either caesarean section (CS) or vaginal deliveries (VD).

Term placentas, n=31		
Mode of birth (%)	CS	61.3
	VD	38.7
Gestational age	weeks ± days	39 ± 9
Placental weight [g]		616 (± 93.4)
Fetal sex (n)	Male	17
	Female	14
Fetal [g]/[cm]	weight	3312.4 (± 348.6)
	length	50.6 (± 2.1)
Maternal [kg/m^2]	pre-pregnancy BMI	21.5 (± 2.4)
	BMI at delivery	26.8 (± 3)

Subjects with a pre-pregnancy recorded disease and/or BMI >26 kg/m2 were excluded. Values are depicted as mean (± SD); n represents number of placentas used in this study.

2.3 DAGLα/β *in situ* hybridization

To detect and discriminate DAGLα and DAGLβ mRNA on cellular level, RNAscope® 2.5 HD Reagent Kit-RED assay (Advanced Cell Diagnostics, Cat#PN 322350) was used according to the manufacturer's protocol. In short, 5 µm thick formaldehyde-fixed paraffin-embedded sections were de-paraffinized and pre-treated under standard pre-treatment conditions with hydrogen peroxide, target retrieval reagents and protease solution. The sections were covered with probe solution and incubated for 2 hours at 40°C using the HybEZ Hybridization System (Advanced Cell Diagnostics, Cat#PN 321710/321720). The sections were treated with AMP 1 to 6 according to the manufacturer´s manual, using the HybEZ Hybridization System. The multi-step hybridization process included hybridization to alkaline phosphatase-labeled probes and resulted in the detection of signal using Fast Red as a substrate. To combine ISH with immunohistochemistry (IHC), after performing ISH IHC was started from the blocking step as described below.

2.4 Immunohistochemistry

Placental tissue sections were blocked with 4% BSA and 10% secondary antibody host serum in PBS/0.3% Triton X100 and incubated overnight with primary antibody solutions. Primary antibodies for cytokeratin 7 (1:500, Abgent, Cat#AJ1229a), CD163 (1:200, Thermo Fisher Scientific, Cat#MA1-82342), and Von Willebrand Factor (1:500, Dako, Cat#A0082) were used. To detect Cytokeratin 7 (CK7) and Von Willebrand Factor (VWF) goat anti-rabbit Alexa Fluor 647 secondary antibody was used (1:500, Cell Signaling Technology, Cat#4414) and displayed in white. CD163 primary antibody incubation was followed by goat anti- mouse Alexa Fluor 488 secondary antibody application (1:500, Invitrogen, Cat#A32723) and displayed in green. Sections were counterstained with DAPI, sealed with a coverslip using VECTASHIELD® Antifade Mounting Medium with DAPI (Vector Laboratories, Cat# H-1200-10) and stored at 4°C until imaged. Representative images were captured on Nikon A1 confocal microscope (original magnification ×40) and prepared using FIJI software v.1.51h.

2.5 Microscopy and signal quantification

For quantitative determination and localization analysis, ten z-stacks of each section were acquired using a Nikon A1 confocal with a ×40 objective at a step size of 0.5 µm. An automated image analysis

was created with the software package FIJI v.1.51h. The analysis entailed a basic pre-processing, generating a maximum intensity projection and mean filter smoothing, followed by application of an algorithm-based threshold. Feature detection of channels containing CK7 or ISH information was achieved employing RenyiEntropy (25), IsoData for the CD163 channel (26) and Otsu for the VWF containing channel (27). Generated regions of interest (ROI) of the ISH were separated by watershed and counted the ROIs of the remaining channels were used to determine the cell type specific ISH localization due to overlap.

2.6 Gel-based activity-based protein profiling

Gel-based ABPP experiments were performed as previously described (28). Frozen tissues were thawed on ice and homogenized in cold lysis buffer (20 mM HEPES pH 7.2, 250 mM sucrose, 1 mM MgCl2, 2.5 U/mL benzonase). After incubation on ice for 15 min, tissue debris was pelleted by centrifugation (2500 × g, 3 min, 4°C) and supernatant was transferred to a clean tube. Subsequently the supernatant was centrifuged at 30.000 × g (90-120 min, 4°C) to pellet the membrane-associated fraction and separate it from the soluble proteome. After removal of the soluble supernatant, the membrane pellet was washed with cold HEPES buffer (20 mM, pH 7.2) followed by resuspension in cold HEPES buffer by pipetting. Concentration of membrane-associated and soluble proteome was quantified (Bradford; BioRad Technologies, CA, USA) and adjusted to desired concentration (2 mg/mL) in HEPES buffer (20 mM, pH 7.2). For direct labeling, proteomes were sequentially treated with one-step activity-based probes DH379 (30 min, 1 µM, Cy3, RT) and FP-Bodipy (15 min, 500 nM, Cy2, RT) or MB064 (30 min, 250 nM, Cy3, RT) alone in a 15 µL total reaction volume. For competitive ABPP experiments, this step was preceded by incubation with DH376 *in vitro* or *ex vivo* and LEI-105 *in vitro* at indicated concentrations. The reactions were quenched by the addition of 5 µL 4x Laemmli-buffer (BioRad Technologies, CA, USA). After separation by SDS-PAGE (10% acrylamide) at 180V for 75 min, samples were visualized by in-gel fluorescence scanning (Cy2 532/28, Cy3 605/50, Cy5 700/50 filter settings) using a flatbed fluorescent scanner ChemiDoc™ MP Imaging System (Bio-Rad, Hercules, CA, USA). Coomassie staining was used to control the protein loading. Gel fluorescence is shown in greyscale, and optical density of the signals was determined using ImageLab 6.1 Biorad.

2.7 DAGLβ activity assay

Membrane fractions of placental tissues were prepared as described above (see Gel-based activity-based protein profiling (ABPP)). Membrane lysates were diluted to 10 ng/µL in assay buffer (50 mM HEPES pH 7.5, 0.0025% Triton X-100). Fluorescent measurements were carried out at RT in a black flat bottom 96-well plate (Thermo Fisher Scientific, MA, USA) in the presence of 0.5 µM EnzChek™ lipase substrate (Thermo Fisher Scientific, Cat#E33955) in 100 µL final volume using a Clariostar plate reader (BMG Labtech, Germany) and excitation/emission wavelengths of 477/525. For competitive experiments placental membrane lysates were pre-incubated with DH376 (100 nM) and LEI-105 (1 µM) for 30 min at RT, respectively. DMSO served as vehicle control and denatured samples (1% SDS, 5 min, 100°C) served as background controls. Background substrate hydrolysis was deducted from each measurement. Each data point is the mean of three technical replicates of n=3 placentas, for concentration testing and n=4 placentas for competitive experiments. The slope t=10 min to t=60 min was used as the enzymatic rate (RFU/min). Enzyme kinetics were plotted as curves in Graph Pad Prism 9 Software (GraphPad Software Inc., CA, USA).

2.8 Chemical proteomics with label-free quantification

Placental tissues were homogenized and prepared as described in Gel-based activity-based protein profiling (ABPP) section. The chemical proteomics workflow is based on previously published protocol (29) and conducted with minor modifications. In short, cytosolic and membrane fractions of placental tissue lysates (250 µg protein, 1 mg/mL, n=5) were incubated with serine hydrolase probe cocktail (10 µM MB108, 10 µM FP-Biotin, 30 min, 37 °C, 300 rpm). A pool of denatured vehicle control samples (1% SDS, 5 min, 100°C) was taken along as a negative control. Following steps were preformed according to protocol, including precipitation, alkylation, avidin enrichment, on-bead digestion, and sample preparation. Dried and desalted peptide samples were stored at -20°C until LC-MS analysis. Prior to measurement, samples were reconstituted in 50 µL 97:3:0.1 solution (H2O, ACN, FA) containing 10 fmol/µL yeast enolase digest (Waters, cat# 186002325) and transferred to LC-MS vials. Additionally, a quality control sample was prepared to prevent overloading the nanoLC system and the automatic gain control (AGC) of the QExactive HF mass spectrometer. LC-MS data was analyzed by MaxQuant software 2.0 applying match between runs. For further analysis, the following cut-offs were used: unique peptides ≥ 2, identified peptides ≥ 2, ratio positive over negative control ≥ 2. Additionally, targets were filtered against a putative probe-target list including human metabolic serine hydrolases.

2.9 *Ex vivo* placental perfusion

Placental perfusion setup is based on the setup published by Schneider et al. (30) and adapted as published by Hirschmugl et al. (31). In short, within 30 min after delivery of the placenta a single placental cotyledon chorionic-artery and vein pair was cannulated and flushed with perfusion buffer, containing DMEM (DMEM, phenol red free, Gibco by Life Technologies, ThermoFisher Scientific, MA, USA) mixed (3:1) with Earl's buffer (6.8 g/L NaCl, 0.4 g/L KCl, 0.14 g/L NaH2PO4, 0.2 g/L MgSO4•7H2O, 0.2 g/L CaCl2, 2.2 g/L NaHCO3, pH 7.4, all Merck, Darmstadt, Germany), amoxicillin (250 mg/L, Sigma-Aldrich, Steinheim, Germany), glucose (2 g/L Merck, Darmstadt, Germany), and essential fatty acid free bovine serum albumin (BSA) (35 g/L, Sigma-Aldrich, Seinheim, Germany). The cannulated cotyledon and surrounding tissue were placed in the pre-warmed perfusion chamber and the fetal circulation

was connected to a magnetic pump (Codan, Salzburg, Austria) with a constant fetal artery inflow of 3 mL/min. The perfusion buffer is constantly fumigated by a gas exchange device (LivingSystems, St. Albans, VT, US) operated with 95% N2 and 5% CO2 on the fetal site during the experiment. A micro catheter pressure sensor (Millar, US) inserted into the fetal arterial cannula recorded the backflow pressure which should not exceed an average of 65 mbar. The impermeability of the perfused cotyledon was monitored within the first 30 min and each cotyledon displayed at least 95% fetal flow recovery. The maternal circulation was established by inserting three rounded needles into the intervillous space of the cotyledon with a flow rate of 9 mL/min. During the experiment, the perfusion buffer was gassed with 5% CO_2, 20% O_2 and 75% N_2 through the gas exchanging device. DH376 (1 µM) was added to the fetal and maternal perfusion buffer reservoirs and the system changed to closed circuit in all inhibitor experiments. During the experiment maternal and fetal perfusates were collected every 30 min *via* a sampling port and oxygen (pO_2), carbon dioxide (pCO_2), pH, lactate production, and glucose consumption measurements were applied by a blood gas analyzer (Radiometer, Copenhagen, Denmark). The data sets obtained by the blood gas analyzer, magnetic pumps, and pressure sensor were registered and recorded *via* LabVIEWbased recording software (Beko engineering, Graz, Austria). After 4h of closed perfusion time, samples of both circuits were collected, centrifuged, and stored at −80°C. The perfused placental tissue was processed in cold PBS and snap frozen in liquid nitrogen until further analysis.

2.10 Lipid analysis by LC-MS

Placenta (pl, ~10 mg powdered), and perfusate (pf, 140 µl) samples were extracted according to Matyash et al. (32). In brief, samples were homogenized using two beads (stainless steel, 6 mm) on a Mixer Mill (Retsch, Haan, GER; 2x10sec, frequency 30/s) in 700 µl methyl-tert-butyl ether (MTBE)/methanol (3/1, v/v) containing 500 pmol butylated hydroxytoluene, 1% acetic acid, and internal standards (IS; pl: 20 pmol 15:0/15:0/15:0 triacylglycerol, 13 pmol rac-17:0/17:0 diacylglycerol, rac-17:0 monoacylglycerol, 50 pmol 17:0/17:0 phosphatidylcholine, Larodan, Solna, Sweden; 133 pmol 17:0/17:0 phosphatidylethanolamine, 30 pmol 17:0/17:0 phosphatidylserine, 8 pmol 17:1 lyso-phosphatidylcholine, 30 pmol 17:1 lyso-phosphatidylethanolamine, Avanti Polar Lipids, Alabaster, AL, USA; cb and pf: 2 nmol 17:0 FA, 800 pmol C21:0 FA, Sigma-Aldrich, St. Louis, MO, USA). Total lipid extraction was performed under constant shaking for 30 min at RT. After addition of 140 µl dH_2O (pl) and further incubation for 30 min at RT, samples were centrifuged at 1,000 x g for 15 min. 500 µl of the upper, organic phase were collected and dried under a stream of nitrogen. Lipids were resolved in 500 µl MTBE/methanol (3/1, v/v). Pl extracts were diluted 1:4 in 2-propanol/methanol/dH_2O (SolA; 7/2.5/1, v/v/v) for LC-MS analysis. To determine fatty acid levels, 200 µl (pf) were derivatized according to Bollinger et al. (33) using the AMP+ MS Kit (Cayman Chemical, Michigan, USA) and resolved in 500 µl SolA for LC-MS analysis. Protein precipitates of the extractions were dried, solubilized in NaOH (0.3 N) at 65°C for 4 h and the protein content was determined using Pierce™ BCA reagent (Thermo Fisher Scientific, MA, USA) and BSA as standard. Chromatographic separation was performed on a 1290 Infinity II LC system (Agilent, CA, USA) equipped with Zorbax RRHD Extend-C18 column (2.1x50 mm, 1.8 µm; Agilent, CA, USA) running a 10 min linear gradient from 60% solvent A (H2O; 10 mM ammonium acetate, 0.1% formic acid, 8 µM phosphoric acid) to 100% solvent B (2-propanol; 10 mM ammonium acetate, 0.1% formic acid, 8 µM phosphoric acid). The column compartment was kept on 50°C. A 6470 Triple Quadrupole mass spectrometer (Agilent, CA, USA) equipped with an ESI source was used for detection of lipids in positive mode. Data acquisition was done by MassHunter Data Acquisition software (B.10, Agilent, CA, USA) either in MRM (glycerol- and glycerophospholipids) or SIM (fatty acid derivatives) mode. Lipidomic data were processed using MassHunter Workstation Quantitative Analysis for QQQ (V.9, Agilent, CA, USA), normalized for recovery, extraction-, and ionization efficacy by calculating analyte/IS ratios (AU) and expressed as AU/µg protein.

2.11 Statistical analysis

Graph Pad Prism 9.02 Software (GraphPad Software Inc., CA, USA) was used for statistical analysis and graph plotting. Data are presented as mean ± SEM. All obtained datasets were tested for normal distribution with the Shapiro-Wilk and Kolmogorov-Smirnov test. Depending on the distribution of datasets parametric or non-parametric statistical tests were applied. If two or more normal distributed groups were compared student`s t-test or one-way ANOVA, including Benjamini- Hochberg *post-hoc* was performed. If the dataset did not show a normal distribution Mann-Whitney U test or Kruskal-Wallis test followed by Benjamini- Hochberg *post hoc* was applied. Two-way ANOVA was applied comparing two or more groups including different variables using Benjamini- Hochberg *post hoc* for multiple comparison correction. All herein presented p-values correspond to a FDR of 1% for multiple testing and p-values below 0.05 were considered statistically significant.

3 Results

3.1 Detection of DAGL mRNA and activity in placental tissue lysates

To elaborate DAGL expression in placental tissues, we first determined DAGLα/β mRNA levels by RT-qPCR. In comparison to DAGLα substantially higher DAGLβ expression was observed (Figure 1A, $p<0.0001$). Serine hydrolase activities in the placenta were examined by gel-based ABPP. To obtain a broad view of placental serine hydrolase activities and DAGL-specific signals, we used a probe cocktail of non- selective FP-Bodipy (34) and the DAGLα/β directed fluorescent probe DH379 (28). Using FP-Bodipy, we detected a broad spectrum of active enzymes in placental lysates. Application of DH379 visualized DAGLβ at the expected molecular weight of ~70 kDa (Figures 1B, C). To confirm the presence of active DAGLβ, competitive ABPP was applied using the DAGL inhibitors DH376 (IC_{50} 3–8 nM) (28) and LEI-105 (IC_{50} ~32 nM) (35). Application of DH376 and LEI-105 reduced DAGLβ activity in a dose-dependent manner. DH376 led to full inhibition at the lowest concentration of

10.3389/fendo.2023.1092024

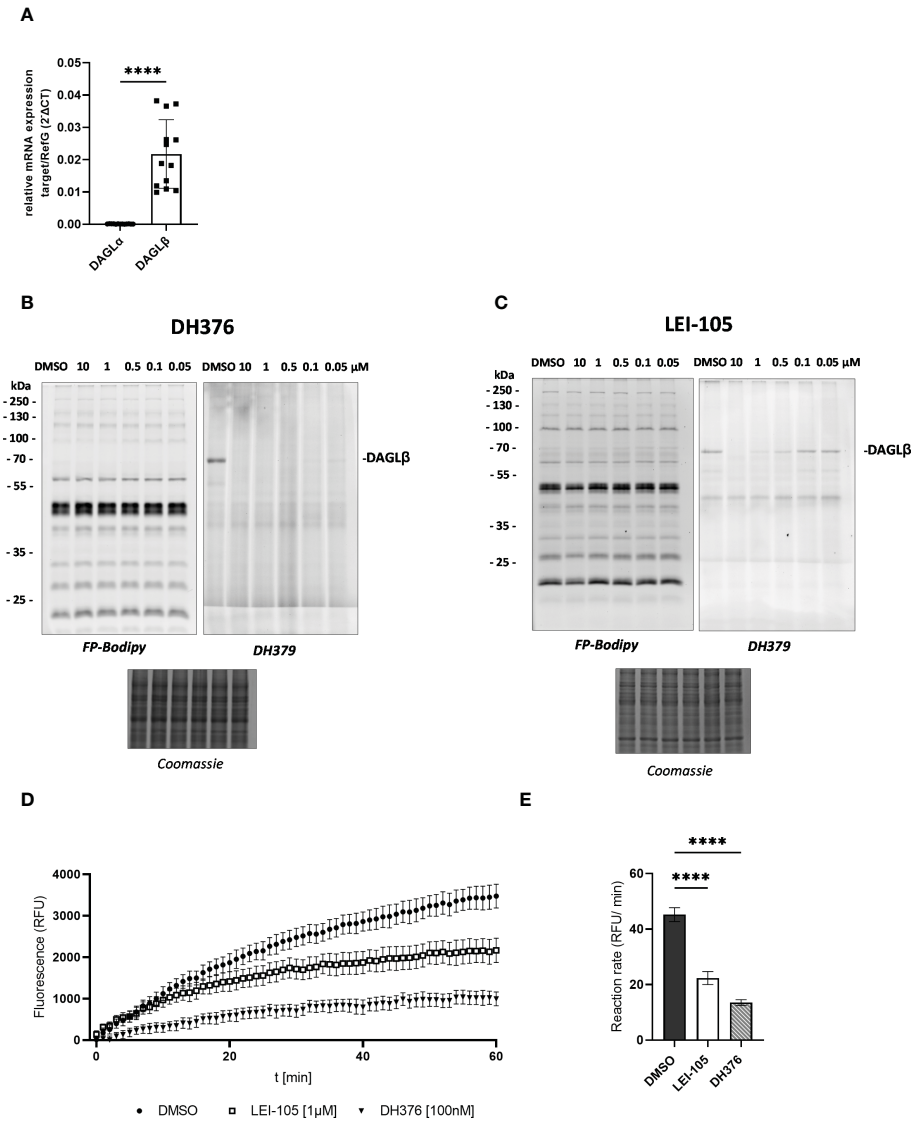


FIGURE 1
Detection of DAGL mRNA and activity in placental tissue lysates. **(A)** Relative DAGLα/β target gene mRNA levels were detected by RT-qPCR. Results were normalized to reference genes (RefG) 18S, RLP30 and HRPT1 detected in each sample and calculated as ΔCT. For statistics student`s t-test was applied and ΔCT values are depicted as 2 -ΔCT (n=13). **(B)**, **(C)** Visualization of DAGLβ activity and selectivity profile of DH376 and LEI-105 using in-gel ABPP. Placental membrane proteomes were profiled by competitive ABPP using a probe cocktail of FP-Bodipy [500 nM] (Cy2, green) and DH379 [1 µM] (Cy3, red). Samples were incubated with indicated inhibitor concentrations or DMSO as a vehicle control. Concentration-dependent inhibition of DAGLβ by DH376 **(B)** and LEI-105 **(C)**. Coomassie staining served as a protein loading control. **(D)** Hydrolase activity was determined using EnzChek™ lipase substrate [0.5µM] and displayed as relative fluorescence units (RFU) per time. DAGLβ activity determined by applying LEI-105 [1 µM] and DH376 [100 nM]. **(E)** The slope of the linear interval t=10 to t=60 min was used to calculate the enzymatic rate (RFU/min). One-way ANOVA for multiple comparisons followed by Benjamini- Hochberg *post hoc* was applied to quantify the differences of enzymatic activities (n=4). Data are depicted in mean ± SEM; ****p ≤ 0.0001.

0.1 µM (Figure 1B), while LEI-105 treatment led to a substantial reduction of DAGLβ signals at a concentration of 0.5 µM (Figure 1C). Notably, we were not able to detect DAGLα activity at the expected molecular weight of ~120 kDa, using the DAGLα tailored probe MB064 (36), likely due to low expression levels compared to DAGLβ (Supplementary Figure 1). DAGLβ activity in placenta tissue lysates was also investigated using the commercially available lipase substrate EnzChek™ (Figure 1D). We applied 100 nM of DH376, which represented the lowest inhibitor concentration leading to potent enzyme inhibition of DAGLβ in-gel (Figure 1B). In comparison to DH376, LEI-105 exhibits lower activity against DAG-lipases and acts as a reversible enzyme inhibitor. Although a substantial reduction in DAGLβ enzyme activity was observed by application of 0.5 µM (Figure 1C), we applied 1 µM LEI-105 to ensure complete enzyme inhibition over time. The application of LEI-105 and DH376 reduced hydrolase activity by 51% and 70%, respectively (Figure 1E). The differences in inhibitor efficacy can be explained by previous observations showing that LEI-105 exhibits higher selectivity for DAGLβ than DH376. At the used inhibitor concentration, DH376 is expected to inhibit α/β hydrolase domain-containing protein 6 (ABHD6), carboxylesterase 1 and 2 (CES1/2), and hormone- sensitive lipase (HSL) (28), which can contribute to the hydrolysis of the EnzChek™ substrate. Gel-based ABPP experiments enabled us to detect specific DAGLβ activity in placental tissue and we could

further decipher DAGL-dependent substrate hydrolysis by administration of DH376 and LEI-105. Overall, our observations indicate that the placenta predominantly expresses DAGLβ, which consequently can affect DAG, MAG, and fatty acid (FA) metabolism.

3.2 Activity profiling of placental metabolic serine hydrolases

ABPP using FP-Bodipy already suggested that the placenta expresses a broad spectrum of serine hydrolases (Figures 1B, C). To get a profile of these enzymes, we performed mass spectrometry-based chemical proteomics utilizing the biotinylated non- selective probes MB108 and FP-Biotin for target identification. While gel-based ABPP experiments strongly rely on specific inhibitors for target identification, MS- based ABPP enables target enrichment and provides high sensitivity. To increase the resolution of proteins, tissue lysates were separated into membrane and cytosolic fraction. This approach resulted in the identification of 38 and 33 different serine hydrolases in membrane and cytosolic fractions, respectively (Figure 2). Activities of several α/β hydrolase domain-containing protein family members (ABHD) and phospholipases such as DDHD2, patatin-like phospholipase domain-containing proteins (PNPLA) and members of the phospholipase A2 family (PLA2) were identified. Furthermore, lipases involved in DAG, MAG and FA metabolism, including HSL, CES1/2 and acyl-coenzyme A thioesterase (ACOT1) were detected. Within the 2-AG biosynthetic active enzymes, we again exclusively detected DAGLβ activity. Taken together, performing chemical proteomics allowed us to generate an overview of the lipolytic proteome of human placental tissue and demonstrated a broad spectrum of metabolic hydrolase activities.

3.3 DAGLβ expression is mainly confined to trophoblasts

As the human placenta is composed of different highly specialized cell types, we aimed to determine the localization of DAGLβ *in situ*, by using specific RNA probes. To localize the transcripts to distinct cell types of the placenta, immunofluorescence (IF) was applied. The visualization of DAGLβ transcripts was combined with cytokeratin 7 (CK7) staining, representing trophoblasts, which are building up the first structural barrier between maternal and fetal compartment and CD163 as a pan macrophage marker (Figure 3A). To identify feto-placental endothelial cells, which are lining placental vessels and are in direct contact with fetal blood, Von- Willebrand Factor (VWF) was applied (Figure 3B). We localized DAGLβ transcripts mainly to CK7 positive trophoblasts (Figure 3A). Quantitative analysis of the signals

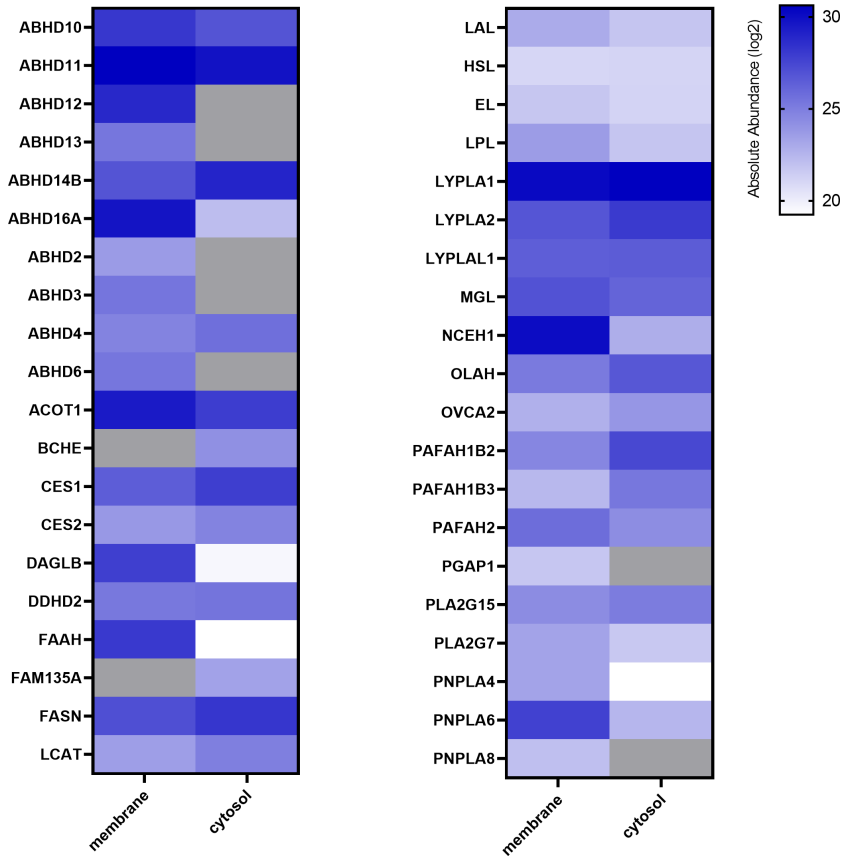


FIGURE 2
Activity profiling of placental metabolic serine hydrolases. Membrane and cytosolic tissue protein fractions were labeled with hydrolase probe cocktail (MB108, FP-Biotin [10 μM]) and analyzed by chemical proteomics. Absolute abundance refers to the mean of LFQ intensities of vehicle perfused placentas and is depicted in alphabetical order as heat map (blue scale, log2), not detected proteins are depicted in grey (n=5).

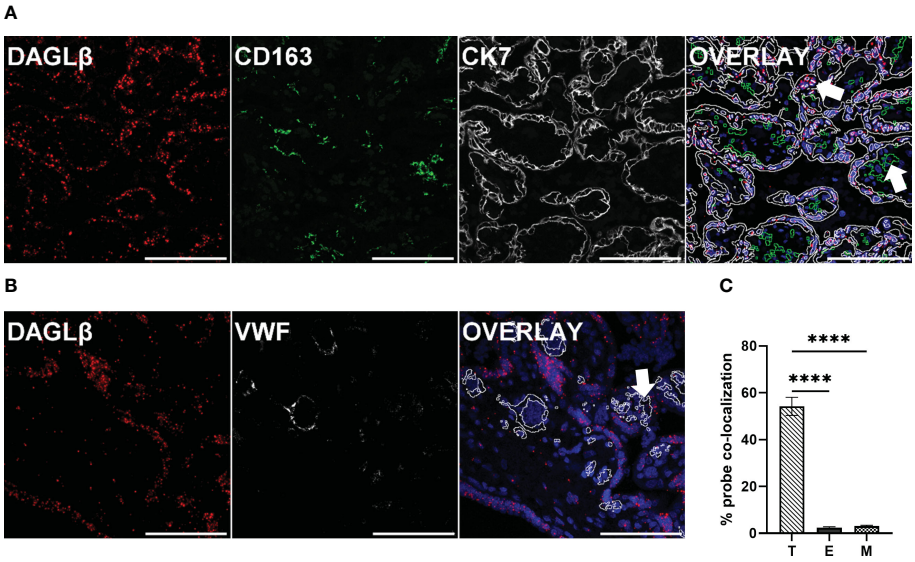


FIGURE 3
DAGLβ expression is mainly confined to trophoblasts. DAGLβ transcripts were detected in placental tissues using RNAscope® 2.5 HD RED assay. **(A)** DAGLβ transcripts detected in CK7 positive trophoblasts and CD163 positive placental macrophages. **(B)** DAGLβ mRNA was localized to VWF stained endothelial cells. Nuclei were counterstained with DAPI (blue). Arrowheads in merged micrographs indicate probe co-localization to different cell types. Magnification x40, Scale bar 100 µm. For quantitative determinations, ten images of four individual placentas were captured on Nikon A1 confocal microscope. Probe co-localization was quantified by Fiji software. **(C)** Relative distribution of DAGLβ transcripts to trophoblasts (T), endothelial cells **(E)** and placental macrophages (M) based on ISH signals (n=4). Statistical analysis was performed using one- way ANOVA, followed by Benjamini-Hochberg *post hoc* test (n=4). Representative stainings are shown in **(A)** and **(B)**. Data are depicted in mean ± SEM; ****p < 0.0001.

revealed that 54% of DAGLβ mRNA was localized to trophoblasts (T), while negligible signals of 2% and 3% were detected in endothelial cells (E) and macrophages (M), respectively (Figure 3C). In contrast to DAGLβ, we could not detect clear signals for DAGLα, confirming our observation that this enzyme is poorly expressed in the human placenta (Supplementary Figure 2).

3.4 Inhibition of DAGLβ activity leads to reduced DAG, MAG and FA levels in perfused placental tissue

To better understand the specific function of DAGLβ in the intact organ, the lipid profile was examined after tissue perfusion with/out inhibitor. First, we examined the extent of DAGLβ inhibition obtained after perfusion by in-gel ABPP. Using DH379, we again identified the DAGLβ band (~70 kDa) in the vehicle perfused proteome (Figure 4A; Supplementary Figure 3). By co-application of DH376 [1µM], signal intensity was strongly reduced by 87%, confirming target engagement (Figure 4B). Thus, our results suggest that the application of DH376 at a concentration of 1 µM in an *ex vivo* setting leads to substantial inhibition of DAGL, which may also be accompanied by changes in the lipid profile. To examine the consequences of DAGLβ inhibition under the applied conditions, we analyzed changes in lipid species in perfused placental tissue. In accordance with the proposed cellular function of DAGL, total MAG levels were decreased by 60% (Figure 4C), resembled by a reduction of all detected MAG species (Figure 4D). Notably, the obtained data further demonstrated significant decreased 2-AG levels (MAG 20:4) upon inhibition of DAGLβ (Figure 4D). Interestingly, decreased MAG levels were not accompanied by augmented DAG concentrations, but a trend to decreased levels could be detected (Figure 4E). In fact, we observed significant reductions in specific DAG species, including DAG 32:0-16:0, DAG 34:2-18:2 and DAG 36:2-18:2 (Figure 4F). Furthermore, FA concentrations showed a downward trend in inhibitor perfused tissues (Figure 4G), of which eicosenoic acid (FA 20:1) was significantly reduced, indicating an effect on the hydrolysis of *sn-1* FA of DAGs (Figure 4H). In contrast, FA levels in the maternal and fetal circuit remained unchanged (Supplementary Figures 4A, B).

4 Discussion

DAG lipases occupy a central role in multiple lipid signaling pathways by regulating DAG (37), endocannabinoid levels and downstream inflammatory mediators (4, 28). Studies in mice demonstrated that acute blockade of DAGL by DH376 *in vivo* led to significant reductions in endocannabinoid-, AA-, and prostaglandin levels in the central nervous system (28). Moreover, it has been shown that pharmacological inhibition and genetic disruption of DAGLα/β suppress induction of 2-AG and prostaglandin levels upon lipopolysaccharide treatment, which was accompanied by decreased pro-inflammatory cytokine secretion (4, 5, 28). Recently, Shin et al. identified DAGLβ as polyunsaturated fatty acid- specific triacylglycerol lipase by demonstrating robust hydrolysis activity for triarachidonin (C20:4 FA) or tridocosahexaenoin (C22:6 FA) *in vitro* (6). Hence, understanding the role of these versatile enzymes in human physiology and disease gained considerable interest. Here, we aimed to study the role of DAGL in placental lipid homeostasis.

ABPP assays were used to screen for serine hydrolase activities in the human placenta and particularly to examine the functional state

10.3389/fendo.2023.1092024

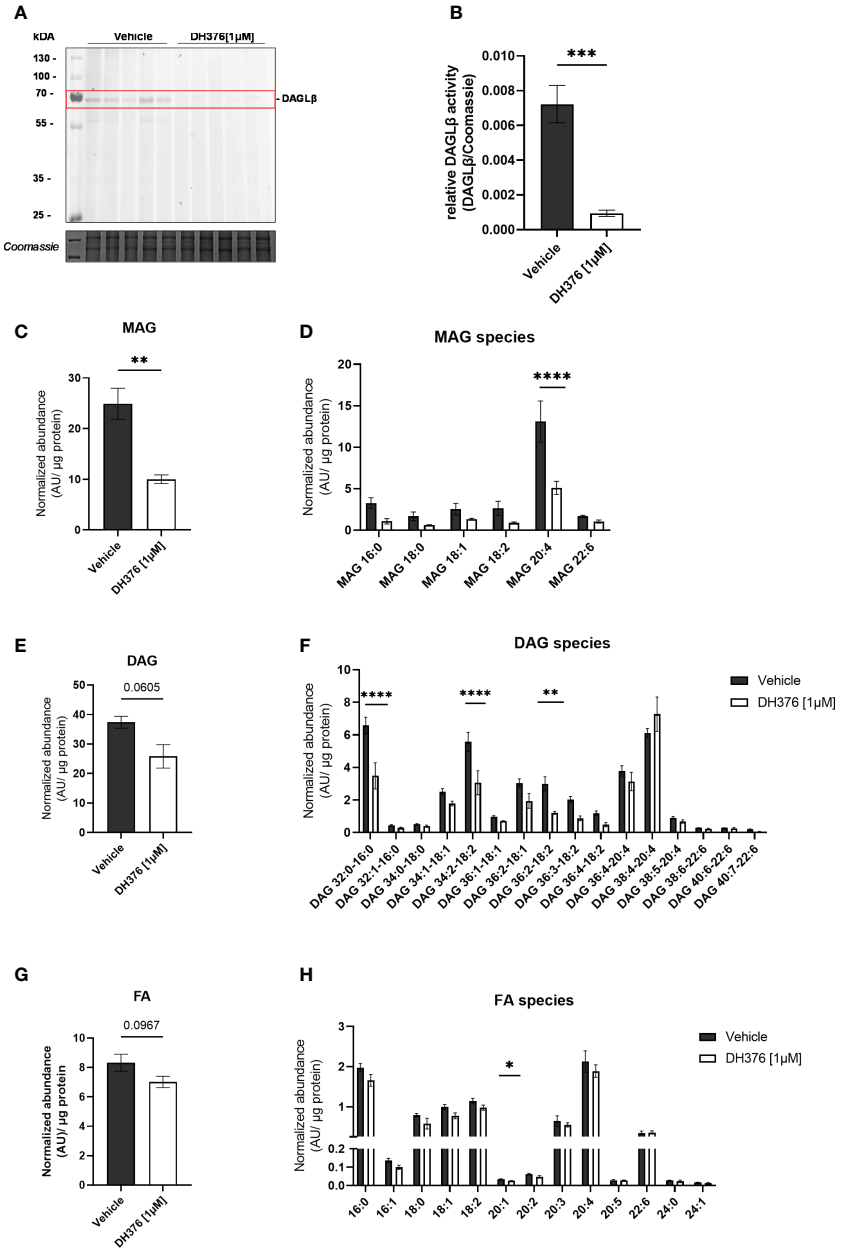


FIGURE 4
Inhibition of DAGLβ activity leads to reduced DAG, MAG and FA levels in perfused placental tissue. **(A)** *In vitro* labeling of enzymes in DH376 [1 µM] and vehicle perfused placental membrane proteomes by direct ABPP using DH379. **(B)** Densiometric quantification of in gel ABPP demonstrated significantly decreased DAGLβ activity in DH376 perfused placentas compared to vehicle controls. Student´s t-test was performed for statistical testing (n=5). **(C)** Total monoacylglycerol (MAG) tissue levels in DH376 [1 µM] and vehicle perfused tissues. **(D)** Depiction of all measured MAG species by LC-MS. **(E)** LC-MS analysis of total diacylglycerol tissue levels (DAG) and diacylglycerol species in vehicle and DH376 perfused placental tissues **(F)**. **(G)** Total tissue FA levels and corresponding FA species **(H)**. Lipid levels are expressed as arbitrary units (AU) and were normalized to total tissue protein (µg). Student´s t-test and multiple t-test followed by Benjamini- Hochberg *post hoc* was performed, respectively (n=3 lipid levels, n=5 FA levels). Data are depicted as mean ± SEM; *p ≤ 0.05, **p ≤ 0.01, ***p ≤ 0.001, ****p< 0.0001.

of DAGL enzymes. The use of a fluorescent DAGL-tailored probe enabled us to detect DAGLβ activity at the corresponding molecular weight of ~70 kDa. Competitive ABPP with selective inhibitors confirmed that the signal was DAGLβ. DH376 has been described as potent, central active and covalent DAGL inhibitor (IC_{50} of 3-8 nM) (28). Since it has been reported that this compound cross-reacts with several other lipases such as CES1/2, HSL and ABHD6, we decided to include LEI-105 to verify our findings. LEI-105 is described as highly selective, but reversible DAGL inhibitor (IC_{50} ~32 nM) (35). Importantly, it has been shown that this compound did not affect the activity of other endocannabinoid-related hydrolases such as ABHD6 (35). Complete enzyme inhibition of placental DAGLβ could be achieved by applying relatively high inhibitor concentrations, as LEI-105 represents a non-covalent inhibitor and shows ~4-fold lower activity against DAGL enzymes compared to DH376. In conclusion, administration of LEI-105 validated our observations in-gel and contributed to the determination of DAGL- dependent substrate hydrolysis. Conversely, DAGLα activity was not detectable

by ABPP, suggesting that DAGLβ is the principal active DAG-lipase in the human term placenta. The predominance of DAGLβ over α in placental tissue was further corroborated on transcriptional level *in vitro* as well as *in situ*. These findings are in accordance with previous studies showing that DAGLβ is mainly found in peripheral metabolically active tissues such as the liver, where DAGLβ-/- mice showed 90% reductions in 2-AG levels (2). As placental tissue is composed of different cell types, we specifically looked at the spatial expression of DAGLβ. DAGLβ transcripts were mainly located to CK7-postive trophoblasts, lining the first cellular barrier between the maternal and fetal circulation. Co-localization of DAGLβ to trophoblasts, which reflect the main site of action upon maternally derived signals, is in concordance with the expression sites of other lipid related enzymes in this organ (38).

In order to assess the importance of DAGL in the spectrum of the lipolytic enzymes in placental tissue we further generated an activity- based profile of serine hydrolases. The chemoproteomic analysis revealed a broad spectrum of hydrolases, which determine lipid metabolism and signaling. Within the 2-AG biosynthetic enzymes we again exclusively detected DAGLβ. Further, specific activity of enzymes involved in degradation of 2-AG, such as MGL, fatty acid amide hydrolase (FAAH), ABHD6 and ABHD12 was detected. It has been shown that beside MGL, which is the main enzyme for 2-AG hydrolysis, ABHD6/12 and FAAH also possess 2-AG hydrolytic activity (39, 40). Blankman et al. suggested that the simultaneous occurrence of different 2-AG hydrolytic enzymes could be explained by the regulation of distinct subcellular 2-AG pools. In accordance with previous observations, ABHD6/12 were exclusively identified in placental membrane preparations, whereas MGL activity was found in the cytosolic and membrane fraction (40). Interestingly, ABHD12 showed the highest activity in our dataset, compared to other 2-AG metabolizing enzymes. The major function of ABHD12 is the hydrolysis of lysophosphatidylserine as shown by genetic depletion in mice (41). The specific role of this enzyme in the placenta remains to be investigated, since only descriptive data is available yet (22). Besides 2-AG, anandamide (AEA) was one of the first discovered endocannabinoids and FAAH is the main catabolic enzyme in this pathway (42). Moreover, ABHD4 activity was detected, which contributes to AEA biosynthesis. In addition, several hydrolases determining lipid and FA metabolism, including (lyso)phospholipases, HSL and CES1/2 were identified.

This study set out with the aim of assessing the importance of DAGLβ activity in the lipid homeostasis of the human term placenta. Therefore, we looked at the functional consequences of pharmacological enzyme inhibition *ex vivo*, by applying DH376 as an inhibitor targeting DAGL activity. Lipidomic analysis of perfused tissue samples showed that acute inhibition of DAGLβ led to significantly reduced total MAG tissue levels, confirming the well-described role of DAGL in DAG catabolism. In fact, we could observe a significant decrease in 2-AG levels and a trend towards reduced saturated as well as mono- and polyunsaturated MAG species. In contrast to previously published data, the decrease in MAG levels was not followed by an increase in respective DAGs, suggesting that DAGs are efficiently metabolized in the absence of DAGL. Interestingly, specific DAG species showed a significant reduction upon DAGLβ inhibition, indicating that the enzyme may possess hydrolase activity against TAGs. In this context, DAGLβ has been previously described as polyunsaturated-specific TAG lipase in mice using genetic and pharmacological approaches (6). The decline in eicosenoic acid (FA 20:1), in inhibitor perfused tissues, suggests that DAGLβ prefers 20:1 species at *sn-1* position of DAGs. Interestingly, we could not detect considerable differences of FA levels neither in the maternal nor in the fetal circulation. In contrast, *in vivo* pharmacological inhibition of DAGLα/β by DH376 led to significant reductions of AA levels in murine central nervous tissues (28). Unchanged AA levels could be explained by compensatory or bypass activities ensuring a constant supply of polyunsaturated fatty acids to the fetus. Furthermore, Hirschmugl et al. demonstrated that only a small proportion of free FA are directly transferred across the placenta and emphasized the tightly regulated release of FA out of metabolic pools of the placenta (31). It is also important to note that DAGLβ is predominantly expressed in trophoblasts and lipid extracts were obtained from whole tissue. Nonetheless, we observed a substantial decrease in MAGs indicating that DAGLβ activity strongly affects lipid homeostasis distinctively in this specific placental cell type.

This study describes for the first time that 2-AG is dramatically reduced after DAGL inactivation in the human placenta. Since 2-AG represents only one of the main endocannabinoids, this study is limited by the lack of information on the potential simultaneous regulation of AEA. Although, both endocannabinoids exhibit distinct synthesis, transport and degradation processes, one may speculate that alterations in lipid levels affect concomitant lipid signaling pathways, and compensatory or bypass mechanisms could be activated to restore lipid homeostasis. In particular, a potential mechanism for synaptic crosstalk and feed-back regulatory mechanisms between the two pathways has already been described in tissues of the central nervous system (43, 44). Furthermore, only one inhibitor concentration and experimental timepoint was used for *ex vivo* experiments. Since DAGLα exhibits a short half- life (< 4 h) and cumulative evidence supports the on-demand model of endocannabinoid biosynthesis (28, 45), it would be of great interest to study the consequences of enzyme blockage on the dynamic composition of placental lipids over time.

In summary, our study demonstrates that the application of small molecule inhibitors in perfusion experiments provides a very useful tool to investigate enzyme function as close as possible to the *in vivo* situation. In addition, ABPP is a powerful technique to visualize the active pool of enzymes and confirm target engagement in such *ex vivo* tissue experiments. The integration of these two approaches provided evidence that inhibition of DAGLβ affects tissue lipid homeostasis with no direct effect on the FA profile in the maternal or fetal compartment. We expect that further experiments by utilizing serine hydrolase inhibitors will strongly improve our understanding of the role of these enzymes in lipid signaling and metabolism at the maternal-fetal interface and reveal important insights related to placental function in normal and compromised pregnancies.

Data availability statement

The mass spectrometry proteomics data have been deposited to the ProteomeXchange Consortium via the PRIDE (46) partner repository with the dataset identifier PXD039930.

Ethics statement

The studies involving human participants were reviewed and approved by Ethical Committee of the Medical University of Graz,

Graz, Austria. The patients/participants provided their written informed consent to participate in this study.

Author contributions

Conceptualization, CW and NB. Methodology, NB, BH, TB, TW, TE and NF. Software, JG. Investigation, NB, TE and NF. Writing – Original Draft, NB, CW, BH and RZ. Funding Acquisition, CW. Resources, MS, RB-G and RZ. Supervision, CW, BH, TW, MS and RZ. All authors contributed to the article and approved the submitted version.

Funding

This work was supported by the Austrian Science Fund FWF (DOC 31-B26, SFB Lipid hydrolysis F73, DK-MCD W1266) and the Medical University of Graz through the PhD Program Inflammatory Disorders in Pregnancy (DP-iDP).

Acknowledgments

We thank T. Schreiner and R. Breinbauer for the synthesis of 1-Oleoyl-2-arachidonoyl-sn-glycerol to test DAGL activity. We acknowledge K. Hsu for kindly providing the HT-01 and FP-TAMRA small molecule probes to establish our ABPP protocols.

Conflict of interest

The authors declare that the research was conducted in the absence of any commercial or financial relationships that could be construed as a potential conflict of interest.

Publisher's note

All claims expressed in this article are solely those of the authors and do not necessarily represent those of their affiliated organizations, or those of the publisher, the editors and the reviewers. Any product that may be evaluated in this article, or claim that may be made by its manufacturer, is not guaranteed or endorsed by the publisher.

Supplementary material

The Supplementary Material for this article can be found online at: https://www.frontiersin.org/articles/10.3389/fendo.2023.1092024/full#supplementary-material

References

1. Bisogno T, Howell F, Williams G, Minassi A, Cascio MG, Ligresti A, et al. Cloning of the first sn1-DAG lipases points to the spatial and temporal regulation of endocannabinoid signaling in the brain. *J Cell Biol* (2003) 163(3):463–8. doi: 10.1083/jcb.200305129

2. Gao Y, Vasilyev DV, Goncalves MB, Howell FV, Hobbs C, Reisenberg M, et al. Loss of retrograde endocannabinoid signaling and reduced adult neurogenesis in diacylglycerol lipase knock-out mice. *J Neurosci* (2010) 30(6):2017–24. doi: 10.1523/JNEUROSCI.5693-09.2010

3. Viader A, Ogasawara D, Joslyn CM, Sanchez-Alavez M, Mori S, Nguyen W, et al. A chemical proteomic atlas of brain serine hydrolases identifies cell type-specific pathways regulating neuroinflammation. *Elife* (2016) 5. doi: 10.7554/eLife.12345

4. Hsu KL, Tsuboi K, Adibekian A, Pugh H, Masuda K, Cravatt BF. DAGLβ inhibition perturbs a lipid network involved in macrophage inflammatory responses. *Nat Chem Biol* (2012) 8(12):999–1007. doi: 10.1038/nchembio.1105

5. Shin M, Buckner A, Prince J, Bullock TNJ, Hsu KL. Diacylglycerol lipase-β is required for TNF-α response but not CD8+ T cell priming capacity of dendritic cells. *Cell Chem Biol* (2019) 26(7):1036–1041.e3. doi: 10.1016/j.chembiol.2019.04.002

6. Shin M, Ware TB, Hsu KL. DAGL-beta functions as a PUFA-specific triacylglycerol lipase in macrophages. *Cell Chem Biol* (2020) 27(3):314–321.e5. doi: 10.1016/j.chembiol.2020.01.005

7. Bitsanis D, Crawford MA, Moodley T, Holmsen H, Ghebremeskel K, Djahanbakhch O. Arachidonic acid predominates in the membrane phosphoglycerides of the early and term human placenta. *J Nutr* (2005) 135(11):2566–71. doi: 10.1093/jn/135.11.2566

8. Brown SHJ, Eather SR, Freeman DJ, Meyer BJ, Mitchell TW. A lipidomic analysis of placenta in preeclampsia: Evidence for lipid storage. *PloS One* (2016) 11(9):e0163972. doi: 10.1371/journal.pone.0163972

9. Basak S, Mallick R, Banerjee A, Pathak S, Duttaroy AK. Maternal supply of both arachidonic and docosahexaenoic acids is required for optimal neurodevelopment. *Nutrients* (2021) 13(6):2061. doi: 10.3390/nu13062061

10. Brittis PA Walsh FS, Doherty PSJ. Fibroblast growth factor receptor function is required for the orderly projection of ganglion cell axons in the developing mammalian retina. *Mol Cell Neurosci* (1996) 8(2/3):120–8. doi: 10.1006/mcne.1996.0051

11. Mitchell MD. Prostaglandins during pregnancy and the perinatal period. *Reproduction* (1981) 62(1):305–15. doi: 10.1530/jrf.0.0620305

12. Szczuko M, Kikut J, Komorniak N, Bilicki J, Celewicz Z, Ziętek M. The role of arachidonic and linoleic acid derivatives in pathological pregnancies and the human reproduction process. *Int J Mol Sci* (2020) 21(24):9628. doi: 10.3390/ijms21249628

13. Phillips RJ, Fortier MA, López Bernal A. Prostaglandin pathway gene expression in human placenta, amnion and choriodecidua is differentially affected by preterm and term labour and by uterine inflammation. *BMC Pregnancy Childbirth* (2014) 14:241. doi: 10.1186/1471-2393-14-241

14. Maccarrone M. Low fatty acid amide hydrolase and high anandamide levels are associated with failure to achieve an ongoing pregnancy after IVF and embryo transfer. *Mol Hum Reprod* (2002) 8(2):188–95. doi: 10.1093/molehr/8.2.188

15. Habayeb OMH, Taylor AH, Evans MD, Cooke MS, Taylor DJ, Bell SC, et al. Plasma levels of the endocannabinoid anandamide in women–a potential role in pregnancy maintenance and labor? *J Clin Endocrinol Metab* (2004) 89(11):5482–7. doi: 10.1210/jc.2004-0681

16. Guida M, Ligresti A, De Filippis D, D'Amico A, Petrosino S, Cipriano M, et al. The levels of the endocannabinoid receptor CB2 and its ligand 2-arachidonoylglycerol are elevated in endometrial carcinoma. *Endocrinology* (2010) 151(3):921–8. doi: 10.1210/en.2009-0883

17. Fügedi G, Molnár M, Rigó J, Schönléber J, Kovalszky I, Molvarec A. Increased placental expression of cannabinoid receptor 1 in preeclampsia: An observational study. *BMC Pregnancy Childbirth* (2014) 14(1):395. doi: 10.1186/s12884-014-0395-x

18. Abán C, Leguizamón GF, Cella M, Damiano A, Franchi AM, Farina MG. Differential expression of endocannabinoid system in normal and preeclamptic placentas: effects on nitric oxide synthesis. *Placenta* (2013) 34(1):67–74. doi: 10.1016/j.placenta.2012.10.009

19. Smith CJ, Baer RJ, Oltman SP, Breheny PJ, Bao W, Robinson JG, et al. Maternal dyslipidemia and risk for preterm birth. *PloS One* (2018) 13(12):e0209579. doi: 10.1371/JOURNAL.PONE.0209579

20. Wojcik-Baszko D, Charkiewicz K, Laudanski P. Role of dyslipidemia in preeclampsia–a review of lipidomic analysis of blood, placenta, syncytiotrophoblast microvesicles and umbilical cord artery from women with preeclampsia. *Prostaglandins Other Lipid Mediat* (2018) 139:19–23. doi: 10.1016/J.PROSTAGLANDINS.2018.09.006

21. Lindegaard MLS, Olivecrona G, Christoffersen C, Kratky D, Hannibal J, Petersen BL, et al. Endothelial and lipoprotein lipases in human and mouse placenta. *J Lipid Res* (2005) 46(11):2339–46. doi: 10.1194/jlr.M500277-JLR200

22. Maia J, Fonseca BM, Cunha SC, Braga J, Gonçalves D, Teixeira N, et al. Impact of tetrahydrocannabinol on the endocannabinoid 2-arachidonoylglycerol metabolism: ABHD6 and ABHD12 as novel players in human placenta. *Biochim Biophys Acta Mol Cell Biol Lipids* (2020) 1865(12):158807. doi: 10.1016/j.bbalip.2020.158807

23. Besenboeck C, Cvitic S, Lang U, Desoye G, Wadsack C. Going into labor and beyond: phospholipase A2 in pregnancy. *Reproduction* (2016) 151(6):R91–102. doi: 10.1530/REP-15-0519

24. Costa MA, Fonseca BM, Keating E, Teixeira NA, Correia-Da-Silva G. 2-arachidonoylglycerol effects in cytotrophoblasts: Metabolic enzymes expression and apoptosis in BeWo cells. *Reproduction* (2014) 147(3):301–11. doi: 10.1530/REP-13-0563

25. Shanbhag AG. Utilization of information measure as a means of image thresholding. *CVGIP Graph Model Image Process* (1994) 56(5):414–9. doi: 10.1006/cgip.1994.1037

26. Ridler TW, Calvard S. Picture Thresholding Using an Iterative Selection Method. *IEE Transactions on Systems, Man, and Cybernetics*. (1978) 8(8):630–2. doi: 10.1109/TSMC.1978.4310039

27. Otsu N. A threshold selection method from Gray-level histograms. *IEEE Trans Systems Man Cybernetics* (1979) 9:62–6. doi: 10.1109/TSMC.1979.4310076

28. Ogasawara D, Deng H, Viader A, Baggelaar MP, Breman A, den Dulk H, et al. Rapid and profound rewiring of brain lipid signaling networks by acute diacylglycerol lipase inhibition. *Proc Natl Acad Sci* (2016) 113(1):26–33. doi: 10.1073/pnas.1522364112

29. van Rooden EJ, Florea BI, Deng H, Baggelaar MP, van Esbroeck ACM, Zhou J, et al. Mapping *in vivo* target interaction profiles of covalent inhibitors using chemical proteomics with label-free quantification. *Nat Protoc* (2018) 13(4):752–67. doi: 10.1038/nprot.2017.159

30. Schneider H, Huch A. Dual *in vitro* perfusion of an isolated lobe of human placenta: method and instrumentation. *Contrib Gynecol Obstet* (1985) 13:40–7. doi: 10.1159/000410668

31. Hirschmugl B, Perazzolo S, Sengers BG, Lewis RM, Gruber M, Desoye G, et al. Placental mobilization of free fatty acids contributes to altered materno-fetal transfer in obesity. *Int J Obes* (2021) 45(5):1114–23. doi: 10.1038/s41366-021-00781-x

32. Matyash V, Liebisch G, Kurzchalia TV, Shevchenko A, Schwudke D. Lipid extraction by methyl-tert-butyl ether for high-throughput lipidomics. *J Lipid Res* (2008) 49(5):1137–46. doi: 10.1194/jlr.D700041-JLR200

33. Bollinger JG, Thompson W, Lai Y, Oslund RC, Hallstrand TS, Sadilek M, et al. Improved sensitivity mass spectrometric detection of eicosanoids by charge reversal derivatization. *Anal Chem* (2010) 82(16):6790–6. doi: 10.1021/ac100720p

34. Janssen APAA, van der Vliet D, Bakker AT, Jiang M, Grimm SH, Campiani G, et al. Development of a multiplexed activity-based protein profiling assay to evaluate activity of endocannabinoid hydrolase inhibitors. *ACS Chem Biol* (2018) 13(9):2406–13. doi: 10.1021/acschembio.8b00534

35. Baggelaar MP, Chameau PJPP, Kantae V, Hummel J, Hsu KL, Janssen F, et al. Highly selective, reversible inhibitor identified by comparative chemoproteomics modulates diacylglycerol lipase activity in neurons. *J Am Chem Soc* (2015) 137 (27):8851–7. doi: 10.1021/jacs.5b04883

36. Baggelaar MP, Janssen FJ, van Esbroeck ACM, den Dulk H, Allarà M, Hoogendoorn S, et al. Development of an activity-based probe and in silico design reveal highly selective inhibitors for diacylglycerol lipase-α in brain. *Angew Chemie Int Ed* (2013) 52(46):12081–5. doi: 10.1002/anie.201306295

37. Eichmann TO, Lass A. DAG tales: The multiple faces of diacylglycerol - stereochemistry, metabolism, and signaling. *Cell Mol Life Sci* (2015) 72:3931–52. doi: 10.1007/s00018-015-1982-3

38. Gauster M, Hiden U, Blaschitz A, Frank S, Lang U, Alvino G, et al. Dysregulation of placental endothelial lipase and lipoprotein lipase in intrauterine growth-restricted pregnancies. *J Clin Endocrinol Metab* (2007) 92(6):2256–63. doi: 10.1210/jc.2006-2403

39. Savinainen JR, Saario SM, Laitinen JT. The serine hydrolases MAGL, ABHD6 and ABHD12 as guardians of 2-arachidonoylglycerol signalling through cannabinoid receptors. *Acta Physiol* (2012) 204(2):267–76. doi: 10.1111/j.1748-1716.2011.02280.x

40. Blankman JL, Simon GM, Cravatt BF. A comprehensive profile of brain enzymes that hydrolyze the endocannabinoid 2-arachidonoylglycerol. *Chem Biol* (2007) 14 (12):1347–56. doi: 10.1016/j.chembiol.2007.11.006

41. Blankman JL, Long JZ, Trauger SA, Siuzdak G, Cravatt BF. ABHD12 controls brain lysophosphatidylserine pathways that are deregulated in a murine model of the neurodegenerative disease PHARC. *Proc Natl Acad Sci USA*. (2013) 110(4):1500–5. doi: 10.1073/PNAS.1217121110/SUPPL_FILE/PNAS.201217121SI.PDF

42. Giang DK, Cravatt BF. Molecular characterization of human and mouse fatty acid amide hydrolases. *Proc Natl Acad Sci USA*. (1997) 94(6):2238–42. doi: 10.1073/pnas.94.6.2238

43. Maccarrone M, Rossi S, Bari M, De Chiara V, Fezza F, Musella A, et al. Anandamide inhibits metabolism and physiological actions of 2-arachidonoylglycerol in the striatum. *Nat Neurosci* (2008) 11(2):152–9. doi: 10.1038/nn2042

44. Musella A, Fresegna D, Rizzo FR, Gentile A, Bullitta S, De Vito F, et al. A novel crosstalk within the endocannabinoid system controls GABA transmission in the striatum. *Sci Rep* (2017) 7(1):7363. doi: 10.1038/s41598-017-07519-8

45. Hashimotodani Y, Ohno-Shosaku T, Tanimura A, Kita Y, Sano Y, Shimizu T, et al. Acute inhibition of diacylglycerol lipase blocks endocannabinoid-mediated retrograde signalling: Evidence for on-demand biosynthesis of 2-arachidonoylglycerol. *J Physiol* (2013) 591(19):4765–76. doi: 10.1113/jphysiol.2013.254474

46. Perez-Riverol Y, Bai J, Bandla C, Hewapathirana S, García-Seisdedos D, Kamatchinathan S, et al. The PRIDE database resources in 2022: A Hub for mass spectrometry-based proteomics evidences. *Nucleic Acids Res* (2022) 50(D1):D543-52.

frontiers | Frontiers in Endocrinology

TYPE Review
PUBLISHED 15 February 2023
DOI 10.3389/fendo.2023.1084986

Check for updates

OPEN ACCESS

EDITED BY
Prashant Rajput,
Banaras Hindu University, India

REVIEWED BY
Nora Saraco,
Garrahan Hospital, Argentina
Rodrigo Azevedo Loiola,
Université d'Artois, France

*CORRESPONDENCE
Delia I. Chiarello
delia.chiarello@uss.cl
Jaime Gutiérrez
jaime.gutierrez@uss.cl

SPECIALTY SECTION
This article was submitted to Developmental Endocrinology, a section of the journal Frontiers in Endocrinology

RECEIVED 31 October 2022
ACCEPTED 30 January 2023
PUBLISHED 15 February 2023

CITATION
Chiarello DI, Ustáriz J, Marín R, Carrasco-Wong I, Farías M, Giordano A, Gallardo FS, Illanes SE and Gutiérrez J (2023) Cellular mechanisms linking to outdoor and indoor air pollution damage during pregnancy. *Front. Endocrinol.* 14:1084986. doi: 10.3389/fendo.2023.1084986

COPYRIGHT
© 2023 Chiarello, Ustáriz, Marín, Carrasco-Wong, Farías, Giordano, Gallardo, Illanes and Gutiérrez. This is an open-access article distributed under the terms of the Creative Commons Attribution License (CC BY). The use, distribution or reproduction in other forums is permitted, provided the original author(s) and the copyright owner(s) are credited and that the original publication in this journal is cited, in accordance with accepted academic practice. No use, distribution or reproduction is permitted which does not comply with these terms.

Cellular mechanisms linking to outdoor and indoor air pollution damage during pregnancy

Delia I. Chiarello[1*], Javier Ustáriz[2], Reinaldo Marín[3], Ivo Carrasco-Wong[1], Marcelo Farías[4], Ady Giordano[5], Felipe S. Gallardo[4], Sebastián E. Illanes[6,7,8] and Jaime Gutiérrez[1*]

[1]Cellular Signaling and Differentiation Laboratory (CSDL), School of Medical Technology, Faculty of Medicine and Science, Universidad San Sebastián, Santiago, Chile, [2]Department of Chemical and Bioprocess Engineering, Pontificia Universidad Católica de Chile, Santiago, Chile, [3]Center for Biophysics and Biochemistry (CBB), Venezuelan Institute for Scientific Research (IVIC), Caracas, Venezuela, [4]Faculty of Medicine, Pontificia Universidad Católica de Chile, Santiago, Chile, [5]Inorganic Chemistry Department, Faculty of Chemistry and of Pharmacy, Pontificia Universidad Católica de Chile, Santiago, Chile, [6]Reproductive Biology Program, Center for Biomedical Research and Innovation (CiiB), Universidad de los Andes, Santiago, Chile, [7]IMPACT, Center of Interventional Medicine for Precision and Advanced Cellular Therapy, Santiago, Chile, [8]Department of Obstetrics and Gynecology, Faculty of Medicine, Universidad de los Andes, Santiago, Chile

Pregnancies are a critical window period for environmental influences over the mother and the offspring. There is a growing body of evidence associating indoor and outdoor air pollution exposure to adverse pregnancy outcomes such as preterm birth and hypertensive disorders of pregnancy. Particulate matter (PM) could trigger oxi-inflammation and could also reach the placenta leading to placental damage with fetal consequences. The combination of strategies such as risk assessment, advise about risks of environmental exposures to pregnant women, together with nutritional strategies and digital solutions to monitor air quality can be effective in mitigating the effects of air pollution during pregnancy.

KEYWORDS

exposome, pregnancy, indoor - outdoor pollution, mitigation strategies, cell damage, $PM_{2.5}$

1 Introduction

Urban daily exposures to chemical mixtures originated from air pollution have a profound effect on health, especially during vulnerable periods of development such as intrauterine life (1, 2). Pregnancy exposome has been emerging as a focal point in developmental origins of diseases, because of its ability to influence the epigenome and thus to affect gene activity and expression, modifying the likelihood of maternal comorbidities and perinatal outcomes risk (2–4). The exposome, defined as the totality of environmental exposure of an individual over the lifespan, is proposed to complement the genome information since the exposome is highly variable and dynamic (5). The exposome includes the general external environment factors, for example, environmental pollution, climate, and sociodemographic factors (6). According to the World Health Organization

(WHO), air pollution (indoor and outdoor) "represents the single largest environmental risk to health globally" (7). Moreover, exposure to air pollutants is emerging as another key factor to determine the susceptibility of an adverse pregnancy outcome (8).

Fetal development is a critical window for every single mammal on earth, including human beings (9). During this period, the embryos depend on the health, nutrition, activities, and emotional status of the mother, which can modify the fetal exposome (2). According to Barker's theory, embryonic development determines the physiological and metabolic responses that the individual will have into adulthood, in a process known as fetal programming. Thus, any stimulus or insult during embryonic development will result in developmental adaptations that produce permanent structural, physiological, and metabolic changes that predispose to cardiovascular, metabolic, and endocrine disease in adult life (10). Epidemiological data associates air pollution exposure during pregnancy with adverse outcomes such as preterm birth (<37 weeks of gestation) (11, 12), low birth weight (< 2500 g at birth) (13), miscarriage (14), preeclampsia and hypertensive disorders of pregnancy (15). Although the mechanisms responsible for the adverse pregnancy outcomes related to air pollution are not elucidated, recent experimental evidence indicates that the placenta is a direct target tissue for air pollution (16, 17). It is suggested that oxidative stress, endocrine disruption, inflammatory response, and DNA damage are the main contributors (18, 19). The immature metabolism and cellular proliferation period that characterizes the growing fetus is highly vulnerable to pollutants exposure (20).

The aim of this review is to provide an updated overview of the evidence linking exposure to outdoor or indoor air pollution during pregnancy with effects at the cellular level and some ways to mitigate these effects will also be discussed.

2 Air pollution

Air pollution is defined as environmental contamination by toxic chemical compounds, gases, and particles that could modify the natural characteristics of the atmosphere with potential adverse health effects (21). Air pollution encompasses a mixture of different pollutants including particulate matter (PM), among many sources of PM, the combustion emissions from fossil fuel engines and degradation of vehicle parts and road surfaces abrasions represent substantial contributions (22). PM are defined according to their aerodynamic diameter as ultrafine particles $PM_{0.1}$ (median aerodynamic diameter <0.1 μm), fine particles $PM_{2.5}$ (median aerodynamic diameter <2.5 μm), coarse particles PM_{10} (median aerodynamic diameter <10 μm) and gaseous components like ozone (O_3), carbon monoxide (CO), sulfur dioxide (SO_2), nitrogen dioxide (NO_2), carbon dioxide (CO_2), black carbon (BC), diesel exhaust fumes, a wide variety of toxic chemicals such as polycyclic aromatic hydrocarbons (PAHs) and volatile and semi-volatile organic compounds (VOCs) (23, 24). Air pollution is a dynamic phenomenon where both outdoor and indoor pollutants interact and affect air quality (25).

The particulate matter often derives from a different source and has different chemical compositions. PM_{10} commonly includes pollen debris, dust from landfills or construction sites, industrial sources, wildfires, brush or waste burning, wind-blown dust from open lands, and microbial fragments (26). $PM_{0.1}$ and $PM_{2.5}$, often linked to biomass and traffic combustion (27, 28), are relevant in rural and urban environments, since they can be inhaled deeply into the lungs and enter the bloodstream, increasing the potential risk for cardiovascular diseases (29), lung cancer (30) and adverse pregnancy outcome (31). $PM_{2.5}$ is composed of a mixture of natural crustal materials (carbonates, silicates), metals (copper, arsenic, and vanadium), inorganic molecules (sulfate, nitrate, sodium, potassium, and ammonium), black carbon and organic compounds (such as polycyclic aromatic hydrocarbons) (32). Polycyclic aromatic hydrocarbons (PAHs) are a large family of organic compounds, formed as products of incomplete combustion from natural (fly ash and soot from wood burning) and anthropogenic sources (motor vehicle exhaust, tobacco smoking, industrial processes, demolition waste), and are often present in the air, soil, and water (33). PAHs are comprised of two or more fused benzene rings in different arrangements (linear, clustered, and angular) highly lipophilic with relatively low solubility in water, that are stable and resistant to hydrolysis (34). Ambient air is one of the major sources of PAHs exposure (35). In the atmosphere, most PAHs present on $PM_{2.5}$ have low volatility (particle-phase), which is characteristic of PAHs containing five or six aromatic rings such as benzo[b]fluoranthene, benzo[g,h,i]perylene, and benzo[a]pyrene (B[a]P). These compounds are linked to mutagenic, teratogenic, and carcinogenic properties (34).

PAHs have short half-lives in the blood (36). Inside the cells, the first phase of biotransformation starts with the recognition of the PAHs by the aryl hydrocarbon receptor (AhR), the complex PAH-AhR is translocated into the nucleus and induces cytochrome P450 *(Cyp)1a1* gene expression, that encodes for xenobiotic-metabolizing enzyme CYP1A. The specific metabolites (several phenols) can bind DNA and form PAH–DNA adducts (37). In the second phase of biotransformation, the resulting phenolic compounds from the metabolization reactions are conjugated to glutathione, glucuronides, and sulfate esters to enhance the aqueous solubility to finally be excreted in urine (38). B[a]P (five-ring) is a member of the PAH family that can accumulate in the placenta (39, 40) inhibiting trophoblast cells differentiation and proliferation (41), disrupting the endocrine placental function (42), disturbing the redox balance (39) and forming DNA adducts (43).

3 Air pollution exposure during pregnancy

3.1 Pregnancy outcomes and outdoor air pollution

Outdoor air pollution exposure during pregnancy has been linked to fetal development problems, preterm birth, and pregnancy complications, including pregnancy-induced hypertensive disorders (44–49). In general, outdoor pollutants refer to exhaust emissions from vehicle emissions, however, in recent years these emissions have been significantly reduced, especially in developed countries (50). While non-exhaust PM emissions have gained interest in the developed countries (51), these emissions are generated by clutch and engine wear, abrasion of wheel bearings, corrosion of other vehicle components, street furniture, crash barriers or resuspension of road dust has been

rising (52). Only a few studies distinguish between exhaust and non-exahust airbone particles. Regarding this, a retrospective population-based cohort study performed in 540 365 singleton births used two pollutant models including source specific $PM_{2.5}$ and found that the magnitude of the association between low birth weight (LBW) and the exhaust $PM_{2.5}$ component was consistently stronger than with non-exhaust $PM_{2.5}$ (53). A cohort study with 34,705 singleton births delivered at Pittsburgh, between 1999 and 2002, reports the association between preeclampsia, gestational hypertension, and preterm delivery with increased exposure to an ambient source of PAHs ($PM_{2.5}$) during the first trimester of pregnancy (54). Non-exhaust emissions contribute primarily to PM_{10} and to a lesser extent $PM_{2.5}$ however the effects have been less explored compared to those of exhaust PM (55). PM_{10} has been associated with fetal overgrowth (56), with preeclampsia, particularly during humid periods (autumn/winter seasons) (57); conversely PM_{10} has also been associated with small for gestational age (a birth weight of less than 10th percentile for gestational age) in twins born between 32 and 36 weeks, but not associated in term twins (58). Suggesting that PM10 increases the risk of abnormal fetal growth (59). Additionally, it has been reported that exposure to PM_{10} during the first trimester can alter the fetal heart response rate without evidence of acidemia or fetal asphyxia (60). Regarding other compounds, several studies have concluded that outdoor SO_2 exposure during the third trimester was associated with early-term births (birth between 37 and 38 weeks) (61). While the associations for NO_2, NO, CO and O_3 were inconclusive in some cases (62), in other cases NO_2 was linked to preterm birth, even among pregnant women living in an area with relatively low average air pollution concentrations (63) and consistently associated with term low birth weight (64). On the other hand, a systematic review of 84 studies found that most types of particulate matter (PM) were associated with low birth weight, but these associations had many inconsistencies in terms of PM sources and the characteristics of the built environment, proximity to traffic, and green spaces near the residence of the pregnant women (65). A recent study that analyzed the records of almost 600,000 pregnant patients demonstrated a positive association between preterm birth and PM_{10}, $PM_{2.5}$, SO_2, NO_2 and CO, where NO_2 was the largest pollutant contributor while the third trimester was identified as the most sensitive exposure window (66). Meanwhile, a recent report showed a positive association between three-month mean residential NO_2 concentrations and maternal hair cortisol as a biomarker for longer-term biological stress during pregnancy (67). Another meta-analysis that included more than 60 studies found that exposure to $PM_{2.5}$, PM_{10}, and O_3 during pregnancy correlates with the risk of preterm birth at 32-35 weeks, 28-31 weeks, and before 28 weeks (68). Exposure to $PM_{2.5}$ pollution during pregnancy is significantly associated with preeclampsia and hypertensive disorders of pregnancy (69). Preeclampsia is a pregnancy pathology associated with placental dysfunction and defined by a new onset of hypertension with or without proteinuria after 20 weeks of gestation (70). A recent meta-analysis performed with data up to March 2020, summarized 9 cohort studies and concluded that maternal exposure to $PM_{2.5}$ during the third trimester of pregnancy elevates the risk of preeclampsia (71). Some epidemiological studies, use the distributed lag linear model, which is a statistical analysis model that distributes the effect of a single exposure event over a specific time period, in order to estimate the lag effect between exposure to ambient air pollutants and a health outcome (72). During pregnancy, several studies have analyzed the lag effect of different air pollutants exposure and its association with the risk of adverse pregnancy outcomes for example, a study reported a significant association between preconceptional air pollution exposure ($PM_{2.5}$, PM_{10}, and O_3) during the cold season and the termination of pregnancy (73). A recent study applied distributed lag nonlinear model to investigate the association between early pregnancy to midpregnancy exposures to $PM_{2.5}$, PM_{10}, and NO_2 and lower birth weight (74). Another study found that the acute and lag effects of high levels $PM_{2.5}$, PM_{10}, NO_2, and SO_2 exposure of the calculated fertilization time was associated with spontaneous abortion preterm birth (75). The identification of critical windows of susceptibility in which exposure to air pollutants may alter pregnancy outcome is key to improve environmental health interventions and prevent vulnerable populations, currently remains inconsistent across studies, further research is needed to investigate the most likely window of exposure, as well as to estimate the lag and acute effect of exposure to air pollutants during pregnancy (76).

3.2 Maternal physiological adaptation during pregnancy and particulate matter exposure

Normal pregnancy implies profound cardiovascular changes necessary to meet the increased demands of the growing fetoplacental unit (77). These changes occur very early in pregnancy, then, the exposure to $PM_{2.5}$ in this period could have a detrimental effect on cardiovascular adaptations during pregnancy leading to the development of hypertensive disorders (78). It has been shown that the smaller particles are more harmful than the larger particles inducing adverse health effects, as the deposition rate is strongly influenced by particle size (79). Fine particles (PM2.5) are stable in the atmosphere with a residence time of 7 to 30 days, being wet deposition by precipitation the predominant removal mechanism (80), in addition dry deposition by gravitational settling has been reported (81). Recent work showed an association between the $PM_{2.5}$ exposure during the first trimester and the development of hypertensive disorders of pregnancy (82) and maternal thyroid dysfunction (75). Since pregnancy is associated with maternal respiratory adaptations, mainly related to significantly increasing tidal volume, pregnant women could inhale more polluted air (83). The acute or chronic exposure to $PM_{2.5}$ causes activation of inflammatory responses (Table 1) together with structural damage to the alveoli, which facilitates the passage of $PM_{2.5}$ into the systemic circulation (84, 104).

3.3 Fetal and maternal vascular alteration by particulate matter exposure

Translocation of inhaled PM2.5 into the systemic circulation has been associated with vascular endothelial cell damage, promoting increased risk of cardiovascular disease (105, 106). The most

TABLE 1 Cellular effects associated to air pollution exposure during pregnancy.

Reference	Study design	Exhaust/ non-exhaust	Pollutants associate to observed effects	Exposure concentration/ time associate to observed effects	Observed effects	Statistics of associations
Smith et al. (53)	Retrospective population-based cohort study. 540 365 singleton term live births	exhaust non-exhaust	$PM_{2.5traffic\ exhaust}$ from London, UK $PM_{2.5traffic\ non\text{-}exhaust}$ from London, UK	>13.8 μg/m^3	Residential exposure to $PM_{2.5}$ traffic exhaust during pregnancy is directly attributable to 3% of term LBW cases in London By analogy, the authors hypothesize that the mechanisms involved may include, oxidative stress, changes in oxygen or nutrition transfer, placental mitochondrial damage, or endocrine disruption	Odds ratio (95% CI) $PM_{2.5traffic\ exhaust}$ 1.04 (1.01 to 1.07)
Zhou et al. (19)	Cohort of 1060 mother-child pairs recruited between April 2016 and December 2018 Sample: maternal blood	mixture	$PM_{2.5}$ from Shanghai, China	Mean 37.74 μg/m^3	$PM_{2.5}$ inorganic constituents, such as Al, Si, K, Mn, and Zn, appear to be responsible for increase in maternal TSH and decreased in maternal serum free thyroxine (fT4) that lead changes in fetal growth measures	% change (95% CI) Maternal TSH: increases of 12.75% (1.01%, 24.61%) Maternal fT4: decreases of 5.82% (8.61%, -2.96%)
Liu et al. (84)	Cell line: Epithelial alveolar cells (A549)	mixture	PM from urban dust (SRM1649b) purchased from NIST (MD, USA)	100 μg/mL/24 h	Increases the expression of ROS, ICAM-1 and the production of interleukin-6 (IL-6)	n.a
Bové et al. (17)	20 mothers Sample: Placenta	exhaust	BC from Belgium	annual means ranging from 0.63 to 2.42 μg per m^3/entire pregnancy	The presence of particles from air pollution within the placenta of all participating mothers was evidenced. The number of placental particles per mm^3 was positively associated with the mothers' residential exposure to BC during pregnancy	Increases (95% CI) Increased placental BC load associated with increased residential BC exposure: $+0.45 \times 10^4$ per mm^3 (0.11×10^4 to 0.80×10^4)
Li et al. (85)	Cell line: HAEC	exhaust	Diesel exhausted particles, collected from a 1998 Kenworth truck	50 μg/ml/4 h	Down-regulation of Zonular Occludin-1 (ZO-1) leading an increase in permeability	n.a
Le et al. (86)	Primary cell culture: HUVEC	mixture	$PM_{2.5}$, China	10 μg/mL/12 h	Increases mRNA and protein levels of TLR2, TLR4 Increase mRNA expression of IL-1 β, and IL-6	n.a
Su et al. (87)	Primary cell culture: HUVEC	mixture	$PM_{2.5}$ from Taiyuan, China	10 μg/$cm^{2/}$6 h	Induced significant structural and functional damage in mitochondria and lysosomes $PM_{2.5}$ internalization is mediated by clathrin and caveolin	n.a
Ma et al. (88)	Cell line: MHC	mixture	$PM_{2.5}$ from Langfan, China	500 μg/mL/48 h	$PM_{2.5}$ induces Endothelial–Mesenchymal Transition (EndMT) by activating the TGF-β1/Smad3/p-Smad3 pathway.	n.a
Xu et al. (117)	Primary cell culture: HUVEC	mixture	$PM_{2.5}$ from Wuhan, China	12.5 μg/mL/24 h	The activation of ERKs, p38 kinase and JNKs mediates the induction of AT1R	n.a
Xu et al. (89)	Primary cell culture: HUVEC	mixture	$PM_{2.5}$ from Wuhan, China	12.5 μg/mL/24 h	Induction of endoplasmic reticulum stress leading to HIF1α transactivation, which in turn mediates endothelial dysfunction by upregulation of components of the ACE/ANGII/AT1R axis in the endothelial cell	n.a
Wauters et al. (90)	12 healthy male volunteers	exhaust	$PM_{2.5}$ from diesel exhaust from PSA DW10 engine (common in Europe)	300 μg/m^3/120 minutes at rest	The acetylcholine/sodium nitroprusside vasodilation ratio decreased after polluted air decreased significantly and was inversely correlated to the total amount of $PM_{2.5}$ inhaled.	Spearman correlation coefficient (r=−0.55, P<0.01)

(Continued)

10.3389/fendo.2023.1084986

TABLE 1 Continued

Reference	Study design	Exhaust/ non-exhaust	Pollutants associate to observed effects	Exposure concentration/ time associate to observed effects	Observed effects	Statistics of associations
					Impairments in microvascular function measured by NO bioavailability decrease and ROS increase.	
Calderón-Garcidueñas et al. (91)	Healthy children, 6–13 years of age	mixture	$PM_{2.5}$ from Mexico City	4000 μg/m^3/h/7-day cumulative outdoor dose	The increase in circulating ET-1 concentrations showed a positive association with the number of daily hours outdoors. An increase in mean pulmonary arterial pressure (PAPM) was observed.	Pearson's correlation (r = 0.31, p = 0.012)
Finch et al. (118)	Young, healthy nonsmokers	mixture	$PM_{2.5}$ from Utah, USA	50 μg/m^3/24 h	Negative association between acute exposure to $PM_{2.5}$ and circulating levels of ET-1	Beta (95% CI) ambient $PM_{2.5}$ and blood ET-1: β −0.773 (−1.18, −0.365)
Grevendonk et al. (92)	293 mother-newborn pairs	mixture	$PM_{2.5}$ and PM10, from Belgium	$PM_{2.5}$, 16.6 μg/$m^{3/}$ entire pregnancy PM_{10}, 21.4 μg/m^3/ entire pregnancy	PM_{10} and $PM_{2.5}$ exposure during the entire pregnancy were positively correlated with mitochondrial 8-OHdG levels in maternal blood	% change (95% CI) $PM_{2.5}$ exposure: increase of mitochondrial 8-OHdG levels in maternal blood 13.9% (0.4 to 29.4%) PM_{10} exposure: increase of mitochondrial 8-OHdG levels in maternal blood 18.3% (5.6 to 33.4%)
Saenen et al. (93)	502 mother-newborn pairs	mixture	$PM_{2.5}$ and BC from Belgium	$PM_{2.5}$, 15.8 μg/$m^{3/}$ first trimester of pregnancy $PM_{2.5}$, 15.3 μg/$m^{3/}$ second trimester of pregnancy BC, 0,90 μg/$m^{3/}$first trimester of pregnancy	Placental nitrosative stress marker, 3-nitrotyrosine (3-NTp) were positively associated with $PM_{2.5}$ and BC exposure levels during gestation	% change (95% CI) Placental 3-NTp increases by each gestational time window of exposure $PM_{2.5}$ first trimestre exposure: 29.0%, (4.9, 58.6); second trimestre exposure: 39.3%, (12.3, 72.7) BC first trimester exposure: 23.6%, (4.4, 46.4)
Dong et al. (40)	64 pregnant women	exhaust	$_{HMW}$PAHs compounds, mainly from the incomplete combustion or pyrolysis of biomass from Kunming, China	n.a.	The low accumulation of PAHs inside the placenta was related to pregnancy complications and increased levels of PAHs in maternal and umbilical cord blood.	n.a.
Familari et al. (94)	Cell line: HTR-8/SVneo cells	mixture	$PM_{2.5}$ from Malmö, Swedenand PM_{10} from Prague, Czech Republic	500-5000 ng/mL/48h	Decreased hCGβ secretion and increased IL-6 secretion	n.a.
Nääv et al. (95)	Cell line: HTR-8/SVneo cells	mixture	$PM_{2.5}$ from Malmö, Sweden	500 ng/mL/48h	Cytotoxicity, increase in progesterone and IL-6 secretion	n.a.
Qin et al. (96)	Cell line: HTR-8/SVneo cells	mixture	$PM_{2.5}$ from Tianjin City, China	120 μg/mL/24 and 48 h	Inhibition of migration and invasion, DNA damage and cell cycle G2/M arrest Higher ROS generation and increasing TIMP1 and TIMP2 expression	n.a.
Agarwal et al. (39)	84 pregnant women Sample: Placental tissue	exhaust	PAHs from Agra, India	$_{LMW}$PAHs 2.047 μg/L/n.a	Negative correlation was observed between low, high, total PAHs and GSH levels, both in placental tissue. The level of MDA was significantly high in	Pearson's correlation GSH and $_{LMW}$PAHs (r = -0.306, p <

(Continued)

10.3389/fendo.2023.1084986

TABLE 1 Continued

Reference	Study design	Exhaust/ non-exhaust	Pollutants associate to observed effects	Exposure concentration/ time associate to observed effects	Observed effects	Statistics of associations
				$_{HMW}$PAHs 3.016 µg/L/n.a total PAHs 5.064 µg/L/n.a	placental tissue and was associated with total PAHs levels. The observed increase in MDA and decrease in GSH suggests an imbalance in oxidant homeostasis	0.01), $_{HMW}$PAHs (r = -0.441, p < 0.001), and TPAHs (r = -0.388, p < 0.001) MDA and total PAHs (r = 0.27, p = 0.0128).
Herbstman et al. (97)	164 pregnant women maternal Sample: umbilical cord blood leukocytes	exhaust	PAHs from New York City, USA	PAHs, including pyrene, 5.314 ng/m^3/third trimester	Maternal exposure to PAHs decreased cord blood global methylation however, B[a]P–DNA adduct formation was associated with higher global DNA methylation in umbilical cord white blood cells	β-values (95% CI) Global methylation in umbilical cord blood and prenatal PAHs exposure: β = −0.11; (−0.21, 0.00) Odds ratio (95% CI) BaP-DNA adducts in umbilical cord blood and increased levels of genomic methylation 2,35; (1,35, 4,09)
Al-Saleh et al. (38)	1578 women Sample: maternal urine and placental tissue	exhaust	PAHs from Al-Kharj, Saudi Arabia	PAHs n.a.	High levels of BaP in the placenta were associated with decreased placental thickness and decreased cord length. A positive relationship was found between the levels of 8-OHdG and 1-HP in maternal urine.	β-values (P) Placental thickness −0.071 (0.018) Cord length −0.074 (0.013) β Weight (P) 8-OHdG and 1-HP 0.303 (<0.001)
van Drooge et al. (98)	Cell line: JEG-3 cells	mixture	Rural and urban PM_1 from Barcelona, Spain	PM_1 11 and 12 m^3 eqAir/mL/24 h	PAHs from PM1 emitted by biomass burning induce cytotoxicity and inhibition of aromatase activity in JEG-3 cells	n.a
Karttunen et al. (43)	12 uncomplicate pregnancies Tissue: Placenta	exhaust	^{3} H-BP (Amersham Biosciences)	0.1 – 1 µM BP/15 min – 6 h	Transfer of BP from the placental maternal side to the fetal circulation was confirmed by placental perfusion experiments BPDE–DNA adducts were found in placental tissue after the perfusion with 1 µM BP	n.a
Wang et al. (99)	Cell line: Swan71 cells	exhaust	Benzo(a)pyren-7,8-dihydrodiol-9,10-epoxide (BPDE)	0.25 – 4 µM BPDE/24 h	BPDE reduces hCG secretion and also prevents trophoblast cell invasion in a dose-dependent manner BPDE induces apoptosis in a dose-dependent manner and induced mitochondrial damage BPDE increase in ROS, MDA, and inflammation, and decrease in SOD	n.a
Wang et al. (100)	Cell line: JEG-3 cells	mixture	$PM_{2.5}$ from Shanxi, China	1 - 10 µg/mL/48 – 96 h	JEG-3 cells exposure to $PM_{2.5}$ increased hCG levels at both 24 h and 48 h Cell proliferation decreased at 24 h	n.a
Wakx et al. (101)	3 healthy mothers with uncomplicated pregnancies Primary cell culture: Ex vivo trophoblasts cells Cell line: JEG-3	exhaust	B[a]P (Sigma, Saint-Quentin Fallavier, France)	0.1 – 10 µM/72 h	In ex vivo placental cells, incubation with 10 µM B[a]P for 48 h did not cause loss of cell viability or DNA fragmentation. JEG-3 cells exposed to 10 µM B[a]P for 72 h leads to cell cycle arrest (G2/M phase) and a significant decrease in cell proliferation and DNA damage.	

(Continued)

10.3389/fendo.2023.1084986

TABLE 1 Continued

Reference	Study design	Exhaust/ non-exhaust	Pollutants associate to observed effects	Exposure concentration/ time associate to observed effects	Observed effects	Statistics of associations
Pidoux et al. (102)	Tissue: Placenta	n.a	[14C]-formaldehyde (50 mCi/ mmol, Perkin-Elmer)	100 µM	Accumulation of formaldehyde in the placenta and the fetal compartments and hormonal dysfunction	n.a
Shen et al. (103)	HUVECs	n.a	Cooking Oil Fumes-derived $PM_{2.5}$	25, 50, 100, 150, and 200 µg/mL	Reduce cells viability, overproduction of ROS, activation of NLRP3 and IL-1β inflammasome, and inhibition of VEGF expression which directly affects angiogenesis	n.a

UK, United Kingdom; LBW, Low birth weight; TSH, thyroid-stimulating hormone; fT4, free thyroxine 4; ROS, Reactive oxygen species; ICAM, Endothelial adhesion molecule; BC, Black carbon; HAEC, Human aortic endothelial cells; HUVEC, Human umbilical vein endothelial cells; TLR2, Toll Like Receptor 2; TLR4, Toll Like Receptor 4; IL-1 β, Interleukin 1β; IL-6, Interleukin 6; MHC, Mouse pulmonary microvascular endothelial cells; TGF-β1, Transforming growth factor-β 1; Smad3, Mothers against decapentaplegic homolog 3; p-Smad3, Phospho-Smad3; ERK, Extracellular signal regulated protein kinase; p38, Family is a highly evolutionarily conserved group of mitogen-activated protein kinases; JNK, c-Jun N-terminal kinases; AT1R, Angiotensin II type 1 receptor; HIF1α, hypoxia inducible factor 1 subunit alpha; ACE, Angiotensin-Converting enzyme; ANGII, Angiotensin II; PSA DW10, diesel engine manufactured by Peugeot S.A; NO, Nitric oxide; ET-1, Endothelin 1; 8-OHdG, 8-Hydroxy-2′-deoxyguanosine; 1-HP, 1-hydroxypyrene; HMWPAHs, High-molecular-weight polycyclic aromatic hydrocarbons; HTR-8/SVneo, Immortalized first trimester human trophoblast cells; hCGβ, Human chorionic gonadotropin β; TIMP1, Tissue inhibitor of metalloproteinase 1; TIMP2, Tissue inhibitor of metalloproteinase 2; G2/M arrest, Cell cycle arrest at the G2/M phase occurs when DNA is damaged; PAHs, Polycyclic Aromatic Hydrocarbons; GSH: Glutathione; LMWPAHs, Low-molecular-weight polycyclic aromatic hydrocarbons; MDA, malondialdehyde; B[a]P–DNA or BaP-DNA, DNA binding by Benzo[a]pyrene; B[a]P or BaP, Benzo[a]pyrene; JEG-3 cells, Human choriocarcinoma cell line; 3H-BP, 3H-benzo(a)pyrene (BP); BPDE-DNA, DNA binding by Benzo(a)pyrene diolepoxide; Swan71 cells, Immortalized human trophoblast cells; hCG, Human chorionic gonadotropin; SOD, Superoxide dismutase; NLRP3, NOD-, LRR- and pyrin domain-containing protein 3; IL-1β, interleukin-1beta; VEGF, Vascular Endothelial Growth Factor; n.a, not available; CI, Confidence interval. Particulate matter from urban samples was understood as a mixture of exhaust and non-exhaust emissions.

prominent mechanisms associated with $PM_{2.5}$ health effects are oxidative stress and inflammation (Table 1) (107).

This crosstalk between altered redox homeostasis and inflammation-related pathways has been termed "oxi-inflammation" to describe the pre-pathological condition (108). This issue requires a special attention for pregnant women since normal pregnancy itself is characterized by systemic inflammatory activity and the placenta is a great source of reactive oxygen species (ROS) (109). In this regard, increased levels of 8-hydroxy-2′-deoxyguanosine (8-OHdG), an indicator of ROS-mediated mitochondrial damage, have been found in both maternal and cord blood during pregnancy in women exposed to both $PM_{2.5}$ and PM_{10} (92). This has been interpreted as that exposure to air pollution in the first years of life plays an important role in the appearance of oxidative stress, both at the mitochondrial and systemic level (92). Furthermore, high levels of 8-OHdG in the cord blood increase the probability of intrauterine growth restriction as compared with newborns below the median level of mitochondrial damage (110). Moreover, HUVEC incubation with 10 µg/cm^2 of $PM_{2.5}$ induces alterations in the mitochondria, leading to an increase in the mitochondrial fusion gene Mfn1 and a decrease in the fission genes Opa1 and Drp1 (87). Authors suggest that fusion-fission imbalance is associated with mitochondrial dysfunction that could induce cardiovascular disease (87), and during pregnancy this imbalance has been associated with preeclampsia (111, 112). *In vitro* experiments in HUVEC demonstrated that $PM_{2.5}$ increases the expression of adhesion proteins (ICAM-1 and VCAM-1) and decreases the expression of a tight junction protein, zonula occludens-1 (ZO-1) leading to endothelial activation and increases the endothelial barrier permeability, respectively (85, 113). In this experimental setup, $PM_{2.5}$ triggers the secretion of inflammatory interleukins such as IL-6 and IL-1β, increasing the inflammatory response (85, 86). A breakdown of intercellular junctions and increased adhesion molecules are characteristic events of inflammation and endothelial dysfunction, which are observed in pregnancy pathologies such as gestational diabetes, preeclampsia and obesity (114). On the other hand, the endothelial damage related to $PM_{2.5}$ exposure involves endothelial-mesenchymal transition (EndMT), triggered by the activation of the transforming growth factor-β (TGF-β) pathway, linked to high levels of reactive oxygen species (ROS) and PAHs (88, 115). Interestingly, it has been reported that EndMT contributes to the development of atherosclerotic lesions, which could explain the role of air pollution in the development and progression of cardiovascular disease (116), where upregulation of angiotensinogen and the angiotensin-converting enzyme has been shown, resulting in increased circulating angiotensin II and activation of the angiotensin II receptor type 1, thus favoring vascular contractility (89, 117). Furthermore, exposure to $PM_{2.5}$ causes a reduction in the bioavailability of NO in the vessel wall, impairing the endothelial-dependent vasorelaxation (90). On the other hand, a study performed in children (7.9 ± 1.3 years of age) chronically exposed to outdoor air pollution showed increased levels of circulating endothelin-1 (ET-1), a potent vasoconstrictor, with a positive correlation with $PM_{2.5}$ exposure levels (91). However, a study conducted in young healthy adults who were exposed to natural variations in $PM_{2.5}$ showed a negative correlation between ET-1 levels and $PM_{2.5}$ exposure levels (118). Another mechanism that

could explain the endothelial dysfunction induced by PM2.5 exposure, is the interleukin 22/interleukin 22 receptor (IL22/IL-22R) pathway (119, 120). The exposure to $PM_{2.5}$ activates the AhR in circulating innate lymphoid cells and induces cytokine IL-22 gene expression (121). IL-22 is a cytokine that plays pro- and anti-inflammatory functions, through interactions with hematopoietic cells, such as macrophages and with endothelial and epithelial cells (122). Endothelial cells express IL-22R, the interaction of IL-22 with its receptor can induce the production of adhesion molecules, endothelial activation, and the secretion of numerous proinflammatory mediators (123). Increased IL-22 has been observed in the blood of pregnant women with preeclampsia and premature rupture of membranes (124, 125).

3.4 Placental tissue and particulate matter exposure

It was reported that black carbon particles from air pollution can translocate from the maternal lungs into the maternal circulation reaching the placenta (17). The $PM_{2.5}$ exposure during the first and second trimesters of gestation has been positively associated with the amount of 3-nitrotyrosine (3-NTp) in the placental tissue from 330 mother-newborn pair cohorts (93). 3-NTp is a well-known biomarker of peroxynitrite because of its positive association with the rate of protein degradation and therefore for a biomarker of both nitrosative and oxidative stress and inflammation (126).

On the other hand, placental methylation status of circadian pathway genes (CLOCK, BMAL1, NPAS2, CRY1-2, and PER1-3) were positively and significantly associated with intrauterine PM2.5 exposure during the third trimester (127). Genetic abnormalities in the molecular circadian pathway have been associated with chronic noncommunicable diseases, such as obesity (128), metabolic syndrome (129) and diabetes (130). It has been reported that the accumulation of PAHs in the placenta from healthy pregnancies decreases the presence of PAHs in fetal blood, suggesting that under normal conditions the placenta acts as a reservoir decreasing the transfer of PAHs from the mother to the fetus (40). While, in placental tissues from pregnancies associated with hypertensive disorders, diabetes, or preterm delivery, PAHs concentration decreases together with an increase of PAHs in fetal blood (40). Familari and colleagues (94) reported that the exposure of HTR-8/SVneo cells (immortalized first trimester trophoblast cell line) to urban pollution particles led to reduced cellular growth, increased proinflammatory cytokines (IL-6), upregulated expression of endocytosis and intracellular transport proteins, as well as an alteration in the amino acid metabolism and autoimmune responses. Similarly, another study showed that the cell line exposed to $PM_{2.5}$ for 48 h, undergoes cytotoxicity, diminution of hCG secretion, and an increase of IL-6 production (95). The exposure of these cells to $PM_{2.5}$ (120 μg/ml) induced cell-cycle arrest and inhibited migration and invasion of HTR-8 cells by up-regulating the expression of tissue inhibitors of metalloproteinases (TIMP1 and TIMP2) and down-regulating Collagen I expression (96).

Elevated levels of B[a]P in placental tissue from women with preterm delivery shows a significant correlation with lower glutathione (GSH) levels and higher levels of thiobarbituric acid-reactive substances (TBARS) in this tissue (39). This has been taken as an indication of a possible contribution of PAHs in preterm delivery through redox imbalance (39). Moreover, PAHs exposure (between 0.24 and 2.47 ng/m^3), during the third trimester of pregnancy, was associated with lower global DNA methylation in umbilical cord white blood cells (97). Additionally, the presence of detectable PAH-DNA adducts in cord blood was shown to be positively associated with global methylation levels. Since both global hypomethylation and hypermethylation of specific genes have been associated with cancer and other diseases in humans, it is remarkable that maternal PAHs exposure can modify genomic DNA methylation status in the fetus (97). In this regard, the presence of PAHs from air pollution in placental tissue is inversely associated with placental weight and cord length (38).

The PAHs are linked with endocrine disruption in trophoblast cells, since a steroidogenic enzyme, aromatase that catalyzes the aromatization of fetal and maternal androgens into estrogens is inhibited in placental JEG-3 cells exposed to organic extracts from biomass burning collected in winter (98). The most abundant and studied PAHs, B[a]P, enters human cells and is metabolized by cytochrome P450 1A1 (CYP1A1) into different compounds. The benzo(a)pyrene-7,8-dihydrodiol-9,10-epoxide (BPDE) metabolite can cross the placenta and reach the fetal compartments leading to toxicity and DNA damage through the generation of BPDE-DNA adducts (43). In addition, the incubation of human trophoblast cells Swan 71 with 2.0 μM of BPDE for 24 h reduces the human chorionic gonadotropin (hCG) secretion, promotes the increase of pro-inflammatory cytokines IL-6 (27.5-fold), TNF-α (51.9-fold), and induces mitochondrial fragmentation and dysfunction due to an increase in mRNA and protein levels of mitochondrial fission genes in these cells (99). On the other hand, JEG-3 cells exposed to $PM_{2.5}$ increase their hCG secretion, and an important inhibition of progesterone synthesis, which could be an indication that $PM_{2.5}$ may directly inhibit the phosphorylation status of Protein Kinase A in JEG-3, with a concomitant inhibition of the protein expression in progesterone-synthesis, leading to a suppression of the progesterone levels (100). Furthermore, placental JEG-3 cells exposed to 10 μM B[a]P for 72 h leads to cell cycle arrest (G2/M phase) and a significant decrease in cell proliferation, likely through the phosphorylation of histone H2A variant H2AX (γ-H2AX) (101).

The exact concentration of $PM_{2.5}$ that reaches the placenta of a woman exposed to air pollution is unknown. It is not valid to convert from the unit used in most experimental studies (μg/ml or ng/ml) to the unit reported by air quality sensors ($\mu g/m^3$). However, one study indicates that levels of 5000 ng/ml (5 μg/ml) could correspond to 25 $\mu g/m^3$ (95). The same study indicates that 10,000 ng/ml (10 ug/ml) could correspond to levels that can be observed in a more polluted city with $PM_{2.5}$ concentrations of 50 $\mu g/m^3$ (95). The reference value for 24 h exposure to $PM_{2.5}$ established by WHO global air quality guidelines is 15 ug/m^3 (7, 131).

3.5 Pregnancy outcomes and indoor air pollution

The main literature on-air quality-related mortality is focused on pollutant measurements taken outdoors. However, the influx of

outdoor air influences indoor air quality, which already includes specific indoor emissions sources, relationships between building systems/construction methods, and occupant behavior (7). According to the United States federal government agency called Environmental Protection Agency (EPA), the levels of indoor air pollutants are often 2 to 5-fold higher than outdoor levels (23). Since people spend most of their time inside, indoor conditions play a prominent part in the overall human exposure to air pollution (132). This is particularly relevant since pregnant women spend most of their time indoors, especially toward the end of pregnancy (133). Indoor pollutants are mostly caused by human interaction at home and in classrooms, but they can also be found in daycare centers, social entertainment settings, and micro-environments, including automobiles, buses, trains, and airplanes (132, 134). Indoor air pollutants can become outdoor air pollutants, resulting in the so-called "neighborhood" pollution effect (132); this is especially relevant in disadvantaged neighborhoods that may use biomass for cooking or heating, which increases the concentration of pollutants in their living area, compared to people living in more socioeconomically advantaged neighborhoods (135). Allergens, mainly house dust mites and insects, pollen, animal sources, molds, and bacterial endotoxins, are examples of biological indoor air pollutants (136). Chemical air pollutants such as gases, particulate matter, formaldehyde, and volatile organic compounds (VOCs) are also present (134). The latter derive from various sources, the most common indoor are burning wood, household chemicals (disinfectants, bleach, dry cleaning fluid, aerosols, air fresheners, paint, varnish, and pesticides), also incense, candles, and cooking (137–140). Cooking with polluting fuels such as gasoline, kerosene, and biomass (wood, charcoal, crop residues, and animal manure) causes household air pollution, which is a global environmental health problem (132). There is evidence that the exposure to labeled carbon particles (less than 100 nm) for 1 min is sufficient to appear in the blood of healthy volunteers and to remain detectable for 60 min (141). However, there are very few studies that have evaluated the effect of indoor exposures to $PM_{2.5}$ on pregnancy and delivery outcomes (142–144). A predominantly indoor air pollutant, formaldehyde has been associated with reduced birth weight (142). The kinetics of transplacental transfer (from the maternal to the fetal compartment) of formaldehyde was studied with a perfused human placental cotyledon model, showing that the compound can accumulate in the placenta and fetus (102). In addition, formaldehyde exposure reduced the synthesis and secretion of the peptide placental hormones (pGH: placental growth hormone, hPL: human placental lactogen, and hCG: human chorionic gonadotrophin), a fact that appears to be mediated by oxidative stress, since hCG production was restored by n-acetylcysteine (102). The cooking oil fumes-derived $PM_{2.5}$, is another source of indoor air pollution that has been associated with preterm birth (145) and low birth weight (57). Human umbilical vein endothelial cells (HUVEC) exposed *in vitro* to PM2.5 derived from cooking oil fumes lead to overproduction of ROS, inflammation, and inhibition of angiogenesis (103).

A study conducted on 68 pregnant women using kerosene stoves, found that cooking with kerosene is associated with reduced birth weight and low levels of micronutrients such as iodine, vitamin B6 and homocysteine in mothers and newborns (146). Solid fuel for cooking has been associated with an increased risk of cesarean delivery, low birth weight, neonatal mortality, and acute respiratory infection among children (147). While another study performed on 695 pregnant women using biomass fuels for cooking in Temuco (Chile) and Bariloche (Argentina), found no association between perinatal morbidity (pre-term birth and low birth weight) and household air pollution exposure; the study highlights that these results may be related to the fact that the studied population cooks in ventilated rooms compared to other studies (148). The link between poor ventilation and persistent indoor air pollution has been explored by different studies, suggesting its association with the development of adverse pregnancy outcomes (147, 149–151). The assessment of exposure to indoor air pollution during intrauterine life has some limitations. For example, some studies have evaluated the personal exposure of pregnant women to various pollutants, however, they do not distinguish indoor and outdoor concentrations of these pollutants and therefore cannot specifically explore associations between indoor air pollutants and birth (142, 152). In this regard, an attempt has been made to evaluate compartmentalized exposure, using passive sampling techniques and surveys that include questions about the types of chemicals used to clean, the type of kitchen, and the time spent indoors (142). When analyzing the personal variability of indoor and outdoor exposures, some of them may be misclassified, furthermore, in many cases, seasonal changes and spatio-temporal variability are not considered during pregnancy exposition measurements (153, 154). The source of individual pollutants is challenging; therefore, it is necessary to apply integrated approaches (*i.e.* survey and exposure models) (155).

4 Mitigation strategies

The most obvious way to avoid the deleterious effect of air pollution is not to be exposed to it. However, this recommendation is not practical since everyone must breathe the available air. We need to reduce the air pollution in our cities, but unfortunately is a long-term process that demands a government commitment, along with education and other strategies related to reduce the sources of pollution. While in some cities it is possible to avoid busy roads or highways at least during pregnancy, however in many cities this is not possible. Thus, individual and public strategies focused to reduce the harmful effects of the available polluted air are needed (Figure 1).

4.1 Behavior actions

Reducing exposure to air pollution during pregnancy is a key opportunity to provide better health to the child (156). A primary prevention measure that can be given to the mother at prenatal care, is to ensure good ventilation to reduce the exposure to indoor air pollution (157). One of the biggest sources of pollution in homes is the use of the kitchen. To reduce or to eliminate air pollution in the kitchen, the American Lung Association recommends using the exhaust fan and ensuring ventilation in the kitchen (158). Another recommendation made by the same association is to get rid of fragrant and scented products such as air fresheners and cleaners, replacing them with natural products such as vinegar, peroxide, and baking

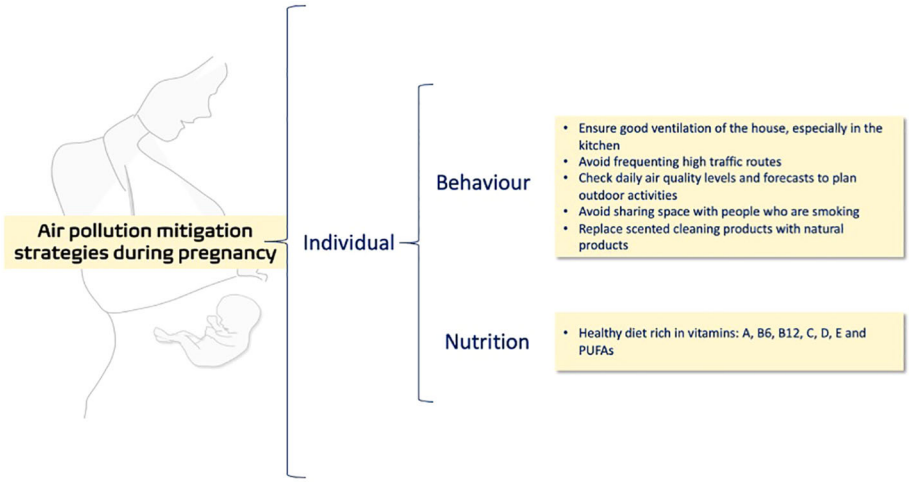


FIGURE 1
Proposed approaches to reduce exposure to air pollution during pregnancy.

soda, or non-toxic brands. Another individual measure is to check daily air quality levels and to perform outdoor activities when pollution levels are lower. It is also recommended that pregnant women avoid sharing space with people who are smoking.

4.2 Nutrition

Since the imbalance in oxidant production is one of the prominent mechanisms leading to cellular damage linked to air pollution, the presence of antioxidants from nutrition represents an opportunity to mitigate the air pollution effects (159–164). According to the Food and Drug Administration antioxidants are substances that, following absorption from the gastrointestinal tract, participate in physiological, biochemical, or cellular processes that inactivate or prevent free radical-initiated chemical reactions (165). The common antioxidants from diet or supplementation, are DL-alpha-tocopherol acetate (vitamin E), ascorbic acid (vitamin C), beta-carotene (vitamin A), omega-3 polyunsaturated fatty acids (omega-3), and selenium, that has been reported to be involved in the deactivation of free radicals (166, 167). About the antioxidant air pollution mitigation, a study conducted in individuals chronically exposed to $PM_{2.5}$ shows that supplementation with omega-3 could modulate the plasma levels of cellular redox systems by increasing glutathione (GSH) and Cu/Zn superoxide dismutase (SOD) activity (168). Additionally, another study shows that oxidized low-density lipoprotein (OxLDL) decreased following the fish oil supplementation in a cohort of healthy university students exposed to the average level of $PM_{2.5}$ of 38 ug/m^3 for four months (169). Simultaneous treatment of human umbilical vein endothelial cells (HUVECs) with vitamin E and $PM_{2.5}$ protects against the reactive oxygen species (ROS) production and the increased levels of lipid peroxidation (161). An epidemiologic cohort study found that women in the first and second trimesters of pregnancy with lower vitamin A intakes have higher negative effects on birth weight due to prenatal $PM_{2.5}$ exposure than women with higher intakes (170). Indeed, concurrent air pollution and poor nutritional status are associated with adverse health and pregnancy outcomes such as low birth weight and preterm birth (171). The lack of vitamin D is mainly due to low exposure to ultraviolet B (UVB) radiation since the skin synthesis provides 90% of all the body's requirements (172). The levels of air pollution influence the percentage of the ground level of UVB (173). In this way, a longitudinal cohort study conducted in 3285 pregnant women, found that the $PM_{2.5}$ exposure during the third trimester and the entire pregnancy was inversely associated with 25(OH)D levels (174). In addition, the mediating effect of total net daily UV-B radiation (radiation reaching ground level) on the inverse association between prenatal PM2.5 exposure and maternal circulating 25(OH)D levels was 70% (174). Similar results were found in a study performed in 375 mother-child cohorts. It was found that the exposure to ambient urban air pollution during late pregnancy may contribute to hypovitaminosis D in the offspring and suggest that this factor could affect the child's risk of developing diseases later in life (175). Epidemiological data associates the presence of urban particulate matter in polluted air with respiratory diseases, and vitamin D deficiency (176). This could be linked to the induction of a proinflammatory and potentially pathogenic T helper 17 cell (Th17) profile (176). Lower levels of vitamin D could increase the risk of low birth weight (177, 178). In addition, the incidence of asthma linked to air pollution exposure is higher among low-term-birthweight children (179). It has been proposed that restoring levels of vitamin D may mitigate the urban particulate matter adverse effect associated with respiratory health (176).

On the other hand, a study found that maternal exposure to NO_2 from traffic-related air pollution, along with low dietary intake of methyl nutrients such as folate, vitamins B6 and B12 are related to the greatest odds of congenital heart defects (180). Recent experimental evidence suggests that vitamin B (folates, vitamin B12, and B6) supplementation in healthy non-smoking volunteers could mitigate the effect of $PM_{2.5}$ exposure on cardiac autonomic dysfunction and

inflammation (181). More data of the same studied population showed that vitamin B supplementation prevents alterations in mitochondrial DNA content in circulating $CD4^+$ Th cell induced by $PM_{2.5}$ exposure (182). Folate (vitamin B9) and vitamin B12 (cyanocobalamin) are hydrosoluble vitamins naturally present in some foods, added to others, and in the dietary supplement (183). Folate together with vitamin B12, acts as a coenzyme in the metabolism of 1-carbon compounds, required for numerous cellular functions such as *de novo* synthesis of purines, thymidylate, and the generation of the methyl groups for the methylation reactions of DNA, RNA, proteins, and lipids (184, 185). Considering all this information, monitoring the levels of vitamin D as well as those of B12 during pregnancy should receive more attention in clinical practice. An important educational campaign could be aimed at raising awareness among pregnant women about the importance of dietary practices to mitigate the health risks of air pollution (164).

5 Concluding remarks

This study reviews the experimental evidence on the effects of indoor and outdoor pollution during pregnancy and discusses some mitigation strategies. The deposition of air pollutants on the air-blood barrier triggers oxidative stress and inflammation, during pregnancy increasing the risk of developing complications that affect the health of the mother and the offspring. Mitigation strategies should include advice to pregnant women on ways to reduce exposure to indoor and outdoor pollution and the importance of this issue during pregnancy. There is a knowledge gap regarding the effects of non-exhaust emissions on intrauterine development. Greater efforts and interaction between different disciplines are needed to develop effective prevention and risk assessment strategies that can significantly reduce the adverse effects of air pollution during pregnancy.

Author contributions

DC, JG, and JU contributed to conception and design of the study. DC and AG organized the database. DC and JU wrote the first draft of the manuscript. RM, IC-W, MF, FG, SI wrote sections of the manuscript. All authors contributed to the article and approved the submitted version.

Funding

FONDECYT 1221362 to JG (Universidad San Sebastián, Chile). CONICYT, PAI Convocatoria Nacional Subvención a Instalación en la Academia, Convocatoria Año 2019, Folio N°PAI77190060 to DC. PAI Convocatoria Nacional Subvención a Instalación en la Academia, Convocatoria Año 2021, Folio N°SA77210087 to IC-W.

Conflict of interest

The authors declare that the research was conducted in the absence of any commercial or financial relationships that could be construed as a potential conflict of interest.

Publisher's note

All claims expressed in this article are solely those of the authors and do not necessarily represent those of their affiliated organizations, or those of the publisher, the editors and the reviewers. Any product that may be evaluated in this article, or claim that may be made by its manufacturer, is not guaranteed or endorsed by the publisher.

References

1. Tonne C, Adair L, Adlakha D, Anguelovski I, Belesova K, Berger M, et al. Defining pathways to healthy sustainable urban development. *Environ Int* (2021) 146:106236. doi: 10.1016/j.envint.2020.106236

2. Wright ML, Starkweather AR, York TP. Mechanisms of the maternal exposome and implications for health outcomes. *ANS Adv Nurs Sci* (2016) 39:E17–30. doi: 10.1097/ANS.0000000000000110

3. Lavigne E, Yasseen AS, Stieb DM, Hystad P, van Donkelaar A, Martin RV, et al. Ambient air pollution and adverse birth outcomes: Differences by maternal comorbidities. *Environ Res* (2016) 148:457–66. doi: 10.1016/j.envres.2016.04.026

4. Ferguson KK, Chin HB. Environmental chemicals and preterm birth: Biological mechanisms and the state of the science. *Curr Epidemiol Rep* (2017) 4:56–71. doi: 10.1007/s40471-017-0099-7

5. Wild CP. Complementing the genome with an "Exposome": The outstanding challenge of environmental exposure measurement in molecular epidemiology. *Cancer Epidemiol Biomarkers Prev* (2005) 14:1847–50. doi: 10.1158/1055-9965.EPI-05-0456

6. Miller GW. The exposome in environmental health sciences and related disciplines. In: *The exposome*. Academic Press (2014), 39–53. doi: 10.1016/B978-0-12-417217-3.00004-5

7. WHO. *Ambient air pollution* (2021). Available at: https://www.who.int/news-room/fact-sheets/detail/ambient-(outdoor)-air-quality-and-health (Accessed 29 October 2021).

8. Koman PD, Hogan KA, Sampson N, Mandell R, Coombe CM, Tetteh MM, et al. Examining joint effects of air pollution exposure and social determinants of health in defining "At-risk" populations under the clean air act: Susceptibility of pregnant women to hypertensive disorders of pregnancy. *World Med Health Policy* (2018) 10:7–54. doi: 10.1002/wmh3.257

9. DiPietro JA. Prenatal development. In: *Encyclopedia of infant and early childhood development* (*Second Edition*). Elsevier (2008). p. 604–7. doi: 10.1016/B978-0-12-809324-5.21831-2

10. Barker DJ. The fetal and infant origins of adult disease. *BMJ* (1990) 301:1111. doi: 10.1136/bmj.301.6761.1111

11. Malley CS, Kuylenstierna JCI, Vallack HW, Henze DK, Blencowe H, Ashmore MR. Preterm birth associated with maternal fine particulate matter exposure: A global, regional and national assessment. *Environ Int* (2017) 101:173–82. doi: 10.1016/j.envint.2017.01.023

12. Porpora M, Piacenti I, Scaramuzzino S, Masciullo L, Rech F, Benedetti Panici P. Environmental contaminants exposure and preterm birth: A systematic review. *Toxics* (2019) 7:11. doi: 10.3390/toxics7010011

13. Lamichhane DK, Leem J-H, Lee J-Y, Kim H-C. A meta-analysis of exposure to particulate matter and adverse birth outcomes. *Environ Health Toxicol* (2015) 30:e2015011. doi: 10.5620/eht.e2015011

14. Linscheid C, Heitmann E, Singh P, Wickstrom E, Qiu L, Hodes H, et al. Trophoblast expression of the minor histocompatibility antigen HA-1 is regulated by oxygen and is increased in placentas from preeclamptic women HHS public access. *Placenta* (2015) 36:832–8. doi: 10.1016/j.placenta.2015.05.018

15. Pedersen M, Halldorsson TI, Olsen SF, Hjortebjerg D, Ketzel M, Grandström C, et al. Impact of road traffic pollution on pre-eclampsia and pregnancy-induced hypertensive disorders. *Epidemiology* (2017) 28:99–106. doi: 10.1097/EDE.0000000000000555

16. Liu A, Qian N, Yu H, Chen R, Kan H. Estimation of disease burdens on preterm births and low birth weights attributable to maternal fine particulate matter exposure in

shanghai, China. *Sci Total Environ* (2017) 609:815–21. doi: 10.1016/j.scitotenv.2017.07.174

17. Bové H, Bongaerts E, Slenders E, Bijnens EM, Saenen ND, Gyselaers W, et al. Ambient black carbon particles reach the fetal side of human placenta. *Nat Commun* (2019) 10(1):3866. doi: 10.1038/s41467-019-11654-3

18. Yan Q, Liew Z, Uppal K, Cui X, Ling C, Heck JE, et al. Maternal serum metabolome and traffic-related air pollution exposure in pregnancy HHS public access. *Environ Int* (2019) 130:104872. doi: 10.1016/j.envint.2019.05.066

19. Zhou Y, Zhu Q, Wang P, Li J, Luo R, Zhao W, et al. Early pregnancy PM2.5 exposure and its inorganic constituents affect fetal growth by interrupting maternal thyroid function. *Environ pollut* (2022) 307:119481. doi: 10.1016/j.envpol.2022.119481

20. Gernand AD, Schulze KJ, Stewart CP, West KP, Christian P. Micronutrient deficiencies in pregnancy worldwide: health effects and prevention. *Nat Rev Endocrinol* (2016) 12:274–89. doi: 10.1038/nrendo.2016.37

21. Sanidas E, Papadopoulos DP, Grassos H, Velliou M, Tsioufis K, Barbetseas J, et al. Air pollution and arterial hypertension. a new risk factor is in the air. *J Am Soc Hypertens* (2017) 11:709–15. doi: 10.1016/j.jash.2017.09.008

22. Stafoggia M, Faustini A. Impact on public health–epidemiological studies. In: *Non-exhaust emissions*. Academic Press (2018). p. 67–88. doi: 10.1016/B978-0-12-811770-5.00003-0

23. Esworthy R. *Air quality: EPA's 2013 changes to the particulate matter (PM) standard*. Congressional Research Service (2015), 7–5700. https://sgp.fas.org/crs/misc/R42934.pdf.

24. Azarmi F, Kumar P, Marsh D, Fuller G. Assessment of the long-term impacts of PM10 and PM2.5 particles from construction works on surrounding areas. *Environ Sci Process Impacts* (2016) 18:208–21. doi: 10.1039/c5em00549c

25. Shrestha PM, Humphrey JL, Carlton EJ, Adgate JL, Barton KE, Root ED, et al. Impact of outdoor air pollution on indoor air quality in low-income homes during wildfire seasons. *Int J Environ Res Public Health* (2019) 16(19):3535. doi: 10.3390/ijerph16193535

26. Fischer PH, Marra M, Ameling CB, Velders GJM, Hoogerbrugge R, de Vries W, et al. Particulate air pollution from different sources and mortality in 7.5 million adults — the Dutch environmental longitudinal study (DUELS). *Sci Total Environ* (2020) 705:135778. doi: 10.1016/j.scitotenv.2019.135778

27. Xue J, Xue W, Sowlat MH, Sioutas C, Lolinco A, Hasson A, et al. Seasonal and annual source appointment of carbonaceous ultrafine particulate matter ($PM_{0.1}$) in polluted California cities. *Environ Sci Technol* (2019) 53(1):39–49. doi: 10.1021/acs.est.8b04404

28. Merk R, Heßelbach K, Osipova A, Popadić D, Schmidt-Heck W, Kim G-J, et al. Particulate matter (PM2.5) from biomass combustion induces an anti-oxidative response and cancer drug resistance in human bronchial epithelial BEAS-2B cells. *Int J Environ Res Public Health* (2020) 17(21):8193. doi: 10.3390/ijerph17218193

29. Vidale S, Campana C. Ambient air pollution and cardiovascular diseases: From bench to bedside. *Eur J Prev Cardiol* (2018) 25:818–25. doi: 10.1177/2047487318766638

30. WHO. *Ambient (outdoor) air quality and health* (2018). Available at: http://www.who.int/en/news-room/fact-sheets/detail/ambient-(outdoor)-air-quality-and-health (Accessed 16 May 2018).

31. Ebisu K, Malig B, Hasheminassab S, Sioutas C, Basu R. Cause-specific stillbirth and exposure to chemical constituents and sources of fine particulate matter. *Environ Res* (2018) 160:358–64. doi: 10.1016/j.envres.2017.10.015

32. Snider G, Weagle CL, Murdymootoo KK, Ring A, Ritchie Y, Stone E, et al. Variation in global chemical composition of PM 2.5 : emerging results from SPARTAN. *Atmos Chem Phys* (2016) 16:9629–53. doi: 10.5194/acp-16-9629-2016

33. Abdel-Shafy HI, Mansour MSM. A review on polycyclic aromatic hydrocarbons: Source, environmental impact, effect on human health and remediation. *Egyptian J Petroleum* (2016) 25:107–23. doi: 10.1016/J.EJPE.2015.03.011

34. Pissinatti R, de Souza SVC. *HC-0A-02: Analysis of polycyclic aromatic hydrocarbons from food*. Singapore: Springer (2017) p. 67–104.

35. Liu YN, Tao S, Dou H, Zhang TW, Zhang XL, Dawson R. Exposure of traffic police to polycyclic aromatic hydrocarbons in Beijing, China. *Chemosphere* (2007) 66:1922–8. doi: 10.1016/j.chemosphere.2006.07.076

36. Barr DB, Wang RY, Needham LL. Biologic monitoring of exposure to environmental chemicals throughout the life stages: requirements and issues for consideration for the national children's study. *Environ Health Perspect* (2005) 113:1083–91. doi: 10.1289/EHP.7617

37. Barouki R, Aggerbeck M, Aggerbeck L, Coumoul X. The aryl hydrocarbon receptor system. *Drug Metabol Drug Interact* (2012) 27(1):3–8. doi: 10.1515/dmdi-2011-0035

38. Al-Saleh I, Alsabbahen A, Shinwari N, Billedo G, Mashhour A, Al-Sarraj Y, et al. Polycyclic aromatic hydrocarbons (PAHs) as determinants of various anthropometric measures of birth outcome. *Sci Total Environ* (2013) 444:565–78. doi: 10.1016/j.scitotenv.2012.12.021

39. Agarwal P, Singh L, Anand M, Taneja A. Association between placental polycyclic aromatic hydrocarbons (PAHS), oxidative stress, and preterm delivery: A case–control study. *Arch Environ Contam Toxicol* (2018) 74:218–27. doi: 10.1007/s00244-017-0455-0

40. Dong X, Wang Q, Peng J, Wu M, Pan B, Xing B. Transfer of polycyclic aromatic hydrocarbons from mother to fetus in relation to pregnancy complications. *Sci Total Environ* (2018) 636:61–8. doi: 10.1016/j.scitotenv.2018.04.274

41. Chen Y, Mi BB, Zhao YL, Yang JM, Tao YL, Yan H. [Prenatal exposure to outdoor air pollution and preterm birth: a meta-analysis]. *Zhonghua Liu Xing Bing Xue Za Zhi* (2016) 37:880–5. doi: 10.1016/j.envres.2021.111654

42. Wierzba W, Radowicki S, Bojar I, Pinkas J. Effects of environmental pollution with aromatic hydrocarbons on endocrine and metabolic functions of the human placenta. *Ann Agric Environ Med* (2018) 25:157–61. doi: 10.26444/aaem/74406

43. Karttunen V, Myllynen P, Prochazka G, Pelkonen O, Segerbäck D, Vähäkangas K. Placental transfer and DNA binding of benzo(a)pyrene in human placental perfusion. *Toxicol Lett* (2010) 197:75–81. doi: 10.1016/j.toxlet.2010.04.028

44. Šrám RJ, Binková B, Dejmek J, Bobak M. Ambient air pollution and pregnancy outcomes: A review of the literature. *Environ Health Perspect* (2005) 113:375–82. doi: 10.1289/ehp.6362

45. Sapkota A, Chelikowsky AP, Nachman KE, Cohen AJ, Ritz B. Exposure to particulate matter and adverse birth outcomes: a comprehensive review and meta-analysis. *Air Qual Atmos Health* (2012) 5:369–81. doi: 10.1007/s11869-010-0106-3

46. Dadvand P, Ostro B, Amato F, Figueras F, Minguillón M-C, Martinez D, et al. Particulate air pollution and preeclampsia: a source-based analysis. *Occup Environ Med* (2014) 71:570–7. doi: 10.1136/oemed-2013-101693

47. Jia L, Liu Q, Hou H, Guo G, Zhang T, Fan S, et al. Association of ambient air pollution with risk of preeclampsia during pregnancy: a retrospective cohort study. *BMC Public Health* (2020) 20:1663. doi: 10.1186/s12889-020-09719-w

48. Khamirchi R, Moslem A, Agah J, Pozo ÓJ, Miri M, Dadvand P. Maternal exposure to air pollution during pregnancy and cortisol level in cord blood. *Sci Total Environ* (2020) 713:136622. doi: 10.1016/j.scitotenv.2020.136622

49. Liu Y, Xu J, Chen D, Sun P, Ma X. The association between air pollution and preterm birth and low birth weight in guangdong, China. *Int J Womens Health* (2020) 12:313–25. doi: 10.1186/s12889-018-6307-7

50. Choma EF, Evans JS, Gómez-Ibáñez JA, Di Q, Schwartz JD, Hammitt JK, et al. Health benefits of decreases in on-road transportation emissions in the united states from 2008 to 2017. *Proc Natl Acad Sci* (2021) 118(51):e2107402118. doi: 10.1073/pnas.2107402118

51. Harrison RM, Allan J, Carruthers D, Heal MR, Lewis AC, Marner B, et al. Non-exhaust vehicle emissions of particulate matter and VOC from road traffic: A review. *Atmos Environ* (2021) 262:118592. doi: 10.1016/j.atmosenv.2021.118592

52. Piscitello A, Bianco C, Casasso A, Sethi R. Non-exhaust traffic emissions: Sources, characterization, and mitigation measures. *Sci Total Environ* (2021) 766:144440. doi: 10.1016/j.scitotenv.2020.144440

53. Smith RB, Fecht D, Gulliver J, Beevers SD, Dajnak D, Blangiardo M, et al. Impact of london's road traffic air and noise pollution on birth weight: retrospective population based cohort study. *BMJ* (2017) 359:j5299. doi: 10.1136/bmj.j5299

54. Lee P-C, Roberts JM, Catov JM, Talbott EO, Ritz B. First trimester exposure to ambient air pollution, pregnancy complications and adverse birth outcomes in Allegheny county, PA. *Matern Child Health J* (2013) 17:545–55. doi: 10.1007/s10995-012-1028-5

55. Timmers VRJH, Achten PAJ. Non-exhaust PM emissions from electric vehicles. *Atmos Environ* (2016) 134:10–7. doi: 10.1016/j.atmosenv.2016.03.017

56. Zhao N, Qiu J, Ma S, Zhang Y, Lin X, Tang Z, et al. Effects of prenatal exposure to ambient air pollutant PM10 on ultrasound-measured fetal growth. *Int J Epidemiol* (2018) 47:1072–81. doi: 10.1093/ije/dyy019

57. Wang L, Hu W, Guan Q, Du G, Chen T, Wu W, et al. The association between cooking oil fume exposure during pregnancy and birth weight: A prospective mother-child cohort study. *Sci Total Environ* (2018) 612:822–30. doi: 10.1016/j.scitotenv.2017.08.031

58. Bijnens EM, Derom C, Gielen M, Winckelmans E, Fierens F, Vlietinck R, et al. Small for gestational age and exposure to particulate air pollution in the early-life environment of twins. *Environ Res* (2016) 148:39–45. doi: 10.1016/j.envres.2016.03.006

59. Guo P, Chen Y, Wu H, Zeng J, Zeng Z, Li W, et al. Ambient air pollution and markers of fetal growth: A retrospective population-based cohort study of 2.57 million term singleton births in China. *Environ Int* (2020) 135:105410. doi: 10.1016/j.envint.2019.105410

60. Morokuma S, Michikawa T, Yamazaki S, Nitta H, Kato K. Association between exposure to air pollution during pregnancy and false positives in fetal heart rate monitoring. *Sci Rep* (2017) 7:12421. doi: 10.1038/s41598-017-12663-2

61. Chen Q, Ren Z, Liu Y, Qiu Y, Yang H , Zhou Y, et al. The association between preterm birth and ambient air pollution exposure in Shiyan, China 2015–2017. *Int J Environ Res Public Health* (2021) 18(8):4326. doi: 10.3390/ijerph18084326

62. Shah PS, Balkhair T. Air pollution and birth outcomes: A systematic review. *Environ Int* (2011) 37:498–516. doi: 10.1016/j.envint.2010.10.009

63. Siddika N, Rantala AK, Antikainen H, Balogun H, Amegah AK, Ryti NRI, et al. Short-term prenatal exposure to ambient air pollution and risk of preterm birth - a population-based cohort study in Finland. *Environ Res* (2020) 184:109290. doi: 10.1016/j.envres.2020.109290

64. Zou Z, Liu W, Huang C, Cai J, Fu Q, Sun C, et al. Gestational exposures to outdoor air pollutants in relation to low birth weight: A retrospective observational study. *Environ Res* (2021) 193:110354. doi: 10.1016/j.envres.2020.110354

65. Tsoli S, Ploubidis GB, Kalantzi O-I. Particulate air pollution and birth weight: A systematic literature review. *Atmos pollut Res* (2019) 10:1084–122. doi: 10.1016/j.apr.2019.01.016

66. Zhou G, Wu J, Yang M, Sun P, Gong Y, Chai J, et al. Prenatal exposure to air pollution and the risk of preterm birth in rural population of henan province. *Chemosphere* (2022) 286:131833. doi: 10.1016/j.chemosphere.2021.131833

67. Verheyen VJ, Remy S, Lambrechts N, Govarts E, Colles A, Poelmans L, et al. Residential exposure to air pollution and access to neighborhood greenspace in relation to hair cortisol concentrations during the second and third trimester of pregnancy. *Environ Health* (2021) 20(1):11. doi: 10.1186/s12940-021-00697-z

68. Ju L, Li C, Yang M, Sun S, Zhang Q, Cao J, et al. Maternal air pollution exposure increases the risk of preterm birth: Evidence from the meta-analysis of cohort studies. *Environ Res* (2021) 202:111654. doi: 10.1016/j.envres.2021.111654

69. Daniel S, Kloog I, Factor-Litvak P, Levy A, Lunenfeld E, Kioumourtzoglou M-A. Risk for preeclampsia following exposure to PM2.5 during pregnancy. *Environ Int* (2021) 156:106636. doi: 10.1016/j.envint.2021.106636

70. Duhig KE, Shennan AH. Recent advances in the diagnosis and management of pre-eclampsia. *F1000Prime Rep* (2015) 7:24. doi: 10.12703/P7-24

71. Yu H, Yin Y, Zhang J, Zhou R. The impact of particulate matter 2.5 on the risk of preeclampsia: an updated systematic review and meta-analysis. *Environ Sci pollut Res* (2020) 27:37527–39. doi: 10.1007/s11356-020-10112-8

72. Kriit HK, Andersson EM, Carlsen HK, Andersson N, Ljungman PLS, Pershagen G, et al. Using distributed lag non-linear models to estimate exposure lag-response associations between long-term air pollution exposure and incidence of cardiovascular disease. *Int J Environ Res Public Health* (2022) 19:2630. doi: 10.3390/ijerph19052630

73. Sun S, Wang X, Ding L, Zhang Q, Li N, Sui X, et al. Association between preconceptional air pollution exposure and medical purposes for selective termination of pregnancy. *Environ Res* (2021) 202:111743. doi: 10.1016/j.envres.2021.111743

74. Niu Z, Habre R, Chavez TA, Yang T, Grubbs BH, Eckel SP, et al. Association between ambient air pollution and birth weight by maternal individual- and neighborhood-level stressors. *JAMA Netw Open* (2022) 5:e2238174. doi: 10.1001/jamanetworkopen.2022.38174

75. Zhou W, Ming X, Chen Q, Liu X, Yin P. The acute effect and lag effect analysis between exposures to ambient air pollutants and spontaneous abortion: a case-crossover study in China 2017–2019. *Environ Sci pollut Res* (2022) 29:67380–9. doi: 10.1007/s11356-022-20379-8

76. Gómez-Roig MD, Pascal R, Cahuana MJ, García-Algar O, Sebastiani G, Andreu-Fernández V, et al. Environmental exposure during pregnancy: Influence on prenatal development and early life: A comprehensive review. *Fetal Diagn Ther* (2021) 48:245–57. doi: 10.1159/000514884

77. Cornette JMJ, Roos-Hesselink JW. Normal cardiovascular adaptation to pregnancy. In: *Evidence-based cardiology consult*. Springer-Verlag London Ltd (2013). p. 423–32. doi: 10.1007/978-1-4471-4441-0_29

78. Ferrari L, Carugno M, Bollati V. Particulate matter exposure shapes DNA methylation through the lifespan. *Clin Epigenet* (2019) 11(1):129. doi: 10.1186/s13148-019-0726-x

79. Schraufnagel DE. The health effects of ultrafine particles. *Exp Mol Med* (2020) 52:311–7. doi: 10.1038/s12276-020-0403-3

80. Thuy NTT, Dung NT, Sekiguchi K, Thuy LB, Hien NTT, Yamaguchi R. Mass concentrations and carbonaceous compositions of PM0.1, PM2.5, and PM10 at urban locations of Hanoi, Vietnam. *Aerosol Air Qual Res* (2018) 18:1591–605. doi: 10.4209/aaqr.2017.11.0502

81. Wu Y, Liu J, Zhai J, Cong L, Wang Y, Ma W, et al. Comparison of dry and wet deposition of particulate matter in near-surface waters during summer. *PloS One* (2018) 13:e0199241. doi: 10.1371/journal.pone.0199241

82. Su X, Zhao Y, Yang Y, Hua J. Correlation between exposure to fine particulate matter and hypertensive disorders of pregnancy in shanghai, China. *Environ Health* (2020) 19:101. doi: 10.1186/s12940-020-00655-1

83. Chang J, Streitman D. Physiologic adaptations to pregnancy. *Neurol Clin* (2012) 30:781–9. doi: 10.1016/j.ncl.2012.05.001

84. Liu C-W, Lee T-L, Chen Y-C, Liang C-J, Wang S-H, Lue J-H, et al. PM2.5-induced oxidative stress increases intercellular adhesion molecule-1 expression in lung epithelial cells through the IL-6/AKT/STAT3/NF-κB-dependent pathway. *Part Fibre Toxicol* (2018) 15:4. doi: 10.1186/s12989-018-0240-x

85. Li R, Ning Z, Cui J, Yu F, Sioutas C, Hsiai T. Diesel exhaust particles modulate vascular endothelial cell permeability: Implication of ZO-1 expression. *Toxicol Lett* (2010) 197(3):163–8. doi: 10.1016/j.toxlet.2010.05.017

86. Le Y, Hu X, Zhu J, Wang C, Yang Z, Lu D. Ambient fine particulate matter induces inflammatory responses of vascular endothelial cells through activating TLR-mediated pathway. *Toxicol Ind Health* (2019) 35(10):670–8. doi: 10.1177/0748233719871778

87. Su R, Jin X, Li H, Huang L, Li Z. The mechanisms of PM2.5 and its main components penetrate into HUVEC cells and effects on cell organelles. *Chemosphere* (2020) 241:125127. doi: 10.1016/j.chemosphere.2019.125127

88. Ma K, Li C, Xu J, Ren F, Xu X, Liu C, et al. LncRNA Gm16410 regulates PM2.5-induced lung endothelial-mesenchymal transition *via* the TGF-β1/Smad3/p-Smad3 pathway. *Ecotoxicol Environ Saf* (2020) 205:111327. doi: 10.1016/j.ecoenv.2020.111327

89. Xu X, qimuge A, Wang H, Xing C, Gu Y, Liu S, et al. IRE1α/XBP1s branch of UPR links HIF1α activation to mediate ANGII-dependent endothelial dysfunction under particulate matter (PM) 2.5 exposure. *Sci Rep* (2017) 7:13507. doi: 10.1038/s41598-017-13156-y

90. Wauters A, Dreyfuss C, Pochet S, Hendrick P, Berkenboom G, van de Borne P, et al. Acute exposure to diesel exhaust impairs nitric oxide–mediated endothelial vasomotor function by increasing endothelial oxidative stress. *Hypertension* (2013) 62 (2):352–8. doi: 10.1161/HYPERTENSIONAHA.111.00991

91. Calderón-Garcidueñas L, Vincent R, Mora-Tiscareño A, Franco-Lira M, Henríquez-Roldán C, Barragán-Mejía G, et al. Elevated plasma endothelin-1 and pulmonary arterial pressure in children exposed to air pollution. *Environ Health Perspect* (2007) 115(8):1248–53. doi: 10.1289/ehp.9641

92. Grevendonk L, Janssen BG, Vanpoucke C, Lefebvre W, Hoxha M, Bollati V, et al. Mitochondrial oxidative DNA damage and exposure to particulate air pollution in mother-newborn pairs. *Environ Health* (2016) 15:10. doi: 10.1186/s12940-016-0095-2

93. Saenen ND, Vrijens K, Janssen BG, Madhloum N, Peusens M, Gyselaers W, et al. Placental nitrosative stress and exposure to ambient air pollution during gestation: A population study. *Am J Epidemiol* (2016) 184(6):442–9. doi: 10.1093/aje/kww007

94. Familari M, Näätv Å, Erlandsson L, de Iongh RU, Isaxon C, Strandberg B, et al. Exposure of trophoblast cells to fine particulate matter air pollution leads to growth inhibition, inflammation and ER stress. *PloS One* (2019) 14(7):e0218799. doi: 10.1371/journal.pone.0218799

95. Nääv Å, Erlandsson L, Isaxon C, Åsander Frostner E, Ehinger J, Sporre MK, et al. Urban PM2.5 induces cellular toxicity, hormone dysregulation, oxidative damage, inflammation, and mitochondrial interference in the HRT8 trophoblast cell line. *Front Endocrinol (Lausanne)* (2020) 11:75. doi: 10.3389/fendo.2020.00075

96. Qin Z, Hou H, Fu F, Wu J, Han B, Yang W, et al. Fine particulate matter exposure induces cell cycle arrest and inhibits migration and invasion of human extravillous trophoblast, as determined by an iTRAQ-based quantitative proteomics strategy. *Reprod Toxicol* (2017) 74:10–22. doi: 10.1016/j.reprotox.2017.08.014

97. Herbstman JB, Tang D, Zhu D, Qu L, Sjödin A, Li Z, et al. Prenatal exposure to polycyclic aromatic hydrocarbons, benzo[a]pyrene-DNA adducts, and genomic DNA methylation in cord blood. *Environ Health Perspect* (2012) 120:733–8. doi: 10.1289/ehp.1104056

98. van Drooge BL, Marqueño A, Grimalt JO, Fernández P, Porte C. Comparative toxicity and endocrine disruption potential of urban and rural atmospheric organic PM1 in JEG-3 human placental cells. *Environ pollut* (2017) 230:378–86. doi: 10.1016/j.envpol.2017.06.025

99. Wang W, Wang R, Zhang Q, Mor G, Zhang H. Benzo(a)pyren-7,8-dihydrodiol-9,10-epoxide induces human trophoblast swan 71 cell dysfunctions due to cell apoptosis through disorder of mitochondrial fission/fusion. *Environ pollut* (2018) 233:820–32. doi: 10.1016/j.envpol.2017.11.022

100. Wang C, Yang J, Hao Z, Gong C, Tang L, Xu Y, et al. Suppression of progesterone synthesis in human trophoblast cells by fine particulate matter primarily derived from industry. *Environ pollut* (2017) 231:1172–80. doi: 10.1016/j.envpol.2017.08.029

101. Wakx A, Regazzetti A, Dargère D, Auzeil N, Gil S, Evain-Brion D, et al. New *in vitro* biomarkers to detect toxicity in human placental cells: The example of benzo[A] pyrene. *Toxicol In Vitro* (2016) 32:76–85. doi: 10.1016/j.tiv.2015.11.022

102. Pidoux G, Gerbaud P, Guibourdenche J, Thérond P, Ferreira F, Simasotchi C, et al. Formaldehyde crosses the human placenta and affects human trophoblast differentiation and hormonal functions. *PloS One* (2015) 10:e0133506. doi: 10.1371/journal.pone.0133506

103. Shen C, Liu J, Zhu F, Lei R, Cheng H, Zhang C, et al. The effects of cooking oil fumes-derived PM2.5 on blood vessel formation through ROS-mediated NLRP3 inflammasome pathway in human umbilical vein endothelial cells. *Ecotoxicol Environ Saf* (2019) 174:690–8. doi: 10.1016/j.ecoenv.2019.03.028

104. Li T, Hu R, Chen Z, Li Q, Huang S, Zhu Z, et al. Fine particulate matter (PM2.5): The culprit for chronic lung diseases in China. *Chronic Dis Transl Med* (2018) 4:176–86. doi: 10.1016/j.cdtm.2018.07.002

105. Liang S, Zhang J, Ning R, Du Z, Liu J, Batibawa JW, et al. The critical role of endothelial function in fine particulate matter-induced atherosclerosis. *Part Fibre Toxicol* (2020) 17(1):61. doi: 10.1186/s12989-020-00391-x

106. Miller MR. Oxidative stress and the cardiovascular effects of air pollution. *Free Radic Biol Med* (2020) 151:69–87. doi: 10.1016/j.freeradbiomed.2020.01.004

107. Thangavel P, Park D, Lee Y-C. Recent insights into particulate matter (PM2.5)-mediated toxicity in humans: An overview. *Int J Environ Res Public Health* (2022) 19:7511. doi: 10.3390/ijerph19127511

108. Valacchi G, Virgili F, Cervellati C, Pecorelli A. OxInflammation: From subclinical condition to pathological biomarker. *Front Physiol* (2018) 9:858. doi: 10.3389/fphys.2018.00858

109. Scaife PJ, Simpson A, Kurlak LO, v. BL, DS G, Broughton Pipkin F, et al. Increased placental cell senescence and oxidative stress in women with pre-eclampsia and normotensive post-term pregnancies. *Int J Mol Sci* (2021) 22:7295. doi: 10.3390/ijms22147295

110. Rossner P, Tabashidze N, Dostal M, Novakova Z, Chvatalova I, Spatova M, et al. Genetic, biochemical, and environmental factors associated with pregnancy outcomes in newborns from the Czech republic. *Environ Health Perspect* (2011) 119:265–71. doi: 10.1289/ehp.1002470

111. Ausman J, Abbade J, Ermini L, Farrell A, Tagliaferro A, Post M, et al. Ceramide-induced BOK promotes mitochondrial fission in preeclampsia. *Cell Death Dis* (2018) 9:298. doi: 10.1038/s41419-018-0360-0

112. Marín R, Chiarello DI, Abad C, Rojas D, Toledo F, Sobrevia L. Oxidative stress and mitochondrial dysfunction in early-onset and late-onset preeclampsia. *Biochim Biophys Acta (BBA) - Mol Basis Dis* (2020) 1866:165961. doi: 10.1016/j.bbadis.2020.165961

113. Montiel-Dávalos A, Alfaro-Moreno E, López-Marure R. PM $_{2.5}$ and PM $_{10}$ induce the expression of adhesion molecules and the adhesion of monocytic cells to human

umbilical vein endothelial cells. *Inhal Toxicol* (2007) 19(Suppl 1):91–8. doi: 10.1080/08958370701495212

114. Echeverria C, Eltit F, Santibanez JF, Gatica S, Cabello-Verrugio C, Simon F. Endothelial dysfunction in pregnancy metabolic disorders. *Biochim Biophys Acta (BBA) - Mol Basis Dis* (2020) 1866:165414. doi: 10.1016/j.bbadis.2019.02.009

115. Xu Z, Ding W, Deng X. PM2.5, fine particulate matter: A novel player in the epithelial-mesenchymal transition? *Front Physiol* (2019) 10:1404. doi: 10.3389/fphys.2019.01404

116. Evrard SM, Lecce L, Michelis KC, Nomura-Kitabayashi A, Pandey G, Purushothaman K-R, et al. ARTICLE endothelial to mesenchymal transition is common in atherosclerotic lesions and is associated with plaque instability. *Nat Commun* (2016) 7:11853. doi: 10.1038/ncomms11853

117. Xu X, Xu H, qimuge A, Liu S, Wang H, Hu M, et al. MAPK/AP-1 pathway activation mediates AT1R upregulation and vascular endothelial cells dysfunction under PM2.5 exposure. *Ecotoxicol Environ Saf* (2019) 170:188–94. doi: 10.1016/j.ecoenv.2018.11.124

118. Finch J, Riggs D W, O'Toole T E, Arden Pope IIIC, Bhatnagar A, J. Conklin D. Acute exposure to air pollution is associated with novel changes in blood levels of endothelin-1 and circulating angiogenic cells in young, healthy adults. *AIMS Environ Sci* (2019) 6(4):265–76. doi: 10.3934/environsci.2019.4.265

119. Che Y, Su Z, Xia L. Effects of IL-22 on cardiovascular diseases. *Int Immunopharmacol* (2020) 81:106277. doi: 10.1016/j.intimp.2020.106277

120. Xuan X, Zhang L, Tian C, Wu T, Ye H, Cao J, et al. Interleukin-22 and connective tissue diseases: emerging role in pathogenesis and therapy. *Cell Biosci* (2021) 11:2. doi: 10.1186/s13578-020-00504-1

121. Xue J, Nguyen DTC, Habtezion A. Aryl hydrocarbon receptor regulates pancreatic IL-22 production and protects mice from acute pancreatitis. *Gastroenterology* (2012) 143:1670–80. doi: 10.1053/j.gastro.2012.08.051

122. Alabbas SY, Begun J, Florin TH, Oancea I. The role of IL-22 in the resolution of sterile and nonsterile inflammation. *Clin Transl Immunol* (2018) 7:e1017. doi: 10.1002/cti2.1017

123. Luo J-W, Hu Y, Liu J, Yang H, Huang P. Interleukin-22: a potential therapeutic target in atherosclerosis. *Mol Med* (2021) 27:88. doi: 10.1186/s10020-021-00353-9

124. Bersani I, de Carolis MP, Foell D, Weinhage T, Rossi ED, de Carolis S, et al. Interleukin-22: Biomarker of maternal and fetal inflammation? *Immunol Res* (2015) 61:4–10. doi: 10.1007/s12026-014-8568-2

125. Behram M, Oğlak SC, Başkıran Y, Süzen Çaypınar S, Akgöl S, Tunç Ş, et al. Maternal serum IL-22 concentrations are significantly upregulated in patients with preterm premature rupture of membranes. *Ginekol Pol* (2021) 92(9):631–6. doi: 10.5603/GP.a2021.0036

126. Lin A, Biscop E, Breen C, Butler SJ, Smits E, Bogaerts A. Critical evaluation of the interaction of reactive oxygen and nitrogen species with blood to inform the clinical translation of nonthermal plasma therapy. *Oxid Med Cell Longev* (2020) 2020:1–10. doi: 10.1155/2020/9750206

127. Nawrot TS, Saenen ND, Schenk J, Janssen BG, Motta V, Tarantini L, et al. Placental circadian pathway methylation and *in utero* exposure to fine particle air pollution. *Environ Int* (2018) 114:231–41. doi: 10.1016/j.envint.2018.02.034

128. Maury E, Navez B, Brichard SM. Circadian clock dysfunction in human omental fat links obesity to metabolic inflammation. *Nat Commun* (2021) 12:2388. doi: 10.1038/s41467-021-22571-9

129. Shimizu I, Yoshida Y, Minamino T. A role for circadian clock in metabolic disease. *Hypertens Res* (2016) 39:483–91. doi: 10.1038/hr.2016.12

130. Javeed N, Matveyenko Av. Circadian etiology of type 2 diabetes mellitus. *Physiology* (2018) 33:138–50. doi: 10.1152/physiol.00003.2018

131. WHO. . *world health organization. (2021). WHO global air quality guidelines: particulate matter (PM2.5 and PM10), ozone, nitrogen dioxide, sulfur dioxide and carbon monoxide* (2022). World Health Organization. Available at: https://apps.who.int/iris/bitstream/handle/10665/345329/9789240034228-eng.pdf?sequence=1&isAllowed=y (Accessed 19 March 2022).

132. Rosário Filho NA, Urrutia-Pereira M, D'Amato G, Cecchi L, Ansotegui IJ, Galán C, et al. Air pollution and indoor settings. *World Allergy Organ J* (2021) 14:100499. doi: 10.1016/j.waojou.2020.100499

133. Ouidir M, Giorgis-Allemand L, Lyon-Caen S, Morelli X, Cracowski C, Pontet S, et al. Estimation of exposure to atmospheric pollutants during pregnancy integrating space–time activity and indoor air levels: Does it make a difference? *Environ Int* (2015) 84:161–73. doi: 10.1016/j.envint.2015.07.021

134. Schraufnagel DE, Balmes JR, Cowl CT, de Matteis S, Jung S-H, Mortimer K, et al. Air pollution and noncommunicable diseases. *Chest* (2019) 155:409–16. doi: 10.1016/j.chest.2018.10.042

135. Brazil N. Environmental inequality in the neighborhood networks of urban mobility in US cities. *Proc Natl Acad Sci* (2022) 119(17):e2117776119. doi: 10.1073/pnas.2117776119

136. Tran V, Park D, Lee Y-C. Indoor air pollution, related human diseases, and recent trends in the control and improvement of indoor air quality. *Int J Environ Res Public Health* (2020) 17(8):2927. doi: 10.3390/ijerph17082927

137. Ding J, Zhong J, Yang Y, Li B, Shen G, Su Y, et al. Occurrence and exposure to polycyclic aromatic hydrocarbons and their derivatives in a rural Chinese home through biomass fuelled cooking. *Environ pollut* (2012) 169:160–6. doi: 10.1016/j.envpol.2011.10.008

138. Manoukian A, Quivet E, Temime-Roussel B, Nicolas M, Maupetit F, Wortham H. Emission characteristics of air pollutants from incense and candle burning in indoor atmospheres. *Environ Sci pollut Res* (2013) 20(7):4659–70. doi: 10.1007/s11356-012-1394-y

139. Seguel JM, Merrill R, Seguel D, Campagna AC. Indoor air quality. *Am J Lifestyle Med* (2017) 11(4):284–95. doi: 10.1177/1559827616653343

140. Zulauf N, Dröge J, Klingelhöfer D, Braun M, Oremek GM, Groneberg DA. Indoor air pollution in cars: An update on novel insights. *Int J Environ Res Public Health* (2019) 16:2441. doi: 10.3390/ijerph16132441

141. Nemmar A, Hoet PHM, Vanquickenborne B, Dinsdale D, Thomeer M, Hoylaerts MF, et al. Passage of inhaled particles into the blood circulation in humans. *Circulation* (2002) 105:411–4. doi: 10.1161/hc0402.104118

142. Franklin P, Tan M, Hemy N, Hall GL. Maternal exposure to indoor air pollution and birth outcomes. *Int J Environ Res Public Health* (2019) 16:1364. doi: 10.3390/ijerph16081364

143. Younger A, Alkon A, Harknett K, Jean Louis R, Thompson LM. Adverse birth outcomes associated with household air pollution from unclean cooking fuels in low- and middle-income countries: A systematic review. *Environ Res* (2022) 204:112274. doi: 10.1016/j.envres.2021.112274

144. Jayaraj NP, Rathi A, Taneja DK. Exposure to household air pollution during pregnancy and birthweight. *Indian Pediatr* (2019) 56:875–6. doi: 10.1007/s13312-019-1616-1

145. Hu P, Wang C, Ding P, He Y-H, Xie C, Tian F-Y, et al. Placental weight mediates association between prenatal exposure to cooking oil fumes and preterm birth. *J Maternal-Fetal Neonatal Med* (2021) 35(25):7248–58. doi: 10.1080/14767058.2021.1946783

146. Arinola G, Dutta A, Oluwole O, Olopade C. Household air pollution, levels of micronutrients and heavy metals in cord and maternal blood, and pregnancy outcomes. *Int J Environ Res Public Health* (2018) 15(12):2891. doi: 10.3390/ijerph15122891

147. Khan MN, Nurs CZ B, Mofizul Islam M, Islam MR, Rahman MM. Household air pollution from cooking and risk of adverse health and birth outcomes in Bangladesh: a nationwide population-based study. *Environ Health* (2017) 16(1):57. doi: 10.1186/s12940-017-0272-y

148. Rey-Ares L, Irazola V, Althabe F, Sobrino E, Mazzoni A, Serón P, et al. Lower tract respiratory infection in children younger than 5 years of age and adverse pregnancy outcomes related to household air pollution in bariloche (Argentina) and temuco (Chile). *Indoor Air* (2016) 26(6):964–75. doi: 10.1111/ina.12274

149. Naeher LP, Smith KR, Leaderer BP, Neufeld L, Mage DT. Carbon monoxide as a tracer for assessing exposures to particulate matter in wood and gas cookstove households of highland Guatemala. *Environ Sci Technol* (2001) 35(3):575–81. doi: 10.1021/es991225g

150. Pope DP, Mishra V, Thompson L, Siddiqui AR, Rehfuess EA, Weber M, et al. Risk of low birth weight and stillbirth associated with indoor air pollution from solid fuel use in developing countries. *Epidemiol Rev* (2010) 32:70–81. doi: 10.1093/epirev/mxq005

151. Nazaroff WW. Exploring the consequences of climate change for indoor air quality. *Environ Res Lett* (2013) 8(1). doi: 10.1088/1748-9326/8/1/015022

152. Schembari A, Triguero-Mas M, de Nazelle A, Dadvand P, Vrijheid M, Cirach M, et al. Personal, indoor and outdoor air pollution levels among pregnant women. *Atmos Environ* (2013) 64:287–29. doi: 10.1016/j.atmosenv.2012.09.053

153. Steinle S, Reis S, Sabel CE, Semple S, Twigg MM, Braban CF, et al. Personal exposure monitoring of PM 2.5 in indoor and outdoor microenvironments. *Sci Total Environ* (2015) 508:383–94. doi: 10.1016/j.scitotenv.2014.12.003

154. Blanchard O, Deguen S, Kihal-Talantikite W, François R, Zmirou-Navier D. Does residential mobility during pregnancy induce exposure misclassification for air pollution? *Environ Health* (2018) 17(1):72. doi: 10.1186/s12940-018-0416-8

155. Shezi B, Mathee A, Cele N, Ndabandaba S, Street RA. Occupational exposure to fine particulate matter (PM4 and PM2.5) during hand-made cookware operation: Personal, indoor and outdoor levels. *Int J Environ Res Public Health* (2020) 17:7522. doi: 10.3390/ijerph17207522

156. Megahed NA, Ghoneim EM. Indoor air quality: Rethinking rules of building design strategies in post-pandemic architecture. *Environ Res* (2021) 193:110471. doi: 10.1016/j.envres.2020.110471

157. Jin Z-Y, Wu M, Han R-Q, Zhang X-F, Wang X-S, Liu A-M, et al. Household ventilation may reduce effects of indoor air pollutants for prevention of lung cancer: A case-control study in a Chinese population. *PloS One* (2014) 9(7):e102685. doi: 10.1371/journal.pone.0102685

158. American Lung Association. *Ventilation: How buildings breathe* (2020). Available at: https://www.lung.org/clean-air/at-home/ventilation-buildings-breathe.

159. Péter S, Holguin F, Wood L, Clougherty J, Raederstorff D, Antal M, et al. Nutritional solutions to reduce risks of negative health impacts of air pollution. *Nutrients* (2015) 7(12):10398–416. doi: 10.3390/nu7125539

160. Schulz AJ, Mentz GB, Sampson NR, Dvonch JT, Reyes AG, Izumi B. Effects of particulate matter and antioxidant dietary intake on blood pressure. *Am J Public Health* (2015) 105(6):1254–61. doi: 10.2105/AJPH.2014.302176

161. Bo L, Jiang S, Xie Y, Kan H, Song W, Zhao J. Effect of vitamin e and omega-3 fatty acids on protecting ambient PM2.5-induced inflammatory response and oxidative stress in vascular endothelial cells. *PloS One* (2016) 11(3):e0152216. doi: 10.1371/journal.pone.0152216

162. Lim CC, Hayes RB, Ahn J, Shao Y, Silverman DT, Jones RR, et al. Mediterranean Diet and the association between air pollution and cardiovascular disease mortality risk. *Circulation* (2019) 139(15):1766–75. doi: 10.1161/CIRCULATIONAHA.118.035742

163. McLoughlin RF, Berthon BS, Williams EJ, Wood LG. Vitamin e and air pollution. In: *Vitamin e in human health*. Cham: Springer International Publishing (2019).

164. Barthelemy J, Sanchez K, Miller MR, Khreis H. New opportunities to mitigate the burden of disease caused by traffic related air pollution: Antioxidant-rich diets and supplements. *Int J Environ Res Public Health* (2020) 17(2):630. doi: 10.3390/ijerph17020630

165. FDA. *Guidance for industry food labeling; nutrient content claims; definition for "High potency" and definition for "Antioxidant" for use in nutrient content claims for dietary supplements and conventional foods*. Guidance for Industry Food Labeling (2008). Available at: https://www.govinfo.gov/app/details/FR-1997-09-23/97-24732.

166. van Meeteren ME, Teunissen CE, Dijkstra CD, van Tol EAF. Antioxidants and polyunsaturated fatty acids in multiple sclerosis. *Eur J Clin Nutr* (2005) 59(12):1347–61. doi: 10.1038/sj.ejcn.1602255

167. Dewell A, Tsao P, Rigdon J, Gardner CD. Antioxidants from diet or supplements do not alter inflammatory markers in adults with cardiovascular disease risk. A pilot randomized controlled trial. *Nutrition Res* (2018) 50:63–72. doi: 10.1016/j.nutres.2017.10.017

168. Romieu I, Garcia-Esteban R, Sunyer J, Rios C, Alcaraz-Zubeldia M, Velasco SR, et al. The effect of supplementation with omega-3 polyunsaturated fatty acids on markers of oxidative stress in elderly exposed to $PM_{2.5}$. *Environ Health Perspect* (2008) 116 (9):1237–42. doi: 10.1289/ehp.10578

169. Lin Z, Chen R, Jiang Y, Xia Y, Niu Y, Wang C, et al. Cardiovascular benefits of fish-oil supplementation against fine particulate air pollution in China. *J Am Coll Cardiol* (2019) 73(16):2076–85. doi: 10.1016/j.jacc.2018.12.093

170. Jedrychowski W, Masters E, Choi H, Sochacka E, Flak E, Mroz E, et al. Pre-pregnancy dietary vitamin a intake may alleviate the adverse birth outcomes associated with prenatal pollutant exposure: Epidemiologic cohort study in Poland. *Int J Occup Environ Health* (2007) 13(2):175–80. doi: 10.1179/oeh.2007.13.2.175

171. Hennig B, Ettinger AS, Jandacek RJ, Koo S, McClain C, Seifried H, et al. Using nutrition for intervention and prevention against environmental chemical toxicity and associated diseases. *Environ Health Perspect* (2007) 115:493–5. doi: 10.1289/ehp.9549

172. Hosseinpanah F, Pour SH, Heibatollahi M, Moghbel N, Asefzade S, Azizi F. The effects of air pollution on vitamin d status in healthy women: a cross sectional study. *BMC Public Health* (2010) 10:519. doi: 10.1186/1471-2458-10-519

173. Hoseinzadeh E, Taha P, Wei C, Godini H, Ashraf GM, Taghavi M, et al. The impact of air pollutants, UV exposure and geographic location on vitamin d deficiency. *Food Chem Toxicol* (2018) 113:241–54. doi: 10.1016/j.fct.2018.01.052

174. Zhao Y, Wang L, Liu H, Cao Z, Su X, Cai J, et al. Particulate air pollution exposure and plasma vitamin d levels in pregnant women: A longitudinal cohort study. *J Clin Endocrinol Metab* (2019) 104(8):3320–26. doi: 10.1210/jc.2018-02713

175. Baïz N, Dargent-Molina P, Wark JD, Souberbielle J-C, Slama R, Annesi-Maesano I. Gestational exposure to urban air pollution related to a decrease in cord blood vitamin d levels. *J Clin Endocrinol Metab* (2012) 97(11):4087–95. doi: 10.1210/jc.2012-1943

176. Mann EH, Ho T-R, Pfeffer PE, Matthews NC, Chevretton E, Mudway I, et al. Vitamin d counteracts an IL-23–dependent IL-17A $^{+}$ IFN- γ^{+} response driven by urban particulate matter. *Am J Respir Cell Mol Biol* (2017) 57:355–66. doi: 10.1165/rcmb.2016-0409OC

177. Khalessi N, Kalani M, Araghi M, Farahani Z. The relationship between maternal vitamin d deficiency and low birth weight neonates. *J Family Reprod Health* (2015) 9:113–7.

178. Larqué E, Morales E, Leis R, Blanco-Carnero JE. Maternal and foetal health implications of vitamin d status during pregnancy. *Ann Nutr Metab* (2018) 72(3):179–92. doi: 10.1159/000487370

179. Sbihi H, Tamburic L, Koehoorn M, Brauer M. Perinatal air pollution exposure and development of asthma from birth to age 10 years. *Eur Respir J* (2016) 47:1062–71. doi: 10.1183/13993003.00746-2015

180. Stingone JA, Luben TJ, Carmichael SL, Aylsworth AS, Botto LD, Correa A, et al. Maternal exposure to nitrogen dioxide, intake of methyl nutrients, and congenital heart defects in offspring. *Am J Epidemiol* (2017) 186:719–29. doi: 10.1093/aje/kwx139

181. Zhong J, Karlsson O, Wang G, Li J, Guo Y, Lin X, et al. B vitamins attenuate the epigenetic effects of ambient fine particles in a pilot human intervention trial. *Proc Natl Acad Sci U.S.A.* (2017) 114:3503–8. doi: 10.1073/pnas.1618545114

182. Zhong J, Trevisi L, Urch B, Lin X, Speck M, Coull BA, et al. B-vitamin supplementation mitigates effects of fine particles on cardiac autonomic dysfunction and inflammation: A pilot human intervention trial. *Sci Rep* (2017) 7:45322. doi: 10.1038/srep45322

183. Sanchez H, Hossain MB, Lera L, Hirsch S, Albala C, Uauy R, et al. High levels of circulating folate concentrations are associated with DNA methylation of tumor suppressor and repair genes p16, MLH1, and MGMT in elderly chileans. *Clin Epigenet* (2017) 9:74. doi: 10.1186/s13148-017-0374-y

184. Castaño E, Piñuñuri R, Hirsch S, Ronco AM. [Folate and pregnancy, current concepts: It is required folic acid supplementation]? *Rev Chil Pediatr* (2017) 88:199–206. doi: 10.4067/S0370-41062017000200001

185. Smith AD, Warren MJ, Refsum H. Vitamin B12. *Adv Food Nutr Res* (2018) 83:215–79. doi: 10.1016/bs.afnr.2017.11.005

frontiers | Frontiers in Endocrinology

TYPE Original Research
PUBLISHED 03 March 2023
DOI 10.3389/fendo.2023.1021640

Check for updates

OPEN ACCESS

EDITED BY
Cilia Abad,
Charles University, Czechia

REVIEWED BY
Priyadarshini Pantham,
University of California, San Diego, United States
Melanie Smith,
Flinders University, Australia
Reinaldo Marín,
Instituto Venezolano de Investigaciones Científicas (IVIC), Venezuela

*CORRESPONDENCE
Udo R. Markert
udo.markert@med.uni-jena.de
Diana M. Morales-Prieto
diana.morales@med.uni-jena.de

SPECIALTY SECTION
This article was submitted to Developmental Endocrinology, a section of the journal Frontiers in Endocrinology

RECEIVED 17 August 2022
ACCEPTED 07 February 2023
PUBLISHED 03 March 2023

CITATION
Murrieta-Coxca JM, Barth E, Fuentes-Zacarias P, Gutiérrez-Samudio RN, Groten T, Gellhaus A, Köninger A, Marz M, Markert UR and Morales-Prieto DM (2023) Identification of altered miRNAs and their targets in placenta accreta. *Front. Endocrinol.* 14:1021640. doi: 10.3389/fendo.2023.1021640

COPYRIGHT
© 2023 Murrieta-Coxca, Barth, Fuentes-Zacarias, Gutiérrez-Samudio, Groten, Gellhaus, Köninger, Marz, Markert and Morales-Prieto. This is an open-access article distributed under the terms of the Creative Commons Attribution License (CC BY). The use, distribution or reproduction in other forums is permitted, provided the original author(s) and the copyright owner(s) are credited and that the original publication in this journal is cited, in accordance with accepted academic practice. No use, distribution or reproduction is permitted which does not comply with these terms.

Identification of altered miRNAs and their targets in placenta accreta

José M. Murrieta-Coxca[1], Emanuel Barth[2,3], Paulina Fuentes-Zacarias[1], Ruby N. Gutiérrez-Samudio[1], Tanja Groten[1], Alexandra Gellhaus[4], Angela Köninger[4,5], Manja Marz[2,6], Udo R. Markert[1*] and Diana M. Morales-Prieto[1*]

[1]Department of Obstetrics, Placenta Lab, Jena University Hospital, Jena, Germany, [2]Friedrich Schiller University Jena, Faculty of Mathematics and Computer Science, RNA Bioinformatics and High Throughput Analysis, Jena, Germany, [3]Faculty of Mathematics and Computer Science, Bioinformatics Core Facility, Friedrich Schiller University Jena, Jena, Germany, [4]Department of Gynecology and Obstetrics, University of Duisburg-Essen, Essen, Germany, [5]University Department of Gynecology and Obstetrics, Hospital St. Hedwig of the Order of St. John, University Medical Center Regensburg, Regensburg, Germany, [6]Fritz Lipman Institute (FLI), Leibniz Institute for Age Research, Jena, Germany

Placenta accreta spectrum (PAS) is one of the major causes of maternal morbidity and mortality worldwide with increasing incidence. PAS refers to a group of pathological conditions ranging from the abnormal attachment of the placenta to the uterus wall to its perforation and, in extreme cases, invasion into surrounding organs. Among them, placenta accreta is characterized by a direct adhesion of the villi to the myometrium without invasion and remains the most common diagnosis of PAS. Here, we identify the potential regulatory miRNA and target networks contributing to placenta accreta development. Using small RNA-Seq followed by RT-PCR confirmation, altered miRNA expression, including that of members of placenta-specific miRNA clusters (e.g., C19MC and C14MC), was identified in placenta accreta samples compared to normal placental tissues. *In situ* hybridization (ISH) revealed expression of altered miRNAs mostly in trophoblast but also in endothelial cells and this profile was similar among all evaluated degrees of PAS. Kyoto encyclopedia of genes and genomes (KEGG) analyses showed enriched pathways dysregulated in PAS associated with cell cycle regulation, inflammation, and invasion. mRNAs of genes associated with cell cycle and inflammation were downregulated in PAS. At the protein level, NF-κB was upregulated while PTEN was downregulated in placenta accreta tissue. The identified miRNAs and their targets are associated with signaling pathways relevant to controlling trophoblast function. Therefore, this study provides miRNA:mRNA associations that could be useful for understanding PAS onset and progression.

KEYWORDS

pregnancy, placenta accreta spectrum, microRNA, RNA-sequencing, miRNA targets, placenta, trophoblast, mRNA

1 Introduction

Placenta Accreta Spectrum (PAS) is the term that integrates the different grades of abnormal placental adherence and invasion (1, 2). The most current classification of PAS includes three grades: 1. Placenta accreta or adherenta, 2. Placenta increta and 3. Placenta percreta. In adherent placenta accreta, the decidua basalis is partly or completely lost so that the trophoblast layer is directly apposed to the myometrial tissue, but without invading it. Placenta increta is defined by deep invasion of trophoblast cells into the myometrium, and placenta percreta when trophoblast cells invade and penetrate the uterine serosa (2, 3). An additional classification recently suggested by FIGO included the subclassification of grade 3a: Placenta percreta limited to the uterine serosa grade 3b: Placenta percreta with urinary bladder invasion; and grade 3c: Placenta percreta with the involvement of pelvic organs (2–4). PAS severity can be evaluated during pregnancy by ultrasound examinations (5, 6), but many cases remain undiagnosed antepartum and are later classified based on the intraoperative situation and histological findings related to partial or complete loss of decidua basalis and the depth of myometrial trophoblast cell invasion (2, 3, 5). The most common diagnosis of PAS cases is placenta accreta (>70%), followed by increta (~15%) and percreta (10%) (5, 7, 8).

The differences in the clinical and histopathological criteria used to define PAS in previous studies make it difficult to compare data and reach a consensus on the etiology of the disease. A failure in normal decidualization caused by previous endometrial damage is currently the most favored hypothesis, but the abnormal invasive capacities of trophoblast cells may also contribute to the disease (9, 10). PAS is frequently associated with a previous cesarean section, which is increasingly applied, thus, the worldwide prevalence of PAS has risen over the last four decades (11, 12). However, only a few investigations have focused on the molecular mechanisms associated with PAS that may also explain its development in women during their first pregnancy. As PAS does not naturally occur in animals and due to its uniqueness to human pregnancy (3, 13), its study in animal models is highly constricted despite one published mouse model (14).

A recent study reported a very low correlation between transcriptome and proteome profiling of PAS samples suggesting a significant role of post-transcriptional regulation (15), which may be mediated by non-coding RNAs including miRNAs. The human placenta harbors miRNAs (20-22 nucleotides size), which regulate its development and functionality (16). This regulation is further demonstrated by the fact that placenta-specific and -associated miRNAs have particular expression patterns during different stages of pregnancy (17–19). As demonstrated in several pioneer studies, dysregulation of specific miRNAs is associated with pregnancy pathologies, including PAS (20–23). Some of the altered miRNAs are linked with intracellular signaling networks implicated in angiogenesis (24), trophoblast apoptosis (20), and epithelial-mesenchymal transition (23).

In this study, next-generation sequencing was used to screen the miRNA signature of PAS placentas and compare it to healthy pregnancies. Altered miRNAs, as well as their targets, were validated and localized in placental tissues. Our results offer molecular elements for understanding the etiology of PAS and promote the identification of markers in PAS.

2 Material and methods

The Placenta Lab strictly applies quality management and is certified after DIN EN ISO 9001.

2.1 Patient samples

Patients were recruited for the study from the Department of Obstetrics, University Hospital Jena and the Department of Gynecology and Obstetrics, University Hospital Essen, Germany, between 2014 and 2018. The respective ethics committees approved the study according to the Helsinki Declaration on ethical principles for medical research involving human subjects by obtaining consent forms (Amendment to No: 1509-03/05 Jena and 12-5212-BO Essen). Multiple pregnancies, fetal anomalies, and infections were excluded from the study.

Samples obtained in Jena were collected intraoperatively in cases where a postpartum curettage had to be performed due to incomplete placenta or retention of the placenta after delivery, even under administration of uterotonic drugs or controlled cord traction. An additional sample was taken during cesarean section of a patient with placenta praevia, intraoperatively diagnosed to be an abnormal adherent placenta. Placenta tissue samples were taken in all cases from the suspected sight of detachment failure. Histopathological findings such as loss of decidua basalis or the direct trophoblast apposition to the myometrial tissue without invasion were used as confirmers for the diagnosis of placenta accreta. For controls, placental chorionic tissue was collected from normally delivered placentas including (for ISH and IF) or excluding decidua (RNA analysis). Samples were immediately washed with sterile phosphate buffer solution (PBS) and placed in RNA later (cat. No. AM7021; Invitrogen Life Technologies, Darmstadt, Germany) overnight and then stored in cryotubes at -80°C until RNA extraction, or fixed in 4% formalin overnight before paraffin-embedding. A sub-set of 17 samples was used for the initial RNA-Seq analysis and a complete set of 26 samples to perform the validation PCR. Samples for immunostaining and *in situ* hybridization were also selected from the complete set. Clinical characteristics are summarized in Table 1.

Placental tissue from Essen was obtained at the time of vaginal delivery or caesarian section from cases where PAS was diagnosed at the third stage of delivery or based on antepartum ultrasound measurements. Samples were classified into placenta accreta, increta or percreta (each n=1) according to the criteria defined by Cali et al. (6) and following the International Federation of Gynecology and Obstetrics (FIGO) guidelines based on intraoperative situation and histological findings (2). Intraoperatively, the area of placental tissue with the highest degree of invasion was chosen for analysis and was collected including surrounding tissue (decidua, myometrium, uterine serosa, broad ligament tissue). In the cases

10.3389/fendo.2023.1021640

TABLE 1 Clinical characteristics of PAS samples.

	Initial RNA-Seq			PCR Validation cohort			Immunostaining			ISH		
	NP (n=9)	PAS (n=8)	p-Value	NP (n=14)	PAS (n=12)	p-Value	NP (n=3)	PAS (n=3)	p-Value	NP (n=4)	PAS (n=6)	p-Value
Maternal age (y)	28.9 ± 3.0	30.2 ± 7.5	0.62	30.4 ± 3.5	30.6 ± 6.8	0.91	31.3 ± 10.0	38.7 ± 2.9	0.29	30.8 ± 7.2	37.8 ± 2.3	0.05
Gestational age (w)	39.8 ± 0.7	39.4 ± 2.2	0.58	39.2 ± 1.5	39.6 ± 1.8	0.51	39.5 ± 1.6	37.9 ± 3.3	0.50	40.1 ± 1.4	36.6 ± 4.7	0.19
Placenta weight (g)	641.5 ± 93.2	509.5 ± 45.5	*<0.05	632.8 ± 116.6	536.3 ± 56.9	0.07	664.3 ± 90.7	527.3 ± 112.8	0.18	654.8 ± 70.2	527.3 ± 112.8 #	0.12
Birth weight (g)	3512.2 ± 295.2	3164.4 ± 434.4	0.07	3469.3 ± 375.9	3429.2 ± 570.0	0.83	3481.7 ± 123.9	3016.7 ± 767.9	0.36	3598.8 ± 215.6	2814.2 ± 918.8.9	0.14
Size birth (cm)	51.7 ± 2.0	51.4 ± 2.0	0.73	51.5 ± 2.4	52.2 ± 2.0	0.38	53.0 ± 1.7	49.2 ± 0.8	0.02	52.5 ± 1.7	49.2 ± 0.8	*<0.05
Neonate gender (% male)	33.3	87.5		37.5	83.3		66.7	33.3		50	50	
Delivery mode (% Cesarean)	44.4	25		64.3	16.6		66.7	33.3		50	Accreta: 25 Increta:100 Percreta: 100	
Gravida	1.8 ± 1.1	1.8 ± 0.9	0.95	2.4 ± 1.6	2.1 ± 1.2	0.54	4.3 ± 3.0	3.7 ± 1.2	0.74	2.8 ± 2.9	4.3 ± 1.6	0.29
Parity	1.7 ± 0.9	1.5 ± 0.5	0.64	2.0 ± 1.4	1.7 ± 0.9	0.39	3.0 ± 2.0	1.3 ± 0.6	0.24	2.2 ± 1.9	2.9 ± 1.5	0.82
PAS disorder	None (9)	Accreta (8)		None (14)	Accreta (12)		None (3)	Accreta (3)		None (4)	Accreta (4) Increta (1) Percreta (1)	

Values are presented as the mean ± SD. NP, Normal pregnancy; PAS, placenta accreta spectrum. PCR Validation set includes samples of the initial set. *p<0.05 #: Information of placenta weight is missing for placenta increta and percreta cases.

of placenta increta and percreta, the specimens were obtained by focal resection of the placenta or hysterectomy. Tissue samples were fixed in 4% formalin overnight followed by standard processing to obtain paraffin-embedded sections for ISH. The clinical characteristics are summarized in Table 1.

2.2 RNA isolation

Total RNA was isolated using a mirVana™ miRNA Isolation Kit (cat. No. AM1561; Invitrogen), according to the manufacturer's protocol. Approximately 100 mg placenta tissue per sample was transferred to a Medicon (cat. No. 340591; BD Biosciences, Franklin Lakes NJ, USA) disposable for biological sample disaggregation containing 1 ml of lysis buffer (provided in the kit) and processed in a Medimachine (Dako; BD) for 20 s. Tissue suspension was collected, and Total RNA concentration was determined in a high-speed microfluidic UV/VIS spectrophotometer (QIAxpert System, Qiagen Hilden, Germany). Samples with A260/A280 ratio >1.8 were stored at −80°C until further processing.

2.3 Next-generation sequencing

GATC Biotech AG, Konstanz, Germany, performed the next-generation sequencing. The small RNA libraries were created using Illumina's small RNA sample preparation protocol (TruSeq Small RNA Sample Prep Kits; Illumina, San Diego, CA, USA) with minor adaptations to the manufacturer's instructions. Single read sequencing of the libraries was performed on a HiSeq 2500 (Illumina) according to the manufacturer's protocol. At least 10 million reads per sample were generated.

2.4 Small RNA-Seq library processing, mapping, and differential expression analysis

First, the RA2 adapter sequences (5'-TGGAATTCTCGGGTG CCAAGG) of the TruSeq small RNA preparation kit were clipped from all reads, using cutadapt (25) (version 2.0), and all reads shorter than 15 bp or with a mean quality lower than 20 were removed subsequently. Read quality was monitored using FastQC (v0.11.3; http://www.bioinformatics.babraham.ac.uk/projects/fastqc). Quality reports of the raw and processed RNA-Seq libraries can be found at https://osf.io/8wq9h. Mapping was performed using TopHat2 (26) (version 2.1.1) with standard parameters onto the human reference genome (Ensembl release 98), and read counting was done using the respective Ensembl gene annotation. For counting, featureCounts (27) (version 1.6.3) with the parameters -M, -O 0.5 was used to count reads for the mature miRNA annotations of each human pre-miRNA separately. Analysis of differentially expressed miRNAs

(DEmiRNAs), as well as plotting PCA, was performed by the Bioconductor R package DESeq2 (28) (version 1.10.0). Multiple testing adjustment of the resulting p-values was performed using Benjamini and Hochberg's FDR approach (29). Mature miRNA loci with an identified adjusted p-value < 0.05 were considered differentially expressed. RNA-Seq datasets including DEmiRNA results and the count values are available at NCBI's GEO database https://www.ncbi.nlm.nih.gov/geo/ under the accession IDGSE216742.

2.5 Biological pathway analysis and interaction network of miRNA targets

Target mRNAs of DEmiRNAs were obtained from the miRTarBase (30) (release 8.0) to get a non-redundant list of experimentally verified genes being potentially altered in PAS. Following the strategy used in our earlier study (31), DEmiRNA targets were assigned within the human regulatory pathways of the KEGG database. KEGG pathways were ranked individually according to the number of targeted genes within each pathway. The hypergeometric test was used to assess if specific pathways were significantly targeted by calculating the corresponding p-values for each pathway. Analysis of sub-pathways was performed by manually identifying key altered regions. To estimate which of the genes of the sub-pathway were most likely affected by the altered DEmiRNAs in PAS, an impact score was calculated based on the frequencies of the genes within the enriched pathways and the amount of DEmiRNAs targeting each gene.

2.6 Confirmation of DEmiRNAs

Expression levels of representative miRNAs were analyzed using the TaqMan™ Advanced miRNA cDNA Synthese-Kit (cat. No. A28007, Applied Biosystems, Darmstadt, Germany) and the TaqMan™ Fast Advanced Master Mix, no UNG (cat. No. A44360, Applied Biosystems) according with the manufacturer's protocol with specific miRNA probes (hsa-miR-193b-3p, Assay ID: 478314_mir; hsa-miR-519d-3p, Assay ID: 478986_mir; hsa-miR-331-3p Assay ID: 478323_mir; hsa-miR-3074-5p Assay ID: 479606_mir; hsa-miR-24-3p Assay ID: 477992_mir; hsa-miR-382-3p Assay ID: 479458_mir; hsa-miR-376c-3p Assay ID: 478459_mir; hsa-miR-495-3p Assay ID: 478136_mir; hsa-miR-370-3p Assay ID: 478326_mir; hsa-miR-423-3p Assay ID: 478327_mir; hsa-miR-222-3p Assay ID: 477982_mir; hsa-miR-106b-3p Assay ID: 477866_mir; hsa-miR-4732-3p Assay ID: 478118_mir; hsa-miR-454-5p Assay ID: 478919_mir; hsa-mir-3615-3p Assay ID: 478837_mir; hsa-miR-16-2-3p Assay ID: 477931_mir; hsa-miR-39-3p Assay ID: 478293_mir). The *Caenorhabditis elegans* miRNA cel-miR-39 (Assay ID: 000200; 5′-UCACCGGGUGUAAAUCAGCUUG) was added at a concentration of 1.6 x 10^8 copies/µL and used as spike-in control. PCR reactions were run in duplicates including no-template controls in 96-well plates on a Mx3005P qPCR System (Applied Biosystems) using 40 cycles, at the following conditions: 95°C for 3 sec and anneal/extend at 60°C for 20 sec. Fold changes were calculated by the formula $2^{-\Delta Ct}$ using cel-miR-39 as normalizer.

2.7 *In situ* localization of DEmiRNA

Representative miRNAs were localized in the placenta tissue by using the microRNA *in situ* hybridization (ISH) Buffer Set for formalin-fixed paraffin-embedded (FFPE) tissue samples (cat. No. 339457; Qiagen). Specific miRCURY LNA™ microRNA detection probes (cat. No. 339501; Qiagen), as well as positive and negative controls, were purchased from Qiagen (cat. No 339451). The one-day microRNA ISH protocol was carried out according to the supplier's recommendations. In brief, paraffin blocks were cut into 6 µm-thick sections. Slides were dewaxed in a train of different percentages of xylene and ethanol solutions ending in phosphate-buffered saline (PBS) (cat No. 14190-094; Gibco, Schwerte, Germany). Following, slides were incubated with Proteinase-K for 10 min at 37°C in a CytoBrite Duo slide incubation system (SciGene; Sunnyvale, CA, USA) and then washed twice with PBS. Hybridization mix containing 10 nM of double-DIG LNA™ microRNA probe (miR-519d-3p, miR-193b-3p, miR-106b-3p, miR-370-3p or the negative control scramble probe SCR, which represents random sequence) was added to the slides and hybridized for 1 h. Slides were then washed in a slide rack with different concentrations of 5xSSC buffer (cat. No. 15557-044; Invitrogen) and placed in PBS. A hydrophobic barrier was created around the tissue sections using a Dako-Pen (Cat. No. H-4000; Vector Laboratories, Newark, CA, USA), and slides were incubated in a humidifying chamber with a blocking solution for 15 min. The blocking solution was removed, anti-DIG reagent (cat. No. 11093274910; Sigma Aldrich; Taufkirchen, Germany) was applied on the slides for 60 min incubation at RT. Sections were incubated with freshly prepared alkaline phosphatase substrate (cat. No. 11697471001; Merck, Darmstadt, Germany) for 2 h at 30°C, protected from light in the humidifying chamber. The reaction was stopped by incubating slides in KTBT buffer (Potassium-Tris Buffer with Triton). Nuclear Fast Red™ (cat. No. H-3403; Vector Laboratories) was applied for 1 min for nuclear counterstaining. Slides were dehydrated in ethanol solutions and mounted with 1-2 drops of mounting medium (cat. No. 03989; Sigma Aldrich), avoiding air-drying. The precipitate was allowed to settle overnight, and slides were analyzed using an Axio Imager A2 microscope and Zen Blue software (Carl Zeiss Microscopy GmbH, Jena Germany).

2.8 Expression of target mRNAs

Total RNA (300 ng) from NP and placenta accreta samples PAS was used to analyze the expression of selected mRNAs by reverse transcription using High-Capacity RNA-to-cDNA™ Kit (cat. No.

4368814; Applied Biosystems). Quantitative real-time PCR was performed using TaqMan assays (ERK1, Assay ID: Hs00385075_m1; NFKB1, Assay ID: Hs00765730_m1; AKT1, Assay ID: Hs00178289_m1; PTEN, Assay ID: Hs02621230_s1; STAT3, Assay ID: Hs00374280_m1; TGFB1, Assay ID: Hs00171257_m1; and GAPDH, Assay ID: Hs03929097_g1) and TaqMan Universal PCR Master Mix reagents (cat. No. 4440040; Applied Biosystems). qPCR was run on a Mx3005P qPCR System (Applied Biosystems). mRNA expression was normalized using the $2^{-\Delta Ct}$ method relative to GAPDH.

2.9 Immunofluorescence staining

Paraffin-embedded tissue sections were deparaffinized, hydrated in a graded ethanol series, and quenched by antigen retrieval with a citrate buffer (10 mM Sodium citrate, 0.05% Tween 20, pH 6.0) at >95° C for 10 min. Tissue sections were blocked with 0.1% BSA for 20 min and incubated with the primary antibodies mouse-anti-cytokeratin-7 (cat. no. MA1-06316; Invitrogen), rabbit-anti-PTEN (cat. No. 9559S; Cell Signaling, Danvers, MA, USA), and rabbit-anti-NF-κB (cat. No. SC-109; Santa Cruz Biotechnology, Heidelberg, Germany) for 2 h at 37°C in a humid atmosphere followed by incubation with the secondary antibodies goat anti-mouseAF488 (cat. No. A11017; Invitrogen) or goat anti-rabbitAF647 (cat. No. A21246; Invitrogen). All antibodies diluted 1:200 were applied and incubated 1 h at 37°C under humidity. DAPI (1 µg/mL) (cat. No. D9542; Sigma Aldrich) was used for nuclei staining. Fluorescence was visualized and recorded using a Zeiss LSM 710 confocal laser scanning microscope (Carl Zeiss Microscopy GmbH).

2.10 Statistical analysis

Unpaired Student t-test with Mann-Whitney test was applied to assess differences between groups using Prism software version 9 (GraphPad, San Diego, CA) as indicated at every figure legend. A p-value < 0.05 was considered significant.

3 Results

3.1 Identification of DEmiRNA in placenta accreta by high-throughput small RNA-Seq

Normal (NP; n=9) and adherent accreta (PAS; n=8) placentas were analyzed by sRNA-Seq. At least 10 million reads per sample were obtained and used for library processing and mapping. Principal component analysis (PCA) revealed a separation of samples belonging to NP and PAS groups with some overlaps (Figure 1A). Most small RNA molecules were identified as miRNA species (39.9%), followed by small nucleolar RNAs (snoRNA; 22.2%) and long non-coding RNAs (lncRNA; 16.3%). A minor proportion included small nuclear RNAs (snRNA; 5.3%) and ribosomal RNA (rRNA; 2.0%) (Figure 1B). To identify the significant genes in PAS ($p< 0.05$), the DESeq2 R package was used. Placental tissues of NP and PAS shared a common miRNA signature consisting of 994 active miRNAs. Exclusively expressed were 95 miRNA species in NP and 37 in PAS placentas (Figure 1C). A total of 147 mature miRNAs were up- and 151 were downregulated in PAS compared to NP (Figure 1D). A selective analysis of miRNAs (17, 32–34) revealed DEmiRNAs in the

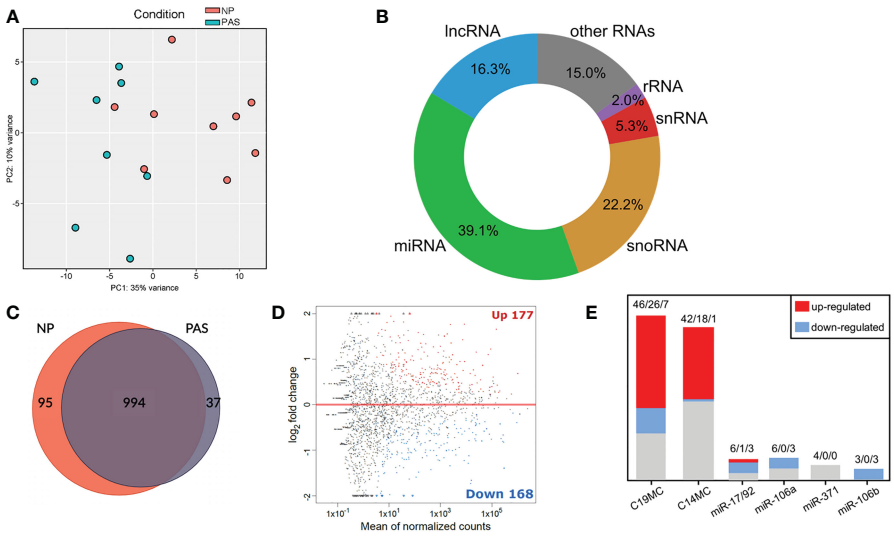


FIGURE 1
Small RNA-Seq analysis reveals a distinct expression pattern of miRNAs in placenta accreta samples. **(A)** PCA of the investigated samples based on all detected miRNAs. **(B)** Mapped sRNA reads were sorted into RNA classes. **(C)** Overlap of the actively transcribed miRNA genes in NP and PAS samples. **(D)** MA plot showing mature DEmiRNAs in PAS relative to NP. The x-axis is the log2 average expression over all samples, and the y-axis is the log2 fold change between PAS and NP groups. Red and blue dots represent respectively the significant differentially up- and down-expressed miRNAs. **(E)** Number of DEmiRNAs in PAS that belong to placental miRNA clusters. Numbers indicate total miRNA species in the cluster/miRNAs upregulated/miRNAs downregulated. NP, Normal pregnancy; PAS, Placenta Accreta Spectrum; C19MC, chromosome 19 miRNA cluster; C14MC, chromosome 14 miRNA cluster.

10.3389/fendo.2023.1021640

placenta-associated clusters including the chromosome 19 miRNA cluster (C19MC; 33 out of 46 miRNA species in the cluster), the chromosome 14 miRNA cluster (C14MC; 19 out of 42), the miR-17/92 cluster (4 out of 6), the miR-106a cluster (3 out of 6), and the miR-106b cluster (3 out of 3), but not the miR-371 cluster (Figure 1E). A full list of miRNAs included in the clusters is presented in Supplementary Table. 1.

3.2 Validation of DEmiRNAs in placenta accreta

DEmiRNAs were sorted according to the adjusted p-value, and a group of 16 DEmiRNAs exhibiting fold-change > 2.0, and good abundance (base mean > 100) were selected for individual validation using RT-qPCR in a larger cohort of samples (NP:14; Placenta accreta PAS:12) that includes the ones used for RNA-Seq. In this group, members of the C19MC (miR-519d-3p) and C14MC (miR-370-3p and miR-454-5p), as well as miRNAs not reported in PAS were included. Small RNA-Seq data was successfully validated in eight out of eight selected upregulated miRNAs in PAS samples: miR-24-3p, miR-193b-3p, miR-331-3p, miR-376c-3p, miR-382-3p, miR-495-3p, miR-519d-3p and miR-3074-5p (Figure 2A). Among downregulated miRNAs in PAS, five out of eight miRNA species were validated by RT-PCR (miR-106b-3p, miR-222-3p, miR-370-3p, miR-454-5p, and miR-3615-3p (Figure 2B).

3.3 DEmiRNAs localize mainly in trophoblast but also in endothelial cells

To determine the possibility of cell-specific expression, localization of DEmiRNAs in PAS was examined by ISH within placental villous tissue (Figure 3). Tissue sections of placenta accreta, placenta increta and percreta were stained with hematoxylin and eosin (H&E) to visualize morphological differences. Abnormally deep anchoring of the placental villi, as well as fibrin and trophoblast cells invaded into decidual tissue, were present in PAS samples (Figure 3). According to CK7 expression by IHC, extravillous trophoblast cells (EVTs) deeply infiltrating the decidual tissue were often observed in invasive PAS but not in NP samples (red arrows in Figure 3). To investigate the location of DEmiRNAs in the tissue, *in situ* hybridization was performed using digoxigenin-labeled LNA probes, which bind specifically to their target miRNA or that contain a random non-genomic scramble sequence (SCR) as negative control. ISH revealed miR-193b-3p signal in STB of both PAS and NP placentas, elevated miR-193b-3p expression was observed in PAS compared to NP samples, especially in the EVTs and areas of trophoblast invasiveness into the decidual tissue. The expression of miR-519d-3p, a placenta-specific miRNA, was restricted to trophoblast cells and strongly present on invasive trophoblast cells of PAS tissue. In NP tissue, the expression of miR-106b-3p and miR-370-3p was found mainly delimited in trophoblast cells, although endothelial cells were also positive for miR-370-3p. In PAS, miR-370-3p was highly expressed by invasive trophoblast cells. Contrary to PCR results, a downregulation of miR-106b-3p and miR-370-3p was not observable in PAS compared to NP samples.

3.4 Biological pathway analysis identifies cell cycle and inflammation pathways as networks of DEmiRNAs in placenta accreta

To explore alterations in gene expression, a hypergeometric test was run to identify KEGG pathways that the identified DEmiRNAs

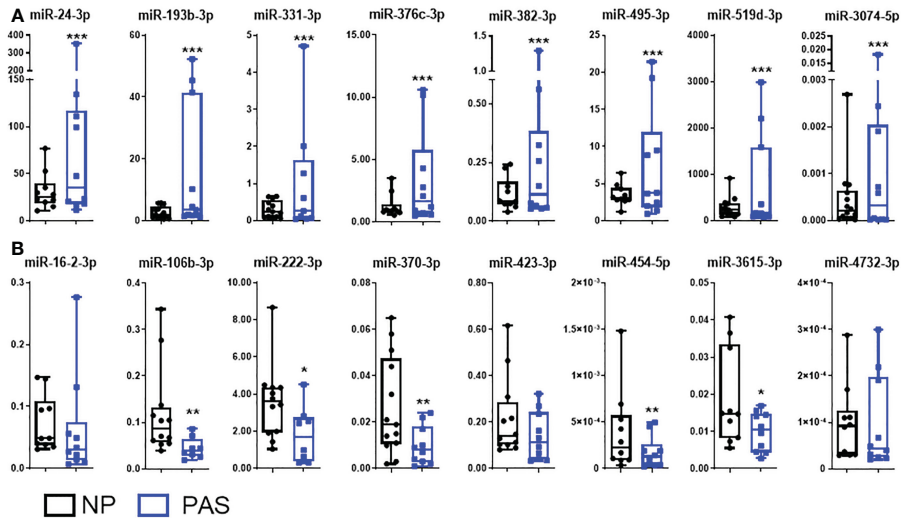


FIGURE 2
Validation of DEmiRNAs in placenta accreta samples. Expression patterns of differentially expressed miRNAs (DEmiRNAs) identified by RNA-Seq were validated by qRT-PCR in a larger sample cohort NP (n = 14) and PAS (n = 12). **(A)** Upregulated miRNAs and **(B)** downregulated miRNAs. The relative expression of each unique miRNA was normalized to the value of the exogenous cel-miR-39 using the $2^{-\Delta Ct}$ formula. Data are shown as the mean ± SE. Significant differences were determined by unpaired t- and Mann-Whitney test. ****p < 0.001, **p < 0.01, *p < 0.05*.

10.3389/fendo.2023.1021640

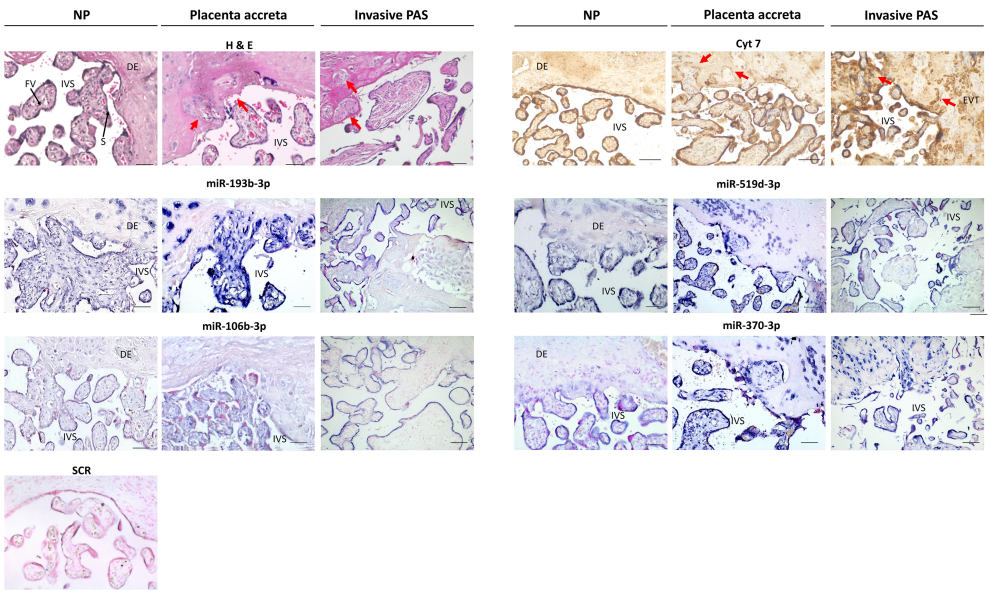


FIGURE 3
Differentially expressed miRNAs visualized by *in situ* hybridization in normal placenta (NP), placenta accreta, and placenta increta and percreta samples (invasive PAS). Areas containing villi and uterine tissue have been selected, in placenta accreta and invasive PAS with implanted villi and extravillous trophoblast cells (EVTs). The hematoxylin and eosin (H&E) staining shows nuclei in blue, cytoplasm in pink; cytokeratin-7 (CK7) staining marks positive cells brown (mainly syncytiotrophoblast and trophoblast cells) red arrows show areas of deep trophoblast infiltration; *in situ* hybridization of miR-193b-3p, miR-519d-3p, miR-106b-3p, and miR-370-3p shows positive cells in blue. Sections were counterstained with Nuclear Red. IVS, intervillous space; DE, decidua; FV, fetal vessel; S, Syncytiotrophoblast. Scale bar: 100 μm.

could alter. This analysis is based on the number of genes involved in each pathway which the DEmiRNAs can potentially regulate. As a result, 87 potentially altered pathways were identified. An additional inspection of these pathways allowed the identification of 7 shared sub-pathways, including cell cycle control, actin regulation, TGF-β, MAPK, PI3K-AKT, NF-κB, and the JAK-STAT signaling pathways (Figure 4A). A representative gene from each pathway was selected for validation by PCR. No significant expression difference was found for ERK1 and AKT mRNA (MAPK and PI3K-AKT signaling pathways are targeted by miR-382-3p and miR-495-3p), but a significant reduction of NF-κB mRNA was confirmed in PAS samples. As a representative of the JAK-STAT pathway with high invasion-inducing capacities (35), STAT3 expression was investigated but was not altered in PAS. Among the TGF-β pathway, TGF-β1 was downregulated in PAS samples. PTEN mRNA, which is involved in the cell cycle control pathway and a potential target of miR-106b-3p, miR-222-3p, and miR-519d-3p (36), was also decreased in PAS compared to NP samples (Figure 4B).

3.5 PTEN is down- while NF-κB is upregulated in placenta accreta

Based on the network of signaling pathways described above, two main transcription factors were selected for further investigation: PTEN, which is involved in cell cycle functions including proliferation, migration, and metabolism (37), and NF-κB, which is involved in the expression of inflammatory factors (38). To localize these proteins in placental tissues from NP and placenta accreta PAS samples, double immunofluorescence staining was carried out as described in the method section. In NP, the placenta villi appeared well delimitated by CK7 positive STB as observed in IHC staining. In contrast, PAS tissue showed zones with unorganized STB and the presence of large areas of EVT infiltration in the decidual tissue (Figure 5). In NP and PAS placenta, NF-κB was expressed in STB and the stroma of placental villi. Additionally, focal expression in areas of column-like EVTs was also observed in PAS (Figure 5A, white arrow). Contrary to the mRNA analysis, the fluorescence intensity of NF-kB protein was higher in PAS than NP (Figure 5C). In NP, PTEN was localized mainly in STB, endothelial cells surrounding fetal blood vessels, and in minor proportion in the stroma. Contrarily, in PAS samples, PTEN localized mainly in the stroma, partially in Hofbauer cells (white arrowheads), and in minor proportion in STB and EVTs (Figure 5B). In agreement with the mRNA validation, PTEN protein expression was reduced in PAS compared to NP tissues (Figure 5C).

3.6 Regulation of trophoblast invasion and migration are the most common functions of DEmiRNAs in PAS

To clarify the function of DEmiRNAs, literature was screened for investigations in physiological or pathological pregnancies. Among the confirmed DEmiRNAs, only miR-495-3p has not been reported as differentially expressed in any pathological pregnancy. Several DEmiRNAs have been previously identified

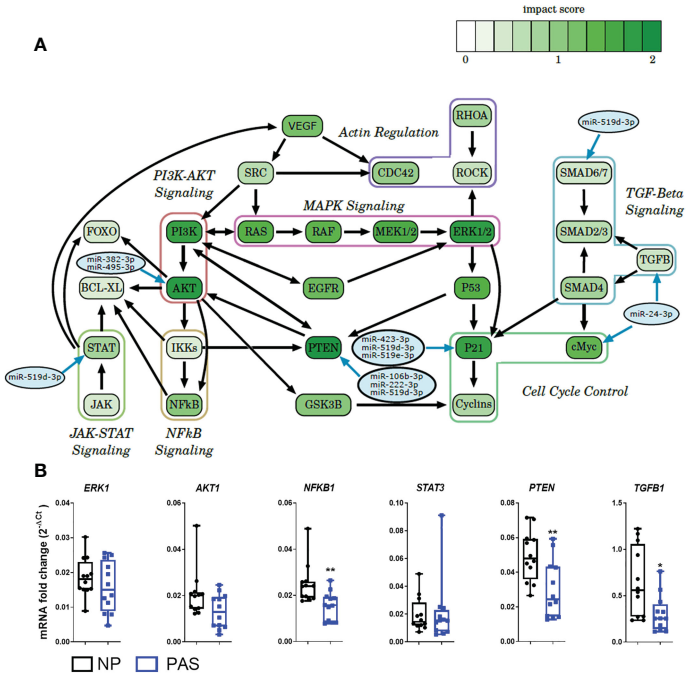


FIGURE 4
Expression of potential DEmiRNA targets in PAS. **(A)** Enriched pathways found in the KEGG analysis and putative DEmiRNAs targeting components of the pathway. The score assigned to each gene roughly describes the probability that this gene is regulated by the DEmiRNAs. The higher the score, the greater the influence of the DEmiRNAs on the gene within the pathway. **(B)** Expression of DEmiRNA mRNA targets by qRT-PCR in NP (n = 14) and PAS placentas (n = 12). The relative expression of each unique mRNA was normalized using the formula $2^{-\Delta Ct}$ with GAPDH as endogenous control. Data are shown as the mean ± SE. Significant differences were determined by the unpaired t- and Mann-Whitney test. **P < 0.05, **P < 0.01.*.

altered in preeclampsia (PE), pre-term birth (PTB), fetal growth restriction (FGR), or gestational diabetes mellitus (GDM). To the best of our knowledge, no reports on PAS regarding the here described DEmiRNAs exist. Target genes confirmed in this study (e.g., TGF-β, MAPK, PETN) have been reported as validated targets of DEmiRNAs in other studies supporting the network associations proposed here. Most of the found studies described miRNA functions in trophoblast cells, and reported their association with cell migration, proliferation and epithelial-mesenchymal transition (Table 2).

4 Discussion

The definition of PAS has been constantly revised in the last century because of the heterogeneous histological and clinical characteristics of deliveries complicated by placental retention. The currently recommended terminology includes different degrees of abnormal placentation from abnormally adherent villi towards extended EVT invasion into the uterine wall and beyond into adjacent organs (1). The incidence of this life-threatening disease is increasing rapidly, affecting at least 1 in 817 pregnancies worldwide and approximately 1 in 500 pregnancies in developed countries. A recent report indicates an incidence as high as 1 in 272 pregnancies (10).

In contrast to placenta accreta, the etiology of severe PAS (placenta increta/percreta) remains largely well defined since in nearly all cases a surgical damage of the decidua preceded. Currently, the most accepted hypothesis is a combination of scarred endometrium caused by damage prior to gestation and the subsequent abnormal invasion of trophoblast cells (74). Consequently, the most common risk factor for PAS is a history of cesarean deliveries and/or previous uterine surgeries (myomectomy, operative hysteroscopic procedures, dilation, and curettage, etc.), followed by assisted reproductive technology, especially *in vitro* fertilization and embryo transfer (IVF-ET) and advanced maternal age (75, 76). In our hands, the number of previous pregnancies was similar among the control and PAS groups, but all women with placenta increta or percreta presented previous uterine surgery. In contrast, several women included in the PAS group that suffered from adherent placenta accreta were primigravida, supporting the role of additional factors other than previous cesarean sections play a role in placenta accreta etiology.

Advanced clinical examinations, including ultrasound and in some cases also magnetic resonance imaging, may allow the diagnosis of severe PAS (placenta increta and percreta) with high sensitivity (88-97%) when used by skilled personnel (6). However, antenatal identification of adherent placenta accreta is limited and is reported as low as in only 33% of the cases (5). Making the diagnosis can be more challenging when patients are not considered at risk because they have no placenta previa or no history of previous uterine surgery (77). Likewise, these measures are insufficient to reliably predicting the exact extent of trophoblast invasion (78, 79). Consecutively, the final decision on the optimal method to deliver the placenta depends on the knowledge of the degree of placental invasion, that often only can be decided intraoperatively. Therefore,

10.3389/fendo.2023.1021640

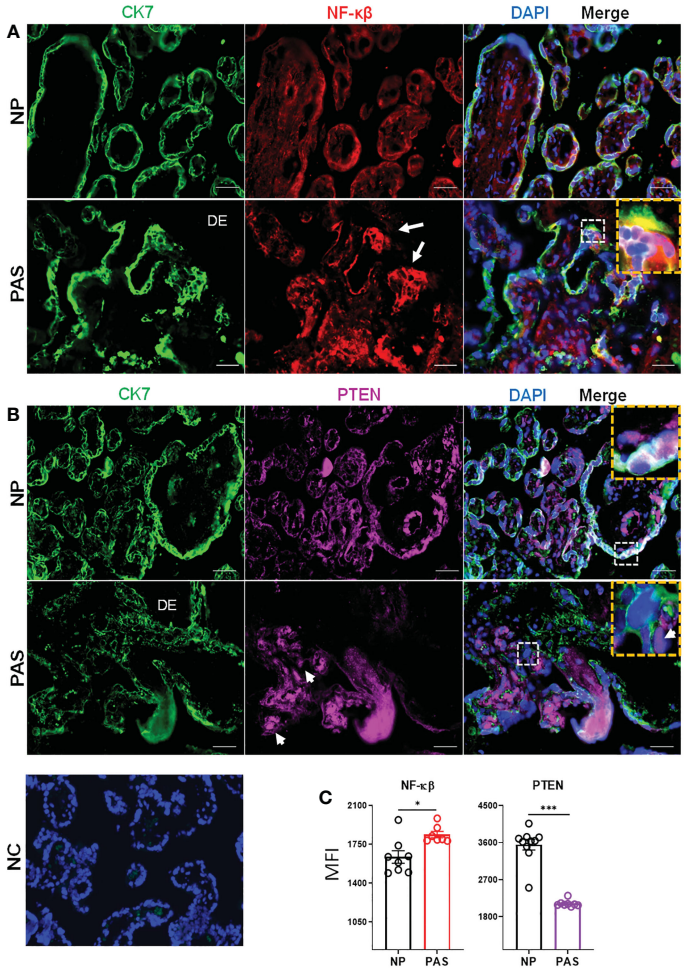


FIGURE 5
Immunolocalization of NF-κB and PTEN in normal and placenta accreta samples. Double immunolabelling of cytokeratin-7 (CK7, pseudo-green) with **(A)** NF-κB (pseudo-red) or **(B)** PTEN (pseudo-violet). Yellow boxes show the zoom-in area of white dotted boxes. White arrows and arrowheads indicate respectively invasive trophoblast columns and potential hofbauer cells. The scale bar represents 100 µm. **(C)** Extracted fluorescent intensity from representative pictures (n=3-5) in slides of NP (n=3) and PAS (n=3). Significant differences were determined by unpaired t- and Mann-Whitney test ****p < 0.001, *p < 0.05*. DE, Decidua; NC, Negative control; NP, normal pregnancy; PAS, placenta accreta spectrum.

several authors attempted to identify biomarkers, including placental proteins (e.g., PAPP-A, AFP), hormones (e.g., hCG and human placenta lactogen), and, more recently, cell-free fetal DNA and cell-free placental mRNA, that could improve the accuracy of antenatal diagnosis of PAS [revised in (80, 81)]. Although these factors may be altered in PAS, there is a significant overlap with their concentration in unaffected pregnancies, which limits their applicability. Combining these with other markers such as miRNAs may potentially improve the diagnosis and clinical management of PAS. A deeper knowledge about the clinical behavior of PAS trophoblast cells may offer better surgical treatment or preventative procedures.

In the last years, miRNAs have been widely accepted as critical players in placental development. miRNA dysregulation is found in pregnancy complications such as preeclampsia (PE), early pregnancy loss, and fetal growth retardation (FGR) (82–84), but very few studies have sought to identify the miRNA expression profile in PAS. Here, we found that the placental expression of miRNAs differs between the adherent PAS and control groups. Although the statistical tool DESeq2 was initially designed to identify differential expression of mRNA and not miRNA genes, its basic model and normalization assumptions hold true for the investigated RNA-Seq datasets, e.g., most genes are not differentially expressed and there is a balance of over- and under-expression (28) (see Figure 1D). An independent study showed that DESeq2 could maintain a reasonable false-positive rate without a significant loss of power, even when executed on a dataset with a relatively low number of highly expressed genes, which is the case for most sRNA-Seq datasets (85). Using this strategy, a group of DEmiRNAs was identified which includes some members of the placenta-associated miRNA clusters C19MC, C14MC, miR-106a, miR-106b, and miR-17-92. These miRNA clusters regulate trophoblast functions, cell-cell communication, and are involved in viral infection responses and placental homeostasis (17, 32–34). In our hands, validation PCR for specific miRNAs carried out in a larger cohort of placenta accreta samples confirmed the differential expression of 13 miRNAs (8 upregulated and 5 downregulated), previously not reported concerning a role in PAS development.

These miRNAs were localized by *in situ* hybridization revealing that they are expressed mainly by trophoblast cells and, in some cases, overexpressed by the invasive EVTs, especially observed in PAS placentas strengthening their role as regulators of trophoblast function. Remarkably, for ten of these miRNAs (miR-331-3p, -193b-3p, -376c-3p, -3074-5p, -222-3p, -519d-3p, -106b-3p, -3615, -16-2-3p und -454-5p, see Table 2), *in vitro* studies have already been carried out in trophoblastic cell lines, and they are reported to control trophoblast invasion and migration. Some of these miRNAs are also altered in PE, FGR, or other pregnancy disorders, suggesting their central role in placental functions and potentially a common alteration of trophoblast regulation in distinct pathologies. However, it cannot be ruled out that these miRNAs regulate different mRNAs to promote PAS development since there are certain redundancies and compensation effects among miRNAs (86). Likewise, the presence of DEmiRNAs considered of trophoblast origin (e.g., miR-519d-3p) in other cell types such as endothelial cells could indicate intercellular transfer from trophoblast to other placental cell types, which may cause alteration in the function of recipient cells. In the context of PAS, the relevance of this mechanism has not been addressed yet and could contribute to clarifying its etiology.

The majority of here identified miRNAs have been already tested in pregnancy-related pathologies at the placental level (Table 2), but researchers are now seeking to determine whether these miRNAs may serve as serum biomarkers. For instance, plasma miR-139-3p, miR-196a-5p, miR-518a-3p, and miR-671-3p were found downregulated in serum of patients diagnosed with placenta increta or percreta compared to healthy pregnancies (87). In our hands, miR-139-3p and miR-671-3p were also found downregulated in placenta accreta compared to NP placentas, which may support their use as biomarkers. However, miR-518a-3p appeared upregulated in our study. Likewise, the assessment of the secretory form of clusterin combined with the expression of either miR-21-5p, miR-92a-3p or miR-320a-3p in plasma of pregnant women were reported as potential predictors for the development of different forms of PAS with high specificity and sensibility (88). While no changes in miR-21-5p or miR-320a-3p were identified in our study, miR-92a-3p was found downregulated and not upregulated as suggested by that publication. Likewise, while our results showed increased miR-382-3p and decreased miR-423-5p expression in placenta tissue from adherent PAS, their serum levels appeared unchanged in the aforementioned studies (87, 88). Other miRNAs such as miR-24 and miR-519d were found here upregulated in PAS tissue and their plasma levels were found upregulated in other pathologies such as preeclampsia (89). Considering that placental miRNA expression changes with the gestation age (90) and the samples included in this study were taken after delivery, the low correlation with the reported alterations in plasma may be due to the differences in the gestational age at sampling. Therefore, although having the potential, more comprehensive studies are needed to determine whether the DEmiRNAs reported in this study may in fact serve as early diagnostic markers for PAS.

To further examine the biological relevance of DEmiRNAs in PAS, an *in silico* analysis was carried out to assign functional meaning for regulation at the mRNA level. To improve the interpretation of biological phenomena related to the extensive list of enriched KEGG pathways, analysis of local regions or sub-pathways has been achieved following a similar strategy as that published by others (91) and in our previous study (31). In the context of PAS, these bioinformatic strategies allowed the identification of biological pathways involved in angiogenesis, embryonic development, cell migration and adhesion, and tumor-related pathways that are deregulated in serum of PAS patients (87). Using a similar strategy, a network of lncRNAs, miRNAs and mRNAs implicated in reduced angiogenesis has been reported in PAS placentas (24). Here, seven sub-pathways, including cell cycle control, actin regulation, TGF-β, MAPK, PI3K-AKT, NF-κB, and the JAK-STAT signaling, were consistently mapped as targets of DEmiRNAs in the enriched KEGG pathways, which highlights them as the major cascades affected in PAS pathophysiology. Some molecules within these pathways have been previously reported as affected in PAS. For instance, an investigation by us reported increased mRNA and protein expression of cell cycle mediators (p21, p16, and CyclinD1) in PAS placentas compared to NP. However, this effect was reported to be significant only when delivery occurred after week 34, suggesting an additional temporary regulation (92). Other factors previously reported in PAS include TGF-β, which regulates cellular growth, motility, tumorigenesis, and trophoblastic EMT. It suppresses trophoblast invasion by regulating the transcription factors zinc finger protein SNAI (SNAIL) and Twist family basic helix-loop-helix transcription factor (TWIST) (93–95). In addition, silencing TGF-β type 1 receptor (TGFBR1) expression in trophoblastic cells significantly enhanced their trophoblastic invasiveness related to EMT promotion. Congruently, TGF-β negatively regulates trophoblast invasion by upregulating miR-7 in a SMAD2-dependent manner supporting the repression of EMT (96). Consistent with our findings, a significant decrease in relative TGF-β1 mRNA expression in tissue of PAS versus NP placenta has been reported (97). *TGFB* genes have been proposed in literature as targets of three DEmiRNAs identified in this study (miR-24-3p, miR-193b-3p and miR-3615-3p) (42) (71). Because miR-24-3p and miR-193b-3p were upregulated while miR-3615-3p was downregulated in PAS samples, it is unfeasible to estimate the contribution of each of these miRNAs to the overall decrease in TGF-β1 mRNA expression nor to the development of PAS. Therefore, these observations reinforce the need to consider larger miRNA:mRNA networks as causative of PAS rather than the association of a single miRNA and its targets reported *in vitro*.

Abnormal expression of other genes identified in sub-pathway analyses has been reported in pregnancy malignancies. For instance, dysregulated PTEN expression in blastocyst implantation, spontaneous abortion, and PE has been reported suggesting its critical role during pregnancy (98–101). Although NF-κB signaling is mainly involved in regulating inflammatory factors, there is evidence that it negatively regulates cell cycle and cell proliferation (102). Several studies have reported associations between PTEN and NF-κB. Increased PTEN, dependent on the AP-1/NF-κB pathway, impairs human trophoblast cell invasion and is related to PE development (103). Furthermore, PTEN has been

TABLE 2 Previous reports of DEmiRNAs in PAS.

miRNA	Chr. Location	Expression in healthy and pathological pregnancy	Target gene(s)	Reported function	Reference
miR-24-3p	chr9: 95,086,064-95,086,085 chr19: 13,836,289-13,836,310	Upregulated in PE	TGF-β, MAPK, CDK, PI3K, p85, MYC, MM14	Regulation of actin organization. Cell migration and proliferation.	(39, 40)
		Upregulated in PPROM and PTB			(41)
miR-193b-3p	chr16: 14,304,017-14,304,038	Upregulated in PE	TGF-β2	Promotes trophoblast (HTR-8/SVneo) cell motility, migration and motion	(42–44)
		Upregulated in FGR			(45)
miR-331-3p	chr12: 95,308,420-95,308,513	Downregulated in PE	TGF-βR1	Regulates the invasion of human trophoblastic HTR-8/SVneo cells	(46, 47)
miR-376c-3p	chr14: 101,039,732-101,039,752 (miR-379/miR-656 cluster)	Upregulated at term labor	PHLDA2, HBEGF, TGF-β1R (ALK5 and ALK7)	Promotes trophoblast outgrowth and invasion	(48)
		Present in umbilical cord serum-derived exosomes			(49)
		Downregulated in PE			(50–52)
miR-382-3p	chr14: 101,054,352-101,054,372	Upregulated in PE	STAT1, NEAT1, ROCK1, PTEN	Inhibits cell proliferation and migration and its downregulation promotes invasiveness in cancer models	(53–55)
miR-495-3p	chr14: 101,033,804-101,033,825	Not reported yet			
miR-519d-3p	chr19: 53,713,400-53,713,421 (C19MC cluster)	Expressed almost exclusively in placenta tissue	CXCL6, NR4A2, FOXL2, PDCD4, PTEN, MMP-2	Reduces trophoblast cell migration and invasion Downregulates the EVT invasive phenotype	(56, 57)
		Upregulated in PE		Suppresses invasion and migration of trophoblast cells by targeting MMP-2	(58)
miR-3074-5p	chr9: 95,086,063-95,086,083	Upregulated in placental villi from recurrent miscarriage Low expressed in placental villi from NP	BCL2, FGF1, P27, BCL-G, DLST, GAP43, CCR3, RUNX2	Promotes apoptosis but inhibits invasion of HTR-8/SVneo cell line	(59, 60)
miR-16-2-3p	chr3: 160,404,797-160,404,818	Upregulated in placental villi and decidua from recurrent spontaneous abortion	VEGF	Regulates placental angiogenesis and development	(61)
		Upregulated in DICE-deficient HTR-8/SVneo trophoblast cell line	COL1A2	Reduces invasion of HTR-8/SVneo cell line	(62)
miR-106b-3p	chr7: 100,094,002-100,094,023	Upregulated in PE	MMP-2	Inhibits the invasion and proliferation of JAR and JEG3 cells	(63)
miR-222-3p	chrX: 45,747,036-45,747,056	Upregulated in PE	BCL2L11	Promotes apoptosis of mesenchymal stem cells in response to hypoxia	(64)
			HDAC6	Inhibits trophoblast proliferation and migration	(65)
miR-370-3p	chr14: 100,911,186-100,911,207	Dysregulated in GTD Upregulated in FGR Downregulated in first-trimester healthy placenta		Involved in regulating proliferation, migration, and invasion of cancer cells	(19, 66, 67)
miR-423-3p	chr17: 30,117,131-30,117,153	Upregulated in early onset PE	MAPK signaling pathway		(68, 69)
miR-454-5p	chr17: 59,137,828-59,137,849	Downregulated in PE	ALK7	Promotes proliferation reduces apoptosis and increases invasion of trophoblast cells	(70)
miR-3615-3p	chr17: 74,748,663-74,748,683	Upregulated in plasma exosomes from PTB	TGF-β signaling	Possibly involved in trophoblast proliferation	(71)
miR-4732-3p	chr17: 28,861,668-28,861,688	Dysregulated in serum from PE Downregulated in GDM		Possibly involved in cellular development and cellular movement	(72, 73)

shown to promote NF-κB activation or suppression in other cell systems (104, 105). In our study presented here, we have found downregulated PTEN and NFKB mRNA in placenta accreta samples, while PTEN protein was downregulated and NF-κB protein was upregulated (in EVTs). Previously, we have reported that overexpression of miR-519d-3p in trophoblast cell lines is related to AKT upregulation but PTEN downregulation. We found miR-519d-3p associated with augmented trophoblast proliferation but reduced migration (56). Here, PAS samples showed high expression of miR-519d-3p, reinforcing its link with the PTEN/AKT/NF-κB system, which constitutes a vital cell cycle signaling pathway involved in trophoblast proliferation and metabolism. PTEN has been demonstrated as a common target of numerous miRNAs, including miR-21, miR-214, and miR-217, which are involved in regulating several cancer types (106, 107). In our study, in addition to miR-519d-3p, PTEN appears to be a potential target of miR-222-3p and miR-106b-3p and AKT of miR-382-3p and miR-495-3p.

In summary, this study provides a set of miRNAs as potential biomarkers for the diagnosis of PAS, especially for placenta accreta. Additionally, these miRNAs and their targets are associated with signaling pathways relevant for controlling trophoblast function, providing preliminary evidence for their role in the pathogenesis of PAS.

Data availability statement

The data presented in the study are deposited in the OSF (https://osf.io/) and NIH (https://www.ncbi.nlm.nih.gov/geo/) repositories, accession numbers: https://osf.io/8wq9h 2022-12-08 and GSE216742 2022-11-01, respectively.

Ethics statement

The studies involving human participants were reviewed and approved by the ethics committees from the Jena University Hospital and the Department of Gynecology and Obstetrics, University Hospital Essen, Germany. Experiments in the study were approved according to the Helsinki Declaration on ethical principles for medical research involving human subjects by obtaining consent forms (Amendment No: 1509-03/05 Jena and 12-5212-BO Essen). The patients/participants provided their written informed consent to participate in this study.

Author contributions

Conceptualization, DM-P and UM. Formal analysis, JM-C, EB, RG-S, and DM-P. Funding acquisition, UM and DM-P. Investigation, JM-C, EB, PF-Z and RG-S. Project administration, DM-P. Supervision, MM, UM and DM-P. Resources, TG, AG, AK und MM. Visualization, JM-C, EB, P-FZ, RG-S and DM-P. Writing—original draft. JM-C and DM-P. Writing—review and editing, JM-C, EB, TG, AG, AK, MM, UM and DM-P. All authors contributed to the article and approved the submitted version.

Funding

This work has been supported by the German Research Foundation (DFG, German Research Foundation)- Project number 255955419- Mo2017/2 and Mo2017/3). UM, MM and AG were additionally supported by the German Research Foundation (DFG, grants Ma1550/12-1- Project number 315156279, MA5082/9-1 and GE-2223/2-1 to UM, MM, and AG, respectively), and DM-P by the Interdisciplinary Center for Clinical Research of the Medical Faculty Jena, (IZKF, DMMP FF05). JM-C has received a postgraduate grant from CONACyT (CVU: 446429) and from DAAD (Ref. 91655120). PF-Z received a grant from DAAD (Ref. 91771964). EB received financial support from the Ministry for Economics, Sciences and Digital Society of Thuringia (TMWWDG), under the framework of the Landesprogramm ProDigital (DigLeben-5575/10-9). MM was additionally supported by the Carl-Zeiss-Stiftung (grant FKZ 0563-2.8/738/2). Carl-Zeiss-Stiftung was not involved in the study design, analysis, interpretation of data, the writing of this article or the decision to submit it for publication. We acknowledge support by the German Research Foundation Projekt-Nr. 512648189 and the Open Access Publication Fund of the Thueringer Universitaets- und Landesbibliothek Jena.

Acknowledgments

The authors thank the patients who donated their placentas for research and also the physicians and midwives from the Department of Obstetrics, Jena University Hospital and the Department of Gynecology and Obstetrics, University Hospital Essen, Germany, for patient care and support during placenta collection.

Conflict of interest

The authors declare that the research was conducted in the absence of any commercial or financial relationships that could be construed as a potential conflict of interest.

Publisher's note

All claims expressed in this article are solely those of the authors and do not necessarily represent those of their affiliated organizations, or those of the publisher, the editors and the reviewers. Any product that may be evaluated in this article, or claim that may be made by its manufacturer, is not guaranteed or endorsed by the publisher.

Supplementary material

The Supplementary Material for this article can be found online at: https://www.frontiersin.org/articles/10.3389/fendo.2023.1021640/full#supplementary-material

References

1. Hecht JL, Baergen R, Ernst LM, Katzman PJ, Jacques SM, Jauniaux E, et al. Classification and reporting guidelines for the pathology diagnosis of placenta accreta spectrum (PAS) disorders: recommendations from an expert panel. *Mod Pathol* (2020) 33(12):2382–96. doi: 10.1038/s41379-020-0569-1

2. Jauniaux E, Ayres-de-Campos D, Langhoff-Roos J, Fox KA, Collins S. FIGO classification for the clinical diagnosis of placenta accreta spectrum disorders. *Int J Gynaecol Obstet* (2019) 146(1):20–4. doi: 10.1002/ijgo.12761

3. Jauniaux E, Collins S, Burton GJ. Placenta accreta spectrum: pathophysiology and evidence-based anatomy for prenatal ultrasound imaging. *Am J Obstet Gynecol* (2018) 218(1):75–87. doi: 10.1016/j.ajog.2017.05.067

4. Jauniaux E, Chantraine F, Silver RM, Langhoff-Roos J. FIGO consensus guidelines on placenta accreta spectrum disorders: Epidemiology. *Int J Gynaecol Obstet* (2018) 140(3):265–73. doi: 10.1002/ijgo.12407

5. Bluth A, Schindelhauer A, Nitzsche K, Wimberger P, Birdir C. Placenta accreta spectrum disorders-experience of management in a German tertiary perinatal centre. *Arch Gynecol Obstet* (2021) 303(6):1451–60. doi: 10.1007/s00404-020-05875-x

6. Cali G, Giambanco L, Puccio G, Forlani F. Morbidly adherent placenta: evaluation of ultrasound diagnostic criteria and differentiation of placenta accreta from percreta. *Ultrasound Obstet Gynecol* (2013) 41(4):406–12. doi: 10.1002/uog.12385

7. Bailit JL, Grobman WA, Rice MM, Reddy UM, Wapner RJ, Varner MW, et al. Morbidly adherent placenta treatments and outcomes. *Obstet Gynecol* (2015) 125 (3):683–9. doi: 10.1097/AOG.0000000000000680

8. Matsuzaki S, Mandelbaum RS, Sangara RN, McCarthy LE, Vestal NL, Klar M, et al. Trends, characteristics, and outcomes of placenta accreta spectrum: a national study in the united states. *Am J Obstet Gynecol* (2021) 225(5):534 e1–534 e38. doi: 10.1016/j.ajog.2021.04.233

9. Jauniaux E, Burton GJ. Pathophysiology of placenta accreta spectrum disorders: A review of current findings. *Clin Obstet Gynecol* (2018) 61(4):743–54. doi: 10.1097/GRF.0000000000000392

10. Gynecologists, A.C.o.O.a and S.f.M.-F. Medicine. Obstetric care consensus no. 7: Placenta accreta spectrum. *Obstet Gynecol* (2018) 132(6):e259–75. doi: 10.1097/AOG.0000000000002983

11. Jauniaux E, Bunce C, Grønbeck L, Langhoff-Roos J. Prevalence and main outcomes of placenta accreta spectrum: a systematic review and meta-analysis. *Am J Obstet Gynecol* (2019) 221(3):208–18. doi: 10.1016/j.ajog.2019.01.233

12. Wu S, Kocherginsky M, Hibbard JU. Abnormal placentation: twenty-year analysis. *Am J Obstet Gynecol* (2005) 192(5):1458–61. doi: 10.1016/j.ajog.2004.12.074

13. Chuong EB, Hannibal RL, Green SL, Baker JC. Evolutionary perspectives into placental biology and disease. *Appl Transl Genom* (2013) 2:64–9. doi: 10.1016/j.atg.2013.07.001

14. Zhou J, Chen H, Xu X, Liu Y, Chen S, Yang S, et al. Uterine damage induces placenta accreta and immune imbalance at the maternal-fetal interface in the mouse. *Placenta* (2022) 119:8–16. doi: 10.1016/j.placenta.2022.01.002

15. Li N, Hou R, Liu C, Yang T, Qiao C, Wei J, et al. Integration of transcriptome and proteome profiles in placenta accreta reveals trophoblast over-migration as the underlying pathogenesis. *Clin Proteomics* (2021) 18(1):31. doi: 10.1186/s12014-021-09336-8

16. Liang Y, Ridzon D, Wong L, Chen C. Characterization of microRNA expression profiles in normal human tissues. *BMC Genomics* (2007) 8:166. doi: 10.1186/1471-2164-8-166

17. Morales-Prieto DM, Ospina-Prieto S, Chaiwangyen W, Schoenleben M, Markert UR, et al. Pregnancy-associated miRNA-clusters. *J Reprod Immunol* (2013) 97(1):51–61. doi: 10.1016/j.jri.2012.11.001

18. Mayor-Lynn K, Toloubeydokhti T, Cruz AC, Chegini N. Expression profile of microRNAs and mRNAs in human placentas from pregnancies complicated by preeclampsia and preterm labor. *Reprod Sci* (2011) 18(1):46–56. doi: 10.1177/1933719110374115

19. Morales-Prieto DM, Chaiwangyen W, Ospina-Prieto S, Schneider U, Herrmann J, Gruhn B, et al. MicroRNA expression profiles of trophoblastic cells. *Placenta* (2012) 33(9):725–34. doi: 10.1016/j.placenta.2012.05.009

20. Gu Y, Bian Y, Xu X, Wang X, Zuo C, Meng J, et al. Downregulation of miR-29a/b/c in placenta accreta inhibits apoptosis of implantation site intermediate trophoblast cells by targeting MCL1. *Placenta* (2016) 48:13–9. doi: 10.1016/j.placenta.2016.09.017

21. Umemura K, Ishioka S, Endo T, Ezaka Y, Takahashi M, Saito T, et al. Roles of microRNA-34a in the pathogenesis of placenta accreta. *J Obstet Gynaecol Res* (2013) 39 (1):67–74. doi: 10.1111/j.1447-0756.2012.01898.x

22. Gu Y, Meng J, Zuo C, Wang S, Li H, Zhao S, et al. Downregulation of MicroRNA-125a in placenta accreta spectrum disorders contributes antiapoptosis of implantation site intermediate trophoblasts by targeting MCL1. *Reprod Sci* (2019) 26 (12):1582–9. doi: 10.1177/1933719119828040

23. Li N, Hou R, Yang T, Liu C, Wei J. miR-193a-3p mediates placenta accreta spectrum development by targeting EFNB2 via epithelial-mesenchymal transition pathway under decidua defect conditions. *Front Mol Biosci* (2020) 7:613802. doi: 10.3389/fmolb.2020.613802

24. Yang T, Li N, Hou R, Qiao C, Liu C. Development and validation of a four-microRNA signature for placenta accreta spectrum: an integrated competing endogenous RNA network analysis. *Ann Transl Med* (2020) 8(15):919. doi: 10.21037/atm-20-1150

25. Martin M. Cutadapt removes adapter sequences from high-throughput sequencing reads. *EMBnet.journal* (2011) 17(1):3. doi: 10.14806/ej.17.1.200

26. Kim D, Pertea G, Trapnell C, Pimentel H, Kelley R, Salzberg SL, et al. TopHat2: accurate alignment of transcriptomes in the presence of insertions, deletions and gene fusions. *Genome Biol* (2013) 14(4):R36. doi: 10.1186/gb-2013-14-4-r36

27. Liao Y, Smyth GK, Shi W. featureCounts: an efficient general purpose program for assigning sequence reads to genomic features. *Bioinformatics* (2014) 30(7):923–30. doi: 10.1093/bioinformatics/btt656

28. Love MI, Huber W, Anders S. Moderated estimation of fold change and dispersion for RNA-seq data with DESeq2. *Genome Biol* (2014) 15(12):550. doi: 10.1186/s13059-014-0550-8

29. Benjamini Y, Drai D, Elmer G, Kafkafi N, Golani I. Controlling the false discovery rate in behavior genetics research. *Behav Brain Res* (2001) 125(1-2):279–84. doi: 10.1016/S0166-4328(01)00297-2

30. Huang HY, Lin YC, Li J, Huang KY, Shrestha S, Hong HC, et al. miRTarBase 2020: updates to the experimentally validated microRNA-target interaction database. *Nucleic Acids Res* (2020) 48(D1):D148–54. doi: 10.1093/nar/gkz896

31. Morales-Prieto DM, Barth E, Murrieta-Coxca JM, Favaro RR, Gutiérrez-Samudio RN, Chaiwangyen W, et al. Identification of miRNAs and associated pathways regulated by leukemia inhibitory factor in trophoblastic cell lines. *Placenta* (2019) 88:20–7. doi: 10.1016/j.placenta.2019.09.005

32. Malnou EC, Umlauf D, Mouysset M, Cavaillé J. Imprinted MicroRNA gene clusters in the evolution, development, and functions of mammalian placenta. *Front Genet* (2018) 9:706. doi: 10.3389/fgene.2018.00706

33. Chen DB, Wang W. Human placental microRNAs and preeclampsia. *Biol Reprod* (2013) 88(5):130. doi: 10.1095/biolreprod.113.107805

34. Ouyang Y, Bayer A, Chu T, Tyurin VA, Kagan VE, Morelli AE, et al. Isolation of human trophoblastic extracellular vesicles and characterization of their cargo and antiviral activity. *Placenta* (2016) 47:86–95. doi: 10.1016/j.placenta.2016.09.008

35. Fitzgerald JS, Poehlmann TG, Schleussner E, Markert UR. Trophoblast invasion: the role of intracellular cytokine signalling via signal transducer and activator of transcription 3 (STAT3). *Hum Reprod Update* (2008) 14(4):335–44. doi: 10.1093/humupd/dmn010

36. Chaiwangyen W, Ospina-Prieto S, Photini SM, Schleussner E, Markert UR, Morales-Prieto DM, et al. Dissimilar microRNA-21 functions and targets in trophoblastic cell lines of different origin. *Int J Biochem Cell Biol* (2015) 68:187–96. doi: 10.1016/j.biocel.2015.08.018

37. Chen CY, Chen J, He L, Stiles BL. PTEN: Tumor suppressor and metabolic regulator. *Front Endocrinol (Lausanne)* (2018) 9:338. doi: 10.3389/fendo.2018.00338

38. Liu T, Zhang L, Joo D, Sun SC. NF-κB signaling in inflammation. *Signal Transduct Target Ther* (2017) 2:e17023. doi: 10.1038/sigtrans.2017.23

39. Luizon MR, Conceição IMCA, Viana-Mattioli S, Caldeira-Dias M, Cavalli RC, Sandrim VC, et al. Circulating MicroRNAs in the second trimester from pregnant women who subsequently developed preeclampsia: Potential candidates as predictive biomarkers and pathway analysis for target genes of miR-204-5p. *Front Physiol* (2021) 12:678184. doi: 10.3389/fphys.2021.678184

40. Wu L, Zhou H, Lin H, Qi J, Zhu C, Gao Z, et al. Circulating microRNAs are elevated in plasma from severe preeclamptic pregnancies. *Reproduction* (2012) 143 (3):389–97. doi: 10.1530/REP-11-0304

41. Hromadnikova I, Kotlabova K, Krofta L. A history of preterm delivery is associated with aberrant postpartal MicroRNA expression profiles in mothers with an absence of other pregnancy-related complications. *Int J Mol Sci* (2021) 22(8):4033. doi: 10.3390/ijms22084033

42. Zhou X, Li Q, Xu J, Zhang X, Zhang H, Xiang Y, et al. The aberrantly expressed miR-193b-3p contributes to preeclampsia through regulating transforming growth factor-beta signaling. *Sci Rep* (2016) 6:19910. doi: 10.1038/srep19910

43. Xu P, Zhao Y, Liu M, Wang Y, Wang H, Li YX, et al. Variations of microRNAs in human placentas and plasma from preeclamptic pregnancy. *Hypertension* (2014) 63 (6):1276–84. doi: 10.1161/HYPERTENSIONAHA.113.02647

44. Betoni JS, Derr K, Pahl MC, Rogers L, Muller CL, Packard RE, et al. MicroRNA analysis in placentas from patients with preeclampsia: comparison of new and published results. *Hypertens Pregnancy* (2013) 32(4):321–39. doi: 10.3109/10641955.2013.807819

45. Ostling H, Kruse R, Helenius G, Lodefalk M. Placental expression of microRNAs in infants born small for gestational age. *Placenta* (2019) 81:46–53. doi: 10.1016/j.placenta.2019.05.001

46. Shan L, Hou X. Circular RNA hsa_circ_0026552 inhibits the proliferation, migration and invasion of trophoblast cells via the miR3313p/TGFbetaR1 axis in preeclampsia. *Mol Med Rep* (2021) 24(5):798. doi: 10.3892/mmr.2021.12438

47. Yi Y, Cheng JC, Klausen C, Leung PCK. TGF-beta1 inhibits human trophoblast cell invasion by upregulating cyclooxygenase-2. *Placenta* (2018) 68:44–51. doi: 10.1016/j.placenta.2018.06.313

48. Yadava SM, Feng A, Parobchak N, Wang B, Rosen T. miR-15b-5p promotes expression of proinflammatory cytokines in human placenta by inhibiting apelin signaling pathway. *Placenta* (2021) 104:8–15. doi: 10.1016/j.placenta.2020.11.002

49. Jia L, Zhou X, Huang X, Xu X, Jia Y, Wu Y, et al. Maternal and umbilical cord serum-derived exosomes enhance endothelial cell proliferation and migration. *FASEB J* (2018) 32(8):4534–43. doi: 10.1096/fj.201701337RR

50. Li J, Du J, Wang Z, Wang C, Bai J, Zhang S, et al. Expression of miR-376 in blood of pregnant women with preeclampsia and its effect on 25-hydroxyvitamin d. *Exp Ther Med* (2018) 16(3):1701–6. doi: 10.3892/etm.2018.6394

51. Yang HL, Zhang HZ, Meng FR, Han SY, Zhang M. Differential expression of microRNA-411 and 376c is associated with hypertension in pregnancy. *Braz J Med Biol Res* (2019) 52(4):e7546. doi: 10.1590/1414-431x20197546

52. Fu G, Ye G, Nadeem L, Ji L, Manchanda T, Wang Y, et al. MicroRNA-376c impairs transforming growth factor-beta and nodal signaling to promote trophoblast cell proliferation and invasion. *Hypertension* (2013) 61(4):864–72. doi: 10.1161/HYPERTENSIONAHA.111.203489

53. Zhang H, Zhu C, He Z, Chen S, Li L, Sun C, et al. LncRNA PSMB8-AS1 contributes to pancreatic cancer progression via modulating miR-382-3p/STAT1/PD-L1 axis. *J Exp Clin Cancer Res* (2020) 39(1):179. doi: 10.1186/s13046-020-01687-8

54. Liu Y, Wang Y, Fu X, Lu Z. Long non-coding RNA NEAT1 promoted ovarian cancer cells' metastasis through regulation of miR-382-3p/ROCK1 axial. *Cancer Sci* (2018) 109(7):2188–98. doi: 10.1111/cas.13647

55. Wang J, Luo J, Liu G, Li X. Circular RNA hsa_circ_0008285 inhibits colorectal cancer cell proliferation and migration via the miR-382-5p/PTEN axis. *Biochem Biophys Res Commun* (2020) 527(2):503–10. doi: 10.1016/j.bbrc.2020.03.165

56. Chaiwangyen W, Murrieta-Coxca JM, Favaro RR, Photini SM, Gutiérrez-Samudio RN, Schleussner E, et al. MiR-519d-3p in trophoblastic cells: Effects, targets and transfer to allogeneic immune cells via extracellular vesicles. *Int J Mol Sci* (2020) 21(10):3458. doi: 10.3390/ijms21103458

57. Xie L, Mouillet JF, Chu T, Parks WT, Sadovsky E, Knöfler M, et al. C19MC microRNAs regulate the migration of human trophoblasts. *Endocrinology* (2014) 155(12):4975–85. doi: 10.1210/en.2014-1501

58. Ding J, Huang F, Wu G, Han T, Xu F, Weng D, et al. MiR-519d-3p suppresses invasion and migration of trophoblast cells via targeting MMP-2. *PloS One* (2015) 10(3):e0120321. doi: 10.1371/journal.pone.0120321

59. Gu Y, Shi Y, Yang Q, Gu WW, He YP, Zheng HJ, et al. miR-3074-5p promotes the apoptosis but inhibits the invasiveness of human extravillous trophoblast-derived HTR8/SVneo cells in vitro. *Reprod Sci* (2018) 25(5):690–9. doi: 10.1177/1933719117725823

60. Gu Y, Zhang X, Yang Q, Wang J, He Y, Sun Z, et al. Aberrant placental villus expression of miR-486-3p and miR-3074-5p in recurrent miscarriage patients and uterine expression of these MicroRNAs during early pregnancy in mice. *Gynecol Obstet Invest* (2015) 81:112–7. doi: 10.1159/000435879

61. Zhu Y, Lu H, Huo Z, Ma Z, Dang J, Dang W, et al. MicroRNA-16 inhibits feto-maternal angiogenesis and causes recurrent spontaneous abortion by targeting vascular endothelial growth factor. *Sci Rep* (2016) 6:35536. doi: 10.1038/srep35536

62. Tang L, Yang M, Qin L, Li X, He G, Liu X, et al. Deficiency of DICER reduces the invasion ability of trophoblasts and impairs the pro-angiogenic effect of trophoblast-derived microvesicles. *J Cell Mol Med* (2020) 24(9):4915–30. doi: 10.1111/jcmm.14917

63. Li J, Wang JM, Liu YH, Zhang Z, Han N, Wang JY, et al. [Effect of microRNA-106b on the invasion and proliferation of trophoblasts through targeting MMP-2]. *Zhonghua Fu Chan Ke Za Zhi* (2017) 52(5):327–32. doi: 10.3760/cma.j.issn.0529-567X.2017.05.007

64. Qu HM, Qu LP, Pan XZ, Mu LS. Upregulated miR-222 targets BCL2L11 and promotes apoptosis of mesenchymal stem cells in preeclampsia patients in response to severe hypoxia. *Int J Clin Exp Pathol* (2018) 11(1):110–9.

65. Liu T, Li W, Zhang J, Zhang Y. MiR-222-3p inhibits trophoblast cell migration and alleviates preeclampsia in rats through inhibiting HDAC6 and Notch1 signaling. *Reprod Sci* (2021) 29(5):1486–97. doi: 10.1007/s43032-021-00793-y

66. Zhao JR, Cheng WW, Wang YX, Cai M, Wu WB, Zhang HJ, et al. Identification of microRNA signature in the progression of gestational trophoblastic disease. *Cell Death Dis* (2018) 9(2):94. doi: 10.1038/s41419-017-0108-2

67. Wen H, Chen L, He J, Lin J. MicroRNA expression profiles and networks in placentas complicated with selective intrauterine growth restriction. *Mol Med Rep* (2017) 16(5):6650–73. doi: 10.3892/mmr.2017.7462

68. Lykoudi A, Kolialexi A, Lambrou GI, Braoudaki M, Siristatidis C, Papaioanou GK, et al. Dysregulated placental microRNAs in early and late onset preeclampsia. *Placenta* (2018) 61:24–32. doi: 10.1016/j.placenta.2017.11.005

69. Vashukova ES, Glotov AS, Baranov VS. MicroRNAs associated with preeclampsia. *Russian J Genet* (2020) 56(1):1–16. doi: 10.1134/S1022795419080167

70. Shi Z, She K, Li H, Yuan X, Han X, Wang Y, et al. MicroRNA-454 contributes to sustaining the proliferation and invasion of trophoblast cells through inhibiting Nodal/ALK7 signaling in pre-eclampsia. *Chem Biol Interact* (2019) 298:8–14. doi: 10.1016/j.cbi.2018.10.012

71. Menon R, Debnath C, Lai A, Guanzon D, Bhatnagar S, Kshetrapal PK, et al. Circulating exosomal miRNA profile during term and preterm birth pregnancies: A longitudinal study. *Endocrinology* (2019) 160(2):249–75. doi: 10.1210/en.2018-00836

72. Srinivasan S, Treacy R, Herrero T, Olsen R, Leonardo TR, Zhang X, et al. Discovery and verification of extracellular miRNA biomarkers for non-invasive prediction of pre-eclampsia in asymptomatic women. *Cell Rep Med* (2020) 1(2):100013. doi: 10.1016/j.xcrm.2020.100013

73. Ding R, Guo F, Zhang Y, Liu XM, Xiang YQ, Zhang C, et al. Integrated transcriptome sequencing analysis reveals role of miR-138-5p/ TBL1X in placenta from gestational diabetes mellitus. *Cell Physiol Biochem* (2018) 51(2):630–46. doi: 10.1159/000495319

74. Jauniaux E, Jurkovic D, Hussein AM, Burton GJ. New insights into the etiopathology of placenta accreta spectrum. *Am J Obstetrics Gynecology* (2022) 227(3):384–91. doi: 10.1016/j.ajog.2022.02.038

75. Eshkoli T, Weintraub AY, Sergienko R, Sheiner E. Placenta accreta: risk factors, perinatal outcomes, and consequences for subsequent births. *Am J Obstet Gynecol* (2013) 208(3):219.e1–7. doi: 10.1016/j.ajog.2012.12.037

76. Baldwin HJ, Patterson JA, Nippita TA, Torvaldsen S, Ibiebele I, Simpson JM, et al. Antecedents of abnormally invasive placenta in primiparous women: Risk associated with gynecologic procedures. *Obstet Gynecol* (2018) 131(2):227–33. doi: 10.1097/AOG.0000000000002434

77. Comstock CH. Antenatal diagnosis of placenta accreta: a review. *Ultrasound Obstet Gynecol* (2005) 26(1):89–96. doi: 10.1002/uog.1926

78. D'Antonio F, Palacios-Jaraquemada J, Timor-Trisch I, Cali G. Placenta accreta spectrum disorders: Prenatal diagnosis still lacks clinical correlation. *Acta Obstet Gynecol Scand* (2018) 97(7):773–5. doi: 10.1111/aogs.13374

79. Morel O, van Beekhuizen HJ, Braun T, Collins S, Pateisky P, Calda P, et al. Performance of antenatal imaging to predict placenta accreta spectrum degree of severity. *Acta Obstet Gynecol Scand* (2021) 100 Suppl 1:21–8. doi: 10.1111/aogs.14112

80. Bartels HC, Postle JD, Downey P, Brennan DJ. Placenta accreta spectrum: A review of pathology, molecular biology, and biomarkers. *Dis Markers* (2018) 2018:1507674. doi: 10.1155/2018/1507674

81. Li J, Zhang N, Zhang Y, Hu X, Gao G, Ye Y, et al. Human placental lactogen mRNA in maternal plasma play a role in prenatal diagnosis of abnormally invasive placenta: yes or no? *Gynecol Endocrinol* (2019) 35(7):631–4. doi: 10.1080/09513590.2019.1576607

82. Choi SY, Yun J, Lee OJ, Han HS, Yeo MK, Lee MA, et al. MicroRNA expression profiles in placenta with severe preeclampsia using a PNA-based microarray. *Placenta* (2013) 34(9):799–804. doi: 10.1016/j.placenta.2013.06.006

83. Gunel T, Hosseini MK, Gumusoglu E, Kisakesen HI, Benian A, Aydinli K, et al. Expression profiling of maternal plasma and placenta microRNAs in preeclamptic pregnancies by microarray technology. *Placenta* (2017) 52:77–85. doi: 10.1016/j.placenta.2017.02.019

84. Hosseini MK, Gunel T, Gumusoglu E, Benian A, Aydinli K.. MicroRNA expression profiling in placenta and maternal plasma in early pregnancy loss. *Mol Med Rep* (2018) 17(4):4941–52. doi: 10.3892/mmr.2018.8530

85. Dillies MA, Rau A, Aubert J, Hennequet-Antier C, Jeanmougin M, Servant N, et al. A comprehensive evaluation of normalization methods for illumina high-throughput RNA sequencing data analysis. *Brief Bioinform* (2013) 14(6):671–83. doi: 10.1093/bib/bbs046

86. Plotnikova O, Baranova A, Skoblov M. Comprehensive analysis of human microRNA-mRNA interactome. *Front Genet* (2019) 10:933. doi: 10.3389/fgene.2019.00933

87. Chen S, Pang D, Li Y, Zhou J, Liu Y, Yang S, et al. Serum miRNA biomarker discovery for placenta accreta spectrum. *Placenta* (2020) 101:215–20. doi: 10.1016/j.placenta.2020.09.068

88. Timofeeva AV, Fedorov IS, Pirogova MM, Vasilchenko ON, Chagovets VV, Ezhova LS, et al. Clusterin and its potential regulatory microRNAs as a part of secretome for the diagnosis of abnormally invasive placenta: Accreta, increta, and percreta cases. *Life (Basel)* (2021) 11(4):270. doi: 10.3390/life11040270

89. Li H, Ge Q, Guo L, Lu Z. Maternal plasma miRNAs expression in preeclamptic pregnancies. *BioMed Res Int* (2013) 2013:970265. doi: 10.1155/2013/970265

90. Morales Prieto DM, Markert UR. MicroRNAs in pregnancy. *J Reprod Immunol* (2011) 88(2):106–11. doi: 10.1016/j.jri.2011.01.004

91. Li X, Shen L, Shang X, Liu W. Subpathway analysis based on signaling-pathway impact analysis of signaling pathway. *PloS One* (2015) 10(7):e0132813. doi: 10.1371/journal.pone.0132813

92. Duan L, Schimmelmann M, Wu Y, Reisch B, Faas M, Kimmig R, et al. CCN3 signaling is differently regulated in placental diseases preeclampsia and abnormally invasive placenta. *Front Endocrinol (Lausanne)* (2020) 11:597549. doi: 10.3389/fendo.2020.597549

93. Karmakar S, Das C. Regulation of trophoblast invasion by IL-1beta and TGF-beta1. *Am J Reprod Immunol* (2002) 48(4):210–9. doi: 10.1034/j.1600-0897.2002.01151.x

94. Haque S, Morris JC. Transforming growth factor-β: A therapeutic target for cancer. *Hum Vaccin Immunother* (2017) 13(8):1741–50. doi: 10.1080/21645515.2017.1327107

95. Cheng JC, Chang HM, Leung PC. Transforming growth factor-beta1 inhibits trophoblast cell invasion by inducing snail-mediated down-regulation of vascular endothelial-cadherin protein. *J Biol Chem* (2013) 288(46):33181–92. doi: 10.1074/jbc.M113.488866

96. Shih JC, Lin HH, Hsiao AC, Su YT, Tsai S, Chien CL, et al. Unveiling the role of microRNA-7 in linking TGF-beta-Smad-mediated epithelial-mesenchymal transition with negative regulation of trophoblast invasion. *FASEB J* (2019) 33(5):6281–95. doi: 10.1096/fj.201801898RR

97. El-Hussieny M, Mohammed EM, Zenhom NM, Refaie MM, Okasha AM, Tawab MAE, et al. Possible role of TGF-. *Fetal Pediatr Pathol* (2021) 40(3):222–32. doi: 10.1080/15513815.2020.1843574

98. Makker A, Goel MM, Nigam D, Mahdi AA, Das V, Agarwal A, et al. Aberrant akt activation during implantation window in infertile women with intramural uterine fibroids. *Reprod Sci* (2018) 25(8):1243–53. doi: 10.1177/1933719117737844

99. Tokyol C, Aktepe F, Hüsniye Dilek F, Yilmazer M. Comparison of placental PTEN and beta1 integrin expression in early spontaneous abortion, early and late normal pregnancy. *Ups J Med Sci* (2008) 113(2):235–42. doi: 10.3109/2000-1967-231

100. Xiao J, Tao T, Yin Y, Zhao L, Yang L, Hu L. miR-144 may regulate the proliferation, migration and invasion of trophoblastic cells through targeting PTEN in preeclampsia. *BioMed Pharmacother* (2017) 94:341–53. doi: 10.1016/j.biopha.2017.07.130

101. Lou CX, Zhou XT, Tian QC, Xie HQ, Zhang JY. Low expression of microRNA-21 inhibits trophoblast cell infiltration through targeting PTEN. *Eur Rev Med Pharmacol Sci* (2018) 22(19):6181–9. doi: 10.26355/eurrev_201810_16023

102. Araki K, Kawauchi K, Tanaka N. IKK/NF-kappaB signaling pathway inhibits cell-cycle progression by a novel Rb-independent suppression system for E2F transcription factors. *Oncogene* (2008) 27(43):5696–705. doi: 10.1038/onc.2008.184

103. Xue P, Zheng M, Diao Z, Shen L, Liu M, Gong P, et al. miR-155* mediates suppressive effect of PTEN 3'-untranslated region on AP-1/NF-kappaB pathway in HTR-8/SVneo cells. *Placenta* (2013) 34(8):650–6. doi: 10.1016/j.placenta.2013.04.015

104. Xie M, Fu Z, Cao J, Liu Y, Wu J, Li Q, et al. MicroRNA-132 and microRNA-212 mediate doxorubicin resistance by down-regulating the PTEN-AKT/NF-kappaB signaling pathway in breast cancer. *BioMed Pharmacother* (2018) 102:286–94. doi: 10.1016/j.biopha.2018.03.088

105. Tian Y, Li H, Qiu T, Dai J, Zhang Y, Chen J, et al. Loss of PTEN induces lung fibrosis via alveolar epithelial cell senescence depending on NF-kappaB activation. *Aging Cell* (2019) 18(1):e12858. doi: 10.1111/acel.12858

106. Yang H, Kong W, He L, Zhao JJ, O'Donnell JD, Wang J, et al. MicroRNA expression profiling in human ovarian cancer: miR-214 induces cell survival and cisplatin resistance by targeting PTEN. *Cancer Res* (2008) 68(2):425–33. doi: 10.1158/0008-5472.CAN-07-2488

107. Kato M, Putta S, Wang M, Yuan H, Lanting L, Nair I, et al. TGF-beta activates akt kinase through a microRNA-dependent amplifying circuit targeting PTEN. *Nat Cell Biol* (2009) 11(7):881–9. doi: 10.1038/ncb1897

frontiers | Frontiers in Endocrinology

TYPE Original Research
PUBLISHED 16 March 2023
DOI 10.3389/fendo.2023.1149786

Check for updates

OPEN ACCESS

EDITED BY
Reinaldo Marín,
Instituto Venezolano de Investigaciones Científicas (IVIC), Venezuela

REVIEWED BY
Mikihiro Yoshie,
Tokyo University of Pharmacy and Life Sciences, Japan
Martin Mueller,
University Hospital Bern, Switzerland

*CORRESPONDENCE
Ellen Menkhorst
ellen.menkhorst@unimelb.edu.au

SPECIALTY SECTION
This article was submitted to Developmental Endocrinology, a section of the journal Frontiers in Endocrinology

RECEIVED 23 January 2023
ACCEPTED 03 March 2023
PUBLISHED 16 March 2023

CITATION
Menkhorst E, So T, Rainczuk K, Barton S, Zhou W, Edgell T and Dimitriadis E (2023) Endometrial stromal cell miR-19b-3p release is reduced during decidualization implying a role in decidual-trophoblast cross-talk. *Front. Endocrinol.* 14:1149786. doi: 10.3389/fendo.2023.1149786

COPYRIGHT
© 2023 Menkhorst, So, Rainczuk, Barton, Zhou, Edgell and Dimitriadis. This is an open-access article distributed under the terms of the Creative Commons Attribution License (CC BY). The use, distribution or reproduction in other forums is permitted, provided the original author(s) and the copyright owner(s) are credited and that the original publication in this journal is cited, in accordance with accepted academic practice. No use, distribution or reproduction is permitted which does not comply with these terms.

Endometrial stromal cell miR-19b-3p release is reduced during decidualization implying a role in decidual-trophoblast cross-talk

Ellen Menkhorst[1,2]*, Teresa So[1,2], Kate Rainczuk[3], Siena Barton[1,2], Wei Zhou[1,2], Tracey Edgell[3] and Evdokia Dimitriadis[1,2,3]

[1]Embryo Implantation Laboratory, Department of Obstetrics and Gynecology, The University of Melbourne, Parkville, VIC, Australia, [2]Gynecology Research Centre, The Royal Women's Hospital, Parkville, VIC, Australia, [3]Centre for Reproductive Health, Hudson Institute of Medical Research, Clayton, VIC, Australia

Introduction: A healthy pregnancy requires successful blastocyst implantation into an adequately prepared or 'receptive' endometrium. Decidualization of uterine endometrial stromal fibroblast cells (hESF) is critical for the establishment of a healthy pregnancy. microRNAs (miRs) are critical regulators of cellular function that can be released by a donor cell to influence the physiological state of recipient cells. We aimed to determine how decidualization affects hESF miR release and investigated the function of one decidualization regulated miR, miR-19b-3p, previously shown to be associated with recurrent pregnancy loss.

Method: miR release by hESF was determined by miR microarray on culture media from hESF decidualized *in vitro* for 3 and 14 days by treatment with oestradiol and medroxyprogesterone acetate. Cellular and whole endometrial/decidual tissue miR expression was quantified by qPCR and localized by in situ hybridization. The function of miR-19b-3p in HTR8/Svneo trophoblast cells was investigated using real time cell analysis (xCELLigence) and gene expression qPCR.

Results: From our miR screen we found that essentially all hESF miR release was reduced following in vitro decidualization, significantly so for miR-17-5p, miR-21-3p, miR-34c-3p, miR-106b-5p, miR-138-5p, miR-296-5p, miR-323a-3p, miR-342-3p, miR-491-5p, miR-503-5p and miR-542-5p. qPCR demonstrated that miR-19b-3p, 181a-2-3p and miR-409-5p likewise showed a significant reduction in culture media following decidualization but no change was found in cellular miR expression following decidualization. *In situ* hybridization localized miR-19b-3p to epithelial and stromal cells in the endometrium and qPCR identified that miR-19b-3p was significantly elevated in the cycling endometrium of patients with a history of early pregnancy loss compared to normally fertile controls. Functionally, overexpression of miR-19b-3p significantly reduced HTR8/Svneo trophoblast proliferation and increased HOXA9 expression.

10.3389/fendo.2023.1149786

Discussion: Our data demonstrates that decidualization represses miR release by hESFs and overexpression of miR-19b-3p was found in endometrial tissue from patients with a history of early pregnancy loss. miR-19b-3p impaired HTR8/Svneo proliferation implying a role in trophoblast function. Overall we speculate that miR release by hESF may regulate other cell types within the decidua and that appropriate release of miRs by decidualized hESF is essential for healthy implantation and placentation.

KEYWORDS

decidua, decidualization, microRNA release, miR-19b-3p, trophoblast, early pregnancy loss

1 Introduction

A healthy pregnancy requires successful blastocyst implantation into an adequately prepared or 'receptive' endometrium. Decidualization of human uterine human uterine endometrial stromal fibroblast (hESF) is critical for the establishment of a healthy pregnancy (1, 2); impaired decidualization is associated with poor pregnancy outcomes including recurrent early pregnancy loss and preeclampsia (3–5). Decidualization is initiated post-ovulation by corpus luteum-secreted progesterone and involves the reprogramming of hESF, including significant phenotypic and functional changes: hESF become rounded, highly secretory and with altered extellular matrix expression (1). In women, decidualization begins each menstrual cycle regardless of the presence of a functional blastocyst (1). Decidual cells interact with the implanting blastocyst to facilitate implantation and placentation: they regulate extravillous trophoblast (EVT) proliferation, migration and invasion (6–8), shield the conceptus from environmental stress signals (1), regulate the recruitment and differentiation of the uterine-resident immune cell population (9–11) and are thought to 'sense' the quality of the conceptus, facilitating rejection of incompetent embryos (12, 13).

microRNAs (miRs) are critical regulators of cellular function and have been most intensively investigated in cancer, where they regulate metastasis, angiogenesis and inflammation (14, 15). miRs can also act as 'hormones' – donor cells (which release the miR) can influence the physiological state of recipient cells (cells which take up the miR) over short (cell to neighboring cell) and long (effects on a different organ) distances (15, 16). In pregnancy, miRs are produced by cells within the decidua (decidual cells, leucocytes and endothelial cells) (17) and placental villous trophoblast (18). miR expression is altered in the decidua of early pregnancy loss compared to healthy pregnancies (18).

Less is known about miRs during endometrial remodelling. *In vitro*, decidual cellular miRs regulate decidualization (19), however little known about how secreted endometrial miRs may regulate other cells within the decidua including trophoblast. We aimed to determine how decidualization affected hESF miR release and determine the expression and function of one hESF released miR, miR-19b-3p, previously associated with recurrent early pregnancy loss (20).

2 Methods

2.1 Primary tissue collection

This study followed the NHMRC guidelines for ethical conduct in human research. Ethics approvals for this study were provided by The Royal Women's Hospital and Monash Health Human Research and Ethics Committees (#90317B, #06014C and #03066B). Written and informed consent was obtained from each participant.

Endometrial biopsies were collected by dilatation and curettage (n=26 women; Table 1). Five biopsies were used for decidualization experiments (1 with history of early pregnancy loss), 3 for *in situ* (2

TABLE 1 Characteristics of non-pregnant participants.

	Normally fertile (n=17)	Pregnancy Loss (n=9)
Maternal age (years)[a]	35.5+/-1.5 (26-46)	37.3+/-1.3 (33-41)
Gravidity[b]	2.3+/-0.2 (1-3)	3.7+/-1.2 (2-6)
Parity median[c]	2.0 (0-3)	0.0 (0-1)
Number of previous losses[d]	0	3.3+/-0.9 (2-5)

Data provided as the mean ± SEM; range given in brackets.
[a]data unavailable for 3 fertile patients; 2 pregnancy loss patients.
[b]data unavailable for 6 fertile patients; 6 pregnancy loss patients.
[c]data unavailable for 5 fertile patients; 4 pregnancy loss patients.
[d]data unavailable for 6 fertile patients; 6 pregnancy loss patients – defined as 'multiple' only.

with history of early pregnancy loss) and 18 for RNA extraction (12 fertile, 6 with a history of early pregnancy loss). The women had no hormonal treatment for ≥ 3 months before tissue collection.

First trimester products of conception were collected following elective termination of pregnancy by evacuation for psychosocial reasons (n=4; amenorrhea 6-11 weeks). Term placental villous and decidual tissue was donated by healthy women following spontaneous labor at term (>37 weeks; n=4).

Serum was collected from women aged >18 years (n=5/group) attending an IVF clinic, who had successful pregnancies following IVF and those who had repeated pregnancy loss following IVF. Serum was collected from women undergoing oocyte collection, two days after induction of ovulation by human chorionic gonadotrophin. Subsequent details of outcomes of embryo transfer in the same cycle were recorded.

2.2 Cell culture

All cells were cultured at 37°C in a 5% CO_2 humidified culture incubator. hESF were maintained in DMEM/F12 (Gibco, Thermo Fisher Scientific, Inc.) plus 10% charcoal stripped Fetal Bovine serum (FBS; Gibco, Thermo Fisher Scientific, Inc.) and 1% antibiotics (penicillin, streptomycin, amphoceterin B; Gibco, Thermo Fisher Scientific, Inc.). HTR8/SVneo cells (CRL-3271) were from the ATCC and cultured with RPMI (Gibco, Thermo Fisher Scientific, Inc.) plus 10% heat inactivated FBS (Gibco, Thermo Fisher Scientific, Inc.).

2.3 Decidualization

hESF were isolated using collagenase digestion and filtration as previously described (21), resulting in a 97% stromal fibroblast population (22). hESF were decidualized as previously described (21) by treatment for 14 days with oestradiol (E, 10^{-8}M; Sigma) and medroxyprogesterone acetate (MPA, 10^{-7}M; Sigma) in DMEM/F12 containing 2% charcoal stripped FBS and 1% antibiotics. The media was refreshed every 2-3 days, on a Monday, Wednesday and Friday. Cells and culture media were collected on Day 3 and Day 14, both after 72h of culture. Cells were pelleted by centrifugation at 500x*g* then snap-frozen. Culture media was centrifuged at 500x*g* for 5 minutes to pellet cell debris then the supernatant snap-frozen.

2.4 Prolactin ELISA

PRL secretion by decidualized hESF (culture media collected on days 3 and 14) was quantified by ELISA as per the manufacturer's instructions (DuoSet kit #DY682, R&D systems) (23).

2.5 RNA isolation

Decidual culture media: RNA was isolated from 200uL culture media collected on Day 3 and Day 14 of culture and media only control using the RNeasy Micro Kit (Qiagen) according to the manufacturer's instructions.

hESF & HTR8/Svneo cells, endometrial and decidual tissue: RNA extraction was performed as previously described using Tri Reagent according to the manufacturer's instructions (Sigma-Aldrich, Merck).

Serum: RNA extraction (from 250uL serum) was performed using the TRIzol LS reagent (Ambion, Life Technologies) as per the manufacturer's instructions.

Genomic DNA was removed from isolated RNA using the DNAfree kit (Ambion; Thermo Fisher Scientific, Inc.) according to the manufacturer's protocol. A spectrophotometer (Nanodrop Technologies; Thermo Fisher Scientific, Inc.), was used at an absorbance ratio of 260/280 nm to analyze RNA sample concentration, yield and purity.

2.6 microRNA array

cDNA synthesis was performed using the miRCURY LNA™ Universal RT microRNA PCR system (Qiagen) and microRNA PCR Human Panel (I) as previously described (24). cDNA products diluted 60-fold were plated on the microRNA PCR Human Panel (I) plate and qPCR was performed using a 7900HT thermocycler (Applied Biosystems) using the recommended parameters (Qiagen). Raw CT values were normalized (ΔCT) to the average of the control wells (UniSP3) on the plate, then ΔΔCT calculated by normalizing the ΔCT to the average of the day 3 samples for each gene (Supplementary Table 1). A media only control was run to enable exclusion of miRs present in the treatment media.

2.7 miR RT-qPCR

cDNA was synthesized from 10ng total RNA using the TaqMan reverse transcription kit (Applied Biosystems; Thermo Fisher Scientific, Inc), and specific TaqMan miR primer sets (cat no. #4427975; miR-19b-3p #000396; miR-181a-2-3p #002317; miR-409-5p #002331; rnU6, #001973; Applied Biosystems; Thermo Fisher Scientific, Inc.) on the Veriti 7 fast block real-time qPCR system (Applied Biosystems). miR qPCR was performed in triplicate (final reaction volume, 10 µl) in 384-well micro- optical plates (Applied Biosystems; Thermo Fisher Scientific, Inc.) on the ABI 7900HT fast block or Viia 7 qPCR systems (Applied Biosystems; Thermo Fisher Scientific, Inc.). A template-free negative control and RNase-free water only was added for each run. The qPCR conditions were: 95°C for 10 min and 40 cycles of 95°C for 15s followed by 60°C for 1 min. Relative expression levels were calculated as per the manufacturer's instructions using the comparative cycle threshold method (ΔΔCT).

2.8 mRNA RT-qPCR

Total RNA (250ng) was reverse transcribed using Superscript III (Invitrogen) (0.5 µL per reaction) as previously described (25).

qPCR was performed as previously described (25) using Power SYBR Green master mix (Applied Biosystems) on the Veriti 7 fast block real-time qPCR system (Applied Biosystems). Primer sequences are as follows: *18s* Fwd: 5`GATCCATTG GAGGGCAAGTCT3`, Rev: 5`CCAAGATCCACCTACGA GCTT3`; Fwd: *HOXA9* 5`TACGTGGACTCGTTCCTGCT3`, Rev: 5`CGTCGCCTTGGACTGGAAG3`; *PTEN* Fwd: 5`TCC ATCCTGCAGAAGAAGCC3`, Rev: 5`AGGATATTGTGCA ACTCTGCAA3`; (Sigma-Aldrich). A template-free negative control in the presence of primers and RNase-free water only negative controls were added for each run. The qPCR conditions were: 95°C for 10 min and 40 cycles of 95°C for 15s followed by 60° C for 1 min. Relative expression levels (normalized to *18s* ribosomal RNA) were calculated as per the manufacturer's instructions using the comparative cycle threshold method (ΔΔCT).

2.9 *In situ* hybridization

In situ hybridization was performed as previously described (26). Briefly, 4 µm thickness endometrial sections were deparaffinized and rehydrated in xylene, neat ethanol, 96% ethanol, and 70% ethanol and then placed in PBS Proteinase K (15 µg/mL) digestion was performed at 37°C for 15 min. Following PBS wash, 100 nM miR-19b-3p detection probe (#339111, YD00619863-BCG; Qiagen) or scramble control probe (cat no. #339111 YD00699004-BCG) was applied to sections and placed in a 60°C incubator for 1 h. Slides were then washed in 5x sodium-saline citrate (SSC), 1x SSC and 0.2x SSC buffers at 60°C for 5 min, and 0.2x SSC at room temperature (RT) for 5 min, then placed in PBS. Blocking solution of 10% CAS block (008120, Thermo), 2% sheep serum, 1% bovine serum albumin (BSA) in PBS-Tween (T) was applied to sections and incubated at RT for 15 min. After incubation, sections were treated with anti-DIG-fluorescein 1:50 in 0.5% BSA/PBS at RT for 1 h. Following additional washes in PBS-T, sections were counterstained with DAPI to indicate the cell nuclei (blue). Sections were visualized using Olympus BX63 fluorescence microscope and cellSense software. All images were taken under the same exposure and settings.

2.10 Real time cell analysis

The real-time cell analyser (RTCA) MP xCELLigence instrument (ACEA Biosciences; Agilent Technologies GmbH) was used to interrogate the effect of miR-19b-3p on HTR8/Svneo adhesion and proliferation. HTR8/Svneo were transfected with 100nM miR-19b-3p mimic (cat no. 339173 YM00470545-ADB) or negative control (cat no. 339173 YM00479902-ADB) using Lipofectamine RNAiMAX (13778100, Thermo Fisher) and Opti-MEM medium (11524456, Fisher) following manufacturer's instructions for 72 h. After transfection cells were seeded into E-plate 96 (ACEA Biosciences; Agilent Technologies GmbH) at ~10,000 cells/well in RPMI supplemented with 5% FCS. Data was collected ever 15 minutes for a total of 96h.

2.11 Statistical analysis

Statistical analyses were performed using GraphPad Prism 9.5.0. Paired t-tests, one-way ANOVA and repeated measures ANOVA were performed. All data is presented as mean ± SEM. $P<0.05$ was considered statistically significant.

3 Results

3.1 hESF miR release is repressed by decidualization

We identified 98 miRs released by hESF into the culture media (Figure 1A; Supplementary Table 1). The most highly expressed miRs were miR-125b-5p, -23a-3p and let-7b-5p. miR release into the culture media was highly repressed following *in vitro* hESF decidualization (Figure 1A): 11 miRs showed a significant reduction at Day 14 of *in vitro* decidualization (Figure 1B). Decidualization was confirmed by PRL secretion (Figure 1C).

To confirm the array data, we investigated the expression of 3 different miRs in hESF matched cellular and culture media RNA (Figures 1D–F). Interestingly, although the cellular levels of miRs-19b-3p, -181a-2-3p and -409-5p were not altered by decidualization, miR concentration in culture media was significantly reduced (Figures 1D–F). In contrast when we investigated whether decidualization altered miR-19b-3p, -181a-2-3p or -409-5p expression in whole endometrial tissue biopsies (non-decidualized: proliferative endometrium; decidualized: late secretory endometrium, 1st trimester or term decidua) (Figures 1G–I) we found no difference in expression between non-decidualized and decidualized tissue, although miR-181a-2-3p was significantly elevated in term decidua compared to late secretory endometrium (Figure 1H) and miR-409-5p was significantly elevated in 1st trimester decidua compared to late secretory endometrium (Figure 1I).

3.2 Endometrial miR-19b-3p is increased in women with a history of early pregnancy loss

In situ hybridization of cycling endometrial tissue biopsies localized miR-19b-3p to most cell types in the endometrium, although endometrial glandular epithelial cell expression was variable even within adjacent glands (Figure 2A). Using qPCR, we found that expression miR-19b-3p in endometrial tissue biopsies was significantly increased in patients with a history of early pregnancy loss compared to fertile controls (Figure 2B). This

10.3389/fendo.2023.1149786

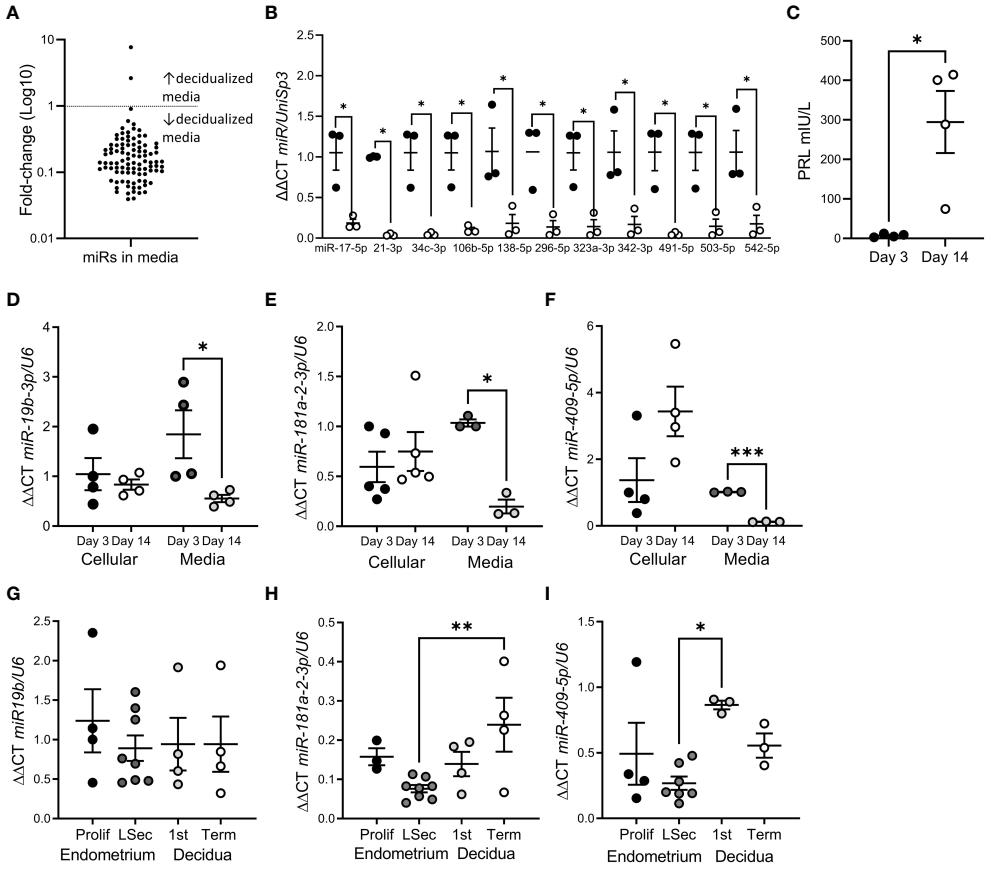


FIGURE 1
miR release was reduced following hESF decidualization. **(A)** Fold-change of all miRs identified in hESF culture media by microarray from Day 3 to Day 14. **(B)** miRs with significantly reduced levels in hESF culture media between Day 3 and Day 14. **(C)**. Prolactin (PRL) secretion by hESF on Day 3 and Day 14 of decidualization. **(D–F)**. qPCR of miR-19b-3p **(D)**, miR-181a-2-3p **(E)** and miR-409-5p **(F)** in hESF cells and culture media on Day 3 and Day 14 of decidualization. **(G–I)**. qPCR of miR-19b-3p **(G)**, miR-181a-2-3p **(H)** and miR-409-5p **(I)** in whole tissue biopsies collected during the proliferative (prolif) and late secretory (LSec) stages of the menstrual cycle and 1st trimester and term decidua. Data shows mean ± SEM; *P<0.05; **P<0.01; ***P<0.001; **(C–F)**, paired t-test; **(G–I)**, one-way ANOVA.

increase was not found in serum from women undergoing IVF with a history of repeated early pregnancy loss (Figure 2C).

3.3 miR-19b-3p reduces HTR8/Svneo trophoblast proliferation

As impaired decidualization is associated with recurrent pregnancy loss and miR-19b-3p release was suppressed by decidualization, we investigated the effect of miR-19b-3p on trophoblast function using the HTR8/Svneo cell line. HTR8/Svneo transfected with miR-19b-3p mimic showed elevated miR-19b-3p expression in the cell pellet (Figure 3A), suggesting that miR-19b-3p is taken up from the media. Using a Real-Time Cell Analysis system (xCELLigence) we found there was no effect of miR-19b-3p on HTR8/Svneo adhesion (Figure 3B) but after 60h miR-19b-3p significantly inhibited HTR8/Svneo proliferation compared to control (Figure 3C). We investigated whether transfection with the miR-19b-3p affected HTR8/Svneo production of predicted miR-19b-3p targets (27, 28): miR-19b-3p increased *HOXA9* mRNA but had no effect on *PTEN* mRNA (Figure 3D).

4 Discussion

Here we showed for the first time that decidualization was associated with a global repression of miR release by hESFs. We found that endometrial tissue collected from women with a history of early pregnancy loss had significantly higher mir-19b-3p production conmpared to fertile controls and transfection of miR-19b-3p mimic to HTR8/Svneo trophoblast cells significantly impaired cell proliferation and increased *HOXA9* mRNA production.

Our observation that global miR release was reduced in decidualized hESF is striking. Released miRs can be transferred to another cell, triggering actions in target cells (15). Certainly, decidualized cell secretions promote decidualization of surrounding stromal cells (1), regulate uterine-resident lympocyte recruitment and differentiation (29) and promote trophoblast invasion (8, 30, 31). We hypothesize hESF-released miRs would

10.3389/fendo.2023.1149786

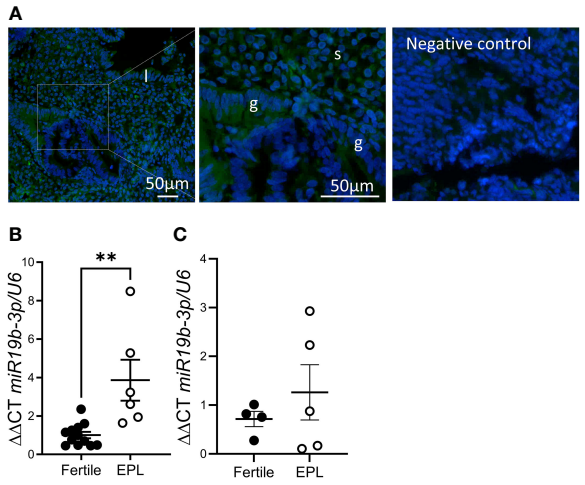


FIGURE 2
miR-19b-3p expression is elevated in endometrium from women with a history of early pregnancy loss. **(A)** *In situ* hybridization of miR-19b-3p in endometrium. Localization of miR-19b-3p indicated by green fluorescent staining. DAPI (blue) counterstaining identifies nuclei. **(B)** qPCR of miR-19b-3p in endometrium from fertile patients and patients with a history of early pregnancy loss (EPL). **(C)** qPCR of miR-19b-3p in serum from fertile patients and patients with a history of early pregnancy loss. g, glandular epithelium; l, luminal epithelium; s, stroma; Data shows mean ± SEM; **P<0.01; **(B, C)**, paired t-test.

be taken up by surrounding cells (eg. other decidual cells, trophoblast, immune and endothelial cells) and our data suggests that decidualization may release these other cells from hESF mediated control. We did not investigate the mechanism by which this repression in miR release occurs, however extracellular vesicle production is increased following decidualization with cAMP (32), suggesting that there may be a change in other methods of release (eg argonaute proteins). Whether argonaute proteins in hESF are regulated by decidualization has not been investigated.

It was somewhat surprising that we didn't see a change in cellular miRs using this *in vitro* model as have been seen in other models that investigated only cellular miRs following *in vitro* decidualization, including miR-181a (downregulated 3-fold) and miR-409-5p (upregulated 2.3-fold) (17). We saw a non-significant trend to increased miR-409-5p cellular expression and a significant increase in production in the 1st trimester decidua compared to late secretory phase endometrium. To exclude the direct effect of oestradiol or MPA on miR release in this study we collected cells and culture media 3 days after initiating the decidualization treatments. Although there is negligible PRL secretion on day 3, it is possible that alterations to miR production are initiated early in decidualization and we may have seen an effect on miR production if we compared hESF before and after decidualization hormone treatment as is done in other studies.

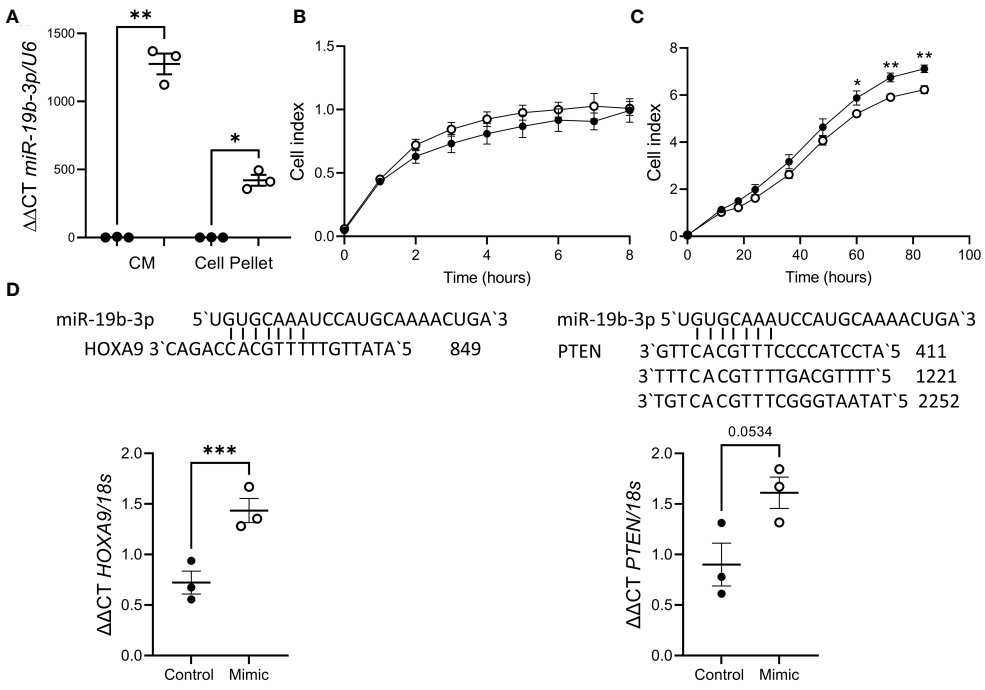


FIGURE 3
miR-19b-3p overexpression in HTR8/Svneo cells impaired proliferation. **(A)** Treatment with miR-19b-3p mimic (○) significantly increased miR-19b-3p levels in HTR8/Svneo culture media (CM) and cell pellet compared to scramble control (●). **(B)** miR-19b-3p mimic had no effect on HTR8/Svneo adhesion (n=3/group). **(C)** miR-19b-3p mimic significantly reduced HTR8/Svneo proliferation after 60h (n=3/group). **(D)** miR-19b-3p mimic significantly increased *HOXA9* expression but had no effect on *PTEN*. Alignment of miR-19b-3p and the 3`UTR of HOXA9 and PTEN is also shown. Data shows mean ± SEM; *P<0.05; **P<0.01; ***P<0.001; **(A–C)**, repeated measures ANOVA; **(D)**, paired t-test.

Collectively, previous studies and our results suggest that dysregulated miR-19b-3p production may be involved in the etiology of recurrent pregnancy loss. We found that miR-19b-3p was significantly elevated in the cycling endometrium of patients with a history of early pregnancy loss and Tian et al. showed that miR-19b-3p is decreased in the placental villous of patients with a history of recurrent early pregnancy loss (20). Furthermore, miR-19b-3p is dysregulated in monocytes from patients with antiphospholipid syndrome (33), an acquired thrombophilia diagnosed in 15-20% of patients with recurrent early pregnancy loss (5).

The function of miR-19b-3p appears highly cell type specific. In trophoblast miR-19b-3p overexpression prevents syncytialization of primary human cytotrophoblasts (34), decreased PTEN production in JEG-3 (20) and here we found miR-19b-3p impaired HTR8/Svneo trophoblast proliferation. In other tissues miR-19b-3p mostly promotes proliferation (35–39). The inhibition of proliferation by miR-19b-3p mimic seen here may be due to the increase in *HOXA9* production also stimulated by the miR-19b-3p mimic: HOXA9 inhibits HTR8/Svneo proliferation (40), migration and invasion (41).

A role for miR-19b-3p in inflammation is also proposed, however again the function of miR-19b-3p in regulating inflammatory responses is not clear. miR-19b-3p increases apoptosis and intracellular reactive oxygen species in endothelial cells (42), enhances Th1/M1 inflammatory responses (43–45) and inhibits Treg differentiation (43), but may also promote M2 polarization (46, 47). That miR-19b-3p may be pro-inflammatory in pregnancy is suggested by elevated levels in maternal plasma of pregnancies with gestational diabetes mellitus (48, 49), and preterm birth (50), both inflammatory conditions. Loss of miR-19b-3p in the endometrium during decidualization therefore may be crucial to promote trophoblast differentiation and maternal tolerance.

In conclusion, we found that *in vitro* decidualization was associated with reduced miR release and that overexpression of miR-19b-3p was found in endometrial tissue from patients with history of early pregnancy loss. Finally, we found that miR-19b-3p impaired HTR8/Svneo proliferation implying a role for this decidual-released miR in trophoblast function. Overall we speculate that decidualization may act to reduce endometrial stromal cell regulation of other cell types within the decidua, particularly trophoblast, enabling healthy implantation and placentation during early pregnancy.

Data availability statement

The original contributions presented in the study are included in the article/Supplementary Material, Further inquiries can be directed to the corresponding author/s.

Ethics statement

The studies involving human participants were reviewed and approved by Royal Women's Hospital Research Ethics Committee Monash Health Human Research Ethics Committee. The patients/participants provided their written informed consent to participate in this study.

Author contributions

EM conception, design, experiments, wrote manuscript. TS experiments. KR experiments. SB experiments. WZ experiments, edited manuscript. TE design, samples, edited manuscript. ED design, edited manuscript. All authors contributed to the article and approved the submitted version.

Funding

This work was supported by the Rebecca L Cooper Medical Research Foundation (project grant PG2018130 to EM), the Trevor B. Kilvington Bequest, the NHMRC (Australia) Fellowship (#550905 to ED) and the Victorian Government's Operational Infrastructure support. The funders had no involvement in the conduct of research, preparation of the manuscript or the decision to publish.

Acknowledgments

We are grateful to the women who donated tissue and thank Emily-Jane Bromley RN, Judi Hocking RN and Leilani Santos for their contribution to this manuscript.

Conflict of interest

The authors declare that the research was conducted in the absence of any commercial or financial relationships that could be construed as a potential conflict of interest.

Publisher's note

All claims expressed in this article are solely those of the authors and do not necessarily represent those of their affiliated organizations, or those of the publisher, the editors and the reviewers. Any product that may be evaluated in this article, or claim that may be made by its manufacturer, is not guaranteed or endorsed by the publisher.

Supplementary material

The Supplementary Material for this article can be found online at: https://www.frontiersin.org/articles/10.3389/fendo.2023.1149786/full#supplementary-material

References

1. Evans J, Salamonsen LA, Winship A, Menkhorst E, Nie G, Gargett CE, et al. Fertile ground: human endometrial programming and lessons in health and disease. *Nat Rev Endocrinol* (2016) 12:654–67. doi: 10.1038/nrendo.2016.116

2. Mori M, Bogdan A, Balassa T, Csabai T, Szekeres-Bartho J. The decidua - the maternal bed embracing the embryo-maintains the pregnancy. *Sem Immunopath* (2016) 38:635–49. doi: 10.1007/s00281-016-0574-0

3. Founds S, Conley YP, Lyons-Weiler JF, Jeyabalan A, Allen Hogge W, Conrad KP. Altered global gene expression in first trimester placentas of women destined to develop preeclampsia. *Placenta* (2009) 30:15–24. doi: 10.1016/j.placenta.2008.09.015

4. Lucas ES, Dyer NP, Murakami K, Lee YH, Chan YW, Grimaldi G, et al. Loss of endometrial plasticity in recurrent pregnancy loss. *Stem Cells* (2016) 34:346–56. doi: 10.1002/stem.2222

5. Dimitriadis E, Menkhorst E, Saito S, Kutteh WH, Brosens JJ. Recurrent pregnancy loss. *Nat Rev Dis Primers* (2020) 6:98. doi: 10.1038/s41572-020-00228-z

6. Graham CH, Lysiak JJ, McCrae KR, Lala PK. Localization of transforming growth factor-β at the human fetal-maternal interface: Role in trophoblast growth and Differentiation1. *Biol Reproduction.* (1992) 46:561–72. doi: 10.1095/biolreprod46.4.561

7. Xu G, Guimond M-J, Chakraborty C, Lala PK. Control of proliferation, migration, and invasiveness of human extravillous trophoblast by decorin, a decidual Product1. *Biol Reprod* (2002) 67:681–9. doi: 10.1095/biolreprod67.2.681

8. Menkhorst EM, Van Sinderen M, Correia J, Dimitriadis E. Trophoblast function is altered by decidual factors in gestational-dependant manner. *Placenta* (2019) 80:8–11. doi: 10.1016/j.placenta.2019.03.013

9. Keskin D, Allan DSJ, Rybalov B, Andzelm MM, Stern JNH, Kopcow HD, et al. TGFβ promotes conversion of CD16+ peripheral blood NK cells into CD16- NK cells with similarities to decidual NK cells. *PNAS* (2007) 104:3378–83. doi: 10.1073/pnas.0611098104

10. Xu X, Wang Q, Deng B, Wang H, Dong Z, Qu X, et al. Monocyte chemoattractant protein-1 secreted by decidual stromal cells inhibits NK cells cytotoxicity by up-regulating expresssion of SOCS3. *PloS One* (2012) 7:e41869. doi: 10.1371/journal.pone.0041869

11. Wheeler K, Jena MK, Pradhan BS, Nayak N, Das S, Hsu C-D, et al. VEGF may contribute to macrophage recruitment and M2 polarization in the decidua. *PloS One* (2018) 13:e0191040. doi: 10.1371/journal.pone.0191040

12. Salker M, Teklenburg G, Molokhia M, Lavery S, Trew G, Aojanepong T, et al. Natural selection of human embryos: impaired decidualization of endometrium disables embryo-maternal interactions and causes recurrent pregnancy loss. *PloS One* (2010) 5:e10287. doi: 10.1371/journal.pone.0010287

13. Brosens JJ, Salker MS, Teklenburg G, Nautiyal J, Salter S, Lucas ES, et al. Uterine selection of human embryos at implantation. *Sci Rep* (2014) 4:3894–4. doi: 10.1038/srep03894

14. Chew C, Conos S, Unal B, Tergaonkar V. Noncoding RNAs: master regulators of inflammatory signaling. *Trends Mol Med* (2018) 24:66–84. doi: 10.1016/j.molmed.2017.11.003

15. Fabbri M. MicroRNAs and miRceptors: a new mechanism of action for intercellular communication. *Philos Trans R Soc Lond B Biol Sci* (2018) 373:20160486.2016040486. doi: 10.1098/rstb.2016.0486

16. Park Y. MicroRNA exocytosis by vesicle fusion in neuroendocrine cells. *Front Endocrinol* (2017) 8:355. doi: 10.3389/fendo.2017.00355

17. Estella C, Herrer I, Moreno-Moya JM, Quiñonero A, Martínez S, Pellicer A, et al. miRNA signature and dicer requirement during human endometrial stromal decidualization *in vitro*. *PloS One* (2012) 7:e41080–0. doi: 10.1371/journal.pone.0041080

18. Wang JM, Gu Y, Zhang Y, Yang Q, Zhang X, Yin L, et al. Deep-sequencing identification of differentially expressed miRNAs in decidua and villus of recurrent miscarriage patients. *Arch Gynecol Obstet* (2016) 293:1125–35. doi: 10.1007/s00404-016-4038-5

19. Hong L, Yu T, Xu H, Hou N, Cheng Q, Lai L, et al. Down-regulation of miR-378a-3p induces decidual cell apoptosis: a possible mechanism for early pregnancy loss. *Hum Reprod* (2018) 33:11–22. doi: 10.1093/humrep/dex347

20. Tian S, Yu J, Zhang Y, Bian Y, Ma J, Yan J. Overexpression of PTEN regulated by miR-19b and miR-494 in the villous of recurrent spontaneous abortion patients. *J Reprod Immunol* (2020) 140:103133. doi: 10.1016/j.jri.2020.103133

21. Menkhorst EM, Van Sinderen ML, Rainczuk K, Cuman C, Winship A, Dimitriadis E. Invasive trophoblast promote stromal fibroblast decidualization *via* profilin 1 and ALOX5. *Sci Rep* (2017) 7:8690. doi: 10.1038/s41598-017-05947-0

22. Dimitriadis E, Robb L, Salamonsen LA. Interleukin 11 advances progesterone-induced decidualization of human endometrial stromal cells. *Mol Hum Reprod* (2002) 8:636–43. doi: 10.1093/molehr/8.7.636

23. Grbac E, So T, Varshney S, Williamson N, Dimitriadis E, Menkhorst E. Prednisolone alters endometrial decidual cells and affects decidual-trophoblast interactions. *Front Cell Dev Biol* (2021) 9:647496. doi: 10.3389/fcell.2021.647496

24. Cuman C, Van Sinderen M, Gantier MP, Rainczuk K, Sorby K, Rombauts L, et al. Human blastocyst secreted microRNA regulate endometrial epithelial cell adhesion. *EBioMedicine* (2015) 2:1528–35. doi: 10.1016/j.ebiom.2015.09.003

25. Menkhorst E, Zhou W, Santos L, Delforce S, So T, Rainczuk K, et al. Galectin-7 impairs placentation and causes preeclampsia features in mice. *Hypertension* (2020) 76:1185–94. doi: 10.1161/HYPERTENSIONAHA.120.15313

26. Barton S, Zhou W, Santos L, Menkhorst E, Yang G, Tinn Teh W, et al. miR-23b-3p regulates human endometrial epithlial cell adhesion implying a role in implantation. *Reproduction* (2023) 165:407–16. doi: 10.1530/REP-22-0338

27. Liu W, Wang X. Prediction of functional microRNA targets by integrative modeling of microRNA binding and target expression data. *Genome Biol* (2019) 20:18. doi: 10.1186/s13059-019-1629-z

28. Chen Y, Wang X. miRDB: an online database for prediction of functional microRNA targets. *Nucleic Acids Res* (2020) 48:D127–d131. doi: 10.1093/nar/gkz757

29. Vinketova K, Mourdjeva M, Oreshkova T. Human decidual stromal cells as a component of the implantation niche and a modulator of maternal immunity. *J Pregnancy* (2016) 2016:8689436. doi: 10.1155/2016/8689436

30. Menkhorst EM, Lane N, Winship AL, Li P, Yap J, Meehan K, et al. Decidual-secreted factors alter invasive trophoblast membrane and secreted proteins implying a role for decidual cell regulation of placentation. *PloS One* (2012) 7:e31418. doi: 10.1371/journal.pone.0031418

31. Menkhorst E, Winship A, Van Sinderen M, Dimitriadis E. Human extravillous trophoblast invasion: intrinsic and extrinsic regulation. *Reprod Fertil Dev* (2016) 28:406–15. doi: 10.1071/RD14208

32. Ma Q, Beal JR, Bhurke A, Kannan A, Yu J, Taylor RN, et al. Extracellular vesicles secreted by human uterine stromal cells regulate decidualization, angiogenesis, and trophoblast differentiation. *PNAS* (2022) 119:. doi: 10.1073/pnas.2200252119

33. Juárez-Vicuña Y, Guzmán-Martín CA, Martínez-Martínez LA, Hernández-Díazcouder A, Huesca-Gómez C, Gamboa R, et al. miR-19b-3p and miR-20a-5p are associated with the levels of antiphospholipid antibodies in patients with antiphospholipid syndrome. *Rheumatol Int* (2021) 41:1329–35. doi: 10.1007/s00296-021-04864-w

34. Kumar P, Luo Y, Tudela C, Alexander JM, Mendelson CR. The c-myc-regulated microRNA-17~92 (miR-17~92) and miR-106a~363 clusters target hCYP19A1 and hGCM1 to inhibit human trophoblast differentiation. *Mol Cell Biol* (2013) 33:1782–96. doi: 10.1128/MCB.01228-12

35. Jiang T, Ye L, Han Z, Liu Y, Yang Y, Peng Z, et al. miR-19b-3p promotes colon cancer proliferation and oxaliplatin-based chemoresistance by targeting SMAD4: validation by bioinformatics and experimental analyses. *J Exp Clin Cancer Res* (2017) 36:131–1. doi: 10.1186/s13046-017-0602-5

36. Daguia Zambe JC, Zhai Y, Zhou Z, Du X, Wei Y, Ma F, et al. miR-19b-3p induces cell proliferation and reduces heterochromatin-mediated senescence through PLZF in goat male germline stem cells. *J Cell Physiol* (2018) 233:4652–65. doi: 10.1002/jcp.26231

37. Xiaoling G, Shuaibin L, Kailu L. MicroRNA-19b-3p promotes cell proliferation and osteogenic differentiation of BMSCs by interacting with lncRNA H19. *BMC Med Genet* (2020) 21:11–1. doi: 10.1186/s12881-020-0948-y

38. Wang Q, Dong Y, Wang H. microRNA-19b-3p-containing extracellular vesicles derived from macrophages promote the development of atherosclerosis by targeting JAZF1. *J Cell Mol Med* (2022) 26:48–59. doi: 10.1111/jcmm.16938

39. Li ZL, Li D, Yin GQ. MiR-19b-3p promotes tumor progression of non-small cell lung cancer *via* downregulating HOXA9 and predicts poor prognosis in patients. *Histol Histopathol* (2022) 37:779–89. doi: 10.14670/HH-18-448

40. Shi Z, Liu B, Li Y, Liu F, Yuan X, Wang Y. MicroRNA-652-3p promotes the proliferation and invasion of the trophoblast HTR-8/SVneo cell line by targeting homeobox A9 to modulate the expression of ephrin receptor B4. *Clin Exp Pharmacol Physiol* (2019) 46:587–96. doi: 10.1111/1440-1681.13080

41. Liu X, Liu X, Liu W, Luo M, Tao H, Wu D, et al. HOXA9 transcriptionally regulates the EPHB4 receptor to modulate trophoblast migration and invasion. *Placenta* (2017) 51:38–48. doi: 10.1016/j.placenta.2017.01.127

42. Xue Y, Wei Z, Ding H, Wang Q, Zhou Z, Zheng S, et al. MicroRNA-19b/221/222 induces endothelial cell dysfunction *via* suppression of PGC-1α in the progression of atherosclerosis. *Atherosclerosis* (2015) 241:671–81. doi: 10.1016/j.atherosclerosis.2015.06.031

43. Jiang S, Li C, Olive V, Lykken E, Feng F, Sevilla J, et al. Molecular dissection of the miR-17-92 cluster's critical dual roles in promoting Th1 responses and preventing inducible treg differentiation. *Blood* (2011) 118:5487–97. doi: 10.1182/blood-2011-05-355644

44. Yin L, Song C, Zheng J, Fu Y, Qian S, Jiang Y, et al. Elevated expression of miR-19b enhances CD8+ T cell function by targeting PTEN in HIV invected long term non-progressors with sustained viral suppression. *Front Immunol* (2019) 9:3140. doi: 10.3389/fimmu.2018.03140

45. Lv L-L, Feng Y, Wu M, Wang B, Li Z-L, Zhong X, et al. Exosomal miRNA-19b-3p of tubular epithelial cells promotes M1 macrophage activation in kidney injury. *Cell Death Differ* (2020) 27:210–26. doi: 10.1038/s41418-019-0349-y

46. Chen J, Zhang K, Zhi Y, Wu Y, Chen B, Bai J, et al. Tumor-derived exosomal miR-19b-3p facilitates M2 macrophage polarization and exosomal LINC00273 secretion to promote lung adenocarcinoma metastasis *via* hippo pathway. *Clin Transl Med* (2021) 11:e478–8. doi: 10.1002/ctm2.478

47. Jiahui C, Jiadai Z, Nan Z, Rui Z, Lipin H, Jian H, et al. miR-19b-3p/PKNOX1 regulates viral myocarditis by regulating macrophage polarization. *Front Genet* (2022) 13:902453. doi: 10.3389/fgene.2022.902453

48. Zhu Y, Tian F, Li H, Zhou Y, Lu J, Ge Q. Profiling maternal plasma microRNA expression in early pregnancy to predict gestational diabetes mellitus. *Int J Gynecology Obstetrics* (2015) 130:49–53. doi: 10.1016/j.ijgo.2015.01.010

49. Li J, Gan B, Lu L, Chen L, Yan J. Expression of microRNAs in patients with gestational diabetes mellitus: a systematic review and meta-analysis. *Acta Diabetol* (2022). doi: 10.1007/s00592-022-02005-8

50. Cook J, Bennett PR, Kim SH, Teoh TG, Sykes L, Kindinger LM, et al. First trimester circulating MicroRNA biomarkers predictive of subsequent preterm delivery and cervical shortening. *Sci Rep* (2019) 9:5861–1. doi: 10.1038/s41598-019-42166-1

frontiers | Frontiers in Endocrinology

TYPE Review
PUBLISHED 03 May 2023
DOI 10.3389/fendo.2023.1087845

Check for updates

OPEN ACCESS

EDITED BY
Reinaldo Marín,
Instituto Venezolano de Investigaciones Científicas (IVIC), Venezuela

REVIEWED BY
Frank Hills,
Middlesex University, United Kingdom
Leonardo Ermini,
University of Siena, Italy

*CORRESPONDENCE
Julio C. Bueno-Sánchez
julio.bueno@udea.edu.co

SPECIALTY SECTION
This article was submitted to Developmental Endocrinology, a section of the journal Frontiers in Endocrinology

RECEIVED 02 November 2022
ACCEPTED 03 March 2023
PUBLISHED 03 May 2023

CITATION
Bueno-Sánchez JC, Gómez-Gutiérrez AM, Maldonado-Estrada JG and Quintana-Castillo JC (2023) Expression of placental glycans and its role in regulating peripheral blood NK cells during preeclampsia: a perspective. *Front. Endocrinol.* 14:1087845. doi: 10.3389/fendo.2023.1087845

COPYRIGHT
© 2023 Bueno-Sánchez, Gómez-Gutiérrez, Maldonado-Estrada and Quintana-Castillo. This is an open-access article distributed under the terms of the Creative Commons Attribution License (CC BY). The use, distribution or reproduction in other forums is permitted, provided the original author(s) and the copyright owner(s) are credited and that the original publication in this journal is cited, in accordance with accepted academic practice. No use, distribution or reproduction is permitted which does not comply with these terms.

Expression of placental glycans and its role in regulating peripheral blood NK cells during preeclampsia: a perspective

Julio C. Bueno-Sánchez[1,2,3]*, Alejandra M. Gómez-Gutiérrez[1], Juan G. Maldonado-Estrada[4] and Juan C. Quintana-Castillo[5]

[1]Reproduction Group, Department of Physiology and Biochemistry, School of Medicine, Universidad de Antioquia, Medellín, Colombia, [2]Department of Obstetrics and Gynecology, School of Medicine, Universidad de Antioquia, Medellín, Colombia, [3]Red Iberoamericana de Alteraciones Vasculares en Trastornos del Embarazo (RIVATREM), Chillan, Chile, [4]One Health and Veterinary Innovative Research & Development (OHVRI) Research Group, Escuela de Medicina Veterinaria, Universidad de Antioquia, Medellín, Colombia, [5]Grupo Infettare, Facultad de Medicina, Universidad Cooperativa de Colombia, Medellín, Colombia

Preeclampsia is a pregnancy-related multisystem disorder characterized by altered trophoblast invasion, oxidative stress, exacerbation of systemic inflammatory response, and endothelial damage. The pathogenesis includes hypertension and mild-to-severe microangiopathy in the kidney, liver, placenta, and brain. The main mechanisms involved in its pathogenesis have been proposed to limit trophoblast invasion and increase the release of extracellular vesicles from the syncytiotrophoblast into the maternal circulation, exacerbating the systemic inflammatory response. The placenta expresses glycans as part of its development and maternal immune tolerance during gestation. The expression profile of glycans at the maternal–fetal interface may play a fundamental role in physiological pregnancy changes and disorders such as preeclampsia. It is unclear whether glycans and their lectin-like receptors are involved in the mechanisms of maternal–fetal recognition by immune cells during pregnancy homeostasis. The expression profile of glycans appears to be altered in hypertensive disorders of pregnancy, which could lead to alterations in the placental microenvironment and vascular endothelium in pregnancy conditions such as preeclampsia. Glycans with immunomodulatory properties at the maternal–fetal interface are altered in early-onset severe preeclampsia, implying that innate immune system components, such as NK cells, exacerbate the systemic inflammatory response observed in preeclampsia. In this article, we discuss the evidence for the role of glycans in gestational physiology and the perspective of glycobiology on the pathophysiology of hypertensive disorders in gestation.

KEYWORDS

glycosylation, preeclampsia, syncitiotrophoblast, NK cells activity, sialic acid (*N*-Acetyl neuraminic acid)

1 Introduction

Preeclampsia is the most common hypertensive disorder in pregnancy, characterized by mild-to-severe microangiopathy of the placenta, kidney, liver, and brain (1–3). Before clinical signs of the disease appear, altered placental development exacerbates the local and systemic inflammatory status targeting the vascular endothelium (4–6). The systemic inflammatory response and clinical signs of preeclampsia end shortly after the fetus and placenta are removed during cesarean section, though hypertensive episodes may persist in some patients beyond the postpartum period. This situation increases the risk of renal disease or new episodes of preeclampsia in the subsequent gestation (7–9).

Preeclampsia is defined as a new onset of maternal hypertension after 20 weeks of gestation and systemic endothelial dysfunction manifested by new onset proteinuria (though not in all patients), hepatic dysfunction, and thrombocytopenia, among other symptoms (10, 11). Furthermore, preeclampsia exhibits diverse clinical manifestations, such as mild or severe, early or late onset (>34 weeks), or the presence or absence of intrauterine growth restriction (12–14). Pathological features of preeclampsia include shallow trophoblast invasion and poor spiral artery remodeling, resulting in placental hypoperfusion and intrauterine growth restriction (15, 16). These events occur during the first trimester of pregnancy and initially compromise the maternal–fetal interface, resulting in increased anti-angiogenic (17) and inflammatory factor production (18–22). Two pathophysiological stages have been proposed (23) to understand better the underlying mechanisms of preeclampsia: The first stage includes poor placentation, placental hypoperfusion, hypoxia, and trophoblast oxidative damage, followed by endothelial dysfunction and hypertensive clinical signs in the second stage (21, 24–26). Endothelial activation is intrinsic to the exacerbated systemic inflammatory response in severe preeclampsia (27), which involves NK cell activation rather than monocyte or lymphocyte activation (28, 29), resulting in coagulation dysfunction, insulin resistance, and hyperlipidemia (30).

In this context, the etiopathogenesis of preeclampsia is unknown, and the factors triggering its onset and progression to a multisystemic syndrome are unpredictable. Preeclampsia pathophysiology has traditionally focused on abnormal trophoblastic invasion, vascular inflammation, and the systemic inflammatory response (Croci et al., 2014). A more comprehensive approach is required to understand the occurrence of the multisystem syndrome (31). In this review, we focused on glycan recognition by peripheral NK cells and modulation of activation toward the cytotoxic phenotype to uncover new insights into molecular communication mechanisms between the trophoblast and the peripheral innate immune system. In the last two decades, a glycobiological perspective on pregnancy has emerged (32–35), and these new approaches have the potential to provide critical insights into the pathogenesis of preeclampsia and the development of severe clinical forms of the disease (36–43).

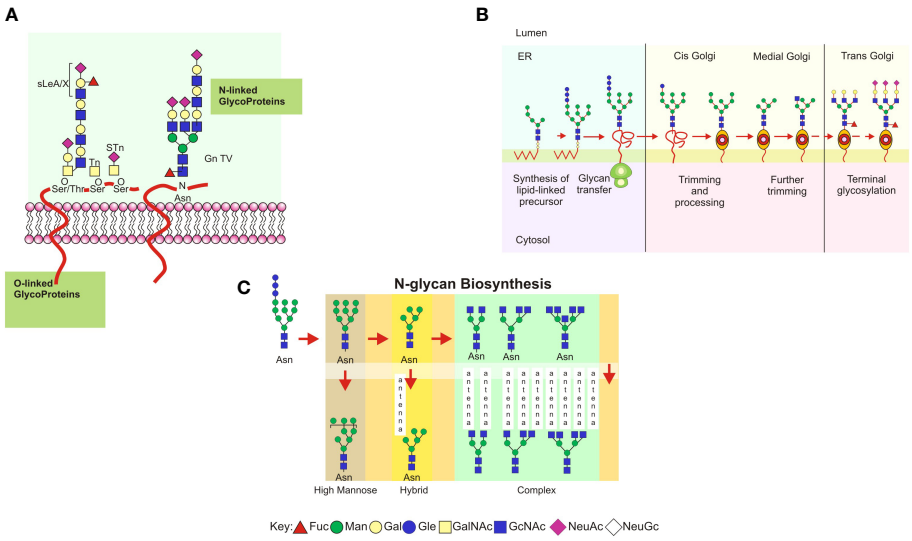


FIGURE 1
(A) Schematic representation of the main types of glycoproteins expressed in mammalian glycocalyx. Types of cell-surface glycans, including *N*-linked and *O*-linked glycans from glycoproteins. Each glycan has a common core whose terminal or internal sequences can vary, leading to a complex diversity among cells or defined microenvironments. **(B)** A consensus sequence for *N*-glycosylation (Asp-X-Ser/Thr, designated sequon) is used as an acceptor in polypeptide chains of a preformed oligosaccharide attached to a dolichol phosphate in the endoplasmic reticulum. The oligosaccharide glucose$_3$–mannose$_9$–*N*–acetylglucosamine$_2$ is transferred to the protein chain by an oligosaccharyltransferase acting as a chaperone and modulating its folding to transport toward the Golgi complex. Trimming and processing of the attached glycan are performed in Golgi compartments by specific glycosyltransferases and glycosidases for each nucleotide sugar donor. It is in the Golgi apparatus that glycans become oligomeric and branched. **(C)** Eukaryotic *N*-glycan biosynthesis in the endoplasmic reticulum and Golgi complex. Processing intermediates of *N*-glycans preserve a unique sequence core Manα1-6 (Manα1-3) Manβ1-4GlcNAcβ1-4GlcNAcβ1-Asn-X-Ser/Thr. Three types of N-glycans are found: oligomannose, complex, and hybrid.

1.1 The role of glycans in cell-to-cell communication

The glycocalyx is the cell's outermost layer of glycoconjugates, mainly glycoproteins and proteoglycans. The glycans bound to these glycoconjugates participate in ligand–receptor interactions in biological processes involving cell-to-cell interaction and function as a barrier and filter in endothelia (44, 45). In turn, the set of glycoprotein modifications complements the glycocalyx, and its more complex structure is encoded by nearly 10% of the transcribed genes that comprise the so-called glycome (46). The glycocalyx conformation may vary depending on the cell type, its activation and differentiation state, the cellular microenvironment, and the physiological or pathological conditions of the cells (47). Therefore, two of the systems in which the physiological role of glycocalyx has been studied are the immune system (reviewed in 48) and the vascular endothelium (reviewed in 49), particularly in pathological conditions (reviewed in 47, 50).

1.2 Structure of glycans

The glycocalyx is made up of monosaccharides or carbohydrates. In this review, glycan is preferred over carbohydrates because, unlike carbohydrates, not all glycans are monomers. Additionally, carbohydrate is often used interchangeably with components of intermediary metabolism. Glycans are composed of one carbonyl group, and the rest of the carbons contain hydroxyl groups. Carbonyl position and hydroxyl group orientation of atoms in asymmetric carbon determine monosaccharide structure. The anomeric carbon is derived from the carbonyl group; depending on the orientation of the anomeric carbon's hydroxyl group, the monosaccharide exists in either a or b anomer (48). The identity, variety, and functions of glycans are determined by chemical modifications of the hydroxyl groups, such as oxidation, *N*-acetylation, and sulfation (51, 52). Finally, when glycans combine to form linear and branched glycan structures, the variety of glycans exponentially increases. The diversity of glycans is estimated to be 1.05 × 1012 of linear and branched glycan structures (53). The most common monosaccharides found in mammalian cells include glucose (Glc), galactose (Gal), mannose (Man), *N*-acetylneuraminic acid (NeuAc), *N*-acetylglucosamine (GlcNAc), *N*-acetylgalactosamine (GalNAc), glucuronic acid (GlaA), xylose (Xyl), and fucose (Fuc) (48).

The DNA code does not determine protein modifications by enzymatic glycosylation because cellular enzymatic expression varies between species, cellular microenvironments, and cell types (54). Besides, glycosylation is a remarkably well-conserved enzymatic process (55). Specific changes in each glycan sequence will depend on the expression of glycosidases and glycosyltransferases, the availability of nucleotide sugar donor sources, and external influences mediated by cytokines and hormones in the cell microenvironment (56, 57). Glycosidases are enzymes that catalyze the hydrolysis of a bond linking a sugar of a glycoside to alcohol or another radical in the glycan molecule, whereas glycosyl transferases are enzymes that catalyze the transfer of glycosyl groups in biochemical reactions (58).

The structural diversity of the mammalian glycome is supported by the synthesis of glycans and their enzymatic regulation, which occurs in the endoplasmic reticulum and Golgi apparatus when added to proteins. If the glycan binds to the nitrogen of asparagine in the protein, it is called *N*-glycosylation or *N*-glycan; if it binds to the oxygen of a serine or threonine, it is called *O*-glycosylation or *O*-glycan (Figure 1A). In the case of proteoglycans, an unbranched polysaccharide chain composed of disaccharide units of a sulfated amino sugar (*N*-acetylglucosamine or *N*-acetylgalactosamine) and uronic acid (iduronic or glucuronic) is attached to a large protein core in a serine residue (59–61).

1.3 *N*-linked glycosylation

In *N*-glycosylation, a series of glycosyltransferases use nucleotide-activated sugar donors as substrates to form the mannose oligosaccharide 5-*N*-acetylglucosamine (Figure 1A). Oligosaccharide portions formed in the endoplasmic reticulum, specifically terminal glucose, and mannose, combined with molecular chaperones and thiol-disulfide oxidoreductases, help to fold newly synthesized proteins (62). The *N*-glycosylated polypeptide is delivered into the Golgi apparatus following interaction with cargo receptors in the vesicular transport system (63). If the protein is misfolded, it is translocated to the cytosol, deglycosylated by the enzyme peptide *N*-glycanase, or degraded by the ubiquitin/proteasome. In this pathway, glycosidases and mannosidases in the endoplasmic reticulum trim the *N*-glycans bound to the nascent protein, resulting in intermediate processing forms (Figure 1B; 64). The mannose residues are trimmed in the endoplasmic reticulum and subsequently in the Golgi complex, where the processed glycans undergo the addition of *N*-acetylglucosamine (*N*-acetylglucosaminylation), galactose (galactosylation), sialic acid (sialylation), or sulfate (sulfation). The intermediate forms of *N*-glycans share a common glycan core consisting of Manα1-6 (Manα1-3) Manβ1-4GlcNAcβ1-4GlcNAcβ1-Asn-X-Ser/Thr and have been classified into three types: (a) oligomannose, in which the mannose residues are attached to the core; (b) complex, in which the mannose residues are trimmed and replaced by *N*-acetylglucosamine, resulting in new elongated branches attached to the *N*-acetylglucosamine residues called "antennae"; and (c) a hybrid, in which only the mannose residues attached to Manα1-6 are conserved, while the mannose attached to Manα1-3 is trimmed and replaced in an antennae sequence by a branched *N*-acetylglucosamine (Figure 1C; reviewed in 64, 65).

1.4 *O*-linked glycosylation

O-linked glycosylation involves the formation of *O*-glycosidic bonds between oligosaccharide chains *via* *N*-acetylgalactosamine

and GalNAc (1β-3), which is found in mucin glycoproteins (Figure 1A) (66). These glycans are mucins with GalNAc *O*-linked to Ser or Thr. *O*-glycosylation occurs in mucin domains containing many serine, threonine, and proline sequences. *O*-glycan processing occurs in the Golgi apparatus and has little impact on the early stages of protein folding. In mammalian mucins, the first attached GalNAc can be replaced by GlcNAc, GalNAc (linkage 1α-3), or Gal, forming up to eight different core structures: core 1: Galβ1-3GalNAc; core 2: GlcNAcβ1-6(Galb1-3)GalNAc; core 3: GlcNAcβ1-3GalNAc; core 4: GlcNAcβ1-6(GlcNAcβ1-3)GalNAca; core 5: GalNAcα1-3GalNAc; core 6: GlcNAcβ1-6GalNAc; core 7: GalNAcα1-6GalNAc; and core 8: Galα1-3GalNAc (67). The most common core sequences are 1 and 2; cores 3 and 4 are only found in mucins. The core structures can be substituted or elongated with sialic acid residues. *O*-glycan biosynthesis is initiated by the enzyme *O*-GalNAc transferase, which transfers the GalNAc residue of UDP-GalNAc to serine or threonine residues in a protein with the α-configuration (68). *O*-glycan processing does not require dolichol derivatives or specific glycosidases, and the mRNA levels of glycosyltransferases are critical factors for their assembly (69). Additionally, glycosyltransferases may form complexes with other proteins, influencing their activities, or metal ion concentrations in the Golgi apparatus may regulate them. The presence of an unsubstituted GalNAc on *O*-glycoproteins forms the Tn antigen in tumor metastasis (70), and GalNAC can be directly substituted with sialic acid to form the sialyl-Tn (STn) antigen. These glycans are truncated and not used in subsequent elongation reactions (68, 70–72).

1.5 Glycan receptors and ligand-receptor interactions

Glycan receptors are proteins with carbohydrate recognition domains (CRDs) called lectins. Lectins bind to clustered CRDs with high affinity *via* (a) binding to multiple epitopes on a single oligosaccharide or polysaccharide, (b) multiple glycans attached to a single protein scaffold, and (c) binding to adjacent glycoproteins or glycolipids in the cell membrane. Plants produce the well-known lectins, followed by those isolated from animals and pathogenic microorganisms (73). The various types of CRDs are classified into four major lectin groups: (a) Siglecs (short for sialic acid binding immunoglobulin-type lectins) or I-type lectins, in which the CRDs are formed by an immunoglobulin domain fold (sialic acid is the major glycocalyx component related to immune system regulation); (b) galectins (predominantly binding to *β*-galactosidase), which contain CRDs formed from a beta-like fold of the protein; (c) C-type lectins, in which the sugars bind directly to a calcium ion attached to the CRD; and (d) lectins containing R-type CRDs, whose structure is related to the plant toxin ricin (reviewed in 74). The most important biological functions of ligand–receptor interactions between glycan ligands and lectin-like receptors include cell adhesion, intracellular trafficking, glycoprotein elimination and turnover, cell signaling, and pathogen recognition (48, 65, 74).

1.6 Trophoblast differentiation in human placental development, hypoxia, and glycan expression

The human placenta is an autonomous and transient anatomical structure that allows the mother and fetus to exchange nutritional, gas, and waste products. The trophoblast layer mediates fetal growth and maternal pregnancy adaptation generating a new vascular bed in the placental interface. These trophoblast cells are the first to separate from the developing blastocyst, giving rise to cytotrophoblast stem cells (75, 76). Placental villous tissue develops from primary to secondary and tertiary villous tissue with the progressive development of villous tree circulation complexity. Primary villi containing cytotrophoblast and syncytiotrophoblast cells predominate during the first four weeks of gestation. Secondary villi develop in the fifth week of gestation, with the extraembryonic mesoderm forming villi and covering the surface of the chorionic sac to provide a framework for intra-villi blood circulation. In the third stage of chorionic villi development, which occurs during the sixth week of gestation, mesenchyme differentiates into blood vessels and cells, resulting in the arteriocapillary framework that fuses with placental vessels into the connecting stalk (reviewed in 77). Besides, they develop with greater complexity, resulting in the formation of (a) stem villi or anchoring villi, from which cytotrophoblast cells migrate into the decidua and become extravillous cytotrophoblast (Figure 2A); (b) branched villi, which grow from the stem villi and represent the most critical portion for exchange with maternal blood from the placental bed through the intervillous spaces (Figure 2B); (c) terminal villi, which consist of protrusions caused by trophoblast proliferation due to the coiling of the fetal capillaries within the mature intermediate villi beginning in the third trimester of gestation; and (d) chorionic plate, which is the region at the base of the villi through which the placental arteries and vein pass (Figure 2A; 78–80). The villous cytotrophoblast stem cell population supports the differentiation of trophoblast into two major cell lineages, syncytiotrophoblast and the invasive trophoblast (named extravillous trophoblast [EVT]; 76, 81–83). The most invasive trophoblast wave occurs when EVT cells infiltrate the endothelium of maternal spiral arteries to come into direct contact with systemic circulation, forming placental villi and a maternal–fetal interface (78). The cell layer responsible for maternal–fetal nutrient and gas exchange is the well-differentiated syncytiotrophoblast cells, which cover the anchoring, branched, and terminal villi (84–86).

One of the most intriguing aspects of placental development during the first trimester is that the partial occlusion of the maternal spiral artery lumen by the extravillous invading endothelial trophoblast (see 87) results in a temporary condition of placental hypoxia, with approximately 20-mm Hg O2 concentration during the first trimester compared with 60 and 40-mm Hg during the second and third trimesters, respectively (Figure 2C) (88). During the first trimester of gestation, hypoxia at the maternal–fetal interface shapes placental development, which involves cellular and molecular adaptations to compensate for the low oxygen

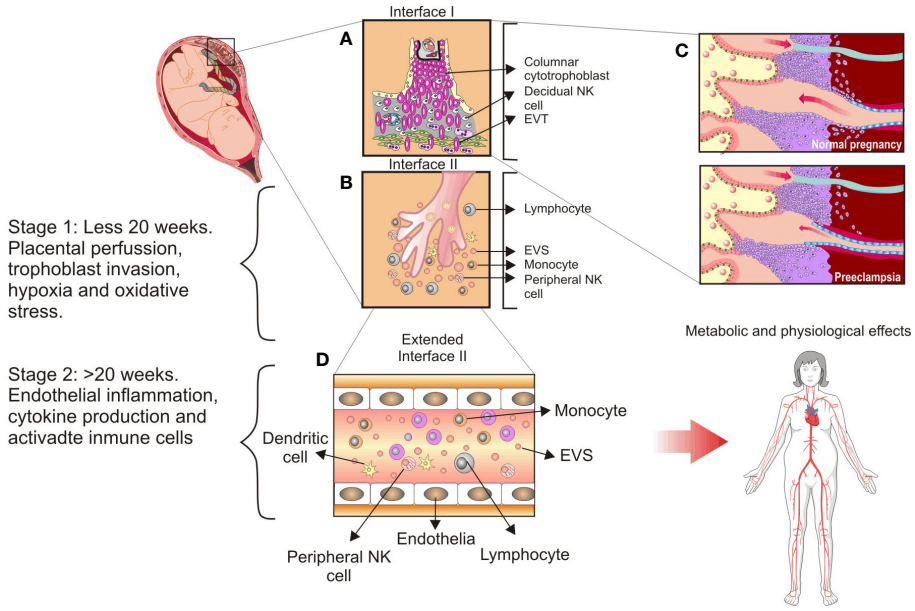


FIGURE 2
Main cellular components found at the maternal–fetal interface and the proposed stages of preeclampsia. **(A)**, Interface I: Villous tree represents a tertiary villous and its predominant cellular components at interface: Columnar cytotrophoblast, anchoring trophoblast, and extravillous trophoblast subsets. **(B)**, Interface II: Floating villi are in contact with maternal blood flow and release syncytiotrophoblast extracellular vesicles into circulation. Peripheral Natural Killer (NK) cells are highlighted as a significant maternal innate immune system component. **(C)**, Spiral arteries remodeling in the placental bed occurs extensively in a normal pregnancy but not in preeclampsia. **(D)**, Extended interface II: Syncytiotrophoblast extracellular vesicles are delivered into maternal circulation and promote the systemic inflammatory response observed during normal pregnancy. This inflammatory response is exacerbated in the case of women with preeclampsia, and it is linked to abnormal placental invasion, low placental perfusion, and increased oxidative stress accompanied by chronic hypoxia. CC, columnar cytotrophoblast; DC, dendritic cells; EVs, syncytiotrophoblast extracellular vesicles; EVT, extravillous trophoblast. This figure is adapted from Sargent et al. (232).

tension. As a result, trophoblast cells are a highly dynamic cellular type responsible for proper placental development. However, these processes are disrupted during pathological gestation conditions, resulting in a loss of placental architecture and abnormalities in fetal growth and development (Figure 2C) (89).

Extravillous trophoblast cells exhibit an invasive phenotype that shares molecular mechanisms with tumor cells, such as binding to the extracellular matrix, extracellular matrix degradation by metalloproteases, and migration through the extracellular matrix mediated by *N*-linked complex-type glycans (90–92). Truncated forms of *O*-glycans, such as core 1 (the Thomsen–Friedenreich [T or TF] antigen) and core 1 with a sialic acid substitution at the α2-3 bond to Gal and at the α2-3 bond to GalNAc to form the sialyl-T antigens, are associated with metastasis in some tumors (93, 94). Furthermore, the environment of tumor cells and EVTs are hypoxic, which confers invasive characteristics. About 60% of solid tumors have an oxygen partial pressure of less than 10 mm Hg compared with 50- to 60-mm Hg observed in adjacent non-tumor tissues (95). These values are comparable with the hypoxic state of the maternal–fetal interface during the first trimester of gestation (96–99). Hung and Burton (100) and Robins et al. (99) identified fluctuations in placental oxygen tension as a determinant of trophoblast invasion and differentiation associated with maternal spiral artery endothelial remodeling and placental angiogenesis.

There is low intrauterine oxygen tension at early implantation, and these oxygen levels are maintained during the first trimester of pregnancy. However, when the placental vascular bed is established, the degree of differentiation of trophoblasts to EVTs and interstitial and endovascular EVT subsets between 8 and 24 weeks of gestation promote increased oxygen tension (97, 99, 101, 102). Besides, the microenvironment into which the EVT invades the decidual stroma influences the release of soluble factors (e.g., immunomodulatory, pro-inflammatory, and anti-inflammatory cytokines, growth, and angiogenic factors), and oxygen concentration influences changes in the invasion process. As previously mentioned, physiologically hypoxic conditions (2%–3% compared with the usual 20% oxygen) in the first trimester promote differentiation toward an invasive pathway and establish a new placental vascular bed (96, 103).

Kang et al. (21) proposed that a failure of trophoblast invasion causes preeclampsia, and Goldman, Wohl, and Yagel (24) proposed that preeclampsia is caused by complex pathological events related to shallow invasion of endovascular and interstitial trophoblast, which reduces the transformation of spiral arteries into low-capacitance vessels (Figure 2C). Despite all evidence, it is inconclusive that the diseases have a distinct placental etiology. Thus, Staff (26) revised the concepts of the two-stage placental model of preeclampsia, which proposed a stage 1 caused by placental dysfunction and a stage 2 related to maternal clinical syndrome (25). In stage 1, maternal factors include a lack of tolerance to allogeneic trophoblasts, impaired placentation, altered spiral artery remodeling, and an oxidative stress state of the placenta. In stage 2, the impaired placenta and trophoblast stress send stress signals to the maternal endothelium, resulting in widespread vascular inflammation and the clinical signs of early-

onset and late-onset preeclampsia (26). These concepts have recently been validated by evidence of atherosclerosis and spiral artery remodeling failure as determinants of preeclampsia and other pathological gestation conditions. Furthermore, Staff et al. (104) reaffirmed their proposal for a multistage placental model of preeclampsia.

1.7 HIF and hypoxia-related signaling

Low oxygen tension at the maternal–fetal interface promotes the accumulation of hypoxia-inducible factor, HIF-1, a regulator of oxygen homeostasis (105). HIF-1 is a heterodimeric protein composed of a constitutively expressed β subunit and an α subunit regulated by the partial oxygen pressure (pO2; 106). Low oxygen concentrations promote cell invasion and progressions by activating more than 60 putative genes after HIF-1 receptor activation (HIF-R) (107–109). Human cytotrophoblast cells express HIF-1α (20, 110), which regulates the expression of target genes in cells subjected to hypoxia, including transferrin receptor (TfR1), vascular endothelial growth factor (VEGF), erythropoietin, endothelin-1, leptin, and glucose transporter 1 (106). HIF-1α regulates the iron and 2-oxoglutarate-dependent dioxygenase family enzymes known as prolyl hydroxylases (PHD1, PHD2, and PHD3) and asparaginyl hydroxylases (95). The PHD2 enzyme is responsible for hydroxylating one of the two proline residues present in HIF-1α (pro402 and pro564), promoting its interaction with the von Hippel-Lindau protein (pVHL) and subsequent polyubiquitination and degradation in the proteasome (103). When a cell is deprived of its oxygen supply, hydroxylation, and subsequent degradation of HIF-1α are significantly reduced, resulting in accumulation (111). HIF-1α accumulates in the nucleus, where it forms a complex with HIF-1β (HIF-1α/HIF-1β heterodimer) that is selectively expressed in the placenta (112, 113). The HIF-1α/HIF-1β heterodimer binds to hypoxia-responsive elements, acting as transcription factors for genes involved in cellular stress response (114). Thus, hypoxia stimulates tumor cell and trophoblast migration and invasion, and the invasive phenotype is activated *via* multiple mechanisms, including direct and indirect regulation of the epithelial to mesenchymal transition and upregulation of proteolytic enzymes, primarily matrix metalloproteinases (115, 116).

During the first trimester of gestation, hypoxic conditions stimulate the production of soluble factors associated with placental angiogenesis and immune tolerance to trophoblast invasion at the maternal–fetal interface (117). However, hypoxia in the second or third trimester may promote an increase in placental apoptosis and a significant decrease in trophoblast invasion, exacerbating the pro-inflammatory state at the maternal–fetal interfaces (99, 101, 118). The significant reduction in maternal spiral artery remodeling during the trophoblastic invasion and the consequent decrease in placental perfusion could correlate with overexpression of HIF-1α, VEGF, soluble FMS-like tyrosine kinase (sFlt1), and soluble VEGF receptor (sVEGFR-1), all elicited by HIF (119, 120). Failure to detect low oxygen tension has been proposed as a cause of early-onset preeclampsia (121), supporting the concept of abnormal placental development as one of the triggering processes (122).

1.8 Glycans as mediators between the placenta and peripheral circulation

The glycosylation profile of trophoblast and glycans do change during endometrium trophoblast invasion. Because of their molecular versatility, they form new affinities and cell–to-cell crossovers and develop complex intercellular structures supporting trophoblast differentiation (123). Changes in glycan profiles could be new biomarkers for diseases such as preeclampsia (124, 125). These changes involve the underexpression and overexpression of naturally occurring glycans in response to the environment- or stress-induced signaling (126). Thus, glycosylation of glycoproteins may contain previously unknown patterns that control stem cell differentiation, phenotype changes, invasion, and mobilization (60, 127), vasculogenesis (128, 129), and extravillous trophoblast invasion (130). The maternal immune system regulates trophoblast differentiation and invasion at multiple levels: locally in the maternal–fetal interface I by uterine NK-to-dendritic cell interaction and systemically in the maternal–fetal interface II by trophoblast-derived extracellular vesicles (EVs) (Figure 2D) or in the vascular compartment by VEGF production (Figures 2A–D; 131, 132). In this regard, Clark et al. (133) proposed that the human embryo–fetus' primary defense mechanism for protecting itself from maternal immune system recognition and rejection is the induction of specific immunosuppressive oligosaccharides in glycoconjugates of placental tissues (133). The syncytiotrophoblast in the full-term placenta expresses up to 95% *N*-linked oligosaccharides with complex sugars, with the remaining 5% being high mannose type (134). These glycan structures were immunosuppressive because the oligosaccharide membrane fraction isolated from syncytiotrophoblast decreased 3H thymidine uptake in a mixed leucocyte reaction (135).

Glycosylation changes can manifest in various ways, including impairing naturally occurring glycans through the influence of environmental or stress-induced signaling pathways. These changes can lead to either under-expression or overexpression of glycans. Additionally, the expression of glycans that are typically restricted to embryonic tissues can occur during the development of a tumor phenotype. (94). Changes in glycosyltransferase levels can lead to modifications in the core structure of N-linked and O-linked glycans, e. g. the oligosaccharide size and branching of N-linked glycans. The increased activity of N-acetylglucosaminyltransferase V (GlcNAc-TV, or MGAT5; the enzyme that leads to β1,6GlcNAc branching) promotes β1-6- linked branching and the invasive phenotype in transfected non-metastatic clones of murine mammary carcinoma (136). The placentation process resembles cancer metastasis in the invasion waves during the first trimester. Therefore, the expression of β1-6- linked branching increases in the trophoblast layer when it is detected by phytohemagglutinin lectin blotting (137). The increased branching creates additional sites for terminal sialic acid residues, which, in conjunction with the corresponding upregulation of sialyltransferases, ultimately leads to an increase in global sialylation. *N*-glycan structures obtained from syncytiotrophoblast proteins are

highly sialylated during pregnancy, as was confirmed by mass spectrometry (43), which could explain syncytiotrophoblast resistance to NK cell—and other cytolytic leukocytes—mediated cytolysis (138). These patterns of glycosylation were confirmed later by Chen et al. (43), who proposed that biantennary bisecting type *N*-glycans(a particular type of glycan modification consisting of four-linked β1 GlcNAc structure attached to the core β-mannose residue expressed in syncytiotrophoblast), could protect class I MHC non-expressing trophoblast cells from NK cell-mediated cytotoxicity. However, further experimental evidence is needed to confirm this. A knockdown of the MGAT5 enzyme increases the migration capacities of first-trimester human placental villi, which are correlated with the upregulation of metalloproteases (MMP-9) and the downregulation of the invasion inhibitor TIMP1/2 (139). Furthermore, the ischemia-reperfusion insult of the placenta may promote the shallow trophoblastic invasion observed in preeclamptic pregnancies, whereas specific changes in *N*-glycans could be involved in migration and differentiation processes. Thus, N-acetylglucosaminyltransferase III (GnT-III) catalyzes the bisecting GlcNAcβ1 modification, which can suppress the processing and branching of the glycan catalyzed by GnT-V (140).

Reduction of biantennary de-sialylated non-fucosylated *N*-glycans was reported in first-trimester decidual tissue as a normal finding (141), but no reports on the expression by placental villi tissue were found. Furthermore, Whyte and Loke (142) reported increased sialylation of trophoblast glycoproteins compared with fetal and tumor cells. According to Jeschke et al. (143), one possible mechanism of immunosuppression in human gestation is the expression of TF antigen at sites of trophoblast invasion.

Placental proteins have different glycosylation patterns depending on gestational age or extracellular cell microenvironmental changes. For instance, Dell et al. (56) reported that glycodelin-A —a potent immunosuppressive protein in the human placenta— expresses biantennary *N*-glycans with the bisecting GlcNAc sequence and sialylated complex *N*-glycans (143–145). The syncytiotrophoblast layer of chorionic villi produces human chorionic gonadotrophin (hCG) throughout human pregnancy (146). hCG, an *N*-glycan glycoprotein, is also secreted by EVT during trophoblast invasion in a hyperglycosylated form, exerting potent immunomodulatory effects (147, reviewed in 146).

Changes in glycosylation profiles of placental glycoproteins associated with preeclampsia have been proposed to be related to oxidative stress-promoting hypoxia in the placental bed and the consequent accumulation of the HIF heterodimer, as mentioned above. For example, Lewis*Y*, a well-recognized glycan associated with angiogenesis, was found in cytotrophoblast cells and villous trophoblastic cells in cases of severe preeclampsia (148) and unexplained miscarriage (149). These results could be explained by a compensatory mechanism triggered by an increase in angiogenic factors, common in pregnancy-related hypertensive disorders, such as preeclampsia (28, 150). Besides, changes in glycan expression at the maternal–fetal interface caused by chronic hypoxia could be associated with increased lectin expression in preeclampsia. This is the case with galectins (Gal), soluble non-glycosylated proteins with a unique sequence motif in their CRDs that show an increased affinity for *N*-acetylated disaccharides such as *N*-acetyl-galactosamine (LacNAc; Galβ1,4GlcNAc) and similar structures. In murine models, Gal-1 exhibits proangiogenic functions during the early stages of pregnancy, promoting decidual vascular expansion *via* VEGF receptor 2 (VEGR2) signaling. A specific blockage of Gal-1 promotes defective trophoblast invasion and impaired maternal spiral artery remodeling, resulting in a PE-like syndrome (151). Gal-1 expression was significantly upregulated in the decidua of preeclamptic placentas and the villous trophoblast of placentas in women with hemolysis, elevated liver enzymes, and low platelet (HELLP), which is consistent with previous findings (144).

1.9 Changes in glycosylation are mediated by hypoxia and inflammation

As mentioned above, hypoxia affects metabolism cells and glycosyltransferase expression in placenta and tumors (139, 140, 152) such as colon cancer cell lines (153, 154) and the immortalized prostate cell line RWPE1 (155). It also promotes the transcription of genes encoding fucosyltransferases and sialyltransferases. Although the role of HIF-1α in placental glycosylation remains unknown, indirect evidence in tumor tissues indicates that HIF-1α upregulation increased fucosyltransferases (FUT)-1-2 mRNA levels and overexpression of fucosylated proteins on the surface of pancreatic adenocarcinoma cells (156). Hypoxia appears to alter endothelial cell glycosylation, inducing the expression of *N*-glycoproteins containing glycans with less α2,6-linked sialic acid, elongated poly-LacNAc (Gal-GlcNAc) residues, and β1,6-linked *N*-glycan structures branching (157, 158). Furthermore, pathophysiological changes of the endothelial surface layer occur following a variety of insults, among these, hypoxia associated with ischemia/reperfusion injury (159). The oxidative and inflammatory stress accompanying hypoxic insult promotes glycocalyx damage *via* reactive oxygen species (Ros), increasing vascular permeability and perivascular inflammation. These ROs-mediated changes to the glycocalyx are dependent on Ca2+ signaling and possibly matrix metalloproteinase activation (160). However, another signaling pathway could be implied in the hypoxic insult associated with glycosyltransferase expression.

Additionally, HIF-1 activates tumor and placental infla mmatory signaling, particularly nuclear factor-kappa B (NF-κB) transcription. Inhibitory IκB dissociates from NF-κB during inflammation, allowing for nuclear translocation and multiple gene transcriptions, mainly IL-6, cycloxygenase-2, and matrix metalloproteinase 9 (161, 162). These findings imply that HIF-1 and NF-κB interaction activates the transcription factors of these genes. In preeclampsia, NFκB expression may stimulate pro-inflammatory and anti-angiogenic protein production, promoting oxidative stress, inflammation, and vascular dysfunction. On the contrary, in normal pregnancies, NFκB promotes placental cellular migration, invasion, and angiogenic protein production (163). In preeclamptic women, local placental inflammation and oxidative stress are associated with placental hyperactivation of NfκB and its release into the maternal circulation, with levels nearly 10-fold higher than in normal pregnancies (163, 164).

Abnormal placental blood perfusion increases hypoxia-induced placental-derived circulating agents and sFlt1 production (120). HIF-1α, the primary regulator of oxygen hemostasis in the placenta, induces TGF-β production (165, 166). The β3 isoform of TGF-β suppresses trophoblast trans-differentiation, reducing its differentiation toward EVT and invasive capacity (165). Therefore, reduced growth of maternal–fetal interfaces 1 and 2 could restrict blood perfusion and promote EV release into the general circulation, contributing to the exacerbated pro-inflammatory status observed after 20 weeks of gestation (167). Placental hypoxia occurs in diseases such as gestational iron deficiency anemia, associated with increased accumulation of HIF-1α, similar to preeclampsia. Additionally, alterations in iron status have been associated with hypertensive disorders of pregnancy (168–171). Glycosylation profiles induced by hypoxia and placental inflammation have been proposed to alter the exchange of macronutrients and micronutrients across the syncytiotrophoblast (172, 173). Iron is transferred from the mother to the fetus *via* the placenta after being taken up by TfR1 at the apical membrane of the syncytiotrophoblast (174–177). TfR1 contains three *N*-glycan and O-glycan chains in its extracellular domain (178–180). TfR1 expression may be altered in hypoxic conditions, such as in women with diabetes, due to post-translational modifications, including glycosylation (181). Thus, women with preeclampsia whose placenta is exposed to prolonged hypoxia may have elevated levels of TfR1, one of the HIF-1 target genes. In preeclamptic women, the galactose-*N*-acetylglucosamine and terminal mannose patterns detected by DSA and GNA lectins, respectively, were overexpressed in TfR1. In addition, TfR1 expressed α2-3 sialic acid rather than α2-6 sialic acid, and preeclamptic placentas overexpressed α2-3 sialic acid (182). Depleting α2-6 sialic acid may promote increased binding of gal-3 to terminal galactose in TfR1 and formation of the transferrin–iron–TfR1 complex during iron uptake (183, 184). Furthermore, overexpression of α2-3 sialic acid in TfR1 of preeclamptic placentas may be associated with resistance to cell membrane scission, which is consistent with the findings of Rutledce and Enns (185), where removal of α2-3 sialic acid released TfR1 protein into the culture medium. We wonder if differences in TfR1 glycosylation patterns in preeclamptic women have implications for TfR1 exportation to the cell membrane or ligand affinity modifications, events that could affect iron uptake by the placenta resulting in impaired fetal nutritional status and, in some cases, intrauterine growth restriction.

1.10 Role of glycan recognition by cells of innate immunity in the pathogenesis of the exacerbated systemic inflammatory response in preeclampsia

Because preeclampsia is a preclinical condition characterized by a prolonged hypoxic state, it may be associated with an increased release of EVs and soluble factors capable of initiating a systemic inflammatory response and impairing endothelial function (131). Murrieta-Coxca et al. (186) recently proposed that EVs could play a critical regulator of feto-maternal tolerance by transferring allogeneic material from fetal to maternal immune cells to remodel their function (in the context of fetal allograft tolerance) and fetal–maternal microchimerism. Darmochwal-Kolarz et al. (187) reported that in preeclamptic patients, there was an imbalance of pro-inflammatory cytokines (IL-2 and IFN-γ) compared with the anti-inflammatory profile (IL-4 and IL-10) characteristic of mitogen-activated CD4+/CD8+ T lymphocytes and NK cells. However, studies on cytokine production by NK cells in preeclampsia used chemical stimulation with Phorbol Myristate Acetate (PMA) and Ca2+ ionophores, which could alter the cytokine profile observed in these assays (188).

The pro-inflammatory profile of NK cells could be induced by lectin-mediated glycan recognition at maternal–fetal interface 2, where peripheral immune cells come into contact with the syncytiotrophoblast layer in circulating microvilli. Under hypoxic conditions, for example, the glycan profile of invasive tumor cells and tumors may change, revealing truncated glycans such as Tn antigen or polysialylated *N*-glycan complexes (93, 189, 190). Recognition of these glycans by NK cells is mediated mainly by lectin-like and immunoglobulin-like receptors (called Siglecs; 191). On the other hand, the functional profile of peripheral NK cells is known to depend on their CD56 phenotype. Therefore, the CD56bright NK cell subset can promote the PMA and the Ca2+ ionophore-induced IFN-γ and TNF-α intracellular production (192). In non-pregnant women, the major NK cell subset is IFN-γ or TNF-α producing NK cells (NK1 profile), and IL-4, IL-5, and IL-13 producing NK cells (NK2 profile) or IL-10/TGF-β non-producing PMA-stimulated CD56bright and CD56dim NK cells (193–195). In pregnant women, the cytokine profile observed in NK cells changes to IL-10-producing NK cells; IFN-γ, TNF-α, IL-4, IL-5, or TGF β-producing CD56dim and CD56bright subsets corresponding to NK regulatory and NK3 profiles, respectively, with no difference between these subsets (194). This way, we evaluated the activation of peripheral NK cells before the more advanced stages of preeclampsia in women with early-onset severe preeclampsia without HELLP syndrome. Monocytes, T lymphocytes, NKT cells, and NK cell proportions were not significantly different compared with healthy pregnant women. Moreover, CD56dim and CD56bright NK cell subsets from the early-onset of severely preeclamptic women significantly produced more intracellular cytokines than NK cells from healthy pregnant women, with no cytokine imbalance. However, peripheral NK cells demonstrated increased cytotoxic activity *in vitro* (28), consistent with reports of increased NK cell cytotoxic activity in NK cells from mild preeclampsia cases (196). Besides, an increased percentage of NK cells bearing the CD96-NKGA/C receptors and CD56bright–NKG2C and NKG2A positive in NKdim and NKbright subsets (28). CD96-NKG2 heterodimers are lectin-like receptors that recognize protein-bound terminal glycans. They are members of the C-type lectin-like receptor superfamily, which includes six NKG2 molecular species (A, B, C, D, E, and H).

The heterodimer CD94/NKG2A is an inhibitory receptor with intracellular motifs that negatively regulates activation signaling for cytotoxic activity and anti-inflammatory cytokine production (197). Both CD94/NKG2 heterodimers can bind to non-classical HLA

molecule HLA-E; however, their affinity varies: CD94/NKG2A binds to HLA-E with low affinity and very rapid association and dissociation rates, whereas CD94/NKG2C binds to HLA-E with nearly 10-fold lower affinity than CD94/NKG2A (198). This affinity is determined by the peptide sequence bound to HLA-E. However, evidence suggests a direct recognition of NKG2A/C receptors mediated by α2-3 sialic acid, a terminal residue of sialic acid monosaccharide-containing glycoproteins (199). NKG2A and NKG2C receptor expression on peripheral blood NK cells was reduced in women with preeclampsia (200). EA.hy296 endothelial cell line expresses HLA-E, and serum from severely preeclamptic women increased its expression (201). In severe preeclampsia, NK cell adhesion to the endothelium is significantly higher than in normal pregnancy, implying an interaction with an overexpressed HLA-E in the endothelial cell membrane (202). Endothelial HLA-E recognition by peripheral NK cells most likely modifies NK cell activity toward a low cytotoxic profile and promotes the production of pro-inflammatory cytokines such as TNF-α and IFN-γ (203, 204). A possible role of terminal α2-3 sialic acid in the HLA-E α1-domain could be relevant to explain this activation profile in peripheral NK cells mediated by NKG2 receptor activation in severe stages of preeclampsia. We wonder if changes in the endothelium and innate response cell (mainly NK cells) activation and cytokine influence the systemic inflammatory response observed during pregnancy. Although the putative role of cytokines produced by peripheral NK cells in the systemic inflammatory response of hypertensive disorders in pregnancy remains unknown, we propose that peripheral NK cells modulate their cytokine profile in preeclampsia *via* HLA-E signaling or lectin-like receptors such as members of NKG2 family, as previously reported (29).

There is little knowledge about glycan recognition in the context of NK cell activation. Previous studies identified glycophorin A, glycodelin-A, and sialic acid-related structures (sialyl Lewis X, among others) as negative modulators of NK cell-mediated cytolysis (205–207). Indirect evidence suggests that glycan recognition may activate NK cells during systemic inflammatory response in preeclampsia, including differential expression of lectin-like receptors or sialic acid-recognition receptors from the Siglec family (208, 209). Ibeto et al. (210) evaluated the glycosylation profile of hCG isolated in urine from women at 7 and 20 weeks of gestation (first and second trimesters, respectively) and urine samples from women suffering from gestational trophoblastic disease. Ibeto et al. (210) found mono-antennary, bi-antennary, tri-antennary, and tetra-antennary *N*-glycans in serum hCG from early and late gestation and significantly lower hCG containing bisected *N*-glycans in patients with the gestational trophoblastic disease. Ibeto et al. (210) suggested that hCG-related bisected type *N*-glycans may directly suppress NK cell cytotoxicity, consistent with the report of Chen et al. (43).

Campuzano et al. (211) investigated the effects of placental glycans on NK cell activity using a peripheral NK cell with a full-term human villous tissue co-culture system to assess whether changes in glycosylation profile could account for differences in cytokine production and cytotoxicity. Peripheral mononuclear leukocytes-containing NK cells co-cultured with fresh villous tissue or BeW0 cells showed that CD56Bright NK cells did significantly produce higher concentrations of IFN-γ and TGF-β than CD56Dim NK cells, consistent with a previous report in which circulating CD56dim and CD56bright NK cells exhibited predominantly cytotoxic and cytokine-producing phenotypes, respectively (211). Besides, blocking glycosylation in a BeWo cell syncytialization model using *N*-glycosylation inhibitors (e.g., castanomycin and tunicamycin) revealed differences in intracellular IFN-γ production by CD56Bright NK cells in co-culture (211). It demonstrated that co-culture of primary placental villous tissue with the choriocarcinoma cell line BeWo modulates NK cell function through specific glycan expression. Tunicamycin specifically inhibits N-linked glycosylation by preventing core oligosaccharide addition to the nascent protein, and thereby, it may interfere with specific ligand-receptor interaction by a decrease of the trophoblast protein synthesis (Surani, 1979). Additionally, castanospermine is a potent inhibitor of alpha- and beta-glucosidases and alters the distribution of insulin-like growth factor (IGF) receptors in villous tissue explants, which reduces the effect of IGF (212).

Based on this, it has been proposed that end-glycans of glycoproteins participate in the syncytiotrophoblast–NK cell interaction during pregnancy inflammatory response regulation (Figures 3A, B). Thus, increased expression of sialic acid binding immunoglobulin-like lectin-6, a unique sialic acid receptor in the placenta, was found during severe preeclampsia (213), and its concentrations were related to the severity of the pathology (214, 215). A case report of a woman presenting gestational diabetes mellitus, overweight, and severe PE, lower staining of Gal-GlcNAc (detected by the DSA lectin), mannose (detected by the GNA lectin), and Sia α2-3 (detected by the MAA lectin) was found in TfR. Accordingly, we propose that increased α2-3 sialyltransferase activity in this woman could explain the increased sialylation in TfR from placental villi (182).

The improved protein stability conferred by sialic acid may be advantageous because there is an increase in inflammatory status ROs production in preeclampsia (reviewed in 216–218). Protein stability is influenced by ROs (219). In placental malaria, increased chorionic villi α2,6 sialylation may influence intervillous placental parasite density as a compensatory response to *Plasmodium falciparum* infection (220). Preeclampsia and placental malaria are diseases with a placental and systemic inflammatory response in which NK cell activity increases progressively throughout gestation and may affect the communication between syncytiotrophoblast and immune cells (123, 221–223).

1.11 An emerging role of EVs in the physiology of the maternal-fetal interface and the exacerbated systemic inflammatory responses?

During the differentiation of cytotrophoblast and fusion to form the syncytiotrophoblast, glycosylation patterns change in a carbohydrate-driven pattern to provide the immunosuppressive microenvironment required for successful placentation, which appears impaired in pathological conditions of gestation. The released EVs from syncytiotrophoblast also carry various

10.3389/fendo.2023.1087845

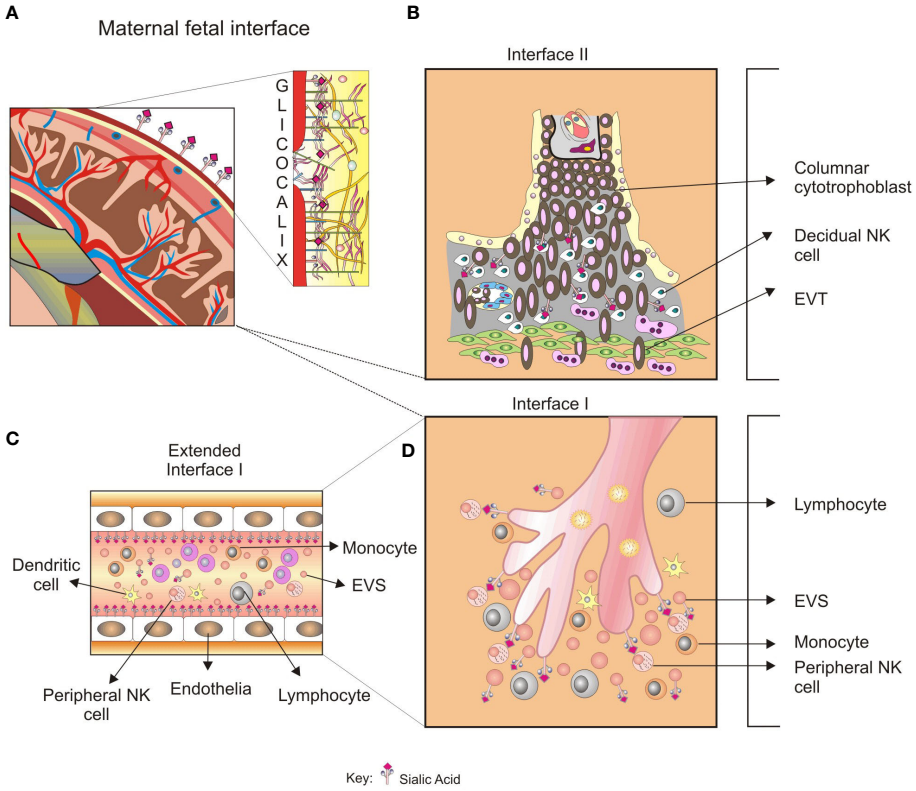


FIGURE 3
A glycobiological view of the systemic inflammatory response in preeclampsia. **(A)**, Sialylated glycoproteins and glycoproteins with LacNAc glycotopes, among others glycoconjugates in the trophoblast glycocalyx, are expressed in maternal–fetal interface II. **(B)**, The recognition by LacNAc by Gal-1 promotes angiogenesis in the placental bed, and impaired balance in the Gal-1 function results in a PE-like syndrome. Furthermore, defective trophoblast invasion has been associated with specific blocking of Gal-1. **(C)**, Glycoconjugates could be recognized by peripheral NK cells in the maternal–fetal interface I, modulating the NK cell activity. The released syncytiotrophoblast EVs found in preeclampsia could transport glycoproteins with immunomodulatory activity and increase the systemic inflammatory response. **(D)**, EVs released from maternal–fetal interface II spread into the systemic circulation and promote endothelial activation. The type and quantity of VES found in preeclampsia could initiate endothelial damage and exacerbate inflammation. The role of glycan recognition in syncytiotrophoblast VES-mediated endothelial damage is not elucidated yet.

conjugated molecules in the maternofetal interface II context. Their size ranges from 30 to 150 nm, increasing in patients with an exacerbated systemic inflammatory response (224, 225). Studies have shown that levels of EVs increase in patients with systemic inflammatory response (224, 225), and this increase is even more pronounced in preeclampsia, where EVs have been found to increase three-fold compared to normal gestation (226, 227). To better understand the composition of EVs in placenta from normal and preeclamptic women, researchers have used perfusion systems to identify their main components (227). These EVs appear to play a role in the transfer of intercellular biomolecules such as flt1, the VEGF membrane receptor, as suggested by recent studies (228, 229). Thus, the exacerbated systemic inflammatory response in EP is associated with the number and variety of EVs found in healthy pregnancies (226, 227). The preeclampsia-associated chronic placental hypoxia and inflammatory status promote EVs shedding from syncytiotrophoblast to the maternal–fetal interface 2 and increase the systemic inflammatory response (230–233). Research suggests that glycans play a crucial role in EVs biogenesis, cellular recognition, and cell receptor interaction. In particular, mannosylated and sialylated N-glycans, with their antennae structures, are believed to mediate important biological functions such as inflammatory cascade activation and other paracrine events (234, 235) Thus, some glycan biomarkers, such as α-2-6 sialic acid and Gal or terminal GlcNAc in complex N-glycans, have been identified in syncytiotrophoblast-derived EVs (236). However, despite advancements in understanding the roles of syncytiotrophoblast-derived EVs glycans, their functional capabilities and interactions with target endothelial cells in both the glomerular filtration barrier and cerebral microcirculation remain largely unknown. Research conducted by our group has shown that serum from women with preeclampsia can affect the function of the glomerular filtration barrier in an *in vitro* model (237–239). This effect appears to be caused by a reduction in the anionic charge of the glomerular endothelium, allowing selective filtration of blood components into the urine. This raises the question of whether the glycans present in EVs from the placenta of women with preeclampsia could modify the permeability of the glomerular endothelium and cerebral microvasculature to albumin, and if they could affect endothelial integrity (43, 145, 240).

These EVs could explain the connection between the maternal–fetal interface and target organs such as the blood–brain barrier and

the glomerular filtration barrier, where glycans are the most promising exchange molecules for research purposes. Further research is needed to fully decipher the complex mechanisms at play in these important physiological processes.

1.12 Perspectives on the role of glycans in gestation and preeclampsia: Connecting the network

Gérard Chaouat proposed nearly a decade ago that the specific immune system evolved to be adapted to vertebrate placentation (in the sense of subordination) as a critical feature of successful vertebrate reproduction (241). Decidual and circulating immune cells must undergo a series of molecular adaptations to avoid conceptus rejection and allow successful embryo and fetus development. The profile of glycan expression at the maternal–fetal interface, the phenotype and functional profile of innate immune cells present in the decidua, the presence of regulatory T cells (242, 243), and the production of soluble factors related to apoptosis, among others, may be responsible for such adaptation process (243–245).

The presence of immunomodulatory glycans in trophoblast is one fundamental mechanism supporting successful placental reproduction, along with the selective expression of "friendly" natural killer cells and low expression and activity of effector T cells capable of exerting cytotoxic activity. Most cellular and molecular mechanisms of the effector adaptive immune response are absent or regulated at the maternal–fetal interface. On the contrary, decidual NK cells are the primary immune cell population in up to 85% of decidua and are responsible for decidualization in early human pregnancy. Interestingly, one of the most abundant proteins produced by syncytiotrophoblast is β-hCG, a placental hormone sharing *N*-glycans coupled to asparagine residues that function as a potent immunomodulatory and angiogenic glycoprotein inducing decidual NK proliferation *via* mannose receptor activation (127, 246, 247). In healthy dynamics that support placental angiogenesis, decidualization, and establishing the maternal–fetal interface, uterine dendritic cells recruit decidual NK cells. Thus, the placenta of pregnant mice depleted of decidual NK cells shows a reduced expression of α2,3-sialylation and O-glycans, whereas the expression of branched *N*-glycans and Gal-1 increased. Ablation of decidual NK cells in the pre-implantation period could influence VEGF-mediated angiogenesis changes and depend on GAL-1 signaling. Experimental murine models of abnormal pregnancy show that changes in trophoblast glycosylation patterns precede poor pregnancy outcomes such as intrauterine growth restriction (248–250).

In conclusion, the fact that fetal and maternal cells exchange, at least in specific windows and compartments during the gestation

TABLE 1 Hypothetical and confirmed role of glycans in physiological and complicated pregnancy.

Organ	Source	Glycan	Condition	Function/pathogenesis	Reference
Placenta	Extravillous trophoblast	TF antigen	Normal pregnancy	Probably migration through the extracellular matrix for promoting invasion	(93, 94)
	Sera samples	hCG (N-glycan glycoprotein)	Normal pregnancy	Promotes trophoblast invasion by its immunomodulatory action	(146, 147)
	Syncytiotrophoblast	highly sialylated N-glycan structures	Normal pregnancy	Syncytiotrophoblast resistance to NK cell—and other cytolytic leukocytes—mediated cytolysis	(43, 135)
	Terminal Villi	Mannose, sialic acid, and β-galactose	Severe preeclampsia	Increased expression	(251)
	Stromal cells/Stroma	Glycodelin-A	Normal pregnancy	Biantennary N-glycans with the bisecting GlcNAc sequence and sialylated complex N-glycans	(143–145)
	Cytotrophoblast/ Villous trophoblast	Lewis*Y*	Preeclampsia Unexplained miscarriage	Angiogenesis-related glycan	(148, 149)
	Syncitialized BeWo cells	Reduced α(2-3) sialylation	Choriocarconoma BeW0 cells	Immunorregulation of peripheral NK cell cytokine production	(211)
	Chorionic Villi	Gal-1	HELLP syndrome	Defective trophoblast invasion	(144)
	Capillary Endothelium	Increased Mannose and β-galactose; decreased sialic acid	Severe preeclampsia	Placentation and angiogenesis	(251)
Decidua	Decidual stroma	Biantennary de-sialylated non-fucosylated N-glycans	Normal pregnancy	Reduced expression	(141)
	Decidual stroma	Gal-1	Upregulated in Preeclampsia	Defective trophoblast invasion	(144)
	Placental tissues (decidua and trophoblast)	Bisecting GlcNAc	Early-onset severe preeclampsia	Reduced expression	(172, 182)

period, adds to our understanding of the complex interplay between the maternal endocrine and immune systems as part of the maternal, placental, and fetal physiological environments and the maintenance of a balanced, functional immune response. Furthermore, evidence supports the theory of the involvement of the innate immune response in mediating critical processes required for early placental development and maintenance, such as decidual growth-supported placental development. In that context—and evolutionary highly conserved—glycans emerged as crucial innate immune cell regulators that support the maintenance of gestation. Because glycan expression profiles are essential modulators of adaptive and effector immune functions, critical advances in understanding successful human and mammalian gestation may provide a comprehensive understanding of normal and pathological pregnancy conditions (Figures 3C, D). We contributed to the discussion on the role of glycans in the pathophysiology of hypertensive disorders of gestation, as proposed by Gérard Chaouat in criticizing the pitfalls of the old immunotropic hypothesis. The main findings are summarized in the Table 1.

This manuscript was edited and proofread before being sent to Gerard Chaouat for final review and approval. However, we did have the misfortune of his death. Therefore, this is our tribute to "Gégé" (Gérard C. Chaouat, 1944–2021).

Author contributions

JB-S conceived and wrote the manuscript and designed the cited studies. AG-G performed cited studies and discussed their results. JM-E. participated in the critical review and reduction of the manuscript. JQ-C. participated in the critical review and reduction of the manuscript and study design. All authors contributed to the article and approved the submitted version.

Funding

Universidad de Antioquia, Vicerrectoría de Investigación, through the calls for support for consolidated research groups (Grupo Reproducción) and groups in consolidation 2020–2021 (Grupo OHVRI). This study was funded by Universidad Cooperativa de Colombia (INV2719-Dirección Nacional de Investigación), Sistema General de Regalías-Minciencias, Cod BPIN 2020000100488.

Acknowledgments

Authors thank the Office for Research and Development at the University of Antioquia (CODI and Vicerrectoría de Investigación, Estrategia de Consolidación de grupos 2020-2021), Corporación Universitaria Remington (CUR), and Universidad Cooperativa de Colombia (Dirección Nacional de Investigación) for funding research groups and projects supporting the cited papers. Special thanks to Minciencias, Colombia, for the financial support.

In Memoriam

In Memoriam: Gérard C. Chaouat (1944–2021).

Conflict of interest

The authors declare that the research was conducted in the absence of any commercial or financial relationships that could be construed as a potential conflict of interest.

Publisher's note

All claims expressed in this article are solely those of the authors and do not necessarily represent those of their affiliated organizations, or those of the publisher, the editors and the reviewers. Any product that may be evaluated in this article, or claim that may be made by its manufacturer, is not guaranteed or endorsed by the publisher.

References

1. Gilstrap L, Ramin S. ACOG practice bulletin. diagnosis and management of preeclampsia and eclampsia. *Obs. Gynecol* (2002) 99:159–67.

2. Kornacki J, Boroń D, Gutaj P, Mantaj U, Wirstlein P, Wender-Ozegowska E. Diagnosis of preeclampsia in women with diabetic kidney disease. *Hypertens Pregnancy* (2021), 1–8. doi: 10.1080/10641955.2021.1987454

3. Magee LA, Nicolaides KH, von Dadelszen P. Preeclampsia. *N Engl J Med* (2022) 386:1817–32. doi: 10.1056/NEJMRA2109523

4. Brosens I, Puttemans P, Benagiano G. Placental bed research: I. the placental bed: from spiral arteries remodeling to the great obstetrical syndromes. *Am J Obstet. Gynecol* (2019) 221:437–56. doi: 10.1016/j.ajog.2019.05.044

5. Harris LK, Benagiano M, D'Elios MM, Brosens I, Benagiano G. Placental bed research: II. functional and immunological investigations of the placental bed. *Am J Obstet Gynecol* (2019) 221:457–69. doi: 10.1016/j.ajog.2019.07.010

6. Romero Infante XC, Uriel M, Rincón Franco. S, Ibáñez Pinilla EA, Rojas NA. First trimester placental growth factor in maternal blood and placenta related disorders. *J Matern. Fetal. Neonatal Med* (2021) 1:8. doi: 10.1080/14767058.2021.1960966

7. Yücesoy G, Ozkan S, Bodur H, Tan T, Calişkan E, Vural B, et al. Maternal and perinatal outcome in pregnancies complicated with hypertensive disorder of pregnancy: a seven year experience of a tertiary care center. *Arch Gynecol. Obstet* (2005) 273:43–9. doi: 10.1007/s00404-005-0741-3

8. Giannubilo SR, Landi B, Ciavattini A. Preeclampsia: what could happen in a subsequent pregnancy? *Obstet. Gynecol. Surv* (2014) 69:747–62. doi: 10.1097/OGX.0000000000000126

9. Coban U, Takmaz T, Unyeli OD, Ozdemir S. Adverse outcomes of preeclampsia in previous and subsequent pregnancies and the risk of recurrence. *Sisli. Etfal. Hastan. Tip. Bul* (2021) 55:426–31. doi: 10.14744/SEMB.2020.56650

10. ACOG (American College of Obstetris and Gynecology). Gestational hypertension and preeclampsia: ACOG Practice Bulletin, number 222. *Obstet Gynecol* (2020) 135:1492–5. doi: 10.1097/AOG.0000000000003892

11. Roberts JM, et al. *Hypertension in pregnancy - ACOG* (2013). Available at: https://www.acog.org/Clinical-Guidance-and-Publications/Task-Force-and-Work-Group-Reports/Hypertension-in-Pregnancy.

12. Sibai B, Dekker G, Kupferminc M. Pre-eclampsia. *Lancet* (2005) 365:785–99. doi: 10.1016/S0140-6736(05)17987-2

13. Robillard P-Y, Chaouat G, Le Bouteiller P, Fournier T, Barau G, Roman H, et al. [Current debates on immunology of preeclampsia. report of the sixth international workshop of reunion island (Indian ocean, December 2008)]. *Gynécologie Obs. Fertil* (2009) 37:570–8. doi: 10.1016/j.gyobfe.2009.03.028

14. Moussa HN, Sibai BM. Management of hypertensive disorders in pregnancy. *Womens Health (Lond)* (2014) 10:385–404. doi: 10.2217/whe.14.32

15. Roberts DJ, Post MD. The placenta in preeclampsia and intrauterine growth restriction. *J Clin Pathol* (2008) 61:1254–60. doi: 10.1136/JCP.2008.055236

16. Huppertz B. Maternal–fetal interactions, predictive markers for preeclampsia, and programming. *J Reprod Immunol* (2015) 108:26–32. doi: 10.1016/J.JRI.2014.11.003

17. Levine RJ, Lam C, Qian C, Yu KF, Maynard SE, Sachs BP, et al. Soluble endoglin and other circulating antiangiogenic factors in preeclampsia. *N Engl J Med* (2006) 355:992–1005. doi: 10.1056/NEJMoa055352

18. Lash GE, Schiessl B, Kirkley M, Innes BA, Cooper A, Searle RF, et al. Expression of angiogenic growth factors by uterine natural killer cells during early pregnancy. *J Leukoc. Biol* (2006) 80:572–80. doi: 10.1189/jlb.0406250

19. Schiessl B. Inflammatory response in preeclampsia. *Mol Aspects Med* (2007) 28:210–9. doi: 10.1016/j.mam.2007.04.004

20. Huppertz B. Placental origins of preeclampsia: challenging the current hypothesis. *Hypertension* (2008) 51:970–5. doi: 10.1161/HYPERTENSIONAHA.107.107607

21. Kang JH, Song H, Yoon JA, Park DY, Kim SH, Lee KJ, et al. Preeclampsia leads to dysregulation of various signaling pathways in placenta. *J Hypertens* (2011) 29:928–36. doi: 10.1097/HJH.0b013e328344a82c

22. Weiner E, Feldstein O, Tamayev L, Grinstein E, Barber E, Bar J, et al. Placental histopathological lesions in correlation with neonatal outcome in preeclampsia with and without severe features. *Pregnancy Hypertens* (2018) 12:6–10. doi: 10.1016/j.preghy.2018.02.001

23. Roberts JM, Hubel CA. The two stage model of preeclampsia: Variations on the theme. *Placenta* (2009) 30:S32. doi: 10.1016/J.PLACENTA.2008.11.009

24. Goldman-Wohl D, Yagel S. Preeclampsia–a placenta developmental biology perspective. *J Reprod Immunol* (2009) 82:96–9. doi: 10.1016/j.jri.2009.05.002

25. Staff AC, Johnsen GM, Dechend R, Redman CWG. Preeclampsia and uteroplacental acute atherosis: immune and inflammatory factors. *J Reprod Immunol* (2014) 101e2:120–6. doi: 10.1016/j.jri.2013.09.001

26. Staff AC. The two-stage placental model of preeclampsia: An update. *J Reprod Immunol* (2019) 134–135:1–10. doi: 10.1016/j.jri.2019.07.004

27. Redman CWG, Staff AC. Preeclampsia, biomarkers, syncytiotrophoblast stress, and placental capacity. *Am J Obstet. Gynecol* (2015) 213:S9.e1–4. doi: 10.1016/j.ajog.2015.08.003

28. Bueno-Sánchez JC, Agudelo-Jaramillo B, Escobar-Aguilerae LF, Lopera A, Cadavid-Jaramillo AP, Chaouat G, et al. Cytokine production by non-stimulated peripheral blood NK cells and lymphocytes in early-onset severe preeclampsia without HELLP. *J Reprod Immunol* (2013) 97:223–31. doi: 10.1016/j.jri.2012.11.007

29. Vinnars MT, Björk E, Nagaev I, Ottander U, Bremme K, Holmlund U, et al. Enhanced Th1 and inflammatory mRNA responses upregulate NK cell cytotoxicity and NKG2D ligand expression in human pre-eclamptic placenta and target it for NK cell attack. *Am J Reprod Immunol* (2018) 80:e12969. doi: 10.1111/aji.12969

30. Murthi P, Pinar AA, Dimitriadis E, Samuel CS. Inflammasomes-a molecular link for altered immunoregulation and inflammation mediated vascular dysfunction in preeclampsia. *Int J Mol Sci* (2020) 21:1406. doi: 10.3390/ijms21041406

31. Giachini FR, Galaviz-Hernandez C, Damiano AE, Viana M, Cadavid A, Asturizaga P, et al. Vascular dysfunction in mother and offspring during preeclampsia: Contributions from Latin-American countries. *Curr Hypertension Rep* (2017) 19(10):83. doi: 10.1007/s11906-017-0781-7

32. Clark GF. The role of glycans in immune evasion: The human fetoembryonic defence system hypothesis revisited. *Mol Hum Reprod* (2014) 20:185–99. doi: 10.1093/molehr/gat064

33. Ziganshina MM, Yarotskaya EL, Bovin NV, Pavlovich SV, Sukhikh GT. Can endothelial glycocalyx be a major morphological substrate in pre-eclampsia? *Int J Mol Sci* (2020) 21:3048. doi: 10.3390/IJMS21093048.b

34. Kulikova GV, Ziganshina MM, Shchegolev AI, Sukhikh GT. Comparative characteristics of the expression of fucosylated glycans and morphometric parameters of terminal placental villi depending on the severity of preeclampsia. *Bull Exp Biol Med* (2021) 172:90–5. doi: 10.1007/s10517-021-05338-6

35. Ziganshina MM, Dolgushina NV, Kulikova GV, Fayzullina NM, Yarotskaya EL, Khasbiullina NR, et al. Epithelial apical glycosylation changes associated with thin endometrium in women with infertility - a pilot observational study. *Reprod Biol Endocrinol* (2021) 19:73. doi: 10.1186/s12958-021-00750-z

36. Patankar MS, Ozgur K, Oehninger S, Dell A, Morris H, Seppala M, et al. Expression of glycans linked to natural killer cell inhibition on the human zona pellucida. *Mol Hum Reprod* (1997) 3:501–5. doi: 10.1093/molehr/3.6.501

37. Easton RL, Patankar MS, Clark GF, Morris HR, Dell A. Pregnancy-associated changes in the glycosylation of tamm-horsfall glycoprotein. expression of sialyl lewis(x) sequences on core 2 type O-glycans derived from uromodulin. *J Biol Chem* (2000) 275:21928–38. doi: 10.1074/jbc.M001534200

38. Jang-Lee J, North SJ, Sutton-Smith M, Goldberg D, Panico M, Morris H, et al. Glycomic profiling of cells and tissues by mass spectrometry: fingerprinting and sequencing methodologies. *Methods Enzymol* (2006) 415:59–86. doi: 10.1016/S0076-6879(06)15005-3

39. Pang P-C, Tissot B, Drobnis EZ, Sutovsky P, Morris HR, Clark GF, et al. Expression of bisecting type and Lewisx/Lewisy terminated *N*-glycans on human sperm. *J Biol Chem* (2007) 282:36593–602. doi: 10.1074/jbc.M705134200

40. Lee C-L, Pang P-C, Yeung WSB, Tissot B, Panico M, Lao TTH, et al. Effects of differential glycosylation of glycodelins on lymphocyte survival. *J Biol Chem* (2009) 284:15084–96. doi: 10.1074/jbc.M807960200

41. Clark GF, Schust DJ. Manifestations of immune tolerance in the human female reproductive tract. *Front Immunol* (2013) 4:26. doi: 10.3389/fimmu.2013.00026

42. Passaponti S, Pavone V, Cresti L, Ietta F. The expression and role of glycans at the feto-maternal interface in humans. *Tissue Cell* (2021) 73:101630. doi: 10.1016/j.tice.2021.101630

43. Chen Q, Pang P-C, Cohen ME, Longtine MS, Schust DJ, Haslam SM, et al. Evidence for differential glycosylation of trophoblast cell types. *Mol Cell Proteomics* (2016) 15:1857–66. doi: 10.1074/mcp.M115.055798

44. Jones CJP, Aplin JD. Reproductive glycogenetics-a critical factor in pregnancy success and species hybridisation. *Placenta* (2009) 30:216–9. doi: 10.1016/j.placenta.2008.12.005

45. Ziganshina MM, Kulikova GV, Fayzullina NM, Yarotskaya EL, Shchegolev AI, Le Pendu J, et al. Expression of fucosylated glycans in endothelial glycocalyces of placental villi at early and late fetal growth restriction. *Placenta* (2020) 90:98–102. doi: 10.1016/j.placenta.2019.12.005.a

46. Haslam SM, Julien S, Burchell JM, Monk CR, Ceroni A, Garden OA, et al. Characterizing the glycome of the mammalian immune system. *Immunol Cell Biol* (2008) 86:564–73. doi: 10.1038/icb.2008.54

47. Wautier JL, Wautier MP. Vascular permeability in diseases. *Int J Mol Sci* (2022) 23:3645. doi: 10.3390/ijms23073645

48. Möckl L. The emerging role of the mammalian glycocalyx in functional membrane organization and immune system regulation. *Front Cell Dev Biol* (2020) 8:253. doi: 10.3389/fcell.2020.00253

49. Jedlicka J, Becker BF, Chappell D. Endothelial glycocalyx. *Crit Care Clin* (2020) 36:217–32. doi: 10.1016/j.ccc.2019.12.007

50. Puchwein-Schwepcke A, Genzel-Boroviczény O, Nussbaum C. The endothelial glycocalyx: Physiology and pathology in neonates, infants and children. *Front Cell Dev Biol* (2021) 9:733557. doi: 10.3389/fcell.2021.733557

51. Pomin VH. Sulfated glycans in inflammation. *Eur J Med Chem* (2015) 92C:353–69. doi: 10.1016/j.ejmech.2015.01.002

52. Pomin VH. Phylogeny, structure, function, biosynthesis and evolution of sulfated galactose-containing glycans. *Int J Biol Macromol* (2016) 84:372–9. doi: 10.1016/J.IJBIOMAC.2015.12.035

53. Laine RA. A calculation of all possible oligosaccharide isomers both branched and linear yields 1.05 x 10(12) structures for a reducing hexasaccharide: the isomer barrier to development of single-method saccharide sequencing or synthesis systems. *Glycobiology* (1994) 4:759–67. doi: 10.1093/glycob/4.6.759

54. Määttänen P, Gehring K, Bergeron JJM, Thomas DY. Protein quality control in the ER: The recognition of misfolded proteins. semin. *Cell Dev Biol* (2010) 21:500–11. doi: 10.1016/j.semcdb.2010.03.006

55. Hirata T, Kizuka Y. *N*-Glycosylation. *Adv Exp Med Biol* (2021) 1325:3–24. doi: 10.1007/978-3-030-70115-4_1

56. Dell A, Morris HR, Easton RL, Panico M, Patankar M, Oehniger S, et al. Structural analysis of the oligosaccharides derived from glycodelin, a human glycoprotein with potent immunosuppressive and contraceptive activities. *J Biol Chem* (1995) 270:24116–26. doi: 10.1074/jbc.270.41.24116

57. Scott DW, Vallejo MO, Patel RP. Heterogenic endothelial responses to inflammation: Role for differential n-glycosylation and vascular bed of origin. *J Am Hear. Assoc Cardiovasc Cerebrovasc. Dis* (2013) 2:e000263. doi: 10.1161/JAHA.113.000263

58. Xu Y, Uddin N, Wagner GK. Covalent probes for carbohydrate-active enzymes: From glycosidases to glycosyltransferases. *Methods Enzymol* (2018) 598:237–65. doi: 10.1016/BS.MIE.2017.06.016

59. Cummings RD. *Handbook of glycomics (Google eBook)*. Academic Press (2009). p. 512.

60. Dennis JW, Lau KS, Demetriou M, Nabi IR. Adaptive regulation at the cell surface by *N*-glycosylation. *Traffic* (2009) 10:1569–78. doi: 10.1111/j.1600-0854.2009.00981.x

61. Cummings RD, Pierce JM. The challenge and promise of glycomics. *Chem Biol* (2014) 21:1–15. doi: 10.1016/j.chembiol.2013.12.010

62. Mariño K, Bones J, Kattla JJ, Rudd PM. A systematic approach to protein glycosylation analysis: a path through the maze. *Nat Chem Biol* (2010) 6:713–23. doi: 10.1038/nchembio.437

63. Orberger G, Fuchs H, Geyer R, Gessner R, Köttgen E, Tauber R. Structural and functional stability of the mature transferrin receptor from human placenta. *Arch Biochem Biophys* (2001) 386:79–88. doi: 10.1006/abbi.2000.2177

64. Lattová; EL, Bryant J, Skř J, Zdráhal Z, et al. Efficient procedure for *N*-Glycan analyses and detection of endo h-like activity in human tumor specimens. *Proteome Res* (2016) 15:2777–86. doi: 10.1021/acs.jproteome.6b00346

65. Cummings RD. Stuck on sugars - how carbohydrates regulate cell adhesion, recognition, and signaling. *Glycoconj J* (2019) 36:241–57. doi: 10.1007/s10719-019-09876-0

66. Inoue M, Takahashi S, Yamashina I, Kaibori M, Okumura T, Kamiyama Y, et al. High density O-glycosylation of the MUC2 tandem repeat unit by *N*-acetylgalactosaminyltransferase-3 in colonic adenocarcinoma extracts. *Cancer Res* (2001) 61:950–6.

67. Wada Y, Dell A, Haslam SM, Tissot B, Canis K, Azadi P, et al. Comparison of methods for profiling O-glycosylation: Human proteome organisation human disease Glycomics/Proteome initiative multi-institutional study of IgA1. *Mol Cel. Proteomics* (2010) 9:719–27. doi: 10.1074/mcp.M900450-MCP200

68. Brockhausen I. Pathways of O-glycan biosynthesis in cancer cells. *Biochim Biophys Acta* (1999) 1473:67–95. doi: 10.1016/S0304-4165(99)00170-1

69. García-Vallejo JJ, Van Dijk W, Van Het Hof B, Van Die I, Engelse MA, Van Hinsbergh VWM, et al. Activation of human endothelial cells by tumor necrosis factor-alpha results in profound changes in the expression of glycosylation-related genes. *J Cell Physiol* (2006) 206:203–10. doi: 10.1002/jcp.20458

70. Brooks SA, Hall DM, Buley I. GalNAc glycoprotein expression by breast cell lines, primary breast cancer and normal breast epithelial membrane. *Br J Cancer* (2001) 85:1014–22. doi: 10.1038/sj.bjc.6692028

71. Brown NS, Bicknell R. Hypoxia and oxidative stress in breast cancer. oxidative stress: its effects on the growth, metastatic potential and response to therapy of breast cancer. *Breast Cancer Res* (2001) 3:323–7. doi: 10.1186/bcr315

72. Yue T, Goldstein IJ, Hollingsworth M, Kaul K, Brand RE, Haab BB. The prevalence and nature of glycan alterations on specific proteins in pancreatic cancer patients revealed using antibody-lectin sandwich arrays. *Mol Cell Proteomics* (2009) 8:1697–707. doi: 10.1074/mcp.M900135-MCP200

73. Taylor ME, Drickamer K, Schnaar RL, Etzler ME, Varki A. Discovery and classification of glycan-binding proteins. In: Varki A, Cummings RD, Esko JD, Stanley P, Hart GW, Aebi M, Darvill AG, Kinoshita T, Packer NH, Prestegard JH, Schnaar RL, Seeberger PH, editors. *Essentials of glycobiology*, *3rd ed*. Cold Spring Harbor (NY: Cold Spring Harbor Laboratory Press (2017). p. 2015–7.

74. Taylor ME, Drickamer K. Mammalian sugar-binding receptors: known functions and unexplored roles. *FEBS J* (2019) 286(10):1800–14. doi: 10.1111/febs.14759

75. Bischof P, Irminger-Finger I. The human cytotrophoblastic cell, a mononuclear chameleon. int. j. biochem. *Cell Biol* (2005) 37:1–16. doi: 10.1016/j.biocel.2004.05.014

76. Lunghi L, Ferretti ME, Medici S, Biondi C, Vesce F. Control of human trophoblast function. *Reprod Biol Endocrinol* (2007) 5:6. doi: 10.1186/1477-7827-5-6

77. Kojima J, Ono M, Kuji N, Nishi H. Human chorionic villous differentiation and placental development. *Int J Mol Sci* (2022) 23:8003. doi: 10.3390/ijms23148003

78. Castellucci M, Kosanke G, Verdenelli F, Huppertz B, Kaufmann P. Villous sprouting: fundamental mechanisms of human placental development. *Hum Reprod* (2000) 6:485–94. doi: 10.1093/humupd/6.5.485

79. Caniggia I, Winter JL. Adriana and luisa castellucci award lecture 2001. hypoxia inducible factor-1: oxygen regulation of trophoblast differentiation in normal and preeclamptic pregnancies–a review. *Placenta* (2002) 23 Suppl A:S47–57. doi: 10.1053/plac.2002.0815

80. Gupta AK, Rusterholz C, Huppertz B, Malek A, Schneider H, Holzgreve W, et al. A comparative study of the effect of three different syncytiotrophoblast micro-particles preparations on endothelial cells. *Placenta* (2005) 26:59–66. doi: 10.1016/j.placenta.2004.04.004

81. Kliman HJ, Nestler JE, Sermasi E, Sanger JM, Strauss JF3rd. Purification, characterization, and *in vitro* differentiation of cytotrophoblasts from human term placentae. *Endocrinology* (1986) 118:1567–82. doi: 10.1210/endo-118-4-1567

82. Tarrade A, Lai Kuen R, Malassiné A, Tricottet V, Blain P, Vidaud M, et al. Characterization of human villous and extravillous trophoblasts isolated from first trimester placenta. *Lab Investig* (2001) 81:1199–211. doi: 10.1038/labinvest.3780334

83. Gude NM, Roberts CT, Kalionis B, King RG. Growth and function of the normal human placenta. *Thromb Res* (2004) 114:397–407. doi: 10.1016/j.thromres.2004.06.038

84. Vargas A, Moreau J, Landry S, LeBellego F, Toufaily C, Rassart E, et al. Syncytin-2 plays an important role in the fusion of human trophoblast cells. *J Mol Biol* (2009) 392:301–18. doi: 10.1016/j.jmb.2009.07.025

85. Fischer I, Redel S, Hofmann S, Kuhn C, Friese K, Walzel H, et al. Stimulation of syncytium formation *in vitro* in human trophoblast cells by galectin-1. *Placenta* (2010) 31:825–32. doi: 10.1016/j.placenta.2010.06.016

86. Guo L, Gu F, Xu Y, Zhou C. Increased copy number of syncytin-1 in the trophectoderm is associated with implantation of the blastocyst. *PeerJ* (2020) 8:e10368. doi: 10.7717/PEERJ.10368

87. James JL, Boss AL, Sun C, Allerkamp HH, Clark AR. From stem cells to spiral arteries: A journey through early placental development. *Placenta* (2022) 125:68–77. doi: 10.1016/j.placenta.2021.11.004

88. Burton GJ, Cindrova-Davies T, Yung HW, Jauniaux E. Hypoxia and reproductive health: Oxygen and development of the human placenta. *Reproduction* (2021) 161:F53–65. doi: 10.1530/REP-20-0153

89. Soares MJ, Iqbal K, Kozai K. Hypoxia and placental development. *Birth Defects Res* (2017) 109:1309–29. doi: 10.1002/bdr2.1135

90. Graham CH, Hawley TS, Hawley RG, MacDougall JR, Kerbel RS, Khoo N, et al. Establishment and characterization of first trimester human trophoblast cells with extended lifespan. *Exp Cell Res* (1993) 206:204–11. doi: 10.1006/excr.1993.1139

91. Hamilton GS, Bond SL, McCrae KR, Shepherd T, Khoo NKS, Lala PK, et al. SV40 tag transformation of the normal invasive trophoblast results in a premalignant phenotype. i. mechanisms responsible for hyperinvasivess and resistance to anti-invasive action of TGFβ. *Int J Cancer* (2002) 77:429–39. doi: 10.1002/(sici)1097-0215(19980729)77:3<429::aid-ijc20>3.3.co;2-q

92. Lala PK, Lee BP, Xu G, Chakraborty C. Human placental trophoblast as an *in vitro* model for tumor progression 1 , 2. *Society* (2002) 149:142–9. doi: 10.1139/Y02-006

93. Rye PD, Fodstad O, Emilsen E, Bryne M. Invasion potential and *N*-acetylgalactosamine expression in a human melanoma model. *Int J Cancer* (1998) 75:609–14. doi: 10.1002/(sici)1097-0215(19980209)75:4<609::aid-ijc19>3.0.co;2-3

94. Dube DH, Bertozzi CR. Glycans in cancer and inflammation-potential for therapeutics and diagnostics. *Nat Rev Drug Discovery* (2005) 4:477–88. doi: 10.1038/nrd1751

95. Zhao HX, Li XY, Yao H, Wu Y, Yang R, Zhao RR, et al. The up-regulation of hypoxia-inducible factor-1alpha by hypoxic postconditioning reduces hypoxia/reoxygenation-induced injury in heart-derived H9c2 cells. *Sheng Li Xue Bao* (2013) 65:293–300.

96. Genbacev O, Joslin R, Damsky CH, Polliotti BM, Fisher SJ. Hypoxia alters early gestation human cytotrophoblast differentiation/invasion *in vitro* and models the placental defects that occur in preeclampsia. *J Clin Invest* (1996) 97:540–50. doi: 10.1172/JCI118447

97. Gratton RJ, Gandley RE, Genbacev O, McCarthy JF, Fisher SJ, McLaughlin MK. Conditioned medium from hypoxic cytotrophoblasts alters arterial function. *Am J Obstet. Gynecol* (2001) 184:984–90. doi: 10.1067/mob.2001.110499

98. Maltepe E, Krampitz GW, Okazaki KM, Red-Horse K, Mak W, Simon MC, et al. Hypoxia-inducible factor-dependent histone deacetylase activity determines stem cell fate in the placenta. *Development* (2005) 132:3393–403. doi: 10.1242/dev.01923

99. Robins JC, Heizer A, Hardiman A, Hubert M, Handwerger S. Oxygen tension directs the differentiation pathway of human cytotrophoblast cells. *Placenta* (2007) 28:1141–6. doi: 10.1016/j.placenta.2007.05.006

100. Hung TH, Burton GJ. Hypoxia and reoxygenation: a possible mechanism for placental oxidative stress in preeclampsia. *Taiwan J Obs. Gynecol* (2006) 45:189–200. doi: 10.1016/S1028-4559(09)60224-2

101. Benyo DF, Miles TM, Conrad KP. Hypoxia stimulates cytokine production by villous explants from the human placenta. *J Clin Endocrinol Metab* (1997) 82:1582–8. doi: 10.1210/jc.82.5.1582

102. Genbacev O, Zhou Y, Ludlow JW, Fisher SJ. Regulation of human placental development by oxygen tension. *Science* (1997) 277:1669–72. doi: 10.1126/science.277.5332.1669

103. Pringle KG, Kind KL, Sferruzzi-Perri AN, Thompson JG, Roberts CT. Beyond oxygen: complex regulation and activity of hypoxia inducible factors in pregnancy. *Hum Reprod* (2009) 16:415–31. doi: 10.1093/humupd/dmp046

104. Staff AC, Fjeldstad HE, Fosheim IK, Moe K, Turowski G, Johnsen GM, et al. Failure of physiological transformation and spiral artery atherosis: their roles in preeclampsia. *Am J Obstet. Gynecol* (2022) 226:S895–906. doi: 10.1016/j.ajog.2020.09.026

105. Ikeda R, Tabata S, Tajitsu Y, Nishizawa Y, Minami K, Furukawa T, et al. Molecular basis for the regulation of hypoxia-inducible factor-1alpha levels by 2-deoxy-D-ribose. *Oncol Rep* (2013) 30:1444–8. doi: 10.3892/or.2013.2572

106. Cowden Dahl KD, Fryer BH, Mack FA, Compernolle V, Maltepe E, Adelman DM, et al. Hypoxia-inducible factors 1alpha and 2alpha regulate trophoblast differentiation. *Mol Cell Biol* (2005) 25:10479–91. doi: 10.1128/MCB.25.23.10479-10491.2005

107. Wang GL, Semenza GL. Characterization of hypoxia-inducible factor 1 and regulation of DNA binding activity by hypoxia. *J Biol Chem* (1993) 268:21513–8. doi: 10.1016/S0021-9258(20)80571-7

108. Krishnamachary B, Berg-Dixon S, Kelly B, Agani F, Feldser D, Ferreira G, et al. Regulation of colon carcinoma cell invasion by hypoxia-inducible factor 1. *Cancer Res* (2003) 63:1138–43.

109. Gilkes DM, Semenza GL. Role of hypoxia-inducible factors in breast cancer metastasis. *Futur Oncol* (2013) 9:1623–36. doi: 10.2217/fon.13.92

110. Huppertz B, Gauster M, Orendi K, König J, Moser G. Oxygen as modulator of trophoblast invasion. *J Anat* (2009) 215:14–20. doi: 10.1111/j.1469-7580.2008.01036.x

111. Resnik ER, Herron JM, Lyu S-C, Cornfield DN. Developmental regulation of hypoxia-inducible factor 1 and prolyl-hydroxylases in pulmonary vascular smooth muscle cells. *Proc Natl Acad Sci U. S. A* (2007) 104:18789–94. doi: 10.1073/pnas.0706019104

112. Chung JW, Shin JE, Han KW, Ahn JH, Kim YJ, Park JW, et al. Up-regulation of hypoxia-inducible factor-1 alpha by cobalt chloride prevents hearing loss in noise-exposed mice. *Env. Toxicol Pharmacol* (2011) 31:153–9. doi: 10.1016/j.etap.2010.10.002

113. Shay JE, Imtiyaz HZ, Sivanand S, Durham AC, Skuli N, Hsu S, et al. Inhibition of hypoxia-inducible factors limits tumor progression in a mouse model of colorectal cancer. *Carcinogenesis* (2014) 35:1067–77. doi: 10.1093/carcin/bgu004

114. Min J-H, Yang H, Ivan M, Gertler F, Kaelin WGJ, Pavletich NP. Structure of an HIF-1alpha -pVHL complex: hydroxyproline recognition in signaling. *Science* (2002) 296:1886–9. doi: 10.1126/science.1073440

115. Airley R, Loncaster J, Davidson S, Bromley M, Roberts S, Patterson A, et al. Glucose transporter glut-1 expression correlates with tumor hypoxia and predicts metastasis-free survival in advanced carcinoma of the cervix. *Clin Cancer Res* (2001) 7:928–34.

116. Xing F, Okuda H, Watabe M, Kobayashi A, Pai SK, Liu W, et al. Hypoxia-induced Jagged2 promotes breast cancer metastasis and self-renewal of cancer stem-like cells. *Oncogene* (2011) 30:4075–86. doi: 10.1038/onc.2011.122

117. Skoura A, Sanchez T, Claffey K, Mandala SM, Proia RL, Hla T. Essential role of sphingosine 1-phosphate receptor 2 in pathological angiogenesis of the mouse retina. *J Clin Invest* (2007) 117:2506–16. doi: 10.1172/JCI31123

118. Schoots MH, Gordijn SJ, Scherjon SA, van Goor H, Hillebrands J-L. Oxidative stress in placental pathology. *Placenta* (2018) 69:153–61. doi: 10.1016/j.placenta.2018.03.003

119. Munaut C, Lorquet S, Pequeux C, Blacher S, Berndt S, Frankenne F, et al. Hypoxia is responsible for soluble vascular endothelial growth factor receptor-1 (VEGFR-1) but not for soluble endoglin induction in villous trophoblast. *Hum Reprod* (2008) 23:1407–15. doi: 10.1093/humrep/den114

120. Foidart JM, Schaaps JP, Chantraine F, Munaut C, Lorquet S. Dysregulation of antiangiogenic agents (sFlt-1, PLGF, and sEndoglin) in preeclampsia–a step forward but not the definitive answer. *J Reprod Immunol* (2009) 82:106–11. doi: 10.1016/j.jri.2009.09.001

121. Rolfo A, Many A, Racano A, Tal R, Tagliaferro A, Ietta F, et al. Abnormalities in oxygen sensing define early and late onset preeclampsia as distinct pathologies. *PloS One* (2010) 5:e13288. doi: 10.1371/journal.pone.0013288

122. Rajakumar A, Brandon HM, Daftary A, Ness R, Conrad KP. Evidence for the functional activity of hypoxia-inducible transcription factors overexpressed in preeclamptic placentae. *Placenta* (2004) 25:763–9. doi: 10.1016/J.PLACENTA.2004.02.011

123. Lee CL, Chiu PC, Pang PC, Chu IK, Lee KF, Koistinen R, et al. Glycosylation failure extends to glycoproteins in gestational diabetes mellitus: evidence from reduced alpha2-6 sialylation and impaired immunomodulatory activities of pregnancy-related glycodelin-A. *Diabetes* (2011) 60:909–17. doi: 10.2337/db10-1186

124. Godfrey-Smith P. Information in biology. In *The Cambridge Guide to the Philosophy of Biology*, ed. Hull DL, Ruse M. (2007) 103–19. Cambridge: Cambridge University Press.

125. Mian IS, Rose C. Communication theory and multicellular biology. *Integr Biol* (2011) 3:350–67. doi: 10.1039/c0ib00117a

126. Veillon L, Zhou S, Mechref Y. Quantitative glycomics: A combined analytical and bioinformatics approach. *Methods Enzymol* (2017) 585:431–77. doi: 10.1016/bs.mie.2016.11.006

127. Elliott MM, Kardana A, Lustbader JW, Cole LA. Carbohydrate and peptide structure of the alpha- and beta-subunits of human chorionic gonadotropin from normal and aberrant pregnancy and choriocarcinoma. *Endocrine* (1997) 7:15–32. doi: 10.1007/BF02778058

128. Harfouche R, Hentschel DM, Piecewicz S, Basu S, Print C, Eavarone D, et al. Glycome and transcriptome regulation of vasculogenesis. *Circulation* (2009) 120:1883–92. doi: 10.1161/CIRCULATIONAHA.108.837724

129. Piecewicz S, Sengupta S. The dynamic glycome microenvironment and stem cell differentiation into vasculature. *Stem Cells Dev* (2011) 20:749–58. doi: 10.1089/scd.2010.0454

130. Yamamoto E, Ino K, Miyoshi E, Inamori K, Abe A, Sumigama S, et al. *N*-acetylglucosaminyltransferase V regulates extravillous trophoblast invasion through glycosylation of alpha5beta1 integrin. *Endocrinology* (2009) 150:990–9. doi: 10.1210/en.2008-1005

131. Borzychowski AM, Sargent IL, Redman CW. Inflammation and pre-eclampsia. *Semin Fetal Neonatal Med* (2006) 11:309–16. doi: 10.1016/j.siny.2006.04.001

132. Huang S, Ernberg I, Kauffman S. Cancer attractors: A systems view of tumors from a gene network dynamics and developmental perspective. *Semin Cell Dev Biol* (2009) 20:869–76. doi: 10.1016/j.semcdb.2009.07.003

133. Clark GF, Oehninger S, Patankar MS, Koistinen R, Dell A, Morris HR, et al. A role for glycoconjugates in human development: the human feto-embryonic defence system hypothesis. *Hum Reprod* (1996) 11:467–73. doi: 10.1093/HUMREP/11.3.467

134. Arkwright PD, Redman CW, Williams PJ, Dwek RA, Rademacher TW. Syncytiotrophoblast membrane protein glycosylation patterns in normal human pregnancy and changes with gestational age and parturition. *Placenta* (1991) 12:637–51. doi: 10.1016/0143-4004(91)90498-5

135. Arkwright P, Rademacher T, Marshall J, Dwek R, Redman C. Glycoprotein glycosylation and the immunosuppressive effects of human pregnancy serum. *J Reprod Immunol* (1992) 21:97–102. doi: 10.1016/0165-0378(92)90043-4

136. Dennis JW, Laferté S. Recognition of asparagine-linked oligosaccharides on murine tumor cells by natural killer cells. *Cancer Res* (1985) 45:6034–40.

137. Tomiie M, Isaka S, Miyoshi E, Taniguchi N, Kimura T, Ogita K, et al. Elevated expression of *N*-acetylglucosaminyltransferase V in first trimester human placenta. *Biochem Biophys Res Commun* (2005) 330:999–1004. doi: 10.1016/j.bbrc.2005.02.186

138. Arkwright PD, Rademacher TW, Boutignon F, Dwek RA, Redman CW. Suppression of allogeneic reactivity *in vitro* by the syncytiotrophoblast membrane glycocalyx of the human term placenta is carbohydrate dependent. *Glycobiology* (1994) 4(1):39–47. doi: 10.1093/glycob/4.1.39

139. Deng Q, Chen Y, Yin N, Shan N, Luo X, Tong C, et al. N-acetylglucosaminyltransferase V inhibits the invasion of trophoblast cells by attenuating MMP2/9 activity in early human pregnancy. *Placenta* (2015) 36:1291–9. doi: 10.1016/j.placenta.2015.08.014

140. Deng Q, Liu X, Yang Z, Xie L. Expression of N-Acetylglucosaminyltransferase III Promotes Trophoblast Invasion and Migration in Early Human Placenta. *Reprod Sci.* (2019) 26:1373–81. doi: 10.1177/1933719118765967

141. Jones CJ, Aplin JD, Burton GJ. First trimester histiotrophe shows altered sialylation compared with secretory phase glycoconjugates in human endometrium. *Placenta* (2010) 31:576–80. doi: 10.1016/j.placenta.2010.04.011

142. Whyte A, Loke YW. Increased sialylation of surface glycopeptides of human trophoblast compared with fetal cells from the same conceptus. *J Exp Med* (1978) 148:1087–92. doi: 10.1084/jem.148.4.1087

143. Jeschke U, Richter DU, Hammer A, Briese V, Friese K, Karsten U. Expression of the thomsen-friedenreich antigen and of its putative carrier protein mucin 1 in the human placenta and in trophoblast cells *in vitro*. *Histochem Cell Biol* (2002) 117:219–26. doi: 10.1007/s00418-002-0383-5

144. Jeschke U, Mayr D, Schiessl B, Mylonas I, Schulze S, Kuhn C, et al. Expression of galectin-1, -3 (gal-1, gal-3) and the thomsen-friedenreich (TF) antigen in normal, IUGR, preeclamptic and HELLP placentas. *Placenta* (2007) 28:1165–73. doi: 10.1016/j.placenta.2007.06.006

145. Clark GF, Dell A, Morris HR, Patankar M, Oehninger S, Seppälä M. Viewing AIDS from a glycobiological perspective: potential linkages to the human fetoembryonic defence system hypothesis. *Mol Hum Reprod* (1997) 3:5–13. doi: 10.1093/molehr/3.1.5

146. Gridelet V, Perrier d'Hauterive S, Polese B, Foidart JM, Nisolle M, Geenen V. Human chorionic gonadotrophin: New pleiotropic functions for an "Old" hormone during pregnancy. *Front Immunol* (2020) 11:343. doi: 10.3389/fimmu.2020.00343

147. Norris W, Nevers T, Sharma S, Kalkunte S. Review: hCG, preeclampsia and regulatory T cells. *Placenta* (2011) 32 Suppl 2:S182–185. doi: 10.1016/j.placenta.2011.01.009

148. Minas V, Mylonas I, Schiessl B, Mayr D, Schulze S, Friese K, et al. Expression of the blood-group-related antigens sialyl Lewis a, sialyl Lewis x and Lewis y in term placentas of normal, preeclampsia, IUGR- and HELLP-complicated pregnancies. *Histochem Cell Biol* (2007) 128:55–63. doi: 10.1007/s00418-007-0293-7

149. Ma Z, Yang H, Peng L, Kuhn C, Chelariu-Raicu A, Mahner S, et al. Expression of the carbohydrate Lewis antigen, sialyl Lewis a, sialyl Lewis X, Lewis X, and Lewis y in the placental villi of patients with unexplained miscarriages. *Front Immunol* (2021) 12:679424. doi: 10.3389/fimmu.2021.679424

150. Jeschke U, Toth B, Scholz C, Friese K, Makrigiannakis A. Glycoprotein and carbohydrate binding protein expression in the placenta in early pregnancy loss. *J Reprod Immunol* (2010) 85:99–105. doi: 10.1016/j.jri.2009.10.012

151. Freitag N, Tirado-Gonzaĺez I, Barrientos G, Herse F, Thijssen VLJL, Weedon-Fekjær SM, et al. Interfering with gal-1-mediated angiogenesis contributes to the pathogenesis of preeclampsia. *Proc Natl Acad Sci U. S. A* (2013) 110:11451–6. doi: 10.1073/PNAS.1303707110

152. Ferrer CM, Lynch TP, Sodi VL, Falcone JN, Schwab LP, Peacock DL, et al. O-GlcNAcylation regulates cancer metabolism and survival stress signaling via regulation of the HIF-1 pathway. *Mol Cell* (2014) 54:820–31. doi: 10.1016/j.molcel.2014.04.026

153. Koike T, Kimura N, Miyazaki K, Yabuta T, Kumamoto K, Takenoshita S, et al. Hypoxia induces adhesion molecules on cancer cells: A missing link between warburg effect and induction of selectin-ligand carbohydrates. *Proc Natl Acad Sci U. S. A* (2004) 101:8132–7. doi: 10.1073/PNAS.0402088101

154. Miyata S, Noda A, Ozaki N, Hara Y, Minoshima M, Iwamoto K, et al. Insufficient sleep impairs driving performance and cognitive function. *Neurosci Lett* (2010) 469:229–33. doi: 10.1016/j.neulet.2009.12.001

155. Nonaka M, Fukuda MN, Gao C, Li Z, Zhang H, Greene MI, et al. Determination of carbohydrate structure recognized by prostate-specific F77 monoclonal antibody through expression analysis of glycosyltransferase genes. *J Biol Chem* (2014) 289:16478–86. doi: 10.1074/JBC.M114.559047

156. Belo AI, Van Vliet SJ, Maus A, Laan LC, Nauta TD, Koolwijk P, et al. Hypoxia inducible factor 1a down regulates cell surface expression of a1,2-fucosylated glycans in human pancreatic adenocarcinoma cells. (2015) 589:2359–66. doi: 10.1016/j.febslet.2015.07.035

157. Croci DO, Cerliani JP, Dalotto-Moreno T, Méndez-Huergo SP, Mascanfroni ID, Dergan-Dylon S, et al. Glycosylation-dependent lectin-receptor interactions preserve angiogenesis in anti-VEGF refractory tumors. *Cell* (2014) 156:744–58. doi: 10.1016/J.CELL.2014.01.043

158. Croci DO, Cerliani JP, Pinto NA, GMorosi L, Rabinovich GA. Regulatory role of glycans in the control of hypoxia-driven angiogenesis and sensitivity to antiangiogenic treatment. *Glycobiology* (2014) 24:1283–90. doi: 10.1093/glycob/cwu083

159. Alphonsus CS, Rodseth RN. The endothelial glycocalyx: a review of the vascular barrier. *Anaesthesia* (2014) 69:777–84. doi: 10.1111/anae.12661

160. Jackson-Weaver O, Friedman JK, Rodriguez LA, Hoof MA, Drury RH, Packer JT, et al. Hypoxia/reoxygenation decreases endothelial glycocalyx via reactive oxygen species and calcium signaling in a cellular model for shock. *J Trauma Acute Care Surg* (2019) 87:1070–6. doi: 10.1097/TA.0000000000002427

161. Haddad JJ, Harb HL. Cytokines and the regulation of hypoxia-inducible factor (HIF)-1alpha. *Int Immunopharmacol* (2005) 5:461–83. doi: 10.1016/j.intimp.2004.11.009

162. Bruning U, Fitzpatrick SF, Frank T, Birtwistle M, Taylor CT, Cheong A. NFκB and HIF display synergistic behaviour during hypoxic inflammation. *Cell Mol Life Sci* (2012) 69:1319–29. doi: 10.1007/s00018-011-0876-2

163. Vaughan JE, Walsh SW. Activation of NF-κB in placentas of women with preeclampsia. *Hypertens Pregnancy* (2012) 31:243–51. doi: 10.3109/10641955.2011.642436

164. Litang Z, Hong W, Weimin Z, Xiaohui T, Qian S. Serum NF-κBp65, TLR4 as biomarker for diagnosis of preeclampsia. *Open Med* (2017) 12:399–402. doi: 10.1515/med-2017-0057

165. Schäffer L, Scheid A, Spielmann P, Breymann C, Zimmermann R, Meuli M, et al. Oxygen-regulated expression of TGF-beta 3, a growth factor involved in trophoblast differentiation. *Placenta* (2003) 24:941–50. doi: 10.1016/s0143-4004(03)00166-8

166. Nishi H, Nakada T, Hokamura M, Osakabe Y, Itokazu O, Huang LE, et al. Hypoxia-inducible factor-1 transactivates transforming growth factor-beta3 in trophoblast. *Endocrinology* (2004) 145:4113–8. doi: 10.1210/en.2003-1639

167. Alijotas-Reig J, Palacio-Garcia C, Farran-Codina I, Ruiz-Romance M, Llurba E, Vilardell-Tarres M. Circulating cell-derived microparticles in severe preeclampsia and in fetal growth restriction. *Am J Reprod Immunol* (2012) 67:140–51. doi: 10.1111/j.1600-0897.2011.01072.x

168. Escudero C, Calle A. Hierro, oxígeno y desarrollo placentario en la génesis de la preeclampsia. Efectos de la altura en Ecuador [Iron, oxygen and placental development in the etiology of preeclampsia. Effects of high altitude in Ecuador]. *Rev Med Chil* (2006) 134:491–8. Spanish. doi: 10.4067/s0034-98872006000400014

169. Serdar Z, Gür E, Develioğlu O. Serum iron and copper status and oxidative stress in severe and mild preeclampsia. *Cell Biochem Funct* (2006) 24:209–15. doi: 10.1002/CBF.1235

170. Toldi G, Stenczer B, Molvarec A, Takáts Z, Beko G, Rigó JJr., et al. Hepcidin concentrations and iron homeostasis in preeclampsia. *Clin Chem Lab Med* (2010) 48:1423–6. doi: 10.1515/CCLM.2010.290

171. Siddiqui IA, Jaleel A, Kadri HM, Saeed WA, Tamimi W. Iron status parameters in preeclamptic women. *Arch Gynecol. Obstet* (2011) 284:587–91. doi: 10.1007/S00404-010-1728-2

172. Gómez-Gutiérrez AM, Parra-Sosa BE, Bueno-Sánchez JC. Glicanos de la vellosidad trofoblástica en la anemia ferropénica y la preeclampsia grave. *Rev Chil. Nutr* (2015) 42:121–30. doi: 10.4067/S0717-75182015000200002

173. Gómez-Gutiérrez AM, Parra-Sosa BE, César Bueno-Sánchez J. Function of receptor 1 in uptaking transferrin and its relation to iron deficiency and iron gestational preeclampsia. *Rev Cuba. Obstet. Ginecol* (2013) 39:33–42.

174. Gambling L, Danzeisen R, Fosset C, Andersen HS, Dunford S, Srai SKS, et al. Iron and copper interactions in development and the effect on pregnancy outcome. *J Nutr* (2003) 133:1554S–6S. doi: 10.1093/jn/133.5.1554S

175. Bastin J, Drakesmith H, Rees M, Sargent I, Townsend A. Localisation of proteins of iron metabolism in the human placenta and liver. *Br J Haematol* (2006) 134:532–43. doi: 10.1111/J.1365-2141.2006.06216.X

176. McArdle HJ, Andersen HS, Jones H, Gambling L. Copper and iron transport across the placenta: regulation and interactions. *J Neuroendocrinol* (2008) 20:427–31. doi: 10.1111/j.1365-2826.2008.01658.x

177. Corrales-Agudelo V, Bueno-Sanchez J, Arboleda B–, Cardona-Ospina A, Lopez-Rojas E, Escobar L, et al. Transferrin receptor 1 and ferroportin expression in the full-term human placenta and its association with maternal and neonatal iron status: A pilot study. *J Clin Nutr Metab* (2018) 3:1–7. doi: 10.4172/JCNM.1000123

178. Ralton JE, Jackson HJ, Zanoni M, Gleeson PA. Effect of glycosylation inhibitors on the structure and function of the murine transferrin receptor. *Eur J Biochem* (1989) 186:637–47. doi: 10.1111/j.1432-1033.1989.tb15254.x

179. Do SI, Enns C, Cummings RD. Human transferrin receptor contains O-linked oligosaccharides. *J Biol Chem* (1990) 265:114–25. doi: 10.1016/S0021-9258(19)40203-2

180. Do S, Cummings RD. Presence of O-linked oligosaccharide on a threonine residue in the human transferrin receptor. *Glycobiology* (1992) 2:345–53. doi: 10.1093/GLYCOB/2.4.345

181. Georgieff MK, Petry CD, Mills MM, McKay H, Wobken JD. Increased *N*-glycosylation and reduced transferrin-binding capacity of transferrin receptor isolated from placentae of diabetic women. *Placenta* (1997) 18:563–8. doi: 10.1016/0143-4004(77)90011-x

182. Gómez-Gutiérrez AM, Parra-Sosa BE, Bueno-Sánchez JC. Glycosylation profile of the transferrin receptor in gestational iron deficiency and early-onset severe preeclampsia. *J Pregnancy* (2019) 2019:9514546. doi: 10.1155/2019/9514546

183. Zhuo Y, Bellis SL. Emerging role of α2,6-sialic acid as a negative regulator of galectin binding and function. *J Biol Chem* (2011) 286:5935. doi: 10.1074/JBC.R110.191429

184. Carlsson MC, Bengtson P, Cucak H, Leffler H. Galectin-3 guides intracellular trafficking of some human serotransferrin glycoforms. *J Biol Chem* (2013) 288:28398. doi: 10.1074/JBC.M113.487793

185. Rutledce EA, Enns CA. Cleavage of the transferrin receptor is influenced by the composition of the 0-linked carbohydrate at position 104. *J Cell Physiol* (1996) 168:284–293. doi: 10.1002/(SICI)1097-4652(199608)168:2

186. Murrieta-Coxca JM, Fuentes-Zacarias P, Ospina-Prieto S, Markert UR, Morales-Prieto DM. Synergies of extracellular vesicles and microchimerism in promoting immunotolerance during pregnancy. *Front Immunol* (2022) 13:837281. doi: 10.3389/fimmu.2022.837281

187. Darmochwal-Kolarz D, Rolinski J, Leszczynska-Goarzelak B, Oleszczuk J. The expressions of intracellular cytokines in the lymphocytes of preeclamptic patients. *A. J Reprod Immunol* (2002) 48:381–6. doi: 10.1034/j.1600-0897.2002.01089.x

188. Van Nieuwenhoven ALV, Moes H, Heineman MJ, Santema J, Faas MM. Cytokine production by monocytes, NK cells, and lymphocytes is different in preeclamptic patients as compared with normal pregnant women. *Hypertension Pregnancy* (2008) 27:207–24. doi: 10.1080/10641950701885006

189. Liao WC, Chen CH, Liu CH, Huang MJ, Chen CW, Hung JS, et al. Expression of GALNT2 in human extravillous trophoblasts and its suppressive role in trophoblast invasion. *Placenta* (2012) 33:1005–11. doi: 10.1016/j.placenta.2012.08.007

190. Hromatka BS, Drake PM, Kapidzic M, Stolp H, Goldfien GA, Shih I, et al. Polysialic acid enhances the migration and invasion of human cytotrophoblasts. *Glycobiology* (2013) 23:593–602. doi: 10.1093/glycob/cws162

191. Masilamani M, Nguyen C, Kabat J, Borrego F, Coligan JE. CD94/NKG2A inhibits NK cell activation by disrupting the actin network at the immunological synapse. *J Immunol* (2006) 177:3590–6. doi: 10.4049/jimmunol.177.6.3590

192. Jacobs R, Hintzen G, Kemper A, Beul K, Kempf S, Behrens G, et al. CD56 bright cells differ in their KIR repertoire and cytotoxic features from CD56 dim NK cells. *Eur J Immunol* (2001) 31:3121–7. doi: 10.1002/1521-4141(2001010)31:10<3121::aid-immu3121>3.0.co;2-4

193. Saito S, Sakai M. Th1/Th2 balance in preeclampsia. *J Reprod Immunol* (2003) 59:161–73. doi: 10.1016/S0165-0378(03)00045-7

194. Higuma-Myojo S, Sasaki Y, Miyazaki S, Sakai M, Siozaki A, Miwa N, et al. Cytokine profile of natural killer cells in early human pregnancy. *Am J Reprod Immunol* (2005) 54:21–9. doi: 10.1111/j.1600-0897.2005.00279.x

195. Saito S, Shigeru S, Nakashima A, Akitoshi N, Myojo-Higuma S, Subaru M-H, et al. The balance between cytotoxic NK cells and regulatory NK cells in human pregnancy. *J Reprod Immunol* (2008) 77:14–22. doi: 10.1016/j.jri.2007.04.007

196. Zhang Z, Gong F, Jia L, Chang C, Hou L, Yang R, et al. Studies on activity of NK cells in preeclampsia patients. *J Huazhong Univ Sci Technolog. Med Sci* (2004) 24:473–5.

197. Petrie EJ, Clements CS, Lin J, Sullivan LC, Johnson D, Huyton T, et al. CD94-NKG2A recognition of human leukocyte antigen (HLA) -e bound to an HLA class I leader sequence. *J Exp Med* (2008) 205:725–35. doi: 10.1084/jem.20072525

198. Valés-Gómez M, Reyburn HT, Erskine RA, López-Botet M, Strominger JL. Kinetics and peptide dependency of the binding of the inhibitory NK receptor CD94/NKG2-a and the activating receptor CD94/NKG2-c to HLA-e. *EMBO J* (1999) 18:4250–60. doi: 10.1093/emboj/18.15.4250

199. Xin X, Higai K, Imaizumi Y, Suzuki C, Ito K, Itoh A, et al. Natural killer group 2A (NKG2A) and natural killer group 2C (NKG2C) bind to sulfated glycans and a 2,3-NeuAc-containing glycoproteins. *Biol Pharm Bull* (2011) 34:480–5. doi: 10.1248/bpb.34.480

200. Hamad RR, Berg L, Bachmayer N, Sohlberg E, Sundstro Y, Sverremark-ekstro E, et al. Women with preeclampsia have an altered NKG2A and NKG2C receptor expression on peripheral blood natural killer cells. *Am J Reprod Immunol* (2009) 62:147–57. doi: 10.1111/j.1600-0897.2009.00724.x

201. Bueno-Sánchez JC, Peña-Alzate S, Peña RB, Agudelo-Jaramillo B, Cadavid-Jaramillo AP, Chaouat G, et al. Sera from early-onset, severely preeclamptic women directly modulate HLA-e expression in the EA.hy296 endothelial cell line. *J Reprod Immunol* (2014) 104-105:68–79. doi: 10.1016/j.jri.2014.03.004

202. Wei J, Satomi M. Effect of sera on the adhesion of natural killer cells to the endothelium in severe preeclampsia. *J Obstet. Gynaecol. Res* (2006) 32:443–8. doi: 10.1111/j.1447-0756.2006.00444.x

203. Damle NK, Doyle LV. IL-2-activated human killer lymphocytes but not their secreted products mediate increase in albumin flux across cultured endothelial monolayers. implications for vascular leak syndrome. *J Immunol* (1989) 142:2660–9. doi: 10.4049/jimmunol.142.8.2660

204. Coupel S, Moreau A, Hamidou M, Horejsi V, Soulillou J-P, Charreau B. Expression and release of soluble HLA-e is an immunoregulatory feature of endothelial cell activation. *Blood* (2007) 109:2806–14. doi: 10.1182/blood-2006-06-030213

205. Ohyama C, Tsuboi S, Fukuda M. Dual roles of sialyl Lewis X oligosaccharides in tumor metastasis and rejection by natural killer cells. *EMBO J* (1999) 18:1516–25. doi: 10.1093/emboj/18.6.1516

206. Sol M, Vacaresse N, Lule J, Davrinche C, Gabriel B, Teissie J, et al. *N*-linked oligosaccharides can protect target cells from the lysis mediated by NK cells but not by cytotoxic T lymphocytes: role of NKG2-a. *Tissue Antigens* (1999) 54:113–21. doi: 10.1034/j.1399-0039.1999.540201.x

207. Pang P, Drobnis EZ, Morris HR, Dell A, Clark GF. Analysis of the human seminal plasma glycome reveals the presence of immunomodulatory carbohydrate functional groups research articles. *J Proteome Res* (2009) 8:4906–15. doi: 10.1021/pr9001756

208. Moebius JM, Widera D, Schmitz J, Kaltschmidt C, Piechaczek C. Impact of polysialylated CD56 on natural killer cell cytotoxicity. *BMC Immunol* (2007) 8:13. doi: 10.1186/1471-2172-8-13

209. Pearce OMT, Läubli H. Sialic acids in cancer biology and immunity. *Glycobiology* (2016) 26:111–28. doi: 10.1093/glycob/cwv097

210. Ibeto L, Antonopoulos A, Grassi P, Pang PC, Panico M, Bobdiwala S, et al. Insights into the hyperglycosylation of human chorionic gonadotropin revealed by glycomics analysis. *PloS One* (2020) 15:e0228507. doi: 10.1371/JOURNAL.PONE.0228507

211. Campuzano M, Bueno-Sánchez J, Agudelo-Jaramillo B, Quintana-Castillo JC, Chaouat GC, Maldonado-Estrada JG. Glycan expression in chorionic villi from histocultures of women with early-onset preeclampsia: Immunomodulatory effects on peripheral natural killer cells. *J Reprod Immunol* (2020) 142:103212. doi: 10.1016/J.JRI.2020.103212

212. Saul R, Molyneux RJ, Elbein AD. Studies on the mechanism of castanospermine inhibition of alpha- and beta-glucosidases. *Arch Biochem Biophys* (1984) 230:668–75. doi: 10.1016/0003-9861(84)90448-x

213. Winn VD, Gormley M, Paquet AC, Kjaer-Sorensen K, Kramer A, Rumer KK, et al. Severe preeclampsia-related changes in gene expression at the maternal-fetal interface include sialic acid-binding immunoglobulin-like lectin-6 and pappalysin-2. *Endocrinology* (2009) 150:452–62. doi: 10.1210/en.2008-0990

214. Friese K, Schiessl B, Schulze S, Kuhn C, Jeschke U, Lomba I, et al. Expression of glycodelin a in decidual tissue of preeclamptic, HELLP and intrauterine growth-restricted pregnancies. *Virchows Arch* (2005) 446:360–8. doi: 10.1007/s00428-004-1201-3

215. Dundar B, Dincgez Cakmak B, Aydin Boyama B, Karadag B, Ozgen G. Maternal serum glycodelin levels in preeclampsia and its relationship with the severity of the disease. *J Matern. Fetal. Neonatal Med* (2018) 31:2884–92. doi: 10.1080/14767058.2017.1359530

216. Hussain T, Murtaza G, Metwally E, Kalhoro DH, Kalhoro MS, Rahu BA, et al. The role of oxidative stress and antioxidant balance in pregnancy. *Mediators Inflammation* (2021) 2021:9962860. doi: 10.1155/2021/9962860

217. Mukherjee I, Dhar R, Singh S, Sharma JB, Nag TC, Mridha AR, et al. Oxidative stress-induced impairment of trophoblast function causes preeclampsia through the unfolded protein response pathway. *Sci Rep* (2021) 11:18415. doi: 10.1038/s41598-021-97799-y

218. Vaka R, Deer E, Cunningham M, McMaster KM, Wallace K, Cornelius DC, et al. Characterization of mitochondrial bioenergetics in preeclampsia. *J Clin Med* (2021) 10:5063. doi: 10.3390/jcm10215063

219. Chandra PK, Cikic S, Rutkai I, Guidry JJ, Katakam PVG, Mostany R, et al. Effects of aging on protein expression in mice brain microvessels: ROS scavengers, mRNA/protein stability, glycolytic enzymes, mitochondrial complexes, and basement membrane components. *Geroscience* (2021) 44:371–88. doi: 10.1007/s11357-021-00468-1

220. Jones CJP, Owens S, Senga E, van Rheenen P, Faragher B, Denton J, et al. Placental expression of α2,6-linked sialic acid is upregulated in malaria. *Placenta* (2008) 29:300–4. doi: 10.1016/j.placenta.2007.12.007

221. Agudelo O, Bueno J, Villa A, Maestre A. High IFN-gamma and TNF production by peripheral NK cells of Colombian patients with different clinical presentation of plasmodium falciparum. *Malar. J* (2012) 11:38. doi: 10.1186/1475-2875-11-38

222. Agudelo OM, Aristizabal BH, Yanow SK, Arango E, Carmona-Fonseca J, Maestre A. Submicroscopic infection of placenta by plasmodium produces Th1/Th2 cytokine imbalance, inflammation and hypoxia in women from north-west Colombia. *Malar J* (2014) 13:122. doi: 10.1186/1475-2875-13-122

223. Arango EM, Samuel R, Agudelo OM, Carmona-Fonseca J, Maestre A, Yanow SK. Molecular detection of malaria at delivery reveals a high frequency of submicroscopic infections and associated placental damage in pregnant women from northwest Colombia. *Am J Trop Med Hyg* (2013) 89:178–83. doi: 10.4269/ajtmh.12-0669

224. Jin J, Menon R. Placental exosomes: A proxy to understand pregnancy complications. *Am J Reprod Immunol* (2018) 79:e12788. doi: 10.1111/aji.12788

225. Zhang Y, Zhao C, Wei Y, Yang S, Cui C, Yang J, et al. Increased circulating microparticles in women with preeclampsia. *Int J Lab Hematol* (2018) 40(3):352–8. doi: 10.1111/IJLH.12796

226. Sargent IL. Microvesicles and pre-eclampsia. pregnancy hypertension. *Int J Women's Cardiovasc Health* (2013) 3(2):58. doi: 10.1016/J.PREGHY.2013.04.004

227. Dragovic RA, Collett GP, Hole P, Ferguson DJP, Redman CW, Sargent IL, et al. Isolation of syncytiotrophoblast microvesicles and exosomes and their characterisation by multicolour flow cytometry and fluorescence nanoparticle tracking analysis. *Methods* (2015) 87:64–74. doi: 10.1016/j.ymeth.2015.03.028

228. Condrat CE, Varlas VN, Duică F, Antoniadis P, Danila CA, Cretoiu D, et al. Pregnancy-related extracellular vesicles revisited. *Int J Mol Sci* (2021) 22:3904. doi: 10.3390/IJMS22083904

229. Laresgoiti-Servitje E, Gomez-Lopez N. The pathophysiology of preeclampsia involves altered levels of angiogenic factors promoted by hypoxia and autoantibody-mediated mechanisms. *Biol Reprod* (2012) 87:36. doi: 10.1095/biolreprod.112.099861

230. Goswami D, Tannetta DS, Magee LA, Fuchisawa A, Redman CWG, Sargent IL, et al. Excess syncytiotrophoblast microparticle shedding is a feature of early-onset pre-eclampsia, but not normotensive intrauterine growth restriction. *Placenta* (2006) 27 (1):56–61. doi: 10.1016/j.placenta.2004.11.007

231. Redman CWG, Sargent IL. Immunology of pre-eclampsia. *Am J Reprod Immunol* (2010) 63:534–43. doi: 10.1111/j.1600-0897.2010.00831.x

232. Sargent IL, Borzychowski AM, Redman CWG. NK cells and human pregnancy–an inflammatory view. *Trends Immunol* (2006) 27:399–404. doi: 10.1016/j.it.2006.06.009

233. Sargent IL, Borzychowski AM, Redman CWG. Immunoregulation in normal pregnancy and pre-eclampsia: an overview. *Reprod Biomed Online* (2006) 13:680–6. doi: 10.1016/s1472-6483(10)60659-1

234. Williams C, Royo F, Aizpurua-Olaizola O, Pazos R, Boons GJ, Reichardt NC, et al. Glycosylation of extracellular vesicles: current knowledge, tools and clinical perspectives. *J Extracell. Vesicles* (2018) 7:1442985. doi: 10.1080/20013078.2018.1442985

235. Harada Y, Ohkawa Y, Maeda K, Kizuka Y, Taniguchi N. Extracellular vesicles and glycosylation. *Adv Exp Med Biol* (2021) 1325:37–149. doi: 10.1007/978-3-030-70115-4_6

236. Tannetta D, Masliukaite I, Vatish M, Redman C, Sargent I. Update of syncytiotrophoblast derived extracellular vesicles in normal pregnancy and preeclampsia. *J Reprod Immunol* (2017) 119:98–106. doi: 10.1016/J.JRI.2016.08.008

237. Henao DE, Mathieson PW, Saleem MA, Bueno JC, Cadavid A. A novel renal perspective of preeclampsia: a look from the podocyte. *Nephrol Dial Transplant* (2007) 22:1477. doi: 10.1093/ndt/gfl804

238. Henao DE, Saleem MA, Cadavid AP. Glomerular disturbances in preeclampsia: disruption between glomerular endothelium and podocyte symbiosis. *Hypertens Pregnancy* (2010) 29:10–20. doi: 10.3109/10641950802631036

239. Henao DE, Saleem MA. Proteinuria in preeclampsia from a podocyte injury perspective. *Curr Hypertens Rep* (2013) 15:600–5. doi: 10.1007/s11906-013-0400-1

240. Singh A, Satchell SC, Neal CR, McKenzie E, Tooke JE, Mathieson PW. Glomerular endothelial glycocalyx constitutes a barrier to protein permeability. *J Am Soc Nephrol* (2007) 18:2885–93. doi: 10.1681/ASN.2007010119

241. Chaouat G. Inflammation, NK cells and implantation: friend and foe (the good, the bad and the ugly?): replacing placental viviparity in an evolutionary perspective. *J Reprod Immunol* (2013) 97:2–13. doi: 10.1016/j.jri.2012.10.009

242. Chaouat G, Ledée-Bataille N, Dubanchet S. Immunological similarities between implantation and preeclampsia. *Am J Reprod Immunol* (2005) 53:222–9. doi: 10.1111/J.1600-0897.2005.00269.X

243. Clark DA, Chaouat G, Wong K, Gorczynski RM, Kinsky R. Tolerance mechanisms in pregnancy: a reappraisal of the role of class I paternal MHC antigens. *Am J Reprod Immunol* (2010) 63:93–103. doi: 10.1111/j.1600-0897.2009.00774.x

244. Chaouat G, Petitbarat M, Bulla R, Dubanchet S, Valdivia K, Ledée N, et al. Early regulators in abortion and implications for a preeclampsia model. *J Reprod Immunol* (2009) 82:131–40. doi: 10.1016/j.jri.2009.08.004

245. Robillard P, Dekker G, Chaouat G, Elliot MG, Scioscia M, Néonatologie S, et al. High incidence of early onset preeclampsia is probably the rule and not the exception worldwide . 20th anniversary of the reunion workshop . a summary. *J Reprod Immunol* (2019) 133:30–6. doi: 10.1016/j.jri.2019.05.003

246. Kane N, Kelly R, Saunders PTK, Critchley HOD. Proliferation of uterine natural killer cells is induced by human chorionic gonadotropin and mediated *via* the mannose receptor. *Endocrinology* (2009) 150:2882–8. doi: 10.1210/en.2008-1309

247. Berndt S, Blacher S, Munaut C, Detilleux J, Perrier d'Hauterive S, Huhtaniemi I, et al. Hyperglycosylated human chorionic gonadotropin stimulates angiogenesis through TGF-β receptor activation. *FASEB J* (2013) 27:1309–21. doi: 10.1096/fj.12-213686

248. Blois SM, Ilarregui JM, Tometten M, Garcia M, Orsal AS, Cordo-Russo R, et al. A pivotal role for galectin-1 in fetomaternal tolerance. *Nat Med* (2007) 131450–7. doi: 10.1038/nm1680

249. Molvarec A, Blois SM, Stenczer B, Toldi G, Tirado-Gonzalez I, Ito M, et al. Peripheral blood galectin-1-expressing T and natural killer cells in normal pregnancy and preeclampsia. *Clin Immunol* (2011) 139:48–56. doi: 10.1016/j.clim.2010.12.018

250. Borowski S, Tirado-Gonzalez I, Freitag N, Garcia MG, Barrientos G, Blois SM. Altered glycosylation contributes to placental dysfunction upon early disruption of the NK cell-DC dynamics. *Front Immunol* (2020) 11:1316. doi: 10.3389/fimmu.2020.01316

251. Sukhikh GT, Ziganshina MM, Nizyaeva NV, Kulikova GV, Volkova JS, Yarotskaya EL, et al. Differences of glycocalyx composition in the structural elements of placenta in preeclampsia. *Placenta* (2016) 43:69–76. doi: 10.1016/j.placenta.2016.05.002

frontiers | Frontiers in Endocrinology

TYPE Review
PUBLISHED 19 May 2023
DOI 10.3389/fendo.2023.1130139

Check for updates

OPEN ACCESS

EDITED BY
Lawrence Merle Nelson,
Mary Elizabeth Conover Foundation, Inc.,
United States

REVIEWED BY
Shujie Liao,
Huazhong University of Science and Technology, China
Stepan Feduniw,
University Zürich, Switzerland

*CORRESPONDENCE
Enrique Guzmán-Gutiérrez
eguzman@udec.cl
Juan Araya
jarayaq@udec.cl

RECEIVED 22 December 2022
ACCEPTED 04 May 2023
PUBLISHED 19 May 2023

CITATION
Mennickent D, Rodríguez A, Opazo MC, Riedel CA, Castro E, Eriz-Salinas A, Appel-Rubio J, Aguayo C, Damiano AE, Guzmán-Gutiérrez E and Araya J (2023) Machine learning applied in maternal and fetal health: a narrative review focused on pregnancy diseases and complications. *Front. Endocrinol.* 14:1130139. doi: 10.3389/fendo.2023.1130139

COPYRIGHT
© 2023 Mennickent, Rodríguez, Opazo, Riedel, Castro, Eriz-Salinas, Appel-Rubio, Aguayo, Damiano, Guzmán-Gutiérrez and Araya. This is an open-access article distributed under the terms of the Creative Commons Attribution License (CC BY). The use, distribution or reproduction in other forums is permitted, provided the original author(s) and the copyright owner(s) are credited and that the original publication in this journal is cited, in accordance with accepted academic practice. No use, distribution or reproduction is permitted which does not comply with these terms.

Machine learning applied in maternal and fetal health: a narrative review focused on pregnancy diseases and complications

Daniela Mennickent[1,2,3], Andrés Rodríguez[3,4], Ma. Cecilia Opazo[5,6], Claudia A. Riedel[6,7], Erica Castro[8], Alma Eriz-Salinas[9], Javiera Appel-Rubio[1], Claudio Aguayo[1], Alicia E. Damiano[10,11], Enrique Guzmán-Gutiérrez[1,3]* and Juan Araya[2,3]*

[1]Departamento de Bioquímica Clínica e Inmunología, Facultad de Farmacia, Universidad de Concepción, Concepción, Chile, [2]Departamento de Análisis Instrumental, Facultad de Farmacia, Universidad de Concepción, Concepción, Chile, [3]Machine Learning Applied in Biomedicine (MLAB), Concepción, Chile, [4]Departamento de Ciencias Básicas, Facultad de Ciencias, Universidad del Bío-Bío, Chillán, Chile, [5]Instituto de Ciencias Naturales, Facultad de Medicina Veterinaria y Agronomía, Universidad de Las Américas, Santiago, Chile, [6]Millennium Institute on Immunology and Immunotherapy, Santiago, Chile, [7]Departamento de Ciencias Biológicas, Facultad de Ciencias de la Vida, Universidad Andrés Bello, Santiago, Chile, [8]Departamento de Obstetricia y Puericultura, Facultad de Ciencias de la Salud, Universidad de Atacama, Copiapó, Chile, [9]Departamento de Obstetricia y Puericultura, Facultad de Medicina, Universidad de Concepción, Concepción, Chile, [10]Cátedra de Biología Celular y Molecular, Departamento de Ciencias Biológicas, Facultad de Farmacia y Bioquímica, Universidad de Buenos Aires, Buenos Aires, Argentina, [11]Laboratorio de Biología de la Reproducción, Instituto de Fisiología y Biofísica Bernardo Houssay (IFIBIO-Houssay)- CONICET, Universidad de Buenos Aires, Buenos Aires, Argentina

Introduction: Machine learning (ML) corresponds to a wide variety of methods that use mathematics, statistics and computational science to learn from multiple variables simultaneously. By means of pattern recognition, ML methods are able to find hidden correlations and accomplish accurate predictions regarding different conditions. ML has been successfully used to solve varied problems in different areas of science, such as psychology, economics, biology and chemistry. Therefore, we wondered how far it has penetrated into the field of obstetrics and gynecology.

Aim: To describe the state of art regarding the use of ML in the context of pregnancy diseases and complications.

Methodology: Publications were searched in PubMed, Web of Science and Google Scholar. Seven subjects of interest were considered: gestational diabetes mellitus, preeclampsia, perinatal death, spontaneous abortion, preterm birth, cesarean section, and fetal malformations.

Current state: ML has been widely applied in all the included subjects. Its uses are varied, the most common being the prediction of perinatal disorders. Other ML applications include (but are not restricted to) biomarker discovery, risk estimation, correlation assessment, pharmacological treatment prediction, drug screening,

data acquisition and data extraction. Most of the reviewed articles were published in the last five years. The most employed ML methods in the field are non-linear. Except for logistic regression, linear methods are rarely used.

Future challenges: To improve data recording, storage and update in medical and research settings from different realities. To develop more accurate and understandable ML models using data from cutting-edge instruments. To carry out validation and impact analysis studies of currently existing high-accuracy ML models.

Conclusion: The use of ML in pregnancy diseases and complications is quite recent, and has increased over the last few years. The applications are varied and point not only to the diagnosis, but also to the management, treatment, and pathophysiological understanding of perinatal alterations. Facing the challenges that come with working with different types of data, the handling of increasingly large amounts of information, the development of emerging technologies, and the need of translational studies, it is expected that the use of ML continue growing in the field of obstetrics and gynecology.

KEYWORDS

machine learning, artificial intelligence, pregnancy diseases, pregnancy complications, adverse perinatal outcomes

1 Introduction

Pregnancy is a physiological process that provides all conditions for normal fetus growth and subsequent birth. Due to certain circumstances, a seemingly normal pregnant woman starts with physiological disorders that can trigger pregnancy diseases (e.g. gestational diabetes mellitus and preeclampsia) or other perinatal complications (e.g. stillbirth, cesarian section, macrosomia and respiratory distress). The search for new strategies for early diagnosis, screening and risk determination could reduce the severity of these alterations and also the negative impact in both mother's and offspring's health. Interestingly, in recent years, machine learning (ML) has been used to find solutions for these problems.

ML corresponds to a wide variety of methods that use mathematics, statistics and computational science to learn from multivariate data. By means of pattern recognition performed on various measured variables, different algorithms are able to find correlations, often hidden to the human eye, and perform accurate predictions about different conditions, such as the belonging of an individual to a certain group or class, or the concentration of a particular biomarker in a sample of interest.

Multivariate methods (i.e. those employed to analyze the behavior of multiple variables simultaneously) have been used for several decades to solve problems in different areas of knowledge, such as psychology, economics, biology, chemistry, etc. However, in the clinical field these tools have begun to penetrate only recently. Remarkably, the use of these tools has received different names throughout history depending on the area of application, i.e. psychometrics in psychology, biometrics in biology, chemometrics in chemistry, etc. In the last years it has become popular to address to these methods as artificial intelligence, ML, data mining, or in a more general sense, data science. The boundaries between the scopes of these different terms are still a subject of debate, and several different opinions and definitions can be found in specialized literature (1, 2). However, unconcerned of this debate, it seems that ML has been the preferred name used in healthcare-related studies, therefore that will be the term used in this manuscript.

One of the most common applications of ML in biomedicine is the detection or prediction of particular pathological conditions (3). It seems logical that in pregnancy the focus has also been in diagnostics (4, 5). However, as it has been evidenced in different disciplines, ML can also be used for other purposes, such as identification of important variables in a system or process, correlation analysis, data management and extraction, noise removal, dimensionality reduction, among others (6, 7). Given the success ML has had in other areas of science, we wondered how far it has penetrated into the field of obstetrics and gynecology. In this review we propose to describe the state of art regarding the use of ML in the context of pregnancy diseases and complications, including its capability for early diagnosis, screening and risk determination, and also other applications of this versatile tool.

2 Methodology

2.1 Type of study and search strategy

This is a narrative review. Publications regarding the use of ML in maternal and fetal health were searched in different databases,

including PubMed, Web of Science and Google Scholar. Seven subjects of interest were considered as representative conditions of the vast domain of obstetrics and gynecology, due to their prevalence and clinical relevance (8): gestational diabetes mellitus, preeclampsia, perinatal death, spontaneous abortion, preterm birth, cesarean section, and fetal malformations.

2.2 Information synthesis

The papers main results were summarized in tables, comprising input, ML technique and output. Tables should be understood as follows: each table is associated with a specific pregnancy disease or complication, as stated on the table's title. For every table, each row refers to a particular study. For each reference (first column), the input, the ML technique and the output (third, fourth and fifth columns, respectively) are directly linked to the ML application (second column) of that study. Most of the tabulated information is written and further extended in the text related to each table.

2.3 Manuscript organization

This manuscript is organized as follows: section 3 gives a general overview on ML-related definitions and concepts, section 4 describes different ML applications in the context of pregnancy diseases and complications, addressed from the highest to the lowest prevalence, section 5 discusses the current state and future challenges in the field, and section 6 rounds off with a brief conclusion.

3 ML: definitions and concepts

ML models can have varied purposes. The most typical one is early detection, but they can also be used for alternative screening, risk estimation, correlation assessment, biomarker discovery, among other possible applications.

In very simple terms, the development of a ML model requires three main parts: the input, the ML technique and the output.

The input is the data that is used to build the ML model. It consists of samples (usually in the biomedical field, the subjects) and variables, which can be very diverse. There is discrete data, e.g. the information retrieved from questionaries; the clinical and biochemical data found in physical and electronic health records (EHR); and the metabolites, peptides/proteins, transcripts or genes identified as relevant in omics studies. Likewise, there is continuous data, e.g. the traces obtained by Doppler ultrasonography, electrohysterography (EHG) or cardiotocography (CTG); and the images recorded by ultrasonography, computed tomography (CT) or echocardiography. The type of data determines what kind of pretreatment has to be performed prior to ML analysis, an aspect that is described in detail elsewhere (9, 10).

The selection of the ML technique depends on the purpose of the study. Non-supervised techniques are used to explore the data, i.e. to assess if there is any spontaneous clustering or correlation between samples and/or variables. Typical examples of non-supervised techniques are principal component analysis (PCA) and K-means. In contrast, supervised techniques are used to predict a property. In the ML field, the word "prediction" refers to the forecast of future behaviors or unobserved outcomes (11). In particular, classification ML techniques allow to predict a class or category, e.g. healthy or diseased; whereas regression ML techniques allow to predict a continuous quantity, e.g. the concentration of a specific biomarker. Moreover, supervised techniques can be linear or non-linear, depending on the nature of the mathematical function that underlies the classification or regression task. The most common linear classifiers are logistic regression (LR) and linear discriminant analysis (LDA), while some examples of linear regression techniques are linear regression and partial least squares (PLS). On the other hand, random forest (RF), support vector machines (SVM) and neural networks (NN) are classical examples of non-linear ML techniques that allow to perform both classification and regression analyses.

The output is the result of having applied the ML model. The most common outputs are those that account for the model predictive performance. In classification, the performance is typically expressed using parameters such as sensitivity, specificity, accuracy and area under the receiver operating characteristic curve (AUC). In regression, other parameters, such as mean absolute error and root mean squared error (RMSE), are used. These and other performance metrics are well described in literature (12, 13). It is important to mention that the aforementioned metrics can be calculated in different stages of the model's development: training, internal validation and external validation. The ideal situation is that the model is tested in all the three stages, to ensure it will be accurate and useful in different populations. This idea has been discussed in greater depth by other authors (14, 15). Another very common output is variable importance. This information allows to identify the variables that contribute the most to predict the property under study, which is useful to identify new biomarkers for a certain condition. There are other possible outputs, depending on the ML application. They are addressed and discussed throughout section 4.

4 ML in pregnancy diseases and complications: applications

4.1 Pregnancy diseases

4.1.1 Gestational diabetes mellitus

The American Diabetes Association defines gestational diabetes mellitus (GDM) as a "diabetes diagnosed in the second or third trimester of pregnancy that was not clearly overt diabetes prior to gestation" (16). This disease has been related to several negative outcomes on maternal and fetal health. In the short-term, it increases the risk of pre-eclampsia, preterm delivery, macrosomia and clinical neonatal hypoglycemia; and in the long-term, of maternal prediabetes, maternal diabetes, offspring obesity and offspring impaired fasting glucose (17).

ML has been applied in GDM research, for diverse purposes (Table 1).

4.1.1.1 ML for GDM prediction

Numerous studies that have applied ML in the context of GDM, have used it to predict this disease at early stages of pregnancy (32). Some of them have based their predictive models on a small number of variables. For example, Xiong et al. assessed hepatic, renal and coagulation function biochemical data to predict GDM at 10-19 gestational weeks (18). Univariate analysis showed that coagulation parameters differed between GDM and control women, so they combined two of them, patient prothrombin time and reference activated partial thromboplastin time, to build different ML predictive models. They achieved AUCs of 99.83% and 99.74% by light gradient boosting and SVM, respectively. Likewise, Zheng et al. used known GDM clinical and biochemical risk factors to predict it at 8-20 gestational weeks (19). By Bayesian adaptive sampling, they selected four maternal variables, maternal age, pre-pregnancy body mass index (BMI), fasting plasma glucose and triglycerides, and then used them to generate a multivariate Bayesian logistic regression model. They got an AUC of 0.766. In contrast, some articles have based their predictive models on a large number of variables. For instance, Wu et al. assessed 73 maternal clinical and biochemical variables and different ML techniques for GDM prediction before 12 gestational weeks (20). Their deep neural networks (DNN) model achieved an AUC of 0.80. Furthermore, they built a simpler model in order to facilitate clinical application. By using seven sequential feature selection chosen variables and LR they got an AUC of 0.77. Similarly, Artzi et al. used 2355 variables from EHR and gradient boosting (GB) to predict GDM before 20 gestational weeks, and obtained an AUC of 0.85 (21). They also built a simpler model to ease clinical implementation. Their nine questions based model yielded an AUC of 0.80. Interestingly, both the full and the simplified models outperformed a baseline score, which involved seven GDM known risk factors and got an AUC of 0.68.

It is worth mentioning that some papers that have sought GDM prediction, have also revealed GDM novel risk factors. That is the case of Artzi et al. study, in which the most important predictor of their full model was the prior pregnancy glucose challenge test result, a previously unreported risk factor for GDM (21). Likewise, Balani et al. used clinical data and different ML techniques to predict GDM in obese pregnant women at 14-17 gestational weeks (22). Their RF model achieved an accuracy of 77.53%, and showed

TABLE 1 ML applications in GDM research.

Reference	ML application	Input	ML technique	Main output
(18)	Disease prediction	Biochemical markers	Light GB	AUC = 99.83%, Se = 92.5% and Sp = 99.2%
(19)	Disease prediction	Clinical and biochemical factors	Bayesian LR	AUC = 0.766, Ac = 0.64, Se = 0.66 and Sp = 0.75
(20)	Disease prediction	Electronic health records	DNN	AUC = 0.80, Se = 63%, Sp = 82% and YI = 0.45
(21)	Disease prediction	Electronic health records	GB	AUC = 0.850 and AUPR = 0.324
(22)	Disease prediction	Clinical parameters	RF	Ac = 77.53%
(23)	Disease prediction, independent of diagnostic criteria	Clinical and biochemical factors	PLS	RMSE = 23.1, RE = 20.7% and r = 0.259 for post load glycemia prediction
(24)	Biomarker discovery	Metabolomics data	OPLS-DA	Formic acid, dimethylamine and galactose as novel biomarkers
(25)	Biomarker discovery	Transcriptomics data	LR	miR-223 and miR-23a as novel biomarkers
(26)	Biomarker discovery	Genomics data	LR	CC2D2B, NAT10, SIPA1, ZNF565, ZNF552, WDR35, MICALL1, CTNNB1, CLOCK, BCKDHB and TGIF2LY as novel biomarkers
(27)	Biomarker discovery	Epigenomics data	LR	cg11169102, cg21179618 and cg21620107 as novel biomarkers
(28)	Risk estimation	Physical activity questionnaire data	SL-EL	2.1 fewer cases of GDM per 100 women for moderate to vigorous intensity exercise
(29)	Disease screening	Spectrochemical data	LDA	Ac = 100%, Se = 100% and Sp = 100%
(30)	Correlation assessment	Clinical and biochemical factors	PCA	Strong correlation between maternal thyroid profile and GDM
(31)	Pharmacological treatment prediction	Mobile real-time collected data	LR	AUC = 0.8

ML, machine learning; GDM, gestational diabetes mellitus; GB, gradient boosting; LR, logistic regression; DNN, deep neural networks; RF, random forest; PLS, partial least squares; OPLS-DA, orthogonal PLS discriminant analysis; SL-EL, SuperLearner with extra learners; LDA, linear discriminant analysis; PCA, principal component analysis; AUC, area under the receiver operating characteristic curve; Se, sensitivity; Sp, specificity; Ac, accuracy; YI, Youden index; AUPR, area under the precision-recall curve; RMSE, root mean squared error; RE, relative error.

that the most relevant predictor was visceral fat mass, a previously unknown risk factor for GDM.

In addition, it is interesting to notice that all the aforementioned studies reported models that allow to predict GDM, but that are restricted to do so under a particular diagnostic criteria. Recently, Mennickent et al. reported a novel strategy that overcomes that limitation (23). The authors used first trimester clinical and biochemical data and PLS to predict the very post load glycemia value that pregnant women would have at 24-28 gestational weeks. Since the predicted value can be interpreted as control or GDM with any diagnostic criteria, the prediction of GDM is no longer restricted to a particular criteria. Their best model allowed to predict the second trimester post load glycemia with a RMSE of 23.1 and a relative error of 20.7% in cross-validation analyses.

4.1.1.2 ML for GDM biomarker discovery

Several studies have applied ML to search new biological markers for GDM. This has been typically done by means of omics techniques. For example, Scott et al. used ^{1}H-NMR metabolomics and 14-27 gestational weeks urine samples to find novel biomarkers for GDM (24). Their statistically significant metabolites, identified through variable importance analysis based on random variable combination, were tested for classification by orthogonal partial least squares discriminant analysis, and achieved an AUC of 0.803. The top three metabolic markers for that model were formic acid, dimethylamine and galactose, which were downregulated in GDM. Similarly, Yoffe et al. applied a targeted transcriptomics approach and 9-11 gestational weeks plasma samples to identify miRNAs that could serve as early biomarkers for GDM (25). Based on multiplex expression assays and RT-qPCR data and DESeq2 analyses, they found two differentially expressed miRNAs, miR-223 and miR-23a, which were upregulated in GDM. These miRNA markers were combined and assessed for classification by LR, and reached an AUC of 0.91. Another case is the study of Guo et al., who used a genomics strategy and 18 or less gestational weeks plasma samples to find cfDNA biosignatures that could be useful for GDM detection at early stages of pregnancy (26). Based on whole-genome sequencing and qPCR promoter profiling data, they identified 800 differentially expressed genes between GDM and control women. Eleven of those genes, CC2D2B, NAT10, SIPA1, ZNF565, ZNF552, WDR35, MICALL1, CTNNB1, CLOCK, BCKDHB and TGIF2LY, were selected by a step-wise feature selection method, and then combined and tested for classification by LR. The eleven marker based model yielded an overall accuracy of 72.1%. Likewise, Liu et al. applied an epigenomics approach to identify CpG markers for GDM (27). They used DNA methylation data from two previous studies, in which placenta samples from GDM and control mothers, and blood samples from children born in GDM and control pregnancies were analyzed. By an overlapped CpGassoc epigenome-wide association study they identified nine differentially methylated CpGs between GDM and control subjects. The LR model built with five of them revealed that the most important CpGs for GDM and control samples differentiation were cg11169102, cg21179618 and cg21620107. The combination of those three biomarkers was assessed for classification by the same ML technique, and achieved an AUC of 0.8519.

4.1.1.3 Other ML applications in GDM research

Some GDM studies have used ML for other purposes, such as risk estimation, screening, correlation assessment and management. For instance, Ehrlich et al. aimed to evaluate the effect of exercise during the first trimester of pregnancy on the risk of GDM (28). Data from a pregnancy physical activity questionnaire, effected at 10-13 gestational weeks, were analyzed by different ML techniques. Their targeted maximum likelihood estimation (TMLE) and SuperLearner (SL) method with extra learners model showed that meeting or exceeding the cohort's 75th percentile of moderate to vigorous intensity exercise reduced the risk of GDM by 2.1 fewer cases per 100 women. Another example is Bernardes-Oliveira et al. study. They intended to develop a fast and low-cost screening tool for GDM, using 9-39 gestational weeks plasma samples, attenuated total reflection Fourier-transform infrared spectroscopy and ML techniques (29). Their genetic algorithm with LDA model, which comprised ten wavenumbers mainly from lipids and proteins spectral regions, achieved an accuracy of 100%. A different case is the study of Araya et al., who meant to determine whether there was a correlation between the maternal thyroid profile and GDM (30). Using clinical and biochemical data registered at 10-14 and 24-28 gestational weeks, and PCA, they demonstrated that maternal thyroid-related hormones from the first and the second trimesters of pregnancy were strongly correlated with GDM. Finally, Velardo et al. aimed to develop a ML tool capable to improve the timeliness of GDM management (31). They used mobile health real-time collected data and different ML techniques to automatically evaluate the switch from diet-based management to pharmacological treatment. Data included blood glucose levels measured at different time points, maternal age, BMI and other GDM clinical risk factors. Their lasso feature selection LR model allowed to predict the timing of initiation of pharmacotherapy with an AUC of 0.8.

4.1.2 Preeclampsia

Preeclampsia (PE) is a pregnancy syndrome that presents two different clinical scenarios, both characterized by the development of maternal hypertension from the 20th week of gestation, an alteration that persists throughout pregnancy. The first of the scenarios is characterized by a moderate form of PE, which symptoms become evident late, from 34 weeks of gestation. It is characterized by blood pressure ≥140/90 mmHg, and other symptoms that indicate liver or renal damage, thrombocytopenia or proteinuria ≥3g/24h, and by not inducing alterations on fetal growth. The second of the scenarios correspond to a severe form of PE, which symptoms become evident before 34 weeks of gestation. It is characterized by blood pressure ≥160/110 mmHg, multisystemic damage and/or proteinuria ≥5g/24h, and for being generally associated with intrauterine growth retardation (IUGR) (33). These conditions can also lead to more serious situations than PE alone, such as HELLP syndrome and eclampsia, which is a severe form of PE accompanied by seizures (34). Severe forms of PE

are associated with at least two times the risk of IUGR, and fetal and neonatal death (35). The origin of PE is still unknown, however, the most accepted hypothesis indicates that the placenta does not form properly. The latter would not allow a correct flow of maternal blood towards the placenta, triggering a compensatory response that would increase blood pressure to meet the metabolic requirements of the fetus in gestation. This process would begin during the first trimester of pregnancy, producing serious effects on the mother, and affecting the fetus during the second and third trimesters of pregnancy (36). Thus, the early detection of PE, i.e. before the appearance of adverse symptoms in the mother, is necessary.

The early detection of PE has been assessed through the determination of the levels of human chorionic gonadotropin (37), anti-Müllerian hormone (38), sFlt-1 (39), the soluble form of Endoglin (40), among others, with sensitivities between 20 and 80%, and specificities between 40 and 90%. Interestingly, algorithms mediated by ML have been proposed as new strategies to predict this pathology earlier (Table 2). Various ML models have been developed for PE prediction using different types of variables, such as metabolites (41), proteins (42), plasma DNA (26) and circular RNA (43), but by far the most common approaches are based on maternal medical data (44–51).

Some ML-based studies have aimed to predict PE before 20 weeks of pregnancy. For example, Marić et al. used clinical and biochemical maternal data and different ML techniques to predict this pregnancy complication before 16 gestational weeks. Their elastic net (EN) model achieved an AUC of 0.79 for all cases of PE,

TABLE 2 ML applications in PE research.

Reference	ML application	Input	ML technique	Main output
(41)	Disease prediction	Metabolomics data	LR	AUC = 0.868, Se = 75.1% and Sp = 83.0%
(42)	Disease prediction	Proteomics data	LDA	AUC = 0.96, Se = 0.90 and Sp = 0.90 for early-onset cases with maternal vascular malperfusion
(26)	Disease prediction	Genomics data	LR	AUC = 0.825, Ac = 83.0%, Se = 81.7% and Sp = 83.3%
(43)	Disease prediction	Transcriptomics data and biochemical markers	LR	AUC = 0.940, Se = 86.67% and Sp = 96.67%
(44)	Disease prediction	Biochemical markers	BPNN	Ac = 79.8%
(45)	Disease prediction	Electronic health records	Stochastic GB	AUC = 0.924, Ac = 0.973, Se = 0.603, Sp = 0.991 and DR = 0.771 for late-onset cases
(46)	Disease prediction	Electronic health records	EN	AUC = 0.89, Se = 72.3% and Sp = 91.2% for early-onset cases
(47)	Disease prediction	Clinical and biochemical factors	LR	AUC = 0.962, Se = 79.3%, Sp = 97.7%, PPV = 92% and NPV = 93.4%
(48)	Disease prediction	Clinical and biochemical factors	LR	AUC = 0.68, Se = 30.6% and Sp = 90% for early-onset cases
(49)	Disease prediction	Clinical and biochemical factors	RF	AUC = 0.976, AUPR = 0.958, Ac = 92.6%, Se = 91% and Sp = 93% for placental dysfunction-related disorders
(50)	Disease prediction	Clinical parameters	RF	AUC = 0.90, Se = 0.70, Sp = 0.89 and Pr = 0.88
(51)	Disease prediction	Ultrasound images	CNN	Se = 70.6% and Sp = 76.6% for hypertension disorders of pregnancy
(52)	Biomarker discovery	Genomics data	SVM	IL7R, IL18, CCL2, HLA-DRA, CD247, ITK, CD2, IRF8, CD48, GZMK, CCR7, HLA-DPA1, LEP, IL1B, CD8A, CD3D and GZMA as novel biomarkers
(53)	Biomarker discovery	Transcriptomics data	C4.5, AB and MLP	HTRA4, PROCR, MYCN, ERO1A, EAF1, PPP1R16B, CRH, FLNB, PIK3CB, PLAAT3, FBN2, RFLNB, and TKT as novel biomarkers
(54)	Risk estimation	Food frequency questionnaire data	SL	3.2 and 4.0 fewer cases of PE per 100 births for high density fruit and vegetable intake
(55)	Drug screening	Drug databases information	TPOTC	Estradiol, estriol, vitamins E and D, lynestrenol, mifrepristone, simvastatin, ambroxol, and some antibiotics and antiparasitics as potential drugs for PE

ML, machine learning; PE, preeclampsia; LR, logistic regression; LDA, linear discriminant analysis; BPNN, back-propagation neural networks; GB, gradient boosting; EN, elastic net; RF, random forest; CNN, convolutional neural networks; SVM, support vector machines; AB, adaptative boosting; MLP, multilayer perceptron; SL, SuperLearner; TPOTC, tree-based pipeline optimization tool classifier; AUC, area under the receiver operating characteristic curve; Se, sensitivity; Sp, specificity; Ac, accuracy; DR, detection rate; PPV, positive predictive value; NPV, negative predictive value; AUPR, area under the precision-recall curve; Pr, precision.

and an AUC of 0.89 for early-onset PE, showing that ML approaches can become a powerful early prediction tool for this obstetric disorder (46). Sandstrom et al. also used clinical and biochemical maternal variables and different ML techniques to predict PE, but before 15 weeks of gestation. Their LR model with 12 pre-specified variables yielded AUCs of 0.68, 0.68 and 0.67 for PE with delivery <34, <37 and ≥37 weeks of pregnancy, respectively (48). A different example is the study of Gupta et al., who aimed to predict hypertensive disorders of pregnancy, including PE, with placenta ultrasound images from the first trimester of gestation. The analysis of abnormal placental image texture with deep convolutional neural networks (CNN) achieved a sensitivity of 70.6% and a specificity of 76.6% (51). In contrast to the aforementioned articles, other ML-based studies have intended to predict PE from 20 weeks of gestation onwards. For instance, Han et al. measured 25 parameters of maternal clinical chemistry before PE clinical diagnosis, and combined them to predict this pregnancy disorder. Their back-propagation neural networks (BPNN) model, which strongest predictors were ALB, MPV, BUN, LDH and TG, displayed an accuracy of 79.8% (44). Likewise, Jhee et al. retrieved maternal data (collected between 14 and 34 weeks of pregnancy) from EHR and tested them to predict late-onset PE. Their ML models, based on decision trees (DT), naïve Bayes (NB), SVM, RF, stochastic GB, and LR reached AUCs of 0.857, 0.776, 0.573, 0.894, 0.924 and 0.806, respectively (45).

Other PE-related studies have applied ML in additional contexts, such as biomarker identification, risk estimation and drug screening. For example, Liu et al. analyzed microarray data to identify hub genes as diagnostic biomarkers of PE. Their bioinformatics approach revealed 17 differentially expressed hub genes between PE and control subjects: IL7R, IL18, CCL2, HLA-DRA, CD247, ITK, CD2, IRF8, CD48, GZMK, CCR7, HLA-DPA1, LEP, IL1B, CD8A, CD3D and GZMA. Those hub genes were combined and assessed for classification by SVM. Their model reached an AUC of 0.958 in the training set, and an AUC of 0.834 in the test set (52). Similarly, Guo et al. screened placental mRNA data to identify PE biomarkers. Their ML-based approach allowed them to select a subset of 13 mRNA features: HTRA4, PROCR, MYCN, ERO1A, EAF1, PPP1R16B, CRH, FLNB, PIK3CB, PLAAT3, FBN2, RFLNB, and TKT, which were combined and tested for PE and control subjects classification by ML. Their model, which fused three ML classifiers, C4.5, AdaBoost and multilayer perceptron, yielded an accuracy of 82.2% (53). A different case is the study of Bodnar et al., who aimed to assess the effect of fruit and vegetable intake and dietary synergy on the risk of various adverse pregnancy outcomes. Their SL with TMLE ML model revealed that high fruit and vegetable densities were associated with 3.2 and 4.0 fewer cases of PE per 100 births, respectively (54). A final example is the article of Tejera et al., who developed a ML-based strategy to identify currently existing drugs that could be repurposed for PE management. Their approach was built on pharmacological targets of drugs under clinical trial for PE, and was designed to exclude those that have shown negative effects in pregnancy. Their ML-based virtual screening identified estradiol, estriol, vitamins E and D, lynestrenol, mifrepristone, simvastatin, ambroxol, and some antibiotics and antiparasitics as potential drugs for PE treatment (55).

4.2 Pregnancy complications

4.2.1 Perinatal death

The World Health Organization (WHO) defines perinatal deaths as those that occur from late stillbirth, i.e. after 28 weeks of gestation, up to 28 days of extra-uterine life, including late neonatal deaths (56). Worldwide, more than 5 million perinatal deaths happen every year (57). Progress in reducing the high numbers of stillbirths and neonatal deaths has been slow. Even though the rate of perinatal deaths has been lowered in developed countries, its reduction in low- and middle-income countries has been insufficient. Indeed, low- and middle-income countries present the highest rates and the slowest reduction (58, 59). The Sustainable Development Goals set by the United Nations General Assembly include to put an end to the avoidable deaths of newborns by 2030 (60), however, during 2019 there were approximately 7000 newborns deaths each day (61). These numbers highlight the necessity to implement new methods and techniques to identify high-risk pregnancies, early enough to be able to provide them personalized attention so as to improve prevention, or reduce risk and perinatal death.

4.2.1.1 Stillbirth

Studies to predict pregnancies with high risk of perinatal death have been difficult due to small sample size (62). This, along with the difficulty posed by a relatively high percentage of missing data, forces researchers to look for strategies to impute missing data or lose variables to avoid biased results (63). Routinely collected perinatal records have a great potential to improve the risk assessment of perinatal death, by providing massive databases that are available for researchers to develop and test ML-based models (Table 3). These records are commonly composed of maternal demographic and medical history information, which can be used as predictors. The high amount of data available in these records also allows to have appropriate validation sets to assess the quality of the prediction. Koivu et al. used publicly available data obtained from the US Centers for Disease Control and Prevention, to build ML-based risk prediction models for early stillbirth, late stillbirth and preterm birth (PTB) pregnancies (64). Using only maternal demographic and medical history data (pregnancy and sexual transmitted diseases) from almost 16 million pregnancies, of which 92,753 were infant deaths, they achieved AUCs of 0.76 for early stillbirth, 0.63 for late stillbirth and 0.64 for PTB. Those results were obtained using an algorithm based on self-normalizing neural networks. An important highlight of this study is that model validation was performed using an external set from a different population, which is the strictest and most reliable type of validation, often resulting in lower performances compared to other more permissive validation methods (such as resampling methods), which are prone to overfitting.

TABLE 3 ML applications in perinatal death research.

Reference	ML application	Input	ML technique	Main output
(62)	Complication prediction	Clinical parameters	Extreme GB	AUC = 0.842, Ac = 94.71%, Se = 45.3%, Sp = 95%, PPV = 4.81%, NPV = 99.68%, +LR = 9.03 and -LR = 0.58 for stillbirth
(63)	Complication prediction	Clinical parameters	LR	AUC = 0.82 for stillbirth
(64)	Complication prediction	Clinical parameters	SNNN	AUC = 0.76, Se = 38% and Sp = 90% for early stillbirth
(65)	Complication prediction	Clinical parameters	LR	AUC = 0.872 for neonatal death
(66)	Complication prediction	Clinical parameters	RF	AUC = 0.79, Ac = 0.87, Se = 0.54, Sp = 0.88, PPV = 0.15 and NPV = 0.98
(67)	Complication prediction	Clinical parameters	DT, GB, LR, RF and SVM	AUC = 90.00%, Ac = 90.56%, Se = 91.37%, Sp = 88.10%, Pr = 88.02% and F1 = 90.58% for stillbirth before delivery and during labor
(68)	Complication prediction	Clinical parameters	MLP	AUC = 95.99%, Ac = 96.79%, Se = 86.20%, Sp = 98.37%, RMSE = 0.1702 and RRSE = 47.47% for neonatal death
(69)	Complication prediction	Clinical parameters	SL	AUC = 0.89 and U = -0.0003 for neonatal death
(70)	Complication prediction	Clinical parameters	RF	AUC = 0.922, Ac = 0.903, Se = 0.674, Sp = 0.919, PPV = 0.377, F1 = 0.477 and mean F1 = 0.712 for neonatal death
(71)	Complication prediction	Clinical parameters	ANN	AUC = 0.92, Ac = 0.86, Se = 0.86, Sp = 0.83, Pr = 0.96 and F1 = 0.91 for neonatal death

ML, machine learning; GB, gradient boosting; LR, logistic regression; SNNN, self-normalizing neural networks; RF, random forest; DT, decision tree; SVM, support vector machines; MLP, multilayer perceptron; SL, SuperLearner; ANN, artificial neural networks; AUC, area under the receiver operating characteristic curve; Ac, accuracy; Se, sensitivity; Sp, specificity; PPV, positive predictive value; NPV, negative predictive value; +LR, positive likelihood ratio; -LR, negative likelihood ratio; Pr, precision; RMSE, root mean squared error; RRSE, root relative squared error.

Using a similar approach, Malacova et al. developed stillbirth risk prediction models using different ML algorithms (62). The study population was a cohort from Western Australia, consisting in almost 1 million births, of which 5,788 were stillbirths. The variables used to build the models were a combination of maternal socio-demographic characteristics, medical history, congenital anomalies and, more importantly, current pregnancy complications, which helped to achieve the greatest sensitivity. Different models were built, since not all subjects had the same amount of information available. For all models AUC varied from 0.59 to 0.84, which suggests the importance of variable selection to achieve better performances. The best results were obtained using XGBoost, resulting in a correct prediction of 45% of all stillbirths.

Shukla et al. also performed ML-based predictive modeling for perinatal mortality, but in a wider population, a cohort of near half million pregnancies in low- and middle-income countries located in South Asia, Africa and Central America (65). They developed different models using prenatal and post-delivery variables up to two days after birth, to predict outcomes from intrapartum stillbirth and neonatal death at different time frames. The variables used included maternal, socio-demographic, and medical information along with delivery and neonatal variables (the last two for neonatal death prediction only). They observed that the prediction of perinatal deaths using just prenatal and predelivery information reached AUC values of 0.72 or less, and that the predictive accuracy of the model improved as more post-delivery variables were included. Indeed, their best results were obtained with post-delivery data, which allowed to predict neonatal deaths with an AUC value of 0.87 by LR.

Mboya et al. studied a cohort of 42,319 singleton deliveries in Tanzanian population (66) and build ML models to predict both stillbirth and neonatal death (defined as death of live births within 7 days of life) using data available in the birth registry, i.e. mainly sociodemographic characteristics. The best results were achieved using RF, NB and Boosting with an AUC of 0.79. Khatibi et al., used a two-step ensemble classifier ML-based method (including DT, GB, LR, RF and SVM) to predict both stillbirth before delivery and stillbirth during labor occurred in Iran in a population of almost 1,5 million births (67). They used a combination of maternal socio-demographic features, labor descriptors, delivery properties and clinical history of the mother and fetus, and achieved an average AUC of 0.9. Although this value is much higher than the previously discussed studies, the aim of the authors was not early prediction, but to predict stillbirth at labor-delivery instead, therefore they used variables that are not available in early prediction studies.

A common result in these studies is that gestational age and fetal height are the two most important features to discriminate livebirth from stillbirth (65–67). Some authors suggest that risk prediction models that only use demographic and medical history could be further improved with the addition of biochemical and/or biophysical variables, however to the date these approaches are yet to be explored.

4.2.1.2 Neonatal death

Regarding neonatal death prediction, a recent work published in early 2021 made a systematic review on ML models used to predict neonatal mortality (72). They focused on works with a high amount of subjects (n>500 individuals) that analyzed both perinatal and neonatal factors, and excluded studies using exclusively antenatal factors, and in which neonatal mortality was not the primary outcome of study. They found eleven publications that met their criteria, among which the AUC value varied from 0.58 to 0.97. The most used ML methods were artificial neural networks (ANN), RF and LR, although the best overall model was obtained using LDA. Interestingly, from all studies reviewed in that work, only two conducted an external validation, which ensures a higher reliability. This fact also stresses the necessity of appropriate analytical methodologies and validations in future studies to ease their application by health care providers.

Other research groups, not covered in the aforementioned systematic review, have reported the prediction of neonatal death using ML-based models, with relatively high success (AUC of 95.99% for the best results) (68–70). In a different study conducted in Iran, different ML-based models were built to predict neonatal deaths in neonatal intensive care units (71). This work stands out since its models were prospectively applied and evaluated in a new cohort of neonates. Seventeen variables considered important in neonatal mortality prediction were used and different ML methods were tested, such as ANN, DT, SVM, Bayesian network and ensemble classifier. The highest AUC was achieved by the RF, SVM and ensemble models with a value of 0.98, however, when they prospectively applied the models for mortality prediction in new neonates, the best overall performance was obtained using ANN, with an AUC of 0.92, whereas the highest precision and specificity were obtained using DTs (0.97 and 0.87 respectively).

4.2.2 Spontaneous abortion

Spontaneous abortion (SA) is defined as the loss of pregnancy before the 20th week of gestation (73). It is often referred also as miscarriage, but according to literature, miscarriage is considered to occur before the 24th week of gestation (74). Both situations imply a common and serious pregnancy complication that has a significant psychological impact on the mother and the family. For this reason, and due to its complicated etiology (75), SA has become a hot topic in scientific research and gynecology.

Recent advances in technology, particularly in the artificial intelligence field, have allowed the use of the increasing amount of data that can be obtained in biomedical studies to improve patients' outcomes. This is consistent with the notion of precision medicine, that is, the need of a more personalized medicine to improve or predict the medical outcome (76), in this case, of a pregnant woman.

Interestingly, ML has been applied in the context of SA and miscarriage (Table 4). In 2013, Bottomley at al., developed a score based on demographic data, symptom variables and ultrasound data to predict the likelihood of a woman to have a successful pregnancy by performing a retrospective study (74). The ML method used was LR. Interestingly, the authors found that the combination of all the factors was able to provide a more accurate prediction of pregnancy viability than the obtained by analyzing the factors in a separated way, with an AUC of 0.924. This score model worked, but at that time it was not proven if it would be able to prevent miscarriage and, as the authors pointed out, the psychological morbidity associated with pregnancy loss should be integrated to the analyses. A distinct approach was made in 2019 using next generation sequencing to analyze 200 DNA samples of 100 couples presenting recurrent miscarriages (RM) (77). This work aimed to develop an algorithm based on the genetic analysis of the HLA protein codifying genes, considering the relationship of the HLA antigen sharing between couples and SA (81) in the context of immune interactions as a possible cause of SA and RM. It has been described that when the mother and the father share HLA antigens, the mother and the fetus will be homozygous for several of these loci. This issue alters the mother immunologic protection to the fetus inducing immunologic rejection and consequently SA (82). The SVM-based algorithm was able to correctly classify 67% of the total subjects, with an AUC of 0.71 and a false positive rate of 57%, which negatively affected the algorithm performance. Interestingly, this study is one of the first to predict RM probabilities in a case-by case basis, having a potential use in couple genetic counseling before

TABLE 4 ML applications in SA research.

Reference	ML application	Input	ML technique	Main output
(74)	Complication prediction	Clinical parameters	LR	AUC = 0.924, Se = 0.922, Sp = 0.733, PPV = 84.7% and NPV = 85.4%
(77)	Complication prediction	Genomics data	SVM	AUC = 0.71, Ac = 67%, Se = 86% and Sp = 43%
(78)	Complication prediction	Proteomics data	DT	AUC = 1, Ac = 100%, Se = 100%, Sp = 100%, Kappa = 1, PPV = 1 and NPV = 1 for recurrent SA with prethrombotic state
(79)	Complication prediction	Clinical parameters	RF	AUC = 0.99, Ac = 0.99, Pr = 0.99, Re = 0.99, F1 = 0.99
(80)	Complication prediction	Electronic health records	SC	AUC = 0.909 and Ac = 89.7% for live birth

ML, machine learning; SA, spontaneous abortion; LR, logistic regression; SVM, support vector machines; DT, decision tree; RF, random forest; SC, sparse coding; AUC, area under the receiver operating characteristic curve; Se, sensitivity; Sp, specificity; PPV, positive predictive value; NPV, negative predictive value; Ac, accuracy; Pr, precision; Re, recall.

conception. A different example is the study of Wu et al., who aimed to predict recurrent SA with prethrombotic state (PTS) serum biomarkers. PTS is known as one of the possible causes of SA. Wu et al. work was based on the analysis of different PTS-related proteins using multiplex array technology (78). They were able to distinguish control and affected individuals with high accuracy and precision using IL-24, exotoxin-3 and epidermal growth factor. Indeed, their DT model got an AUC of 1.000. Despite this excellent result, the cohort used for this study needs to be incremented to evaluate the real diagnostic power of this promising model.

In vitro fertilization embryo transfer (IVF-ET) is nowadays an alternative for couples with difficulties to conceive. This procedure implies high risks of miscarriage, being psychologically stressful for couples. Therefore, it becomes necessary to find a way or system that allows the prediction of the transfer outcome, and the early detection of possible problems (83). Recently, Liu et al. developed a ML-based model with historic data obtained by transvaginal ultrasonography from females that underwent IVF-ET. The study only considered women with viable singleton and 6-12 weeks of pregnancy (79). The authors were able to predict embryonic development after transfer using six different ML-classifiers, with AUCs ranging from 0.91 to 0.97 when fetal heart rate (FHR) was included among the predictors. The most accurate prediction was obtained by RF at the 10th week after embryo transfer, with an AUC of 0.99. Other example is the article of Huang et al., who used deep learning to predict pregnancy outcomes in patients with recurrent reproductive failure (RRF), including recurrent pregnancy loss (RPL) and recurrent implantation failure (RIF). The study defined RPL as two or more SA before 20 weeks of pregnancy, and RIF as couples unable to conceive after multiple IVF-ET cycles. The authors analyzed EHR data with sparse coding, and predicted four pregnancy outcomes: biochemical pregnancy, clinical pregnancy, ongoing pregnancy and live birth. They got testing accuracies that ranged between 54.2% and 89.7% for the different pregnancy outcomes. Notably, the best model for the prediction of biochemical pregnancy was obtained with a panel of 10 endometrial immunological markers, while the best models for the other three outcomes, were obtained with a panel of 15 autoantibodies. The authors discussed that this knowledge could help clinicians to plan a more personalized diagnosis and treatment for patients with RRF (80).

4.2.3 Preterm birth

The WHO defines PTB as the delivery of alive babies before 37 weeks of pregnancy are completed (56). Based on gestational age, it can be sub-categorized as: extremely preterm, before 28 weeks; very preterm, between 28 and 32 weeks; and moderate to late preterm, between 32 and 37 weeks. Most of preterm deliveries are spontaneous, although some are provider-initiated (56).

PTB is the main cause of death in children under 5 years of age worldwide. Furthermore, it has short and long-term consequences on newborns' health, which imply a significant psychological and economic burden to families and health systems (84). The development of PTB predictive tests could be useful to identify high risk pregnancies, which could guide the healthcare personnel to offer prophylactic interventions and make antenatal management decisions (85).

ML has already been applied to develop predictive models for PTB (Table 5). For instance, Khatibi et al. aimed to predict spontaneous and provider-initiated PTB with data from the Iranian Maternal and Neonatal registry, which includes information of more than 1,400,0000 deliveries and 112 features. The authors used different big data ML algorithms to classify pregnant women in two steps. In the first step, all subjects were classified into term or PTB; and in the second step, the subjects classified as PTB in the first step, were then sub-classified as spontaneous or provider-initiated. Their best model, an ensemble of DT, SVM and RF, achieved a weighted average accuracy of 81%, and an AUC of 68% (86). Similarly, Belaghi et al. used first and second trimester information from the Ontario's Better Outcomes Registry and Network database, and different ML methods to predict overall and spontaneous PTB. The investigation considered 112,963 pregnancies. For overall cases, the best models were obtained by ANN, and reached AUCs of 60.3% and 79.8% in the validation cohort at the first and second trimester, respectively. For spontaneous cases, the best results were obtained by LR, and got validation AUCs of 59.4% and 64.5% at the first and second trimester, respectively (87). A different approach was followed by Gao et al., who used EHR text data and deep learning ML methods to predict extreme PTB. Their dataset involved 10 years of EHR information from 25,689 deliveries at the Vanderbilt University Medical Center. The long short-term memory (LSTM) recurrent neural networks (RNN) ensemble model allowed to predict extreme PTB with an AUC of 0.744 in the validation cohort, greater than the obtained by LR, SVM and GB (88). This is an interesting result, although this work didn't differentiate spontaneous from provider-initiated cases. Likewise, Zhang et al. aimed to predict PTB with continuous EHR data and LSTM. Their dataset included first and second trimester medical parameters from more than 25,000 pregnant women who received antenatal care and had vaginal delivery at the Hangzhou Women's Hospital. Notably, the time-series deep learning technique LSTM achieved a better predictive performance than the traditional cross-sectional ML technique XGBoost, with cross-validation AUCs of 0.651 and 0.516-0.601, respectively (89).

All the aforementioned studies based their predictive models on clinical and biochemical maternal information available in databases. However, other articles have assessed alternative types of data to predict PTB. Such studies are very useful to find novel biomarkers for PTB, and to propose informed hypotheses about its causes and underlying mechanisms, which are not fully understood (84, 85). For instance, Aung et al. measured an extensive set of 65 urine and plasma biomarkers, and combined them with ML to predict PTB at 26 weeks of gestation. They tested three ML methods: LR, adaptive EN and RF. The best validation results were obtained with the latter. The combination of all the biomarkers with RF yielded AUCs of 0.85 and 0.79 for overall and spontaneous PTB, respectively. Then, the authors divided the biomarkers into five groups, i.e. DNA damage markers, angiogenic factors, protein damage markers, inflammatory markers and lipid damage markers. The best predictive performances were obtained

TABLE 5 ML applications in PTB research.

Reference	ML application	Input	ML technique	Main output
(86)	Complication prediction	Clinical and biochemical factors	DT, SVM and RF	AUC = 68% and Ac = 81% for spontaneous and provider-initiated cases
(87)	Complication prediction	Clinical and biochemical factors	ANN	AUC = 79.8%, Se = 62.7%, Sp = 84.6%, PPV = 23.2% and NPV = 97.0%
(88)	Complication prediction	Electronic health records	LSTM	AUC = 0.744, Se = 0.682, Sp = 0.743 and PPV = 0.028 for extreme cases
(89)	Complication prediction	Electronic health records	LSTM	AUC = 0.651, Ac = 0.739, Se = 0.407 and Sp = 0.982
(90)	Biomarker discovery	Biochemical markers	RF	PGA2, 15DO12,14-PGJ2, BCPGE2, 13,14DHK-PGF2a, RVD1, LTE4, LTB4, linolenic acid and IL-10 as novel biomarkers
(91)	Biomarker discovery	Metabolomics data	RF	FA(17:1), FA(24:6), FA(14:2), CAR(18:2), hexanoylcarnitine, FA(14:0(Ke)), FA(26:1), raffinose, PC(18:0/16:3), FA(16:3), glycocholic acid, PC(33:4), FA(22:5), FA(14:1(Ke)), heptadecanoic acid, FA(19:1) and FA(14:1) as novel biomarkers
(92)	Biomarker discovery	Metabolomics, proteomics and transcriptomics data	RF	IL-6, IL-1RA, G-CSF, RARRES2, CCL3, ANGPTL4, PAD12, TfR, and metabolites from glutamine/glutamate metabolism, and valine/leucine/isoleucine biosynthesis pathways as novel biomarkers
(93)	Complication prediction	Electrohysterography recordings	RF	AUC = 0.999, Ac = 99.23%, Se = 98.40%, Sp = 99.76% and Pr = 95.86%
(94)	Complication prediction	Clinical parameters	KNN; RF	AUC = 1.00, Ac = 0.95, Se = 0.67, Sp = 1.00, G-means = 0.82 for PTB and the potential value of performing cervical cerclage to prolong the pregnancy; MAE = 3.521, MSE = 4.560 and R = 0.752 for timing of spontaneous delivery

ML, machine learning; PTB, preterm birth; DT, decision tree; SVM, support vector machines; RF, random forest; ANN, artificial neural networks; LSTM, long short-term memory; KNN, k-nearest neighbors; AUC, area under the receiver operating characteristic curve; Ac, accuracy; Se, sensitivity; Sp, specificity; PPV, positive predictive value; NPV, negative predictive value; Pr, precision; MAE, mean absolute error; MSE, mean squared error.

with lipid damage markers and RF, with AUCs of 0.84 and 0.79 for overall and spontaneous cases, respectively. Furthermore, the study identified the enzymatic pathway that contributed the most to that prediction: the eicosanoid lipoxygenase pathway. The combination of 15 lipoxygenase metabolites with RF got AUCs of 0.83 and 0.82 for overall and spontaneous PTB, respectively (90). Another example is the study of Chen et al., who applied untargeted LC-MS plasma metabolomics to identify metabolites that could be related to PTB, at 24-28 gestational weeks. The authors identified 17 and 16 biomarkers for overall and spontaneous cases, respectively, and tested their predictive performance with seven ML classifiers. The best results were obtained by RF, with AUCs of 0.92 and 0.89 in the testing dataset. Interestingly, most of the identified biomarkers were fatty acids, which suggests their involvement in the pathogenesis of PTB (91). Similarly, Jehan et al. performed an early pregnancy multiomics characterization of PTB. The authors applied untargeted transcriptomics and targeted proteomics on plasma samples, and untargeted metabolomics on urine specimens. They used a 2-step ML algorithm, in which a model was first trained for each omics dataset, and then combined into a final model. The integrated model achieved a cross-validation AUC of 0.83, higher than the obtained for the different omics datasets alone. The work also identified the features that were more associated with PTB: a proteomics inflammatory module, including IL-6, IL-1RA, G-CSF, RARRES2 and CCL3; and an urine metabolomic module, enriched for glutamine and glutamate metabolism, and valine, leucine and isoleucine biosynthesis pathways (92).

Some less common approaches have also been applied in the context of PTB prediction. For example, Despotovic et al. tested EHG recordings to predict PTB. They built ML models using k-nearest neighbors (KNN), SVM, RF, RF with synthetic minority oversampling technique (SMOTE), and RF with adaptative synthetic (ADASYN) sampling. Their RF-ADASYN model allowed to predict PTB at 22-25 weeks of pregnancy, with an accuracy of 99.23% and an AUC of 0.999 in cross-validation (93). A different case is the work of Rawashdeh et al., who combined 19 clinical maternal parameters with ML methods to predict PTB in a high risk cohort. They developed two different strategies to analyze their data. The first one aimed to predict whether the pregnancy would continue beyond 26 gestational weeks (the lower limit for PTB in this study) and the potential value of performing cervical cerclage to prolong the pregnancy. For this first aim, the authors tested four different classification ML methods, DT, RF, KNN and NN; solo and with SMOTE. The highest testing AUC was obtained by the KNN-SMOTE model, with a value of 1.000. The second strategy of the authors aimed to predict the timing of spontaneous delivery after cervical cerclage, an approach that wasn't assessed in any of the previously discussed articles. For this second aim, they tested five different regression ML methods, linear regression, Gaussian process, RF, K-star and locally weighted learning. The best correlation with the actual gestational age at delivery was obtained by the RF model, with a value of 0.752 in the testing dataset. Such a regression ML model could help physicians to define prophylactic interventions timely, and reduce PTB-related perinatal morbidity and mortality (94).

4.2.4 Cesarean section

Cesarean section is an effective mean to solve medical and surgical complications during dystocia and severe pregnancy disorders, and has an irreplaceable role (95). Delivery through cesarean section reduces the risk of maternal-fetal morbidity and mortality, when is medically indicated (96). Emergency cesarean section (EMCS) can be a procedure that saves lives if pregnant women experience abnormal conditions during vaginal delivery, such as fetal suffering, eclampsia or severe preeclampsia (97). Deciding to perform an EMCS is a complicated process, occurring only in specific obstetric conditions, and requires awareness and rapid assessment of the risk of the situation (98). Failure to perform EMCS on time can lead to postpartum mental disorders and other severe adverse maternal and fetal outcomes (99, 100). Recognizing an acute situation during pregnancy, labor or delivery, that can be life threatening and that could require an EMCS, is considered one of the most challenging tasks in obstetrics (101).

Visual inspection of CTG traces by obstetricians and midwives is the gold standard for monitoring the wellbeing of the fetus during antenatal care (102). One of the areas in which mathematical and computational tools for data analysis, such as ML methods, excel is in the analysis of instrumental continuous signals (Table 6). Several output data from instruments used in clinical diagnosis or monitoring are composed of this type of signals, in which between any two points there can be a large amount of data points, as large as allowed by the signal resolution, or even an infinite amount in the case of analog instruments. CTG traces are a great example of this type of data in obstetrics. The problem with this type of data is that its visual interpretation is highly dependent on the observer's experience and can be strongly subjective. Most importantly, clinical decisions such as pregnancy intervention through cesarean section are made using visual inspection of CTG traces. It has been reported that the positive predictive value produced by obstetricians to anticipate negative outcomes that require cesarean section deliveries is only 30% (110). However, although human eye may fail to provide a reliable and objective interpretation, mathematical tools for pattern recognition are not subjected to the observer's bias.

Two different articles published by the same group in Liverpool have addressed the observer variability of CTG traces using a ML approach (102, 103). The authors applied signal processing techniques to extract relevant features from CTG traces and modeled the data using different ML methods, such as DNN, LDA, RF, SVM and ensemble classifiers. They were able to classify cesarean section and vaginal deliveries from CTG traces with cross-validation AUC values of 96-99%. Other study performed by an Italian research group used a similar methodology and obtained consistent results, that is, a cross-validation AUC value of 96.7% by RF (104). Likewise, a Chinese study that proposed a comparable strategy to classify normal and abnormal CTG traces reported an AUC of 0.95 by CNN in cross-validation (105). Their results demonstrate that ML methods significantly improve the prediction efficiency of necessary cesarean sections, and that their use provide a valuable decision support tool to minimize subjective interpretations of CTG traces from medical practitioners.

Besides CTG traces analysis, ML methods have been applied on EHR information to predict cesarean section and identify important variables, as well as to understand the interaction between those variables. The model developed by Clark et al. using a classification and regression tree had an AUC value of 0.7, which was considered acceptable (106). The three features that contributed the most to that model were hospital type, maternal BMI and intrapartum oxytocin dose.

Other uses of ML have been tested in the context of cesarean sections. For example, a decision-support ML-based model for assessing intrathecal hyperbaric bupivacaine dose using physical

TABLE 6 ML applications in cesarean section research.

Reference	ML application	Input	ML technique	Main output
(102)	Complication prediction	Cardiotocography traces	DNN	AUC = 99%, Se = 94%, Sp = 91%, F1 = 100% and MSE = 1%
(103)	Complication prediction	Cardiotocography traces	LDA, RF and SVM	AUC = 96%, Se = 87%, Sp = 90% and MSE = 9%
(104)	Complication prediction	Cardiotocography traces	RF	AUC = 96.7%, Ac = 91.1%, Se = 90.0%, Sp = 92.2% and Pr = 92.1%
(105)	Complication prediction	Cardiotocography traces	CNN	AUC = 0.95, Ac = 94.70%, Pr = 94.71% and Re = 94.68%
(106)	Complication prediction	Electronic health records	CART	AUC = 0.7
(107)	Anesthesia dose prediction	Clinical parameters	LASSO	MSE = 0.0087 and R^2 = 0.8070
(108)	Surgical site infection prediction	Clinical parameters and mobile images	LR	AUC = 1.0, Ac = 100%, Se = 1.0 and Sp = 1.0
(109)	Later vaginal birth prediction	Electronic health records	RF	AUC = 0.69, Ac = 70.0%, Se = 97.9% and Sp = 6.9%

ML, machine learning; DNN, deep neural networks; LDA, linear discriminant analysis; RF, random forest; SVM, support vector machines; CNN, convolutional neural networks; CART, classification and regression tree; LASSO, least absolute shrinkage and selection operator; LR, logistic regression; AUC, area under the receiver operating characteristic curve; Se, sensitivity; Sp, specificity; MSE, mean squared error; Ac, accuracy; Pr, precision; Re, recall.

variables during cesarean section was developed, providing the anesthesiologists a new tool that gives new insights into the potential impact of controversial parameters (107). The least absolute shrinkage and selection operator regression model got a mean squared error of 0.0087. ML has also been applied to predict surgical site infection in cesarean section wounds, which is a leading cause of mortality and an important health concern in low-resource countries (108). The best model was obtained with mobile device images and LR, and achieved an AUC of 1.0. Prediction of likelihood of a successful vaginal birth after former cesarean deliveries has also been addressed using ML, which may help as a decision-making tool that could contribute to a reduction in cesarean deliveries rates (109). The EHR-based RF model reached an AUC of 0.69, better than the obtained by DT and LR.

4.2.5 Fetal malformations

4.2.5.1 General congenital diseases

Congenital anomalies are seen in 1–3% of the population, and approximately 60–70% of the anomalies can be diagnosed *via* ultrasonography, while the remaining 30–40% can be diagnosed after childbirth. An e-Health android application was developed by comparing the performance of nine binary ML classification models (averaged perceptron, boosted DT, Bayes point machine, decision forest, decision jungle, locally-deep SVM, LR, NN, SVM) (Table 7). The models were trained with the clinical dataset of 96 pregnant women and used to predict fetal anomaly status based on maternal clinical data. The decision forest model reached the best performance, with 89.5% of accuracy, 75% of F1-Score and 95% of AUC. An external validation testing with 16 users, showed that the classification algorithm accuracy was 87.5%. This estimate is

TABLE 7 ML applications in fetal malformations research.

Reference	ML application	Input	ML technique	Main output
(111)	Complication prediction	Mobile collected data	DF	Ac = 87.5%
(112)	Complication prediction	Computed tomography images	LDA	Ac = 95.7%, Se = 92.7% and Sp = 98.9% for craniosynostosis
(113)	Complication prediction	Ultrasound images	SVM	AUC = 0.89, Ac = 88.63%, Se = 95%, Sp = 82% and +LR = 5.25 for craniosynostosis
(114)	Complication differentiation	Stereophotogrammetry images	PCA	Clear differentiation between craniosynostosis and control patients
(115)	Data acquisition	Ultrasound videos	RF	Estimation of heart position, orientation, viewing plane and cardiac phase
(116)	Data acquisition	Electrocardiography recordings	ICA and DT	Reconstruction of fetal electrocardiogram
(117)	Data acquisition	Electrocardiography recordings	SDAE	Reconstruction of fetal electrocardiogram
(118)	Data extraction	Ultrasound videos	SVM	Detection of fetal presentation and heartbeat
(119)	Data extraction	Cardiotocography recordings	EMD	Extraction of fetal heart rate
(120)	Data extraction	Electrocardiography recordings	CNN and LSTM	Extraction of fetal heart rate
(121)	Data extraction	Electrocardiography recordings	CNN and LSTM	Extraction of fetal heart rate
(122)	Data extraction	Doppler ultrasound recordings	EMD	Extraction of fetal heart rate
(123)	Complication prediction	Cardiotocography recordings	CNN	AUC = 97.82%, Ac = 98.34%, Se = 98.22%, Sp = 94.87% and QI = 96.53% for fetal acidemia caused by hypoxia
(124)	Decision making support	Cardiotocography recordings	Infant software	Identification of fetal status
(125)	Decision making support	Cardiotocography recordings	PeriCALM software	Identification of fetal status

(Continued)

TABLE 7 Continued

Reference	ML application	Input	ML technique	Main output
(126)	Decision making support	Cardiotocography recordings and ultrasound measurements	Foetos software	Identification of fetal status
(127)	Complication prediction	Ultrasound measurements	NN	Ac = 95% for intrauterine growth restriction
(128)	Complication prediction	Cardiotocography recordings	SVM	Ac = 78,26%, Se = 0.78 and Sp = 0.79 for intrauterine growth restriction
(129)	Complication prediction	Ultrasound images	ANN	Ac = 91-94% for intrauterine growth restriction
(130)	Complication prediction	Echocardiography images	FINE software	Se = 98%, Sp = 93%, +LR = 14 and -LR: 0.02 for congenital heart disease
(131)	Complication prediction	Echocardiography images	CON	Ac = 99.0%, Se = 75%, Sp = 99.6%, PPV = 99% and NPV = 88.5% for congenital heart disease
(132)	Biomarker discovery	Transcriptomics data	PCA and K-means	miR-1647, miR-3064, mirR-3533, miR-6544, miR-6590, miR-6593, miR-6602, miR-6604, miR-6639, miR-6667, miR-6706, miR-6710, miR-1650, miR-1665, miR-6542, miR-6565, miR-6619 and miR-6706 as novel biomarkers for fetal alcohol spectrum disorder
(133)	Complication prediction	Clinical parameters	LR	AUC = 0.880, Se = 1.00, Sp = 0.49, PPV = 0.03 and NPV = 1.00 for macrosomia
(134)	Complication prediction	Electronic health records	LSTM	Ac = 93.3% for small, appropriate and large for gestational age
(135)	Drug teratogenicity prediction	Drug databases information	t-SNE and GB	AUC = 0.8

ML, machine learning; DF, decision forest; LDA, linear discriminant analysis; SVM, support vector machines; PCA, principal component analysis; RF, random forest; ICA, independent component analysis; DT, decision tree; SDAE, stacked denoising autoencoder; EMD, empirical mode decomposition; CNN, convolutional neural networks; LSTM, long short-term memory; NN, neural networks; ANN, artificial neural networks; CON, compound network; LR, logistic regression; t-SNE, t-distributed stochastic neighbor embedding; GB, gradient boosting; Ac, accuracy; Se, sensitivity; Sp, specificity, AUC, area under the receiver operating characteristic curve; +LR, positive likelihood ratio; QI, quality index; -LR, negative likelihood ratio; PPV, positive predictive value; NPV, negative predictive value.

enough to give a general overview of fetal health before the patient visits the physician (111).

4.2.5.2 Craniosynostosis

Craniosynostosis is a congenital condition characterized by a premature fusion of the fetal cranial sutures, which induces one or more cranial bones in a fetal skull to join too early. Since this happens before the fetal brain is fully formed, as the brain grows, the skull can become deformed. Craniosynostosis is a common cause of pediatric skull deformities, affecting 1 of every 2000 to 2500 live births worldwide. This birth defect occurs in a predictable pattern because of localized fusions and the compensatory expansion of the cranial vault (136). It is usually detected early in life, both due to its cosmetic manifestations and functional consequences, as it can result in limited brain growth, elevated intra-cranial pressure, and respiratory and visual impairment. Early diagnosis is crucial for management, prevention of complications, and consideration for early surgical correction (112). In parallel with the growing understanding of the pathophysiology of craniosynostosis, new advances include the improvement of existing technologies such as ultrasound, and the introduction of new technologies such as ML and augmented reality (137).

Various algorithms and mathematical models have been developed to allow the computer to reliably and accurately predict specific outcomes, based on premature fusion suture input data. Using data from CT-derived measurements of cranial suture fusion, cranial deformation and curvature discrepancy, different ML methods (RF, LDA and SVM) were tested to determine the presence or absence of craniosynostosis. The best classification performance was obtained by the LDA model, with 92.7% of sensitivity, 98.9% of specificity and the probability of correctly classifying a new subject of 95.7% (112). In a different study, SVM and RF were used on ultrasound images in order to decrease the user error involved in the interpretation of craniosynostosis diagnostic imaging. They got a diagnostic accuracy of 88.63% and an AUC of 0.89 by SVM (113). Finally, PCA has proven effective in differentiating between healthy controls, scaphocephalic, and trigonocephalic patients, when applied on images obtained *via* stereophotogrammetry (114).

4.2.5.3 Congenital heart disease

The incidence of congenital heart disease (CHD) has been estimated between 0.6% and 1.2% among live births (138); however, it has been reported an increased incidence of 8.3% when stillborn infants of ≥26 weeks of gestation are included (139). There could be an even higher incidence in early gestation, given spontaneous and elective pregnancy termination. A multitude of factors are associated with an increased risk of identifying CHD in the fetus, which are related to familial, maternal, or fetal conditions. The leading reason of referral for fetal cardiac evaluation is the suspicion of a structural heart abnormality on obstetric ultrasound, which results in a diagnosis of CHD in 40% to 50% of the referred fetuses. In general, subjects with risk levels exceeding ≥2% should have a detailed fetal echocardiogram by a trained examiner.

Fetal echocardiology has evolved from the description of cardiac anatomical abnormalities toward the quantitative assessment of cardiac dimensions, shape, and function. It has been demonstrated to be useful in the diagnosis and monitoring of fetuses with a compromised cardiovascular system, which may be related to several fetal conditions, such as IUGR, twin-to-twin transfusion syndrome, and CHD (140, 141). Different ultrasound approaches are currently used to evaluate fetal cardiac structure and function, including conventional 2D imaging, and M-mode and tissue Doppler imaging, among others (142). However, assessing fetal cardiac function is still challenging due to fetus involuntary movements, the small size of the heart, the high heart rate, the limited access to the fetus, and the lack of expertise in fetal echocardiography of some sonographers. After having obtained an optimal image, various measurements must be performed to extract relevant cardiac features related to remodeling and functional status. Therefore, the use of new technologies to improve the primary acquired images, or to help extract and standardize measurements is of great importance for optimal assessment of the fetal heart. ML techniques can help to optimize three different aspects of fetal echocardiology: acquisition, quantification and features extraction, and fetal diagnosis.

4.2.5.3.1 Acquisition

ML-powered methods can speed up the acquisition process, decreasing the learning curve, standardizing the resulting images and increasing data quality. In such case, standardization occurs with minimal human intervention. In this regard, Bridge et al. implemented a framework for tracking key features from healthy fetal heart ultrasound videos through RF (115); and Yu et al. and Muduli et al. used independent component analysis along with a DT (116) and a stacked denoising autoencoder neural networks-based deep learning approach (117) to reconstruct fetal electrocardiography (ECG) signals from abdominal ECG recordings.

4.2.5.3.2 Quantification and feature extraction

The vast majority of the research in this field focuses on automatically measuring the heartbeat. Some examples are the detection of fetal cardiac activity from maternal abdomen ultrasound videos using SVM (118), the extraction of FHR features from CTG recordings applying empirical mode decomposition (EMD) (119), the extraction of FHR from fetal ECG signals employing a combination of CNN and LSTM RNN (120, 121), and the detection of fetal heart beats from continuous Doppler ultrasound signals by EMD (122).

4.2.5.3.3 Fetal diagnosis

One of the subfields in which ML has been extensively applied is the improvement of the diagnosis of fetal hypoxia or acidemia, based on CTG analyses. For example, Zhao et al. used CNN and got an AUC value of 97.82% for fetal acidemia caused by hypoxia (123). There have also been some attempts to translate these methods into clinical practice *via* the development of software that could provide additional support in the interpretation of CTG signals and, therefore, improve the assessment of fetal status. Some examples are Infant (124), PeriCALM (125) and Foetos (126).

ML has also been assessed to improve the diagnosis of IUGR, a pathology that affects about 10% of pregnancies and that has been associated with cardiac remodeling *in utero* (143). IUGR early detection models have been developed using ultrasound biometric measurements and NN (127), CTG data and SVM (128), and 2D ultrasound images and ANN (129). Such strategies got classification accuracies of 95%, 78% and 91-94%, respectively.

Finally, ML has been recently applied to improve heart diseases prenatal diagnosis. Yeo et al. presented an intelligent ML navigation method called FINE, to automatically obtain different echocardiography anatomical views of the fetal heart and identify abnormalities within the cardiac anatomy (130). Their method allowed to predict CHD with a sensitivity of 98% and a specificity of 93%. Moreover, Han et al. used an artificial intelligence algorithm based on a compound network to segment echocardiography images, and then screen for fetal CHD during pregnancy. Their method achieved an accuracy of 99.0% (131).

4.2.5.4 Fetal alcohol spectrum disorder (FASD)

Gestational alcohol exposure is the most important known cause of neurodevelopmental disability, affecting nearly 5% of children in the US. It leads to complex epigenetic and transcriptomic modifications, which subsequently impair signaling pathways in neural and morphological development (144). In this regard, identifying transcriptomic mechanisms that regulate alcohol's teratogenicity during embryonic development is crucial to understand different phenotypic outcomes, and may allow future therapeutic interventions that could mediate alcohol's effects. In order to understand transcriptomic changes in FASD, spanning gene, exon and splicing variants, ML approaches can be used to corroborate traditional statistical methods, and to

robust genomic functional studies. For example, Al-Shaer. applied PCA and K-means clustering on transcriptome sequencing (RNA-Seq) data. They identified 6857 differentially expressed exons, which represented 1251 gene IDs that deviated from baseline expression, and 18 miRNAs with significantly different expression profiles in response to alcohol. Several of those exons regulate focal adhesion, FoxO signaling, insulin signaling and Wnt signaling (132).

4.2.5.5 Macrosomia

Fetal macrosomia is diagnosed when fetal growth is beyond a specific threshold, regardless of the gestational age. In developed countries, the most used threshold is a weight above 4,000 g (145). Macrosomia is associated with an increased risk of several maternal and newborn delivery complications, like shoulder dystocia, brachial plexus injury, asphyxia, prolonged labor, postpartum hemorrhage, and laceration of the anal sphincter (146). Predicting macrosomia is important for making decisions about induction or cesarean delivery before the start of labor. For example, Shigemi et al. developed LR and RF ML models to predict macrosomia using maternal clinical parameters. The generated LR risk scoring system allowed to determine the association of each predictor with macrosomia, and achieved an AUC value of 0.880 (133). Likewise, Tao et al. tested different ML techniques to predict fetal birthweight from EHR data. They considered three categorical outcomes: small for gestational age (SGA), appropriate for gestational age (AGA) and large for gestational age (LGA). SGA was defined as birthweight lower than 2,500 g; AGA as birthweight between 2,500 and 4,000 g; and LGA as birthweight greater than 4,000 g. Remarkably, the time-series deep learning technique LSTM achieved a classification accuracy of 93.3%, outperforming the traditional cross-sectional ML techniques LR, BPNN, CNN and RF (134).

4.2.5.6 Teratogenicity

Teratogenicity is the most serious manifestation of iatrogenic fetal toxicity. Developing fetuses are especially sensitive to chemical exposures. Teratogens lead to fetal malformation and are implicated in lifelong physical and/or mental disabilities (135). Teratogenicity scoring for small molecules is unsystematic, and is performed outside the clinical environment (147). Moreover, prescribing behavior for gravid patients is based on limited human data and conflicting cases of adverse outcomes, due to the exclusion of pregnant populations from randomized controlled trials (148). Using unsupervised t-distributed stochastic neighbor embedding and supervised GB ML methods, Challa et al. demonstrated that small molecule drug structure is a good predictor of teratogenicity. The application of such methods also allowed to discover relationships between chemical functionalities within drugs prescribable in pregnancy and existing teratogenicity information. Three chemical functionalities that predispose a drug towards increased teratogenicity and two moieties with potentially protective effects were discovered. The ML algorithm predicted three clinically relevant classes of teratogenicity with an AUC of 0.8, and nearly double the predictive accuracy of a blind control for the same task, suggesting a successful modeling (135).

5 ML in pregnancy diseases and complications: current state and future challenges

5.1 Current state

ML has been widely applied in all the seven subjects considered in this review: gestational diabetes mellitus, preeclampsia, perinatal death, spontaneous abortion, preterm birth, cesarean section, and fetal malformations. The applications are varied, including early detection, alternative screening, biomarker discovery, risk estimation, correlation assessment, pharmacological treatment prediction, drug screening, data acquisition, data extraction, among others. We observed that the most common ML use is the prediction of perinatal diseases or complications. This is in line with what was described in two recent reviews on ML and pregnancy care. The scoping review of Abuelezz et al. explored the contribution of artificial intelligence in pregnancy, and categorized the applications in "prediction of pregnancy disorders/complications", "treatment and management" and "assist with patients' safety outcome". 75% of the reviewed studies fell into the first category (4). Likewise, the systematic review of Islam et al. dug into the use of ML to predict pregnancy outcomes. They categorized the reviewed articles according to their scope: "predicting pregnancy risks/complications", "exploring pregnancy factors", "predicting mode of delivery", "predicting outcome of IVF treatment", "predicting labor outcome" and "comparing two birth weight groups". The most common was the first category, with a frequency of 35% (5). Furthermore, we noted that the number of studies employing ML in pregnancy has increased over time, with most of the reviewed articles being published in the last five years. This tendency was also identified by previous reviews in the field (4, 5, 149).

Depending on the type of data available, different ML methods are preferred for studying pregnancy-related alterations. When the data available come from medical records, the information available is rich in socio-demographic characteristics, medical history variables and anthropometric measurements. We observed that when this is the case, the researchers usually have a massive amount of data (patients) available, obtained from the aforementioned medical records, to train the ML model. In this scenario, the most used ML methods correspond to non-linear methods, such as SVM, NN, DT, ensemble methods, etc. This could be explained by the fact that correlations between this type of data and the diseases or complications we focused on in this review are complex, not directly or linearly correlated. Non-linear and non-parametrical methods seem to be more suitable in such scenario, in which data is affected by a higher amount of variability and uncertainty. This is especially true when data from medical questionnaires and other surveys are used, in which the answers and values obtained thereof are highly dependent on the patient's perception. Appropriate variable selection and validation of the models is perhaps even more important in those cases. In several studies reviewed in this work, the authors used some level of validation to test their models, and therefore, the accuracies they

reported demonstrate a certain relationship between the data used and the pathology studied, even though that relationship is not necessarily linear. Therefore, it is possible to obtain adequate ML models to study adverse perinatal outcomes from data already available. This adds value to currently existing medical records databases.

A fundamental precept in data science is that, in order to predict a property (e.g. a pathology, or the concentration of a particular biomarker) the data must contain information related to that property, and the stronger the correlation, the better the performance of the model. In this regard, it has been suggested that prediction models could be improved when using biochemical or biophysical variables (64). This type of data is less affected by human bias and is more directly related to the physiology of an individual, or the pathophysiology of a disease. Most variables of this type correspond to biochemical analytes or ultrasonography parameters. In this scenario, the type of variables used are not too different from the data used in chemical, environmental or pharmaceutical sciences. Analytical chemists have been successfully using chemometrics (i.e. ML applied in chemistry) for several decades to extract relevant information from chemical data, to find correlations or predict a sample property. In essence, the exercise to identify the origin of certain wine from its metal profile, an example of a common application of chemometrics in analytical chemistry, would be no different than predicting a pathology based on the characteristic multivariate pattern of a blood biochemical profile. Likewise, biophysical variables such as the continual recording of FHR through CTG are very similar to the graphical outputs obtained from the analytical instruments used in chemistry (e.g. chromatogram or spectrogram), in the sense that an analytical signal is continuously recorded from an instrument. Therefore, the robust chemometrical platform used in analytical chemistry for the analysis of this type of data could also be exploited in biomedical science. In chemometrics, the most used methods are linear, i.e. are based on linear combinations of the original variables, with which they find hidden correlations that can be used to predict a particular property. Methods such as PCA, partial least squares regression, soft independent modeling of class analogies, discriminant analysis, or variations of them, are among the most used in chemistry (6, 7). These methods are more intuitive than the non-linear methods mentioned before. Furthermore, they usually provide valuable information about the importance or weight of the variables on the prediction of a certain property, as well as variable-variable and variable-sample relationships, which are some of the reasons they are preferred in chemical analysis. Curiously, in this review we observed that these methods are not common in pregnancy-related applications, where non-linear methods are the trend and LR seems to be almost the only linear method chosen. This observation is consistent with the systematic review and meta-analysis of Sufriyana et al., who found that the most common ML techniques in prognostic prediction studies for pregnancy care are LR (64.8%) and ANN (14.1%) (150). As clinical chemistry can be considered as a type of analytical chemistry, a more widespread application in biomedicine of the linear ML methods used in chemistry could be highly beneficial, whenever biochemical data is available.

5.2 Future challenges

It is difficult to think of a field of knowledge in which ML has not been applied. Consequently, it is quite challenging to be innovative regarding the use of ML in the context of pregnancy diseases and complications. An aspect that could be improved is data management, for example by automating their recording, storage and update in both medical and research settings. The later could ease data extraction, analysis and posterior interpretation. Even though EHR are common in developed countries, they are not frequent in low- or middle- income countries (151, 152). Therefore, the spread of EHR and their adaptation to different realities is an important task for the scientific community in the near future. Moreover, it is necessary to adapt ML applications to the emerging technologies in biomedical sciences, with which novel and more complex types of data can be obtained (153). This could be employed not only to develop more accurate predictive models, but also to find new biomarkers that could help to better understand the pathophysiology of a particular disease or complication, which could in turn lead to an improvement in its prevention, management or treatment. Furthermore, although there are a lot of published ML models aiming to improve maternal and fetal health, many of them have never been validated, nor subjected to impact analysis. This translational issue was also identified by a recent systematic review on ML-based clinical decision support systems in the context of pregnancy care (154). To be considered suitable for clinical implementation, ML models have to exhibit a good predictive performance in both internal and external validation, and also prove to foster positive changes in medical settings (e.g. improve patients outcomes, reduce management costs, etc.) without impairing care quality and patient satisfaction (14). Hence, besides developing new ML tools in the field of pregnancy alterations, it is necessary to carry out studies to test the already published models in different populations and healthcare facilities. This would allow to know if it is really worthwhile to implement them in clinical practice. To perform such studies is a demanding task, since the recruitment and follow-up of large cohorts of subjects require a very well-coordinated multidisciplinary work, and both time and financial resources are spent. However, it is the only way to lead ML models closer to real medical applications.

Pregnancy lasts only nine months, and the first three have been proposed as the ideal time frame for the early detection, treatment and management of gestational alterations (155–157). This window of time is narrow, but represents a great opportunity to exploit all the advantages that are associated with the use of ML, i.e. finishing

complex assignments rapidly, dealing with multiple tasks efficiently, and predicting short- and long- term outcomes accurately (158, 159). Indeed, this review widely demonstrates that ML methods have a great potential to be applied in such a context, and to contribute to reducing the impact of pregnancy diseases and complications on maternal and fetal health.

5.3 Strengths of this review

This review is not restricted to a particular ML application on pregnancy diseases and complications. There are a couple of recent systematic reviews that are similar to our work, however they focus on a specific ML application in the field of pregnancy care, such as the screening of adverse perinatal outcomes (160) and the prediction of perinatal complications (149). In contrast, this review covers the wide variety of applications that ML may have on maternal and fetal health, including not only the screening or prediction of perinatal alterations, but also biomarker discovery, risk estimation, correlation assessment, pharmacological treatment prediction, drug screening, data acquisition, data extraction, among others, in the context of such alterations. Moreover, this review has a marked clinical focus. There are some recent narrative and systematic reviews that describe different pregnancy-related ML applications, but their emphases are on the applications themselves, and not on specific perinatal pathologies (4, 5, 161, 162). On the contrary, this review focuses on particular diseases and complications, and gives a broad overview of ML applications for each, which allows to visualize how much ML has penetrated into specific areas of the field of obstetrics and gynecology. Finally, this review covers a considerable body of literature. Most of the reviews found in literature regarding ML and perinatal care include a small number of references (4, 5, 149, 160, 162). Contrarily, this review comprises an important number of scientific articles, which ensures giving a comprehensive overview of the state of art regarding the use of ML in the context of pregnancy diseases and complications.

5.4 Limitations of this review

Due to the narrative nature of this review, the search and selection of articles was not performed by means of a systematic protocol. Hence, it could be subjected to bias. In addition, this review was restricted to seven selected pregnancy diseases and complications, and English-written articles. Hence, we may have missed some promising ML applications in the field of maternal and fetal health.

6 Conclusion

The use of ML methods in the context of pregnancy diseases and complications is fairly recent, and is becoming increasingly popular. The applications are varied, and go beyond diagnosis. Indeed, ML has been used to improve the management, treatment, and also the understanding of the pathophysiological mechanisms underlying different perinatal alterations. Facing the challenges that come with working with different types of data, the handling of increasingly large amounts of information, the development of emerging technologies, and the need of translational studies, it is expected that the use of ML methods continue growing in the field of obstetrics and gynecology in the coming years.

Author contributions

DM, AR, CO, CR, EC, AE-S, JA-R, EG-G, and JA tabulated literature information; DM and JA wrote the manuscript; DM, CA, AD, EG-G, and JA improved the manuscript. All authors contributed to the article and approved the submitted version.

Funding

This work was financially supported by ANID through PhD scholarship 21190736 (DM), FONDECYT 11181153 (JA) and FOVI210057 (EG-G); and UdeC/MINEDUC *via* Proyecto UCO 1866 (DM).

Conflict of interest

The authors declare that the research was conducted in the absence of any commercial or financial relationships that could be construed as a potential conflict of interest.

Publisher's note

All claims expressed in this article are solely those of the authors and do not necessarily represent those of their affiliated organizations, or those of the publisher, the editors and the reviewers. Any product that may be evaluated in this article, or claim that may be made by its manufacturer, is not guaranteed or endorsed by the publisher.

References

1. Helm JM, Swiergosz AM, Haeberle HS, Karnuta JM, Schaffer JL, Krebs VE, et al. Machine learning and artificial intelligence: definitions, applications, and future directions. *Curr Rev Musculoskelet Med* (2020) 13:69–76. doi: 10.1007/s12178-020-09600-8

2. Amigo JM. Data mining, machine learning, deep learning, chemometrics. definitions, common points and trends (Spoiler alert: VALIDATE your models!). *Braz J Anal Chem* (2021) 8:45–61. doi: 10.30744/brjac.2179-3425.AR-38-2021

3. Goecks J, Jalili V, Heiser LM, Gray JW. How machine learning will transform biomedicine. *Cell* (2020) 181:92–101. doi: 10.1016/j.cell.2020.03.022

4. Abuelezz I, Hassan A, Jaber BA, Sharique M, Abd-Alrazaq A, Househ M, et al. Contribution of artificial intelligence in pregnancy: a scoping review. *Stud Health Technol Inform* (2022) 289:333–6. doi: 10.3233/SHTI210927

5. Islam MN, Mustafina SN, Mahmud T, Khan NI. Machine learning to predict pregnancy outcomes: a systematic review, synthesizing framework and future research agenda. *BMC Pregnancy Childbirth* (2022) 22:1–19. doi: 10.1186/s12884-022-04594-2

6. Brereton RG. *Applied chemometrics for scientists*. Chichester, UK: Wiley (2007). doi: 10.1002/9780470057780

7. Otto M. *Chemometrics*. Weinheim, Germany: Wiley-VCH Verlag GmbH & Co. KGaA (2016). doi: 10.1002/9783527699377

8. Gibbs RS, Karlan BY, Haney AF, Nygaard IE. *Danforth's obstetrics and gynecology. 10th ed*. Baltimore, MD: Lippincott Williams & Wilkins (2008).

9. Daszykowski M, Kaczmarek K, Vander Heyden Y, Walczak B. Robust statistics in data analysis {{/amp]]mdash; a review. *Chemom Intell Lab Syst* (2007) 85:203–19. doi: 10.1016/j.chemolab.2006.06.016

10. Engel J, Gerretzen J, Szymańska E, Jansen JJ, Downey G, Blanchet L, et al. Breaking with trends in pre-processing? *TrAC Trends Anal Chem* (2013) 50:96–106. doi: 10.1016/j.trac.2013.04.015

11. Bzdok D, Altman N, Krzywinski M. Statistics versus machine learning. *Nat Methods* (2018) 15:233–4. doi: 10.1038/nmeth.4642

12. Ballabio D, Grisoni F, Todeschini R. Multivariate comparison of classification performance measures. *Chemom Intell Lab Syst* (2018) 174:33–44. doi: 10.1016/j.chemolab.2017.12.004

13. Botchkarev A. A new typology design of performance metrics to measure errors in machine learning regression algorithms. *Interdiscip J Information Knowledge Manag* (2019) 14:045–76. doi: 10.28945/4184

14. McGinn TG, Guyatt GH, Wyer PC, Naylor CD, Stiell IG, Richardson WS, et al. Users' guides to the medical literature. *JAMA* (2000) 284:79. doi: 10.1001/jama.284.1.79

15. Cowley LE, Farewell DM, Maguire S, Kemp AM. Methodological standards for the development and evaluation of clinical prediction rules: a review of the literature. *Diagn Progn Res* (2019) 3:16. doi: 10.1186/s41512-019-0060-y

16. ADA. 2. classification and diagnosis of diabetes: standards of medical care in diabetes–2021. *Diabetes Care* (2021) 44:S15–33. doi: 10.2337/dc21-S002

17. McIntyre HD, Catalano P, Zhang C, Desoye G, Mathiesen ER, Damm P. Gestational diabetes mellitus. *Nat Rev Dis Prim* (2019) 5:47. doi: 10.1038/s41572-019-0098-8

18. Xiong Y, Lin L, Chen Y, Salerno S, Li Y, Zeng X, et al. Prediction of gestational diabetes mellitus in the first 19 weeks of pregnancy using machine learning techniques. *J Matern Neonatal Med* (2022) 35:2457–63. doi: 10.1080/14767058.2020.1786517

19. Zheng T, Ye W, Wang X, Li X, Zhang J, Little J, et al. A simple model to predict risk of gestational diabetes mellitus from 8 to 20 weeks of gestation in Chinese women. *BMC Pregnancy Childbirth* (2019) 19:252. doi: 10.1186/s12884-019-2374-8

20. Wu Y-TT, Zhang C-JJ, Mol BW, Kawai A, Li C, Chen L, et al. Early prediction of gestational diabetes mellitus in the Chinese population *via* advanced machine learning. *J Clin Endocrinol Metab* (2021) 106:e1191–205. doi: 10.1210/clinem/dgaa899

21. Artzi NS, Shilo S, Hadar E, Rossman H, Barbash-Hazan S, Ben-Haroush A, et al. Prediction of gestational diabetes based on nationwide electronic health records. *Nat Med* (2020) 26:71–6. doi: 10.1038/s41591-019-0724-8

22. Balani J, Hyer S, Shehata H, Mohareb F. Visceral fat mass as a novel risk factor for predicting gestational diabetes in obese pregnant women. *Obstet Med* (2018) 11:121–5. doi: 10.1177/1753495X17754149

23. Mennickent D, Ortega-Contreras B, Gutiérrez-Vega S, Castro E, Rodríguez A, Araya J, et al. Evaluation of first and second trimester maternal thyroid profile on the prediction of gestational diabetes mellitus and post load glycemia. *PloS One* (2023) 18: e0280513. doi: 10.1371/journal.pone.0280513

24. Scott HD, Buchan M, Chadwick C, Field CJ, Letourneau N, Montina T, et al. Metabolic dysfunction in pregnancy: fingerprinting the maternal metabolome using proton nuclear magnetic resonance spectroscopy. *Endocrinol Diabetes Metab* (2021) 4:1–10. doi: 10.1002/edm2.201

25. Yoffe L, Polsky A, Gilam A, Raff C, Mecacci F, Ognibene A, et al. Early diagnosis of gestational diabetes mellitus using circulating microRNAs. *Eur J Endocrinol* (2019) 181:565–77. doi: 10.1530/EJE-19-0206

26. Guo Z, Yang F, Zhang J, Zhang Z, Li K, Tian Q, et al. Whole-genome promoter profiling of plasma DNA exhibits diagnostic value for placenta-origin pregnancy complications. *Adv Sci* (2020) 7:1901819. doi: 10.1002/advs.201901819

27. Liu Y, Wang Z, Zhao L. Identification of diagnostic cytosine-phosphate-guanine biomarkers in patients with gestational diabetes mellitus *via* epigenome-wide association study and machine learning. *Gynecol Endocrinol* (2021) 37:857–62. doi: 10.1080/09513590.2021.1937101

28. Ehrlich SF, Ferrara A, Hedderson MM, Feng J, Neugebauer R. Exercise during the first trimester of pregnancy and the risks of abnormal screening and gestational diabetes mellitus. *Diabetes Care* (2021) 44:425–32. doi: 10.2337/dc20-1475

29. Bernardes-Oliveira E, de Freitas DLD, de Morais CdeLM, de Mesquita Cornetta MdaC, Camargo JD, de AS, et al. Spectrochemical differentiation in gestational diabetes mellitus based on attenuated total reflection Fourier-transform infrared (ATR-FTIR) spectroscopy and multivariate analysis. *Sci Rep* (2020) 10:19259. doi: 10.1038/s41598-020-75539-y

30. Araya J, Rodriguez A, Lagos-SanMartin K, Mennickent D, Gutiérrez-Vega S, Ortega-Contreras B, et al. Maternal thyroid profile in first and second trimester of pregnancy is correlated with gestational diabetes mellitus through machine learning. *Placenta* (2021) 103:82–5. doi: 10.1016/j.placenta.2020.10.015

31. Velardo C, Clifton D, Hamblin S, Khan R, Tarassenko L, Mackillop L. Toward a multivariate prediction model of pharmacological treatment for women with gestational diabetes mellitus: algorithm development and validation. *J Med Internet Res* (2021) 23:e21435. doi: 10.2196/21435

32. Mennickent D, Rodríguez A, Farías-Jofré M, Araya J, Guzmán-Gutiérrez E. Machine learning-based models for gestational diabetes mellitus prediction before 24–28 weeks of pregnancy: a review. *Artif Intell Med* (2022) 132:102378. doi: 10.1016/j.artmed.2022.102378

33. Ababneh M. Management of pre-eclampsia/eclampsia. *Middle East J Anaesthesiol* (2004) 17:939–50.

34. ACOG. Hypertension in pregnancy. *Obstet Gynecol* (2013) 122:1122–31. doi: 10.1097/01.AOG.0000437382.03963.88

35. Mureşan D, Rotar IC, Stamatian F. The usefulness of fetal Doppler evaluation in early versus late onset intrauterine growth restriction. review of the literature. *Med Ultrason* (2016) 18:103. doi: 10.11152/mu.2013.2066.181.dop

36. Gyselaers W, Mullens W, Tomsin K, Mesens T, Peeters L. Role of dysfunctional maternal venous hemodynamics in the pathophysiology of pre-eclampsia: a review. *Ultrasound Obstet Gynecol* (2011) 38:123–9. doi: 10.1002/uog.9061

37. Keikkala E, Vuorela P, Laivuori H, Romppanen J, Heinonen S, Stenman U-H. First trimester hyperglycosylated human chorionic gonadotrophin in serum – a marker of early-onset preeclampsia. *Placenta* (2013) 34:1059–65. doi: 10.1016/j.placenta.2013.08.006

38. Birdir C, Fryze J, Vasiliadis H, Nicolaides KH, Poon LC. Maternal serum anti-müllerian hormone at 11–13 weeks' gestation in the prediction of preeclampsia. *J Matern Neonatal Med* (2015) 28:865–8. doi: 10.3109/14767058.2014.937418

39. Stepan H, Unversucht A, Wessel N, Faber R. Predictive value of maternal angiogenic factors in second trimester pregnancies with abnormal uterine perfusion. *Hypertension* (2007) 49:818–24. doi: 10.1161/01.HYP.0000258404.21552.a3

40. Stepan H, Geipel A, Schwarz F, Krämer T, Wessel N, Faber R. Circulatory soluble endoglin and its predictive value for preeclampsia in second-trimester pregnancies with abnormal uterine perfusion. *Am J Obstet Gynecol* (2008) 198:175.e1–6. doi: 10.1016/j.ajog.2007.08.052

41. Lee SM, Kang Y, Lee EM, Jung YM, Hong S, Park SJ, et al. Metabolomic biomarkers in midtrimester maternal plasma can accurately predict the development of preeclampsia. *Sci Rep* (2020) 10:16142. doi: 10.1038/s41598-020-72852-4

42. Tarca AL, Romero R, Benshalom-Tirosh N, Than NG, Gudicha DW, Done B, et al. The prediction of early preeclampsia: results from a longitudinal proteomics study. *PloS One* (2019) 14:e0217273. doi: 10.1371/journal.pone.0217273

43. Jiang M, Lash GE, Zhao X, Long Y, Guo C, Yang H. CircRNA-0004904, CircRNA-0001855, and PAPP-a: potential novel biomarkers for the prediction of preeclampsia. *Cell Physiol Biochem* (2018) 46:2576–86. doi: 10.1159/000489685

44. Han Q, Zheng W, Guo XD, Zhang D, Liu HF, Yu L, et al. A new predicting model of preeclampsia based on peripheral blood test values. *Eur Rev Med Pharmacol Sci* (2020) 24:7222–9. doi: 10.26355/eurrev_202007_21874

45. Jhee JH, Lee S, Park Y, Lee SE, Kim YA, Kang S-W, et al. Prediction model development of late-onset preeclampsia using machine learning-based methods. *PloS One* (2019) 14:e0221202. doi: 10.1371/journal.pone.0221202

46. Marić I, Tsur A, Aghaeepour N, Montanari A, Stevenson DK, Shaw GM, et al. Early prediction of preeclampsia *via* machine learning. *Am J Obstet Gynecol MFM* (2020) 2:100100. doi: 10.1016/j.ajogmf.2020.100100

47. Mello G, Parretti E, Ognibene A, Mecacci F, Cioni R, Scarselli G, et al. Prediction of the development of pregnancy-induced hypertensive disorders in high-risk pregnant women by artificial neural networks. *Clin Chem Lab Med* (2001) 39:801–5. doi: 10.1515/CCLM.2001.132

48. Sandström A, Snowden JM, Höijer J, Bottai M, Wikström A-K. Clinical risk assessment in early pregnancy for preeclampsia in nulliparous women: a population based cohort study. *PloS One* (2019) 14:e0225716. doi: 10.1371/journal.pone.0225716

49. Sufriyana H, Wu Y-W, Su EC-Y. Prediction of preeclampsia and intrauterine growth restriction: development of machine learning models on a prospective cohort. *JMIR Med Inf* (2020) 8:e15411. doi: 10.2196/15411

50. Sufriyana H, Wu Y-W, Su EC-Y. Artificial intelligence-assisted prediction of preeclampsia: development and external validation of a nationwide health insurance dataset of the BPJS kesehatan in Indonesia. *EBioMedicine* (2020) 54:102710. doi: 10.1016/j.ebiom.2020.102710

51. Gupta K, Balyan K, Lamba B, Puri M, Sengupta D, Kumar M. Ultrasound placental image texture analysis using artificial intelligence to predict hypertension in pregnancy. *J Matern Neonatal Med* (2022) 35:5587–94. doi: 10.1080/14767058.2021.1887847

52. Liu K, Fu Q, Liu Y, Wang C. An integrative bioinformatics analysis of microarray data for identifying hub genes as diagnostic biomarkers of preeclampsia. *Biosci Rep* (2019) 39:866–75. doi: 10.1042/BSR20190187

53. Guo R, Teng Z, Wang Y, Zhou X, Xu H, Liu D. Integrated learning: screening optimal biomarkers for identifying preeclampsia in placental mRNA samples. *Comput Math Methods Med* (2021) 2021:1–7. doi: 10.1155/2021/6691096

54. Bodnar LM, Cartus AR, Kirkpatrick SI, Himes KP, Kennedy EH, Simhan HN, et al. Machine learning as a strategy to account for dietary synergy: an illustration based on dietary intake and adverse pregnancy outcomes. *Am J Clin Nutr* (2020) 111:1235–43. doi: 10.1093/ajcn/nqaa027

55. Tejera E, Pérez-Castillo Y, Chamorro A, Cabrera-Andrade A, Sanchez ME. A multi-objective approach for drug repurposing in preeclampsia. *Molecules* (2021) 26:777. doi: 10.3390/molecules26040777

56. WHO. *Making every baby Count : audit and review of stillbirths and neonatal deaths*. Geneva, Switzerland. WHO Press. (2016).

57. WHO. *The WHO application of ICD-10 to deaths during the perinatal period: ICD-PM*. Geneva, Switzerland. WHO Press (2016).

58. Liu L, Oza S, Hogan D, Perin J, Rudan I, Lawn JE, et al. Global, regional, and national causes of child mortality in 2000–13, with projections to inform post-2015 priorities: an updated systematic analysis. *Lancet* (2015) 385:430–40. doi: 10.1016/S0140-6736(14)61698-6

59. Blencowe H, Cousens S, Jassir FB, Say L, Chou D, Mathers C, et al. National, regional, and worldwide estimates of stillbirth rates in 2015, with trends from 2000: a systematic analysis. *Lancet Glob Heal* (2016) 4:e98–e108. doi: 10.1016/S2214-109X(15)00275-2

60. Willcox ML, Price J, Scott S, Nicholson BD, Stuart B, Roberts NW, et al. Death audits and reviews for reducing maternal, perinatal and child mortality. *Cochrane Database Syst Rev* (2020) 2020. doi: 10.1002/14651858.CD012982.pub2

61. Abebe H, Adane D, Shitu S. Essential newborn care practice and its associated factors in southwest Ethiopia. *Arch Public Heal* (2021) 79:42. doi: 10.1186/s13690-021-00568-6

62. Malacova E, Tippaya S, Bailey HD, Chai K, Farrant BM, Gebremedhin AT, et al. Stillbirth risk prediction using machine learning for a large cohort of births from Western australia 1980–2015. *Sci Rep* (2020) 10:5354. doi: 10.1038/s41598-020-62210-9

63. Kayode GA, Grobbee DE, Amoakoh-Coleman M, Adeleke IT, Ansah E, de Groot JAH, et al. Predicting stillbirth in a low resource setting. *BMC Pregnancy Childbirth* (2016) 16:274. doi: 10.1186/s12884-016-1061-2

64. Koivu A, Sairanen M. Predicting risk of stillbirth and preterm pregnancies with machine learning. *Heal Inf Sci Syst* (2020) 8:14. doi: 10.1007/s13755-020-00105-9

65. Shukla VV, Eggleston B, Ambalavanan N, McClure EM, Mwenechanya M, Chomba E, et al. Predictive modeling for perinatal mortality in resource-limited settings. *JAMA Netw Open* (2020) 3:e2026750. doi: 10.1001/jamanetworkopen.2020.26750

66. Mboya IB, Mahande MJ, Mohammed M, Obure J, Mwambi HG. Prediction of perinatal death using machine learning models: a birth registry-based cohort study in northern Tanzania. *BMJ Open* (2020) 10:e040132. doi: 10.1136/bmjopen-2020-040132

67. Khatibi T, Hanifi E, Sepehri MM, Allahqoli L. Proposing a machine-learning based method to predict stillbirth before and during delivery and ranking the features: nationwide retrospective cross-sectional study. *BMC Pregnancy Childbirth* (2021) 21:202. doi: 10.1186/s12884-021-03658-z

68. Rezaeian A, Rezaeian M, Khatami SF, Khorashadizadeh F, Moghaddam FP. Prediction of mortality of premature neonates using neural network and logistic regression. *J Ambient Intell Humaniz Comput* (2022) 13:1269–77. doi: 10.1007/s12652-020-02562-2

69. Cooper JN, Minneci PC, Deans KJ. Postoperative neonatal mortality prediction using superlearning. *J Surg Res* (2018) 221:311–9. doi: 10.1016/j.jss.2017.09.002

70. Jaskari J, Myllarinen J, Leskinen M, Rad AB, Hollmen J, Andersson S, et al. Machine learning methods for neonatal mortality and morbidity classification. *IEEE Access* (2020) 8:123347–58. doi: 10.1109/ACCESS.2020.3006710

71. Sheikhtaheri A, Zarkesh MR, Moradi R, Kermani F. Prediction of neonatal deaths in NICUs: development and validation of machine learning models. *BMC Med Inform Decis Mak* (2021) 21:131. doi: 10.1186/s12911-021-01497-8

72. Mangold C, Zoretic S, Thallapureddy K, Moreira A, Chorath K, Moreira A. Machine learning models for predicting neonatal mortality: a systematic review. *Neonatology* (2021) 118:394–405. doi: 10.1159/000516891

73. Larsen EC, Christiansen OB, Kolte AM, Macklon N. New insights into mechanisms behind miscarriage. *BMC Med* (2013) 11:154. doi: 10.1186/1741-7015-11-154

74. Bottomley C, Van Belle V, Kirk E, Van Huffel S, Timmerman D, Bourne T. Accurate prediction of pregnancy viability by means of a simple scoring system. *Hum Reprod* (2013) 28:68–76. doi: 10.1093/humrep/des352

75. Mu Y, Yuan Y, Han W, Pian P, Li L, Wang D, et al. Exploring the molecular mechanism and biomarker of recurrent spontaneous abortion based on RNA sequencing analysis. *Clin Lab* (2020) 66:2055–61. doi: 10.7754/Clin.Lab.2020.200222

76. Toh C, Brody JP. Applications of machine learning in healthcare. In: *Smart manufacturing - when artificial intelligence meets the Internet of things*. London, UK: IntechOpen (2021). doi: 10.5772/intechopen.92297

77. Mora-Sánchez A, Aguilar-Salvador D-I, Nowak I. Towards a gamete matching platform: using immunogenetics and artificial intelligence to predict recurrent miscarriage. *NPJ Digit Med* (2019) 2:12. doi: 10.1038/s41746-019-0089-x

78. Wu Y, Xin M, Han Q, Wang J, Yin X, He J, et al. Extensive serum biomarker analysis in the prethrombotic state of recurrent spontaneous abortion. *J Cell Mol Med* (2021) 25:6679–94. doi: 10.1111/jcmm.16671

79. Liu L, Jiao Y, Li X, Ouyang Y, Shi D. Machine learning algorithms to predict early pregnancy loss after *in vitro* fertilization-embryo transfer with fetal heart rate as a strong predictor. *Comput Methods Programs BioMed* (2020) 196:105624. doi: 10.1016/j.cmpb.2020.105624

80. Huang C, Xiang Z, Zhang Y, Tan DS, Yip CK, Liu Z, et al. Using deep learning in a monocentric study to characterize maternal immune environment for predicting pregnancy outcomes in the recurrent reproductive failure patients. *Front Immunol* (2021) 12:642167. doi: 10.3389/fimmu.2021.642167

81. Meuleman T, Lashley LELO, Dekkers OM, van Lith JMM, Claas FHJ, Bloemenkamp KWM. HLA associations and HLA sharing in recurrent miscarriage: a systematic review and meta-analysis. *Hum Immunol* (2015) 76:362–73. doi: 10.1016/j.humimm.2015.02.004

82. Berger DS, Hogge WA, Barmada MM, Ferrell RE. Comprehensive analysis of HLA-G: implications for recurrent spontaneous abortion. *Reprod Sci* (2010) 17:331–8. doi: 10.1177/1933719109356802

83. Medenica S, Zivanovic D, Batkoska L, Marinelli S, Basile G, Perino A, et al. The future is coming: artificial intelligence in the treatment of infertility could improve assisted reproduction outcomes–the value of regulatory frameworks. *Diagnostics* (2022) 12. doi: 10.3390/diagnostics12122979

84. Chawanpaiboon S, Vogel JP, Moller A-B, Lumbiganon P, Petzold M, Hogan D, et al. Global, regional, and national estimates of levels of preterm birth in 2014: a systematic review and modelling analysis. *Lancet Glob Heal* (2019) 7:e37–46. doi: 10.1016/S2214-109X(18)30451-0

85. Suff N, Story L, Shennan A. The prediction of preterm delivery: what is new? *Semin Fetal Neonatal Med* (2019) 24:27–32. doi: 10.1016/j.siny.2018.09.006

86. Khatibi T, Kheyrikoochaksarayee N, Sepehri MM. Analysis of big data for prediction of provider-initiated preterm birth and spontaneous premature deliveries and ranking the predictive features. *Arch Gynecol Obstet* (2019) 300:1565–82. doi: 10.1007/s00404-019-05325-3

87. Arabi Belaghi R, Beyene J, McDonald SD. Prediction of preterm birth in nulliparous women using logistic regression and machine learning. *PloS One* (2021) 16:e0252025. doi: 10.1371/journal.pone.0252025

88. Gao C, Osmundson S, Velez Edwards DR, Jackson GP, Malin BA, Chen Y. Deep learning predicts extreme preterm birth from electronic health records. *J BioMed Inform* (2019) 100:103334. doi: 10.1016/j.jbi.2019.103334

89. Zhang Y, Lu S, Wu Y, Hu W, Yuan Z. The prediction of preterm birth using time-series technology-based machine learning: retrospective cohort study. *JMIR Med Inf* (2022) 10:e33835. doi: 10.2196/33835

90. Aung MT, Yu Y, Ferguson KK, Cantonwine DE, Zeng L, McElrath TF, et al. Prediction and associations of preterm birth and its subtypes with eicosanoid enzymatic pathways and inflammatory markers. *Sci Rep* (2019) 9:17049. doi: 10.1038/s41598-019-53448-z

91. Chen Y, He B, Liu Y, Aung MT, Rosario-Pabón Z, Vélez-Vega CM, et al. Maternal plasma lipids are involved in the pathogenesis of preterm birth. *Gigascience* (2022) 11:1–11. doi: 10.1093/gigascience/giac004

92. Jehan F, Sazawal S, Baqui AH, Nisar MI, Dhingra U, Khanam R, et al. Multiomics characterization of preterm birth in low- and middle-income countries. *JAMA Netw Open* (2020) 3:e2029655. doi: 10.1001/jamanetworkopen.2020.29655

93. Despotovic D, Zec A, Mladenovic K, Radin N, Turukalo TL. A machine learning approach for an early prediction of preterm delivery. *2018 IEEE 16th Int Symp Intell Syst Inf* (2018), 265–70. doi: 10.1109/SISY.2018.8524818

94. Rawashdeh H, Awawdeh S, Shannag F, Henawi E, Faris H, Obeid N, et al. Intelligent system based on data mining techniques for prediction of preterm birth for women with cervical cerclage. *Comput Biol Chem* (2020) 85:107233. doi: 10.1016/j.compbiolchem.2020.107233

95. Ye J, Zhang J, Mikolajczyk R, Torloni M, Gülmezoglu A, Betran A. Association between rates of caesarean section and maternal and neonatal mortality in the 21st century: a worldwide population-based ecological study with longitudinal data. *BJOG Int J Obstet Gynaecol* (2016) 123:745–53. doi: 10.1111/1471-0528.13592

96. Martinez LD, Glynn LM, Sandman CA, Wing DA, Davis EP. Cesarean delivery and infant cortisol regulation. *Psychoneuroendocrinology* (2020) 122:104862. doi: 10.1016/j.psyneuen.2020.104862

97. Gosset M, Ilenko A, Bouyou J, Renevier B. Emergency caesarean section. *J Visc Surg* (2017) 154:47–50. doi: 10.1016/j.jviscsurg.2016.09.012

98. David M, Scherer K, Henrich W, Breckenkamp J. Does an immigrant background affect the indication, incidence or outcome of emergency cesarean section? results of the prospective data collection of 111 births. *Geburtshilfe Frauenheilkd* (2018) 78:167–72. doi: 10.1055/s-0044-100147

99. Ryding EL, Wijma K, Wijma B. Psychological impact of emergency cesarean section in comparison with elective cesarean section, instrumental and normal vaginal delivery. *J Psychosom Obstet Gynecol* (1998) 19:135–44. doi: 10.3109/01674829809025691

100. Yang X-J, Sun S-S. Comparison of maternal and fetal complications in elective and emergency cesarean section: a systematic review and meta-analysis. *Arch Gynecol Obstet* (2017) 296:503–12. doi: 10.1007/s00404-017-4445-2

101. Wangel A-M, Molin J, Östman M, Jernström H. Emergency cesarean sections can be predicted by markers for stress, worry and sleep disturbances in first-time mothers. *Acta Obstet Gynecol Scand* (2011) 90:no–o. doi: 10.1111/j.1600-0412.2010.01056.x

102. Fergus P, Hussain A, Al-Jumeily D, Huang D-S, Bouguila N. Classification of caesarean section and normal vaginal deliveries using foetal heart rate signals and advanced machine learning algorithms. *BioMed Eng Online* (2017) 16:89. doi: 10.1186/s12938-017-0378-z

103. Fergus P, Selvaraj M, Chalmers C. Machine learning ensemble modelling to classify caesarean section and vaginal delivery types using cardiotocography traces. *Comput Biol Med* (2018) 93:7–16. doi: 10.1016/j.compbiomed.2017.12.002

104. Ricciardi C, Improta G, Amato F, Cesarelli G, Romano M. Classifying the type of delivery from cardiotocographic signals: a machine learning approach. *Comput Methods Programs BioMed* (2020) 196:105712. doi: 10.1016/j.cmpb.2020.105712

105. Tang H, Wang T, Li M, Yang X. The design and implementation of cardiotocography signals classification algorithm based on neural network. *Comput Math Methods Med* (2018) 2018:1–12. doi: 10.1155/2018/8568617

106. Clark RRS, Hou J. Three machine learning algorithms and their utility in exploring risk factors associated with primary cesarean section in low-risk women: a methods paper. *Res Nurs Health* (2021) 44:559–70. doi: 10.1002/nur.22122

107. Wei C, Wang L, Chang X, Zhou Q. A prediction model using machine-learning algorithm for assessing intrathecal hyperbaric bupivacaine dose during cesarean section. *BMC Anesthesiol* (2021) 21:116. doi: 10.1186/s12871-021-01331-8

108. Fletcher RR, Olubeko O, Sonthalia H, Kateera F, Nkurunziza T, Ashby JL, et al. Application of machine learning to prediction of surgical site infection. *2019 41st Annu Int Conf IEEE Eng Med Biol Soc (EMBC)* (2019), 2234–7. doi: 10.1109/EMBC.2019.8857942

109. Lipschuetz M, Guedalia J, Rottenstreich A, Novoselsky Persky M, Cohen SM, Kabiri D, et al. Prediction of vaginal birth after cesarean deliveries using machine learning. *Am J Obstet Gynecol* (2020) 222:613.e1–613.e12. doi: 10.1016/j.ajog.2019.12.267

110. Pinas A, Chandraharan E. Continuous cardiotocography during labour: analysis, classification and management. *Best Pract Res Clin Obstet Gynaecol* (2016) 30:33–47. doi: 10.1016/j.bpobgyn.2015.03.022

111. Akbulut A, Ertugrul E, Topcu V. Fetal health status prediction based on maternal clinical history using machine learning techniques. *Comput Methods Programs BioMed* (2018) 163:87–100. doi: 10.1016/j.cmpb.2018.06.010

112. Mendoza CS, Safdar N, Okada K, Myers E, Rogers GF, Linguraru MG. Personalized assessment of craniosynostosis *via* statistical shape modeling. *Med Image Anal* (2014) 18:635–46. doi: 10.1016/j.media.2014.02.008

113. Wu JY, Tuomi A, Beland MD, Konrad J, Glidden D, Grand D, et al. Quantitative analysis of ultrasound images for computer-aided diagnosis. *J Med Imaging* (2016) 3:14501. doi: 10.1117/1.JMI.3.1.014501

114. Meulstee JW, Verhamme LM, Borstlap WA, van der Heijden F, De Jong GA, Xi T, et al. A new method for three-dimensional evaluation of the cranial shape and the automatic identification of craniosynostosis using 3D stereophotogrammetry. *Int J Oral Maxillofac Surg* (2017) 46:819–26. doi: 10.1016/j.ijom.2017.03.017

115. Bridge CP, Ioannou C, Noble JA. Automated annotation and quantitative description of ultrasound videos of the fetal heart. *Med Image Anal* (2017) 36:147–61. doi: 10.1016/j.media.2016.11.006

116. Yu Q, Yan H, Song L, Guo W, Liu H, Si J, et al. Automatic identifying of maternal ECG source when applying ICA in fetal ECG extraction. *Biocybern BioMed Eng* (2018) 38:448–55. doi: 10.1016/j.bbe.2018.03.003

117. Muduli PR, Gunukula RR, Mukherjee A. (2016). A deep learning approach to fetal-ECG signal reconstruction, in: *2016 Twenty Second National Conference on Communication (NCC) (IEEE)*. Guwahati, India, . pp. 1–6. doi: 10.1109/NCC.2016.7561206

118. Maraci MA, Bridge CP, Napolitano R, Papageorghiou A, Noble JA. A framework for analysis of linear ultrasound videos to detect fetal presentation and heartbeat. *Med Image Anal* (2017) 37:22–36. doi: 10.1016/j.media.2017.01.003

119. Krupa N, MA M, Zahedi E, Ahmed S, Hassan FM. Antepartum fetal heart rate feature extraction and classification using empirical mode decomposition and support vector machine. *BioMed Eng Online* (2011) 10:6. doi: 10.1186/1475-925X-10-6

120. Fotiadou E, van Sloun RJG, van Laar JOEH, Vullings R. A dilated inception CNN-LSTM network for fetal heart rate estimation. *Physiol Meas* (2021) 42:045007. doi: 10.1088/1361-6579/abf7db

121. Fotiadou E, Xu M, van Erp B, van Sloun RJG, Vullings R. (2020). Deep convolutional long short-term memory network for fetal heart rate extraction, in: *2020 42nd Annual International Conference of the IEEE Engineering in Medicine & Biology Society (EMBC)*, Montreal, Canada. pp. 1–4. doi: 10.1109/EMBC44109.2020.9175442

122. Al-Angari HM, Kimura Y, Hadjileontiadis LJ, Khandoker AH. A hybrid EMD-kurtosis method for estimating fetal heart rate from continuous Doppler signals. *Front Physiol* (2017) 8:641. doi: 10.3389/fphys.2017.00641

123. Zhao Z, Deng Y, Zhang Y, Zhang Y, Zhang X, Shao L. DeepFHR: intelligent prediction of fetal acidemia using fetal heart rate signals based on convolutional neural network. *BMC Med Inform Decis Mak* (2019) 19:286. doi: 10.1186/s12911-019-1007-5

124. Brocklehurst P. A study of an intelligent system to support decision making in the management of labour using the cardiotocograph – the INFANT study protocol. *BMC Pregnancy Childbirth* (2016) 16:10. doi: 10.1186/s12884-015-0780-0

125. Parer JT, Hamilton EF. Comparison of 5 experts and computer analysis in rule-based fetal heart rate interpretation. *Am J Obstet Gynecol* (2010) 203:451.e1–7. doi: 10.1016/j.ajog.2010.05.037

126. Alonso-Betanzos A, Moret-Bonillo V, Hernandez-Sande C. Foetos: an expert system for fetal assessment. *IEEE Trans BioMed Eng* (1991) 38:199–211. doi: 10.1109/10.76387

127. Gurgen F, Onal E, Varol FG. IUGR detection by ultrasonographic examinations using neural networks. *IEEE Eng Med Biol Mag* (1997) 16:55–8. doi: 10.1109/51.585518

128. Magenes G, Pedrinazzi L, Signorini MG. (2004). Identification of fetal sufferance antepartum through a multiparametric analysis and a support vector machine, in: *The 26th Annual International Conference of the IEEE Engineering in Medicine and Biology Society (IEEE)*, San Francisco, USA. pp. 462–5. doi: 10.1109/IEMBS.2004.1403194

129. Gadagkar AV, Shreedhara KS. (2014). Features based IUGR diagnosis using variational level set method and classification using artificial neural networks, in: *2014 Fifth International Conference on Signal and Image Processing (IEEE)*, Bangalore, India. pp. 303–9. doi: 10.1109/ICSIP.2014.54

130. Yeo L, Romero R. Fetal intelligent navigation echocardiography (FINE): a novel method for rapid, simple, and automatic examination of the fetal heart. *Ultrasound Obstet Gynecol* (2013) 42:268–84. doi: 10.1002/uog.12563

131. Han G, Jin T, Zhang L, Guo C, Gui H, Na R, et al. Adoption of compound echocardiography under artificial intelligence algorithm in fetal congenial heart disease screening during gestation. *Appl Bionics Biomech* (2022) 2022:1–8. doi: 10.1155/2022/6410103

132. Al-Shaer AE, Flentke GR, Berres ME, Garic A, Smith SM. Exon level machine learning analyses elucidate novel candidate miRNA targets in an avian model of fetal alcohol spectrum disorder. *PloS Comput Biol* (2019) 15:e1006937. doi: 10.1371/journal.pcbi.1006937

133. Shigemi D, Yamaguchi S, Aso S, Yasunaga H. Predictive model for macrosomia using maternal parameters without sonography information. *J Matern Neonatal Med* (2019) 32:3859–63. doi: 10.1080/14767058.2018.1484090

134. Tao J, Yuan Z, Sun L, Yu K, Zhang Z. Fetal birthweight prediction with measured data by a temporal machine learning method. *BMC Med Inform Decis Mak* (2021) 21:26. doi: 10.1186/s12911-021-01388-y

135. Challa AP, Beam AL, Shen M, Peryea T, Lavieri RR, Lippmann ES, et al. Machine learning on drug-specific data to predict small molecule teratogenicity. *Reprod Toxicol* (2020) 95:148–58. doi: 10.1016/j.reprotox.2020.05.004

136. Guimarães-Ferreira J, Miguéns J, Lauritzen C. Advances in craniosynostosis research and management. In: *Advances and technical standards in neurosurgery* Vienna, Austria. Springer (2004). p. 23–83. doi: 10.1007/978-3-7091-0558-0_2

137. Safran T, Gorsky K, Viezel-Mathieu A, Kanevsky J, Gilardino MS. The role of ultrasound technology in plastic surgery. *J Plast Reconstr Aesthetic Surg* (2018) 71:416–24. doi: 10.1016/j.bjps.2017.08.031

138. Wren C. Temporal variability in birth prevalence of cardiovascular malformations. *Heart* (2000) 83:414–9. doi: 10.1136/heart.83.4.414

139. Moons P, Sluysmans T, De Wolf D, Massin M, Suys B, Benatar A, et al. Congenital heart disease in 111 225 births in Belgium: birth prevalence, treatment and survival in the 21st century. *Acta Paediatr* (2009) 98:472–7. doi: 10.1111/j.1651-2227.2008.01152.x

140. Rychik J, Tian Z, Bebbington M, Xu F, McCann M, Mann S, et al. The twin-twin transfusion syndrome: spectrum of cardiovascular abnormality and development of a cardiovascular score to assess severity of disease. *Am J Obstet Gynecol* (2007) 197:392.e1–8. doi: 10.1016/j.ajog.2007.06.055

141. Garcia-Canadilla P, Sanchez-Martinez S, Crispi F, Bijnens B. Machine learning in fetal cardiology: what to expect. *Fetal Diagn Ther* (2020) 47:363–72. doi: 10.1159/000505021

142. Crispi F, Valenzuela-Alcaraz B, Cruz-Lemini M, Gratacós E. Ultrasound assessment of fetal cardiac function. *Australas J Ultrasound Med* (2013) 16:158–67. doi: 10.1002/j.2205-0140.2013.tb00242.x

143. Cruz-Lemini M, Crispi F, Valenzuela-Alcaraz B, Figueras F, Sitges M, Bijnens B, et al. Fetal cardiovascular remodeling persists at 6 months in infants with intrauterine growth restriction. *Ultrasound Obstet Gynecol* (2016) 48:349–56. doi: 10.1002/uog.15767

144. Resendiz M, Mason S, Lo C-L, Zhou FC. Epigenetic regulation of the neural transcriptome and alcohol interference during development. *Front Genet* (2014) 5:285. doi: 10.3389/fgene.2014.00285

145. Langer O, Berkus MD, Huff RW, Samueloff A. Shoulder dystocia: should the fetus weighing ≥4000 grams be delivered by cesarean section? *Am J Obstet Gynecol* (1991) 165:831–7. doi: 10.1016/0002-9378(91)90424-P

146. Oral E, Cağdaş A, Gezer A, Kaleli S, Aydinli K, Öçer F. Perinatal and maternal outcomes of fetal macrosomia. *Eur J Obstet Gynecol Reprod Biol* (2001) 99:167–71. doi: 10.1016/S0301-2115(01)00416-X

147. Garg RC, Bracken WM, XXXM. Hoberman A. Reproductive and developmental safety evaluation of new pharmaceutical compounds. In: *Reproductive and developmental toxicology*. Oxford, UK: Elsevier (2011). p. 89–109. doi: 10.1016/B978-0-12-382032-7.10008-6

148. Kim JH, Scialli AR. Thalidomide: the tragedy of birth defects and the effective treatment of disease. *Toxicol Sci* (2011) 122:1–6. doi: 10.1093/toxsci/kfr088

149. Bertini A, Salas R, Chabert S, Sobrevia L, Pardo F. Using machine learning to predict complications in pregnancy: a systematic review. *Front Bioeng Biotechnol* (2022) 9:780389. doi: 10.3389/fbioe.2021.780389

150. Sufriyana H, Husnayain A, Chen YL, Kuo CY, Singh O, Yeh TY, et al. Comparison of multivariable logistic regression and other machine learning algorithms for prognostic prediction studies in pregnancy care: systematic review and meta-analysis. *JMIR Med Inf* (2020) 8:1–26. doi: 10.2196/16503

151. Kumar M, Mostafa J. Research evidence on strategies enabling integration of electronic health records in the health care systems of low- and middle-income countries: a literature review. *Int J Health Plann Manage* (2019) 34:e1016–25. doi: 10.1002/hpm.2754

152. Shapiro LM, Kamal RN. Implementation of electronic health records during global outreach: a necessary next step in measuring and improving quality of care. *J Handb Surg Am* (2022) 47:279–83. doi: 10.1016/j.jhsa.2021.09.016

153. Sobti RC, Rai J, Prakash A. Introduction to emerging technologies in biomedical sciences. In: *Biomedical translational research*. Singapore: Springer Nature Singapore (2022). p. 1–22. doi: 10.1007/978-981-16-4345-3_1

154. Du Y, McNestry C, Wei L, Antoniadi AM, McAuliffe FM, Mooney C. Machine learning-based clinical decision support systems for pregnancy care: a systematic review. *Int J Med Inform* (2023) 173:105040. doi: 10.1016/j.ijmedinf.2023.105040

155. Sweeting A, Park F, Hyett J. The first trimester: prediction and prevention of the great obstetrical syndromes. *Best Pract Res Clin Obstet Gynaecol* (2015) 29:183–93. doi: 10.1016/j.bpobgyn.2014.09.006

156. Poon LC, McIntyre HD, Hyett JA, da Fonseca EB, Hod M. The first-trimester of pregnancy – a window of opportunity for prediction and prevention of pregnancy complications and future life. *Diabetes Res Clin Pract* (2018) 145:20–30. doi: 10.1016/j.diabres.2018.05.002

157. Bouariu A, Panaitescu AM, Nicolaides KH. First trimester prediction of adverse pregnancy outcomes–identifying pregnancies at risk from as early as 11–13 weeks. *Medicina (B Aires)* (2022) 58:332. doi: 10.3390/medicina58030332

158. Ngiam KY, Khor IW. Big data and machine learning algorithms for health-care delivery. *Lancet Oncol* (2019) 20:e262–73. doi: 10.1016/S1470-2045(19)30149-4

159. Khanzode KCA, Sarode RD. Advantages and disadvantages of artificial intelligence and machine learning: a literature review. *Int J Libr Inf Sci* (2020) 9:30–6. doi: 10.17605/OSF.IO/GV5T4

160. Feduniw S, Golik D, Kajdy A, Pruc M, Modzelewski J, Sys D, et al. Application of artificial intelligence in screening for adverse perinatal outcomes–a systematic review. *Healthc* (2022) 10:1–20. doi: 10.3390/healthcare10112164

161. Davidson L, Boland MR. Towards deep phenotyping pregnancy: a systematic review on artificial intelligence and machine learning methods to improve pregnancy outcomes. *Brief Bioinform* (2021) 22:1–29. doi: 10.1093/bib/bbaa369

162. Ramakrishnan R, Rao S, He JR. Perinatal health predictors using artificial intelligence: a review. *Women's Heal* (2021) 17:1–7. doi: 10.1177/17455065211046132

frontiers | Frontiers in Endocrinology

TYPE Review
PUBLISHED 11 July 2023
DOI 10.3389/fendo.2023.1172831

Check for updates

OPEN ACCESS

EDITED BY
Alicia E. Damiano,
University of Buenos Aires, Argentina

REVIEWED BY
Deanne Helena Hryciw,
Griffith University, Australia
Mauricio Castro-Parodi,
University of Buenos Aires, Argentina
Reinaldo Marín,
Instituto Venezolano de Investigaciones Científicas (IVIC), Venezuela

*CORRESPONDENCE
Antonio Pérez-Pérez
aperez14@us.es
Víctor Sánchez-Margalet
margalet@us.es

†These authors share first authorship

RECEIVED 23 February 2023
ACCEPTED 14 June 2023
PUBLISHED 11 July 2023

CITATION
Guadix P, Corrales I, Vilariño-García T, Rodríguez-Chacón C, Sánchez-Jiménez F, Jiménez-Cortegana C, Dueñas JL, Sánchez-Margalet V and Pérez-Pérez A (2023) Expression of nutrient transporters in placentas affected by gestational diabetes: role of leptin.
Front. Endocrinol. 14:1172831.
doi: 10.3389/fendo.2023.1172831

COPYRIGHT
© 2023 Guadix, Corrales, Vilariño-García, Rodríguez-Chacón, Sánchez-Jiménez, Jiménez-Cortegana, Dueñas, Sánchez-Margalet and Pérez-Pérez. This is an open-access article distributed under the terms of the Creative Commons Attribution License (CC BY). The use, distribution or reproduction in other forums is permitted, provided the original author(s) and the copyright owner(s) are credited and that the original publication in this journal is cited, in accordance with accepted academic practice. No use, distribution or reproduction is permitted which does not comply with these terms.

Expression of nutrient transporters in placentas affected by gestational diabetes: role of leptin

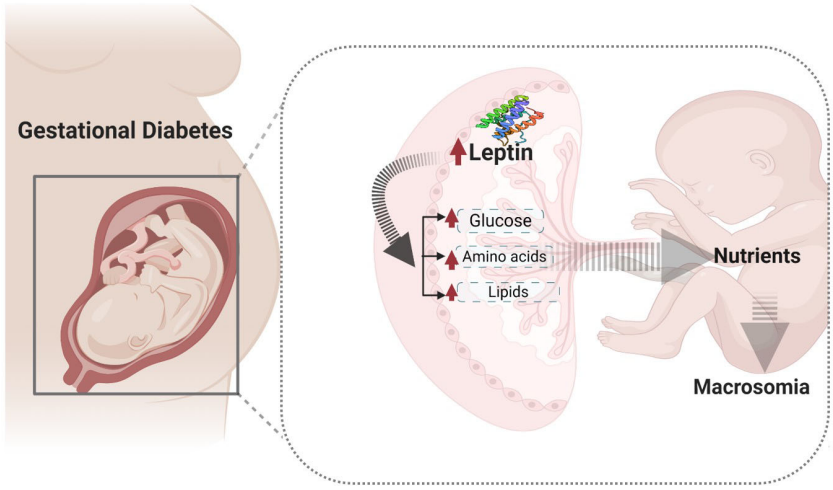
Pilar Guadix[1†], Isabel Corrales[1†], Teresa Vilariño-García[2], Carmen Rodríguez-Chacón[3], Flora Sánchez-Jiménez[3], Carlos Jiménez-Cortegana[3], José L. Dueñas[1], Víctor Sánchez-Margalet[3*] and Antonio Pérez-Pérez[3*]

[1]Obstetrics and Gynecology Service, Virgen Macarena University Hospital, School of Medicine, University of Seville, Seville, Spain, [2]Clinical Biochemistry Service, Virgen del Rocio University Hospital, School of Medicine, University of Seville, Seville, Spain, [3]Clinical Biochemistry Service, Virgen Macarena University Hospital and Department of Medical Biochemistry and Molecular Biology and Immunology, School of Medicine, University of Seville, Seville, Spain

Gestational diabetes mellitus (GDM) is the most frequent pathophysiological state of pregnancy, which in many cases produces fetuses with macrosomia, requiring increased nutrient transport in the placenta. Recent studies by our group have demonstrated that leptin is a key hormone in placental physiology, and its expression is increased in placentas affected by GDM. However, the effect of leptin on placental nutrient transport, such as transport of glucose, amino acids, and lipids, is not fully understood. Thus, we aimed to review literature on the leptin effect involved in placental nutrient transport as well as activated leptin signaling pathways involved in the expression of placental transporters, which may contribute to an increase in placental nutrient transport in human pregnancies complicated by GDM. Leptin appears to be a relevant key hormone that regulates placental transport, and this regulation is altered in pathophysiological conditions such as gestational diabetes. Adaptations in the placental capacity to transport glucose, amino acids, and lipids may underlie both under- or overgrowth of the fetus when maternal nutrient and hormone levels are altered due to changes in maternal nutrition or metabolic disease. Implementing new strategies to modulate placental transport may improve maternal health and prove effective in normalizing fetal growth in cases of intrauterine growth restriction and fetal overgrowth. However, further studies are needed to confirm this hypothesis.

KEYWORDS

gestational diabetes mellitus, placental transport, leptin, glucose, amino acids, lipids, fetal macrosomia, nutrient transporters



GRAPHICAL ABSTRACT
Nutrient transport in normal and altered conditions.

1 Introduction

Gestational diabetes mellitus (GDM) is a condition characterized by glucose intolerance that occurs during pregnancy (1). It is one of the most common complications, affecting 3–8% of all pregnancies (1, 2). The prevalence of GDM has increased in recent decades, reaching rates of ≥20% in some parts of the world, due to factors such as increased maternal age and obesity (3). In Spain, the estimated prevalence of GDM ranges from 3 to 5% of pregnancies, depending on factors such as ethnicity, age, fetal sex, and diagnostic criteria. It is considered the leading cause of fetal macrosomia, which is associated with an increased risk of perinatal mortality and neonatal morbidity (4, 5).

The placenta from GDM subjects is often susceptible to altered metabolism, which could change the expression of placental nutrient transporter systems (6). In fact, this change may disrupt fetal growth and expose offspring to long-term consequences of GDM. Consequently, the offspring of women affected by GDM are more likely to suffer from long-term conditions such as obesity, cardiovascular disease, metabolic syndrome, and type 2 diabetes mellitus later in life (7). Therefore, it has been hypothesized that fetal development is more closely linked to altered placental transport resulting from GDM-associated conditions rather than maternal circulation.

An array of maternal circulating factors has been shown to alter placental macronutrient metabolism in pregnancies complicated by GDM (8). For example, a wide range of hormones and cytokines such as insulin, leptin, insulin-like growth factors (IGFs), and molecular signaling pathways, including the mammalian target of rapamycin (mTOR), phosphatidylinositol 3-kinase (PI3K), and mitogen-activated protein kinases (MAPK), have been reported to be activated in the maternal-facing microvillous (MVM) of human placentas affected by GDM (6, 9, 10). Based on these facts, the activity of placental nutrient transport might be modulated by the maternal environment and placental metabolism (11). Therefore, since the human placenta is responsible for the production of adipokines (12), leptin has been implicated in various related pathologies of pregnancy such as GDM, obesity, fetal growth abnormalities, and metabolic dysfunction (6, 13, 14).

Maternal-fetal macronutrient transport is primarily mediated by a family of placental transporters. For example, glucose transport, in particular, is mediated by glucose transporters (GLUTs) (15), while amino acid transport is mediated by several membrane transport proteins, including the sodium-dependent system A transporter, also called the serotonin N-acetyltransferase (SNAT) family and the sodium-independent system L transporter, known as the large neutral amino acid transporters (LATs) family (16, 17). On the other hand, lipid transport is mediated by the free fatty acid transporter (FATB), fatty acid-binding proteins (FABPs), and the activity of lipases in the MVM of syncytiotrophoblast (18).

During pregnancy, placental leptin levels increase in pregnancies complicated by GDM (19). This suggests a physiological role for leptin in the placental uptake of nutrients. However, the mechanism by which leptin may act as a modulator of placental transporter expression in GDM pregnancies is not well understood. Recently, leptin and insulin signaling pathways have been demonstrated in placentas from GDM pregnancies (20), suggesting a role for leptin in the expression of placental transporters in GDM. However, data and evidence on this topic are limited, and therefore it is not fully understood.

Previous studies have shown that leptin increases the glucose uptake rate in cultured trophoblasts by increasing GLUT1 expression in the human placenta BeWo cell line (21, 22). Additionally, leptin increases the expression of Aquaporin-9 (AQP9), an aquaglyceroporin membrane channel, in normal trophoblasts (23), providing a substrate for gluconeogenesis. Increased expression of AQP9 has been found in placental trophoblasts from patients with GDM (24). Leptin has also been

implicated in placental amino acid uptake. In this regard, several studies have reported that leptin stimulates the system A transporter in villous fragments via PI3K and the JAK (Janus tyrosine kinase)-STAT (signal transducer and activator of transcription) (JAK/STAT) pathway in obese pregnant women (25, 26). These data suggest a role of leptin in regulating amino acid metabolism in the human placenta and probably in placentas affected by GDM linked to maternal obesity (7). Concerning placental fatty acid transport, little is known about the leptin effect in GDM. However, in normal pregnancy, it has been shown that leptin increased fatty acid translocase, such as FAT/CD36, expressions in the syncytiotrophoblast of human placentas in primary cell cultures (27).

Taking all these facts together, we aimed to review the reported placental transport changes during GDM and to elucidate the possible role/impact of leptin on placental transporter expressions altered by GDM.

2 Gestational diabetes mellitus

GDM is one of the most common complications of pregnancy (28, 29) and affects 6–25% of pregnant women (depending on diagnostic criteria) (30). Although the GDM phenotype is highly heterogeneous (28), half of its prevalence can be explained by being overweight and obesity (3). GDM is associated with an increased risk of stillbirth and neonatal death, as well as multiple serious morbidities for both the mother and baby (28). The main pathophysiological complications of GDM are due to fetal macrosomia, which is characterized by a larger placenta weight and size to support the increased needs of the macrosomic fetus. The alteration of placental function may be a reason for abnormal fetal growth (29) observed in this pregnancy pathology (30). However, its pathophysiology is not fully clarified yet. In this sense, women with GDM have increased plasma leptin levels (31). Additionally, insulin levels are also increased in GDM, and hyperinsulinemia may mediate an increase in leptin synthesis in the placenta (32). In fact, the role of leptin in the growth and metabolism of the placenta has been demonstrated (9), where the trophic action of leptin may mediate an increase in the size of placentas affected by GDM (6, 33), as both the expression of leptin and its receptor were increased (34).

2.1 Diagnostic criteria of GDM

Unfortunately, there is no scientific consensus on the best way to diagnose GDM due to discrepancies in the definition criteria. Expert professional worldwide organizations acknowledge several acceptable options (35, 36), each with its own advantages and disadvantages. According to the American Diabetic Association and the National Institute for Health and Care Excellence, the diagnosis of GDM is defined as glucose intolerance diagnosed in the second or third trimester of pregnancy. Both criteria consider a fasting plasma glucose level ≥ 5.6 mmol/L or a 2-h plasma glucose level ≥ 7.8 mmol/L (7).

In Spain, a screening approach is used [preferred by the National Diabetes Data Group (NDDG) (37)] for gestational diabetes at week 24 of gestation, employing the O'Sullivan test (oral glucose tolerance test (OGTT) with 50 g of glucose). This includes an initial non-fasting 1-h glucose challenge test (35), which is logistically simpler for patients and can easily be performed as part of a scheduled prenatal visit. Most women do not require further screening. However, approximately 20% of patients fail this screening [values ≥ 140 mg/dL (≥ 7.77 mmol/L)], and a diagnostic test is then carried out using an OGTT of 100 g, with assessment of glycemia at baseline and at 3 h (38). Two or more increased values are diagnostic for GDM.

In the first trimester of pregnancy, and if there are risk factors (family history of diabetes, previous child weighing more than 4,500 g, age > 35 years, or history of gestational diabetes in a previous pregnancy), an O'Sullivan test is required. If the O'Sullivan test is pathological, the OGTT with 100 g is performed. If the result is normal, the OGTT with 100 g would be performed again in the second trimester.

2.2 Risk factors of GDM

GDM is a complex pathophysiological state of pregnancy in which both genetic and environmental factors are involved. Maternal obesity is considered the main risk factor for developing GDM (7). Indeed, obese women have an increased risk of GDM compared to women of normal weight (28). Therefore, both obesity and GDM lead to fetal overgrowth, which is associated with an increased capacity for maternal nutrient supply across the placenta to the fetus (11). Nevertheless, many other factors could contribute to a high risk of GDM, such as a family history of any form of diabetes, advanced maternal age, race (particularly non-white), or having previously given birth to large babies. Moreover, pathologies related to insulin resistance and leptin resistance, such as polycystic ovarian syndrome (PCOS) and pre-eclampsia, may also lead to GDM (39, 40).

The consequences of GDM during pregnancy can have significant impacts on both the mother and the newborn later in life. Castillo et al. have recently described the short-term and long-term complications of GDM in their work (7). Short-term complications may include maternal pre-eclampsia, fetal macrosomia, shoulder dystocia, and higher body fat. Additionally, complications during delivery, such as prolonged labor, caesarean birth, surgical complications, hemorrhage, infection, and extended hospital stays, may also occur in some cases. Moreover, the long-term complications of GDM can increase the risk of both the mother and her child developing type 2 diabetes mellitus, cardiovascular disease, metabolic syndrome, and obesity (7) later in life.

3 Leptin

Leptin is the satiety hormone secreted by adipose tissue and plays a crucial role in regulating energy balance (41). In fact, circulating leptin levels reflect adipose tissue size and also change with the nutritional state. Furthermore, leptin is considered a pleiotropic hormone that regulates not only body weight but also many other functions,

including the immune system and the systemic inflammatory response, as well as the normal physiology of the reproductive system (9, 42). In this sense, leptin is involved in the ovulatory cycle, where it acts to maintain the energy balance linked to this process (43). Therefore, leptin can act as a metabolic switch connecting the nutritional status of the body to high energy-consuming processes. This is especially important in pregnancy, where leptin not only modulates satiety and energy homeostasis in the mother (41), but is also produced by the placenta. This is why, during pregnancy, high leptin secretion levels have been detected in both maternal and fetal circulations, which rise until childbirth (44, 45). The serum leptin concentration is two- to three-fold higher in pregnant women compared to nonpregnant counterparts and peaks at approximately 28–32 weeks of gestation. Immediately after delivery, levels rapidly decrease back to pre-gestational levels (46). This significant increase in maternal circulating leptin during pregnancy is caused by increased leptin production from adipose tissue in connection with weight gain and fat deposition in the mother from the late second trimester onwards, as well as by placental leptin production in the first trimester, which constitutes approximately 15% of the total maternal serum leptin concentration (47). In this sense, leptin modulates the dialogue between fetal and maternal metabolism (48). The leptin expression increases in the human (and non-human primate) placenta as pregnancy proceeds (49).

3.1 Leptin in normal pregnancy

Leptin is not only an adipokine hormone secreted by adipose tissue but also an autocrine trophic factor produced by trophoblast cells to regulate the growth and metabolism of the placenta (50–55). Leptin also plays an essential role in reproduction by regulating gonadotropin-releasing hormone secretion (56). Moreover, overexpression of leptin in animal models has been reported to cause early puberty (57). In humans, maternal leptin levels have been shown to be higher in the early stages of pregnancy (45). This data was later confirmed in 2004 by Nuamah et al., where the authors demonstrated an increase in maternal leptin levels during induced delivery, along with an increase in placental leptin mRNA production (58). The various reproductive functions of leptin include the regulatory control of different processes, such as placental growth, macronutrient transport, placental angiogenesis, trophoblast mitogenesis, and immunomodulation (6, 14), all crucial events for fetal development and adequate placental function.

3.2 Leptin in pathologic pregnancy

During pregnancy, the majority of plasma leptin is secreted by the placenta. The increased level of placental leptin has been linked to several metabolic conditions during pregnancy, such as maternal obesity and gestational diabetes mellitus (GDM) (6). Leptin and its receptors are key regulatory factors implicated in various pregnancy complications. Its role has been further studied in pregnant women with obesity, GDM, and pre-eclampsia. A summary of the more relevant implications of leptin in pregnancy complications is provided in Table 1.

Pregnancies complicated by GDM are under the influence of many regulatory factors such as growth hormones, insulin resistance, and leptin, which may impact placental transport and

TABLE 1 Summary of the most common pregnancy complications and the role of leptin in their pathophysiology.

Pregnancy disease-related	Role of leptin.	Expressions	References
Maternal obesity	Increased leptin levels in obese pregnant women are significantly correlated with fetal overgrowth, leading to macrosomia.	↑	(59)
Pre-eclampsia	Leptin is a predictive marker of pre-eclampsia in obese pregnancies. Increased placental leptin levels in all trimesters of pregnancy represent risk factors for pre-eclampsia. Higher maternal leptin levels increase oxidative stress in high-altitude (HA) residents with pre-eclampsia. Lower serum leptin levels decrease placental production when pre-eclampsia is associated with HIV infection. Lower leptin levels in newborn babies from pre-eclamptic pregnancies are significantly correlated with obesity and oxidative stress.	↓,↑	(60–64)
Intrauterine growth restriction (IUGR)	Higher maternal leptin levels may contribute to fetal distress. Increased leptin concentration in prepubertal males born with IUGR is emerging as an early marker of metabolic syndrome. Maternal serum leptin and endothelin-1 (a highly potent vasoconstrictor released in conditions of hypoxia) was found to be increased and positively correlated with the degree of fetal growth restriction in women with pre-eclampsia. Lower leptin levels are associated with intrauterine growth restriction (IUGR) in discordant dichorionic twins. The evidence strongly correlates lower leptin concentrations with pregnancies complicated by IUGR, leading to fetal malnutrition.	↑,↓	(65–67) (68)
Recurrent miscarriage	Leptin gene polymorphisms at different levels may increase the risk of recurrent spontaneous abortion	↑	(69, 70)
Polycystic ovary syndrome (PCOS)	Hyperleptinemia is significantly associated with PCOS and may lead to an increased free leptin index in young women. Increased leptin levels, along with other biochemical parameters, contribute to increased oxidative stress in adolescent girls with PCOS. The leptin signaling pathway plays a crucial role in the production of male hormones in women with PCOS. Leptin and insulin resistance mediate lower expression of aromatase in granulosa cells from women with PCOS.	↑	(39, 40, 71–73)

↑, increase in expression levels; ↓, decrease in expression levels.

fetal growth (7). Maternal obesity and the differences in diagnosis criteria may also impact the accuracy of the available data related to the involvement of leptin in the regulation of the placental transporter mechanism altered by GDM (7). Currently, several studies consider hyperleptinemia to be a good parameter in predicting GDM in early pregnancy (6, 19, 74). In addition, another group have shown that leptin levels are higher in women with early onset of GDM during pregnancy compared with standard onset and overweight women (75). Moreover, the authors of the same paper mentioned that these women had an inflammatory profile. Therefore, leptin is likely involved in the inflammatory response during pregnancy complicated by GDM.

An array of metabolic and endocrine alterations, such as hyperinsulinemia, hyperleptinemia, and oxidative stress, have been linked to pregnancy complicated by GDM. In this sense, Shang et al. reported that the increase of leptin levels in GDM was significantly correlated with markers of oxidative stress such as malondialdehyde, 8-isoprostane, and xanthine oxidase (76). Furthermore, the increase of leptin levels in GDM is more likely linked to body mass index (BMI) and is probably expected to alter fetal growth, leading to high fat body in GDM offspring. In this context, recent studies have demonstrated that higher leptin levels are associated with insulin-resistance in newborns from mothers with GDM (77, 78). Additionally, Powe et al. have demonstrated that an adjustment of leptin levels in early pregnancy enhances the insulin secretory response in GDM women (79). Such a result may indicate the possible beneficial role of leptin in GDM therapy.

GDM is the most common metabolic disorder that may alter placental nutrients transport. GDM is mainly characterized by insulin-resistance and leptin-resistance (10). Thus, higher concentrations of placental leptin mRNA and protein have been shown in placentas affected by GDM compared to healthy controls (13), and placental leptin production is increased in GDM. In this context, leptin is a regulatory factor that can modulate placenta functions in an autocrine or paracrine manner, involved in many processes such as proliferation and protein synthesis (51, 53, 80–82) and probably placental transporter activity or expression. Thus, the role or impact of leptin on placental transporters of macronutrients such as glucose, amino acids, and lipids in GDM will be further explored in the following sections.

Based on the literature, we hypothesized that the increase of leptin in GDM may enhance placental macronutrient uptake by increasing placental transporter expression. Figure 1. represents the proposal algorithm we have adopted in order to support our hypothesis and provide further insight to the role of leptin in GDM and its impact on placental nutrient availability compared to other pregnancy complications related to hypoleptinemia, such as fetal growth restriction (65–67) and spontaneous miscarriage in the first pregnancy trimester (69, 70), as mentioned in the previous section (see Table 1 for more details).

In order to fulfill the demands of the fetus and normal growth, the human placenta promotes an array of macronutrient transporters, summarized in Figure 1. Their expression and activity in response to leptin and in GDM will be discussed in more detail, and further insight will be provided in the next sections.

3.3Role of leptin in glucose transport in GDM

Glucose is the primary nutrient required for fetal growth and development. Glucose transport across the placenta to the fetus is mediated by a family of facilitated diffusion transporters, named GLUTs, encoded by the solute carrier family 2 and facilitated glucose transporter (SLC2A) family of genes (83). Seven GLUT isoforms have been reported to be expressed in the human placenta at different sites of the syncytiotrophoblast membrane (84). Placental GLUT activity/expression have been found at distinct sites in the human placenta trophoblast. Most placental GLUTs are expressed in both polarized syncytiotrophoblast membranes of the placenta; in the maternal-facing microvillous plasma membrane (MVM) and the fetal-facing basal plasma membrane (BM), see Figure 1 for more detail. Leptin has been shown to increase the

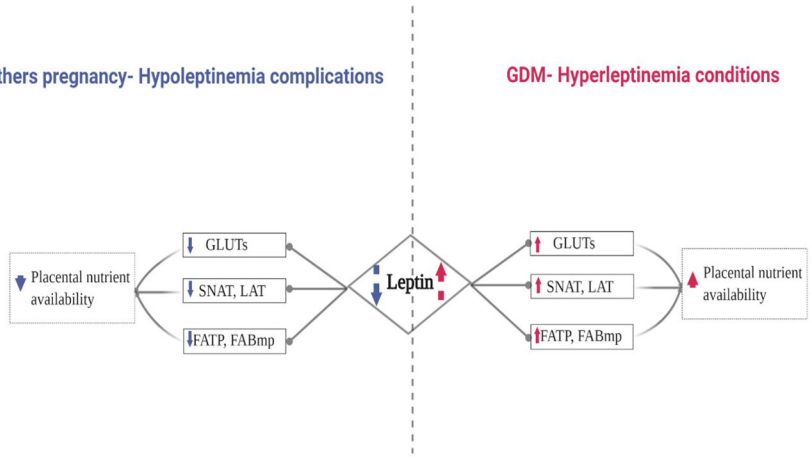


FIGURE 1
Proposed Algorithm: Leptin's Role in the Expression of Placental Transporters in Pregnancy Complicated by GDM.

expression of GLUT1 in human placental trophoblasts under physiological conditions (21). In GDM, leptin could act to further upregulate the expression of GLUT1 and GLUT3 transporters, contributing to hyperglycemia in the fetus.

3.3.1 GLUT1

Glucose transfer from mother to fetus across the placenta takes place primarily through glucose transporter isoform 1 (GLUT1) because of its abundance in both the MVM and BM membranes of the human placenta syncytiotrophoblast (85). GLUT1 plays a regulatory role in the transplacental transport of glucose (86). GLUT1 is the primary glucose transporter protein isoform mediating glucose transport across the syncytiotrophoblast, the transporting epithelium of the human placenta (86). Relevant data related to this isoform have been provided. Thus, the GLUT1 expression is approximately 3-fold greater in the MVM than BM in the syncytiotrophoblast of normal pregnancy conditions (86). On the other hand, conflicting data have been reported, where the activity or expression of GLUT1 differs from first to third trimester of pregnancy (84, 87).

Interestingly, placental GLUT1 mRNA expression was positively correlated with maternal age and inversely correlated with placental weight (88). Moreover, placental GLUT1 protein expression was positively correlated with the pre-pregnancy maternal BMI and umbilical artery glucose levels, but was not associated with umbilical insulin levels (89, 90).

Moreover, GLUT1 activity in the human placenta is likely to be more dependent on maternal glucose metabolism and placenta function. In fact, this may justify the impact of other placental regulatory factors such as leptin, for instance. In term placenta affected by GDM, Gaither et al. reported an increase in GLUT1 expression leading to an increase in glucose uptake in the syncytial BM and no differences with respect to the MVM (85). Regarding the analysis of GLUT1 expression, conflicting studies have demonstrated no differences between placentas affected by GDM and nondiabetic pregnancies (91). Taking all these data in consideration, we can assume that other GDM- related conditions, in addition to insulin-resistance, might be responsible for the altered GLUT1 expression, and that placental leptin or leptin receptor, which are overexpressed in the MVM of human placentas, are affected by GDM, as we have recently shown (20).

GLUT1 expression appears to be inversely related to the maternal glucose concentration; however, within the physiological range, GLUT1 expression is relatively refractory to glucose concentration. Information is still needed on the expression and activity in well-defined conditions of GDM, on the mechanisms and consequences of the changes observed in pregnancy complicated by GDM, and on the role of leptin in regulating placental glucose transport. In this context and regarding GDM, evidence related to the effect of leptin on the expression of GLUT1 is sparse. Thus, the effect of leptin on GLUT1 is indirect. However, as discussed in-depth in recent studies, increased levels of leptin and activation of the leptin receptor in placentas affected by GDM (25–27) may modulate the activity of GLUT1 via the activation of cascade placental signaling pathways such as JAK/STAT or PI3K pathways. Proposal models of this association are shown in Figure 2. However, the direct effect of leptin on GLUT1 expression in GDM is unknown, and further investigation is needed to elucidate this effect.

3.3.2 GLUT3

Glucose transporter isoform 3 (GLUT3) provides high-affinity glucose transport to crucial organs and tissues that are highly dependent on a constant supply of glucose, even during hypoglycemia (92). In human trophoblast cells, GLUT3 is present during the first trimester of pregnancy and is characterized by a

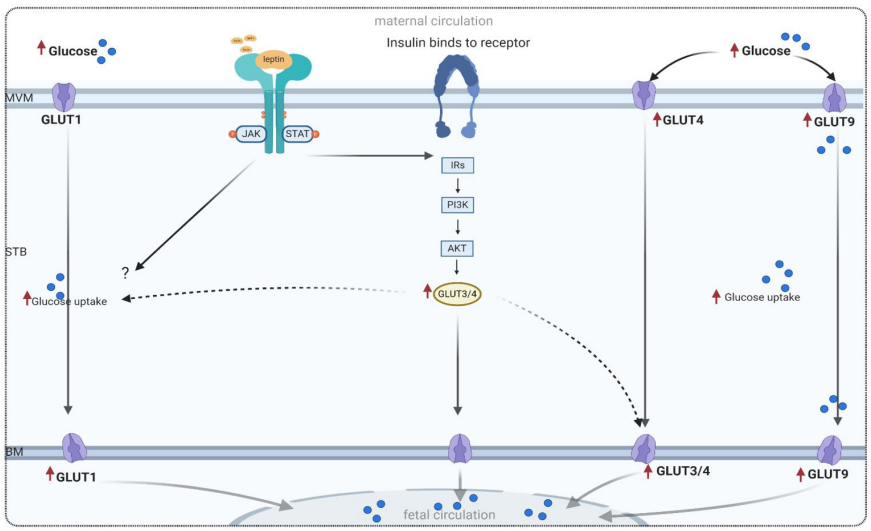


FIGURE 2
Proposed model of glucose transport in a trophoblast cell, adapted from references listed in Table 2. MVM, microvillous plasma membrane; BM, basal plasma membrane; GLUT, glucose transport; PI3K, phosphatidylinositol 3-kinase; IRS, insulin receptor substrate; Akt, protein kinase; mTOR, mammalian target of rapamycin; JAK/STAT, main leptin pathway in trophoblast cell.

higher affinity for glucose compared to GLUT1. GLUT3 is an important isoform that ensures an adequate availability of glucose in fetal tissues early in gestation (93). However, there is limited information available on the activity or expression of GLUT3 in human placentas affected by GDM. Only two groups have reported the expression of GLUT3 in human placentas affected by GDM (94, 95). Some investigators have demonstrated a decrease in GLUT3 expression in diabetic groups (mice and human placentas) compared to normal controls (94). In contrast to this data, other studies conducted on animal models (diabetic rats) have shown that placental GLUT3 mRNA and protein levels were increased four-to-fivefold compared to nondiabetic rats (96). These findings suggest that GLUT3 expression may play a major role in placental glucose uptake in GDM by regulating hyperglycemia. Rong et al. discovered decreased GLUT3 gene methylation and increased mRNA expression in GDM patients compared with control pregnant women (97).

Regarding the effect of leptin or LEPR on placental GLUT3 expression, there is a lack of data. However, data from animal models in obese mothers, without diabetic conditions, have demonstrated that leptin and insulin increase GLUT3 expression via activation of the PI3K pathway (98). It is well-established that maternal obesity increases the risk of GDM. These findings support the possible role of leptin in increased glucose transport in GDM.

3.3.3 GLUT4

Another GLUTs family expressed in human placentas is glucose transporter isoform 4 (GLUT4). What is unique about GLUT4 is that it is an insulin-dependent transporter predominantly expressed in adipose tissue, as well as in skeletal and cardiac muscle (99). GLUT4 is also expressed in the MVM of the syncytiotrophoblast of human placentas (100). Xing et al. detected the colocalization of GLUT4 with insulin receptors in term human placental tissue (101). Zang et al. reported a decrease of GLUT4 expression in pregnancy complicated by GDM due to insulin signaling components (IRS-2) and sex hormone-binding globulin (SHBG) impact (102, 103).

On the other hand, the placental GLUT4 protein density was positively correlated with the fetal birth weight in patients with insulin-dependent GDM (89).

Considering the aforementioned data, the activity or expression of GLUT4 might be influenced by other GDM- related conditions in addition to insulin impact. Interestingly, recent research in non-GDM obese pregnancies conducted by Powell and coworkers demonstrated that maternal insulin stimulates placental glucose transport by promoting GLUT4 trafficking to the fetal-facing syncytiotrophoblast BM (104). A possible interpretation of the mechanism might involve the role of leptin and insulin receptor signaling pathways, whose overexpression in GDM have been shown in human placentas (20).

The role of leptin in GLUT4 expression in human placentas complicated by GDM is unknown. However, other studies on animal models, such as heterozygous C57BL6/J-Lepr(db/+) mice that develop spontaneous GDM, have shown that GLUT4 overexpression markedly improves insulin-signaling in GDM, resulting in increased insulin secretion and improved glycemic control (105). These data may indicate a beneficial role of leptin in future GDM therapy.

3.3.4 GLUT8

Glucose transport isoform 8 (GLUT8) is an insulin-dependent transporter similar to GLUT4. It participates in placental glucose transport. Its activity or expression has been confirmed in the syncytiotrophoblast and endothelium of villous vessels of term placentas (106). Currently, the available data on GLUT8 functions and its relationship with fetal growth complications are based on animal models (106, 107). However, there is no data regarding GLUT8 expression in placentas affected by GDM.

3.3.5 GLUT9

Glucose transport isoform 9 (GLUT9) is the only isoform in the GLUT family of glucose transporters that consists of 2 splice variants: GLUT-9a and GLUT-9b, both of which are responsible for transporting glucose and fructose. Additionally, they participate in urate transfer (91, 108). Both forms of the GLUT9 proteins are expressed in the syncytiotrophoblast of the human placenta. Their expression was significantly increased in diabetic placentas from pregnancies complicated by GDM and pre-gestational diabetes (PGDM) compared to healthy controls. Despite the differences in the expression of both GLUT9 forms (109), in trophoblasts, these findings were confirmed by a significant increase in GLUT9 expression in placentas from patients with insulin-dependent diabetes, GDM, and PGDM (110). These findings suggest that GLUT9 expression may play a role in the long-term consequences of fetal overgrowth associated with GDM. Unfortunately, there is a lack of information regarding the link between leptin and leptin receptor activation and their effect on GLUT9 in GDM.

3.3.6 GLUT10

The glucose transporter isoform 10, also known as GLUT10, is characterized by its high affinity for both D-glucose and D-galactose, but not fructose, unlike GLUT9 (111). Recent studies have indicated that DNA methylation regulates GLUT10 gene expression in the human placenta, which may influence the function of other members of the GLUT family in the placenta during pregnancy and in various disease conditions, as suggested by the authors. Additionally, the GLUT10 gene has been found to be involved in a region of human chromosome 20q12-13.1 associated with type 2 diabetes, indicating a potential role for GLUT10 in glucose metabolism and type 2 diabetes (112). To the best of our knowledge, the expression of GLUT10 in normal placentas or placentas affected by GDM has not yet been investigated. Unfortunately, there is currently no available information regarding the role of leptin in its expression.

3.3.7 GLUT12

Glucose transporter isoform 12 (GLUT12) has been reported to be predominantly expressed in the basal membrane of the syncytiotrophoblast and in extra-villous trophoblast cells of the human placenta during the first trimester of pregnancy (113). However, there is currently no available information regarding

changes in placental GLUT12 expression related to any form of diabetes.

Furthermore, the existing data regarding changes in the expression of GLUTs during pregnancy and the impact of GDM appear to have conflicting reports. This discrepancy may make it difficult to understand the molecular mechanisms of GDM and further elucidate the role of GLUTs in diabetes-associated conditions. Hyperleptinemia, hyperinsulinemia, and fetal overgrowth (macrosomia) are the primary hallmarks of GDM. Therefore, gaining further insight into their role in placental glucose metabolism and GLUTs expression is necessary to develop new interventions or therapeutic approaches that can improve pregnancy outcomes or at least reduce the exposure of pregnant women and newborns to the consequences of GDM, both in the short and long term.

3.4 Role of leptin in amino acids transport in GDM

Concentrations of most amino acids are higher in fetal plasma than in maternal plasma, indicating active accumulation across the syncytiotrophoblast, which is the transporting and hormone-producing epithelium of the human placenta (114). The supply of amino acids to the fetus is critically dependent on the transport capacity of the placenta. This directional transfer requires the coordinated action of over 20 different amino acid transporter proteins, which are localized to both the maternal-facing and fetal-facing plasma membranes of the placental epithelium. These transporters facilitate the uptake of amino acids from the mother and their delivery to the fetus (115, 116). Placental amino acid transport can be categorized based on substrate specificity and sodium dependence, although only two systems have been extensively studied. System A is sodium-dependent and facilitates the uptake of non-essential neutral amino acids, while System L is sodium-independent and facilitates the uptake of essential amino acids in the placenta (17, 117, 118).

3.4.1 System A

The System A transporter is responsible for transporting a wide range of non-essential neutral amino acids, including alanine, serine, and glutamine (119). It is highly regulated and consists of three isoforms (SNAT1, SNAT2, and SNAT4), which are encoded by the SLC38A family of genes and expressed in the human placenta (7, 120). System A facilitates the uptake of non-essential neutral amino acids, and SNAT1 is the major contributor to amino acid uptake in cultured primary human trophoblasts. Higher expression of SNAT1 has been positively correlated with birth weight in human placentas from pregnancies affected by GDM, which is associated with fetal macrosomia (121). Regarding the expression of placental amino acid transporters in GDM, some studies have reported a decrease in the expression of system A amino acid transporters in the microvillous membrane (MVM) of placentas from pregnancies complicated by GDM. This decrease may be attributed to a reduction in the number of amino acid transporters, as suggested by the authors (122). However, contrasting these findings, Jansson et al. demonstrated an increase in placental amino acid uptake in human pregnancies complicated by GDM compared to control pregnancies (123). Additionally, the same investigators reported that leptin is involved in the regulation of placental amino acid transport by stimulating the activity of the system A amino acid transporter in term placentas (26) (Table 2). In line with this, a recent study has reported that leptin modulates the expression of the system A amino acid transporter in normal placentas through the JAK/STAT pathway (126). A theoretical model of this mechanism is proposed in Figure 3.

3.4.2 System L

As mentioned previously, the System L or large neutral amino acid transporter system (LAT) is a sodium-independent obligatory exchanger responsible for the transport of neutral amino acids (17, 135). This system primarily transports essential amino acids, such as L-leucine and L-phenylalanine, across the placenta. The System L of amino acid transport consists of two isoforms: LAT1 (also known as SLC7A5) and LAT2. Both isoforms have been found to be expressed in trophoblast cells of the human placenta, and they are localized in the microvillous membrane (MVM) and basal membrane (BM) of the syncytiotrophoblast (7, 118), as shown in Figure 4.

Increased activity or expression of both System A and System L in GDM have been reported to accelerate fetal growth and contribute to fetal overgrowth in women with GDM (123, 136), thereby affecting placental function. As mentioned earlier, leptin plays a crucial role in cell proliferation and protein synthesis. In human trophoblastic cells, leptin promotes amino acid synthesis through the activation of MAPK and PI3K pathways (51, 82).

However, changes in placental amino acid transporter expression modulated by leptin, whether through direct or indirect mechanisms, have not been well established, and the available data on this topic are limited.

3.5 Role of leptin in lipids transport in GDM

Fatty acids (FAs) play crucial roles in fetal growth and development. An increase in maternal circulating triglycerides (TGs) and dyslipidemia, as well as hyperleptinemia, are associated with GDM complications. These hallmarks of GDM can affect placental FA uptake. The transport of FAs from the maternal circulation to the fetus is mediated by the placenta. Maternal TGs require lipase enzyme activity to cross the placenta as non-esterified fatty acids (NEFAs) and glycerol. Placental NEFAs, under normal conditions, provide the necessary nutrients for fetal development. However, pregnancies complicated by GDM and obesity may be exposed to an excess supply of lipids, leading to an increase in placental FA transporters. This observation has been associated with an increase in fat mass in newborns from mothers with GDM (137).

Maternal FAs can cross the placenta through the microvillous membrane (MVM) of the syncytiotrophoblast via simple diffusion

TABLE 2 Summary of Altered Expressions of Placental Transporters in GDM and Leptin Expressions.

Placental transporters	GDM	Leptin/LEPR	Activated pathways	References
Glucose transporters				
GLUT1	↑	↑ (BeWo cells line)	IRs and PI3K	(85, 95, 119, 124)
GLUT3	↑,↓	NA		(94–96)
GLUT4	↑,↓	↓ (human placenta); ↑ (animal model)	IR and PI3K	(95, 105, 125)
GLUT8	NA	NA	NA	
GLUT9	↑	NA	NA	(91, 109)
GLUT10	NA	NA	NA	
GLUT12	NA	NA	NA	
Amino Acid transporters				
SNAT1	↑	↑	PI3K and mTOR,	(26, 122, 126)
SNAT2	NA	NA	NA	
LAT1-2	↑	↓	PI3K and mTOR,	(119, 127)
Lipids transporters				
FAT/CD36	↑	↑	MAPK	(27, 128)
EL	↑	↑	MAPK & TNF-α	(129)
LPL	↑	NA	NA	(128)
FATP1	↓	NA		(128)
FATP2	↓	↑	NA	(130)
FATP4	↓	NA	NA	(128)
FATP6	↑,↓	↑	NA	(128, 130)
MFSD2A	↓	NA	NA	(131)
FABP1	↑	NA	NA	(132)
FABP4	↑	NA	NA	(128, 133, 134)
FABP5	↑	NA	NA	(133, 134)

↑, increase in expression levels; ↓, decrease in expression levels.
GLUT, glucose transport; SNAT, sodium-coupled or system A for neutral amino acid transporters; LAT, large neutral amino acid transporter; FAT/CD36, fatty acids translocase; EL, endothelial lipase; LPL, lipoprotein lipase; MFSD2A, major superfamily domain 2A; FATP, fatty acid transporter proteins; FABP, plasma membrane fatty acid binding protein; LEPR, leptin receptor; NA, not available or unknown.

or facilitated transport by FA carriers such as FA translocase (FAT/CD36), FA transport proteins (FATPs), and plasma membrane fatty acid binding protein (FABpm) (7, 135). The expression of these transporters in the placenta facilitates the transfer of NEFAs from the placenta to the fetus through the basal membrane (BM) of the syncytiotrophoblast. However, the available data regarding the expression levels of these transporters in both the MVM and BM of the syncytiotrophoblast are unclear and conflicting in normal physiological pregnancies and altered conditions.

Moreover, placental fatty acid (FA) transport in GDM is more complex and has shown to be more susceptible to alterations in placental factors and pathologic pregnancies related to GDM-induced metabolic changes. In this section, we will focus on the most relevant long-chain polyunsaturated fatty acids (LC-PUFAs) and their related transporters involved in fetal growth and development to gain further insight into the molecular mechanisms altered by GDM pregnancy and the possible role of leptin. As mentioned previously, maternal triglycerides (TGs) need to undergo processing by lipases (7, 18), such as lipoprotein lipase (LPL) and endothelial lipase (EL), in order to cross the placental microvillous membrane (MVM) and basal membrane (BM) and reach the fetus as non-esterified fatty acids (NEFAs). LPL and EL activities are likely required to generate NEFAs from maternal TGs. These two lipases have been found to be highly expressed in the human placenta (138); LPL is particularly abundant in the MVM (132), while EL is present in the membrane of capillary endothelial cells in the human placenta (7, 18, 135).

Fatty acid transport proteins (FATPs) are integral placental transporters for long-chain polyunsaturated fatty acids (LC-PUFAs) such as arachidonic acid (AA) and docosahexaenoic acid (DHA), which are both essential for fetal growth and brain development. The FATP family consists of six isoforms, of which five (FATP1-4, 6) are encoded by the SLC27A gene family (7, 139). All of these isoforms have been reported to be expressed in the

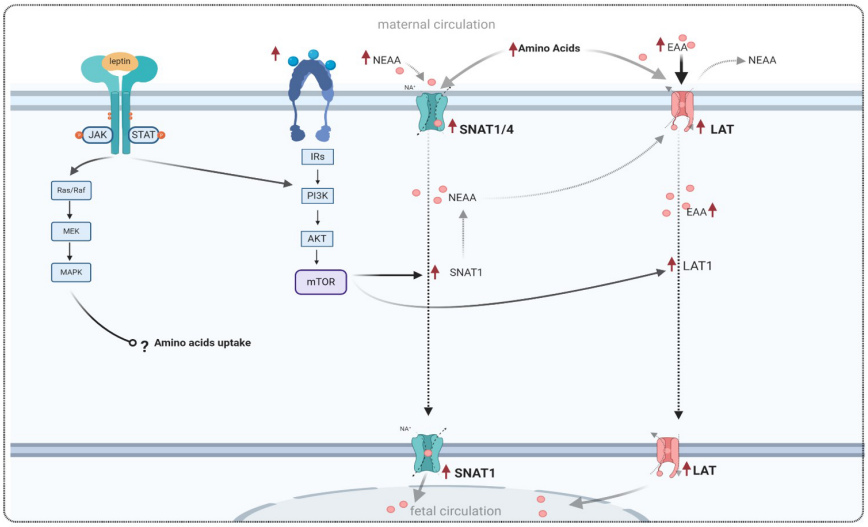


FIGURE 3
Theoretical model of amino acid transport in GDM conditions, and the effect of leptin signaling on amino acid transporters, adapted from references listed in Table 2. Leptin binds to its receptor and activates a cascade of signaling in trophoblast cells, similar to the effects of insulin and the insulin receptor. Leptin and insulin exert their effects by modulating the expression of amino acid transporters via the PI3K and mTOR pathways. NEAA, non-essential neutral amino acid; EAA, essential amino acid; SNAT1, sodium-coupled neutral amino acid transporter 1; LAT1, large neutral amino acid transporter; MAPK, mitogen-activated protein kinases; PI3K, phosphatidylinositol 3-kinase; mTOR, mammalian target of rapamycin.

human placenta (140). Various studies have indicated that FATP isoforms 1 and 4 are the primary transporters of DHA across the human placenta (18). However, recent research has demonstrated that the sodium-dependent lysophosphatidylcholine symporter (MFSD2A) mediates DHA delivery across the human placenta to the fetus, and its expression may affect placental DHA uptake (131).

In contrast to the FATP family, the placental fatty acid binding protein family (FABPpm) is mainly characterized by its high affinity for LC-PUFAs. It consists of five members (FABP1-5) and is exclusively located in the microvillous membrane (MVM) of the syncytiotrophoblast in the human placenta (140–142). Unfortunately, there is a lack of information regarding FABP expression in the human placenta and in pregnancies complicated by GDM. Nevertheless, some data have been reported regarding altered gene expression of FABP in GDM (133).

The expression and activity of proteins involved in fatty acid transport are influenced by insulin, IGF1, and leptin (69–71). In pregnancies complicated by GDM and a high body mass index

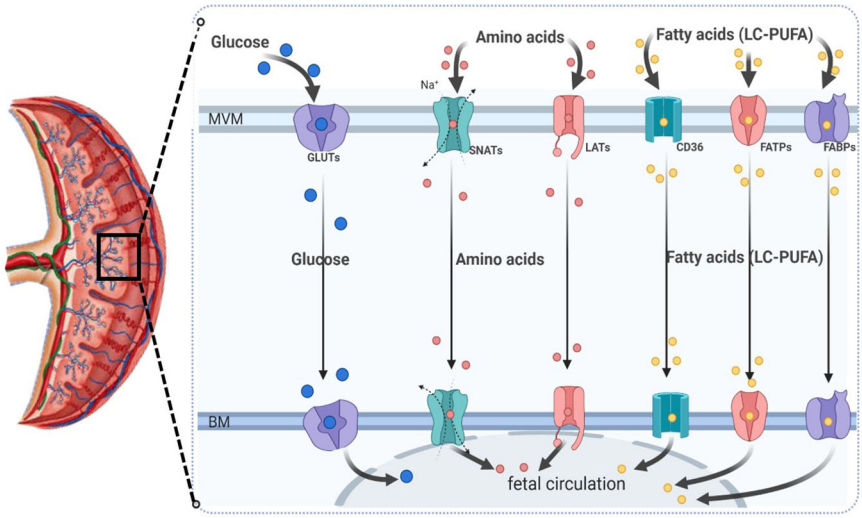


FIGURE 4
Schematic diagram representing the most relevant placental macronutrient transporters for maternal-to-fetal circulation across the human syncytiotrophoblast. MVM, microvillous plasma membrane; BM, basal plasma membrane; GLUTs, glucose transporters; SNATs, sodium-coupled neutral amino acid transporters; LATs, large neutral amino acid transporter (sodium-independent); CD36, fatty acid translocase; FATP, fatty acid transporter proteins; FABPs, plasma membrane fatty acid binding protein; LC-PUFA, long-chain polyunsaturated fatty acids.

(BMI), some alterations in placental fatty acid transport have been observed. These include a decrease in FATP1 and FATP4 expressions, but an increase in FAT/CD36 and FATP6 expressions compared to normal controls (128) (see Table 1 for more details). These findings suggest that GDM and high BMI increase the uptake of fatty acids in the placenta independent of maternal fatty acid supply, which is reported to be the main factor for fatty acid transport in the placenta. Regarding DHA, a decreased level has been observed in pregnancies complicated by GDM due to low expression of the MFSD2A transporter (131). Interestingly, in contrast to these findings, Ortega et al. have demonstrated unaltered levels of both AA and DHA concentrations in pregnant women with GDM. Additionally, the authors have reported a decrease in most fatty acids in cord serum from GDM subjects, except for α-linolenic acid (ALA), which was higher in the GDM group (143). It is important to note that ALA is one of the most important LC-PUFAs required for fetal growth, as the placenta and fetus cannot synthesize adequate amounts of this molecule to sustain normal fetal development (7).

Despite hyperlipidemia associated with GDM and high fetal fat mass, the potential effect of leptin on placental fatty acid transport is not well understood. Leptin and insulin stimulation have been reported to influence fatty acid uptake in BeWo cell placental choriocarcinoma. It has also been shown that an increase in leptin levels leads to an increase in FAT/CD36 expression in cultured samples from the human placenta in obese pregnant women without GDM (27). Leptin may also be related to the antioxidant system. In this context, a recent study has demonstrated that supplementation with 100 mg of alpha-lipoic acid in women with GDM leads to an increase in leptin and adiponectin levels (144). These findings suggest that leptin is likely involved in the regulation of oxidative stress related to GDM. Evidence of this correlation has been mentioned before (76). Figure 5 summarizes the altered expressions of fatty acid transporters in GDM.

3.6 Leptin and GDM: an integrated model of molecular regulatory mechanisms

A wide range of growth factors, pro-inflammatory cytokines, and hormones, including leptin, insulin, and IGF-1, are highly expressed in diabetic placentas in the MVM of the syncytiotrophoblast (10, 82, 122, 137, 145). In pregnancies complicated by GDM, changes in maternal and fetal circulatory levels of leptin are believed to modulate placental functions related to nutrient transport and may potentially alter the expression of placental transporters through intracellular signaling cascades. Therefore, this can be considered the main cause of higher placental nutrient uptake during pregnancy, which can lead to fetal growth disorders such as macrosomia, being large for gestational age (LGA), and an increased risk of metabolic dysfunction in offspring.

Leptin is a proinflammatory factor that modulates the expression of FA and glycerol transporters and mediates placental NEFA uptake by promoting oxidative stress in GDM conditions, as shown in Figure 6. As discussed above, many studies have reported higher leptin levels in GDM pregnancy compared to normal pregnancy. Thus, it is expected that the potential impact of placental leptin signaling on the expression of macronutrient transporters altered in GDM can help elucidate the molecular mechanisms underlying GDM pathophysiology. Furthermore, this may provide insights into the main cause of fetal macrosomia, resulting from changes in the expression pattern of placental transporters.

Leptin serves as both a proinflammatory factor involved in lipid metabolism and GDM pathophysiology, as well as an antiapoptotic factor that acts via the MAPK pathway in the human placenta (50). As mentioned earlier, leptin stimulates system A amino acid transporters through the activation of the JAK2/STAT3 pathway. This provides a compelling reason to investigate other activated signaling pathways through which leptin may modulate glucose uptake and protein synthesis. In this context, the mammalian target of rapamycin (mTOR) is another positive signaling regulator of key

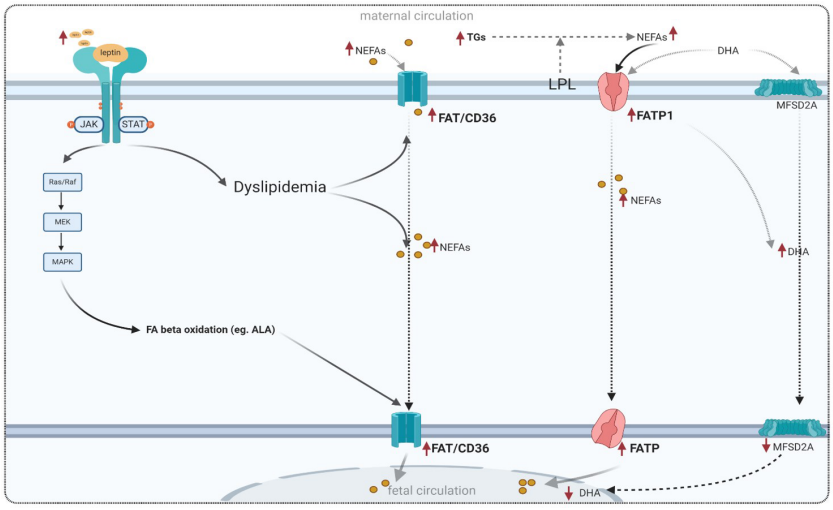


FIGURE 5
Adapted model for placental fatty acid transport in GDM and the role of leptin signaling in lipid metabolism. FAT/CD36, fatty acid translocase; FATP, fatty acid transporter proteins; FABPs, plasma membrane fatty acid binding protein; MFSD2A, major superfamily domain 2A; DHA, docosahexaenoic acid.

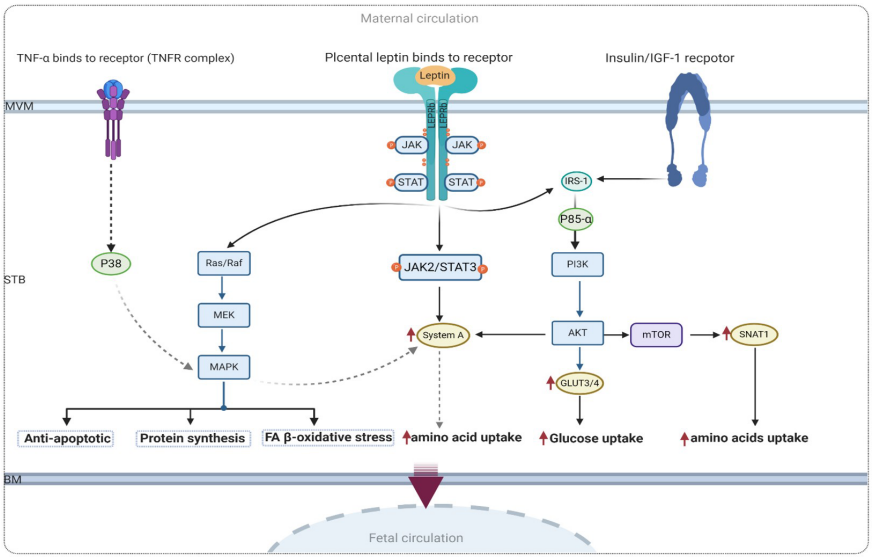


FIGURE 6
Proposed signaling of leptin and insulin in human trophoblastic cell with GDM. IR-1, Insulin receptor substrate 1; AKT, protein kinase; TNFα, tumor necrosis factor-α; MAPK, mitogen-activated protein kinases; PI3K, phosphatidylinositol 3-kinase; mTOR, mammalian target of rapamycin.

placental functions. Given that the mTOR pathway plays a crucial role in nutrient sensing in the human placenta (118), it has been proposed that the activation of placental mTOR signaling may contribute to increased nutrient delivery to the fetus. Therefore, the activation of mTOR and IGF-1 pathways in the placentas of women with GDM who give birth to macrosomic babies has been attributed to the increased expression of SNAT1 (121). A proposed model illustrating the underlying mechanism of mTOR and leptin signaling is presented in Figure 6.

Placental leptin binds to the leptin receptor in the MVM of the syncytiotrophoblast and triggers a variety of intracellular functions in the human placenta via the MAPK pathway. Put simply, placental leptin receptor signaling has been shown to promote the MAPK pathway and processes that are important for regulating amino acid metabolism (82) in human trophoblast cells. A recent study demonstrated that an increase in the proinflammatory cytokine TNF-alpha, observed in maternal obesity and GDM, leads to increased amino acid uptake in cultured primary human trophoblast cells in a MAPK-dependent manner. In the context of obesity, it has been shown that leptin stimulates the production of TNF-α in the human placenta (6, 118). Furthermore, Jansson et al. demonstrated that TNF-α regulates placental amino acid uptake by increasing the protein expression of both SNAT1 and SNAT2 isoforms of system A amino acid transporters via p38 MAPK (145). This evidence highlighting the significant association between leptin and TNF-α as proinflammatory mediators in the pathophysiology of GDM may help elucidate the connection between leptin and the MAPK pathway, as well as its role in amino acid and lipid metabolism in diabetic placentas.

Figure 6 shows the possible molecular mechanism of the link between leptin and proinflammatory TFN-α in the regulation of amino acid metabolism via the MAPK pathway.

4 Conclusion

Nutrient transport across the syncytial epithelium of the placenta is a highly regulated process that depends on various nutritional and hormonal signals. In general, obesity and GDM indicate abundant maternal fuel reserves, which stimulate the placental transport of glucose, amino acids, and lipids, thereby increasing their availability for fetal growth and optimizing offspring fitness. The primary objective of this review was to provide an overview of the expression of placental transporters that are altered by GDM, while also assessing the effect of leptin on these transporters and their expression. However, it should be noted that GDM, as a pathophysiological condition, may impact the accuracy of data related to the effect of leptin on placental transporters. Increases in leptin levels during pregnancy complicated by GDM may be associated with an increase in placental nutrient uptake. Nevertheless, the specific effect of leptin on the expression of GLUTs in human placentas affected by GDM remains unclear. Leptin signaling pathways may serve as crucial targets for new GDM therapies. However, further *in vivo* and *in vitro* experiments are required to evaluate the impact of leptin on placental nutrient transport under normal and altered conditions.

Author contributions

PG, IC and AP-P wrote the paper. All the authors participated in the literature search, in the design of the figures and manuscript revision. All authors have read and agreed to the published version of the manuscript.

Funding

We acknowledge the financial support of the Instituto de Salud Carlos III (ISCIII), Ministerio de Ciencia e Innovación, Spain, Grant n° PI19/01741 funded in part by FEDER Funds, to VS-M and AP-P; and the Consejería de Conocimiento e Investigación, Junta de Andalucía, Spain, Grant n° P20_01253, to VS-M.

Acknowledgments

The authors would like to express their sincere gratitude to James William Bryce for their invaluable assistance in the revision and editing of the English grammar in this manuscript. Their suggestions improved the clarity and readability of the final version.

Conflict of interest

The authors declare that the research was conducted in the absence of any commercial or financial relationships that could be construed as a potential conflict of interest.

Publisher's note

All claims expressed in this article are solely those of the authors and do not necessarily represent those of their affiliated organizations, or those of the publisher, the editors and the reviewers. Any product that may be evaluated in this article, or claim that may be made by its manufacturer, is not guaranteed or endorsed by the publisher.

References

1. Yan B, Yu Y, Lin M, Li Z, Wang L, Huang P, et al. High, but stable, trend in the prevalence of gestational diabetes mellitus: a population-based study in Xiamen, China. *J Diabetes Investig* (2019) 10:1358–64. doi: 10.1111/JDI.13039

2. Ferrara A. Increasing prevalence of gestational diabetes mellitus: a public health perspective. *Diabetes Care* (2007) 30(Suppl 2):S105–11. doi: 10.2337/DC07-S206

3. Kim SY, England L, Wilson HG, Bish C, Satten GA, Dietz P. Percentage of gestational diabetes mellitus attributable to overweight and obesity. *Am J Public Health* (2010) 100:1047–52. doi: 10.2105/AJPH.2009.172890

4. Gortazar L, Flores-Le Roux JA, Benaiges D, Sarsanedas E, Payà A, Mañé L, et al. Trends in prevalence of gestational diabetes and perinatal outcomes in Catalonia, Spain, 2006 to 2015: the diagestcat study. *Diabetes Metab Res Rev* (2019) 35:1–8. doi: 10.1002/DMRR.3151

5. Plows JF, Stanley JL, Baker PN, Reynolds CM, Vickers MH. The pathophysiology of gestational diabetes mellitus. *Int J Mol Sci* (2018) 19(11):3342. doi: 10.3390/ijms19113342

6. Pérez-Pérez A, Toro A, Vilariño-García T, Maymó J, Guadix P, Dueñas JL, et al. Leptin action in normal and pathological pregnancies. *J Cell Mol Med* (2018) 22:716–27. doi: 10.1111/JCMM.13369

7. Castillo-Castrejon M, Powell TL. Placental nutrient transport in gestational diabetic pregnancies. *Front Endocrinol (Lausanne)* (2017) 8:306. doi: 10.3389/FENDO.2017.00306

8. Li L, Lee SJ, Kook SY, Ahn TG, Lee JY, Hwang JY. Serum from pregnant women with gestational diabetes mellitus increases the expression of FABP4 mRNA in primary subcutaneous human pre-adipocytes. *Obstet Gynecol Sci* (2017) 60:274–82. doi: 10.5468/OGS.2017.60.3.274

9. Pérez-Pérez A, Sánchez-Jiménez F, Maymó J, Dueñas JL, Varone C, Sánchez-Margalet V. Role of leptin in female reproduction. *Clin Chem Lab Med* (2015) 53:15–28. doi: 10.1515/CCLM-2014-0387

10. Pérez-Pérez A, Guadix P, Maymó J, Dueñas JL, Varone C, Fernández-Sánchez M, et al. Insulin and leptin signaling in placenta from gestational diabetic subjects. *Horm Metab Res* (2016) 48:62–9. doi: 10.1055/S-0035-1559722

11. Dimasuay KG, Boeuf P, Powell TL, Jansson T. Placental responses to changes in the maternal environment determine fetal growth. *Front Physiol* (2016) 7:12. doi: 10.3389/FPHYS.2016.00012

12. Masuzaki H, Ogawa Y, Sagawa N, Hosoda K, Matsumoto T, Mise H, et al. Nonadipose tissue production of leptin: leptin as a novel placenta- derived hormone in humans. *Nat Med* (1997) 3:1029–33. doi: 10.1038/nm0997-1029

13. Lea RG, Howe D, Hannah LT, Bonneau O, Hunter L, Hoggard N. Placental leptin in normal, diabetic and fetal growth-retarded pregnancies. *Mol Hum Reprod* (2000) 6:763–9. doi: 10.1093/MOLEHR/6.8.763

14. Tessier DR, Ferraro ZM, Gruslin A. Role of leptin in pregnancy: consequences of maternal obesity. *Placenta* (2013) 34:205–11. doi: 10.1016/J.PLACENTA.2012.11.035

15. Day PE, Cleal JK, Lofthouse EM, Hanson MA, Lewis RM. What factors determine placental glucose transfer kinetics? *Placenta* (2013) 34:953–8. doi: 10.1016/J.PLACENTA.2013.07.001

16. Lewis RM, Brooks S, Crocker IP, Glazier J, Hanson MA, Johnstone ED, et al. Review: modelling placental amino acid transfer - from transporters to placental function. *Placenta* (2013) 34:S46–51. doi: 10.1016/j.placenta.2012.10.010

17. Vaughan OR, Rosario FJ, Powell TL, Jansson T. Regulation of placental amino acid transport and fetal growth. *Prog Mol Biol Transl Sci* (2017) 145:217–51. doi: 10.1016/bs.pmbts.2016.12.008

18. Lewis RM, Wadsack C, Desoye G. Placental fatty acid transfer. *Curr Opin Clin Nutr Metab Care* (2018) 21:78–82. doi: 10.1097/MCO.0000000000000443

19. Kautzky-Willer A, Pacini G, Tura A, Bieglmayer C, Schneider B, Ludvik B, et al. Increased plasma leptin in gestational diabetes. *Diabetologia* (2001) 44:164–72. doi: 10.1007/S001250051595

20. Pérez-Pérez A, Guadix P, Maymó J, Dueñas J, Varone C, Fernández-Sánchez M, et al. Insulin and leptin signaling in placenta from gestational diabetic subjects. *Horm Metab Res* (2015) 48:62–9. doi: 10.1055/s-0035-1559722

21. Di Simone N, Di Nicuolo F, Marzioni D, Castellucci M, Sanguinetti M, D'Lppolito S, et al. Resistin modulates glucose uptake and glucose transporter-1 (GLUT-1) expression in trophoblast cells. *J Cell Mol Med* (2009) 13:388–97. doi: 10.1111/J.1582-4934.2008.00337.X

22. Balachandiran M, Bobby Z, Dorairajan G, Gladwin V, Vinayagam V, Packirisamy RM. Decreased maternal serum adiponectin and increased insulin-like growth factor-1 levels along with increased placental glucose transporter-1 expression in gestational diabetes mellitus: possible role in fetal overgrowth: regulation of placental GLUT-1 expression in gestational diabetes mellitus. *Placenta* (2021) 104:71–80. doi: 10.1016/j.placenta.2020.11.008

23. Vilariño-García T, Pérez-Pérez A, Dietrich V, Guadix P, Dueñas JL, Varone CL, et al. Leptin upregulates aquaporin 9 expression in human placenta *in vitro*. *Gynecol Endocrinol* (2018) 34:175–7. doi: 10.1080/09513590.2017.1380184

24. Vilariño-García T, Pérez-Pérez A, Dietrich V, Fernández-Sánchez M, Guadix P, Dueñas JL, et al. Increased expression of aquaporin 9 in trophoblast from gestational diabetic patients. *Horm Metab Res* (2016) 48:535–9. doi: 10.1055/S-0042-105152

25. Farley DM, Choi J, Dudley DJ, Li C, Jenkins SL, Myatt L, et al. Placental amino acid transport and placental leptin resistance in pregnancies complicated by maternal obesity. *Placenta* (2010) 31:718–24. doi: 10.1016/J.PLACENTA.2010.06.006

26. Jansson N, Greenwood SL, Johansson BR, Powell TL, Jansson T. Leptin stimulates the activity of the system a amino acid transporter in human placental villous fragments. *J Clin Endocrinol Metab* (2003) 88:1205–11. doi: 10.1210/JC.2002-021332

27. Mousiolis AV, Kollia P, Skentou C, Messinis IE. Effects of leptin on the expression of fatty acid-binding proteins in human placental cell cultures. *Mol Med Rep* (2012) 5:497–502. doi: 10.3892/MMR.2011.686

28. Powe CE, Allard C, Battista MC, Doyon M, Bouchard L, Ecker JL, et al. Heterogeneous contribution of insulin sensitivity and secretion defects to gestational diabetes mellitus. *Diabetes Care* (2016) 39:1052–5. doi: 10.2337/DC15-2672

29. Osmond DTD, Nolan CJ, King RG, Brennecke SP, Gude NM. Effects of gestational diabetes on human placental glucose uptake, transfer, and utilisation. *Diabetologia* (2000) 43:576–82. doi: 10.1007/S001250051346

30. Jansson N, Pettersson J, Haafiz A, Ericsson A, Palmberg I, Tranberg M, et al. Down-regulation of placental transport of amino acids precedes the development of intrauterine growth restriction in rats fed a low protein diet. *J Physiol* (2006) 576:935–46. doi: 10.1113/JPHYSIOL.2006.116509

31. Lepercq J, Cauzac M, Lahlou N, Timsit J, Girard J, Auwerx J, et al. De overexpression of placental leptin in diabetic pregnancy: a critical role for insulin. *Diabetes* (1998) 47:847–50. doi: 10.2337/DIABETES.47.5.847

32. Sagawa N, Yura S, Itoh H, Mise H, Kakui K, Korita D, et al. Role of leptin in pregnancy - a review. *Placenta* (2002) 23:S80–6. doi: 10.1053/plac.2002.0814

33. Tang L, Li P, Li L. Whole transcriptome expression profiles in placenta samples from women with gestational diabetes mellitus. *J Diabetes Investig* (2020) 11:1307–17. doi: 10.1111/JDI.13250

34. Pérez-Pérez A, Maymó JL, Gambino YP, Guadix P, Dueñas JL, Varone CL, et al. Activated translation signaling in placenta from pregnant women with gestational diabetes mellitus: possible role of leptin. *Horm Metab Res* (2013) 45:436–42. doi: 10.1055/S-0032-1333276

35. Caughey AB, Turrentine M. ACOG practice bulletin no. 190: gestational diabetes mellitus. *Obstet Gynecol* (2018) 131:E49–64. doi: 10.1097/AOG.0000000000002501

36. National Diabetes Data Group. Classification and diagnosis of diabetes: standards of medical care in diabetes-2020. *Diabetes Care* (2020) 43(Suppl. 1):S14–31. doi: 10.2337/DC20-S002

37. National Diabetes Data Group. Classification and diagnosis of diabetes mellitus and other categories of glucose intolerance. national diabetes data group. *Diabetes* (1979) 28:1039–57. doi: 10.2337/DIAB.28.12.1039

38. Coustan DR. Gestational diabetes mellitus. *Clin Chem* (2013) 59:1310–21. doi: 10.1373/CLINCHEM.2013.203331

39. Vilariño-García T, Guadix P, Dorado-Silva M, Sánchez-Martín P, Pérez-Pérez A, Sánchez-Margalet V. Decreased expression of Sam68 is associated with insulin resistance in granulosa cells from PCOS patients. *Cells* (2022) 11(18):2821. doi: 10.3390/cells11182821

40. Vilariño-García T, Pérez-Pérez A, Santamaría-López E, Prados N, Fernández-Sánchez M, Sánchez-Margalet V. Sam68 mediates leptin signaling and action in human granulosa cells: possible role in leptin resistance in PCOS. *Endocr Connect* (2020) 9:479–88. doi: 10.1530/EC-20-0062

41. Friedman JM, Halaas JL. Leptin and the regulation of body weight in mammals. *Nature* (1998) 395:763–70. doi: 10.1038/27376

42. Behnes M, Brueckmann M, Lang S, Putensen C, Saur J, Borggrefe M, et al. Alterations of leptin in the course of inflammation and severe sepsis. *BMC Infect Dis* (2012) 12:217. doi: 10.1186/1471-2334-12-217

43. Chan JL, Mantzoros CS. Role of leptin in energy-deprivation states: normal human physiology and clinical implications for hypothalamic amenorrhoea and anorexia nervosa. *Lancet (London England)* (2005) 366:74–85. doi: 10.1016/S0140-6736(05)66830-4

44. Lin KC. Increase of maternal plasma leptin concentrations during pregnancy: comparison with nonpregnant women. *Kaohsiung J Med Sci*. (1999) 15(11):640–5.

45. Highman TJ, Friedman JE, Huston LP, Wong WW, Catalano PM. Longitudinal changes in maternal serum leptin concentrations, body composition, and resting metabolic rate in pregnancy. *Am J Obstet Gynecol* (1998) 178:1010–5. doi: 10.1016/S0002-9378(98)70540-X

46. Anim-Nyame N, Sooranna SR, Steer PJ, Johnson MR. Longitudinal analysis of maternal plasma leptin concentrations during normal pregnancy and pre-eclampsia. *Hum Reprod* (2000) 15:2033–6. doi: 10.1093/HUMREP/15.9.2033

47. Linnemann K, Malek A, Sager R, Blum WF, Schneider H, Fusch C. Leptin production and release in the dually *in vitro* perfused human placenta. *J Clin Endocrinol Metab* (2000) 85:4298–301. doi: 10.1210/JCEM.85.11.6933

48. Reitman ML, Bi S, Marcus-Samuels B, Gavrilova O. Leptin and its role in pregnancy and fetal development–an overview. *Biochem Soc Trans* (2001) 29:68. doi: 10.1042/0300-5127:0290068

49. Henson MC, Castracane VD. Leptin in pregnancy: an update. *Biol Reprod* (2006) 74:218–29. doi: 10.1095/BIOLREPROD.105.045120

50. Pérez-Pérez A, Maymó J, Dueñas JL, Goberna R, Calvo JC, Varone C, et al. Leptin prevents apoptosis of trophoblastic cells by activation of MAPK pathway. *Arch Biochem Biophys* (2008) 477:390–5. doi: 10.1016/J.ABB.2008.06.015

51. Pérez-Pérez A, Julieta Maymo Y, Gambino É, Dueñas JL, Goberna R, Varone C, et al. Leptin stimulates protein synthesis-activating translation machinery in human trophoblastic cells. *Biol Reprod* (2009) 81:826–32. doi: 10.1095/BIOLREPROD.109.076513

52. Maymó JL, Pérez Pérez A, Gambino Y, Calvo JC, Sánchez-Margalet V, Varone CL. Review: leptin gene expression in the placenta–regulation of a key hormone in trophoblast proliferation and survival. *Placenta* (2011) 32(Suppl 2):S146–53. doi: 10.1016/J.PLACENTA.2011.01.004

53. Toro AR, Maymó JL, Ibarbalz FM, Pérez A, Maskin B, Faletti AG, et al. Leptin is an anti-apoptotic effector in placental cells involving p53 downregulation. *PloS One* (2014) 9(6):e99187. doi: 10.1371/journal.pone.0099187

54. Pérez-Pérez A, Toro AR, Vilarino-Garcia T, Guadix P, Maymó JL, Dueñas JL, et al. Leptin reduces apoptosis triggered by high temperature in human placental villous explants: the role of the p53 pathway. *Placenta* (2016) 42:106–13. doi: 10.1016/J.PLACENTA.2016.03.009

55. Schanton M, Maymó JL, Pérez-Pérez A, Sánchez-Margalet V, Varone CL. Involvement of leptin in the molecular physiology of the placenta. *Reproduction* (2018) 155:R1–R12. doi: 10.1530/REP-17-0512

56. Sagawa N, Yura S, Itoh H, Kakui K, Takemura M, Nuamah MA, et al. Possible role of placental leptin in pregnancy: a review. *Endocrine* (2002) 19:65–71. doi: 10.1385/ENDO:19:1:65

57. Reitman ML, Bi S, Marcus-Samuels B, Gavrilova O. Leptin and its role in pregnancy and fetal development-an overview. *Biochem Soc Trans* (2001) 29:68. doi: 10.1042/0300-5127:0290068

58. Nuamah MA, Yura S, Sagawa N, Itoh H, Mise H, Korita D, et al. Significant increase in maternal plasma leptin concentration in induced delivery: a possible contribution of pro-inflammatory cytokines to placental leptin secretion. *Endocr J* (2004) 51:177–87. doi: 10.1507/ENDOCRJ.51.177

59. Misra VK, Trudeau S. The influence of overweight and obesity on longitudinal trends in maternal serum leptin levels during pregnancy. *Obesity* (2011) 19:416–21. doi: 10.1038/oby.2010.172

60. Bashir SO, Morsy MD, Elkarib AO, Abusham AA, Aboonq MS, Agamy AI. Impact of high altitude on maternal serum leptin level and its correlation with oxidative stress and endothelial inflammatory markers in preeclamptic women. *Chin J Physiol* (2018) 61:50–6. doi: 10.4077/CJP.2018.BAG537

61. Daskalakis G, Bellos I, Nikolakea M, Pergialiotis V, Papapanagiotou A, Loutradis D. The role of serum adipokine levels in preeclampsia: a systematic review. *Metabolism* (2020) 106:154172. doi: 10.1016/j.metabol.2020.154172

62. Thagaard IN, Hedley PL, Holm JC, Lange T, Larsen T, Krebs L, et al. Leptin and adiponectin as markers for preeclampsia in obese pregnant women, a cohort study. *Pregnancy Hypertens* (2019) 15:78–83. doi: 10.1016/j.preghy.2018.12.002

63. Haffejee F, Naicker T, Singh M, Kharsany ABM, Adhikari M, Singh R, et al. Placental leptin mRNA expression and serum leptin levels in pre-eclampsia associated with HIV infection. *J Obstet Gynaecol (Lahore)* (2017) 37:48–52. doi: 10.1080/01443615.2016.1209170

64. Kharb S, Bala J, Nanda S. Markers of obesity and growth in preeclamptic and normotensive pregnant women. *J Obstet Gynaecol (Lahore)* (2017) 37:610–5. doi: 10.1080/01443615.2017.1286463

65. Rabiepoor S, Abedi M, Saboory E, Khalkhali HR. Stress during pregnancy affected neonatal outcomes and changed cortisol and leptin levels both in mothers and newborns. *J Neonatal Perinatal Med* (2019) 12:209–19. doi: 10.3233/NPM-1818

66. Sidiropoulou EJ, Paltoglou G, Valsamakis G, Margeli A, Mantzou A, Papassotiriou I, et al. Biochemistry, hormones and adipocytokines in prepubertal children born with IUGR evoke metabolic, hepatic and renal derangements. *Sci Rep* (2018) 8:15691. doi: 10.1038/s41598-018-34075-6

67. Milenković S, Jankovic B, Mirković L, Jovandaric MZ, Milenković D, Otašević B. Lipids and adipokines in cord blood and at 72 h in discordant dichorionic twins. *Fetal Pediatr Pathol* (2017) 36:106–22. doi: 10.1080/15513815.2016.1242675

68. Nezar MAS, El-Baky AMA, Soliman OAS, Abdel-Hady HAS, Hammad AM, Al-Haggar MS. Endothelin-1 and leptin as markers of intrauterine growth restriction. *Indian J Pediatr* (2009) 76:485–8. doi: 10.1007/S12098-009-0079-0

69. Wang CY, Wang SG, Wang JL, Zhou LY, Liu HJ, Wang YF. Effect of miRNA-27a and leptin polymorphisms on risk of recurrent spontaneous abortion. *Med Sci Monit* (2016) 22:3514–22. doi: 10.12659/MSM.897147

70. Zidan HE, Rezk NA, Alnemr AAA, Moniem MIA. Interleukin-17 and leptin genes polymorphisms and their levels in relation to recurrent pregnancy loss in Egyptian females. *Immunogenetics* (2015) 67:665–73. doi: 10.1007/s00251-015-0876-8

71. Khashchenko E, Vysokikh M, Uvarova E, Krechetova L, Vtorushina V, Ivanets T, et al. Activation of systemic inflammation and oxidative stress in adolescent girls with polycystic ovary syndrome in combination with metabolic disorders and excessive body weight. *J Clin Med* (2020) 9:1399. doi: 10.3390/JCM9051399

72. Rizk NM, Sharif E. Leptin as well as free leptin receptor is associated with polycystic ovary syndrome in young women. *Int J Endocrinol* (2015) 2015:1–10. doi: 10.1155/2015/927805

73. Behboudi-Gandevani S, Ramezani Tehrani F, Bidhendi Yarandi R, Noroozzadeh M, Hedayati M, Azizi F. The association between polycystic ovary syndrome, obesity, and the serum concentration of adipokines. *J Endocrinol Invest* (2017) 40:859–66. doi: 10.1007/S40618-017-0650-X

74. Sweeting AN, Wong J, Appelblom H, Ross GP, Kouru H, Williams PF, et al. Novel early pregnancy risk prediction model for gestational diabetes mellitus. *Fetal Diagn Ther* (2019) 45:76–84. doi: 10.1159/000486853

75. Lobo TF, Torloni MR, Mattar R, Nakamura MU, Alexandre SM, Daher S. Adipokine levels in overweight women with early-onset gestational diabetes mellitus. *J Endocrinol Invest* (2019) 42:149–56. doi: 10.1007/s40618-018-0894-0

76. Shang M, Dong X, Hou L. Correlation of adipokines and markers of oxidative stress in women with gestational diabetes mellitus and their newborns. *J Obstet Gynaecol Res* (2018) 44:637–46. doi: 10.1111/jog.13586

77. Kampmann FB, Thuesen ACB, Hjort L, Bjerregaard AA, Chavarro JE, Frystyk J, et al. Increased leptin, decreased adiponectin and FGF21 concentrations in adolescent offspring of women with gestational diabetes. *Eur J Endocrinol* (2019) 181:691–700. doi: 10.1530/EJE-19-0658

78. Manoharan B, Bobby Z, Dorairajan G, Vinayagam V, Packirisamy RM. Adipokine levels and their association with insulin resistance and fetal outcomes among the newborns of indian gestational diabetic mothers. *Saudi Med J* (2019) 40:353–9. doi: 10.15537/smj.2019.4.24058

79. Powe CE, Huston Presley LP, Locascio JJ, Catalano PM. Augmented insulin secretory response in early pregnancy. *Diabetologia* (2019) 62:1445–52. doi: 10.1007/s00125-019-4881-6

80. Magariños MP, Sánchez-Margalet V, Kotler M, Calvo JC, Varone CL. Leptin promotes cell proliferation and survival of trophoblastic cells. *Biol Reprod* (2007) 76:203–10. doi: 10.1095/BIOLREPROD.106.051391

81. Sánchez-Jiménez F, Pérez-Pérez A, González-Yanes C, Varone CL, Sánchez-Margalet V. Sam68 mediates leptin-stimulated growth by modulating leptin receptor signaling in human trophoblastic JEG-3 cells. *Hum Reprod* (2011) 26:2306–15. doi: 10.1093/HUMREP/DER187

82. Pérez-Pérez A, Gambino Y, Maymó J, Goberna R, Fabiani F, Varone C, et al. MAPK and PI3K activities are required for leptin stimulation of protein synthesis in human trophoblastic cells. *Biochem Biophys Res Commun* (2010) 396:956–60. doi: 10.1016/j.bbrc.2010.05.031

83. Thorens B, Mueckler M. Glucose transporters in the 21st century. *Am J Physiol - Endocrinol Metab* (2010) 298:E141. doi: 10.1152/ajpendo.00712.2009

84. Illsley NP, Baumann MU. Human placental glucose transport in fetoplacental growth and metabolism. *Biochim Biophys Acta - Mol Basis Dis* (2020) 1866:165359. doi: 10.1016/j.bbadis.2018.12.010

85. Gaither K, Quraishi AN, Illsley NP. Diabetes alters the expression and activity of the human placental GLUT1 glucose transporter. *J Clin Endocrinol Metab* (1999) 84:695–701. doi: 10.1210/jc.84.2.695

86. Jansson T, Wennergren M, Illsley NP. Glucose transporter protein expression in human placenta throughout gestation and in intrauterine growth retardation. *J Clin Endocrinol Metab* (1993) 77:1554–62. doi: 10.1210/jcem.77.6.8263141

87. Illsley NP. Glucose transporters in the human placenta. *Placenta* (2000) 21:14–22. doi: 10.1053/plac.1999.0448

88. Sciullo E, Cardellini G, Baroni M, Torresi P, Mazziotti F, Pozzilli P, et al. Glucose transporters (GLUT 1, GLUT 3) mRNA in human placenta of diabetic and non-diabetic pregnancies. *Ann Ist Super Sanita* (1997) 33:361–5.

89. Stanirowski PJ, Szukiewicz D, Pyzlak M, Abdalla N, Sawicki W, Cendrowski K. Analysis of correlations between the placental expression of glucose transporters GLUT-1, GLUT-4 and GLUT-9 and selected maternal and fetal parameters in pregnancies complicated by diabetes mellitus. *J Matern Fetal Neonatal Med* (2019) 32:650–9. doi: 10.1080/14767058.2017.1387897

90. Michelsen TM, Holme AM, Holm MB, Roland MC, Haugen G, Powell TL, et al. Uteroplacental glucose uptake and fetal glucose consumption: a quantitative study in human pregnancies. *J Clin Endocrinol Metab* (2019) 104:873–82. doi: 10.1210/JC.2018-01154

91. Stanirowski PJ, Szukiewicz D, Pazura-Turowska M, Sawicki W, Cendrowski K. Placental expression of glucose transporter proteins in pregnancies complicated by gestational and pregestational diabetes mellitus. *Can J Diabetes* (2018) 42:209–17. doi: 10.1016/j.jcjd.2017.04.008

92. Haber RS, Weinstein SP, O'Boyle E, Morgello S. Tissue distribution of the human GLUT3 glucose transporter. *Endocrinology* (1993) 132:2538–43. doi: 10.1210/ENDO.132.6.8504756

93. Araújo JR, Keating E, Martel F. Impact of gestational diabetes mellitus in the maternal-to-fetal transport of nutrients. *Curr Diab Rep* (2015) 15:569. doi: 10.1007/s11892-014-0569-y

94. Huang B, Huang C, Zhao H, Zhu W, Wang B, Wang H, et al. Impact of GPR1 signaling on maternal high-fat feeding and placenta metabolism in mice. *Am J Physiol Endocrinol Metab* (2019) 316:E987–97. doi: 10.1152/AJPENDO.00437.2018

95. Feng C, Jin Z, Sun L, Wang X, Chi X, Zhang X, et al. Endogenous SHBG levels correlate with that of glucose transporters in insulin resistance model cells. *Mol Biol Rep* (2019) 46:4953–65. doi: 10.1007/S11033-019-04946-W

96. Boileau P, Mrejen C, Girard J, Hauguel-De Mouzon S. Overexpression of GLUT3 placental glucose transporter in diabetic rats. *J Clin Invest* (1995) 96:309–17. doi: 10.1172/JCI118036

97. Rong C, Cui X, Chen J, Qian Y, Jia R, Hu Y. DNA Methylation profiles in placenta and its association with gestational diabetes mellitus. *Exp Clin Endocrinol Diabetes* (2015) 123:282–8. doi: 10.1055/S-0034-1398666

98. Rosario FJ, Kanai Y, Powell TL, Jansson T. Increased placental nutrient transport in a novel mouse model of maternal obesity with fetal overgrowth. *Obesity* (2015) 23:1663–70. doi: 10.1002/oby.21165

99. Gorovits N, Charron MJ. What we know about facilitative glucose transporters: lessons from cultured cells, animal models, and human studies. *Biochem Mol Biol Educ* (2003) 31:163–72. doi: 10.1002/bmb.2003.494031030227

100. Vaughan OR, Thompson F, Lorca RA, Julian CG, Powell TL, Moore LG, et al. Effect of high altitude on human placental amino acid transport. *J Appl Physiol* (2020) 128:127–33. doi: 10.1152/japplphysiol.00691.2019

101. Xing AY, Challier JC, Lepercq J, Caüzac M, Charron MJ, Girard J, et al. Unexpected expression of glucose transporter 4 in villous stromal cells of human placenta. *J Clin Endocrinol Metab* (1998) 83:4097–101. doi: 10.1210/JCEM.83.11.5290

102. Feng C, Jin Z, Chi X, Zhang B, Wang X, Sun L, et al. SHBG expression is correlated with PI3K/AKT pathway activity in a cellular model of human insulin resistance. *Gynecol Endocrinol* (2018) 34:567–73. doi: 10.1080/09513590.2017.1411474

103. Zhang B, Jin Z, Sun L, Zheng Y, Jiang J, Feng C, et al. Expression and correlation of sex hormone-binding globulin and insulin signal transduction and glucose transporter proteins in gestational diabetes mellitus placental tissue. *Diabetes Res Clin Pract* (2016) 119:106–17. doi: 10.1016/j.diabres.2016.07.003

104. James-Allan LB, Teal S, Powell TL, Jansson T. Changes in placental nutrient transporter protein expression and activity across gestation in normal and obese women. *Reprod Sci* (2020) 27, 1758–1769. doi: 10.1007/s43032-020-00173-y

105. Ishizuka T, Klepcyk P, Liu S, Panko L, Liu S, Gibbs EM, et al. Effects of overexpression of human GLUT4 gene on maternal diabetes and fetal growth in spontaneous gestational diabetic C57BLKS/J lepr(db/+) mice. *Diabetes* (1999) 48:1061–9. doi: 10.2337/diabetes.48.5.1061

106. Limesand SW, Regnault TRH, Hay WW. Characterization of glucose transporter 8 (GLUT8) in the ovine placenta of normal and growth restricted fetuses. *Placenta* (2004) 25:70–7. doi: 10.1016/j.placenta.2003.08.012

107. Schmidt S, Joost H-G, Schürmann A. GLUT8, the enigmatic intracellular hexose transporter. *Am J Physiol Metab* (2009) 296:E614–8. doi: 10.1152/ajpendo.91019.2008

108. Bibert S, Hess SK, Firsov D, Thorens B, Geering K, Horisberger J-D, et al. Mouse GLUT9: evidences for a urate uniporter. *Am J Physiol Physiol* (2009) 297:F612–9. doi: 10.1152/ajprenal.00139.2009

109. Bibee KP, Illsley NP, Moley KH. Asymmetric syncytial expression of GLUT9 splice variants in human term placenta and alterations in diabetic pregnancies. *Reprod Sci* (2011) 18:20–7. doi: 10.1177/1933719110380276

110. Stanirowski PJ, Szukiewicz D, Pyzlak M, Abdalla N, Sawicki W, Cendrowski K. Impact of pre-gestational and gestational diabetes mellitus on the expression of glucose transporters GLUT-1, GLUT-4 and GLUT-9 in human term placenta. *Endocrine* (2017) 55:799–808. doi: 10.1007/s12020-016-1202-4

111. Szablewski L. *Human glucose transporters in health and diseases*. (2019) (Cambridge: Scholars Publishing), 245.

112. Novakovic B, Gordon L, Robinson WP, Desoye G, Saffery R. Glucose as a fetal nutrient: dynamic regulation of several glucose transporter genes by DNA methylation in the human placenta across gestation. *J Nutr Biochem* (2013) 24:282–8. doi: 10.1016/j.jnutbio.2012.06.006

113. Gude NM, Stevenson JL, Rogers S, Best JD, Kalionis B, Huisman MA, et al. GLUT12 expression in human placenta in first trimester and term. *Placenta* (2003) 24:566–70. doi: 10.1053/plac.2002.0925

114. Cetin I, Ronzoni S, Marconi AM, Perugino G, Corbetta C, Battaglia FC, et al. Maternal concentrations and fetal-maternal concentration differences of plasma amino acids in normal and intrauterine growth-restricted pregnancies. *Am J Obstet Gynecol* (1996) 174:1575–83. doi: 10.1016/S0002-9378(96)70609-9

115. Regnault TRH, De Vrijer B, Battaglia FC. Transport and metabolism of amino acids in placenta. *Endocrine* (2002) 19:23–41. doi: 10.1385/ENDO:19:1:23

116. Cleal JK, Lewis RM. The mechanisms and regulation of placental amino acid transport to the human foetus. *J Neuroendocrinol* (2008) 20:419–26. doi: 10.1111/J.1365-2826.2008.01662.X

117. Dicke JM, Henderson GI. Placental amino acid uptake in normal and complicated pregnancies. *Am J Med Sci* (1988) 295:223–7. doi: 10.1097/00000441-198803000-00012

118. Gaccioli F, Aye ILMH, Roos S, Lager S, Ramirez VI, Kanai Y, et al. Expression and functional characterisation of system l amino acid transporters in the human term placenta. *Reprod Biol Endocrinol* (2015) 13:57. doi: 10.1186/s12958-015-0054-8

119. Jansson T, Ylvén K, Wennergren M, Powell TL. Glucose transport and system a activity in syncytiotrophoblast microvillous and basal plasma membranes in intrauterine growth restriction. *Placenta* (2002) 23:392–9. doi: 10.1053/plac.2002.0826

120. Johns EC, Denison FC, Reynolds RM. The impact of maternal obesity in pregnancy on placental glucocorticoid and macronutrient transport and metabolism. *Biochim Biophys Acta - Mol Basis Dis* (2020) 1866:165374. doi: 10.1016/j.bbadis.2018.12.025

121. Shang M, Wen Z. Increased placental IGF-1/mTOR activity in macrosomia born to women with gestational diabetes. *Diabetes Res Clin Pract* (2018) 146:211–9. doi: 10.1016/j.diabres.2018.10.017

122. Kuruvilla AG, D'Souza SW, Glazier JD, Mahendran D, Maresh MJ, Sibley CP. Altered activity of the system a amino acid transporter in microvillous membrane vesicles from placentas of macrosomic babies born to diabetic women. *J Clin Invest* (1994) 94:689–95. doi: 10.1172/JCI117386

123. Jansson T, Ekstrand Y, Björn C, Wennergren M, Powell TL. Alterations in the activity of placental amino acid transporters in pregnancies complicated by diabetes. *Diabetes* (2002) 51:2214–9. doi: 10.2337/diabetes.51.7.2214

124. Baumann MU, Deborde S, Illsley NP. Placental glucose transfer and fetal growth. *Endocrine* (2002) 19(1):13–22. doi: 10.1385/ENDO:19:1:13

125. Colomiere M, Permezel M, Riley C, Desoye G, Lappas M. Defective insulin signaling in placenta from pregnancies complicated by gestational diabetes mellitus. *Eur J Endocrinol* (2009) 160:567–78. doi: 10.1530/EJE-09-0031

126. von Versen-Höynck F, Rajakumar A, Parrott MS, Powers RW. Leptin affects system a amino acid transport activity in the human placenta: evidence for STAT3 dependent mechanisms. *Placenta* (2009) 30:361–7. doi: 10.1016/j.placenta.2009.01.004

127. Araújo JR, Correia-Branco A, Ramalho C, Gonçalves P, Pinho MJ, Keating E, et al. L-methionine placental uptake: characterization and modulation in gestational diabetes mellitus. *Reprod Sci* (2013) 20:1492–507. doi: 10.1177/1933719113488442

128. Segura MT, Demmelmair H, Krauss-Etschmann S, Nathan P, Dehmel S, Padilla MC, et al. Maternal BMI and gestational diabetes alter placental lipid transporters and fatty acid composition. *Placenta* (2017) 57:144–51. doi: 10.1016/j.placenta.2017.07.001

129. Gauster M, Hiden U, Van Poppel M, Frank S, Wadsack C, Hauguel-de Mouzon S, et al. Dysregulation of placental endothelial lipase in obese women with gestational diabetes mellitus. *Diabetes* (2011) 60:2457–64. doi: 10.2337/db10-1434

130. Lappas M. Effect of pre-existing maternal obesity, gestational diabetes and adipokines on the expression of genes involved in lipid metabolism in adipose tissue. *Metabolism* (2014) 63:250–62. doi: 10.1016/j.metabol.2013.10.001

131. Prieto-Sánchez MT, Ruiz-Palacios M, Blanco-Carnero JE, Pagan A, Hellmuth C, Uhl O, et al. Placental MFSD2a transporter is related to decreased DHA in cord blood of women with treated gestational diabetes. *Clin Nutr* (2017) 36:513–21. doi: 10.1016/j.clnu.2016.01.014

132. Magnusson AL, Waterman IJ, Wennergren M, Jansson T, Powell TL. Triglyceride hydrolase activities and expression of fatty acid binding proteins in the human placenta in pregnancies complicated by intrauterine growth restriction and diabetes. *J Clin Endocrinol Metab* (2004) 89:4607–14. doi: 10.1210/jc.2003-032234

133. Radaelli T, Lepercq J, Varastehpour A, Basu S, Catalano PM, Hauguel-De Mouzon S. Differential regulation of genes for fetoplacental lipid pathways in pregnancy with gestational and type 1 diabetes mellitus. *Am J Obstet Gynecol* (2009) 201:209.e1–209.e10. doi: 10.1016/j.ajog.2009.04.019

134. Scifres CM, Chen B, Nelson DM, Sadovsky Y. Fatty acid binding protein 4 regulates intracellular lipid accumulation in human trophoblasts. *J Clin Endocrinol Metab* (2011) 96:E1083–91. doi: 10.1210/jc.2010-2084

135. Lager S, Powell TL. Regulation of nutrient transport across the placenta. *J Pregnancy* (2012) 2012:179827. doi: 10.1155/2012/179827

136. Jansson T, Cetin I, Powell TL, Desoye G, Radaelli T, Ericsson A, et al. Placental transport and metabolism in fetal overgrowth - a workshop report. *Placenta* (2006) 27:109–13. doi: 10.1016/j.placenta.2006.01.017

137. Schaefer-Graf UM, Graf K, Kulbacka I, Kjos SL, Dudenhausen J, Vetter K, et al. Maternal lipids as strong determinants of fetal environment and growth in pregnancies with gestational diabetes mellitus. *Diabetes Care* (2008) 31:1858–63. doi: 10.2337/DC08-0039

138. Waterman IJ, Emmison N, Dutta-Roy AK. Characterisation of triacylglycerol hydrolase activities in human placenta. *Biochim Biophys Acta - Lipids Lipid Metab* (1998) 1394:169–76. doi: 10.1016/S0005-2760(98)00105-2

139. Schaiff WT, Bildirici I, Cheong M, Chern PL, Nelson DM, Sadovsky Y. Peroxisome proliferator-activated receptor-γ and retinoid X receptor signaling regulate fatty acid uptake by primary human placental trophoblasts. *J Clin Endocrinol Metab* (2005) 90:4267–75. doi: 10.1210/jc.2004-2265

140. Biron-Shental T, Schaiff WT, Ratajczak CK, Bildirici I, Nelson DM, Sadovsky Y. Hypoxia regulates the expression of fatty acid-binding proteins in primary term human trophoblasts. *Am J Obstet Gynecol* (2007) 197:516.e1–6. doi: 10.1016/j.ajog.2007.03.066

141. Brett KE, Ferraro ZM, Yockell-Lelievre J, Gruslin A, Adamo KB. Maternal–fetal nutrient transport in pregnancy pathologies: the role of the placenta. *Int J Mol Sci* (2014) 15:16153–85. doi: 10.3390/ijms150916153

142. Cunningham P, McDermott L. Long chain PUFA transport in human term placenta. *J Nutr* (2009) 139:636–9. doi: 10.3945/jn.108.098608

143. Ortega-Senovilla H, Schaefer-Graf U, Herrera E. Pregnant women with gestational diabetes and with well controlled glucose levels have decreased concentrations of individual fatty acids in maternal and cord serum. *Diabetologia* (2020) 63:864–74. doi: 10.1007/s00125-019-05054-x

144. Aslfalah H, Jamilian M, Khosrowbeygi A. Elevation of the adiponectin/leptin ratio in women with gestational diabetes mellitus after supplementation with alpha-lipoic acid. *Gynecol Endocrinol* (2019) 35:271–5. doi: 10.1080/09513590.2018.1519795

145. Aye ILMH, Jansson T, Powell TL. TNF-α stimulates system a amino acid transport in primary human trophoblast cells mediated by p38 MAPK signaling. *Physiol Rep* (2015) 3(10):e12594. doi: 10.14814/PHY2.12594

frontiers | Frontiers in Endocrinology

TYPE Original Research
PUBLISHED 18 August 2023
DOI 10.3389/fendo.2023.1177547

Check for updates

OPEN ACCESS

EDITED BY
Reinaldo Marín,
Instituto Venezolano de Investigaciones Científicas (IVIC), Venezuela

REVIEWED BY
Luis Sobrevia,
Pontificia Universidad Católica de Chile, Chile
Noemí García,
Tecnológico de Monterrey, Mexico

*CORRESPONDENCE
Yue Wang
wangyue0900226@126.com

RECEIVED 01 March 2023
ACCEPTED 03 August 2023
PUBLISHED 18 August 2023

CITATION
Zhao Y, Gao Q, Li B, Wang Y and Wang Y (2023) Ferroptosis and its potential role in gestational diabetes mellitus: updated evidence from pathogenesis to therapy. *Front. Endocrinol.* 14:1177547. doi: 10.3389/fendo.2023.1177547

COPYRIGHT
© 2023 Zhao, Gao, Li, Wang and Wang. This is an open-access article distributed under the terms of the Creative Commons Attribution License (CC BY). The use, distribution or reproduction in other forums is permitted, provided the original author(s) and the copyright owner(s) are credited and that the original publication in this journal is cited, in accordance with accepted academic practice. No use, distribution or reproduction is permitted which does not comply with these terms.

Ferroptosis and its potential role in gestational diabetes mellitus: updated evidence from pathogenesis to therapy

Yan Zhao[1], Qianqian Gao[2], Baoxuan Li[1], Yang Wang[1] and Yue Wang[1]*

[1]Department of Obstetrics and Gynaecology, Shengjing Hospital of China Medical University, Shenyang, Liaoning, China, [2]Department of Obstetrics, Weifang People's Hospital, Weifang, ShanDong, China

Background: Studies have demonstrated that high iron status is positively associated with gestational diabetes mellitus (GDM), implying that iron overload and ferroptosis play important roles in the development of GDM. The aim of this study was to explore effective therapeutic drugs from traditional Chinese medicine (TCM)formulas for the treatment of GDM based on ferroptosis.

Methods: In this study, the presence of ferroptosis in the placenta was verified through clinical and experimental data, and key genes were subsequently screened for association with ferroptosis in the development of GDM. The analysis was based on transcriptome sequencing of datasets combined with differentially expressed genes (DEGs) analysis and weighted gene correlation network analysis (WGCNA); functional enrichment analysis was also performed. A protein–protein interaction (PPI) network was constructed and pivotal genes were identified using Cytoscape. Finally, traditional Chinese medicine (TCM) formulas related to treating GDM were collected, then the proteins corresponding to the key genes were molecularly docked with the small molecular structures of clinically proven effective herbal tonics, and molecular dynamic simulations were performed to select the best candidates for pharmacological compounds.

Results: Elevated ferritin levels in patients with GDM were verified using clinical data. The presence of ferroptosis in placental tissues of patients with GDM was confirmed using electron microscopy and western blotting. Ninety-nine key genes with the highest correlation with ferroptosis were identified from DEGs and weighted gene co-expression network analysis (WGCNA). Analysis using the Kyoto Encyclopedia of Genes and Genomes demonstrated that the DEGs were primarily involved in the oxidative phosphorylation pathway. The key genes were further screened by PPI; two key genes, SF3B14 and BABAM1, were identified by combining the gene corresponding to protein structure and function, followed by molecular docking and molecular dynamic simulation. *Coptis chinensis* was proposed as the best candidate for herbal treatment at the molecular level.

Conclusion: This data revealed the presence of ferroptosis in patients with GDM and identified possible modulatory roles of ferroptosis-related genes involved in

the molecular mechanisms of GDM, providing new insights into the pathogenesis of GDM, which also provided new directions for the systematic optimization of TCM formulas for the management and targeted treatment of GDM.

KEYWORDS

gestational diabetes mellitus, ferroptosis, bioinformatic, WGCNA, molecular docking, molecular dynamic simulation

1 Introduction

Gestational diabetes mellitus (GDM) is traditionally defined as glucose intolerance of variable severity, with onset or first detection during pregnancy. The global prevalence of GDM is up to one in seven pregnancies (1). GDM is associated with long-term adverse health outcomes in women and their offspring and is at the center of the "diabetes begetting diabetes" vicious circle (2). For example, women with GDM experience an increased risk of hypertensive disorders in pregnancy, preterm delivery, and an exceptionally high risk for type 2 diabetes, metabolic syndromes, and cardiovascular diseases later in life (3). Children born to pregnant women affected by GDM often experience excess growth during the fetal period, resulting in increased adiposity at birth and an increased risk for obesity and cardiometabolic disorders later in life (2, 4). Current studies have demonstrated that the occurrence and development of GDM is influenced by multiple factors, among which genetic, metabolic and environmental factors are important in the pathogenesis of GDM(5). Currently, we recommend dietary modification and increasing appropriate physical activity to improve gestational diabetes, and when basic methods cannot control blood glucose, insulin therapy (6) or oral hypoglycemic agents, mainly metformin and glibenclamide (7), are mostly used. The majority of current studies have focused on hypoglycemic approaches to treat GDM. However, the efficacy in preventing and stopping further disease progression have not been completely satisfactory. Therefore, identifying women at increased risk of GDM at an early stage and exploring markers to predict GDM can aid in the diagnosis and treatment of GDM.

The average daily iron requirement during pregnancy increases to approximately 1,000–1,200 mg to meet the maternal and fetal placental needs for erythropoiesis, growth, and development (8). Therefore, much attention has been focused on the prevention of iron deficiency, that is anemia, and iron supplementation has become a routine recommendation for all women throughout pregnancy (9). Nonetheless, as early as 20 years ago, studies suggested that iron accumulation increases the risk of glucose intolerance in late pregnancy and iron overload may play a role in the development of GDM (10). Many subsequent clinical studies have demonstrated a correlation between disturbances in iron homeostasis during pregnancy and GDM. A recent meta-analysis included 32 prospective cohort or case-control studies investigating the relationship between serum iron metabolic markers and GDM, and higher levels of serum iron, ferritin, transferrin saturation, ferritin, and hemoglobin were reported in patients with GDM than in those without GDM, suggesting that high serum ferritin and hemoglobin levels are positively associated with the risk of developing GDM (11). Recent studies have questioned the recommendation of routine iron supplementation during pregnancy in iron-sufficient and non-anemic women and have further suggested that excessive iron intake may paradoxically increase the risk of reproductive disorders (12). Several relevant clinical, *in vitro*, and *in vivo* studies have validated the correlation between iron overload and the development of GDM (13, 14); nonetheless, the specific mechanisms by which iron overload causes GDM are not fully understood. Iron death is an iron-dependent process characterized by dysregulation of iron homeostasis, leading to excessive iron death, which is a recently described programmed cell death process mediated by iron-dependent lipid peroxidation of the cell membrane. Iron overload drives iron accumulation and the biological effects thereof (15). Iron overload during pregnancy leads to ferroptosis, which causes GDM (12). Therefore, iron overload may be presumed to play a crucial role in GDM. However, whether iron overload actually causes GDM or is simply a byproduct of iron death remains to be proven.

As a type of programmed cell death, ferroptosis is dependent on iron and induced by the accumulation of oxidatively damaged phospholipids. It is associated with the malfunction of glutathione-dependent antioxidant defenses mediated by glutathione peroxidase 4 (Gpx4) via different pathways (8, 10), resulting in an increased amount of reactive oxygen species (ROS). This in turn leads to a reduction in the metabolism of lipid peroxides catalyzed by Gpx4 and intracellular glutathione, which causes Fe2+ to oxidize lipids in a Fenton-like manner, resulting in the production of large amounts of ROS and promotion of ferroptosis (16). Recently, the importance of ferroptosis has been demonstrated in the antioxidant activity of pancreatic β-cells and insulin resistance (17). However, the specific role of ferroptosis in GDM currently remains elusive.

Traditional Chinese medicine (TCM) is an effective way to treat GDM with chemical diversity, effectiveness and few side effects (18).

Abbreviations: GDM, gestational diabetes mellitus; TCM, traditional Chinese medicine; DEGs, differentially expressed genes; PPI, protein-protein interaction; WGCNA, weighted gene co-expression network analysis; KEGG, Kyoto Encyclopedia of Genes and Genomes; GCMs, gene co-expression modules.

In recent years, TCM has made remarkable progress in the treatment of GDM, and a large number of effective formulas have been accumulated. However, due to the complexity of TCM components, the formulations of TCM vary greatly. Current TCM-related studies have focused on given formulations, herbs or single compounds, and we performed screening of specific core drugs for the treatment of GDM by transcriptomics, network analysis and computer virtualization.

In this study, clinical data were applied to reaffirm the positive association of ferritin with the development of GDM, confirming the occurrence of ferroptosis in the placental tissue of patients with GDM by using electron microscopy, and the expression of GPX4, SLC7A11, and FTH1 was evaluated by western blot analysis. Recent advances in sequencing technology have greatly facilitated genetic studies of GDM. Reliable differentially expressed genes (DEGs) were identified in GDM based on the GSE70493 dataset. A weighted gene co-expression network analysis (WGCNA) in 32 patients with GDM and 31 non-GDM controls was conducted. Compared with traditional methodologies that take every transcript in the microarray alone and only capture two less pieces of information than that provided by the microarray, WGCNA takes correlations among those transcripts into account and identifies potential disease-related gene co-expression modules (GCMs) by considering associations between GCMs and disease traits as well as intramodular associations. A gene module closely associated with ferroptosis was identified and screened for potential biomarkers via a combination of protein–protein interaction (PPI) networks. Wheat-flavored Rehmannia decoction, Astragalus Sijunzi decoction, Radix Astragali and Radix Ophiopogonis decoction, and Shenqi Dihuang decoction have been used for many years in the clinical treatment of GDM with remarkable efficacy. The complexity of Chinese herbal medicine suggests a potential for multiple therapeutic applications. We analyzed the herbs that could be evaluated for the treatment of GDM from the perspective of ferroptosis. In summary, we analyzed the impact of ferroptosis on GDM utilizing a bioinformatics approach and found a significant association between ferroptosis and GDM. In addition, we analyzed the herbs targeted ferroptosis to treat GDM based on molecular docking and molecular dynamic simulation. This study provided new directions for the management and targeted treatment of GDM.

2 Materials and methods

2.1 Collection of clinical data and tissue samples

A procedural flowchart of the study is illustrated in Figure 1. A retrospective analysis was performed from January 2020 to December 2020 at the Shengjing Hospital, China Medical University. Pregnant women who completed the oral glucose tolerance test (OGTT) from 24–28 weeks of pregnancy and received a diagnosis of GDM based on abnormal OGTT defined as per the criteria of the International Association of Diabetes and Pregnancy Study Groups (IADPSG) were included in the study; patients with normal OGTT in the same period were included as controls. A total of 65 GDM patients with ferritin and 153 normal pregnant women with ferritin were included during the first trimester. And 330 GDM patients with ferritin and 920 normal pregnant women with ferritin were included during the second trimester. Detailed information is listed in Supplementary Table 1. Subjects with a history of GDM, smoking before and during pregnancy, and medical conditions, such as hemoglobinopathies, infections, and other chronic diseases, were excluded. Serum ferritin levels were measured during early (8–12 weeks) and mid-pregnancy

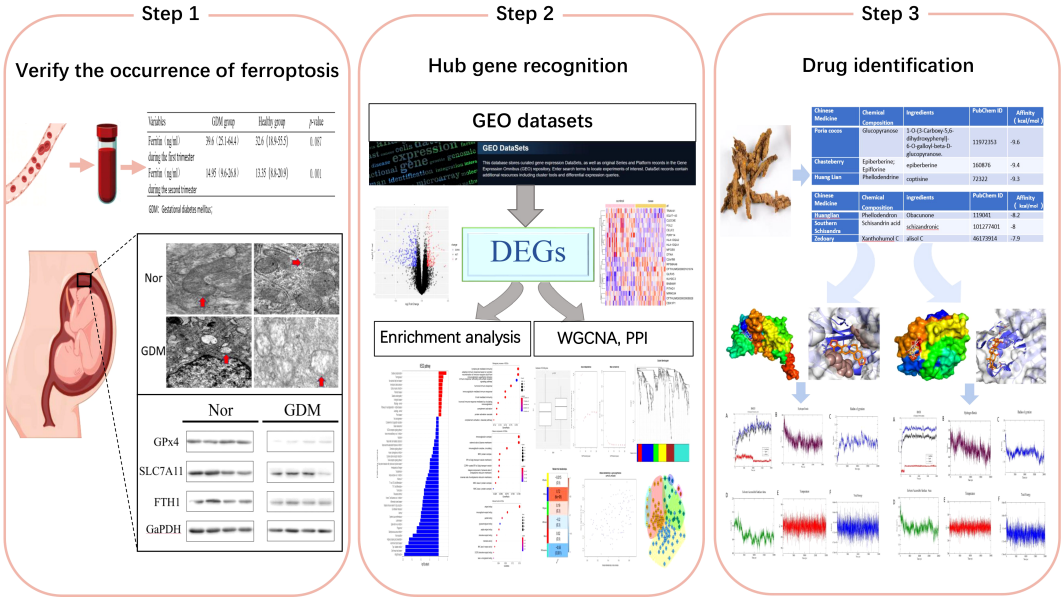


FIGURE 1
Flowchart.

(24–28 weeks). Ferritin and blood glucose levels were measured using ferritin kit for the DXI800 instrument (Beckman Coulter, Brea, CA, USA) and blood glucose kit for the c16000 instrument (Abbott Diagnostics, Abbott Park, IL, USA).

Women with full-term singleton pregnancies who underwent cesarean delivery at the Shengjing Hospital of China Medical University, from January 2021 to June 2021, were selected. GDM was diagnosed based on the criteria of the IADPSG. The exclusion criteria included twin (multiple) pregnancies; diabetes diagnosis prior to pregnancy; pregnancy complications such as preeclampsia; essential (primary) hypertension; hyperthyroidism; hypothyroidism; Cushing's syndrome; smoking; assisted reproduction; and severe liver, kidney, or heart disease. 10 women with GDM and 10 healthy controls were included in the study. Placental tissue samples from women with GDM and healthy women were collected randomly from the substrate (2 cm from the periphery to avoid placental infarction) immediately after delivery for western blotting. The tissue samples were washed repeatedly with phosphate buffered saline (PBS), placed in labeled lyophilized tubes, and stored in liquid nitrogen. Two or three pieces of placental tissue approximately 0.5 cm^3 in size were randomly sampled from the substrate (in the middle of the central tufts of villi connecting to the maternal region) immediately after delivery for electron microscopic evaluation. The placental tissue samples were washed in saline, and the washed placental tissue was immersed in 2.5% glutaraldehyde fixative (0.1 mol/L sodium dimethylarsonate buffer, pH 7.4). The tissue blocks were cut into 1 mm^3 pieces and fixed at 4°C for at least 2 h. Sampling was performed simultaneously by YW and BL. This study was conducted in accordance with the principles of the Declaration of Helsinki and approved by the Research Medical Ethics Committee of Shengjing Hospital of China Medical University (The ethics number of the experiment:2017PS066K).

2.2 Validation of ferroptosis in placental tissues of patients with GDM

Electron microscopy was used to examine mitochondrial changes in placental tissues of patients with GDM. After fixation, the placental tissues were washed with 0.1 mol/L PBS for 30 min and post-fixed with 1% osmium tetroxide fixative for 90 min at 4°C. After rinsing, dehydration, permeabilization, embedding, sectioning, and staining, changes in mitochondrial morphology in the placental tissue cells were observed under an electron microscope (H-7650, Hitachi, Japan) and photographed for sample retention. Protein levels associated with ferroptosis were subsequently evaluated. Placental tissues collected from patients with GDM (n = 10) as well as from normal pregnancies (n = 10) were removed from the liquid nitrogen, and the samples were lysed with RIPA lysis buffer (P0013B, Beyotime, Beijing, China) and phenylmethylsulfonyl fluoride (PMSF). Proteins in the lysates were electrophoresed on 10% sodium dodecyl sulfate-polyacrylamide gel electrophoresis (SDS-PAGE) and subsequently transferred to polyvinylidene fluoride (PVDF) membranes. After closure with 5% skim milk to block non-specific binding, the specific primary antibody was placed and incubated overnight at 4°C, followed by incubation at 37°C for 1 h with horseradish peroxidase-labeled secondary antibodies (Cell Signaling Technology). The following primary antibodies were used: SLC7A11 (1:500; ab175186; Abcam), GPX4 (1:1000; ab231174; Abcam), FTH1 (1:500; ab75972; Abcam), and GAPDH (60004-1-Ig; Proteintech).

Antibody-labeled proteins were detected using chemiluminescence with a LAS-3000 luminescence image analyzer (Fujifilm Holdings Corporation, Tokyo, Japan) and SuperSignal West Femto maximum sensitivity substrate (Thermo Fisher Scientific, Inc., Waltham, MA, USA). Using the gel image processing software image J, the backgrounds were removed, units and assay data were adjusted, and grayscale values were calculated. Values were entered into GraphPad Prism 7 (GraphPad Software 7.0.1, San Diego, CA, USA) for statistical analyses. Experiments were performed in triplicate for each target protein strip. Antibody-labeled proteins were detected using chemiluminescence with a LAS-3000 image analyzer (Fujifilm Holdings Corporation, Tokyo, Japan), and ImageJ was used to remove the background, adjust the units with the assay data, and calculate the grayscale values. The values were entered into GraphPad Prism 7 for statistical analysis. Triplicate experiments were performed for each target protein strip.

2.3 Microarray data source

GSE70493 with the GPL17586 platform was collected from Gene Expression Omnibus (GEO) (https://www.ncbi.nlm.nih.gov/geo/). In total, 63 samples were obtained, including RNA-seq data and clinical data; 32 placenta samples from patients with GDM and 31 placenta samples from patients without GDM, and 253 ferroptosis-related regulators were collected from the FerrDb database (19).

2.4 Identification of differentially expressed genes

Following potent mean background correction, the microarray matrix file was subjected to quantile normalization and expression calculation using Affymetrix to obtain gene expression profiles. The differentially expressed genes (DEGs) between placental samples from 32 patients with GDM and 31 matched pregnancies without GDM were identified using the R package Limma (available online: http://www.bioconductor.org/). The criteria for DEGs considered included $|\log2(FC)| > 0.1$ and a p-value < 0.05. Subsequently, a heatmap of the obtained differential genes was constructed using the pheatmap package (version 1.0.8, https://cran.r-project.org/web/packages/pheatmap).

2.5 Functional enrichment analysis

The Kyoto Encyclopedia of Genes and Genomes (KEGG) pathway and Gene Ontology (GO) analyses were used to investigate underlying potential mechanisms; the GO analysis consisted of biological process (BP), cellular component (CC),

and molecular function (MF). This analysis was performed using the R package ClusterProfiler. In this study, GO and KEGG pathway enrichment analyses were performed for the DEGs obtained. False discovery rate (FDR) <0.05 was identified as the threshold for enrichment analysis.

2.6 Weighted gene co-expression network analysis

A weighted gene co-expression network was constructed to explore the correlation with ferroptosis. The co-expression similarity network was composed of the GSE70493 mRNA expression profile and 253 ferroptosis-related regulators, using the R package WGCNA. The soft thresholding was set at seven. A matrix of weighted adjacency was created using the formula amn = |cmn|β (amn: adjacency between gene m and gene n; cmn: Pearson's correlation; β: soft-power threshold). Subsequently, the clinical trait data were loaded, and scale independence and mean connectivity were estimated. Additionally, the topological overlap measure (TOM) matrix, transformed by the adjacency matrix, was used to estimate the connectivity property in the network. A hierarchical clustering dendrogram of the TOM matrix was constructed using the average distance with a minimum size threshold of 30 to classify similar gene expression profiles into different gene modules. Different module eigengenes (MEs) and clinical traits were then correlated. The gene significance (GS) quantifying the associations of individual genes with the clinically interesting trait and module membership (MM), which acted as the correlation between the MEs and the gene expression profiles, were calculated. As previously reported, if GS and MM were highly correlated, the most important (central) elements in the modules were also tightly associated with the trait. As such, they can be used to construct the PPI network with the use of Cytoscape software to identify hub genes.

2.7 Molecular docking and molecular dynamics analysis

To evaluate whether Wheat-flavored Rehmannia decoction, Astragalus Sijunzi decoction, Radix Astragali and Radix Ophiopogonis decoction, and Shenqi Dihuang decoction tonics can bind to the ferroptosis-related genes and play a therapeutic role, molecular docking of key active ingredients with key targets was performed, and the binding energies were evaluated as evaluation indices. Given the complexity of the active ingredients of herbal medicines, we screened all active ingredients based on multiple commonly used herbal ingredients (https://old.tcmsp-e.com/index.php; http://www.tcmip.cn/TCMIP/index.php/Home/; http://119.3.41.228:8000/tcmid/herb/1138/).The molecular structures of the akey active ingredients of all Chinese medicine components involved in the four tonics were downloaded from the PubChem database (https://pubchem.ncbi.nlm.nih.gov/), along with a total of 218 ingredients. After format conversion using Open Babel, AutoDockTools 1.5.7 was used to process the ligands and receptors. Core target protein structures were downloaded from the protein database (PDB; http://www.rcsb.org/pdb/home/home.do). We used PyMol software to remove water molecules and residues from the receptor proteins, followed by the addition of nonpolar hydrogens to generate coordinate files using AutoDockTools 1.5.7. Protein-binding pockets were predicted using DoGSiteScorer (https://proteins.plus/). Using the key target as the receptor and the corresponding key active ingredient as the ligand, AutoDockTools was used to set the docking box center and the box grid parameters, including the active pocket sites where the small molecule ligand might bind. Molecular docking was performed using AutoDock Vina 1.1.2, maintaining the top 10 ligands with the lowest binding free energy. The lowest energy conformation was selected as the best binding conformation, and the protein-ligand forces were mapped in two dimensions using Poseview. The binding sites, interaction forces between amino acid residues, and binding pocket surfaces were analyzed in three dimensions using PyMOL. The molecular structures of 218 active ingredients were obtained by docking, and the best-scoring-complex conformation was applied for mapping using PyMOL.

Based on the results of molecular docking, molecular dynamic simulations of the obtained protein-ligand complexes were performed using GROMACS 5.0 software (http://www.gromacs.org/); GROMOS was used to generate input files, where the topology files of the small-molecule ligands were generated using the ATB website (http://atb.uq.edu.au/index.py). All simulations were performed using periodic boundaries, and all were placed in a dodecahedral cell box (with a 1 nm edge distance). The simple point charge solvent model was initially added as a water model, and five chloride ions were added to the solventized system to maintain the electrical neutrality. The simulations were performed using a periodic boundary approach with 1,000 steps of energy minimization at 300 K for the protein and small-molecule ligand complexes, followed by 100 ps canonical ensemble (NVT) systemic equilibrium and 100 ps of isothermal–isobaric (NPT) systemic equilibrium for the optimized system, in which the system positions were constrained. Finally, the entire system was maintained at 300 K for 20 ns of kinetic simulations, where the time interval was 2 fs, and the coordinate trace files were saved every 10 ps. The post-simulation analysis included structure comparison (alignment), calculation of root mean square deviation (RMSD), hydrogen bonding (H-bond), solvent accessible surface area (SASA), temperature, total energy, and radius of gyration (Rg). The RMSD was used as an evaluation index of the stability of the complexes; the smaller the average RMSD, the more stable the bonding.

2.8 Statistical analysis

All analyses were performed using R software (version 3.6.1, www.r-project.org). All statistical tests were two-sided, and statistical significance was set at $p < 0.05$. Group comparisons were performed using the independent t-test for normally distributed variables and the Mann–Whitney U test for variables showing an abnormal distribution. The statistical methods and algorithms used were described in the corresponding steps.

3 Results

3.1 Validation of ferroptosis in patients with GDM

Retrospective analysis of ferritin levels measured in early and mid-pregnancy between the GDM and healthy groups (Figure 2A) demonstrated that serum ferritin levels in early pregnancy were positively associated with the risk of GDM and serum ferritin levels in mid-pregnancy were significantly higher in pregnant women with GDM than in non-GDM women ($p < 0.05$). Thus, our results are consistent with the findings of previous studies indicating that high ferritin levels are an important factor in GDM development. To further investigate whether ferroptosis was activated during GDM, western blotting to detect the levels of protein associated with ferroptosis and electron microscopic observation of changes in intracellular mitochondria were performed. As depicted in Figure 2B, western blotting indicated reduced levels of GPx4 ($p < 0.01$), SLC7A11 ($p < 0.01$), and FPN1 ($p < 0.01$) in placental tissues of patients with GDM compared with healthy controls. Mitochondrial morphology was observed using electron microscopy: mitochondria were swollen, and mitochondrial cristae were reduced or absent (Figure 2C). Overall, this evidence suggests that iron death is activated during GDM.

3.2 Identification of DEGs in GDM

In this study, DEGs and their significant biological characteristics were identified based on GEO mRNA microarray datasets (GSE70493); there were 32 GDM cases and 31 matched pregnancies, without maternal complications. Following gene expression assays, data processing, and normalization, DEGs were screened among each mRNA dataset using the Limma R package with the criteria of $|\log2(FC)| > 0.1$ and a p-value <0.05. The volcano plot contained each of the DEGs in the dataset, and 172 upregulated and 324 downregulated genes were identified (Figure 3A). The DEGs are listed in Supplementary Table 2.

A heatmap was compiled for the top 20 genes with the most significant differential expression from the 63 samples. Cluster analysis suggested that these DEG expression profiles were able to distinctly distinguish GDM from non-GDM samples (Figure 3B).

Subsequently, functional enrichment analysis was performed to identify the signaling pathways differentially affected by GDM using the ClusterProfiler package. The DEGs between the GDM group and the normal group were chiefly enriched in "oxidative phosphorylation" pathways, "thermogenesis" pathways, and "non-alcoholic fatty liver" disease pathways as determined using KEGG analysis, while the group without GDM was highly associated with "allograft rejection" pathways, and "graft-versus-host disease" pathways (Figure 3C). The GO analysis of the DEGs demonstrated that the differential genes were primarily enriched in the "lymphocyte-mediated immune" pathway, "adaptive immune response based on somatic" pathway, and "recombination of immune receptors built from immunoglobulin superfamily domains" pathway in BP (Figure 3D). In terms of cellular components, the DEGs were primarily enriched in the immunoglobulin complex, external side of plasma membrane, and circulating immunoglobulin complex (Figure 3E); with respect to MF, the DEGs were primarily enriched in antigen binding, immunoglobulin receptor binding, and peptide binding (Figure 3F).

A

Variables	GDM group	Healthy group	*p*-value
Ferritin（ng/ml）during the first trimester	39.6（25.1-64.4）	32.6（18.9-55.5）	0. 087
Ferritin（ng/ml）during the second trimester	14.95（9.6-26.8）	13.35（8.8-20.9）	0. 001

GDM：Gestational diabetes mellitus；

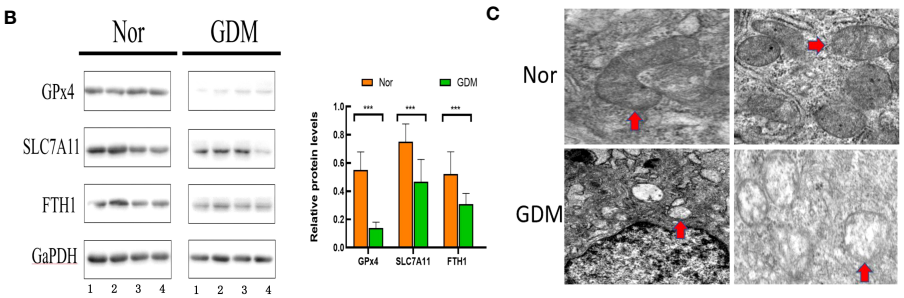


FIGURE 2
Evaluation of ferroptosis in GDM patients. **(A)** ferritin in early and mid-pregnancy between the GDM group and non-GDM group. **(B)** Levels of proteins associated with ferroptosis were assessed using western blot between the GDM group (n = 10) and non-GDM group (n = 10). **(C)** Mitochondrial morphology was observed under electron microscopy between the GDM group and non-GDM group(Red arrows point to changes in mitochondria. Mitochondria in GDM placental tissue conform to ferroptosis changes, with reduced or disappeared mitochondrial cristae and rupture of mitochondrial outer membrane; Mitochondria in normal placental tissue are normal). ***p<0.001.

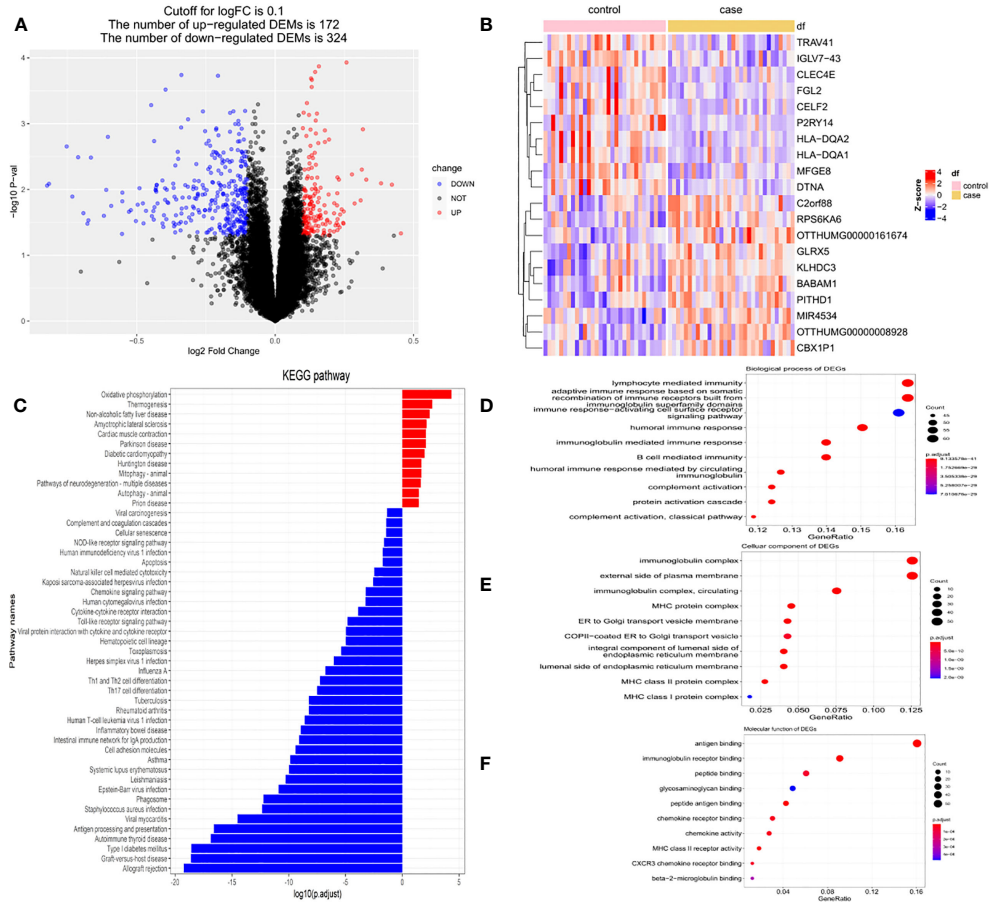


FIGURE 3
The DEGs based on GEO mRNA microarray datasets (GSE70493). **(A)** The volcano plot of DEGs in GSE70493. **(B)**The heatmap of top 200 DEGs in GSE70493. **(C)** KEGG enrichment analysis. **(D)** GO enrichment analysis of biological process. **(E)** GO enrichment analysis of cellular component. **(F)** GO enrichment analysis of molecular function.

3.3 Genes co-expressed with ferroptosis-related genes via WGCNA

To determine whether ferroptosis affects GDM, 253 ferroptosis-related regulators from FerrDb were collected and a co-expression network based on the ferroptosis signature genes and average expression values of 496 differential genes was constructed (Supplementary Table 3). Differences in the expression of ferroptosis signature genes between the two groups was compared. The ferroptosis signature expression was greater in the GDM group than in the non-GDM group (Figure 4A). Then, using 10 as a soft threshold (Figures 4B, C), a co-expression network with six modules using DEGs in the GDM group was constructed with the WGCNA package (Figure 4D). The clustering results between modules demonstrated that the blue module, which contained 99 genes, showed the highest correlation with ferroptosis-related genes (Figure 4E; r = 0.72, P = 6e-06), and genes from this module were selected as ferroptosis co-expression genes.

The correlation between DEGs and the members in the blue module, as well as that between the genes and ferroptosis was analyzed individually; additionally, the two variables were plotted as abscissa and ordinate, and the result was positively correlated. The blue modules were again highly correlated with ferroptosis (Figure 4F).

A PPI network was then constructed to explore the hub genes (Figure 4G). Notably, COX7A2, NDUFA6, UQCR10, UXT, SELT, SF3B14, BABAM1, SUPT4H1, and SCARNA12 were revealed as the top 10 hub genes according to the decreasing order of "Vlength" (illustrated in Supplementary Table 4).

3.4 Identification of potential ferroptosis-related hub gene drug targets

Based on the top 10 hub genes obtained, the proteins corresponding to SF3B14 and BABAM1 were determined to be potential drug targets in terms of protein structure and function. The core target protein structures were downloaded from the PBD protein database (http://www.rcsb.org/pdb/home/home.do). Based on the source of the structure, complexity of the structure, influencing factorsand, We finally chose BABAM1_6H3C and SF3B14_2F9D. Two protein structures were docked with each of the 218 Chinese herbal ingredients in the four tonics. AutoDock evaluated the energy match between the receptor and ligand based

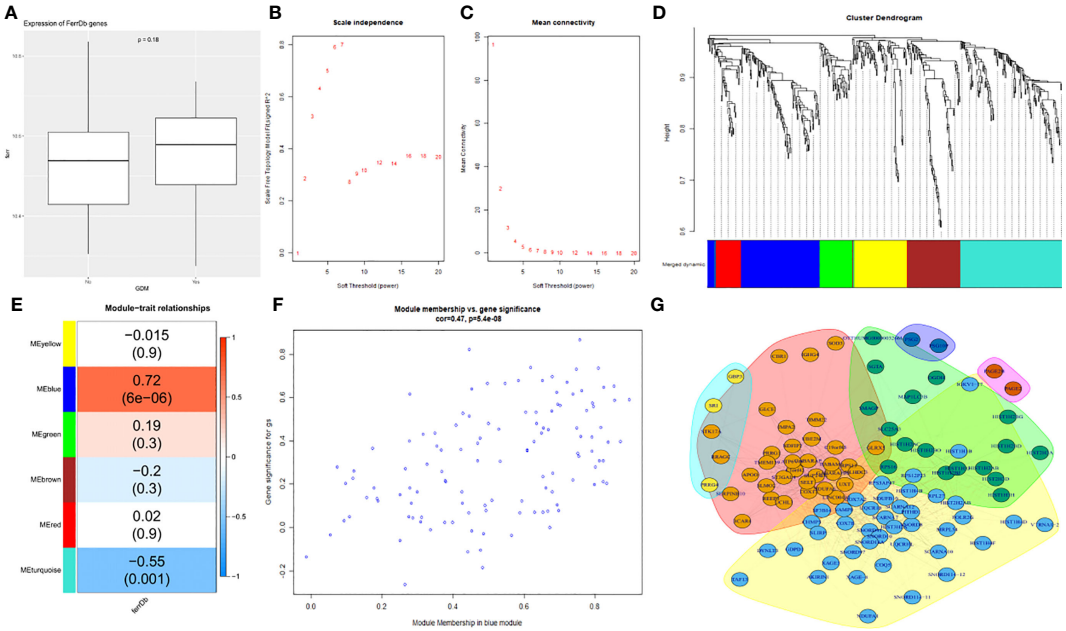


FIGURE 4
Screening of key ferroptosis-related genes using WGCNA and PPI network. **(A)** The differences in expression of ferroptosis signature genes between the two groups. **(B)** The correlation between various soft-thresholding power and scale-free topology model fit index. **(C)** The correlation between various soft-thresholding power and mean connectivity (degree). **(D)**The dendrogram clustered using topological overlap based on ferroptosis signature genes and mean mRNA expression of DEGs. **(E)** The correlation among different modules and traits. **(F)** The analysis of bule module genes and GDM. **(G)** PPI network.

on a semi-empirical free energy calculation method; the smaller the value, the greater the affinity between the ligand and receptor (20). Molecular docking of protein SF3B14_2F9D with 218 herbal components and the top 10 best results for binding free energy are listed in Table 1. The top 10 binding free energy produced negative results for 218 docking experiments, and the binding energy of the best top 3 docking results were -9.6, -9.4, and -9.3 kcal/mol, indicating that protein SF3B14_2F9D had good binding effects with glucopyranoside, epifriedrine, and pyrantel bases. Molecular docking of BABAM1_6H3C with 218 herbal components was then performed, and the top 10 best results for the binding free energy are listed in Table 2. The top 10 binding free energy results were negative among the 218 docking experimental results, and the binding energy of the best top 3 docking results were -8.2, -8, and -7.9 kcal/mol, indicating that protein BABAM1 had good binding effect with *Coptis chinensis*, Nanwuji, and Zedoary.

TABLE 1 The TOP10 docking binding energy between 218 herbal components and the active site of the protein target (SF3B14_2F9D).

Chinese Medicine	Chemical Composition	Ingredients	PubChem ID	Affinity (kcal/mol)
Poria cocos	Glucopyranose	1-O-(3-Carboxy-5,6-dihydroxyphenyl)-6-O-galloyl-beta-D-glucopyranose.	11972353	-9.6
Chasteberry	Epiberberine; Epiflorine	epiberberine	160876	-9.4
Huang Lian	Phellodendrine	coptisine	72322	-9.3
Radix Codonopsis	Chrysoprase	Chrysanthemaxanthin	21160900	-9.3
Fructus Schisandrae	Neonanwort B	neokadsuranic acid B	145709631	-9.2
Yam	Phellodendrin	Doradexanthin	16061189	-9.1
Huanglian	Pawpaw rhubarb dianthrone	Palmidin A	5320384	-9
Cornus officinalis	N	galloyl(-3)[galloyl(-6)]a-All	6398541	-9
Yellow Essence	Diosgenin	diosgenin	99474	-9
Coptis Chinensis	Phellodendron	Obacunone	119041	-9

N, none.

Combining drug efficacy and drug binding efficacy, we determined that *Coptis Chinensis* demonstrated the optimal binding energy.

3.5 Molecular docking and molecular dynamics simulation of targeted drugs

We further validated the stability and biological activity of SF3B14_2F9D with coptisine, a component of *Coptis Chinensis*, BABAM1_6H3C, and berberine, a component of *Coptis Chinensis*. Initially, SF3B14_2F9D was docked with coptisine to form more hydrophobic interactions and predict the location of the protein binding pocket as depicted in Figure 5A, followed by the establishment of the binding surface map (Figure 5B), two-dimensional spatial model (Figure 5C) and three-dimensional spatial model (Figure 5D). As illustrated in the figure, coptisine bound to SF3B14_2F9D in the predicted binding pocket. The molecular dynamics of SF3B14_2F9D with coptisine were then further simulated. In the 20 ns molecular dynamics simulation, the protein SF3B14_2F9D reached the equilibrium state at 0.45 nm, and coptisine reached the equilibrium state (tuA) at 0.075 nm based on RMSD over time (Figure 5E). Molecular dynamic simulations of the equilibrium trajectories were used for further analysis; SF3B14_2F9D and coptisine were able to form 725 hydrogen bonds (Figure 5F). Combining the radius of gyration (Figure 5G), SASA (Figure 5H), temperature (Figure 5I), and total energy (Figure 5J) between SF3B14_2F9D and coptisine, the results suggest that SF3B14_2F9D can stably bind to coptisine and exert potential biological activity.

As with the process above, protein BABAM1_6H3C was again docked with berberine to form more hydrophobic interactions, predict the location of the protein binding pocket as illustrated in Figure 6A, and establish the binding surface map (Figure 6B), two-dimensional spatial model (Figure 6C) and three-dimensional spatial model (Figure 6D). As depicted in the figure, berberine was able to bind to BABAM1_6H3C in the predicted binding pocket. Subsequently, molecular dynamic simulations of BABAM1_6H3C with berberine were performed. In the 20 ns molecular dynamic simulation, protein BABAM1 reached equilibrium at 0.4 nm, and berberine reached equilibrium at 0.075 nm based on RMSD over time (Figure 6E). Subsequently, BABAM1_6H3C and berberine formed 725 hydrogen bonds (Figure 6F). Combining the radius of gyration (Figure 6G), solvent-accessible surface area (Figure 6H), temperature (Figure 6I), and total energy (Figure 6J), the results suggest that BABAM1_6H3C can be stably bound to berberine and exert potential biological activity.

4 Discussion

One of the most common complications of pregnancy worldwide is GDM, and it causes many long-term maternal and neonatal complications affecting 2%–22% of all pregnancies (21). Adverse consequences of GDM for both mother and fetus can lead to damage or functional disorders in various organs of the pregnant woman and are associated with adverse fetal outcomes such as macrosomia, pre-eclampsia, obstructed shoulder birth, stillbirth, neonatal hyperbilirubinemia, neonatal hypoglycemia, and respiratory distress (22, 23). Patients with GDM and newborns with GDM are at increased risk of obesity, type 2 diabetes, and other metabolic diseases in the long term (24). Despite tremendous progress in its treatment, GDM still has adverse effects on the long-term health of both the mother and her offspring. The pathogenesis of GDM is influenced by multiple factors, among which epigenetic alterations are important mechanisms affecting the development of GDM. The placenta serves as an important connecting organ that maintains normal fetal growth and development, providing nutrition, oxygen, and other essential factors to the fetus. The placenta maintains a normal pregnancy by selectively regulating and transporting nutrients and vital ions. A common complication of pregnancy is GDM and various studies have demonstrated a correlation between impaired iron homeostasis and GDM (13, 25). Studies have reported that

TABLE 2 The TOP10 docking binding energy between 218 herbal components and the active site of the protein target (BABAM1_6H3C).

Chinese Medicine	Chemical Composition	ingredients	PubChem ID	Affinity (kcal/mol)
Coptis Chinensis	Phellodendron	Obacunone	119041	-8.2
Southern Schisandra	Schisandrin acid	schizandronic	101277401	-8
Zedoary	Xanthohumol C	alisol C	46173914	-7.9
Huanglian	Phellodendrine; Berberine	coptisine	72322	-7.8
Southern Schisandra	Neo-South schisanic acid	neokadsuranic acid B	145709631	-7.8
Mai Dong	Hydroxymethyl maidenhair flavonoid A	Hydroxymethylophiopogonone A	101238141	-7.7
Mai Dong	Macroisoflavone A	Ophiopogonone A	10087732	-7.5
Yam	Schisandrin; Dihydroquercetin; Flavopiridol; Yewaxanthin;	taxifolin	712316	-7.5
Mai Dong	Maidenhair Flavonoid A	Ophiopogonanone A	92449512	-7.5
Chasteberry	Pinusolitrin; Dihydroquercetin; Flavopiridol; Yewcitrin;	taxifolin	439533	-7.4

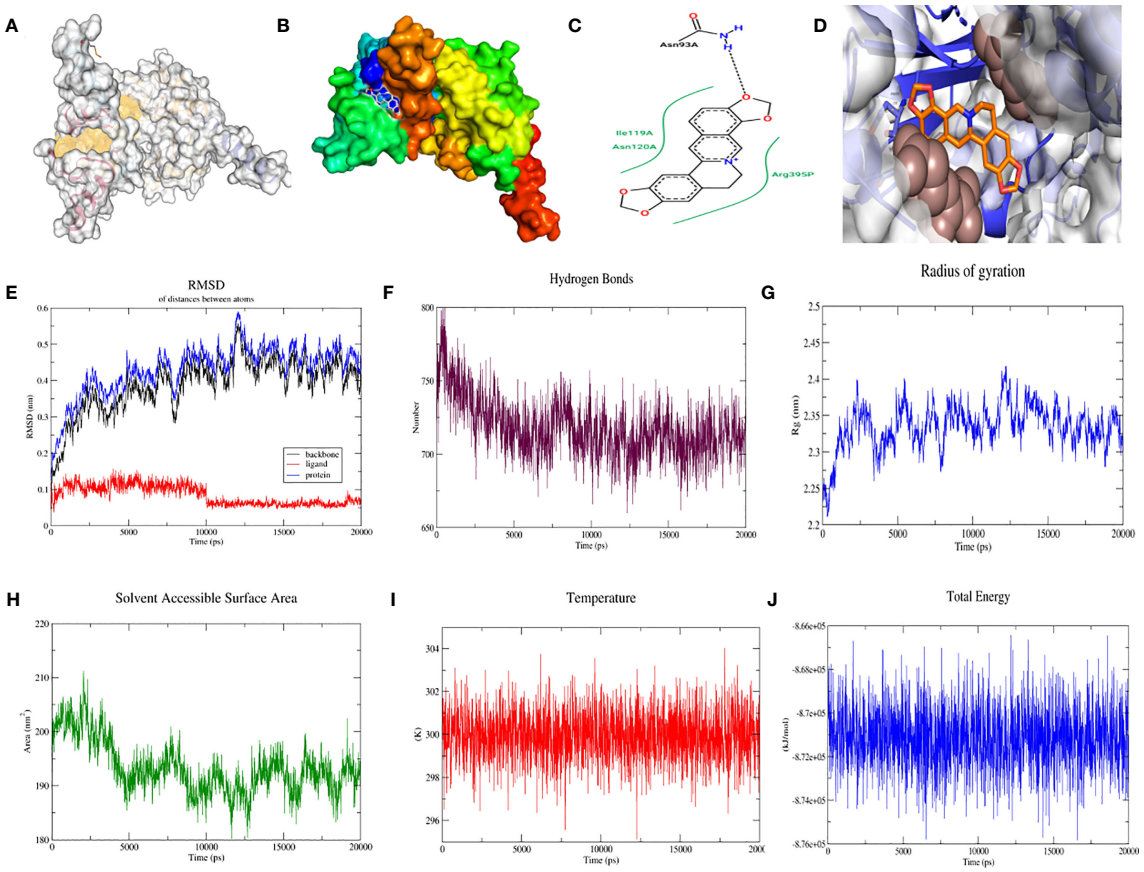


FIGURE 5
Molecular docking and molecular dynamics simulation of SF3B14_2F9D with coptisine. **(A)** Location of the predicted binding pocket of SF3B14_2F9D; **(B)** Surface map of the docking result of SF3B14_2F9D with coptisine; **(C)** Two-dimensional structure of the docking result of SF3B14_2F9D with coptisine; **(D)** Three-dimensional structure of the docking result of SF3B14_2F9D with coptisine; **(E)** RMSD between SF3B14_2F9D and coptisine using molecular dynamics simulation; **(F)** Hydrogen bonding network between SF3B14_2F9D and coptisine using molecular dynamics simulation **(G)** Gyration radius between SF3B14_2F9D and coptisine using molecular dynamics simulation; **(H)** Solvent accessible surface area between SF3B14_2F9D and coptisine using molecular dynamics simulation; **(I)** Temperature between SF3B14_2F9D and coptisine using molecular dynamics simulation; **(J)** Total energy between SF3B14_2F9D and coptisine using molecular dynamics simulation;.

ferroptosis may play a central role in major placenta-related obstetric disorders (26). The results of a meta-analysis that included 10 studies showed that the risk of GDM increased with increasing ferritin (27). Higher levels of ferritin in mid-trimester are significantly associated with risk of GDM and adverse pregnancy outcomes associated with GDM (28). Ferroptosis has been reported to impair islet cell viability and function; ferroptosis inhibitors can reverse this damage (29). Hyperglycemia reportedly leads to impaired iron transport and increased lipid peroxidation. However, treatment with the antioxidant sodium selenite (NaSe) altered the expression of iron homeostasis genes, suggesting that hyperglycemia is involved in the induction of ferroptosis (14). These features suggest that ferroptosis is closely related to the development of GDM. We hypothesized that dysregulation of iron homeostasis genes in placental tissues and ferroptosis are likely potential mechanisms for the development of GDM. The aim of this study was to determine the correlation between GDM and ferroptosis through clinical studies, molecular biological data, and bioinformatics analysis, with the aim of identifying targets for the early treatment of GDM.

In this study, the correlation between GDM and serum ferritin levels was investigated, and increased iron levels inducing the development of ferroptosis in placental tissue and alteration of the protein expression of ferroptosis-related genes were subsequently verified. The results of the clinical correlation analysis demonstrated that serum ferritin levels were higher in patients with GDM than in patients without GDM in both early and mid-pregnancy, and there was a significant difference in mid-pregnancy serum ferritin levels between the two groups. Ferroptosis is characterized by the onset of mitochondrial dysfunction, primarily in the form of mitochondrial swelling, with a reduction in cristae and increased mitochondrial membrane permeability (30). We observed the mitochondrial ultrastructural changes in trophoblasts in the GDM and normal groups using electron microscopy. The mitochondria within trophoblast cells appeared significantly swollen and were accompanied by specific changes in the disappearance or reduction of cristae. Changes in the

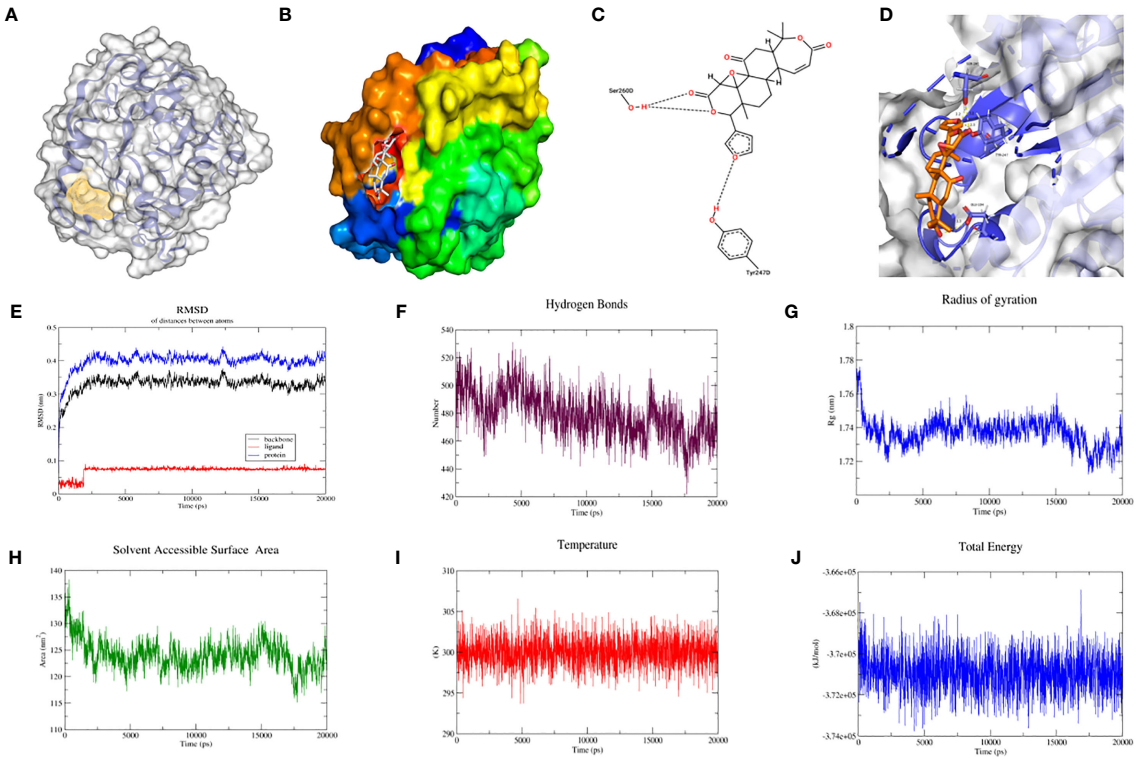


FIGURE 6
Molecular docking and molecular dynamics simulation of BABAM1_6H3C with berberine. **(A)** Location of the predicted binding pocket of BABAM1_6H3C; **(B)** Surface map of the docking result of BABAM1_6H3C with berberine; **(C)** Two-dimensional structure of the docking result of BABAM1_6H3C with berberine; **(D)** Three-dimensional structure of the docking result of BABAM1_6H3C with berberine; **(E)** RMSD between BABAM1_6H3C and berberine using molecular dynamics simulation; **(F)** Hydrogen bonding network between BABAM1_6H3C and berberine using molecular dynamics simulation **(G)** Gyration radius between BABAM1_6H3C and berberine using molecular dynamics simulation; **(H)** Solvent accessible surface area between BABAM1_6H3C and berberine using molecular dynamics simulation; **(I)** Temperature between BABAM1_6H3C and berberine using molecular dynamics simulation; **(J)** Total energy between BABAM1_6H3C and berberine using molecular dynamics simulation;.

expression of ferroptosis-related genes in placental tissues were subsequently measured. Western blotting demonstrated reduced expression of GPx4, SLC7A11, and FTH1 in placental tissues of patients in the GDM group. These results confirm the presence of elevated ferritin levels and occurrence of ferroptosis in placental tissues in patients with GDM. The alteration of expression of ferroptosis-related genes in placental tissues was then verified.

DEGs are generally recognized as an important feature of disease progression. The genes involved in the pathogenesis of GDM and associated with ferroptosis were examined; 172 upregulated and 324 downregulated genes were identified by analyzing the differential expression profiles of placental tissues from GDM and non-GDM samples. Clustering analysis was then performed; it was observed that these DEG profiles clearly distinguished between GDM and non-GDM samples. The differential expression of these genes provides a new direction for further exploration of the underlying molecular mechanisms involved in GDM. To reveal the potential functions of the DEGs, functional enrichment analysis was performed using GO analysis by database for annotation, visualization and integrated discovery and KEGG pathway analysis by gene set enrichment analysis. The functions of DEGs in three components, CC, MF, and BPs, were revealed using GO analysis. Following annotation of the genes themselves, the pathways involved in DEGs were explored using KEGG analysis; this revealed that the "oxidative phosphorylation" pathway was significantly activated in the GDM group. Under aerobic conditions, cells obtain energy mainly through oxidative phosphorylation, and during hypoxia, they undergo glycolysis (31). Mitochondria are an important source of ROS in human cells, and glycolysis is increased when mitochondrial metabolism is reduced. Increased mitochondrial ROS production reportedly promotes ferroptosis, and the application of mitochondria-targeted antioxidants or enzyme inhibitors can inhibit this process (32). The tricarboxylic acid cycle is an enzymatic pathway located in the mitochondrial matrix that transfers electrons to the mitochondrial electron transport chain through a series of redox reactions, resulting in the production of ATP through oxidative phosphorylation. Altered ATP/ADP ratios play a dual role in ferroptosis (32). Deficient oxidative phosphorylation may lead to iron sagging. These findings suggest that the "oxidative phosphorylation" pathway, which is significantly activated by differential genes, is closely related to the occurrence of ferroptosis in GDM. Placental development requires a unique oxidative stress environment, and when an imbalance of oxidative stress occurs in the placenta, lipid metabolism in placental tissues is disrupted, which can promote the onset of ferroptosis. Within the last several years, studies have described the interrelationship between maternal iron status, placental lipid metabolism,

hyperglycemia and oxidative stress, which may be attributed to the effects or outcomes of ferroptosis. It has been found that synergistic mechanism of obesity before and during pregnancy increases inflammation and lipid peroxidation in trophoblasts which triggers a ferroptotic impairment of pancreatic islet function, resulting in GDM. High glucose conditions, reduced glutathione levels, impaired iron transport, and increased lipid peroxidation in trophoblast cells suggest that hyperglycemia causes ferroptosis. Iron accumulation may lead to increased lipid peroxidation and intracellularly generated protein carbonation, which in turn causes ferroptosis. The synergistic relationship between hyperglycemia and altered placental iron homeostasis during pregnancy was suggested as the mechanistic basis for ferroptosis (33). Although several clinical studies have reported a correlation between GDM and elevated maternal iron plasma levels, however, the associated pathophysiologic links and their underlying mechanisms are unclear. The fact that current studies on ferroptosis macrosomia have only scratched the surface of the phenomenon and its outcome remains a challenge for precision medicine, with detailed roles for iron prolapse in the onset and progression of GDM needing in-depth study.

Gene association patterns described by WGCNA explore the relationship between phenotypic data and gene modules based on the endogeneity of gene sets and identify the hub genes in the modules. The PPI network was then used to filter out genes that played a key role in this process. The expression of ferroptosis genes in both groups was analyzed, and the results confirmed the ferroptosis signature expression was greater in the GDM group than in the non-GDM group, and the changes were not statistically significant. Subsequently, WGCNA was applied to rapidly identify GCMs with the highest correlation with ferroptosis characteristics. The clustering results of the six modules constructed demonstrated that the blue module containing 99 genes was included in the PPI network to determine the pivotal genes due to the highest correlation with ferroptosis-related genes. Finally, 10 hub genes were identified. Based on the top 10 hub genes obtained, the use of the proteins corresponding to SF3B14 and BABAM1 as drug targets in terms of protein structure and function was determined. Homo sapiens splicing factor 3b subunit 14(SF3B14), also named SF3B6, encodes a 14 kDa protein subunit of the splicing factor 3b complex. This protein interacts directly with the adenosine that carries out the first transesterification step of splicing at the pre-mRNA branch site. It is well known that splicing of pre-mRNA is a critical step in gene expression and is accomplished by the spliceosome. The spliceosome specifically recognizes pre-mRNA, where U1 snRNP recognizes 5′-SS, U2 snRNP recognizes intronic Branch Site (BS). SF3B6 is involved in mRNA processing and RNA metabolism (34)。 Sf3b6 stabilizes the BS:U2 snRNA duplex, contributing to the recognition of intronic (35). In addition, it has been found that functional knockdown of SF3B14 results in normal mulberry development but failure to form a blastocyst cavity or morphologically differentiated trophoblast ectoderm, which correlates with subsequent placentation (36). Previous studies have found that LUC7L2 is involved in coding for snRNP to affect pre-mRNA splicing and gene expression. The largest differential gene in the splicing analysis after knockdown of LUC7L2 is SLC7A11, which is required for SLC7A11 (xCT) splicing. LUC7L2 deletion leads to a reduction in SLC7A11 (xCT) and controls glycogen and glutamate metabolism (37), and promotes ferroptosis (25). It is reasonable to speculate that SF3B14, which is involved in pre-mRNA splicing, may contribute to ferroptosis by affecting the expression of key proteins for ferroptosis, which deserves to be further investigated in the future. BRISC and BRCA1 A complex member 1(BABAM1), locates in cytosol and nuclear body and involved in several processes, including mitotic G2 DNA damage checkpoint signaling; protein K63-linked deubiquitination; and positive regulation of DNA repair. Previous studies found that BABAM1 is regulated by mTORC2 to initiate DNA damage response, which can lead to ferroptosis (38). In addition, the kinase complex mTORC2 was found to prevent ferroptosis (39). Further studies can be conducted in the future both *in vivo* and *in vitro*.

We further verified the differential expression of SF3B14 and BABAM1 in women with GDM and normal pregnancy based on the GSE70493 dataset. SF3B14 and BABAM1 were significantly elevated in GDM (Supplementary Figure 1). With the rapid development of high-throughput analyses, molecular level targeting therapy has become a major trend in drug development. Molecular docking and molecular dynamic techniques can provide insights into the interactions between molecules and explain the mechanisms of interactions in a visual manner, which have now become important research methods for elucidating biological mechanisms. Additionally, molecular docking and molecular dynamic techniques provide important tools for predicting the binding types and interaction patterns of biomolecular complexes. The mechanisms of action and molecular targets of Wheat-flavored Rehmannia decoction, Astragalus Sijunzi decoction, Radix Astragali and Radix Ophiopogonis decoction, and Shenqi Dihuang decoction for the treatment of GDM are currently largely unknown. To assess whether these traditional Chinese medicines can bind to ferroptosis-related gene loci for preventive and therapeutic effects, the central gene expression proteins were combined as receptors for the downloaded molecular structures of 218 herbal ingredients involved in the four tonics. *Coptis Chinensis* has optimal binding energy when the drug efficacy and drug binding efficacy are combined. Further molecular dynamic simulations demonstrated that SF3B14_2F9D could stably bind and exert potential bioactivity with coptisine, a component of *Coptis Chinensis*, and BABAM1_6H3C could stably bind and exert potential bioactivity with berberine, another component of *Coptis Chinensis*. This result indicates that at the molecular level, *Coptis Chinensis* can bind better to these target proteins, providing a theoretical basis for the treatment of GDM with *Coptis Chinensis*.

There are certain limitations to this study. First, no clear indicator of iron overload was identified, and the ferritin detected in the study was subjected to multiple factors. In addition, Since the retrospective study, pregnant women in the first trimester were mostly examined in the community hospital, so the amount of data and the population was limited. The first trimester and second trimester samples didn't collected from the same patients. Also, women were all in a pool not differentiating whether they were with pre-pregnancy normal weight, overweight or obese and weight gain

during pregnancy due to data limitations. There is some bias in the data, and thus more prospective studies on ferritin and multiple iron-related indicators which need to take into account the pre-pregnancy weight and metabolic condition are needed for more extensive validation. Next, there was limited data available on public databases to screen for relevant genes that met the inclusion criteria; therefore, further validation on a larger scale is anticipated. Only electron microscopy and iron death-related protein alterations were used to verify the occurrence of ferroptosis in GDM placental tissues; hence, further studies are needed to verify the relevance of ferroptosis in the development of GDM. In addition, we selected the optimal PDB IDs and the full selection of active ingredients of herbal tonics currently available on the website for analysis in this article because of technical limitations. Finally, this study lacks validation of SF3B14 and BABAM1 in placental tissues, and related study whether the compound can regulate the expression of ferroptosis related gene. Thus, the genes, proteins, and regulatory mechanisms associated with ferroptosis require further validation.

In conclusion, we verified the elevation of serum ferritin in patients with GDM from a clinical perspective, confirmed the occurrence of ferroptosis in placental tissues in patients with GDM, and proposed an important role of ferroptosis in the pathogenesis of GDM. Next, based on a comprehensive bioinformatics analysis, we screened ferroptosis-related genes with clinical value in GDM, among which SF3B14 and BABAM1 were key genes involved in ferroptosis in the pathogenesis of GDM. Finally, based on the screened proteins corresponding to SF3B14 and BABAM1, we performed molecular docking and molecular dynamic simulations with small molecules that can be bound in clinically proven effective traditional Chinese medicine tonics and proposed the mechanism of action of *Coptis Chinensis* for the treatment of GDM at the molecular level. Thus, our findings provide a theoretical basis for the future clinical application of *Coptis Chinensis*. We have combined a variety of methods to reveal the active ingredients in herbal formulas, and the results might provide new directions for the systematic optimization of TCM formulas for the management and targeted treatment of GDM.

Data availability statement

The datasets presented in this study can be found in online repositories. The names of the repository/repositories and accession number(s) can be found in the article/Supplementary Material.

Ethics statement

The studies involving humans were approved by Ethics Committee of Shengjing Hospital, China Medical University. The studies were conducted in accordance with the local legislation and institutional requirements. The participants provided their written informed consent to participate in this study. Ethical approval was not required for the studies on animals in accordance with the local legislation and institutional requirements because only commercially available established cell lines were used.

Author contributions

YuW conceived the study and critically revised the content of this manuscript. YZ, QG, and BL made significant contributions to the study methods, results, and interpretation. YaW was responsible for collecting the patients' information. QG has done a lot of work on the addition of experiments and the addition of bioinformatics section. All authors contributed to the article and approved the submitted version.

Funding

This work was supported by grants from the Science and Technology Projects of Liaoning Province (2021JH2/10300093).

Conflict of interest

The authors declare that the research was conducted in the absence of any commercial or financial relationships that could be construed as a potential conflict of interest.

Publisher's note

All claims expressed in this article are solely those of the authors and do not necessarily represent those of their affiliated organizations, or those of the publisher, the editors and the reviewers. Any product that may be evaluated in this article, or claim that may be made by its manufacturer, is not guaranteed or endorsed by the publisher.

Supplementary material

The Supplementary Material for this article can be found online at: https://www.frontiersin.org/articles/10.3389/fendo.2023.1177547/full#supplementary-material

References

1. Johns EC, Denison FC, Norman JE, Reynolds RM. Gestational diabetes mellitus: Mechanisms, treatment, and complications. *Trends Endocrinol Metab* (2018) 29:743–54. doi: 10.1016/j.tem.2018.09.004

2. McIntyre HD, Catalano P, Zhang C, Desoye G, Mathiesen ER, Damm P. Gestational diabetes mellitus. *Nat Rev Dis Primers* (2019) 5:47. doi: 10.1038/s41572-019-0098-8

3. Ballesteros M, Gil-Lluís P, Ejarque M, Diaz-Perdigones C, Martinez-Guasch L, Fernández-Veledo S, et al. DNA methylation in gestational diabetes and its predictive value for postpartum glucose disturbances. *J Clin Endocrinol Metab* (2022) 107 (10):2748–57. doi: 10.1210/clinem/dgac462

4. Lowe WL Jr., Lowe LP, Kuang A, Catalano PM, Nodzenski M, Talbot O, et al. Maternal glucose levels during pregnancy and childhood adiposity in the Hyperglycemia and Adverse Pregnancy Outcome Follow-up Study. *Diabetologia* (2019) 62:598–610. doi: 10.1007/s00125-018-4809-6

5. Plows JF, Stanley JL, Baker PN, Reynolds CM, Vickers MH. The pathophysiology of gestational diabetes mellitus. *Int J Mol Sci* (2018) 19:3342. doi: 10.3390/ijms19113342

6. Modzelewski R, Stefanowicz-Rutkowska MM, Matuszewski W, Bandurska-Stankiewicz EM. Gestational diabetes mellitus-recent literature review. *J Clin Med* (2022) 11(19):5736. doi: 10.3390/jcm11195736

7. Oliveira MM, Andrade KFO, Lima GHS, Rocha TC. Metformin versus glyburide in treatment and control of gestational diabetes mellitus: A systematic review with meta-analysis. *Einstein* (2022) 20:eRW6155. doi: 10.31744/einstein_journal/2022RW6155

8. Fisher AL, Nemeth E. Iron homeostasis during pregnancy. *Am J Clin Nutr* (2017) 106:1567S–74S. doi: 10.3945/ajcn.117.155812

9. Peña-Rosas JP, De-Regil LM, Garcia-Casal MN, Dowswell T. Daily oral iron supplementation during pregnancy. *Cochrane Database Syst Rev* (2015) 2015(7): CD004736. doi: 10.1002/14651858.CD004736.pub5

10. Lao TT, Chan PL, Tam KF. Gestational diabetes mellitus in the last trimester - a feature of maternal iron excess? *Diabetes Med* (2001) 18(3):218–23. doi: 10.1046/j.1464-5491.2001.00453.x

11. Yang K, Yang Y, Pan B, Fu S, Cheng J, Liu J. Relationship between iron metabolism and gestational diabetes mellitus: A systemic review and meta analysis. *Asia Pac J Clin Nutr* (2022) 31(2):242–54. doi: 10.6133/apjcn.202206_31(2).0010

12. Petry CJ. Iron supplementation in pregnancy and risk of gestational diabetes: A narrative review. *Nutrients* (2022) 14(22):4791. doi: 10.3390/nu14224791

13. Kataria Y, Wu Y, Horskjær PH, Mandrup-Poulsen T, Ellervik C. Iron status and gestational diabetes-A meta-analysis. *Nutrients* (2018) 10(5):621. doi: 10.3390/nu10050621

14. Zaugg J, Melhem H, Huang X, Wegner M, Baumann M, Surbek D, et al. Gestational diabetes mellitus affects placental iron homeostasis: Mechanism and clinical implications. *FASEB J* (2020) 34(6):7311–29. doi: 10.1096/fj.201903054R

15. Zhang S, Xin W, Anderson GJ, Li R, Gao L, Chen S, et al. Double-edge sword roles of iron in driving energy production versus instigating ferroptosis. *Cell Death Dis* (2022) 13(1):40. doi: 10.1038/s41419-021-04490-1

16. Li J, Cao F, Yin HL, Huang ZJ, Lin ZT, Mao N, et al. Ferroptosis: past, present and future. *Cell Death Dis* (2020) 11:88. doi: 10.1038/s41419-020-2298-2

17. Bao L, Jin Y, Han J, Wang W, Qian L, Wu W. Berberine regulates GPX4 to inhibit ferroptosis of islet β Cells. *Planta Med* (2023) 89(3):254–61. doi: 10.1055/a-1939-7417

18. Zhao Q, Bai J, Chen Y, Liu X, Zhao S, Ling G, et al. An optimized herbal combination for the treatment of liver fibrosis: Hub genes, bioactive ingredients, and molecular mechanisms. *J Ethnopharmacol* (2022) 297:115567. doi: 10.1016/j.jep.2022.115567

19. Zhou N, Bao J. FerrDb: a manually curated resource for regulators and markers of ferroptosis and ferroptosis-disease associations. *Database (Oxford)* (2020) 2020: baaa021. doi: 10.1093/database/baaa021

20. Wang Y, Li B, Zhao Y. Inflammation in preeclampsia: genetic biomarkers, mechanisms, and therapeutic strategies. *Front Immunol* (2022) 13:883404. doi: 10.3389/fimmu.2022.883404

21. Liwei C, Rachel M, Adaire C, Gang H. Gestational diabetes mellitus: its epidemiology and implication beyond pregnancy. *Curr Epidemiol Rep* (2016) 3:11. doi: 10.1007/s40471-016-0063-y

22. Farrar D. Hyperglycemia in pregnancy: prevalence, impact, and management challenges. *Int J Womens Health* (2016) 8:519–27. doi: 10.2147/IJWH.S102117

23. Mashayekh-Amiri S, Mohammad-Alizadeh-Charandabi S, Abdolalipour S, Mirghafourvand M. Myo-inositol supplementation for prevention of gestational diabetes mellitus in overweight and obese pregnant women: a systematic review and meta-analysis. *Diabetol Metab Syndr* (2022) 14(1):93. doi: 10.1186/s13098-022-00862-5

24. Caissutti C, Berghella V. Scientific evidence for different options for gdm screening and management. *BioMed Res Int* (2017) 2017:2746471. doi: 10.1155/2017/2746471

25. Zhang W, Sun Yu, Bai Lu, Zhi L, Yang Y, Zhao Q, et al. RBMS1 regulates lung cancer ferroptosis through translational control of SLC7A11. *J Clin Invest* (2021) 131 (22):e152067. doi: 10.1172/JCI152067

26. Beharier O, Kajiwara K, Sadovsky Y. Ferroptosis, trophoblast lipotoxic damage, and adverse pregnancy outcome. *Placenta* (2021) 108:32–8. doi: 10.1016/j.placenta.2021.03.007

27. Sun C, Wu QJ, Gao SY, Ma ZM, Liu YS, Zhang JY, et al. Association between the ferritin level and risk of gestational diabetes mellitus: A meta-analysis of observational studies. *J Diabetes Investig* (2020) 11(3):707–18. doi: 10.1111/jdi.13170

28. Fan X, Wang L, Jiao R, Song W, Liu Y, Yu T. Correlation between high serum ferritin levels and adverse pregnancy outcomes in women with gestational diabetes mellitus. *Heliyon* (2023) 9(3):e14285. doi: 10.1016/j.heliyon.2023.e14285

29. Bruni A, Pepper AR, Pawlick RL, Gala-Lopez B, Gamble AF, Kin T, et al. Ferroptosis-inducing agents compromise in vitro human islet viability and function. *Cell Death Dis* (2018) 9(6):595. doi: 10.1038/s41419-018-0506-0

30. Dixon SJ, Lemberg KM, Lamprecht MR, Skouta R, Zaitsev EM, Gleason CE, et al. Ferroptosis: an iron-dependent form of nonapoptotic cell death. *Cell* (2012) 149 (5):1060–72. doi: 10.1016/j.cell.2012.03.042

31. Chae YC, Kim JH. Cancer stem cell metabolism:target for cancer therapy. *BMB Rep* (2018) 51(7):319–26. doi: 10.5483/bmbrep.2018.51.7.112

32. Chen X, Kang R, Kroemer G, Tang D. Organelle-specific regulation of ferroptosis. *Cell Death Differ* (2021) 28(10):2843–56. doi: 10.1038/s41418-021-00859-z

33. Zaugg J, Solenthaler F, Albrecht C. Materno-fetal iron transfer and the emerging role of ferroptosis pathways. *Biochem Pharmacol* (2022) 202:115141. doi: 10.1016/j.bcp.2022.115141

34. Shreeve N, Depierreux D, Hawkes D, Traherne JA, Sovio U, Huhn O, et al. The CD94/NKG2A inhibitory receptor educates uterine NK cells to optimize pregnancy outcomes in humans and mice. *Immunity* (2021) 54(6):1231–44. doi: 10.1016/j.immuni.2021.03.021

35. Tholen J, Razew M, Weis F, Galej WP. Structural basis of branch site recognition by the human spliceosome. *Science* (2022) 375(6576):50–7. doi: 10.1126/science.abm4245

36. Maserati M, Dai X, Walentuk M, Mager J. Identification of four genes required for mamMalian blastocyst formation. *Zygote* (2014) 22(3):331–9. doi: 10.1017/S0967199412000561

37. Jourdain AA, Begg BE, Mick E, Shah H, Calvo SE, Skinner OS, et al. Loss of LUC7L2 and U1 snRNP subunits shifts energy metabolism from glycolysis to OXPHOS. *Mol Cell* (2021) 81(9):1905–1919.e12. doi: 10.1016/j.molcel.2021.02.033

38. Kalpongnukul N, Bootsri R, Wongkongkathep P, Kaewsapsak P, Ariyachet C, Pisitkun T, et al. Phosphoproteomic analysis defines BABAM1 as mTORC2 downstream effector promoting DNA damage response in glioblastoma cells. *J Proteome Res* (2022) 21(12):2893–904. doi: 10.1021/acs.jproteome.2c00240

39. Wang Y, Tian Q, Hao Y, Yao W, Lu J, Chen C, et al. The kinase complex mTORC2 promotes the longevity of virus-specific memory CD4+ T cells by preventing ferroptosis. *Nat Immunol* (2022) 23(2):303–17. doi: 10.1038/s41590-021-01090-1

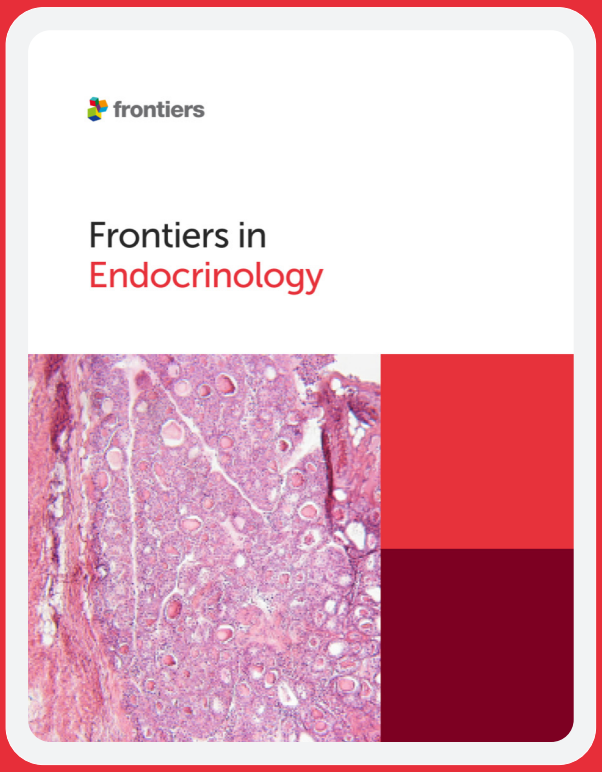
Frontiers in Endocrinology

Explores the endocrine system to find new therapies for key health issues

The second most-cited endocrinology and metabolism journal, which advances our understanding of the endocrine system. It uncovers new therapies for prevalent health issues such as obesity, diabetes, reproduction, and aging.

Discover the latest Research Topics

See more →



Frontiers

Avenue du Tribunal-Fédéral 34
1005 Lausanne, Switzerland
frontiersin.org

Contact us

+41 (0)21 510 17 00
frontiersin.org/about/contact